LYVE-1 and the response of lymphatic vessel endothelium to inflammation

Thesis

UNRESTRICTED

LYVE-1 AND THE RESPONSE OF LYMPHATIC VESSEL ENDOTHELIUM TO INFLAMMATION

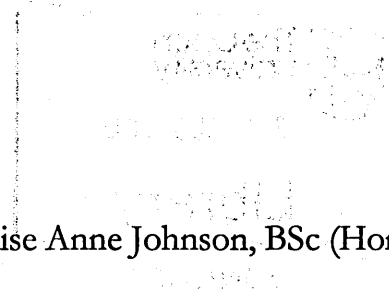

Louise Anne Johnson, BSc (Hons)

Weatherall Institute of Molecular Medicine, Oxford

Thesis for the degree of
Doctor of Philosophy

Open University

2005

DATE OF SUBMISSION 11 MARCH 2005

DATE OF AWARD 8 JULY 2005

Abstract

The lymphatic system provides a conduit for the delivery of antigen-presenting cells from peripheral tissues to draining lymph nodes, both constitutively and during inflammation, when a dramatic increase in the number of trafficking events occurs. This thesis is concerned with the role played by the lymphatic endothelium under pro-inflammatory conditions and the mechanisms regulating entry of leukocytes into the lymphatic capillaries.

Monoclonal antibodies against the lymphatic vessel endothelial-specific receptor for hyaluronan, LYVE-1, were raised in rat against the mouse orthologue, for use both as a marker for lymphatics in mouse tissue and to investigate the physiological role of this protein. LYVE-1 was found to be dramatically and specifically down-regulated by TNFα and TNFβ, by rapid internalisation and transcriptional down-regulation in primary lymphatic endothelial cells. A significant reduction in LYVE-1 expression was also recorded in intact lymphatic vessels in response to TNFα and in an allergen-induced mouse model of skin inflammation. Furthermore, lymphatic endothelial cells were found to respond to this pro-inflammatory cytokine by instigating a distinct expression programme characterised by up-regulation of the key leukocyte adhesion receptors VCAM-1, ICAM-1 and E-selectin; chemokines and other potential regulators of leukocyte entry. Moreover, the major components of this programme were confirmed in dermal lymphatic vessels in the allergen-induced mouse model of skin inflammation, simultaneous with the down-modulation of LYVE-1 and lymphatic accumulation of migrating leukocytes. The results described in this thesis provide the first evidence that lymphatic endothelial cells play an active role in inflammation. In addition these data indicate that the lymphatic and blood vascular systems share components of the same address code for specific vascular targeting.

Acknowledgements

Firstly, I would like to thank Prof. David Jackson for his supervision and advice throughout this PhD. Also, my colleagues in the Jackson lab: Steve, Neale, Remko, Tom, Alastair, Branwen, and (more recently) Jorge and Matt, for sharing their knowledge and brightening my days. Also, I greatly appreciate the guidance I have received from my second supervisor, Prof. Andrew McMichael and am tremendously indebted to Dr. Mike Puklavec, without whom the generation of anti-mouse monoclonal antibodies for this thesis would not have been possible.

My greatest thanks go to my mother and father, for their perpetual support, encouragement and love; and my husband, Gareth who has brought me so much happiness over the last two years.

"Without counsel, purposes are disappointed: but in the multitude of counsellors, they are established." (Prov. 15:22)

Outline

Title page

Abstract

Acknowledgements

Outline

Contents

Abbreviations and Acronyms

Chemokine Nomenclature

Chapter 1. General Introduction

Chapter 2. Materials and Methods

Chapter 3. Generation of Monoclonal Antibodies against Mouse LYVE-1

Chapter 4. Effects of Inflammatory Cytokines on LYVE–1 Expression in Human Lymphatic Endothelial Cells

Chapter 5. An Inflammation-induced Expression Programme in Lymphatic Endothelial Cells

Chapter 6. The Effects of Inflammation on Lymphatic Endothelium in Whole Tissue

Chapter 7. General Discussion

Bibliography

Appendices

Table of Contents

CHAPTER 1

General Introduction 1

1.1 The Lymphatic System 2

1.1.1 The discovery of the lymphatics 2

1.1.2 Anatomy and Physiology 7

1.1.2.1 Lymphatic vessels 7

1.1.2.2 Lymph nodes 10

1.1.3 The origins and development of the lymphatics during embryogenesis 14

1.1.4 Functions of the lymphatics 17

1.2 Hyaluronan and its Receptors: CD44 and LYVE-1 18

1.2.1 Functions of HA 19

1.2.2 HA metabolism and turnover 20

1.2.3 Hyaluronan receptors 21

1.2.4 CD44 24

1.2.4.1 Structure of CD44 24

1.2.4.2 Expression and functions of CD44 25

1.2.5 LYVE-1 29

1.2.5.1 Structure of LYVE-1 29

1.2.5.2 Cloning of the mouse orthologue 30

1.2.5.3 LYVE-1-mediated HA binding and internalisation 32

1.3 Other Endothelium Markers 34

1.3.1 Prox1 34

1.3.2 Podoplanin 35

1.3.3 VEGFR-3 37

1.3.4 CD34 39

1.3.5 CD31 43

1.4 Pathological Conditions of the Lymphatics 49
1.4.1 Metastasis of tumour cells and lymphangiogenesis 49
1.4.2 Lymphatics as an entry for pathogens 52
1.4.3 Lymphoedema 54
1.5 The Migration of Leukocytes Throughout the Vasculature and Lymphatic Systems: in Sickness and in Health 58
1.5.1 The TNF superfamily 59
1.5.1.1 TNFα 59
1.5.1.2 TNFβ 60
1.5.2 Receptors 61
1.5.3 Leukocyte influx into tissues 62
1.5.3.1 Paracellular transmigration 69
1.5.3.2 Transcellular transmigration 76
1.5.4 Recirculation of T cells to the lymph nodes 79
1.5.5 Leukocyte trafficking through afferent lymphatics 81
1.6 Aims of this thesis 88
CHAPTER 2
Methods & Materials 89
2.1 General Reagents 90
2.1.1 Chemicals 90
2.1.2 Molecular biology reagents 90
2.1.2.1 General reagents 90
2.1.2.2 Nucleic acids 91
2.1.2.3 Enzymes 91
2.1.2.4 Radiolabelled reagents 92
2.1.3 Cell culture reagents 92
2.1.3 1 Media 92
2.1.3.2 Transfection reagents 93
2.1.3.3 Reagents for magnetic cell sorting of cells (MACS) 93

2.1.3.4 Tissue culture ware 93
2.1.4 Reagents for the generation of monoclonal antibodies 94
2.2 Antibodies 95
2.2.1 Primary anti-mouse antibodies 95
2.2.2 Primary anti-human antibodies 95
2.2.3 Secondary antibodies and conjugates 97
2.3 Bacterial Culture 98
2.3.1 Bacterial media 98
2.3.2 Bacterial strains 99
2.3.3 Preparation of glycerol stocks 99
2.3.4 Preparation of calcium competent DH5α or MC1061/p3 99
2.3.5 Transformation of calcium competent E.coli 99
2.3.6 Preparation of electrocompetent E. coli 100
2.3.7 Electroporation of E.coli 100
2.4 Molecular Biology Methods 101
2.4.1 RNA 101
2.4.1.1 Extraction of total cellular RNA from tissues 101
2.4.1.2 Extraction of total cellular RNA from cells 102
2.4.1.3 Electrophoresis of RNA through agarose-formalehyde gels 102
2.4.1 4 Northern blotting: Neutral transfer by capillary transfer by upward flow 103
2.4.1.5 Preparation of ^{32}P-labelled DNA probes 103
2.4.1.6 Northern Hybridisation 104
2.4.1.7 Generation of first strand synthesis products 104
2.4.1.8 Affymetrix array analysis 104
2.4.2 DNA 106
2.4.2.1 Plasmids 106
2.4.2.2 Constructs 106
2.4.2.3 Agarose gel electrophoresis 107

2.4.2.4 Digestion of DNA with restriction endonucleases 107
2.4.2.5 Purification of DNA Fragments from Agarose Gels 108
2.4.2.6 Ligation of digested DNA fragments 108
2.4.2.7 PCR (Polymerase Chain Reaction) 108
2.4.2.8 Amplification with Taq Polymerase 108
2.4.2.9 Amplification with Pfu Polymerase 109
2.4.2.10 Amplification Using TaqPlus® Precision PCR System 109
2.4.2.11 Small-scale Preparation of Plasmid DNA (miniprep) 110
2.4.2.12 Large-scale Preparation of Plasmid DNA (maxiprep) 110
2.4.2.13 Southern Blotting: Alkali Transfer by Upward Capillary Transfer 111
2.4.2.14 Southern Hybridisation 111
2.4.2.15 Primer Extension Analysis 112
2.4.2.16 Preparation of genomic DNA 115
2.5 Tissue Culture 117
2.5.1 Cell lines and transfectants 117
2.5.1.1 Transformed cell lines 117
2.5.1.2 Primary cell lines 117
2.5.2 Culture conditions 118
2.5.3 Collagen-coating of tissue culture dishes for mouse LEC 118
2.5.4 Gelatin-coating of tissue culture dishes for human endothelial cells .. 118
2.5.5 Passaging of cells 119
2.5.5.1 293T and RAW 264.7 119
2.5.5.2 NS–1 and Y3 119
2.5.5.3 Endothelial cells 119
2.5.6 Frozen storage of cells 119
2.5.7 Recovery of frozen cells 119
2.5.8 Preparation of mouse LEC from skin 120
2.5.9 Derivation of primary HDLEC from HDMEC 121

2.5.10 Trypan blue dye exclusion assay 122
2.5.11 MTT proliferation assay 122
2.5.12 Tube-formation assay 123
2.5.13 Transfection methods 123
2.5.13 1 Transient transfection of 293T cells by calcium phosphate precipitation 123
2.5.13.2 Electroporation of HUVEC 123
2.5.13.3 Lipofectin transfection of RAW 264.7 124
2.5.14 Expression and purification of soluble Fc fusion proteins 124
2.6 Protein Biochemical Methods 125
2.6.1 Measurement of protein concentration 125
2.6.2 SDS-Polyacrylamide gel electrophoresis (SDS-PAGE) 125
Buffers and solutions 125
2.6.3 Coomassie blue staining of protein gels 126
2.6.4 Western blotting 126
2.6.5 Enzyme-linked immunosorbant assay to quantitate chemokine concentrations 127
2.6.6 Estimation of shed LYVE-1 in culture supernatant 127
2.7 Generation of Polyclonal Antisera 128
2.7.1 Immunisation 128
2.7.2 Assessment of antibody reactivity by ELISA 128
2.8 Generation of Monoclonal Antibodies Against Mouse LYVE–1 129
2.8.1 Testing of sera for myeloma culture 129
2.8.2 Immunisation 130
2.8.3 Testing the titre of antisera 130
2.8.4 Hybridoma fusions 130
2.8.5 Screening of hybridomas for production of antibodies against LYVE-1 131
2.8.5.1 293T-mouse LYVE-1 transfectant assay 131

2.8.5.2 ELISA 132
2.8.6 Re-cloning hybridomas 132
2.8.7 Ig subtyping of LYVE-1 monoclonal antibodies 132
2.8.8. Culture of hybridomas and purification of antibody 132
2.9 Immunohistochemistry and Immunofluorescence Antibody Staining 133
2.9.1 Source of tissue sections 133
2.9.1.1 Frozen human skin sections 133
2.9.1.2 Paraffin-embedded mouse tissues 133
2.9.1.3 Mouse frozen tissue sections 133
2.9.2 Preparation of cytospin slides 134
2.9.3 De-waxing and antigen retrieval of paraffin-embedded sections 134
2.9.4 Single immunoperoxidase staining 134
2.9.5 Flow cytometry 135
2.9.6 Immunofluorescence staining of cells 135
2.9.7 Staining of intracellular antigens 136
2.9.8 Whole mount staining of mouse ears 137
2.9.9 Confocal microscopy 137
2.10 Animal Procedures 138
2.10 1 Animals 138
2.10.2 Mouse ear explants 138
2.10.3 Elicitation of oxazolone-induced contact hypersensitivity in mice ... 138
CHAPTER 3
Generation of Monoclonal Antibodies against 139
Mouse LYVE-1 139
3.1 Introduction 140
3.2 Results 144
3.2.1 Immunisation of rats and testing of antisera 144
3.2.2 Generation and screening of hybridomas 147

3.2.3 Assessing the mAbs for immunoperoxidase staining of paraffin sections 151
3.2.4 Immunofluorescence staining using the newly generated mAbs 153
3.2.5 The use of C1/8 for whole mount staining of tissue 153
3.2.6 Characterisation of the specificity of the LYVE-1 mAbs 158
3.2.7 Determining the effect of the degree of LYVE-1 sialation on mAb binding 160
3.2.8 Preliminary epitope mapping using mouse/human LYVE-1 chimeras 162
3.2.9 Functional assays 162
3.2.9.1 Testing the ability of the mAbs to induce shedding of LYVE-1 162
3.2.9.2 Determining ability of the mAbs to block HA binding 163
3.3 Discussion 167
CHAPTER 4
Effects of Inflammatory Cytokines on LYVE–1 Expression in Human Lymphatic Endothelial Cells 169
4.1 Introduction 170
4.1.1 Blood and lymphatic endothelial cells 170
4.1.2 Possible regulation of LYVE-1 expression in LEC 171
4.1.3 Aims 174
4.2 Results 175
4.2.1 Derivation of human lymphatic endothelial cells (LEC) 175
4.2.1.1 Human dermal endothelial cells from Clonetics, USA 175
4.2.1.2 Human dermal microvascular endothelial cells from PromoCell, Germany 176
4.2.1.3 Characterisation of PromoCell HDLEC 179
4.2.2 Changes in LYVE-1 surface expression in response to culture conditions 181
4.2.3 Effects of TNF on primary HDLEC 185

4.2.3.1 Effect on morphology 185
4.2.3.2 Viability and proliferation 187
4.2.3.3 Effect of TNFα on tube formation by HDLEC in Matrigel™ 190
4.2.3.4 Time course 190
4.2.3.5 Concentration dependence 193
4.2.3.6 Recovery 193
4.2.4 The fate of LYVE-1 following exposure to TNF 196
4.2.4.1 Effects of TNFα stimulation on LYVE-1 protein 196
4.2.4.2 Effects of TNFα stimulation on LYVE-1 mRNA levels 203
4.2.5 Investigating possible involvement of NFkB in TNFα-induced down-regulation of LYVE-1 206
4.2.6 Possible effects of LYVE-1 down-regulation on HA binding 211
4.2.6.1 Effects of TNFα on HA binding by LYVE-1 in HDLEC 211
4.2.6.2 Effects of TNFα on HA binding by LYVE-1 in primary mouse dermal LEC 213
4.2.7 Effect of IL-6 on LYVE-1 expression on HDLEC 216
4.2.7.1 Concentration dependence 216
4.2.7.2 Time-course 216
4.2.8 Effect of hypoxia on HDLEC 219
4.2.9 Effect of PMA on LYVE-1 expression 219
4.2.9.1 The effect of PMA on LYVE-1 shedding in HDLEC 221
4.2.9.2 Involvement of matrix metalloproteases 221
4.3 Discussion 224
4.3.1 Preliminary phenotyping of HDLEC 224
4.3.2 Factors affecting variability of LYVE-1 expression in cultured cells ... 225
4.3.3 Characterisation of TNFα-induced down-regulation of LYVE-1 226
4.3.4 The mechanism for TNFα-mediated LYVE-1 down-regulation 228
4.3.5 Putative down-modulation of LYVE-1 via NFκB 231
4.3.6 Does TNFα activate LYVE-1 to bind HA? 232

4.3.7 Investigating the response of LYVE-1 expression to hypoxia 234
4.3.8 Conclusion 235
CHAPTER 5.
An Inflammation-induced Expression Programme in Lymphatic Endothelial Cells 236
Introduction 237
5.1.1 Inflammation-induced changes in gene expression on blood vascular endothelium 237
5.1.2 Aims 239
Results 240
5.2.1 Effect of proinflammatory cytokines and chemokines on expression of leukocyte adhesion molecules in primary HDLEC 240
5.2.2 Kinetics of adhesion molecule up-regulation in primary HDLEC 243
5.2.3 Effects of TNFα on other key leukocyte adhesion molecules 245
5.2.4 Gene array analysis 250
5.2.5 Kinetics of induction of chemokine synthesis in primary HDLEC 257
5.2.6 Effects of TNFα on mouse LEC 259
5.2.6.1 Isolation of mouse LEC 259
5.2.6.2 Effects of TNFα on mouse LEC morphology 260
5.2.6.3 Effect of TNFα on LYVE-1 expression 263
5.2.6.4 Effects of TNFα on expression of key leukocyte adhesion molecules 268
5.2.6.5 Microarray analysis of resting and TNFα-stimulated mouse LEC 274
5.2.6.6 Effect of TNF on chemokine production by mouse LEC 279
5.3 Discussion 282
5.3.1 Expression of adhesion molecules on LEC 282
5.3.2 Chemokines 285
5.3.4 Matrix metalloproteinases 287
5.3.5 TNF superfamily members 288

5.3.6 LYVE-1 289
5.3.7 Conclusion 290
CHAPTER 6
The Effects of Inflammation on Lymphatic Endothelium in 291
Whole Tissue 291
6.1 Introduction 292
6.1.1 The effects of TNF in the skin 292
6.2 Results 295
6.2.1 Cultured mouse ear tissue 295
6.2.2 TNFα-mediated contact hypersensitivity in mice 302
6.2.2.1 Expression of LYVE-1 following challenge 302
6.2.2.2 Kinetics of LYVE-1 down-regulation in inflamed dermal tissue .. 305
6.2.2.3 Expression of leukocyte adhesion molecules by dermal lymphatic vessel endothelia following oxazolone challenge 310
6.2.2.4 Effects of inflammation on dermal leukocyte trafficking 314
6.2.2.5 Effects of inflammation on dermal chemokines expression 319
6.3 Discussion 323
6.3.1 Expression of adhesion receptors in inflammation 323
6.3.2 The role of chemokines and their receptors in leukocyte trafficking into lymphatic endothelium 324
6.3.3 LYVE-1 327
6.3.4 Conclusion 329
CHAPTER 7
General Discussion 331
7.1 LYVE-1 333
7.1.1 Generation of monoclonal antibodies against mouse LYVE-1 333
7.1.2 Factors regulating LYVE-1 expression 334
7.1.3 The effect of TNFα on LYVE-1 expression in primary LEC 335
7.1.4 HA binding by LYVE-1 337

7.1.5 A putative role for LYVE-1 in regulating reverse transmigration ... 338
7.2 The effects of TNFα on lymphatic endothelial cells *in vitro* and in intact tissue ... 339
7.2.1 TNFα-mediated induction of key leukocyte adhesion molecules ... 339
7.2.2 TNFα-induced change in morphology of lymphatic endothelial cells ... 342
7.2.3 Synthesis of pro-inflammatory chemokines by lymphatic endothelial cells ... 342
7.2.4 Induction of MMPs by lymphatic endothelial cells ... 343
7.2.5 Synthesis of TNF superfamily members by lymphatic endothelial cells ... 344
7.2.6 A model for the inflammation-induced expression programme in lymphatic endothelium ... 345
7.3 Conclusion ... 347

Abbreviations and Acronyms

aa	amino acid residue(s)
Ab	antibody
ADAM	a disintegrin and metalloproteinase
Ang	angiopoetin
APC	antigen presenting cell
APS	ammonium persulphate
ATP	adenosine 5′-triphosphate
bp	base pair
BLAST	basic local alignment search tool
BSA	bovine serum albumin
BRAL1	brain Link protein-1
CCR	chemokine receptor
cDNA	complementary DNA
CD	cluster of differentiation
CH	constant region: heavy chain (of immunoglobulin)
CHO	chinese hamster ovary
CHS	contact hypersensitivity
CLEVER-1	common lymphatic endothelial and vascular endothelial receptor-1
cRNA	complementary RNA
CSF	colony stimulating factor
Ctrl	control
CTP	cytosine 5′-triphosphate
DC	dendritic cell
DMEM	Dulbecco's modified Eagle's medium
DMSO	dimethyl sulphoxide
DNA	deoxyribonucleic acid
DNase	deoxyribonuclease
dNTP	deoxynucleoside triphosphate
ds	double stranded
DTT	dithiothrietol
E. coli	Escherichia coli
EBM-2	endothelial cell basal medium
E-cadherin	epithelial cadherin
ECL	enhanced chemiluminescence
ECM	extracellular matrix
ECM-III	extracellular matrix receptor type III
EDTA	ethylenediaminetetra-acetic acid
EEA	early endosome antigen
EGF	epidermal growth factor
ELC	Epstein-Barr virus-induced molecule 1 ligand chemokine

ELISA	enzyme linked immunosorbant assay
ENA	epithelial cell-derived neutrophil attractant
ER	endoplasmatic reticulum
ERM	ezrin, radixin and moesin
EST	expressed sequence tag
Fab	fragment antigen binding
FACS	fluorescence activated cell sorting
FBS	foetal bovine serum
FCS	foetal calf serum
FEEL-1	Fasciclin, EGF-like, laminin-type EGF-like and Link domain containing scavenger receptor-1
FEL-1	Fasciclin domains, EGF repeats and Link module containing protein-1
FGF	fibroblast growth factor
Fc	fragment crystallisable (hinge, CH2 and CH3 domain from Ig)
FITC	fluorescein isothiocyanate
G418	geneticin
GAG	glycosaminoglycan
G-CSF	granulocyte-colony-stimulating factor
GCP	granulocyte chemotactic protein
GlyCAM	glycan-bearing cell adhesion molecule
GM-CSF	granulocyte-monocyte-colony-stimulating factor
GTP	guanosine 5'-triphosphate
h	hour
HA	hyaluronan
Has	HA synthase
HARE	HA receptor for endocytosis
HDMEC	human dermal microvascular endothelial cells
HDLEC	human dermal lymphatic endothelial cells
HEV	high endothelial venule
HMVEC	human microvascular endothelial cells
HRP	horseradish peroxidase
HUVEC	human umbilical vein endothelial cells
HYAL	hyaluronidase
ICAM	intercellular adhesion molecule
Ig	immunoglobulin
IGF	insulin-like growth factor
IL	interleukin
IFN	interferon
IP-10	interferon-inducible protein-10
JAM	junctional adhesion molecule
kb	kilobase
kDa	kiloDalton

LB	Luria broth
LC	Langerhans cell
LEC	lymphatic endothelial cell
LFA	leukocyte function-associated antigen
LPS	lipopolysaccharide
LYVE-1	lymphatic vessel endothelial hyaluronan receptor-1
mAb	monoclonal antibody
MACS	magnetic cell sorting
MadCAM	mucosal addressin-cell adhesion molecule
MCP	monocyte chemotactic protein
M-CSF	monocyte-colony-stimulating factor
MES	2-[N-morpholino] ethane-sulfonic acid
MEM	minimum essential media
MFI	mean fluorescent intensity
MHC	major histocompatability complex
min	minute
MIP	macrophage inflammatory protein
MMP	matrix metalloproteinase
MOPS	3-(N-morpholino) propanesulfonic acid
mRNA	messenger RNA
NANAse	neuraminidase
NF-κB	nuclear factor-κB
OD	optical density
OPD	*O*-phenylenediamine
OPN	osteopontin
Oxaz	oxazolone
PAC	plasmid artificial chromosome
PBS	phosphate buffered saline
PCR	polymerase chain reaction
PDI	protein disulphide isomerase
PECAM	platelet endothelial cell adhesion molecule
PEG	polyethylene glycol
Pen	penicillin
PFA	paraformaldehyde
Pgp-1	phagocytic glycoprotein-1
PKC	protein kinase C
PMA	phorbol 12-myristate 13-acetate
Prox1	prospero-related homeobox 1
RANTES	regulated upon activation, normal T cell expressed and secreted
RNA	ribonucleic acid
RNase	ribonuclease
RPMI	Roswell Park Memorial Institute (media)
rRNA	ribosomal RNA

RT-PCR	reverse transcriptase PCR
RPM	revolutions per minute
SCID	severe combined immunodeficiency
SDF	stromal cell-derived factor
SDS	sodium dodecyl sulphate
SDS-PAGE	sodium dodecyl sulphate polyacrylamide gel electrophoresis
SLC	secondary lymphoid tissue chemoattractant
Strep	streptomycin
TB	terrific broth
TGF-β	transforming growth factor-β
TEMED	NNN'N'-tetramethylethylenediamine
Tiam1	T cell lymphoma invasion and metastasis
TLR	Toll-like receptor
TGN	trans-Golgi network
TM	transmembrane domain
TNF	tumour necrosis factor
TNFR	tumour necrosis factor receptor
TNFRSF	tumour necrosis factor receptor superfamily
TNFS	tumour necrosis factor superfamily
Tris	tris-hydroxymethylamino methane (C4H11NO3)
tRNA	transfer RNA
TSG-6	tumour necrosis factor inducible gene-6
Tween 20	polyoxyethylene-sorbitan monolaurate
VCAM-1	vascular cell adhesion molecule-1
VEGF	vascular endothelial growth factor
VEGFR	vascular endothelial growth factor receptor
VLA-4	very late antigen-4
UTR	untranslated region
UV	ultra violet
V	volume
VE-cadherin	vascular endothelial cadherin
vWF	von Willebrand factor
v/v	volume per volume
w/v	weight per volume
ZO	zona occludens

Chemokine Nomenclature

SYSTEMATIC NAME	SCY NAME	ALTERNATIVE NAMES	
		HUMAN	MOUSE
C Family			
XCL1	SCYC1	Lptn	Lptn
XCL2	SCYC2	-	-
CX_3C Family			
CX_3C	-	Fractalkine	Fractalkine
CC Family			
CCL1	SCYA1	I-309	TCA-3
CCL2	SCYA2	MCP-1	JE
CCL3	SCYA3	MIP-1β	MIP-1α
CCL4	SCYA4	MIP-1β	MIP-1β
CCL5	SCYA5	RANTES	RANTES
CCL6	SCYA6	-	C10
CCL7	SCYA7	MCP-3	MCP-3
CCL8	SCYA8	MCP-2	MCP-2
CCL9/10	SCYA9	-	MIP-1γ
CCL11	SCYA11	Eotaxin	Eotaxin
CCL12	SCYA12	-	MCP-5
CCL13	SCYA13	MCP-4	-
CCL14	SCYA14	HCC-1	-
CCL15	SCYA15	MIP-1δ	-
CCL16	SCYA16	HCC-4	-
CCL17	SCYA17	TARC	TARC
CCL18	SCYA18	PARC	-
CCL19	SCYA19	MIP-3β (*or* ELC)	MIP-3β (*or* ELC)

SYSTEMATIC NAME	SCY NAME	ALTERNATIVE NAMES	
		HUMAN	MOUSE
CCL20	SCYA20	MIP-3α	MIP-3α
CCL21	SCYA21	SLC (*or* 6Ckine)	SLC (*or* 6Ckine)
CCL22	SCYA22	MDC	MDC
CCL23	SCYA23	MPIF	MPIF
CCL24	SCYA24	Eotaxin-2	Eotaxin-2
CCL25	SCYA25	TECK	TECK
CCL26	SCYA26	Eotaxin-3	-
CCL27	SCYA27	CTACK	CTACK
CCL28	SCYA28	MEC	MEC
CXC Family			
CXCL1	SCYB1	GROα	
CXCL2	SCYB2	GROβ	MIP-2
CXCL3	SCYB3	GROγ	
CXCL4	SCYB4	PF4	PF4
CXCL5	SCYB5	ENA-78	ENA-78
CXCL6	SCYB6	GCP-2	LIX
CXCL7	SCYB7	NAP-2	TCK-1
CXCL8	SCYB8	IL-8	
CXCL9	SCYB9	MIG	MIG
CXCL10	SCYB10	IP10	IP10
CXCL11	SCYB11	I-TAC	I-TAC
CXCL12	SCYB12	SDF-1	SDF-1
CXCL13	SCYB13	BCA-1	BLC
CXCL14	SCYB14	BRAK	BRAK
CXCL15	SCYB15		Lungkine
CXCL16	SCYB16	SRPSOX	SRPSOX

CHAPTER 1

General Introduction

1.1 The Lymphatic System.....2

1.2 Hyaluronan and its Receptors: CD44 and LYVE-1.....18

1.3 Other Endothelium Markers.....34

1.4 Pathological Conditions of the Lymphatics.....49

1.5 The Migration of Leukocytes Throughout the Vasculature and Lymphatic Systems: in Sickness and in Health.....58

1.6 Aims of this thesis.....88

1.1 The Lymphatic System

1.1.1 The discovery of the lymphatics

The early history of the research into the lymphatics is contemporary with the founding of modern medicine. The ancient Greeks first recorded the observation of vessels containing colourless fluid: Hippocrates spoke of "white blood" circa 400BC and the Greek physician Herophilus recorded *vasa chylifera* or lacteals in the mesenteries of the live criminals he dissected (Robinson, 1907). Another Greek physician, Erasistratus (340-280 B. C.) also observed such vessels but mistakenly believed them to be arteries. However the important physiological functions they perform were unreported. No further progress was made until 1622 when an Italian professor of anatomy and surgery, Gasparo Aselli observed white fluid-filled vessels in the mesentery of a well-fed dog. He termed these vessels "milky veins", *lacteis venis* in a descriptive paper published posthumously in 1627 (figure 1.1). The following year the efforts of Nicolas Peiresc, a liberal senator of Aix, resulted in these observations being confirmed in a human subject, a felon who had eaten copiously before execution and whose body was inspected an hour and a half later.

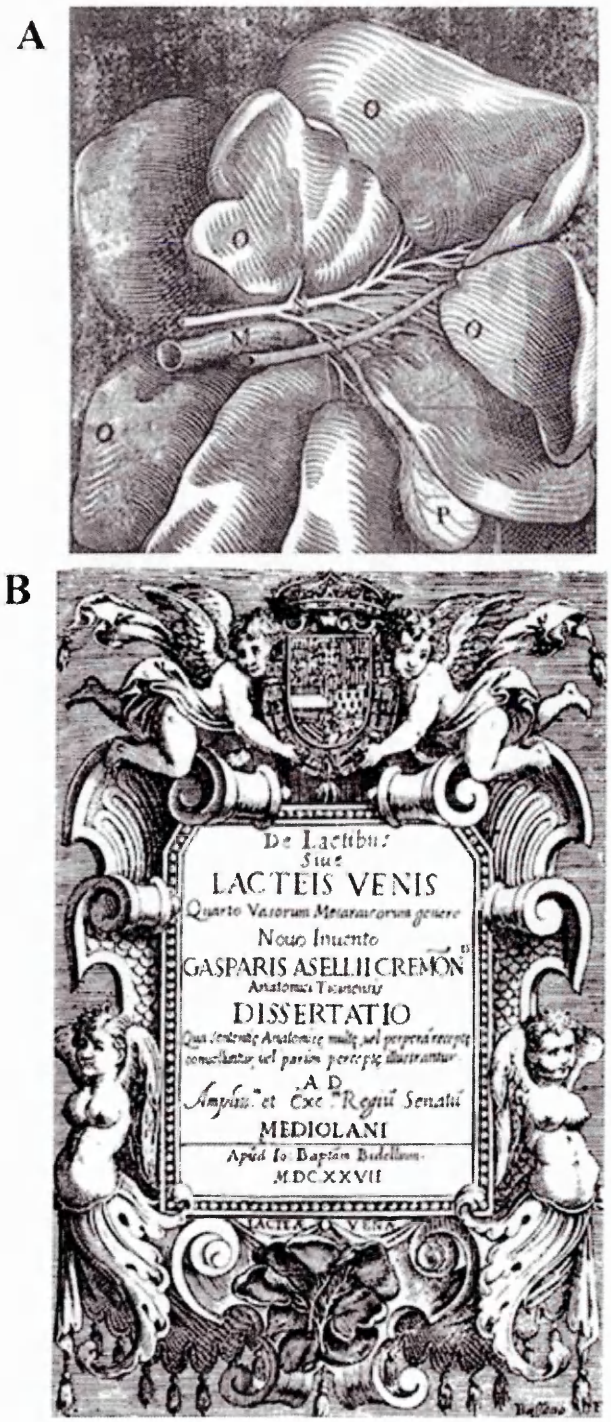

Figure 1.1 Illustrations from the descriptive paper on mesenteric lymphatics by Gasparo Aselli (1627). Upper panel depicts the branching *"lacteis venis"* in canine mesentery. Lower panel shows the highly decorative front cover of this extensive study.

The discovery of the thoracic duct by Jacques Mentel in 1629 and again in 1651 by Jean Pecquet lead to the recognition that lymph drains from the thoracic duct into the blood instead of to the liver, as was previously suggested by Aselli, who postulated that lymph would transform into blood in the liver. However the importance of the lymphatics was not initially acknowledged and it was assumed that their primary role was to enable absorption of food. This concept was revised following the observation of the extensive network of the lymphatics throughout the body, by Olaus Rudbeck in 1651, a young Swede working in Upssala and at the same time by George Joyliffe, an English anatomist and then again in 1653 independently by Thomas Barholin in Copenhagen, who first introduced the term *lymphaticus* (Robinson, 1907). The lymphatics of the large intestine were traced to the thoracic duct, which was found to lead into the subclavian veins.

Development of the technique of intralymphatic injection of mercury, first by Nuck (1692), then modified by Macagni (1784), Cruikshank (1798) and Gerota (1896), permitted the lymphatic system to be outlined in greater detail than was previously possible. Monro *primus* (1732) and Monro *secundus* (1788) were responsible for various accounts of the lymphatic system and detailed plates indicating the location of major lymphatic vessels in the body (figure 1.2), as revealed by the injection of mercury (reviewed by Kaufman, 1999). The modern era of understanding lymphatic function was heralded in 1746 in London, when William Hunter with his brother John Hunter and pupils at the School of Anatomy were able to show that the lymphatic vessels are responsible for absorption throughout the body, instead of only from the gut, as was initially believed. By the end of the century, the anatomy of the larger lymphatic network was correctly elucidated. The fine lymphatic capillaries had to linger on in obscurity until 1862, when the advent of a discovery by von Recklinghausen revolutionised the field. He found that following the application of silver nitrate

to tissues, the borders of endothelial cells stained black (reviewed by Skobe and Detmar, 2000). He went on to disprove the popular theory of the time that lymph passed from the blood stream into the lymphatics through a fine tubular system and demonstrated that the two systems were not directly connected. Instead he theorised that lymphatic capillaries have open endings into which fluid passes from the interstitial space. He was responsible for an accurate description of the network of lymphatic capillaries and revealed that they are lined by a single layer of endothelial cells.

Figure 1.2 Engraving of the lymphatic system, based on the cadaver of a male subject, dissected and injected with mercury in 1788 by Monro *secundus*. Adapted from Kaufman, 1999.

The first suggestion that lymph was a filtrate of blood was by Ludwig in the late 19th century and confirmed by Starling in 1896. Although Starling had realized that capillaries leak protein, the concept was further developed in the early 20th century by Drinker (Skobe and Detmar, 2000). Thus the lymphatic system was recognised as constituting highly permeable absorbing vessels which return fluid and proteins to the blood stream and a cease in this recirculation results in death, (Adair and Guyton, 1985).

The role played by the lymphatics in absorbing digested fats from the intestine was characterised more fully by Allen (1967), who identified the presence of lacteals within the villi of the small intestine, so called due to the milky *(lacte)* white appearance, first observed and recorded 2000 years earlier.

The important immunological functions performed by the lymphatics were not recognised until the 20th century, with the characterisation of lymph nodes and understanding of antigen presentation. The pioneering works of Gowans (1957 and 1964) and later Morris (1961-1972) are credited with paving the way for our modern understanding (reviewed by Young, 1999), as although the presence of cells (*lymphocytes*) within the lymphatics had been noted, it was initially believed that these were newly formed cells. Gowans demonstrated that the cannulation of the thoracic duct in a rat resulted in a progressive loss of lymphocytes in the thoracic duct lymph but that this loss could be reversed by returning the collecting cells to the animal by intravenous injection. He also observed that cells collected and labelled with radioactive tracking agents could later be recovered from the thoracic duct lymph and thus the recirculation of lymph-borne cells was demonstrated. Morris and colleagues continued the studies in sheep, which as a large animal permitted the lymphatic vessels draining individual lymph nodes to be accessed surgically. The other advantage of the ovine model was that sheep lymph nodes do not occur in chains as in humans, where the efferent lymph of

one node contributes to the afferent supply of a second node. Instead, each node is drained by only a single efferent lymphatic. Thus this simplified model has permitted many subsequent researchers to track lymphocyte traffick through a variety of lymphoid and non-lymphoid organs, in normal and pathological conditions (reviewed by Young, 1999).

Over the last 2000 years the inhumane and brutal early anatomical studies of the lymphatics have launched methodical scientific research into furthering understanding of the role of this fascinating circulatory system. With the relatively new discovery of novel, specific markers for lymphatic vessels (described in sections 1.2.5 and 1.3 of this chapter), the next few years can be anticipated to be an exciting time in the chronicles of research into the lymphatics.

1.1.2 Anatomy and Physiology

1.1.2.1 Lymphatic vessels

Lymphatic vessels are present in all tissues except for the central nervous system, bone and bone marrow (Mortimer, 1997). They can be broadly classified as either lymph capillaries (also termed initial capillaries), pre-collectors, collectors or lymphatic trunks. The initial capillaries within the superficial dermis of the skin originate as blind-ended endothelial-lined tubes and drain through a series of enlarging vessels, diminishing in number until they reach the thoracic duct. The initial lymphatics form an extensive network between the papillary and reticular dermis, overlaid by further plexi of arterioles and venules which lie directly beneath the epidermis.

When viewed in histological sections, lymphatic vessels often appear collapsed and distended, with thin attenuated walls of loosely overlapping endothelial

cells and nuclei bulging into the lumen (figure 1.3). Unlike blood vessels they lack a basement membrane or zona occludens (Fawcett, 1986) and possess no fenestrations. Collagen fibres tether the lymphatic vessels to the surrounding matrix and prevent vessel collapse when the fluid pressure in the surrounding interstitium exceeds that within the vessels. The overlaps of cells create valves which prevent fluid leaking back into the tissue once the pressure has increased within the vessel (figure 1.3). In larger vessels, specialised valves composed of endothelium and matrix also assist in the one-way movement of lymph, as do local tissue pressure due to muscular activity and local arterial pulsation (Parson and McMaster,. 1938; reviewed by Swartz, 2001). Lymph fluid must be transported through the vessels against a hydrostatic pressure gradient and against a protein concentration gradient (reviewed by von der Weid and Zawieja, 2003). Collector vessels are surrounded by lymphatic smooth muscles, as are larger lymphatic vessels. These muscles are arranged into one to three layers, interwoven with collagen and elastin fibres and surrounded by an adventitia of fibroblasts, connective tissue and nerve endings. As the vessels progress centrally the amount of smooth muscle increases, with the layers more distinguishable. This smooth muscle exhibits spontaneous and phasic contractions which enable the valve-delineated chambers of the vessel to act as pumps or "primitive hearts". The spontaneous transient depolarisation events which lead to contraction are believed to be of a myogenic origin (von der Weid and Zawieja, 2003). Impaired lymphatic smooth muscle function has been linked to various pathologies including lymphoedema (tissue swelling due to accumulation of protein-rich interstitial fluid resulting from low lymphatic output); interstitial oedema (increased leakage of fluid and protein from the blood, compounded by the inability to increase lymphatic clearance); and potentially inflammatory bowel disease. A study by Kaiserling et al., 2003 used the lymphatic marker podoplanin to demonstrate an increase in the number of

intestinal lymphatic capillaries which may lead to abnormal lymphatic contractile function and impaired lymph flow (von der Weid and Zawieja, 2003).

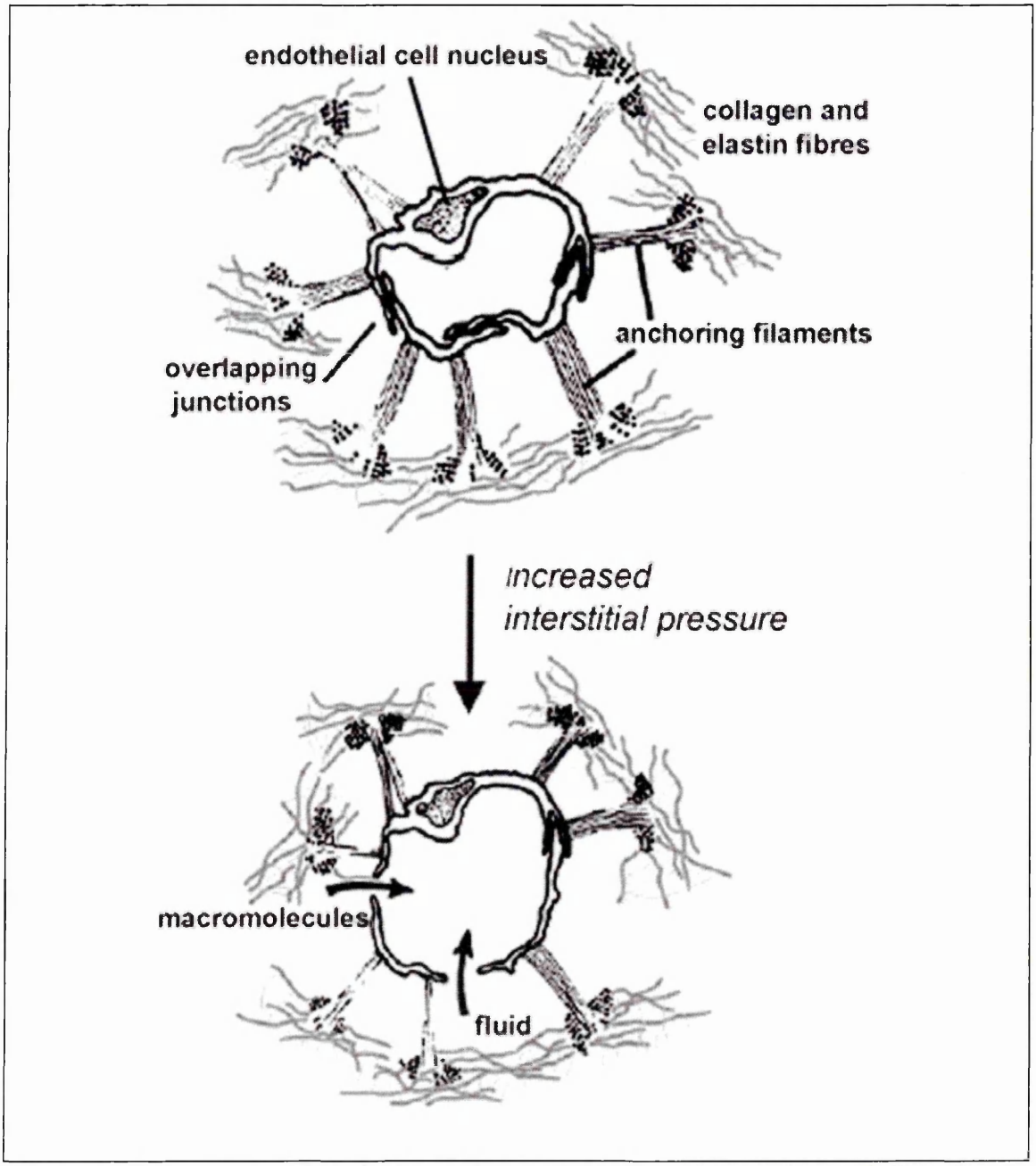

Figure 1.3 Transverse section of a dermal lymphatic capillary. Lymphatic endothelial cells are firmly attached to the collagen and elastin fibres in tissues by anchoring filaments. An increase in interstitial fluid pressure expands the tissue and stretches the fibres. This expansion opens the intercellular junctions between overlapping endothelial cells, allowing passage of fluid and macromolecules into the distended lumen. Adapted from Skobe and Detmar, 2000.

1.1.2.2 Lymph nodes

Lymphatic vessels deliver lymph fluid to the lymph nodes, which are responsible for filtering the fluid to remove cell debris and foreign matter for immune surveillance. There are hundreds of lymph nodes throughout the human body, varying in size from 1 to 10 mm in diameter (reviewed by Swartz, 2001). These are organised in clusters in regions such as the neck (cervical), near the jaw (submaxillary), armpits (axillary), in between the lungs (mediastinary), the abdominal cavity (mesenteric) and groin (inguinal), (figure 1.4).

Each lymph node is bounded by a collagenous capsule but a cross-sectional view reveals that it consists of several layers: the cortex, containing B-cells; the paracortex, rich in T-cells; and a central medulla (figure 1.5). The cortex in larger animals is subdivided into lobules, each separated by fibrous radial bands termed trabeculae (Gretz et al., 1997) whilst the lymph nodes of smaller animals such as mice typically contain only one lobule. B-cells aggregate in the lymphoid follicle of each lobule, with high endothelial venules (HEVs) and cortical sinuses situated in the surrounding cortex area. Macrophages are resident within the node to engulf cell debris and particulate matter and remove it from the lymph. This region is also rich in professional antigen presenting cells (APCs) which have entered through the afferent lymph as lymph node sinuses are the continuation of the lymphatic vessels entering the node. These branch into smaller subcapsular sinuses and the lymph fluid passes on to cortical sinuses within the cortex to reach the underlying sinuses of the medulla (Gretz et al., 1997). Medullary sinuses drain into the terminal sinus and the filtered fluid leaves the node at the hilum via the efferent lymphatic vessel.

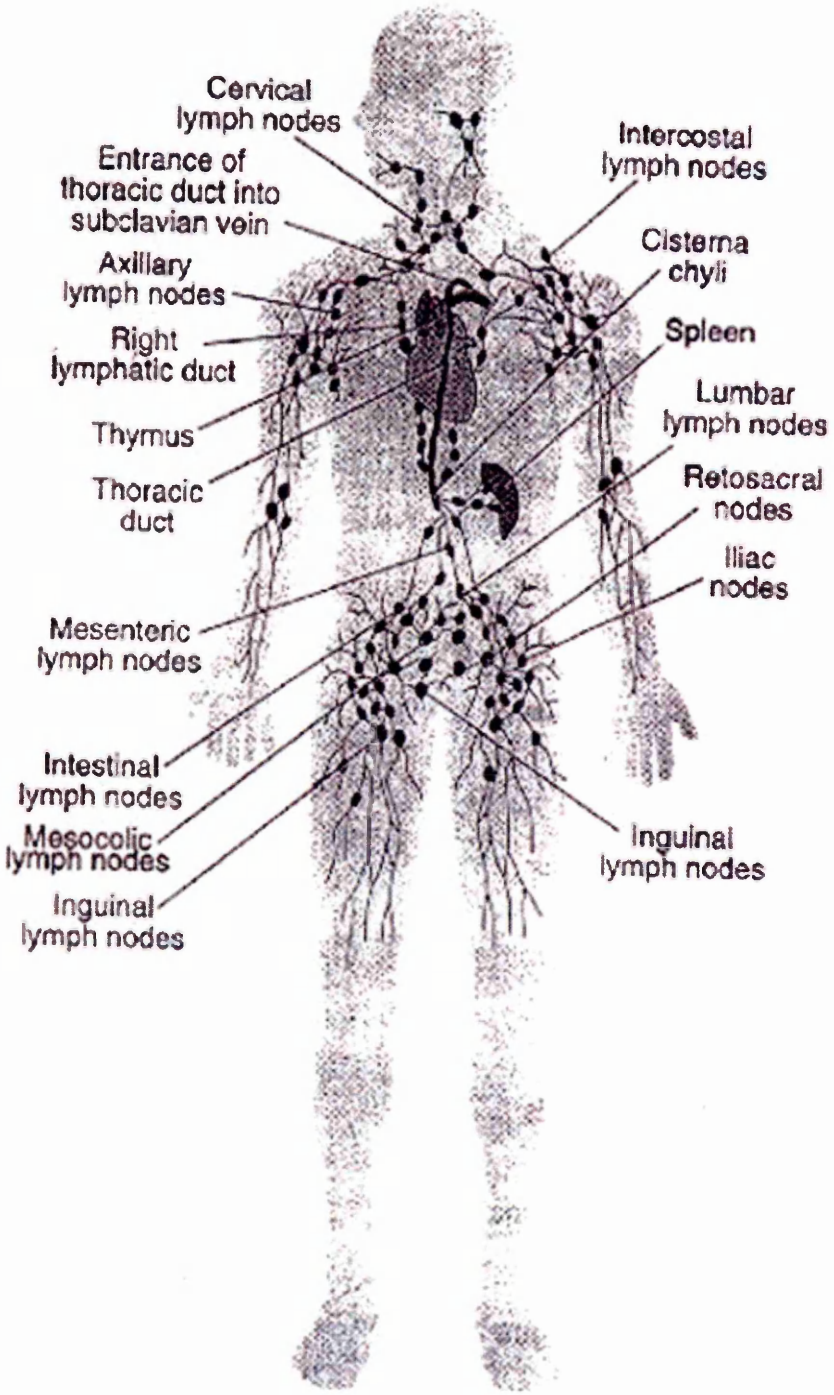

Figure 1.4 Schematic representation of the lymphatic system and lymph nodes.

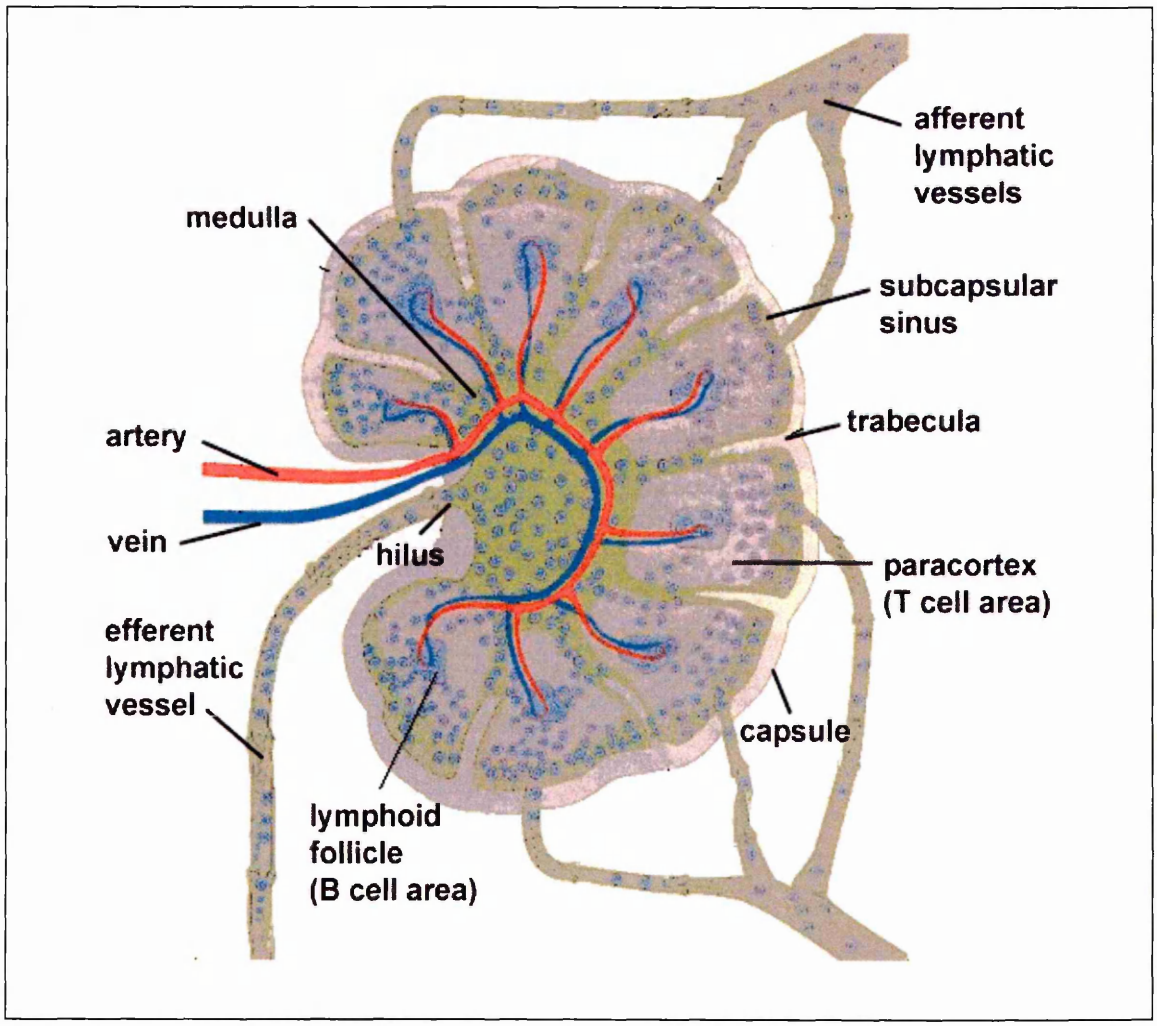

Figure 1.5 Structure of a lymph node. Schematic diagram of a lymph node illustrating the cortex, containing the lymphoid follicles (rich in B lymphocytes) and the surrounding parafollicular cortex which contains T lymphocytes. The inner medulla contains large numbers of macrophages and dendritic cells, with some scattered lymphocytes. Lymph fluid enters from afferent lymphatic vessels and enters the subcapsular sinus. After passing through the node, the filtrate exits through the single efferent lymphatic vessel at the hilus.

The migration of cells through the lymph node is by no means random but rather a carefully orchestrated process known as ecotaxis. This is dependent upon cellular interactions, gradients of soluble factors such as chemokines and the expression of specific structural proteins within the node (reviewed by Young, 1999). The majority of lymphocytes enter the lymph node directly from the bloodstream by extravasation at HEVs (discussed more thoroughly in section 1.5.4 of this chapter) and are localised within B- and T-cell areas. Originally it was believed that lymph-borne antigens percolated through the lymph node cortex but Gretz et al. (2000) demonstrated that a functional barrier exists which restricts access to the cortex. In this study tracers of known molecular weight were injected subcutaneously into rats and mice to demonstrate that high molecular weight tracers were abundant in the subcapsular sinus but absent in the adjacent cortex, whereas low molecular weight tracers were only partially excluded. The authors suggest that this barrier could be significant during microbial infections, where it would isolate the cortex from the microbes themselves and their soluble products, which could perturb immune responses. They also showed that it remained intact even during viral-induced swelling of the lymph node. However such a barrier could restrict the ability of antigen presenting cells (APCs) already in the cortex to acquire lymph-borne antigen. The authors found high molecular weight tracer within the cortex after a delay of four hours from the time of subcutaneous injection and suggest that this is due to cellular uptake and would allow contact with APCs. Restriction of lymph-borne material to HEVs did not occur as low molecular weight tracers were found to highlight the reticular network and HEVs in the cortex. Thus lymph moves from the subcapsular sinus towards HEVs through the reticular network. Each reticular fibre is ensheathed by fibroblastic reticular cells and constitutes an extracellular space distinct from the interstitial space of the parenchyma and continuous with the fibres in the floor of the subcapsular sinus and those enwrapping the HEVs (Moe et al., 1963). Incoming lymphocytes pass from the

HEV lumen to the cortical parenchyma and are bathed in the low molecular weight lymph-borne molecules that arrive via the reticular network. Gretz et al. (2000) speculate that this could be the site where antigen-specific B cells could capture their soluble antigen and transport it to the cortex for presentation to T cells. Chemokines were also found to travel through the reticular network to HEVs and may be immobilised on the endothelium to play a role in the lymphocyte recruitment. This route could also be utilised by pro-inflammatory cytokines, produced within inflamed tissue and passed through the lymph to the draining lymph node to stimulate endothelium at HEVs and perhaps up-regulate adhesion molecules to enhance leukocyte recruitment from the blood.

1.1.3 The origins and development of the lymphatics during embryogenesis

Until 1999, there were two theories concerning the origin of the lymphatics in the developing embryo. Injection experiments carried out by Sabin (1902, 1904) led her to propose that isolated primitive lymphatic sacs originate from endothelial budding from the veins (figure 1.6). An alternative theory, less widely accepted, was put forward by Huntington and McClure in 1910, whereby the initial lymph sacs arise in the mesenchyme and independent to the veins. In 1999, Wigle and Oliver proved Sabin's theory correct. They found that the transcription factor Prox1 is a specific marker for the subpopulation of endothelial cells that bud and sprout from the vasculature of the developing mouse embryo.

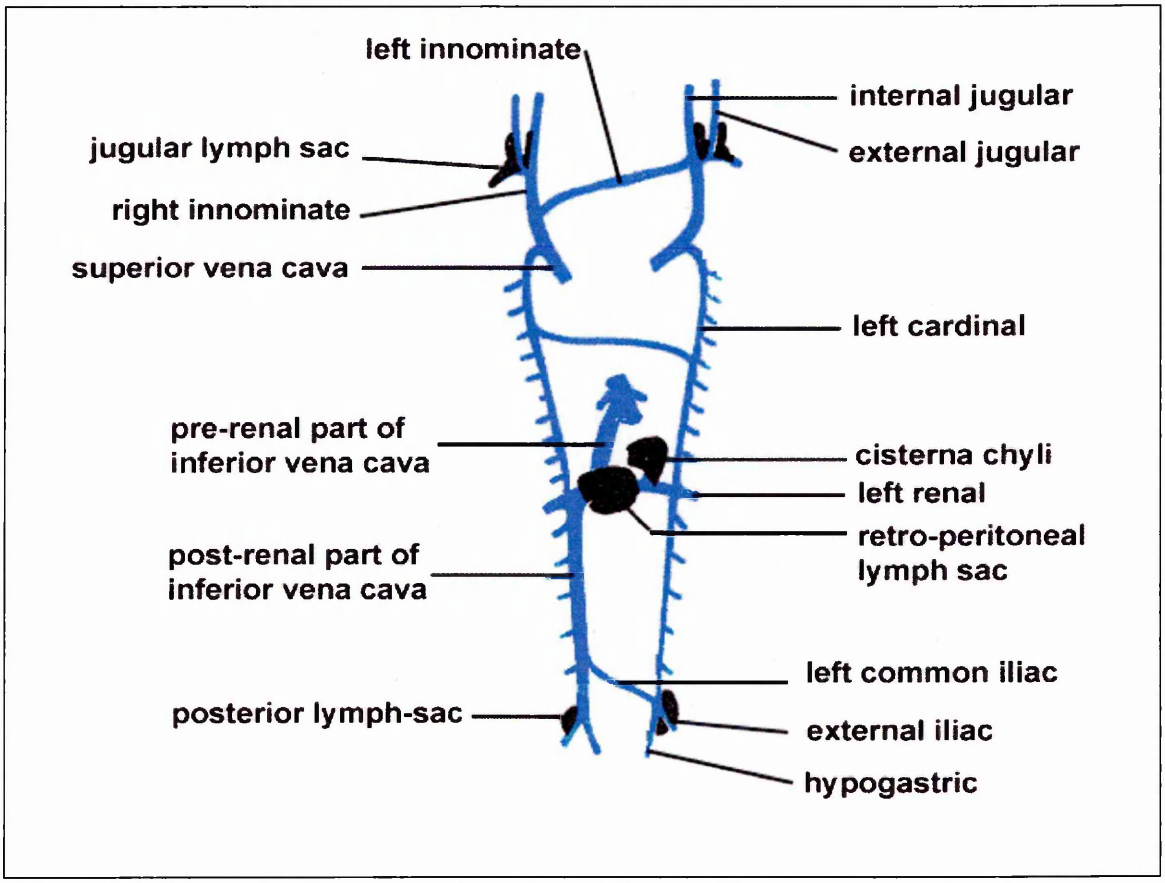

Figure 1.6 Schematic diagram to show the relative positions of primary lymph sacs, as described by Sabin.

At E9.5 in the mouse, a few cells in the region anterior to the developing forelimb were Prox1 positive, becoming more apparent and abundant by E10.5. Prox1 positive cells were found lining one area of the anterior cardinal vein and these cells bud and spread in a clearly polarised manner, moving dorsoanteriorly. Expression of CD31 and VE-cadherin revealed that these cells were of endothelial origin. Thus an initial step must require the formation of endothelial cell precursors before specific growth factors and transcription factors induce arterial and venous formation. The initial budding of lymphatic endothelial cells from the veins is Prox1 independent and may be regulated by the haematopoietic

intracellular signalling proteins SLP-76 and Syk, the loss of which confer an angiogenic phenotype on haematopoietic cells (Abtahian et al., 2003). However Prox1 is required to maintain budding and sprouting of the restricted subpopulation. Also it has been shown that ectopic expression of Prox-1 in cultured primary blood vascular endothelial cells induces lymphatic endothelial cell-specific genes and downregulated blood vessel-specific genes (Petrova et al., 2002; Hong et al., 2002). Once the cells are committed to the lymphatic endothelial lineages, lymphatic vessel sprouting from embryonic veins is dependent upon paracrine VEGF-C signalling through VEGFR-3 and the first lymphatic endothelial cells are believed to migrate to form lymph sacs towards a VEGF-C concentration gradient (Karkkainen et al., 2003). The involvement of VEGFR-3 had been demonstrated earlier by Mäkinen et al. (2001a), who found that expression of soluble VEGFR-3 in transgenic mice during embryonic development inhibited lymphangiogenesis and lead to regression of existing foetal lymphatic vessels. The dermis and subcutaneous fat layer thickened, as in human lymphoedema and a lack of macromolecular transport in the dermis with fluid accumulation in the skin was also observed. However angiogenesis and the blood vascular endothelium were unaffected.

Budding from the cardinal vein gives rise to the jugular lymph sacs, from where capillary plexuses spread to the neck, head, forelimbs and thorax (Wigle and Oliver, 1999). From E12.5 onwards, additional posterior lymph sacs form, probably due to endothelial budding from other veins. Prox1-positive cells arise around other veins of the body, in the trachea, oesophagus, lungs and from the posterior cardinal vein By E14.5, these endothelial cells begin to grow out towards the periphery of the embryo to form lymphatic capillaries. At E15.5 an extensive lymphatic capillary network has developed, covering the dermis of the skin and intermingling with the blood capillaries throughout the entire embryo.

Lymph nodes develop from an accumulation of $CD45^+$ $CD4^+$ $CD3^-$ cells which are in close proximity to MAdCAM-1, VCAM-1 and ICAM-1 expressing cells, seen enclosed within a layer of $LYVE\text{-}1^+$ $MECA32^+$ endothelial cells by E16.5 (Cupedo et al., 2004). Such expression of both lymphatic and blood vascular markers reflects the fact that these cells have recently sprouted from the large veins and are still undergoing transition from a vascular to a lymphatic phenotype. This endothelial cell layer eventually differentiates to form the subcapsular sinus of the lymph node.

1.1.4 Functions of the lymphatics

The functions of lymphatics within the skin can be divided into three broad categories. Firstly it is responsible for carrying triacylglycerols and cholesterol from the intestines to the tissues (Voet and Voet, 1995), the function which originally lead to its discovery. Secondly it has an important immunological function (discussed in more detail in section 1.5 of this chapter). The lymphatics provide a major exit route from the skin for circulating cells such as T-lymphocytes and macrophages, as well as professional antigen presentating cells like dendritic cells. Antigens are transported to the regional lymph node and a primary immune response is initiated as naïve lymphocytes are brought into contact with antigen-presenting cells. The third vital function of the lymphatics is the regulation of homeostasis in the skin, draining excess fluid from the interstitium to maintain constant interstitial volume, returning macromolecules to the circulation to maintain constant colloid osmotic pressure, transporting extracellular matrix components, eliminating unwanted cellular by-products and removing foreign organic and inorganic material (Berne et al., 1998). Each day approximately 50% of the total circulating protein escapes from the blood vessels and as it cannot be reabsorbed through the same route, it is the responsibility of the lymphatic system to return extravasated fluid and macromolecules to the circulation (Skobe and Detmar, 2000).

1.2 Hyaluronan and its Receptors: CD44 and LYVE-1

One of the extracellular matrix components transported by the lymphatics is hyaluronan (HA), a large glycosaminoglycan linear copolymer of D-glucuronic acid and *N*-acetyl-D-glucosamine (Figure 1.7), up to 10^5– 10^7 Da in size (reviewed by Toole, 2004). Other glycosaminoglycans (such as chondroitin sulphate, heparan sulphate and keratan sulphate) are bound to a core protein to form a glycosylated protein, or proteoglycan. However HA is not covalently bound in such a molecule but is secreted as a free polysaccharide.

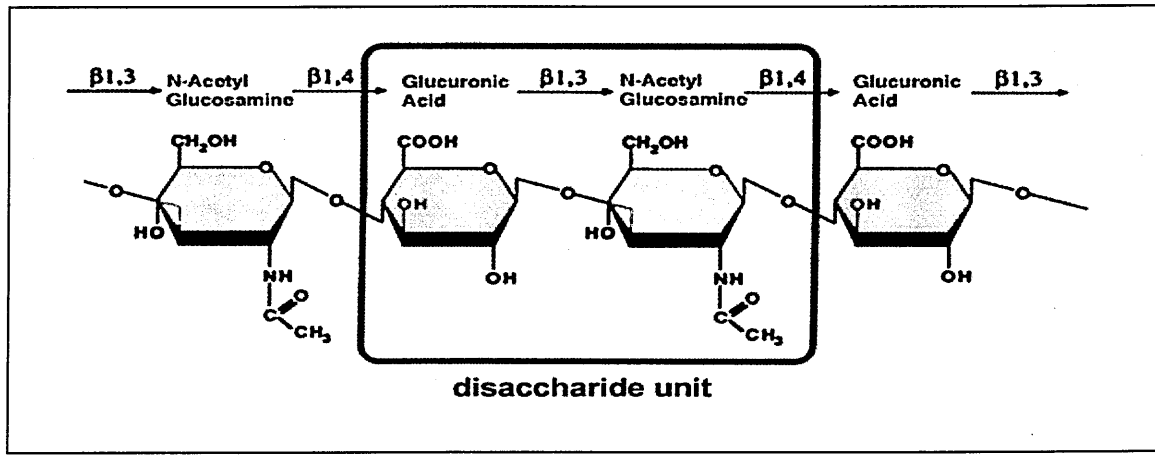

Figure 1.7 Schematic diagram of the structure of hyaluronan. The repeating disaccharide unit consists of alternating units of glucuronic acid and N-acetyl glucosamine (adapted from Laurent and Fraser, 1992).

Karl Meyer is credited with the discovery of HA in 1934, which was found to consist of "a uronic acid and an amino sugar". Thus, as it was isolated from bovine vitreous humour it was named hyaluronic acid from the Greek *hyalos* meaning vitreous (Meyer and Palmer, 1934). The name was later modified to hyaluronan, (Balasz et al., 1986) partly because it is the accepted terminology that names of polysaccharides have the suffix –an. The other reason was a chemical

one: at physiological pH this molecule exists with dissociated carboxyl groups and should thus be termed hyaluronate but the counter ion *in vivo* could not be specified.

Subsequent studies found that HA was present in other soft connective tissues, such as umbilical cord, skin and rooster comb and the latter became a major source for HA (reviewed by Laurent and Fraser, 1992).

1.2.1 Functions of HA

HA is implicated in a wide range of physiological roles, as a structural component and also through its interactions with a cohort of HA binding proteins, discussed in section 1.2.3 of this chapter. HA plays an important structural role in cartilage where it provides support and lubrication. At physiological pH, HA is highly acidic due the presence of carboxyl groups and therefore has a net negative charge. This attracts many positively charged ions, which in turn attract large numbers of water molecules to form a highly hydrated gel. When bound by cartilage Link protein and large proteoglycans such as aggrecan and versican (reviewed by Knudson and Knudson, 1993), the HA-proteoglycan complex forms a porous, hydrated, space-filling gel in the extracellular matrix. Such an HA matrix has been found around cells as a pericellular coat (Knudson et al., 1993), which has been shown to aid cell movement (Evanko et al., 1999). The importance of HA in cell migration is indicated by its up-regulation during embryogenesis, wound healing and inflammation (Knudson and Knudson, 1993). The mechanism by which this occurs is thought to be due to reduced intercellular adhesion, enhancing cell division or migration. An increase in the amount of HA in some cancers has also been noted (reviewed by Toole, 2004), where it correlates with a more aggressive tumour.

Interaction of HA with one of its principal receptors CD44 (described in more detail in section 1.2.4 of this chapter) has been found to promote signal transduction, eliciting a range of responses such as production of pro-inflammatory cytokines and rearrangement of the cytoskeleton.

HA is not restricted to eukaryotes and has also been identified in certain pathogenic bacteria, such as *Streptococcus pyogenes* and *Pasteurella multocida*, which use their hyaluronan coat to evade the host's immune system.

1.2.2 HA metabolism and turnover

HA is synthesised on the inner side of the cell membrane, unlike other GAGs which become covalently linked to a protein backbone within the Golgi complex (Toole et al., 2004). To date, three HA synthase genes, termed *Has1*, *Has2* and *Has3*, have been identified in both mouse and human, spanning the membrane four times with both the C and N-termini located intracellularly. Has2 exhibits more restricted expression in the adult than Has1 or Has3. However, a study by Camenisch et al. (2000) found that Has2 is crucial for normal embryonic development, as the $Has2^{-/-}$ phenotype is embryonic lethal, unlike either Has1 or Has3, with severe defects in vasculature development and a highly compact extracellular matrix, lacking the hydrating and expanding properties of HA.

HA turnover is surprisingly rapid in comparison to most extracellular matrix components, with approximately one third of the body's HA content turned over per day (Fraser et al., 1997). Only one third of this HA is degraded locally (Laurent and Fraser, 1992), by internalisation followed by degradation by intracellular hyaluronidases. The majority of HA is transported through the lymphatic vessels for degradation within the draining lymph nodes. The concentration of HA within the lymph was measured by Laurent and Fraser (1992) as between 8.5 and 18 μg/ml. Serum concentrations of HA are maintained

at very low levels, typically 0.01 to 0.1 μg/ml, in sharp contrast to the concentrations found in certain tissues such as cartilage (1200 μg/ml) and in the dermis of the skin (200 μg/ml). Any HA present within the blood is rapidly transported to either the liver, spleen or kidneys, thus avoiding an increased viscosity of the blood.

The mechanism by which HA is taken into the lymphatics and transported remains unknown. However it may involve receptor-mediated transcytosis or be a case of simple diffusion between gaps in the intercellular junctions. Approximately 90% of HA in the afferent lymph is degraded within the lymph node, but the mechanism by which this occurs is largely uncharacterised (Fraser et al., 1997).

Degradation of HA occurs within lysosomes by the hyaluronidases HYAL1, HYAL2, HYAL3, HYAL4, PH20 and HYALP1. These enzymes are all endo-β-N-acetylhexosaminidases and cleave HA into small oligosaccharides of either 4 or 10 repeating units in length (reviewed by Csoka et al., 2001). Expression of these enzymes varies between tissues. Degradation is completed by two exoglycosidases, β-glucuronidase and β-N-acetylglucosaminidase, which sequentially remove saccharides from the reducing end of the short HA chain.

1.2.3 Hyaluronan receptors

The majority of HA-binding proteins, or hyaladherins within the tissues belong to the Link protein superfamily, characterised by one or more copies of the Link domain (reviewed by Day and Prestwich, 2002). The Link domain acquired its name as it was first identified in Link protein, a component of cartilage, following a report that cartilage proteoglycans interacted with HA (Hardingham and Muir, 1972). The domain is approximately 100 amino acid residues in length and contains four cysteine residues which form two disulphide bridges.

The majority of Link protein superfamily members are components of the extracellular matrix and form a subfamily known as the hyalectans. These include aggrecan, versican, brevican and neurocan. They may be characterised by the G1 domain, containing an Ig fold and two Link modules, a central GAG attachment domain and a G3 domain. Other Link superfamily members include Link protein itself; BRAL1 (brain Link protein-1), identified by a BLAST homology search using brevican sequence; and TSG6 (tumour necrosis factor-stimulated gene-6), a small 277 residue protein which was originally isolated from TNF-treated fibroblasts (reviewed by Day and Prestwich, 2002).

The cell surface Link family members identified to date are CD44, LYVE-1, Stabilin-1 (also known as FEL-1, CLEVER-1 and FEEL-1) and HARE (FEL-2, Stabilin-2 or FEEL-2). CLEVER-1 and HARE are both large transmembrane proteins containing motifs for clathrin-mediated endocytosis. The extracellular domains are composed of alternating EGF-repeat regions and tandem Fasciclin domains with a membrane-proximal Link module.

CD44 has been well characterised over a number of years and plays a variety of roles in diverse physiological settings. LYVE-1 is in a much earlier stage of characterisation and much of the work done to date has been within the laboratory of Prof. David Jackson. However both receptors share a high degree of structural similarity and thus any study on LYVE-1 could not be undertaken without first reviewing CD44 (figure 1.8).

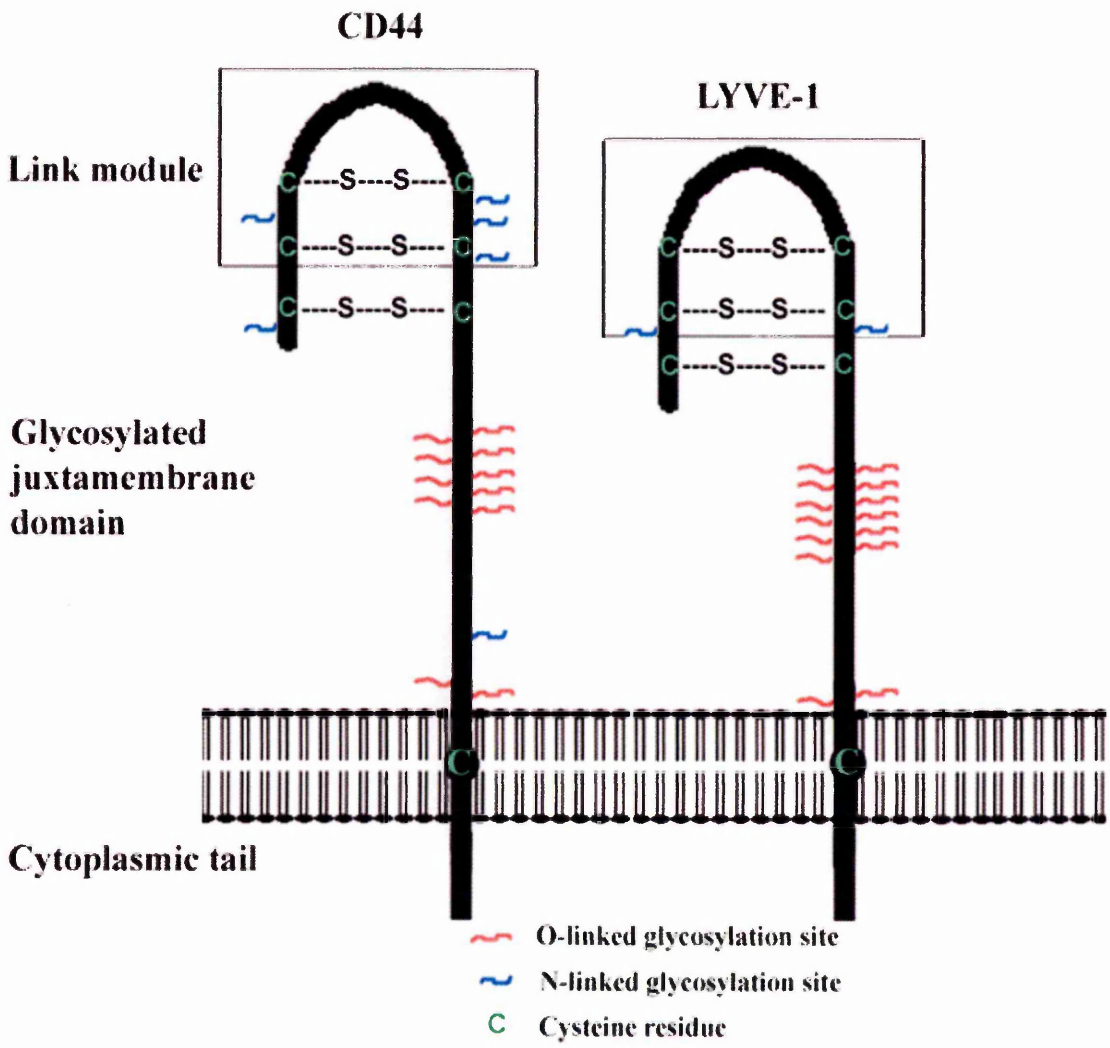

Figure 1.8 Schematic diagram of CD44 and LYVE-1. Both proteins are type I transmembrane receptors with the Link module situated at the N-terminus (indicated by a black box), a glycosylated domain adjacent to the transmembrane domain and a cytoplasmic domain at the C-terminus. The Link module contains two di-sulphide bridges, but both CD44 and LYVE-1 contain an additional cysteine pair which form an extra disulphide bridge outside the Link module and an unpaired cysteine residue within the transmembrane domain.

1.2.4 CD44

CD44 attained its name at the Third International Workshop on Leukocyte Differentiation Antigens (reviewed by Haynes et al., 1989), after repeated discoveries over the previous nine years under several different names. Dalchau et al. (1980) are credited with the first discovery of CD44, when they detected reactivity of a monoclonal antibody, F10.44.2, towards a then unknown antigen on T-cells, granulocytes, cortical thymocytes and in brain homogenate. Subsequent researchers characterised the antigen under various names including Pgp-1 (phagocytic glycoprotein-1), on macrophages and granulocytes; Extracellular Matrix Receptor type III (ECM-III), expressed on fibroblasts and found to bind to collagen types I and VI and fibronectin; and Hermes antigen, identified using the Hermes-3 mAb by Jalkanen et al. (1988) which was found to block the binding of lymphocytes to high endothelial venules (HEVs). The same molecule was found to be recognised by the "cluster" of antibodies used in all these studies and thus attained a "cluster of differentiation" number, CD44.

The reasons behind a long period of independent studies on what were considered different molecules within distinct functional contexts lie in the supremely polymorphic nature of CD44. Alternative splicing and heavy modification by glycosylation permits the molecule to exert a wide range of functions through each of its domains.

1.2.4.1 Structure of CD44

Cloning of CD44 cDNA from lymphoid cell lines by two independent groups in 1989 confirmed that the multitude of antigens originally studied as different proteins were truly products of the same gene (Goldstein et al., 1989; Stamenkovic et al., 1989). Discrepancies between the sequences published are due to the former group cloning a variant isoform with a truncated cytoplasmic

tail and the latter describing what is now considered the standard form. This type I transmembrane protein is 314 amino acid residues in length, following cleavage of the 19 amino acid signal peptide. The extracellular domain is 248 amino acids in length and contains the Link module at the N-terminus, with the characteristic two disulphide bridges. Unlike most other Link superfamily members, CD44 (and also LYVE-1) contain a third disulphide bridge. The extracellular domain is followed by a stretch of 21 hydrophobic residues which make up the transmembrane domain and a 72-residue cytoplasmic tail precedes the carboxy terminus.

The extracellular domain contains six putative N-linked- and six putative O-linked- glycosylation sites (Goldstein et al., 1989), which accounts for the discrepancy between the predicted molecular weight of only 37 kD and observed molecular weight which exceeds 85 kD. The presence of four SG motifs represent potential GAG attachment sites, which may be modified with chondroitin or heparan sulphate (reviewed by Lesley et al., 1993)

1.2.4.2 Expression and functions of CD44

CD44 is widely expressed on cells of epithelial, mesothelial and haematopoietic origin. The few tissues that have been consistently reported as CD44-negative are cardiac muscle, renal tubular epithelium, testis and portions of the skin (Lesley et al., 1993). Given that it is so extensively expressed, it is quite astonishing that the $CD44^{-/-}$ mouse did not exhibit some developmental defect which would cause its demise whilst still an embryo. Instead no embryonic lethality was reported and such mice developed normally, albeit with impaired homing of lymphocytes to the thymus and lymph nodes (Protin et al., 1999) and altered tissue distribution of myeloid progenitors (Schmits et al., 1997). This contrasted considerably with other studies which had shown that CD44 plays a critical role in development and tissue homeostasis. For example the injection of

function blocking CD44 antibodies significantly reduced limb outgrowth (Sherman et al., 1998) and the disruption of CD44 expression in the skin resulted in severe accumulation of HA (Kaya et al., 1997). The absence of such a phenotype in the CD44 deficient mice would suggest that compensatory mechanisms come into play, such as up-regulation of other HA receptors. However the subsequent examination of the knock-out mouse and other studies on function blocking have shed more light on the many varied functions that CD44 performs, both in a normal physiological state and under pathological conditions

The mechanism by which leukocytes extravasate from the blood stream into the tissues is described in detail in section 1.5.3 of this chapter. Interactions between the leukocyte and blood vascular endothelium may be broadly divided into three phases of 1. rolling and initial attachment, mediated by selectins, 2. firmer attachement via integrins and 3. transmigration. The involvement of CD44 in the earlier stage of rolling was demonstrated by Clark et al. (1996), using CD44-positive lymphocytes within a flow chamber coated with hyaluronan or tonsillar stromal cells and by DeGrendele et al. (1996) using a substrate of SV40-transformed lymph node endothelial cells. DeGrendele et al. (1997b) later showed that CD44-HA interactions are of critical importance in the migration of T-cells to sites of inflammation. Numerous studies have shown that anti-CD44 treatment, for example by promoting monoclonal antibody-induced shedding (Zheng et al., 1995) lead to a reduction of inflammation due to the lack of leukocyte infiltrate. More recent studies using the knock-out mouse have confirmed this and have found that this animal does not enjoy the normal healthy phenotype initially believed. Teder et al. (2002) demonstrated that such mice are unable to resolve lung inflammation following bleomycin-induced non-infectious lung injury, due to impaired clearance of apoptotic neutrophils, persistent accumulation of HA fragments and impaired activation of TGFβ1. A

partial reversal of this inflammatory phenotype was performed by reconstituting CD44 deficient mice with bone marrow from $CD44^+$ mice and thus demonstrated a critical role for CD44 in resolving the inflammatory response. It is now generally believed that CD44 plays a role in the regulation of lymphocytes specifically during inflammatory conditions rather than in normal lymphocyte trafficking. Stoop et al. (2002) showed that the increased resistance of CD44 deficient mice to collagen-induced arthritis was most likely due to impaired migration of leukocytes to the inflamed joints. Whereas CD44-positive lymphocytes in arthritic mice migrated to the site of inflammation, lymphocytes from CD44 deficient mice preferentially migrated to the lymph nodes.

CD44 is also believed to play a vital role in maintaining homeostasis within the extracellular matrix, where HA is known to form large complexes with proteoglycans. Transfection of CD44 into COS-7 cells and addition of exogenous HA lead to assembly of a pericellular matrix (Knudson et al., 1993), in a similar manner to that by chondrocytes, which naturally express CD44. CD44 has also been shown to mediate internalisation of HA in a number of cells such as chondrocytes, fibroblasts, macrophages and keratinocytes, via a clathrin- and caveolae-independent pathway (Culty et al., 1992; Hua et al., 1993; Kaya et al., 1997; Tammi et al., 2001). Moreover Kaya et al. (1997) demonstrated that targeted suppression of CD44 in keratinocytes leads to the accumulation of HA in the skin of transgenic mice, which exhibited abnormal epidermal structure and delayed wound healing.

The importance of the cytoplasmic tail to the function of CD44 is becoming increasingly appreciated and the roles in signal transduction dissected out. Bourguignon et al. (1993) demonstrated that binding of HA to CD44 induces an increase in intracellular free calcium concentrations in T-lymphoma cells and thus could trigger signal transduction events within the cell. Association of

CD44 with Src family tyrosine kinases and RhoA has been shown, as have interactions with GTP exchange factors Tiam1 and Vav2, promoting signalling through Rac1 (reviewed by Turley et al., 2002). Such signalling pathways are known to regulate actin assembly that is associated with membrane ruffling, cellular projections and cell motility.

In addition to recruitment of other signalling molecules, signalling activity of the intracellular domain itself has been shown. This domain is proteolytically released from the rest of the molecule in response to stimulation with phorbol ester (Okamoto et al., 2001). The fragment has been shown to translocate to the nucleus and activate transcription via the 12-*O*-tetradecanoylphorbol 13-acetate-responsive element, found in numerous genes including *CD44*, which is induced.

Interactions of the cytoplasmic tail with other proteins have also been reported. The ERM proteins ezrin, radixin and moesin are closely related to each other, sharing approximately 75% homology but are encoded by different genes (Bretscher and Berryman, 1999). They are involved in the attachment of microfilaments to the plasma membrane and are capable of regulated homotypic and heterotypic interactions through their N- and C-terminal domains. The N-termini have been shown to bind *in vitro* to a motif of charged amino acids in the cytoplasmic portion of CD44 (Legg and Isacke, 1998), thus potentially connecting the cytoskeleton with the extracellular matrix.

Thus CD44 plays a critical role in cell adhesion, both in maintaining contact with the extracellular matrix and with other cells. Moreover this cell adhesion may trigger a range of responses within the cell, from activation of gene transcription to intracellular signal transduction cascades and the rearrangement of cytoskeletal proteins.

1.2.5 LYVE-1

Despite the diverse functions of CD44, deletion of this gene in mice produced no immediately obvious abnormalities. Clearly the identities of HA receptors involved in HA homeostasis remained to be identified, prompting Banerji et al. (1999) to search Human Genome Sciences/TIGR expression sequence tag (EST) databases for cDNAs homologous to the full length CD44H. A 2,313-bp EST from a HUVEC library was found to contain an open reading frame encoding a novel type I transmembrane receptor containing an N-terminal Link domain. Upon transfection of this cDNA into fibroblasts, the cells were found to bind HA, demonstrating that this CD44 homologue was a genuine HA receptor and the second cell surface receptor within the Link module superfamily. A soluble fusion protein of the novel homologue was generated and used to raise polyclonal antibodies in rabbits, to determine the expression pattern in tissue. Immunohistochemistry revealed that in sharp contrast to the widely expressed CD44, this protein was exclusively expressed on lymphatic vessels and was hence named LYVE-1 (lymphatic vessel endothelial HA receptor-1).

1.2.5.1 Structure of LYVE-1

The amino acid sequence of LYVE-1 encodes a 322-residue polypeptide, with the typical characteristics of a type I integral membrane glycoprotein (Banerji et al., 1999). Kyte-Doolittle and Goldman hydropathy plots revealed that a sequence of 26 largely hydrophobic residues reside at the NH_2 terminus and probably constitute the leader peptide. These are followed by a hydrophilic sequence of 212 amino acids which encode the extracellular domain. A sequence of 21 hydrophobic residues correspond to the transmembrane anchor, followed by the dibasic motif KR and a highly charged stretch forming the 63-residue cytoplasmic tail. A heavily *O*-glycosylated serine/threonine-rich region, comprising 71 residues lies within the extracellular domain, as do two motifs for

N-linked glycosylation, NFT and NSS, centred on residues 54 and 131 respectively. LYVE-1 shares an overall 43% homology with CD44, although the sequence is more tightly conserved around the HA-binding Link domain. Both LYVE-1 and CD44 contain a single Link domain, composed of two β sheets flanked by two short α helices encapsulating a hydrophobic core (Kohda et al., 1996). The domain is stabilised by four central cysteine residues (C2-C5), with a flanking pair (C1 and C6) spaced at exactly the same distances in both LYVE-1 and CD44 and the two molecules share a much higher sequence homology of 57% between these flanking cysteines. Both molecules also have a cysteine residue within the transmembrane sequence which is believed to be involved in covalent dimerisation of CD44 (Liu et al., 1997) and LYVE-1 (Nightingale and Jackson, unpublished).

Sequence alignment of LYVE-1 from five different species has shown that the cytoplasmic tail is remarkably well conserved (figure 1.9), suggesting that in addition to HA binding, LYVE-1 may perform other functions via this domain.

1.2.5.2 Cloning of the mouse orthologue

Human LYVE-1 amino acid sequence was used to identify the mouse orthologue by BLAST searching the mouse EST data base (Prevo et al., 2001). The cDNA was subsequently cloned from mouse lung and found to contain an open reading frame encoding 318 residues, i.e. 4 residues shorter than the human sequence, due to three amino acids less in the leader peptide and one less in the extracellular domain. Overall the LYVE-1 sequences from the two species share 74% homology, with 79% homology within the Link domain. As in the human, two glycosylation sites exist within the extracellular domain, at N52 and N129, as does the heavily *O*-glycosylated serine/threonine-rich tract between residues 144 and 188. The cysteine residues within the extracellular domain are conserved, as is the unpaired cysteine within the transmembrane domain

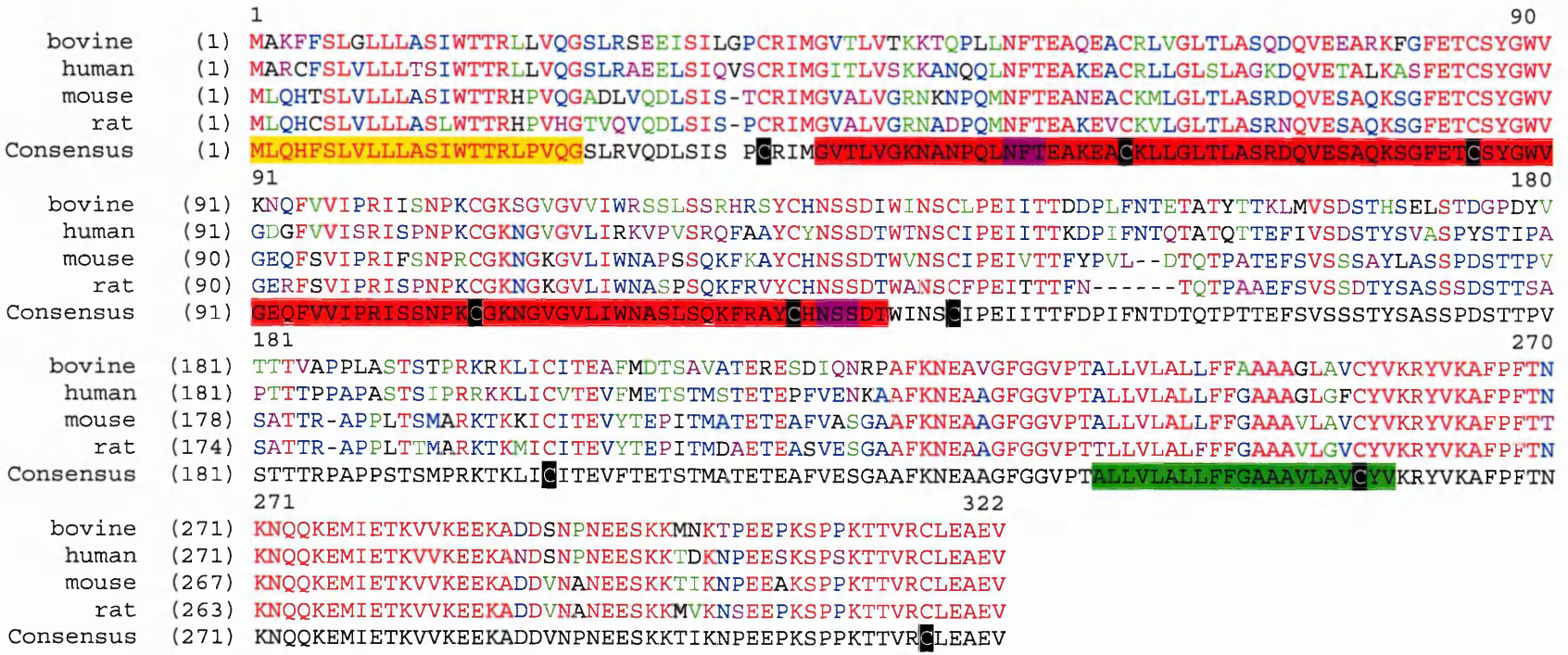

Figure 1.9 LYVE-1 sequence alignments of bovine, human, mouse and rat orthologues from the ClustalW programme. Identical residues are coloured red, consensus residues derived from a block of similar residues are coloured blue, consensus residues derived from the occurence of greater than 50% similar residues are coloured green and weakly similar residues are coloured purple. Non-similar residues are shown in black. On the consensus sequence below, the signal peptide is highlighted in yellow, the Link module in red and the transmembrane domain in green. Cysteine residues are shaded whilst N-linked glycosylation sites are highlighted in purple.

1.2.5.3 LYVE-1-mediated HA binding and internalisation

HA binding by LYVE-1 was first demonstrated in the human by Banerji et al., 1999. They expressed the extracellular domain and leader peptide as a soluble fusion protein with the hinge, CH2 and CH3 domains of human IgG1 and showed that LYVE-1 Fc bound immobilised HA in a concentration dependent manner which was virtually identical to that of CD44 Fc. Control fusion proteins of CD33 Fc and ICAM2 Fc displayed no significant binding. The LYVE-1-immobilised HA interaction was shown to be very sensitive to competition with soluble HA, whereas neither chondroitin -4-SO_4, chondroitin -6-SO_4 or heparin sulphate could compete for HA binding. Thus HA binding by LYVE-1 was shown to be highly specific. Evidence to suggest binding of HA by LYVE-1 *in vivo* was also shown. LYVE-1 was found to associate on the luminal face of tissue lymphatics with HA, in immunofluorescence studies using the HA probe biotinylated HABC (composed of bovine aggrecan and Link protein).

HA binding by mouse LYVE-1 was demonstrated by Prevo et al., 2001, using both transient 293T transfectants and soluble mouse LYVE-1 Fc fusion protein in microplate binding assays. The specificity of murine LYVE-1 for HA was shown, with no detectable binding to chondroitin -4-SO_4, chondroitin -6-SO_4 or heparin sulphate.

Prevo et al. (2001) also demonstrated that both mouse and human LYVE-1 mediate the internalisation of HA in 293T transfectants, through receptor-mediated endocytosis. Immunoelectron microscopy was also used to reveal that murine LYVE-1 is located on both the luminal and abluminal surfaces of lymphatic endothelium. This would suggest an involvement of LYVE-1 in the transport of HA across lymphatic endothelium. The uptake of HA by LYVE-1 is considerably slower than that by the professional scavenger receptor HARE (HA

receptor for endocytosis, Zhou et al., 2000), which would suggest that LYVE-1 does not play a role in the rapid uptake and degradation of lymphatic HA.

More recent work by Tom Nightingale (DPhil thesis, University of Oxford, 2004) has sought to address the molecular mechanism by which LYVE-1 binds HA. Curiously the default binding state of LYVE-1 on lymphatic endothelium, both in the mouse and human, is "off". Removal of terminal sialic acid residues from carbohydrate chains linked to the protein via *N*-glycosidic linkages is required before LYVE-1 can bind HA. Moreover the LYVE-1 knockout mouse did not show any obvious abnormality of the lymphatics or HA metabolism. It is possible that more HA receptors remain to be identified and these play compensatory roles in both the $CD44^{-/-}$ and $LYVE\text{-}1^{-/-}$ mice. However it is also highly possible that LYVE-1 may have another physiological function besides that of an HA binding molecule. This would explain why HA binding requires a specific mechanism whereby it is "switched off", instead of just simply down-regulating protein expression. If LYVE-1 is to serve as a highly specific marker for the lymphatics, expression under various physiological and pathological conditions must be carefully characterised. Such studies require the use of a second lymphatic marker, to demonstrate that the vessels expressing LYVE-1 are truly lymphatic and not blood capillaries.

1.3 Other Endothelium Markers

The study of the lymphatics demands the ability to discriminate between lymphatic vessels and blood vasculature in tissue sections as well as in cultured cells. Research into identifying specific and reliable markers for both blood and lymphatic endothelium has advanced at a rapid pace over the last six years and

although each marker may have its virtues and shortcomings, their use in concert has permitted a variety of exciting, novel studies.

1.3.1 Prox1

The homeobox transcription factor Prox1 was cloned in 1993 by Oliver et al. by homology to the *Drosophila melanogaster* gene, *prospero*, where it controls axonal outgrowth. Functional inactivation of *Prox1* in mice proved to confer embryonic lethality, with phenotypic alterations to the lens and liver (Wigle et al., 1999). However its importance as a specific marker for the lymphatics was first reported by Wigle and Oliver (1999). Heterozygous *Prox1*$^{+/-}$ mice were generated with an in-frame insertion of the β-galactosidase (*lacZ*) gene which permitted detections of *Prox1* expression throughout development. *Prox1*$^{+/-}$ mice died between two and three days after birth, with their intestines filled with chyle, the milky-white fluid transported by lymphatic vessels of the small intestine. Such a phenotype indicated haploinsufficiency and suggested that the development of the enteric lymphatic system was dependent upon the presence of two copies of *Prox1*. The important role that this transcription factor plays during the development of the lymphatics was further demonstrated by studying β-gal expression in the heterozygous embryos. *Prox1* was found to be expressed in a subpopulation of endothelial cells which bud off from the cardinal vein and give rise to the lymphatic system. Moreover in the homozygous *Prox1*$^{-/-}$, although the development of the vasculature proved unaffected, budding and sprouting of the lymphatics did not occur. Thus *Prox1* was shown to be a specific and essential regulator of the development of the lymphatic system.

Prox1 was later shown to be required in maintaining the budding and sprouting of a restricted subpopulation of these endothelial cells rather than responsible for initiating it, (Wigle et al., 2002). The default phenotype of budding endothelial cells was shown to be that of blood vasculature and such cells require *Prox1*

before a lymphatic vasculature phenotype can be adopted. A subsequent study by Petrova et al. (2002) found that *Prox1* is capable of reprogramming endothelial cells, up-regulating lymphatic endothelium-specific genes and inducing proliferation whilst suppressing blood vasculature endothelial genes.

Prox1 has proved a very useful marker for lymphatics in tissues and in cultured lymphatic endothelial cells, with a distinct nuclear localisation.

1.3.2 Podoplanin

Podoplanin is one of the most highly expressed lymphatic-specific genes (Petrova et al., 2002; Hirakawa et al., 2003). It was first cloned from phorbol ester-treated osteoblastic cells and named OTS-8 (Nose et al., 1990). *In vivo* expression in lymphatic endothelium but not on blood vascular endothelium was first reported by Wetterwald et al. (1996) who named it E11 antigen due to its recognition by E11 antibody, a marker for cells of the late osteogenic lineage which binds to osteoblasts and osteocytes. An identical sequence termed T1α was found to be selectively expressed at the apical surface of alveolar epithelial type I cells in rat lung (Dobbs et al., 1988; Rishi et al., 1995). T1α expression was also detected in the choroid plexus, ciliary epithelium of the eye, intestine, kidney, thyroid and oesophagus of the foetal rat (Williams et al., 1996). Most recently the same gene was cloned as podoplanin by Breiteneder-Geleff et al. (1997) who identified it as a 43kDa membrane protein expressed on glomerular epithelial cells in rat kidneys. The researchers found that podoplanin was down-regulated in puromycin aminonucleoside nephrosis (PAN), a rat model of human minimal change nephropathy. Podoplanin acquired its name due to association with this pathological condition, where the arborised foot processes of podocytes are transformed into "flat feet", the Latin term for which is *pes planus*.

Podoplanin is first expressed in the mouse embryonic vascular system between days E10.5 and E11.5 (Schacht et al., 2003) in endothelial cells of the cardinal vein and in the Prox1-positive lymphatic progenitor cells. By parturition, expression was found to be almost completely restricted to lymphatic endothelium, predominantly localised to the luminal plasma membrane of lymphatic vessel endothelial cells. Podoplanin$^{-/-}$ mice died immediately after birth due to respiratory failure, precipitated by impaired formation of alveolar airspace which was associated with a reduction in the number of differentiated type I alveolar epithelial cells in the lung (Ramirez et al., 2003). Such neonates also exhibited cutaneous lymphoedema, dilated cutaneous and intestinal lymphatic vessels and impaired lymphatic transport. However their blood vasculature was unaffected. Schacht et al. (2003) also found that over-expression of podoplanin in cultured vascular endothelial cells promoted the formation of elongated cell extensions. Cell adhesion, migration and tube formation were also found to be significantly increased. Thus podoplanin was shown to be a key regulator of lymphatic vascular formation.

Podoplanin has proved an extremely useful and reliable marker, both in the identification of lymphatic vessels in tissues and in isolating and characterising cultured cells (Kriehuber et al., 2001; Hong et al., 2002 and Petrova et al., 2002, to mention but a few).

1.3.3 VEGFR-3

Vascular endothelial growth factor receptor-3 (VEGFR-3), a tyrosine kinase receptor was first cloned by Aprelikova et al. (1992) from human leukaemia cells and named FLT4 as the tyrosine kinase domain shared 79% homology with the haematopoietic growth factor FLT1 (later re-named VEGFR-1). FLT4 expression was detected in human placenta, lung, heart and kidney. Subsequent studies revealed that both FLT1 and FLT4 contain seven immunoglobulin-like

extracellular domains (Galland et al., 1993; Pajusola et al., 1992), with 12 potential glycosylation sites and two different transcript sizes of 5.8kb and 4.5kb, which differed in their carboxy terminal tails. These two isoforms, termed FLT4s (short) and FLT4l (long) were found to be generated by alternative polyadenylation and subsequent alternative splicing (Padjusola et al., 1993). Borg et al. (1995) demonstrated that FLT4 is highly glycosylated with a molecular weight of approximately 180kDa and provided some evidence that the two forms have different signalling properties.

VEGF-C was identified as a ligand for FLT4 by Joukov et al. (1996), who re-named it VEGFR-3. In the same study VEGF-C binding to VEGFR-3 was found to induce tyrosine autophosphorylation of the receptor. VEGF-D was later identified as a second ligand for VEGFR-3 by Achen et al. (1998). Both ligands are able to induce the proliferation, migration and survival of VEGFR-3-positive cells *in vitro* (Mäkinen et al., 2001b) and are implicated in lymphangiogenesis, discussed in section 1.4.1 of this chapter.

Early studies suggested that VEGFR-3 was absent from blood vascular endothelium (Padjusola et al., 1992). However Kukk et al. (1997) showed that VEGFR-3 is widely expressed in the vascular endothelium in the early stages of development. Also disruption of the VEGFR-3 gene was found to cause disorganization in the large blood vessels (Dumont et al., 1998). The defective lumens of these vessels lead to fluid accumulation in the pericardial cavity and cardiovascular failure at embryonic day 9.5. Clearly the receptor plays an essential role in the development of the embryonic cardiovascular system before the lymphatic system has formed. The importance of VEGFR-3 within the lymphatic system was shown in a study by Irrthum et al., 2000, who identified an intragenic polymorphism in *VEGFR-3* as responsible for Milroy disease, an autosomal dominant, congenital lymphoedema, characterised by a chronic

swelling of limbs. This mis-sense mutation was found to inhibit the autophosphorylation of the receptor. Thus the loss of adequate VEGFR-3 signalling appears to cause diminished or delayed development of lymphatic channels.

Although VEGFR-3 cannot serve as a specific marker for lymphatic endothelium in the embryo, it has been used extensively in studies on both normal and pathogenic adult tissue, for example Lymboussaki et al., 1998. Antibodies against the extracellular domain have also been used to isolate lymphatic endothelial cells from human primary microvascular endothelium, (Mäkinen et al., 2001b). However, in a study by Partanen et al. (2000), although VEGFR-3 was mainly confined to lymphatic endothelium within the adult and absent from large blood vessel endothelium, expression was detected on the endothelium of specific subsets of capillary. Such capillaries were typically found in tissues associated with extensive molecular exchange across the blood vessel wall, such as endocrine glands and the kidney glomeruli. The researchers found that continuous endothelia were usually negative for VEGFR-3 whilst discontinuous endothelia were positive. Thus it was suggested that VEGFR-3 plays a role in the transport functions of more permeable endothelia. Expression of VEGFR-3 at major sites of haematopoiesis or blood cell trafficking was also observed, in the sinusoids of the liver, spleen and bone marrow, implying a role for the receptor in regulating the translocation of cells.

Expression of VEGFR-3 on blood capillaries has also been observed during the neovascularisation of tumours and in chronic inflammatory wounds. Kubo et al. (2000) found that VEGFR-3 is induced in murine vascular endothelial cells upon implantation of tumour cells where it is essential for maintaining the integrity of the endothelium. A study on wound healing in pigs and humans by Paavonen et al. (2000) revealed weak expression on vascular endothelium in chronic wounds

such as within the neovasculature of ulcers and in lower extremity decubitus lesions.

VEGFR-3 is probably the most well-characterised of lymphatic endothelium markers detailed here. However exact sets of circumstances under which VEGFR-3 is expressed on blood capillary endothelium remain to be fully elucidated and therefore as a marker VEGFR-3 must be used with prudence. As many of the studies carried out in this thesis concern inflammation and the administration of inflammatory stimuli, VEGFR-3 is not employed as a marker in any of these experiments. Nevertheless its extensive use in other studies and its emerging role in a variety of physiological and pathological processes mean that this introductory chapter would not be complete without alluding to it.

1.3.4 CD34

The sialomucin CD34 is a heavily glycosylated type I transmembrane protein, expressed on developmentally early lymphohaematopoietic stem and progenitor cells, small-vessel endothelial cells and embryonic fibroblasts (reviewed by Krause et al., 1996). Its molecular weight is estimated at 116 kDa but due to extensive post-translational modifications, the molecular mobility is strongly influenced by its charge and remarkably the amino acid sequence deduced from the human CD34 gene sequence predicts a polypeptide of only 40 kDa (Simmons et al., 1992).

CD34 was first identified in a study by Civin et al. (1984), who sought to analyse and enrich haematopoietic progenitor cells using a mAb they had generated against the KG1a myeloid leukaemia. The gene was cloned in 1992 by Simmons et al. who identified nine potential N-linked glycosylation sites and numerous potential O-linked glycosylation sites within the extracellular domain. Within the cytoplasmic portion they found two consensus protein kinase C

phosphorylation sites and one potential tyrosine kinase phosphorylation site. The CD34 gene was found to span 26kb and possess nine exons (Satterthwaite et al., 1992). Two forms of CD34 have been identified, arising due to alternative splicing. One species contains exons 1 through to 8 and forms the full-length form; alternative splicing results in the insertion of an addional exon, termed exon X, between exons 7 and 8 which introduces a translational stop codon. This results in a truncated form of CD34, with a shorter cytoplasmic domain but identical transmembrane and extracellular regions to the full length protein.

Later studies revealed more about the structural nature of CD34 (reviewed by Krause et al., 1996). The extracellular region is dominated by an amino-terminal mucin-like domain, which is densely substituted with sialylated *O*-linked carbohydrates (Baumhueter et al., 1993), rendering CD34 highly stable and resistant to proteases. Due to this extensive glycosylation, the mucin domain is forced to adopt an extended, rod-like structure. Adjacent to this domain is a globular domain which contains six evenly spaced cysteine residues and could potentially fold into an Ig-like structure (Brown et al., 1991). The cytoplasmic domain is highly conserved between species orthologues, with over 90% amino acid residue homology). This domain also shares the most homology with other members of the growing CD34 family of sialomucins, namely podocalyxin and endoglycan (Sassetti et al., 2000). Such a high degree of conservation implies that this domain is responsible for a vital functional role and due to the presence of potential phosphorylation sites, would suggest that CD34 is involved in cell signalling.

Expression of CD34 on vascular endothelial cells was first identified and published by Fina et al. (1990). In this study, seven CD34 mAb already known to recognise epitopes on human haemopoietic progenitor cells were also found to bind to vascular endothelium. The researchers found that the majority of

capillaries in most tissues were CD34 positive, as was umbilical artery. Less staining was observed on vein endothelium, whilst large vessels and placental sinuses were negative. CD34 was found to be concentrated on membrane processes, particularly at the interdigitations between adjacent endothelial cells. However none was observed on well established cell-cell contacts at tight junctions. Thus it was suggested that CD34 functions as an adhesion molecule on both endothelial cells and haematopoietic progenitors. A study by Schlingemann et al. (1990) very shortly afterwards, found that CD34 was localised at the luminal endothelial membrane but not the abluminal membrane, which was either negative or very weakly positive. However the abluminal microprocesses within tumour stroma were strongly positive and suggestive that CD34 could be used for such microprocesses during neovascularisation.

Expression of CD34 in freshly isolated umbilical vessel endothelial cells was reported by Fina et al., 1990. However they found that with continuous culture, although message could still be detected, CD34 protein could not be. They concluded that this was either due to downregulation or the possibility that the protein was being processed into another form which the antibodies they employed could not recognise. Maintaining expression of CD34 in cultured cells was later found to be possible by restraining cell proliferation and promoting cell contact (Delia et al., 1993), suggesting that CD34 might have a negative modulatory role on adhesion function within endothelial cells.

Within undifferentiated haematopoietic progenitors it would appear that full length CD34 plays a role in the maintenance of a phenotypically plastic state, thus inhibiting differentiation. Fackler et al. (1995) carried out a study on murine myeloid leukaemia cells and found that cytokine-induced differentiation resulted in the down-regulation of CD34. Constitutive expression of recombinant full length CD34 prevented differentiation, although leukaemia cells expressing the

truncated form were found to complete differentiation. Thus inappropriate expression of full-length CD34 in leukaemic cells could contribute to their undifferentiated phenotype.

CD34 at high endothelial venules (HEV) has been identified as a ligand for L-selectin, but only when appropriately glycosylated and thus has a putative role in L-selectin-mediated leukocyte trafficking (Baumhueter et al., 1993; Baumhueter et al., 1994). L-selectin has been shown to bind directly to GlyCAM-1 on murine HEV, to form a chimeric protein which in turn binds to CD34 in a sialic acid-specific and Ca^{2+}-dependent manner. Satomaa et al. (2002) identified the carbohydrate moieties on CD34 extracted from human tonsils and suggested that the sialated *O*-glycans could potentially form multiglycan binding epitopes for L-selectin. No L-selectin binding has been reported on either non-HEV endothelial tissues or haematopoietic progenitor cells, implying that differential glycosylation of CD34 across cell types may affect adhesive interactions, as may expression of different accessory molecules like GlyCAM-1.

Since the early 1990s, CD34 has served as a reliable marker for blood vascular endothelium in tissue sections. Traweek et al., 1991 found that CD34 gave quantitatively and qualitatively stronger staining in vascular neoplasia than von Willebrand Factor, vWf, an alternative marker for vascular endothelium, synthesised in Weibel-Palade bodies. Similarly Miettinen et al., 1994 found that CD34 was a specific and sensitive marker for the diagnosis of angiosarcomas, whereas vWf was less reliable. CD34 is employed in some of the experiments of this thesis in phenotyping cultured endothelial cells, as its expression has been shown to be restricted to prox-1-negative blood vessels in human skin and absent from lymphatic endothelium (Hirakawa et al., 2003). However, it has a limitation as a marker for blood endothelial cells in culture as there is evidence outlined above to suggest that CD34 expression decreases with continuous culturing. Therefore for this reason the absence of CD34 from an endothelial cell

alone cannot be interpreted as an indication that the cell is lymphatic endothelial. Lymphatic endothelial cell markers were used much more extensively to avoid such potential artefacts.

1.3.5 CD31

CD31 or platelet endothelial cell adhesion molecule-1 (PECAM-1) was first identified in a search for novel endothelial cell adhesion molecules (Muller et al, 1989). This immunoglobulin (Ig) superfamily member is widely expressed on haemopoietic and endothelial cells, (reviewed by Jackson, 2003) and was found to be heavily glycosylated, with a relative molecular mass of approximately 130 kDa, up to 40% of which is believed to consist of carbohydrate (Newman et al., 1990). Expression occurs at a high density in endothelial cells where it concentrates at cell-cell borders and up to a million copies of CD31 have been found on such cells (Newman et al., 1994). Much lower expression is found on haematopoietic and immune cells such as macrophages, neutrophils, monocytes, mast cells, natural killer cells, platelets and naïve B and T cells. No CD31 has been detected on fibroblasts, epithelial cells or red blood cells. The open reading frame, encoded on human chromosome 17q23 and mouse chromosome 6 (Gumina et al., 1996) consists of 16 exons encoding a signal peptide, six C2-type Ig domains, a transmembrane region and a cytoplasmic C-terminal. CD31 message is highly expressed in lung, heart and kidney and to a lesser extent in brain and liver. Several alternative splice variants occur, which are expressed in a cell-, tissue- and species-specific pattern and arise as a result of alternative splicing of either the transmembrane or cytoplasmic domain exons. The delta-exon 14 form (Kirschbaum et al., 1994) and delta-exon 13 form (Osawa et al., 1997) may be generated in endothelial cells.

The ligand interactions of CD31 have attracted much interest for research over a number of years as this molecule is capable of both homophilic interactions with

another corresponding CD31 molecule on an adjacent cell and also heterophilic binding to several other ligands. Homophilic interactions have been shown to be mediated by the NH_2 terminal Ig domains 1 and 2, with the other Ig domains and the transmembrane proximal region responsible for maintaining these binding domains in the correct spacial organisation (J. Sun et al., 1996; Newton et al., 1997). Human-mouse chimeric studies by Q. H. Sun et al. (1996) demonstrated the species specificity of these homophilic interactions. CD31 can also dimerise (Newton et al., 1999) and it is believed that the formation of primary *cis* interactions promotes efficient *trans* interactions with CD31 molecules on the neighbouring cell. A zipper model was proposed by Newton et al. (1997), whereby CD31 dimers interdigitate with other dimers on an apposing cell surface. Thus each CD31 molecule interacts with two others in this homophilic manner, with contribution from residues on both faces of the first Ig fold.

Heterophilic interactions with αvβ3 integrin have been found in both the mouse (Piali et al., 1995) and human (Buckley et al., 1996). In the latter publication, the binding was found to be mediated predominantly by the Ig domain 1, with some contribution from domain 2. CD31 binding to CD38 and an unidentified 120 kDa ligand on T cells have also been demonstrated (reviewed by D. E. Jackson, 2003).

As CD31 is capable of both heterophilic and homophilic binding of ligand, tight regulation of binding specificity is essential. J. Sun et al. (1996) suggested that the local level of surface expression of CD31 can alter ligand binding properties: where CD31 expression is high, typically at endothelial cell-cell junctions, homophilic ligand interactions occur. On leukocytes, where CD31 expression is lower and more diffuse, heterophilic interactions are more commonly mediated. A possible molecular mechanism by which this could be occurring was identified in a publication from the same research group, by Yan et al. (1995a). They transfected a series of mouse CD31 splice variants into mouse L cells and

analysed the adhesive properties in an aggregation assay whereby transfectants were mixed with non-transfectants and allowed to aggregate. They found that full length CD31 and all isoforms containing peptide sequences encoded in cytoplasmic exon 14 mediated heterophilic aggregation via a non-CD31 ligand. Deletion of exon 14 resulted in homophilic aggregation. The researchers also found that heterophilic aggregation was sensitive to deglycosylation of CD31, whereas homophilic aggregation was not.

The region of exon 14 responsible for ligand specificity was identified by a series of deletion mutants as a conserved 5 residue motif, VYSEI in the mouse sequence or VYSEV in the human sequence (Famiglietti et al., 1997). The tyrosine residue within this motif was found to be key in determining the mode of aggregation. A construct in which the tyrosine was mutated to a phenylalanine residue was found to induced aggregation in a homophilic manner rather than the heterophilic aggregation observed by the wild-type. Homophilic aggregation was also induced following high levels of tyrosine phosphorylation within the cell. Thus the cell could potentially determine whether CD31 functions as a homophilic or heterophilic adhesion molecule by alternative splicing during synthesis and by the state of phosphorylation in the translated protein.

On endothelial cells CD31 is localised primarily at the cell-cell junctions but research by Bird et al. (1999) have lead to the suggestion that this adhesion molecule does not support strong adhesive interactions but rather acts as an adhesion-dependent signalling receptor and promotes cell adhesion and survival. In a study carried out by J. Sun et al. (2000), the localisation of CD31 to cell-cell junctions was found to be dependent on homophilic binding between adjacent cells and thus intact extracellular and transmembrane domains. A small group of highly charged amino acids (^{599}RKAKAK^{604}) in a membrane proximal region of the cytoplasmic domain were also found to be crucial. These provide

putative docking sites for the recruitment of cytosolic signalling molecules and perhaps also cytoskeletal proteins.

In a study by Bogen et al. (1992) using immunoperoxidase and immunoelectron microsopic techniques, high levels of CD31 were found to be expressed on endothelium-adherent lymphocytes transmigrating across sinusoidal or venular vascular boundaries. Such expression was also detected in draining lymph nodes during the immune response following challenge with a protein antigen, where there are many transmigrating lymphocytes. They also found that leukocyte CD31 was predominantly localised on the surface which was in contact with endothelial cells and postulated that CD31 may play a role in lymphocyte recruitment and transmigration. The requirement for CD31 in transendothelial migration of leukocytes was shown by Muller et al. (1993). They found that anti-CD31 antibodies blocked transmigration when bound to either CD31 on monocytes or to CD31 at the endothelial junction, both in resting cells and following stimulation with proinflammatory cytokines. Neutrophil migration was also found to be blocked by these antibodies, although such migration only occurred across stimulated endothelial cells. As soluble CD31 also blocked migration, the interaction was deemed to be most probably homophilic and thus binding of leukocyte to endothelium was direct. Also, the epitope of the blocking antibody used lay within Ig domains 1 and 2 and was not found to block heterophilic aggregation. Heterophilic aggregation in L-cells was mapped to either Ig domain 2 or Ig domain 6 (Yan et al., 1995b) whilst again the N-terminal Ig domains were shown to be involved in transmigration.

Following stimulation of endothelium with the pro-inflammatory cytokines IFNγ and TNFα, CD31 is redistributed from the intercellular junctions, perhaps as a means of regulating the transmigration of leukocytes (Romer et al., 1995). Also the gene expression decreases (Neubauer et al., 2000), shown in sinusoidal

endothelial cells and monocytes following inflammation in the liver and also in cells *in vitro*. However these phenomena were not shown to reduce monocyte or neutrophil transmigration under flow (Shaw et al., 2001). A study using CD31-deficient mice demonstrated that although no differences in levels of leukocyte rolling or firm adhesion were observed in response to IL-1β, there was a delay in leukocyte transmigration (Thompson et al., 2001). Thus CD31 was shown to play a critical regulatory role in leukocyte migration through vessel walls at sites of inflammation. Such a delay in transmigration in these mice did not occur following TNFα elicitation as this cytokine was found to stimulate leukocytes directly. Thus CD31-independent leukocyte migration may also occur.

In addition to direct interactions as an adhesion molecule, CD31 plays pivotal roles in cell signalling pathways as an agonist receptor. Dangerfield et al. (2002) showed that homophilic interactions between neutrophil CD31 and CD31 at endothelial cell junctions stimulated enhanced expression of α6β1 integrin on the cell surface of transmigrating neutrophils. This is believed to aid their migration through the perivascular basement membrane via interactions with laminin, a major constituent of this barrier. Such up-regulation of the surface expression of this integrin may be due to translocation from granules and degranulation. Other research groups have found that engagement of CD31 can up-regulate β1, β2 and β3 integrin function, (Tanaka et al., 1992; Berman and Muller, 1995; and Varon et al., 1998).

Other functions of CD31 in endothelial cells include the maintenance of a vascular permeability barrier, as shown by enhanced permeability changes in response to histamine by endothelial cells which do not express CD31, (Graesser et al., 2002). A role for CD31 in angiogenesis has also been found by several groups. In a recent study by Solowiej et al. (2003), a sterile and inert object was implanted into mice subcutaneously and the neutrophil infiltrate measured. An

attenuated infiltrate was observed in CD31 knock-out mice and this was found to be due to a decrease in angiogenesis and thereby diminished delivery of leukocytes to the region.

Thus the different domains of CD31 permit this Ig superfamily member to carry out a vast repertoire of diverse function. This protein also serves as an effective marker for endothelial cells, both of the blood vasculature and of the lymphatics, allowing discrimination from epithelial cells and fibroblasts in culture.

Of the endothelial cell markers described above, podoplanin has been used the most extensively in this PhD as its high expression on the surface of lymphatic endothelium makes it ideal for investigating possible variations in LYVE-1 expression. The availability of specific antibodies against both mouse and human podoplanin has permitted the study of LYVE-1 expression on both mouse and human tissue, in cell lines and also in models of pathological conditions within tissues.

1.4 Pathological Conditions of the Lymphatics

1.4.1 Metastasis of tumour cells and lymphangiogenesis

The role of the lymphatics as a conduit for metastasising tumours has been recognised since the early 1700s when Louis Petit reported the spread of breast cancer to axillary lymph nodes (reviewed by Swartz, 2001). Tumours of the breast, lung and gastrointestinal tract are known to result frequently in secondary tumours within draining regional lymph nodes (reviewed by Saharinen et al., 2004); however the mechanism by which this dissemination occurs remains poorly characterised.

An increased expression of VEGF-C has been detected in many human tumours and has been found to correlate with lymph node metastasis in thyroid, prostate, gastric, colorectal and lung cancers. VEGF-C is also implicated in inducing lymphangiogenesis. A model used extensively to investigate this is that of transgenic mice overexpressing VEGF-C under the control of the keratin 14 (K14) promoter, which directs transgene expression to the basal keratinocytes of the skin. Jeltsch et al. (1997) found that K14-VEGF-C mice display a pronounced hyperplasia of cutaneous lymphatic vessels but exhibit no variation in the growth of blood vessels. A later study by Veikkola et al. (2001) generated transgenic mice with K14-VEGF-D and K14-VEGF-C156S, a mutant factor which is a selective agonist of VEGFR-3 and showed that VEGF-D is also lymphangiogenic. In addition they demonstrated that VEGFR-3 alone was responsible for the signal transduction. At around the same time Enholm et al. (2001) used an adenoviral system to show that subcutaneous expression of VEGF-C induces proliferation and enlargement of lymphatic vessels in mice and also strongly up-regulates VEGFR-2 and VEGFR-3 expression in blood vessels. They found that VEGF, in contrast, only induces angiogenesis and the up-

regulation of VEGFR-2. Mandriota et al. (2001) demonstrated that VEGF-C overexpression in pancreatic β-cells of transgenic mice results in extensive lymphatic channel formation around the islets of Langerhans which, as islets are very rarely in direct contact with lymphatics in wild-type mice, indicates *de novo* formation of lymphatics. These mice were crossed with mice from a transgenic model of β-cell carcinogenesis, which develop numerous B-cell tumours that are capable of local invasion but not metastasis. In contrast to the single transgenics, 37% of the mice crossed with those overexpressing VEGF-C developed metastases in the draining regional mesenteric lymph nodes of the pancreata, thus providing evidence for a causal role for VEGF-C-mediated lymphangiogenesis and the dissemination of tumour cells.

The importance of VEGF-C in promoting lymphangiogenesis and metastasis to lymph nodes and lungs has also been shown using MCF-7 and MDA-MB435 human breast cancer cells in immuno-deficient mice (Skobe et al., 2001; Karpanen et al., 2001; Mattila et al., 2002). However in contrast to the animal studies, Williams et al. (2003) were unable to detect dividing lymph vessels in primary human breast carcinoma and found few if any intra-tumoural lymphatic vessels. Dissemination was hypothesised to occur as the cancerous cells invade and destroy existing lymphatic vessels and the recombinant VEGF-C used in the animal studies was expressed at much higher concentrations than would normally occur.

Involvement of VEGF-D was elucidated by Stacker et al. (2001) who used 293EBNA cells expressing VEGF or VEGF-D for subcuaneous injection into SCID mice. They found that VEGF-293 and VEGF-D-293 cells developed into highly vascularised tumours whereas the control 293 cells did not produce such large, vascularised tumours. Oedema was also noted in VEGF-293 tumours, which was not observed in VEGF-D-293 tumours. Moreover the growth of VEGF-D-293

tumours was found to be inhibited by intraperitoneal injections of a mAb specific for the bioactive region of VEGF-D, which blocks binding of VEGF-D to both VEGFR-2 and VEGFR-3. The VEGF-D-293 tumours alone were found to contain LYVE-1-positive lymphatic vessels within the tumour mass as well as in the outer connective tissue capsule region surrounding the tumour and by use of dye injection experiments, these vessels were found to be functional. A massive tumour infiltrate within the lymph nodes was also reported in such animals. Together, these studies demonstrated the lymphangiogenic and angiogenic effect of VEGF-D through VEGFR-3 and VEGFR-2 respectively, as well as showing that VEGF-D-induced lymphangiogenesis can promote metastatic spread of tumour cells through the lymphatic network.

A study by Leu et al. (2000) had investigated functional lymphatics within a murine sarcoma and found that although lymphangiogenic factors VEGF-C and VEGFR-3 were present, functional lymphatic vessels did not form within the tumour, possibly because they collapsed due to solid stress exerted by the growing malignancy. However this study did not measure the expression of VEGF-C and VEGF-D which have been proteolytically processed into active forms. Thus the ability of a tumour to induce lymphangiogenesis of functional lymphatic vessels through which it can disseminate most likely depends upon which VEGF family members it is expressing and processing, as well as the interstitial pressure of the tumour.

The role of VEGF-D was also assessed by Niki et al. (2000), who found that the expression of VEGF-D was inversely correlated with metastatic spread of lung adenocarcinoma to lymph nodes. However this study was based on analysis of RNA from clinical samples by PCR which cannot take into account the extent of VEGF-D proteolytic processing into an active form which can bind VEGFR-2 and VEGFR-3 with high affinity. Nevertheless the possibility of more growth factors

in addition to the VEGF family cannot be ruled out. A later study by Dadras et al. (2003) showed that intra- and peri-tumoural lymphangiogenesis in primary human cutaneous melanomas occurs and can be correlated with metastasis. However, although expression of VEGF-C was detected more frequently in tumour cells of metastatic melanomas than non-metastatic melanomas, these differences were not statistically significant ($P > 0.05$) and the authors suggest that lymphatic vessel growth might be stimulated by other growth factors which are as yet unknown. One possible candidate could be basic fibroblast growth factor (bFGF), which was found to be associated with the presence of peri-tumoral lymphatics in cutaneous melanoma (Straume et al., 2003).

Despite the controversy that remains regarding the functional significance of tumour-stimulated *de novo* growth of lymphatic vessels in clinical cases of cancer, the lymphatics are widely recognised as an important potential conduit for disseminating tumour cells from certain tumours. Once the molecular mechanisms of lymphangiogenesis are better elucidated this may serve as a potential therapeutic target to reduce metastasis of primary tumours.

1.4.2 Lymphatics as an entry for pathogens

Metastasising cancer cells are not the only entities which seek to hijack the lymphatics for purposes which are not in the animal's best interest. The pathogen *Yersinia Pestis*, a facultative anaerobic intracellular Gram-negative coccobacillus is a prime example, an organism known to be responsible for the deaths of nearly 200 million people through the infectious disease termed *plague* or *Black Death* (reviewed by Velendzas et al., 2004). This disease was responsible for at least three pandemics and multiple epidemics. It was during the last pandemic (starting in around 1855 in China) that Alexandre Yersin isolated the plague bacillus and developed an antiserum to combat the disease.

The organism can be transmitted from an animal host to a human via the bite of a vector. More than 200 different species can serve as hosts, frequently rodents but also cats, dogs, deer, rabbits, camels and sheep. The vector is usually the rat flea, *Xenopsylla cheopis* but the human flea *Pulex irritans* as well as ticks and lice can also serve as carriers (Velendzas et al., 2004). The bacillus proliferates in the flea's oesophagus, preventing food from entering the stomach. The flea will try to overcome starvation by fervently attempting to feed more often on its host or an unfortunate human and as it tries to swallow, the distended bacillus-packed oesophagus recoils and deposits the bacillus into the victims' skin. It may then enter the lymphatics either alone or engulfed by an antigen presenting cell and traffick to a nearby draining lymph node. As the bacillus proliferates it induces inflammation and produces the characteristic bubo, a necrotic and haemorrhagic lymph node (figure 1.10). The bacteria may also be ingested by macrophages, in which they will proliferate. From there the bacilli may spread through efferent lymph to the thoracic duct, gaining entry into the vasculature and then potentially every organ, causing septicaemia and haemorrhage throughout the body. Direct inhalation of the bacillus results in pneumonic plague whilst delivery of the bacillus to the vasculature and bypassing the lymphatics results in septicaemic plague. However as bubonic plague has a longer incubation time of 2-6 days (as opposed to pneumonic plague which has a trypical mortality rate of 100% within 24h if left untreated), the potential for infecting more individuals and carriers is much higher. *Yersinia Pestis* is still very much endemic throughout most of the world and between 1967 and 1993, the World Health Organisation reported an annual average of 1666 cases of plague.

Figure 1.10 Swollen lymph nodes in a patient infected with *Yersinia Pestis*, resulting in the characteristic buboes.

1.4.3 Lymphoedema

Clinical oedema results when either the volume of interstitial fluid exceeds the drainage capacity of the lymphatics or the lymphatic vessels become blocked, causing interstitial fluid to accumulate (Berne et al., 1998). Such tissue fluid imbalance may be hereditary and is termed primary lymphoedema, characterised by hypoplastic or aplastic superficial or subcutaneous lymphatic vessels which fail to transport lymphatic fluid into the venous circulation. Non-inherited secondary lymphoedema occurs when the lymphatic vessels are damaged as a result of infection, trauma (from burns or radiation), surgery, tissue grafting or transplantation (reviewed by Swartz, 2001). If this arises in the lungs it is termed pulmonary oedema whilst such excess fluid in the peripheral tissues is known as generalised oedema. Pulmonary oedema is a frequent complication of cardiovascular disease, occurring when pulmonary capillary hydrostatic pressure exceeds plasma oncotic pressure, resulting in serious

interference with gaseous exchange due to fluid accumulation within the pulmonary interstitium or within the alveoli themselves, which can prove lethal.

Lymphatic filariasis is caused by a parasite known as the filaria round-worm. This organism infects the lymph nodes and provokes the growth of connective tissue, leading to the blockage of lymph flow from a limb. As fluid accumulates and oedema develops, the limb swells and grows to enormous proportions, as shown in figure 1.11, (Rischer and Easton, 1995). In such an advanced stage the lymphatics have been damaged irreversibly and the disease is frequently termed *elephantiasis.* The parasitic worm is carried by tropical mosquitoes and poses a great problem in developing countries. Secondary infection by bacteria through "entry lesions" in the skin can provoke acute adenolymphangitis, characterised by a worsening of the condition (reviewed by Shenoy, 2002).

Figure 1.11 Elephantiasis in the right leg of a female patient from Ghana. (Photograph from www.filariasis.org)

Myxoedema is a symptom of hypothyroidism and a lower-than normal metabolic rate (Berne et al., 1998). It is produced by an accretion of mucopolysaccharide in the tissues, which results in an accumulation of fluid. This produces the characterisitic puffy features of a patient with hypothyroidism, coupled with an enlarged tongue, hoarseness, joint stiffness, effusions of the pleural, pericardial and peritoneal spaces; and entrapment of pressure on peripheral and cranial nerves. Other unpleasant symptoms include constipation, loss of hair, menstrual dysfunction and anaemia. The end stage of untreated hypothyroidism is myxoedema coma, an acute medical emergency which, since it frequently occurs in older patients with underlying pulmonary and vascular disease, has a very high associated mortality (Greenspan and Strewler, 1997).

Unfortunately despite the discomfort and danger of lymphoedema, few treatments have been developed and even fewer have proved effective (Swartz, 2001). Oedema resulting from an increase in interstitial osmotic forces due to increased permeability of the blood microcirculation has been treated with some success by drugs such as Coumarin, of the benzopyrone family. These stimulate proteolysis by macrophages, thus reducing oncotic pressure within the interstitium. However sustained oedema elicits reorganisation of the extracellular matrix by fibroblasts. This precipitates an overall decrease in tissue elasticity and may cause protein accumulation which exacerbates the situation.

The advent of gene therapy may herald an era of greater success in treating oedema with fewer side effects. Yoon et al. (2003) used naked plasmid DNA encoding human VEGF-C on rabbit ear and mouse tail models of secondary lymphoedema and found that the increase in lymphangiogenesis that occurred lead to a decrease in thickness and volume of lymphoedema, improved lymphatic function and attenuation of the fibrofatty changes of the skin which

occur with prolonged lymphoedema. Thus VEGF-C gene therapy may represent a novel therapeutic approach to managing this disabling condition.

The study of the lymphatics was neglected for many years, with much more effort concentrated on the blood circulatory system. The lack of markers was blamed, which forced investigators to rely solely on observing morphological differences between blood and lymphatic vessels. Another factor cited as a reason to place less effort on research into the lymphatics was the lack of fatal lymphatic diseases, with the exception of cancer (Mortimer, 1997). However the lymphatics have far reaching implications in a number of diseases and debilitating conditions as described above and these make them very well worth while studying. Also with the explosion in the number of specific lymphatic and blood endothelial cell markers there is no longer an excuse.

1.5 The Migration of Leukocytes Throughout the Vasculature and Lymphatic Systems: in Sickness and in Health.

Although the lymphatic and blood vascular systems are structurally distinct (figure 1.12), they are functionally interconnected and act in concert to maintain homeostasis within the tissues, cell nutrition and removal of metabolic by-products. The two systems also provide transport routes for leukocytes and are thus essential in the systemic effects of both innate and acquired immunity. Leukocytes travel through the blood vasculature to peripheral tissues and to the lymph nodes. The lymphatics are responsible for the trafficking of leukocytes from the tissues to the lymph nodes.

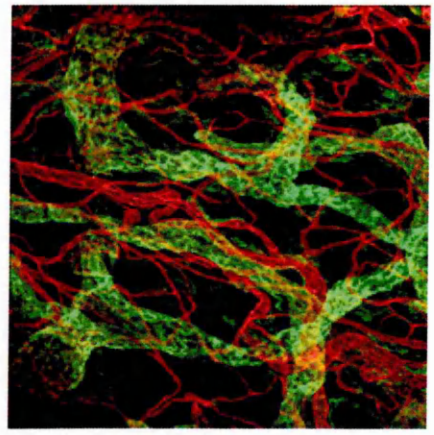

Figure 1.12 The discrete networks of blood vasculature and the lymphatics within peripheral tissue. Whole mount staining of mouse ear tissue of blood capillaries (red, stained with rat anti-mouse CD31) and lymphatic vessels (green, rabbit anti-mouse LYVE-1). Image captured at a magnification of x100.

Both innate and specific immunity are mediated and regulated by cytokines, which regulate the growth and differentitation of leukocyte subsets as well as activate and regulate inflammatory cells. Two of the key pro-inflammatory cytokines are the tumour necrosis factors TNFα and TNFβ, whose effects on lymphatic endothelium have been extensively studied during the course of this PhD.

1.5.1 The TNF superfamily

Evidence to suggest that a tumour necrotizing molecule existed arose from the observation that cancer patients occasionally showed spontaneous regression of their tumours following bacterial infections. Subsequent research indicated that endogenous mediators synthesised in response to bacterial products were likely to be responsible for this effect. In 1975 it was demonstrated that a bacterially-induced circulating factor had strong anti-tumour activity against tumours implanted in the skin of mice (Carswell et al., 1975) and was named tumour necrosis factor (TNF or TNFα). This was the first member of a superfamily of related ligands to be identified, all of which are involved in immune regulation and inflammation, acting through TNF receptors which also constitute a superfamily. This introduction will only mention TNFα and TNFβ, the proinflammatory cytokines of interest in this thesis. However to date the superfamily consists of a total of 17 known members

1.5.1.1 TNFα

TNFα is a non-glycosylated protein which exists in either a soluble (157aa) or membrane-bound (233aa) form (Pennica et al., 1984; Wang et al., 1985; Shirai et al., 1985). When in membrane-bound form, TNFα has a molecular weight of 26 kDa and consists of a 29 residue cytoplasmic domain, a 28 residue transmembrane region and a 176 residue extracellular domain. This is present as a type II transmembrane protein on the cell surface and is believed to associate as

a homotrimer. The soluble protein is created by proteolytic cleavage within the membrane proximal extracellular domain mediated by the 85 kDa metalloproteinase TNF-alpha converting enzyme (TACE), (Black et al., 1997), generating a 157 residue product (Wang et al., 1985; Moss et al., 1997) which circulates as a homotrimer under normal physiological conditions (Smith et al., 1987). Both forms of TNFα are biologically active, although Decoster et al. (1995) have shown (through mutation of the standard TNF cleavage site and generation of a membrane-bound, uncleavable mutant) that soluble TNF is more potent in cytotoxic assays.

The mouse orthologue of TNFα shares 79% sequence identity with human TNFα, although mouse TNFα consists of a longer 235-residue polypeptide with a potential N-glycosylation sequence (Asn-Ser-Ser) at amino acids 7-9 (Pennica et al., 1985; Fransen et al., 1985). However, the two molecules are cross-reactive and have been shown to bind each other's receptors.

TNFα is expressed by a wide range of cells including macrophages, CD4+ and CD8+ T cells (Ware et al., 1992), adipocytes (Kern et al., 1995), keratinocytes (Lisby et al., 1995), mammary and colon epithelium (Varela and Varela, 1996), osteoblasts (Modrowski et al., 1995), mast cells (Bissonnette et al., 1995), dendritic cells (Zhou and Tedder, 1995), pancreatic beta-cells (Yamada et al., 1993), astrocytes (Lee et al., 1993), neurons (Tchelingerian et al., 1996), monocytes (Frankenberger et al., 1996) and steroid-secreting cells within the adrenal zona reticularis (Gonzalez-Hernandez et al., 1996).

1.5.1.2 TNFβ

TNFβ (lymphotoxin-α, LT-α) is another cytotoxic protein with similar biochemical characteristics and biological activities to TNFα, with which it shares 28% amino acid homology (Gray et al., 1984; Pennica et al., 1984; Li et al., 1987).

Cells known to express TNFβ include NK cells, T cells and B cells (Ware et al., 1992).

TNFβ is glycosylated, with a molecular weight of 25 kDa and like TNFα, circulates as a non-covalent linked homotrimer (Eck et al., 1992; Hochman et al., 1995). TNFβ does not have a transmembrane form but it can be membrane-associated due to its binding to membrane-anchored lymphotoxin-β (LTβ), with which it readily forms a trimeric complex, in either 2:1 in favour of LT-β (the major form) or a 1:2 ratio, the minor form (Browning et al., 1993; Hochman et al., 1995).

1.5.2 Receptors

TNF receptor superfamily members (TNFRSF) are all type I transmembrane glycoproteins but may exist in both membrane-bound and soluble forms (Baker and Reddy, 1998). Both TNFRI (also known as p55) and TNFRII (p75) are capable of binding TNFα and TNFβ. TNFRI is a 55 kDa transmembrane glycoprotein comprised of 455 amino acid residues and is expressed by virtually all nucleated mammalian cells (Loetscher et al., 1990; Schall et al., 1990; Gray et al., 1990). Mouse and human TNFRI molecules share 64% sequence identity, with 70% homology in the extracellular domain and have been shown to bind human and mouse TNFα with equal affinity (Barrett et al., 1991). Soluble TNFα binds TNFRI with a K_d of 20-60 pM whilst TNFβ displays a slightly lower affinity, with a K_d of 650 pM (Marsters et al., 1992).

The cytoplasmic region contains an 80 amino acid residue "death domain" that can trigger an apoptotic pathway (Tartaglia et al., 1993). Binding of TNF to TNFRI leads to the recruitment of several proteins such as TRADD (TNFR-associated death domain protein) to the death domain. Other proteins such as RIP (receptor interacting protein) and TRAF2 (TNFR-associated factor 2) may

then also bind to TRADD, resulting in a signal cascade of kinases which leads to the activation of the transcription factors NFκB and AP1. Multiple genes may then be up-regulated and apoptosis is suppressed (reviewed by Baker and Reddy, 1996). However if an alternative protein, FADD (Fas-associated death domain protein) is recruited to TRADD, a caspase cascade is initiated, resulting in apoptosis.

TNFRII is also widely expressed but binds TNFα with a much lower affinity (K_d: 300 pM) than TNFRI does. Since systemic TNFα levels are usually approximately 100 pM, this would suggest that TNFRI is the more physiologically-relevant receptor and mediates most TNFα activity.

The effects of TNFα and TNFβ are critical for local inflammatory responses. For example, a neutralising anti-TNFα antibody was found to reduce joint swelling and leukocyte infiltration into joint fluid in antigen induced arthritis in rabbits (Lewthwaite et al., 1995). Administration of this antibody also led to a decrease in the expression of αMβ2 integrin on cells in the joint fluid. The generation and characterisation of $TNF\alpha^{-/-}$ mice also revealed a vital role for TNFα in the containment and resolution of infection (Marino et al., 1997). The effects of TNFα on vascular endothelium are described in detail in section 1.5.3 of this introduction, whilst the effects on lymphatic endothelium are explored in chapters 4, 5 and 6 of this thesis.

1.5.3 Leukocyte influx into tissues

The extravasation of leukocytes from the vascular lumen into the tissues is dependent upon a series of sequential molecular interactions between these cells and the endothelium. Recruitment of leukocytes to non-inflamed peripheral tissue is required without inflammatory stimulus as macrophages and dendritic cells (DCs) must be present constitutively. These cells originate from the bone

marrow and circulate as monocyte precursors in the blood, from which they must be recruited. One of the chemotactic molecules constitutively expressed and implicated in acting on these circulating monocytes is BRAK (breast and kidney expressed chemokine, CXCL14), (Kurth et al., 2001). However the roles of this chemokine or other chemoattractants have not been examined in the context of non-inflammatory recruitment of monocytes to tissues (reviewed by Imhof and Aurrand-Lions, 2004).

Populations of DCs in the lungs have rapid turnover rates, requiring de novo constitutive migration of precursor cells to constantly replace those which have emigrated to the thoracic lymph nodes (Vermaelen et al., 2001). Schneeberger et al. (2000) used this observation to try to elucidate the molecular mechanisms involved in constitutive migration. They found that mice deficient in ICAM-1, E-selectin or P-selectin or both did not exhibit a reduction of DCs in the lungs. However animals deficient in the expression of CD18 (β2 integrin) showed a marked decrease in the number of DCs in the lungs. CD18 is known to interact with ICAM-1 but clearly interactions with other ligands appear to be occurring, such as ICAM-2. Immature DCs express high levels of DC-SIGN, the human DC adhesion receptor (CD209) and Geijtenbeek et al. (2000a) were able to demonstrate that this receptor interacts with ICAM-2, constitutively expressed on vascular endothelium. They found that these interactions mediated DC rolling and transendothelial migration from the vasculature into the peripheral tissues, both inflamed and normal. The researchers postulate that such interactions could also be important in the exit of DCs from tissues into the lymphatics.

Recruitment of leukocytes to tissues during inflammation has attracted much more interest from researchers and is therefore better characterised. Upon inflammation, proinflammatory cytokines such as TNFα, stimulate vascular

endothelial cell production of prostaglandins and nitric oxide, potent vasodilators which increase local blood flow to optimise delivery of leukocytes to the site of inflammation (Baumann and Gauldie, 1994). The activated endothelium also exhibits increased expression of certain adhesion-mediating cell surface proteins and thus the circulating leukocytes passing through the post-capillary and collecting venules of inflamed tissue experience an increase in the residence time on the venular surface (figure 1.13). The first visible display of this *in vivo* is the slow rolling or sliding of leukocytes along the endothelium. A well-characterised mediator of this is E-selectin, an 110kD glycoprotein also known as CD62E or ELAM-1 (endothelial leukocyte adhesion molecule-1). E-selectin is exclusively expressed on endothelium and can bind complex sialylated carbohydrate groups related to the Lewis-X or Lewis-A family found on various surface proteins of granulocytes, monocytes and certain memory T-cells (reviewed by von Andrian and Mackay, 2000). It is also responsible for the initial attachment of neutrophils (Bevilacqua et al, 1989) and eosinophils (Weller et al, 1991). This tethering is reversible and may be followed by either the release of the leukocyte and its return to circulation or by a firmer interaction.

E-selectin is the first adhesion molecule to be up-regulated on vascular endothelium, typically 1 to 2 h following the onset of antigen challenge. Vascular cell adhesion molecule-1, VCAM-1 is subsequently up-regulated by pro-inflammatory cytokines through NFκB (Neish et al., 1992), and binds to the VLA-4 (α4β1) integrin on leukocytes, marking the beginning of a phase of firmer attachment of the leukocyte to the endothelium (Staunton et al., 1988; Springer, 1990). A second firm interaction is mediated by intercellular adhesion molecule-1, ICAM-1 and its integrin ligand LFA-1, also known as CD11a/CD18 or αLβ2, (Rothlein et al., 1986). ICAM-1 is constitutively expressed on endothelium but expression increases upon NFκB-mediated activation by pro-inflammatory cytokines (Springer, 1990). ICAM-1 and VCAM-1 play reciprocal roles in the

binding of resting T cells to resting endothelium and to endothelium activated by proinflammatory cytokines respectively (Oppenheimer-Marks et al., 1991). ICAM-1 mediates a firm adhesion with the leukocyte through either LFA-1 (Makgoba et al., 1988) or Mac-1 (CD11b/CD18, αMβ2) and this interaction also plays a role in the transmigration of leukocytes across the blood vessel into the tissue. In the absence of LFA-1, T cells retain the ability to bind to endothelium, most likely due to interactions between other receptor-ligand pairs such as VLA-4 and VCAM-1, although migration is substantially reduced (Kavanaugh et al., 1991; Greenwood et al., 1995). Endothelial cells constitutively express ICAM-2, a second ligand for LFA-1 (Staunton et al., 1989) which is down-regulated in response to TNFα. McLaughlin et al. (1999) identified the TNFα response elements within the human ICAM-2 promoter and found that binding sites for NFκB and Ets family members were involved in basal promoter activity but that TNFα-induced down-regulation of ICAM-2 in endothelial cells was mediated by the Ets family member Erg. In the mouse, ICAM-1 and ICAM-2 were shown by Lehmann et al. (2003) to have redundant roles in lymphocyte recirculation through lymph nodes. However ICAM-1 alone was shown to be involved in T cell migration into inflamed skin and in trapping within the lung. Thus it appears that ICAM-2 does not have a role in inflammation but rather is constitutively expressed in normal tissue for lymphocyte recirculation.

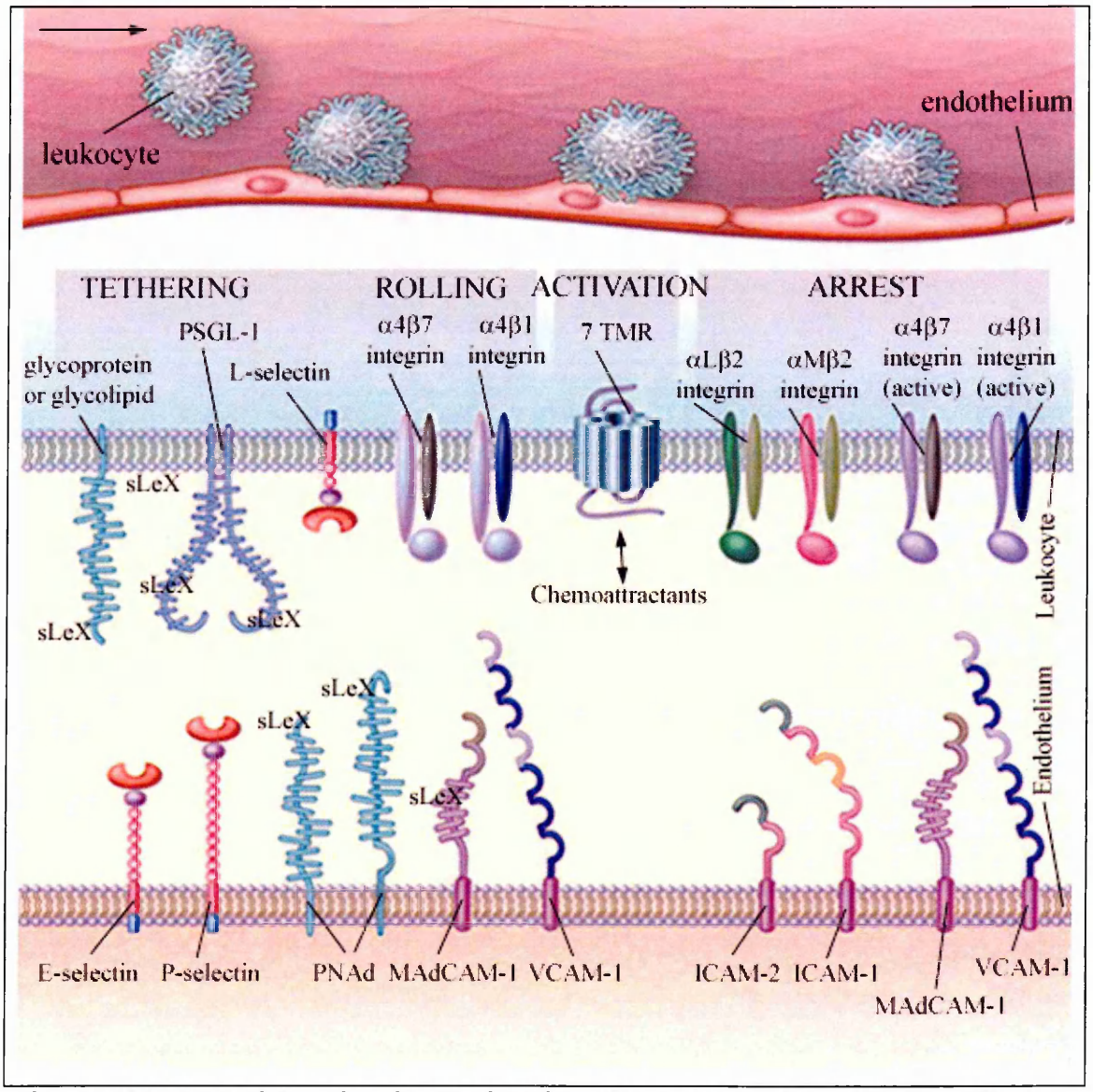

Figure 1.13 Molecular interactions in adhesion of a leukocyte to vascular endothelium. The four phases of adhesion are indicated in capital letters at the top of the diagram, with the predominant interactions of adhesion molecules indicated by arrows. Tethering is facilitated by leukocyte receptors that occur at high density on the tips of microvillous surface protrusions. The selectins are the principal molecules involved in this, interacting with sulphated sialyl-Lewis-X-like sugars. Integrins reduce the velocity of leukocyte rolling. Rolling leukocytes respond to chemoattractants on endothelial cells via seven transmembrane domain receptors (7TMR) and are thus activated. β_2 integrins and α_4 integrins are activated and may bind members of the endothelial Ig superfamily to bring about leukocyte arrest prior to transmigration. These molecules include intercellular adhesion molecule 1 and 2 (ICAM-1 and ICAM-2), vascular cell adhesion molecule 1 (VCAM-1) and mucosal addressin-cell adhesion molecule type 1 (MAdCAM-1). VCAM-1 is not constitutively expressed by endothelium but rather is involved in homing of leukocytes to inflamed tissue throughout the body. MAdCAM-1 is required for homing of leukocytes to gut and associated lymphoid tissue only. Adapted from von Andrian and Mackay, 2000.

The role of CD44 in rolling and adherence of leukocytes to vascular endothelium has become increasingly appreciated over the last few years. Activation of T cells through the T cell receptor induces activation of CD44 and adhesion (DeGrendele et al., 1997a, 1997b; Lesley et al., 1994) and facilitates the extravasation of activated T cells into an inflamed peritoneal site (DeGrendele et al., 1997b). CD44 expression by circulating T cells has also been shown to correlate with autoimmune disease in human (Estess et al., 1998) and in murine models (Brocke et al., 1999). Peripheral blood monocytes constitutively express CD44 but do not bind HA unless stimulated with LPS (Levesque and Haynes, 1996; Levesque and Haynes, 1997). The interactions between CD44 and HA have been shown to be very important in the rolling phase of the leukocyte along the endothelium. Gee et al. (2003) suggested that LPS-induced CD44-mediated HA binding in primary monocytes might be regulated by endogenously produced TNFα and IL-10 via the induction of sialidase activity.

HA is by no means the only molecule that CD44 can interact with and a recent study by Nandi et al. (2004) provided data to show that CD44 also plays a role in cell arrest via interaction with VLA-4. Both mouse and human T cell extravasation is initiated by the activated form of CD44 associating with VLA-4 in a manner dependent upon the cytoplasmic tail of CD44. In the absence of this domain CD44-HA mediated rolling can still occur but the adhesion of VLA-4 to its ligand, VCAM-1 is prevented.

Leukocyte movements are tightly regulated by chemokines, structurally related chemotactic cytokines which are subclassed according to the relative position of conserved cysteine residues. The most numerous CC subfamily have the first two cysteines adjacent, whereas the CXC chemokines have the first two cysteines separated by one amino acid. CX_3C chemokines are characterised by the first two cysteine residues being separated by three intervening amino acids and C

chemokines lack the first and third cysteine residues. Chemokines bind seven-transmembrane-domain receptors which are coupled to heterotrimeric G proteins (reviewed by Thelen, 2001). Activated endothelium and leukocytes already within the tissue secrete chemokines such as RANTES (regulated upon activation, normal T-cell expressed and secreted, CCL5), IL-8 (CXCL8) and MCP-1 (monocyte chemotactic protein-1, CCL2). Gerszten et al. (1999) demonstrated that when IL-8 and MCP-1 were applied to HUVEC monolayers expressing E-selectin, the arrest of rolling monocytes was enhanced. MIP-1β (Macrophage inflammatory protein-1β, CCL3/4), IL-8 and RANTES have been shown to bind to transmembrane heparan sulphate proteoglycans on the luminal surface of vascular endothelial cells and be presented to leukocytes. Tanaka et al. (1993) found that MIP1β induced both chemotaxis and adhesion of T cells to vascular endothelium. They established that it is present on lymph node endothelium and when immobilized by binding to proteoglycan, could also induce binding of T cells to VCAM-1. Spillmann et al. (1998) studied the interaction between a heparan sulphate chain and IL-8 dimer and found that a minimal sequence of 18-20 monosaccharide units were necessary to span the two saccharide-binding sites on the dimer. Halden et al. (2004) later demonstrated that IL-8 can bind syndecan-2 on HUVEC, which is up-regulated following TNFα stimulation. However they also found that binding could occur between IL-8 and a non-glycosylated form of syndecan-2, albeit with a higher K_d value and thus concluded that protein-protein interactions could contribute to chemokine-proteoglycan interactions. Interaction of RANTES with the glycosaminoglycan chains of CD44 was demonstrated by Roscic-Mrkic et al. (2003). They found that such binding induced the formation of a signalling complex composed of CD44, src kinases and adapter molecules, which led to the activation of the p44/42 mitogen-activated protein kinase (MAPK) pathway

When chemokines bind to these proteoglycans, the binding site for chemokine receptors remains exposed (reviewed by Proudfoot et al., 2000), permitting the chemokine to interact with its seven transmembrane spanning G-protein-coupled receptor expressed on a rolling leukocyte which passes over the endothelium. This elicits a rapid integrin-activation signal, dependent upon the individual chemokines and receptor (reviewed by Thelen et al., 2001), which permits the leukocyte to attach more firmly to the endothelium via integrin-VCAM-1 or –ICAM-1 interactions.

Upon activation by contact with the endothelium, leukocytes undergo cytoskeletal rearrangement to permit a morphological change from spherical to flattened, allowing a greater surface area of contact with the endothelium (reviewed by Imhof and Aurrand-Lions, 2004). Vascular endothelial cells also undergo a change in shape and basement remodelling to aid extravasation of leukocytes whilst still maintaining vascular integrity. *In vitro* studies have shown that considerable leukocyte trafficking can occur without an increase in the permeability of the endothelial cell monolayer or a decrease in electrical resistance, (reviewed by Muller, 2003).

1.5.3.1 Paracellular transmigration

A leukocyte poised to take the classical paracellular route across endothelium must breach the large array of endothelial junctions, which are responsible for maintaining the integrity of the endothelium and regulating vascular permeability. To date, three types of endothelial junction have been described: tight junctions, adherens junctions and gap junctions (reviewed by Imhof and Aurrand-Lions, 2004). These junctions resemble those found in epithelium but have a less ordered spacial organisation, which reflects the need for frequent remodelling to permit leukocyte trafficking.

Tight junctions are the most apical of the three, containing occludin, claudins and junctional adhesion molecules (JAMs). Occludin is a 65-kDa protein with four transmembrane domains and a hypothesised topology of two extracellular loops with a short cytoplasmic N-terminus and a long cytoplasmic C-terminus (reviewed by Luscinskas et al., 2002). The C-terminal tail can associate with several cytoplasmic components including zona occludens (ZO)-1, -2 and -3, which in turn link to the actin cytoskeleton (figure 1.14). However, the role of this protein at these junctions remains unknown.

Claudins constitute a large family of proteins, which contain a similar membrane topology to occludin and associate with ZO-1, -2 and -3 but share no amino acid sequence homology with occludin (Furuse et al., 1998). Heterogeneous claudin species form tight junctional strands and the combinations and ratios of abundance of each claudin species is believed to define the permeability of the junction to macromolecules (Furuse et al., 2001). However the roles of claudins in leukocyte transmigration are still under investigation (reviewed by Luscinskas et al., 2002). A study by Poritz et al. (2004) suggested that the TNFα-induced redistribution of claudin-1 and ZO-1 away from the tight junctions of endothelial cells that they observed *in vitro* could explain the increased intestinal permeability associated with the chronic intestinal inflammation which occurs in patients with irritable bowel disease. Thus these proteins may be involved in regulating the permeability of the endothelium.

JAM family members include JAM-A, JAM-B and JAM-C and belong to the immunoglobulin superfamily. JAM-A, the first to be cloned, has two extracellular Ig domains, which are capable of both homophilic interactions and heterophilic interactions with LFA-1. JAM-A is also capable of interactions with several proteins including occludin and ZO-1 through its cytoplasmic tail (reviewed by Imhof and Aurrand-Lions, 2004). Through the use of a monoclonal

antibody with blocking activity, Del Maschio et al. (1999) demonstrated that JAM-A aided monocyte and neutrophil recruitment and transmigration at sites of injury. Stimulation of endothelial cells with inflammatory cytokines was found to induce the redistribution of JAM-A from intercellular junctions to the luminal surface of the cells, resulting in reduced transendothelial migration of leukocytes under static conditions but no change under flow (Shaw et al., 2001). JAM-B and JAM-C have also been shown to interact with ZO-1 and all three JAMS are believed to be involved in the regulation of tight junction formation and cell polarity through recruitment of both ZO-1 and the cell polarity protein PAR-3 (Ebnet et al., 2003). In addition, JAM-B and JAM-C act as receptors for integrins: JAM-B binds α4β1 whilst JAM-C binds αMβ2 and αXβ2. JAM-B and JAM-C may also interact with each other (reviewed by Imhof and Aurrand-Lions, 2004). JAM-B is implicated in facilitating and controlling the transmigration of leukocytes across HEVs, discussed in section 1.5.4 of this chapter (Johnson-Leger et al., 2002). Thus the JAMs appear to be involved in both the structural maintenance of cell-cell junctions and integrin-mediated transmigration.

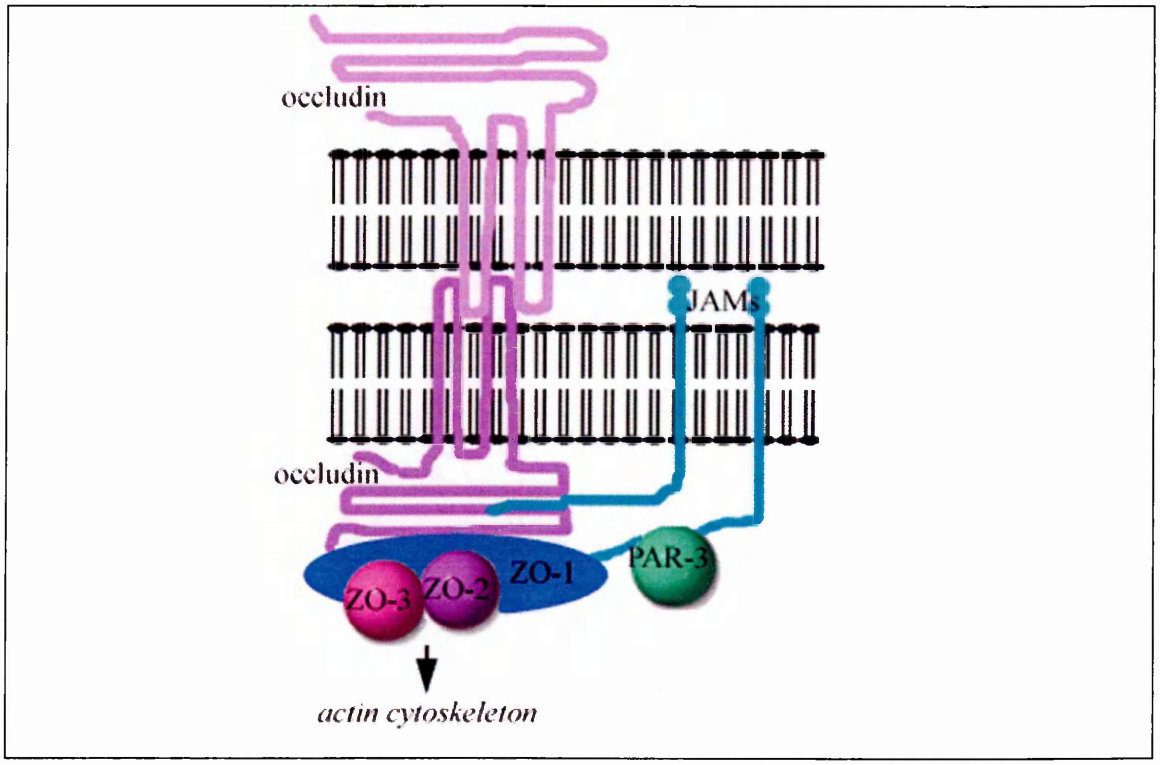

Figure 1.14 Schematic representation of a tight junction. Homophilic interactions occur between occludin molecules on adjacent cells. Occludin has a short N-terminal and an extended C terminal, which interacts with zona occludens molecules ZO-1, ZO-2 and ZO-3. All three JAM molecules may also interact with either occludin or ZO-1, as well as the cell polarity protein PAR-3.

Adherens junctions are cell membrane contacts formed by cadherins, a large family of transmembrane adhesion molecules which act in a homophilic way to connect epithelial or endothelial cells (reviewed by Yagi and Takeichi, 2000). VE-cadherin (also known as cadherin-5) is found on blood vascular endothelial cells and possesses the same organisation typical of other cadherins, consisting of an extracellular domain comprising five repeat motifs (Luscinskas et al., 2002). The extracellular domain is responsible for homophilic interactions while the cytoplasmic tail provides a linkage to the actin cytoskeleton via α- and β-catenins, plakoglobin and p120 and contributes to stable adhesion (figure 1.15). The role of VE-cadherin as a gate keeper which must be pushed aside by transmigrating cells is also widely accepted (reviewed by Muller, 2003). Thus this molecule does not directly participate in the process of leukocyte transmigration but rather contributes to the maintenance of the vascular integrity (Imhof and Aurrand-Lions, 2004).

The other adhesion molecules found at adherens junctions, CD31 and CD99, play much more active roles in transmigration. CD31 (described in detail in section 1.3.5 of this chapter) is actively recruited to sites of monocyte transendothelial migration. Studies where CD31 interactions have been prevented using a blocking mAb have shown an approximately 90% reduction in transmigration, both *in vivo* and *in vitro*, identifying CD31 as a playing a key role in the process. The important role played by CD99 in transmigration was demonstrated by Schenkel et al. (2002). They showed that this heavily O-glycosylated 32 kDa type I transmembrane protein was not only expressed on leukocytes as was previously believed but was also found on endothelium, particularly at intercellular junctions. Furthermore it is able to form homophilic interactions with CD99 molecules on leukocytes and diapedesis of monocytes could be blocked by over 90% in the presence of a CD99 blocking antibody. However,

CD99 is believed to regulate a step in transmigration which is distinct from that controlled by CD31 (Imhof and Aurrand-Lions, 2004).

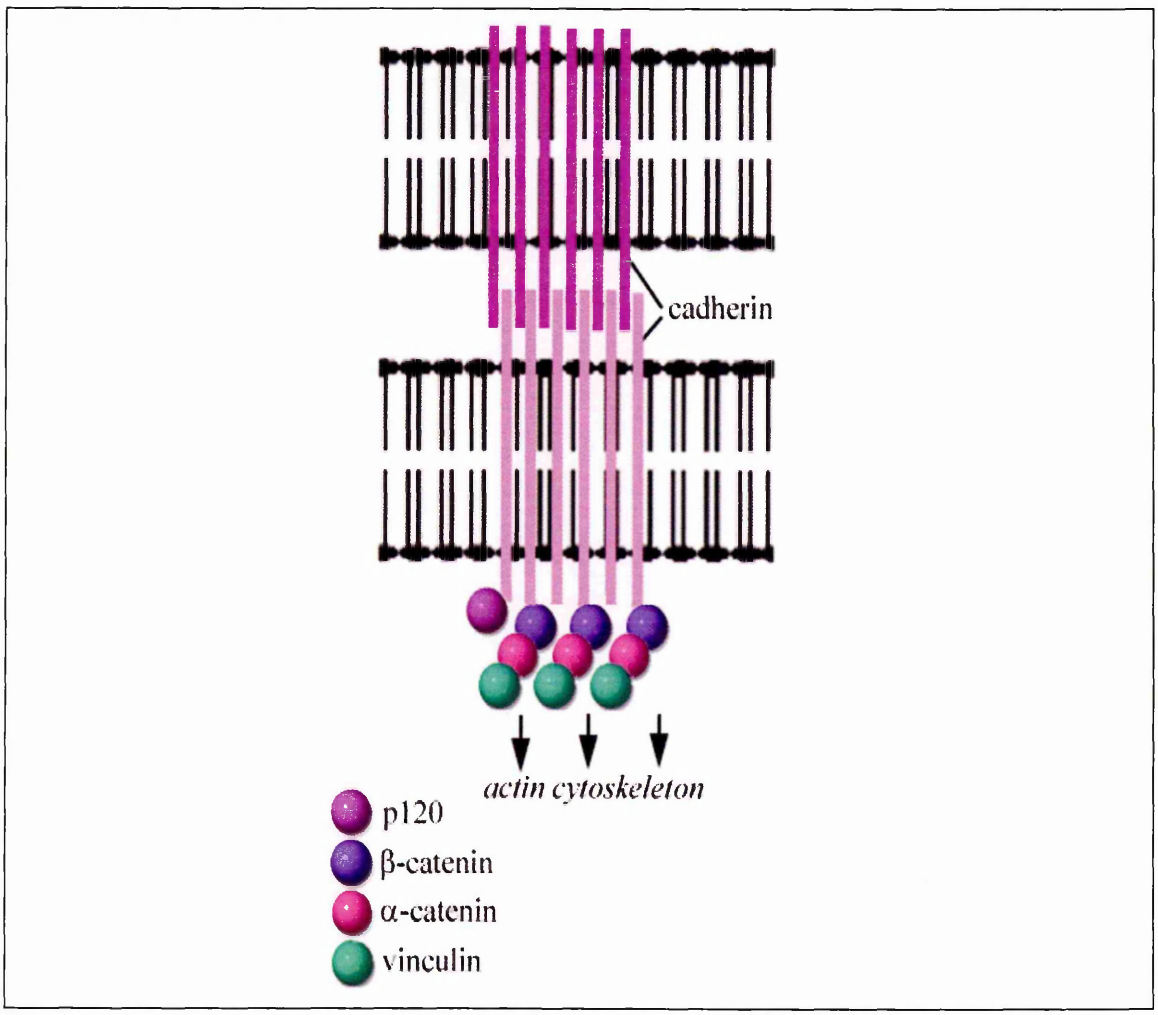

Figure 1.15 Schematic representation of the principal protein interactions at a cadherin-based adherens junction. Homophilic interactions occur between extracellular domains of cadherin on adjacent cells, whilst the intracellular domain of cadherin interacts with catenins and may be linked to the actin cytoskeleton through vinculin. Additional proteins such as p120 stabilise these interactions.

Gap junctions are clusters of hydrophilic transmembrane channels which permit the direct exchange of ions and small molecules (Beyer, 1993). Each channel is composed of six polypeptide subunits, connexins, arranged around a central pore (figure 1.16). Connexins 37, 40 and 43 are constitutively expressed by vascular endothelium and primarily at cell-cell contacts. The gap junctional coupling between leukocytes and the endothelium may have a role in modulating transendothelial migration, although this remains controversial (Imhof and Aurrand-Lions, 2004).

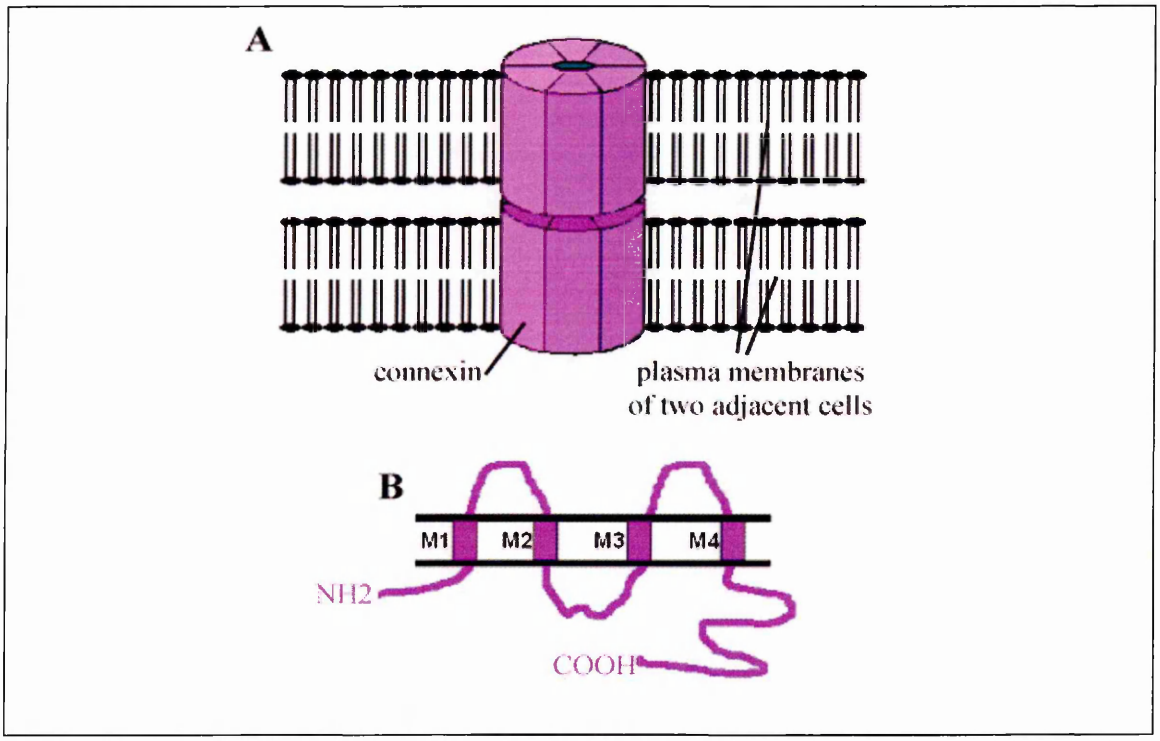

Figure 1.16 Schematic diagram of a gap junction between two adjacent cells. This transmembrane channel is composed of six connexin polypeptides arranged around a central pore (A). Each connexin has four transmembrane domains and intracellular N- and C-termini (B).

The change in morphology of the endothelium also permits some leakage of macromolecules such as fibronectin and fibrin, the insoluble cleavage product of fibrinogen (Abbas, 1997), which form a scaffolding to facilitate leukocyte migration and retention within the tissue.

1.5.3.2 Transcellular transmigration

In addition to the paracellular migration of leukocytes squeezing between adjacent endothelial cells, another pathway for transmigration is also believed to occur, termed transcellular migration. Ultrastructural studies carried out in the 1960s suggested that leukocytes could pass through the body of an endothelial cell (Marchesi and Gowans, 1964). This finding was supported by the work of Feng et al. (1998) who demonstrated that neutrophils stimulated with a chemotactic peptide could emigrate from inflamed venules primarily by a transcytotic pathway. In this study, serial electron microscopic sectioning showed clearly that the course taken by the transmigrating neutrophil did not involve endothelial cell-cell junctions. More recent work has sought to address the molecular interactions that permit and control this form of transmigration.

The preliminary stages of junctional-independent migration are suggested in a paper by Barreiro et al. (2002), who found that the endothelial adhesion molecule VCAM-1 localised to microvilli and microspikes at the apical surface of TNFα-activated human umbilical vascular endothelial cells (figure 1.17). The cytoplasmic tail of VCAM-1 was shown to bind the active N-terminal domain of the actin cytoskeleton linker proteins ezrin and moesin *in vitro*, which were also shown to colocalise within the microvilli-like projections. Additionally, they demonstrated that ICAM-1 colocalised with ezrin and clustered around lymphocytes throughout adhesion and transmigration, whereas VCAM-1 clusters were only observed during adhesion and had disappeared once transmigration had occurred. The authors observed VCAM-1-ezrin docking

structures which were raised above the endothelial surface to form a cup-like structure. The formation of this was found to be associated with the relocation of cytoskeletal components such as the actin bundling protein α-actinin, the focal adhesion protein vinculin and the actin-nucleating protein VASP. Phosphoinositides and the Rho/p160 ROCK pathway (which participate in the activation of ERM proteins) were identified as being involved in the generation and maintenance of the anchoring structure.

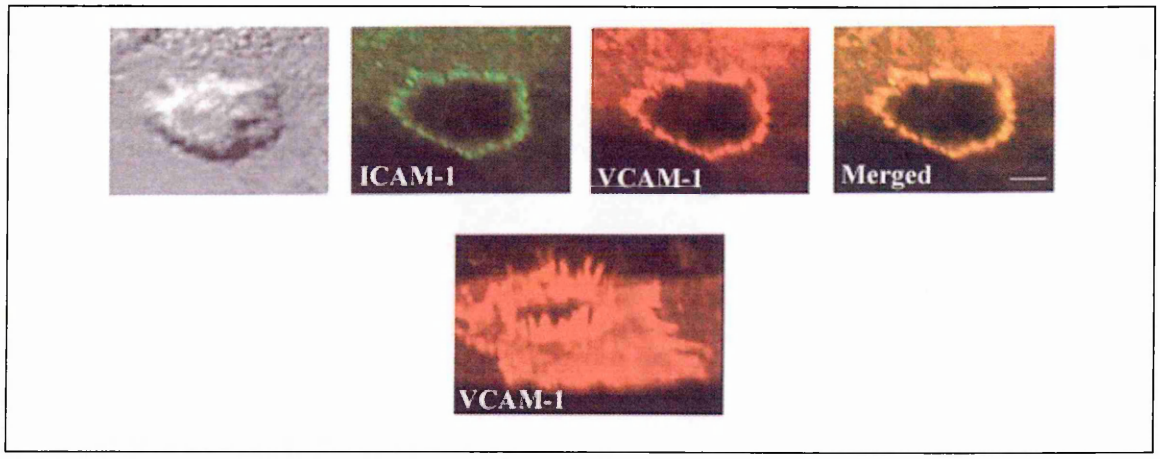

Figure 1.17 Formation of the endothelial docking structure for adhered lymphocytes. Differential interference contrast image of the lymphocyte is shown in the grey-scale panel, with the endothelial ICAM-1 (green) and VCAM-1 (red) forming around it. The VCAM-1-positive projections from the endothelial cell are shown in the lower panel. (Bar represents 3.5μm). Taken from Barreiro et al., 2002.

The role that these microvilli-like projections and cup-like structures could play in transcytosis was suggested by Carman et al. (2003). As in the paper by Barreiro et al. (2002), they also observed the cup-like structures and found that the projections which encircled the leukocyte were ICAM-1-enriched and extended up the sides of the leukocytes and clustered the leukocyte integrin LFA-1 into linear tracks (figure 1.18). Such projections were found to form independently of VCAM-1-VLA-4 interactions; however disruptions of the projections with various cytoskeletal inhibitors did not affect firm adhesion and the authors suggest that such structures are more important in transendothelial migration. They followed up this hypothesis with a subsequent study (Carman and Springer, 2004), in which they provide direct evidence for transcellular diapedesis. By monitoring transmigration of chemokines-activated monocytes, neutrophils and lymphocytes through human umbilical vein endothelial cells, they found that transcellular migration (occurring away from cell-cell junctions) accounts for 7 ± 1%, 5 ± 2% and 11 ± 4% respectively of total migration events, i.e. a minority. However, the authors also mentioned that this could be an underestimation as events occurring near cell-cell junctions were hard to judge and therefore denoted as paracellular. Thus the transmigratory cup appears to provide directional guidance to leukocytes to permit their extravasation and such transcytosis accounts for a least some transmigrational events. The extent to which these occur remains to be accurately determined as the speed of transcellular migration in comparison to paracellular migration is unknown. If one mechanism occurs much more rapidly than the other, its contribution to transmigration could be underestimated when observing what are effectively snap-shots of events following fixation. The mechanisms by which the endothelium "decides" which route for migration it wishes to offer a leukocyte remain to be elucidated. However it is currently accepted that the transcytotic pathway of extravasation is probably not the main route taken by leukocytes (reviewed by Imhof and Aurrand-Lions, 2004).

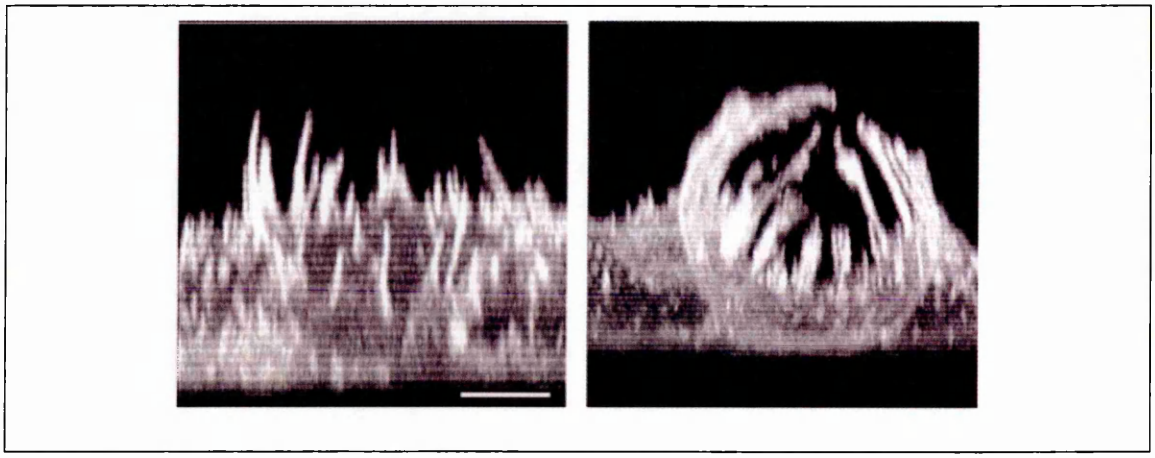

Figure 1.18 ICAM-1-enriched microvilli-like membrane projections formed by a CHO cell encircling a leukocyte (Scale bar, 5 μm.) Taken from Carman et al., 2003.

1.5.4 Recirculation of T cells to the lymph nodes

The homing of naïve T cells from the blood to the stroma of peripheral lymph nodes involves different adhesion molecules and occurs across high endothelial venules, HEVs (Anderson and Anderson, 1976; Anderson et al., 1976). HEVs are modified post-capillary venules which are lined with plump endothelial cells, thus giving the venules their name due to their appearance in transverse sections. Intravital microscopy revealed that the HEV endothelium has greater adhesiveness for circulating lymphocytes and a collision with the vessel wall will result in a loose attachment which may last several seconds. A similar collision occurring with normal vessel walls of the microcirculation would cause the lymphocyte to immediately rebound or adhere very briefly before being swept on by the force of the blood flow (Johnson-Leger et al., 2000). The low affinity attachment with the HEV permits a proportion of T cells to spread out into mobile forms and extravasate into the stroma of the lymph node, perchance to encounter their specific antigen.

Adherence of lymphocytes to HEVs is mediated by homing receptors termed addressins. These are responsible for directing the lymphocytes to their ligands on specific and anatomically distinct sites. L-selectin (CD62L) is considered the most important homing receptor on naïve T cells. This 90-100 kD, variably glycosylated carbohydrate-binding protein is abundant on naïve T cells but has low expression on memory cells. Its ligands include sulphated glycosaminoglycans on GlyCAM-1, a secreted proteoglycan on HEVs; CD34 on endothelial cells; and mucosal addressin cell adhesion molecule-1 (MadCAM-1) on endothelial cells in the gut. L-selectin mediates rapid low-affinity attachment tethering between the leukocyte and endothelium. The integrins mediating the firmer attachment of the lymphocytes and subsequent transmigration are less well characterised. However JAM-B, expressed on HEVs in human tonsil and a subset of human leukocytes is predicted to play a role in this. Johnson-Leger et al. (2002) have demonstrated that in the mouse, leukocytes migrate in much greater numbers across monolayers of endothelioma cells transfected with JAM-B. Moreover in a human model, the researchers found that either an anti-JAM-B antibody or soluble JAM-B were sufficient to block the transmigration of primary human peripheral blood leukocytes across HUVECs expressing endogenous JAM-B.

Monocytes do not adhere to HEVs in lymph nodes that drain non-inflamed tissues but adherence becomes possible after an inflammatory challenge (Imhof and Aurrand-Lions, 2004). Chemokines such as CCL3 and CXCL8 can be transported to the draining lymph nodes, where they are captured on HEVs, subcapsular sinuses and reticular fibres (Gretz et al., 2000). Inflammatory chemokines such as CXCL9 are also transported to lymph nodes from their site of production within inflamed tissue and contribute to the recruitment of monocytes.

Once the naïve T cell is within the lymph node and activated by binding of specific antigen, the cell up-regulates adhesion molecules such as LFA-1 (CD11aCD18), VLA-4 (α4β1 integrin), VLA-5 (α5β1 integrin), VLA-6 (α6β1 integrin) and CD44.

1.5.5 Leukocyte trafficking through afferent lymphatics

Generation of a primary immune response is dependent upon the delivery of antigen to lymphoid organs, either via the blood, lymph or mobile antigen-presenting cells (Zinkernagel, 1996). Dendritic cells (DC) are bone marrow-derived accessory cells present in the interstitium of most organs, including the dermis of the skin. They will phagocytose microorganisms, dead cells and cellular debris prior to migration across the lymphatic endothelium and through afferent lymphatic vessels to the T-cell rich paracortical area of a regional lymph node (figure 1.19). Although other cell types such as macrophages or activated parenchymal cells may drive the activation and proliferation of memory T cells, DCs alone are capable of stimulating the expansion of naïve T cells and thereby initiating primary immune responses (Randolph, 2001). They are abundant in T cell rich areas of lymph nodes and the spleen and found in immature form circulating in the blood as well as scattered throughout the epidermis of the skin, where they are termed Langerhans cells (LC). LC contain the Birbeck granule, a cytoplasmic organelle whose function remains to be determined but enables LC to be distinguished from dermal DC by electron microscopy (Abbas et al, 1997; Weinlich et al, 1997). LC also express the chemokine receptor CCR6, which through interactions with macrophage inflammatory protein 3α (MIP3α) may promote their migration to normal skin (von Andrian and Mackay, 2000). DC endocytose protein antigen, which then undergoes proteolytic processing in either the endosome or lysosome. The peptides are loaded on to an MHC class II molecule within an exocytic vesicle from the Golgi and transported to the cell surface for presentation as MHC class II-peptide complexes. DC display high

levels of expression of MHC class II molecules and thus may be distinguished from monocytes which exhibit lower levels of expression (Weinlich et al, 1997). DC also have distinct morphology, with long, thin cytoplamic processes and a lobulated and excentrically localised nucleus.

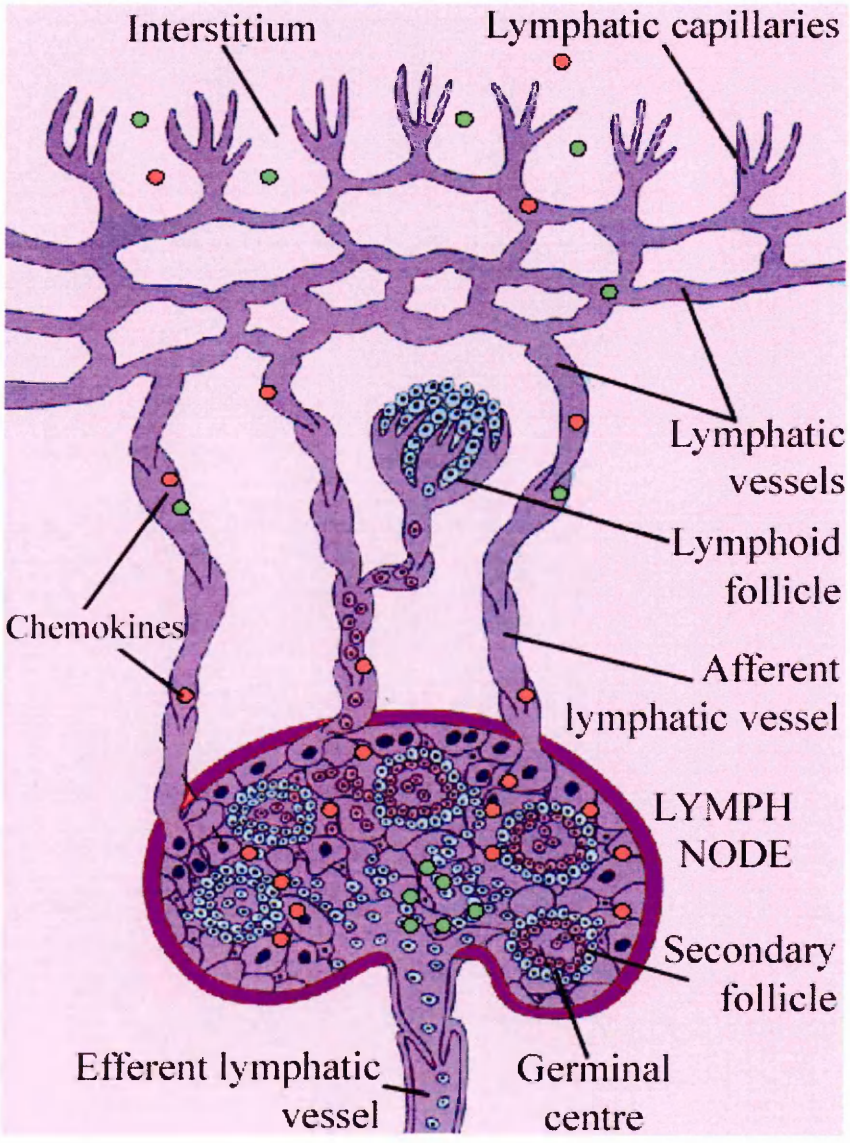

Figure 1.19 The lymphatics as a conduit for leukocytes. Cells such as DCs from the interstitium transmigrate across the lymphatic endothelium to gain access to the lymphatic capillaries and afferent lymphatic vessels before reaching the lymph node. They then home to the T-cell rich paracortical areas and thus an immune response to antigen may be elicited.

DC migrate and home to the T cell areas of lymphoid organs from afferent lymphatic vessels that drain peripheral tissues (Austyn, 1989). Upon reaching a lymph node, DCs down-modulate receptors for inflammatory chemokines and up-regulate receptors for lymphoid chemokines to aid migration to the T-cell area of the node (von Andrian and Mackay, 2000). Naïve T cells collect in the paracortical region of lymph nodes and the spleen, having migrated directly from the vasculature. The murine contact hypersensitivity (CHS) model has been used extensively to study the migration of DC from the skin in response to antigenic challenge. In this model, a skin sensitising agent is applied to an area of mouse skin and is captured by LC or dermal DC, which migrate to lymph nodes in an IL-1 and TNFα-dependent manner (Cumberbatch et al., 2002) and elicit an IL-1-dependent hapten-specific T cell activation (Nakae et al., 2002). Once the mouse has been sensitised and memory T cells are resident throughout the body, a challenge by cutaneous application of the same antigen, typically to the ear, results in local inflammation and oedema. Nakae et al. (2002) used IL-1α/β$^{-/-}$, TNFα$^{-/-}$and IFNγ$^{-/-}$ mice to dissect out the roles of these cytokines in the development of CHS. They found that whilst IL-1 plays a crucial role in antigen-specific T cell activation through CD40L and OX40 induction on T cells, TNFα is key in the elicitation phase. This confirmed the findings of early work by McHale et al. (1999) who demonstrated that neutralising antibodies against TNFα, IL-1α and IL-1β were no more effective at inhibiting the increase in ear thickness and accompanying up-regulation of adhesion molecules than antibodies against TNFα alone. TNFα is produced by keratinocytes and LC within the skin, as well as mast cells. However production by CD4+ T cells was not found to be directly involved (Nakae et al., 2002). TNFα stimulates the up-regulation of ICAM-1, MCP-1, MIP-1α and MIP-1β, leading to the ear swelling which characterises the elicitation phase.

Exogenous administration of proinflammatory factors IL-1β, TNFα or lipopolysaccharide (LPS) promotes the loss of DCs from the periphery within 12h (reviewed by Randolph, 2001) and such migration is known to involve a cohort of chemokines and adhesion molecules. Epidermal LCs have been used in the majority of studies to elucidate the factors involved in DC migration. For such cells to be initially mobilised, their migratory capacity must be triggered by one or more factors, all converging to produce NFκB activation. In addition to the proinflammatory cytokines IL-1β and TNFα, microbial factors and exogenous DNA activate Toll-like receptors, TLRs (O'Neill, 2004). Stimulation with necrotic cells following tissue injury and with CD40L, typically expressed on activated T cells can also trigger maturation. Such stimulated LCs then downregulate E-cadherin, thus permitting their detachment from neighbouring keratinocytes, coupled with up-regulation of adhesion molecules such as α6β1 and CD44, induction of matrix metalloproteinase-9 and *de novo* expression of the chemokines receptor CCR7, which is believed to be essential in permitting DC entry into lymphatic vessels (reviewed by Randolph, 2001) as a lack of migration was observed in mice deficient for CCR7 (Förster et al., 1999) and mice deficient in both ELC (CCL19) and SLC (CCL21), the chemotactic ligands for CCR7 (Gunn et al., 1999; Luther et al., 2000). However CCR7 is also necessary for naïve T cells to enter the lymph node and such mice therefore do not have normal lymph nodes. Thus initially it was considered possible that defective DC migration is secondary to these genetic abnormalities. However further evidence to show that CCR7 was indeed a key regulator was provided by Ohi et al. (2004), who demonstrated that the absence of this chemokine receptor in mice prevented DC migration into dermal lymphatics under both inflammatory conditions and during constitutive trafficking. Martín-Fontecha et al. (2003) analysed factors affecting migration of dendritic cells to the draining lymph nodes in mice and demonstrated that subcutaneous injection of inflammatory cytokines increased DC migration. They claimed that this was due to an increase in SLC expression,

as detected by in situ hybridisation and antibodies. The role of ELC in mediating cysteinyl leukotriene (cysLT)-induced chemotaxis of DCs has been demonstrated more convincingly (Robbiani et al., 2000). cys-LTs are mediators of immediate hypersensitivity reactions and induce DC migration through the lipid transporter multi-drug resistance protein 1 (MDR-1). The researchers were able to show such migration occurs specifically to ELC and that accumulation of DCs in the lymph nodes was blocked using anti-ELC antibodies. However although the paper identifies a role for ELC in DC migration from the epidermis *in vivo*, expression of ELC by lymphatic endothelial cells in the periphery remains to be addressed.

Other possible candidates for DC migration are L-selectin and mannose receptor. Irjala et al. (2001) demonstrated binding of L-selectin on leukocytes to mannose receptor on sinusoidal endothelial cells and suggested that as mannose receptor is also expressed on afferent lymphatic vessels, this interaction may additionally play a role in leukocyte exit from non-lymphoid tissues. Further studies to investigate such binding using dermal lymphatic endothelial cells could assess this putative role in leukocyte trafficking into the lymphatics.

The involvement of the chemotactic protein osteopontin (OPN) in DC migration and its interaction with CD44 and αvβ3 integrin is described in Weiss et al, 2001. OPN was found to be up-regulated in skin and lymph nodes in the sensitization phase of CHS and it induced chemotactic DC migration in microchamber assays. The researchers also generated DC from bone marrow culture and detected expression of two OPN receptors, CD44 and αvβ3 integrin by flow cytometry. mAbs against these two adhesion molecules known to block OPN binding were used to show that DC migration was dependent upon CD44 and αvβ3 integrin interactions with OPN.

Weiss et al (2001) did not demonstrate whether OPN was secreted by microvascular blood endothelial cells or lymphatic endothelium. However, strongly class II positive cells in cords within dermal sheets have been observed by many investigators and Weinlich et al show that these vessels are ICAM-1 negative. The ICAM-1 positive structures had "the typical morphology of blood vessels [and] did not contain DC". In the same publication an immunohistochemical analysis of molecules on DC was carried out on migrating cells in organ culture. The authors found that expression of the CTLA-4 receptor, CD86 was induced, as was increased surface expression of MHC class II.

Lymphatic vessels are also responsible for trafficking other leukocytes in addition to DCs. Mancardi et al (2003) demonstrated that mouse lymphatic endothelial cells derived from experimentally induced lymphangiomas could induce cell migration of neutrophils, lymphocytes and monocyte/macrophages. Moreover they detected message of CXC, CC and C chemokines KC, IP10, Mig-1, BCL, MIP-2, SLC, RANTES, MCP-1, C10 and Lptn. Expression of the CC chemokine receptor D6 by lymphatic endothelium was detected by Nibbs et al. (2001), which could influence chemokine-driven trafficking of leukocytes through the lymphatics.

In recent years extensive work has been undertaken by Gwendalyn Randolph and co-workers into monocyte-derived dendritic cells. They found that the culture of blood mononuclear cells in the presence of HUVEC grown on extracellular matrix resulted in the differentiation of these cells into DCs within 2 days, particularly after phagocytosing particles in subendothelial collagen (Randolph et al., 1998). These DCs then migrated across the endothelium in an ablumenal-to-lumenal direction, as would occur across lymphatic endothelium, termed reverse transmigration. Monocytes which differentiated into macrophages remained in the sub-endothelial matrix. The authors conclude that

this would suggest that the endothelium itself is responsible for initiating monocyte differentiation but full differentiation is dependent upon additional stimulus, such as the uptake of potential antigen. A later study revealed that such monocyte-derived DCs use CCR8 in addition to CCR7 to migrate from the tissues to the lymphatic vessels (Qu et al., 2004).

Much less is known about the constitutive migration of leukocytes to lymph nodes in the absence of inflammatory stimuli. Huang et al. (2000) demonstrated that DCs are capable of transporting apoptotic cells to lymph nodes in the absence of external stimuli and Scheinecker et al (2002) provided evidence that constitutive presentation of self antigen at the draining lymph node was mediated by DCs under non-inflammatory conditions. Also as described above, Vermaelen et al. (2001) have demonstrated that pulmonary derived DCs constitutively migrate to the lymph nodes. The adhesive mechanisms and chemokines involved in these processes, from both uninflamed and inflamed tissue are in the early stages of being understood, although a role for JAM-A has recently been characterised. Cera et al. (2004) detected JAM-A on the surface of DCs and found that DCs from *Jam-A*$^{-/-}$ mice exhibited an increase in random migration and transmigration across lymphatic endothelial cells. Such mice also showed increased localisation to lymph nodes of skin DCs and an enhanced reaction to contact hypersensitivity. The study supported earlier work which found that JAM-A on endothelial cells enhances transmigration, as they reported a decrease in lymph node homing in endothelium-restricted *Jam-A* deficiency. Thus it would appear that endothelial JAM-A has a positive role in promoting cell extravasation whilst DC JAM-A plays a role in limiting cell motility. Although the migration of DC through the lymphatics to the lymph nodes is becoming better understood, the mechanism whereby DC enter the lymphatics remains to be elucidated.

1.6 Aims of this thesis

Since the identification of LYVE-1 in 1999 by Banerji et al. as a novel member of the Link protein superfamily, the majority of investigators from other laboratories have sought to use it as a highly specific marker for lymphatic endothelium. However, the functions and mechanisms by which expression of this protein is regulated have remained unknown and this PhD has sought to characterise them.

- Monoclonal antibodies against mouse LYVE-1 were generated and characterised, as described in chapter 3, to permit investigations into mouse tissue and complement studies carried out using the human monoclonal antibodies already raised by Dr. Remko Prevo.
- Factors regulating LYVE-1 expression were investigated extensively, described in chapter 4, to define limitations that this lymphatic marker may have as well as to shed light on the roles it may play under physiological and pathological conditions.
- The potent effects of proinflammatory cytokines on LYVE-1 expression identified in chapter 4 were further pursued in chapter 5, to examine other molecular changes in inflamed lymphatic endothelium. The expression of adhesion molecules on lymphatic endothelium was of particular interest, because in contrast to the well-characterised protein expression profile of inflamed blood vascular endothelium, no similar studies had been undertaken for lymphatic endothelium.
- Studies into the alteration in expression profile were also pursued in chapter 6 through the use of *in vivo* models of inflammation and the physiological relevance with respect to the trafficking of antigen presenting cells was explored.

CHAPTER 2

Methods & Materials

2.1 General Reagents.....90
2.2 Antibodies.....95
2.3 Bacterial Culture.....98
2.4 Molecular Biology Methods.....101
2.5 Tissue Culture.....117
2.6 Protein Biochemical Methods.....125
2.7 Generation of Polyclonal Antisera.....128
2.8 Generation of mAbs Against Mouse LYVE–1.....129
2.9 Immunohistochemistry & Immunofluorescence Ab Staining133
2.10 Animal Procedures.....138

2.1 General Reagents

2.1.1 Chemicals

BAY 11-7082 was purchased from Chemicon (Harrow, UK) and a stock solution of 20 mM made up in DMSO, storing in aliquots at –20°C.
EDTA: 0.5 M stock was made with ethylenediaminetetraacetate dihydrate (di-sodium salt) in water and adjusted to pH 8.0 with NaOH.
Ilomastat (GM6001), matrix metalloproteinase inhibitor was purchased from Chemicon.
OPD (*O*-Phenylenediamine) substrate and buffer tablets were from SIGMA (Poole, UK).
PBS: 1 tablet of PBS (Phosphate buffered saline, Dulbecco A; from Oxoid Ltd, England) was dissolved per 100 ml H20.
PMA (phorbol 12-myristate 13-acetate) was purchased from Calbiochem (Merke Biosciences Ltd, Nottingham, UK). A 200 µg/ml stock was prepared in DMSO and stored at –20°C.
Saponin (from Quillaja bark) was from SIGMA.
SSC: A 20 x stock solution contained 3 M NaCl, 0.3 M Sodium citrate (pH 7.0).
Tris-HCl buffer: 2 M stock was made from Tris base (Tris-hydroxymethylamino methane) in water and adjusted to pH 8.0 with HCl.

All other chemicals were purchased from either SIGMA (Poole, UK) or BDH (Leicester, UK), unless otherwise stated.

2.1.2 Molecular biology reagents

2.1.2.1 General reagents

Actinomycin D (SIGMA) dissolved in methanol at 5mg/ml and stored at –20°C in the dark.
Agarose was purchased from Invitrogen (Paisley, UK).
Bio 101 GeneClean II kit was from Q-BIOgene-ALEXIS (Nottingham, UK).
Gene Pulser Cuvettes, 0.2cm were purchased from BioRad (Hercules, USA).

Hybond-N+ and Hybond-C+ transfer membranes were purchased from Amersham Pharmacia Biotech (Amersham, UK).
Mixed Bed Resin, Analytical grade was from BioRad.
Pyrococcus furiosus (Pfu) polymerase was from Stratagene (Amsterdam Zudoost, The Netherlands) and was used with the buffer provided.
QIAEX II gel extraction kit was purchased from Qiagen (Crawley, UK).
RNeasy Mini Kit was purchased from Qiagen.
SequaGel sequencing system was purchased from National Diagnostics (Hessle, UK).
TE buffer was prepared, consisting of 10 mM Tris pH 8.0, 1 mM EDTA, both purchased from SIGMA.

2.1.2.2 Nucleic acids

1kb and 100bp DNA Ladders were purchased from New England Biolabs (Hertfordshire, UK) and diluted in glycerol-bromophenol blue loading buffer to 50ng/ml.
ØX174-*Hae*III digest was purchased from New England Biolabs.
Biotin-11-CTP was purchased from Perkin Elmer (Wellesley, USA).
Biotin-16-UTP was purchased from Roche (Lewes, UK).
dNTPs were purchased from Bioline (London, UK) as 100 mM stocks. A 50x (12.5 mM for each dNTP) stock was made in sterile water and stored at –20°C.
RNA Ladder was purchased from New England Biolabs.
tRNA (from brewer's yeast was purchased from Roche.

2.1.2.3 Enzymes

AMV Reverse Transcriptase, 21U/µl was purchase from Cambio (Cambridge, UK)
DNA Polymerase I, Large (Klenow) Fragment was purchased from New England Biolabs.
Pyrococcus furiosus (Pfu) polymerase was from Stratagene and was used with the buffer provided.
Restriction enzymes were purchased from New England Biolabs or Roche and used with the recommended buffers according to manufacturers' instructions.
RNAsin was purchased from Promega (Southampton, UK).

T4 ligase and buffer was from New England Biolabs.
T4 Polynucleotide Kinase was from New England Biolabs.
TaqPlus® Precision PCR System was purchased from Stratagene.
Thermus aquaticus (Taq) polymerase (BioTaq) was purchased from Bioline (London, UK) and used with the buffers provided.

2.1.2.4 Radiolabelled reagents

[α^{32}P]dCTP (~3000 Ci/mmole) and [γ^{32}P]ATP (7000 Ci/mmole) were both purchased from Amersham Pharmacia Biotech.

2.1.3 Cell culture reagents

2.1.3 1 Media

The following reagents were purchased from Gibco (Paisley, UK):-
DMEM (Dulbecco modified Eagle medium),
FCS (Foetal Calf Serum), which was heat inactivated prior to use (20 min 55°C),
G418 (Geneticin), from which a 125 mg/ml stock solution was prepared in RPMI (Roswell Park Memorial Institute) medium (also from Gibco), adjusted to neutral pH with NaOH, filter sterilised and stored at 4°C, and
Trypsin EDTA.

The following reagents were purchased from SIGMA:-
Gentamycin sulphate, from which a 50 mg/ml stock solution was prepared in RPMI and used at a working concentration of 50 µg/ml,
Gelatin 2% (w/v) solution, type B, used at a working concentration of 0.1% (w/v) in PBS,
L-Glutamine, of which a stock solution of 200 mM was prepared, stored at -20°C and used at a working concentration of 2 mM.
Penicillin and Streptomycin, from which stock solutions of penicillin at 100 U/ml) and streptomycin at 5 mg/ml were prepared, stored at -20°C and used at working concentrations of 1 U/ml and 50 µg/ml respectively.

Accutase was purchased from PAA Laboratories (Yeovil, UK) and stored in aliquots at -20°C.
Cytokines and growth factors were purchased from R&D Systems (Oxford) and reconstituted according to the manufacturers recommendations prior to storage at –20°C.
EGM–2 MV BulletKit media was purchased from Cambrex Bioscience (Walkersville, USA), consisting of EBM–2 (Endothelial basal medium) and supplemented with the supplied SingleQuots (Hydrocortisone, EGF, FBS, VEGF, FGF-B, R3-IGF, ascorbic acid and gentamycin/amphotericin-B) prior to use.
Type I collagen (rat tail) was purchased from BD (San Diego, USA)
UltraCHO medium was purchased from BioWhittaker

2.1.3.2 Transfection reagents

HEPES (used for calcium phosphate transfections) was from SIGMA.
HUVEC Nucleofector™ kit (solutions, cuvette and electroporator were from Amaxa Biosystems.
LIPOFECTIN® reagent and serum-free OptiMEM were both purchased from Life Technologies (Roskilde, Denmark).

2.1.3.3 Reagents for magnetic cell sorting of cells (MACS)

Cell strainers, 70µm mesh were purchased from BD Falcon, (Bedford, USA).
MACS columns, (sizes LS and MS), metal stand, pre-separation filters (30µm mesh) and goat anti-rat MACS beads were purchased from Miltenyi Biotec GmbH (Bisley, UK).

2.1.3.4 Tissue culture ware

Tissue culture flasks and multiwell dishes were from Nunc (Roskilde, Denmark).
Tissue culture dishes (14 cm) and 8-chamber slides were from BD Falcon (Bedford, USA).

2.1.4 Reagents for the generation of monoclonal antibodies

FBS (Foetal Bovine Serum), Australian origin, was purchased from GIBCO and batch-tested prior to ordering, to ensure that an individual batch was suitable for supporting hybridoma growth.

HAT (Hypoxanthine, 10mM, Aminopterin, 0.4µM, Thymidine, 16.5µM, L Glycine, 3µM, Sodium pyruvate, 1mM) 100x concentration solution was prepared in water and filter-sterilised, storing in aliquots at 4°C.

GKN isotonic buffer was prepared from sodium chloride, 137 mM; potassium chloride, 5.37 mM; Na2HPO4, 10 mM; NaH2PO4.H2O, 5 mM and glucose, 11 mM, dissolved in water and filter sterilised.

HT, (Hypoxanthine, 10mM, 0.4µM, Thymidine, 16.5µM, L Glycine, 3µM, Sodium pyruvate, 1mM) 100x concentration solution prepared in water and filter-sterilised, storing in aliquots at 4°C.

Polyethylene Glycol (PEG) 1500 was from Roche.

2.2 Antibodies

Antibodies directed against murine and human cell surface receptors, intracellular proteins and chemokines are listed in tables 2.1 and 2.2 below, along with their specificity, host, isotype and source.

2.2.1 Primary anti-mouse antibodies

Specificity	Antibody	Host	Clone	Source
CD31	MEC13-3	Rat	IgG	BD Pharmingen
CD44	IM7	Rat	IgG	BD Pharmingen
ICAM-1	-	Goat	Polyclonal	R&D Systems
ICAM-1	cbl 1331	Rat	IgG	Cymbus Biotechnology
JE/MCP-1	-	Goat	Polyclonal	R and D Systems
LYVE-1	B1/10	Rat	IgG1	*See chapter 3*
LYVE-1	C1/8	Rat	IgG2a	*See chapter 3*
LYVE-1	-	Rabbit	Polyclonal	Prevo et al., 2001
Macrophage mannose receptor	F4/80	Rat	IgG2b	Prof. S. Gordon
MIP-3α	-	Goat	Polyclonal	R and D Systems
Podoplanin	8.1.1	Hamster	IgG	DSHB, Iowa
Podoplanin	*Viennese Nanni*	Rabbit	Polyclonal	Prof. D. Kerjaschki
Prox-1*	-	Rabbit	Polyclonal	RDI
RANTES	-	Goat	Polyclonal	R and D Systems
SLC	-	Goat	Polyclonal	R and D Systems
VCAM-1	429 (MVCAM.A)	Rat	IgG2a	BDPharmingen
VE-Cadherin	11D4.1	Rat	IgG	BDPharmingen

Table 2.1 Primary anti-mouse antibodies.

2.2.2 Primary anti-human antibodies

Specificity	Antibody	Host	Clone	Source
a3 Integrin	1A3	Mouse	IgG1	CR-UK
α4 Integrin	7.2	Mouse	IgG1	CR-UK
α6 Integrin	MP4F10	Mouse	IgG2b	CR-UK
α9β1 Integrin	Y9A2	Mouse	IgG1	Serotec
αvβ3 Integrin	23C6	Mouse	IgG1	CR-UK
αMβ1 Integrin	24	Mouse	IgG1	CR-UK
αMβ1 Integrin	TS2/4.1.1	Mouse	IgG1	CR-UK
β1 Integrin	P5D2	Mouse	IgG1	CR-UK
β1 Integrin	TS2/16	Mouse	IgG2a	CR-UK
Cytochrome C	-	Mouse		Dr. R. Thorne
CD31	JC70A	Mouse	IgG1	DakoCytomation
CD34	581	Mouse	IgG1	BD Pharmingen
CD44	E1/2.8	Mouse	IgG1	CR-UK
CD44	25.32	Mouse	IgG1	CR-UK
CD63	H5B6	Mouse	IgG1	Developmental studies hybridoma bank
E-Selectin	BIIG-E4	Mouse	IgG1	R&D Systems
E-Selectin	62E	Mouse	IgG1	CR-UK
EEA1	14	Mouse	IgG1	BD Pharmingen
ICAM-1	15.2	Mouse	IgG1	Serotec
ICAM-1	PIW16	Mouse	IgG1	CR-UK
ICAM-2	B-T1	Mouse	IgG1	Serotec
ICAM-3	ICAM3.1	Mouse	IgG1	CR-UK
ICAM-3	ICAM3.2	Mouse	IgG1	CR-UK
JAM-1	3b8	Mouse	IgG1	Prof. C. Buckley
LYVE-1	8C	Mouse	IgG1	Dr. R. Prevo
LYVE-1	6A	Mouse	IgG1	Dr. R. Prevo
LYVE-1	3A	Mouse	IgG1	Dr. R. Prevo
LYVE-1	-	Rabbit	Polyclonal	Banerji et al. 1999
PDI	-	Mouse	IgG1	Dr. R. Thorne
Podoplanin	*Viennese Susi*	Rabbit	Polyclonal	Prof. D. Kerjaschki
Podoplanin	D2-40	Mouse	IgG1	Signet
Prox-1*	-	Rabbit	Polyclonal	RDI
Sialoadherin	HSn 7D2	Mouse	IgG1	CR-UK
TIE-2	4g8	Mouse	IgG1	CR-UK
VCAM-1	MCA 907	Mouse	IgG	CR-UK
VCAM-1	51-10C9	Mouse	IgG1	BD Pharmingen
VE-CAD	CAD-5	Mouse	IgG	Prof. C. Buckley

Table 2.2 Primary anti-human antibodies. (*The rabbit anti-Prox1 antisera was raised against human but cross-reacts with mouse)

2.2.3 Secondary antibodies and conjugates

Specificity	Conjugate	Host	Source	Notes[1]
Goat IgG	Alexa568	Donkey	Molecular Probes	red fluorescent (578/603)
Hamster IgG	Alexa568	Goat	Molecular Probes	red fluorescent (578/603)
Human IgG	HRP	Goat	Pierce	used for ELISA
Mouse IgG	Alexa488	Goat	Molecular Probes	green fluorescent (495/519)
Mouse IgG	Alexa568	Goat	Molecular Probes	red fluorescent (578/603)
Mouse IgG	Alexa594	Goat	Molecular Probes	red fluorescent (590/617)
Mouse IgG	HRP	Goat	Pierce	used for ELISA
Mouse IgG	HRP	Goat	DAKO (K4006)	part of Envision system for IHC
Rabbit IgG	Alexa488	Goat	Molecular Probes	green fluorescent (495/519)
Rabbit IgG	Alexa568	Goat	Molecular Probes	red fluorescent (578/603)
Rabbit IgG	Alexa594	Goat	Molecular Probes	red fluorescent (590/617)
Rabbit IgG	HRP	Goat	Pierce	used for ELISA and Westerns
Rabbit IgG	HRP	Goat	DAKO (K4010)	part of Envision system for IHC
Rat IgG	Alexa488	Goat	Molecular Probes	green fluorescent (495/519)
Rat IgG	Alexa568	Goat	Molecular Probes	red fluorescent (578/603)
Rat IgG	Alexa488	Donkey	Molecular Probes	green fluorescent (495/519)

Table 2.3 Secondary antibodies and conjugates.

1) The numbers in brackets refer to wavelengths for fluorescent absorption and fluorescence emission maxima (nm) for fluorescent conjugates (adapted from Molecular Probes Inc).

2.3 Bacterial Culture

2.3.1 Bacterial media

Agar plates were made by adding Bacto-agar (BD) to freshly dissolved LB medium (see below) to a final concentration of 1.6% (w/v) and autoclaving. Appropriate antibiotics were added after the solution had cooled down to approximately 50°C and the solution poured into 9 cm petri dishes. Plates were dried at room temperature and stored at 4°C for up to 1 month.

Ampicillin (D[-]-α-aminobenzylpenicillin) was purchased from SIGMA. A stock of 100 mg/ml was made in water and stored in aliquots at –20°C. A concentration of 100 µg/ml was used for agar plates and liquid medium. When ampicillin was used together with tetracycline, a concentration of 25 µg/ml was used.

LB (Luria broth) medium was made by dissolving 10 g Tryptone (BD), 5 g Yeast extract (BD) and 5 g NaCl in 1 litre water and autoclaving.

SOB medium was made by dissolving 2 g Tryptone, 0.5 g yeast extract, 200 µl 5 M NaCl in 100 ml of water and autoclaving. 1/100 volumes of sterile 1 M MgCl2 and 1/100 volume of sterile 1 M KCl were then added.

SOC medium was made by adding 1/50 volume of 1 M filter-sterilised glucose to autoclaved SOB medium.

Terrific broth (Modified) was purchased as a dried media from SIGMA and prepared according to the manufacturer's instructions.

Tetracycline (Hydrochloride) was purchased from SIGMA and a 7.5 mg/ml stock was made in 50% (v/v) aqueous ethanol. Tetracycline was used at 7.5 µg/ml together with 25 µg/ml ampicillin in agar plates and liquid culture.

2.3.2 Bacterial strains

The following E.coli strains were used:

DH5α, used for transformation with pRcCMV vector and luciferase vectors (see section 2.4.1), which confer resistance to ampicillin.
MC1061/p3, used for transformation with pCDM7Ig vector, which confers resistance to ampicillin and tetracycline.

2.3.3 Preparation of glycerol stocks

A single colony was picked from an agar plate and used to inoculate a liquid culture of LB supplemented with the appropriate antibiotics and grown overnight with shaking at 37°C. The following day 700 µl of the culture was supplemented with 300 µl glycerol and stored at –80°C.

2.3.4 Preparation of calcium competent DH5α or MC1061/p3

Bacteria were streaked out on an agar plate and grown overnight at 37°C. A single colony was then used to inoculate 5ml LB and grown overnight at 37°C with agitation. This was subsequently used to inoculate 500ml LB, which was grown at 37°C with agitation until in mid-log phase (OD600nm between 0.4 and 0.6). The flask was chilled on ice for 15-30 min and then centrifuged at 5000 RPM at 4°C in a Heraeus Megafuge 2.0R in autoclaved tubes. Cells were resuspended in 100ml chilled washing buffer (30 mM Potassium acetate, 50 mM $MnCl_2$, 100 mM KCl, 10mM $CaCl_2$, 15 % Glycerol) and incubated on ice for 15 min. Cells were centrifuged again at 3000 RPM at 4°C and then resuspended in 20ml chilled storage buffer (10 mM MOPS pH 7.0, 75 mM $CaCl_2$, 10 mM KCl, 15 % glycerol) prior to dividing into 200 µl aliquots and snap freezing in a dry-ice ethanol bath. Vials were stored at –80°C.

2.3.5 Transformation of calcium competent E.coli

50 µl of calcium competent *E. coli* were used for each transformation. Plasmid DNA was added on ice (typically 1 µg of DNA of intact plasmid or 5 µl of ligation mix) and incubated on ice for 30 min. Bacteria were heat-shocked at 42°C for 90 sec and then allowed to recover for 1 min on ice. Preheated SOB

(4 x vol) was added and cells were incubated for 1h at 37°C with agitation. 50 µl to 200 µl of culture was spread on agar plates supplemented with the appropriate antibiotics. MC1060/p3 transformed with the pCDM7Ig plasmid were grown on agar plates supplemented with 25 µg/ml ampicillin and 7.5 µg/ml tetracycline. DH5α transformed with either pRcCMV or a luciferase plasmid were grown on agar plates supplemented with 100 µg/ml ampicillin.

2.3.6 Preparation of electrocompetent E. coli

An agar plate was streaked with the desired bacterial strain and grown overnight at 37°C. A single colony was picked and used to inoculate 10 ml LB, growing overnight at 37°C with agitation. This pre-culture was subsequently used to inoculate 1 litre of LB and grown at 37°C with agitation until OD^{600nm} was between 0.5 and 0.8. The flask was chilled on ice for 15-30 min and cells then centrifuged for 15 min at 4200 RPM in a JS 4.2 rotor at 4°C. The pelleted cells were resuspended in 500 ml of ice-cold water and centrifuged again. Cells were resuspended in 20 ml.

2.3.7 Electroporation of E.coli

40 µl electrocompetent *E.coli* were used for each transformation. Plasmid DNA (typically 0.5 µg of intact plasmid or 1 µl of ligation mix) was added to the cells on ice and left for 1 min. The mixture of cells and DNA was transferred to a 0.2 cm chilled cuvette and placed in the pulse chamber of a Bio-Rad electroporation apparatus. One pulse was given at the following settings: 25 µF, 200 Ω, 2.5 kV. 1 ml of SOC medium was then added to the cuvette and the suspension was transferred to a 15 ml round-bottomed Falcon tube. The cells were incubated in the 37°C shaker for one hour. Approximately half of the culture (concentrated to 100 µl by centrifugation) was spread out on agar plates with appropriate antibiotics and grown overnight at 37°C.

2.4 Molecular Biology Methods

2.4.1 RNA

All reagents used were maintained in RNase-free conditions

2.4.1.1 Extraction of total cellular RNA from tissues

(The method used was adapted from Chomczynski and Sacchi, 1987, *Anal. Biochem.* 162, 156-159)

Buffers and solutions

DEPC-treated water

DEPC, 0.1% (v/v) in distilled deionized water was incubated at 37°C overnight to drive off the DEPC and then autoclaved.

Denaturing solution

Guanidine thiocyanate, 4 M
Sodium citrate, 25 mM
Mercaptoethanol, 0.1 M, added just before use.

Procedure

Tissue was homogenised in denaturing solution, 1 ml per 100mg of tissue, using either a small (2 ml) Dounce homogeniser or a EUROTURRAX® T 25 motorised dispersion device, depending on the scale of the RNA preparation. Sodium acetate, pH 4.0, 2M, 0.1 ml per 1 ml solubilised tissue was added, then acid-equilibrated phenol chloroform (5:1), 1.2ml per 1 ml, shaking vigorously and then chilling on ice for 15 minutes. Samples were centrifuged at 10000g for 20 min at 4°C. The upper aqueous layer containing the RNA was transferred to new tubes and an equal volume of isopropanol added. Samples were placed at –20°C for 1 h and the precipitates collected by centrifuging as before. The pellets were redissolved in 0.3 ml denaturing solution and precipitated as before by addition of an equal volume of isopropanol at –20°C for 1 h. RNA pellets were recovered by centrifugation, washing in 75% (v/v) ethanol before vacuum-drying the RNA in a Speed Vac

(Savant) and dissolving in DEPC-treated water by heating to 70°C. RNA was stored at –80°C

2.4.1.2 Extraction of total cellular RNA from cells

Adherent cells were lifted using trypsin-EDTA and washed with PBS. All supernatant was aspirated off and the cell pellet resuspended in RLT lysis buffer from the RNeasy kit (Qiagen), 600 µl/<5 x 10^6 cells according to the manufacturer's instructions. Briefly, cells were lysed by vortexing and an equal volume of 70 % ethanol was added. The sample was then applied to an RNeasy column which was subsequently washed with buffers RW1 and RPE respectively before eluting the RNA in nuclease-free water.

2.4.1.3 Electrophoresis of RNA through agarose-formalehyde gels

Buffers and solutions

Running Buffer, made up as a 10x concentrate stock and diluted to 1x in DEPC-treated water.
0.2 M MOPS
0.05 M Sodium Acetate
5 mM EDTA, pH 8.0

Sample buffer

30% formamide, deionized on mixed bed resin in order that pH > 4
0.67 x concentrate MOPS
4% formaldehyde, deionized on mixed bed resin in order that pH < 7
33.3% glycerol
0.3 mg/ml bromophenol blue
in DEPC-treated water, stored in aliquots at –20°C

Procedure

A 1% (w/v) agarose gel was made by dissolving agarose in 1x running buffer, heating to allow the agarose to dissolve and then cooling to 50°C before adding deionized formaldehyde to a final concentration of 2% (v/v) and pouring into the gel tray. The gel was pre-run at 5V/cm for approximately 5 min before the samples were loaded, with a magnetic stirrer within the tank to permit running buffer to circulate. Typically 10-15 µg of sample was

vacuum dried and resuspended in 20 µl sample buffer supplemented with ethidium bromide at a final concentration of 10 µg/ml. Samples were boiled for 2 min then cooled on ice prior to loading. An RNA ladder (New England Biolabs) was included in a parallel lane to serve as a size standard and prepared according to the manufacturers' recommendations. Electrophoresis was carried out at a constant voltage of 4-5V/cm. RNA was visualized by placing the gel on a UV transilluminator and photographed.

2.4.1 4 Northern blotting: Neutral transfer by capillary transfer by upward flow

Following agarose-formaldehyde electrophoresis, the gel was rinsed in DEPC-treated water and then soaked for 20 min in 5 gel volumes of 0.5 M NaOH. The gel was transferred to 10 gel volumes of 20x concentrated SSC for a further 40 min. Meanwhile, Hybond N+ membrane (Amersham) was immersed in 10x SCC. The gel was inverted and placed on Whatman 3MM paper, with wicks trailing in to 10x SSC and Saran wrap around to prevent short-circuiting. The top right hand corner of the gel was trimmed to aid subsequent orientation and the membrane laid on top with the corresponding corner trimmed. 3 pieces of Whatman 3MM paper were laid on top to the membrane and a pile of tissue paper placed above, with a flat plate on top of the stack and a 500g weight to weigh it down. Upward transfer of RNA was allowed to occur for 4 h. The membrane was washed briefly in 6x SSC prior to Northern hybridisation.

2.4.1.5 Preparation of ^{32}P-labelled DNA probes

DNA probes comprising either full length *LYVE–1* or an approximately 600bp *β-actin* fragment were amplified from human dermal lymphatic endothelial cells (HDLEC) by the primers ActinFwd (AGGCATCCTCACCCTGAAGTAC) and ActinRev (TTGCCAATGGTGATGACCTGGC). Probes were then radiolabelled by random oligonucleotide priming and Klenow polymerase (High Prime DNA Labeling Kit, Roche) whereby a complementary DNA strand is synthesised with the modified deoxyribonucleoside-triphosphate [α^{32}P] dCTP (Redivue, Amersham) incorporated. Briefly, approximately 30 ng DNA probe, either from a digested vector or a PCR product, was

denatured by boiling for 10 min then chilled rapidly in an ice-ethanol bath. dGTP, dATP, dTTP and High Prime reaction mixture were added plus 5 µl (1.85 MBq) of [α-^{32}P] dCTP prior to incubation at 37°C for 10 min. The reaction was stopped by addition of 2 µl 0.2 M EDTA pH 8. The probe was separated from un-incorporated nucleotides on a Sephadex G-25, NAP–5 column (Amersham Pharmacia Biotech) and eluted in 1 ml TE. The eluted probe was mixed with 100 µg sheared salmon testis DNA (SIGMA) and denatured for 5 min at 100°C prior to hybridisation.

2.4.1.6 Northern Hybridisation

The membrane containing the RNA from neutral transfer was placed in ExpressHyb hybridisation solution (Clontech) at 65 °C, rotating slowly in a Hybaid hybridisation oven for 1 h prior to addition of the [α-^{32}P] labelled probe. Hybridisation was carried out overnight at 65°C. The following day, blots were first rinsed and washed at low stringency (2x SSC, 0.05% (w/v) SDS, 2 x 15 min at room temperature) and then washed at high stringency (0.1 x SSC, 0.1% SDS, 2 x 20 min at 50°C) prior to autoradiography for 1 day to one week, as appropriate.

For re-probing, blots were stripped in 0.1% SDS at 100°C, then rinsed in 2x SSC and re-probed with another cDNA probe.

2.4.1.7 Generation of first strand synthesis products

First strand synthesis from total RNA was carried out by oligo-dT priming. 3-5µg total RNA was heated for 10 min with oligo-dT$_{12\text{-}18}$ primers (Collaborative Research), prior to the addition on ice of 0.5µM dNTPs, 0.1M Tris-HCl, pH8.3, 20 U RNasin and 1U/µl AMV reverse transcriptase in a total volume of 50 µl. The reaction mixture was incubated for 90 min at 42°C.

2.4.1.8 Affymetrix array analysis

<u>Preparation of double-stranded cDNA and in vitro transcription</u>

The first approach for preparing biotinylated complementary RNA (cRNA) from total RNA isolated from cultured cells used the MessageAmp™ aRNA kit from Ambion (detailed below). cRNA was prepared for duplicate analysis

of HDLEC (described in chapter 5 of this thesis). However, the quality of RNA yielded by this kit was highly variable and thus this method was replaced by supplying total RNA to the Paterson Institute for Cancer Research, Manchester, where complementary RNA was prepared by an alternative method whereby phenol-chloroform extraction was used to recover nucleic acids from solution, rather than columns supplied in the Ambion kit.

The MessageAmp™ aRNA kit supplied all enzymes, buffers, filter cartridges and other reagents for the preparation of biotinylated complementary RNA. 5 µg of total RNA prepared by RNeasy purification from human LEC cultured in either the presence or absence of human recombinant TNFα, 10ng/ml for 72 h was used for each amplification reaction. RNA and T7 Oligo (dT) primer were heated together to 70°C for 10 min in a thermal cycler prior to first strand synthesis by reverse transcriptase, to synthesise cDNA with a T7 promoter sequence by incubation in a hybridisation oven at 42°C for 2 h. Second strand cDNA synthesis was then carried out by DNA polymerase at 16°C for 2 h in a thermal cycler. The cDNA was purified using a filter cartridge, to remove RNA, primers, enzymes and salts before *in vitro* transcription.

To make biotin labelled cRNA, 7.5 µl of 10 mM biotin-11-CTP (Perkin Elmer) and biotin-16-UTP (Roche) were included in the T7 RNA-polymerase-catalysed reaction, carried out for 13 h at 37°C in a hybridisation oven. The cRNA was purified using a filter cartridge and eluted in nuclease-free water. cRNA was concentrated by vacuum centrifugation and the concentration estimated in a UV spectrophotometer at 260 nm. The typical yield was between 100 and 200 µg from the initial 5 µg total RNA. 2-3 µg were subjected to agarose gel electrophoresis, to ensure that the amplified cRNA was visible as a smear from 100bp to 2Kb, with a brighter region between 500bp and 1Kb.

Fragmentation of complementary RNA

25 µg of cRNA was fragmented in a total volume of 50 µl with 10 µl 5x fragmentation buffer (200 mM Tris-acetate, pH 8.1, 500 mM KOAc. 150 mM MgOAc, filter sterilised) by heating to 94°C in a thermal cycler for 35 min.

The sample was then chilled on ice and stored at –80°C. Biotin-labelled cRNA was also prepared from HDLEC RNA by Dr. Yvonne Hey at the Paterson Institute for Cancer Research.

Affymetrix GeneChip analysis of human transcripts

Biotin-labelled human cRNA target was hybridised to the probe set on the GeneChip® Human Genome U133 Plus 2.0 array at the CR-UK microarray facility at the Paterson Institute for Cancer Research, Manchester. Triplicate sets of data were generated and normalisation of data was performed in Bioconductor and RMA by Dr. Stephen Taylor, Bioinformatics, WIMM.

Micro array analysis of complementary RNA derived from mouse

Mouse LEC were cultured for 12h in either EGM-2 medium alone or supplemented with mouse recombinant TNFα (R and D Systems), 100ng/ml. RNA and biotin-labelled cRNA were prepared at the Paterson Institute for Cancer Research, as from the HDLEC, and applied to the GeneChip® Mouse Expression Set 430 array. Due to limited availability of this primary cell line, only one set of data could be obtained.

2.4.2 DNA

2.4.2.1 Plasmids

pCDM7Ig used for expression of soluble Ig fusion proteins was kindly provided by Dr. Alejandro Aruffo, Bristol-Myers Squibb, Seattle, WA.
pRcCMV used for eukaryotic expression was from InVitrogen.
pGL3-Basic, a luciferase construct was obtained originally from Promega and kindly donated by Dr. John Moore, Cancer Research UK, Weatherall Institute of Molecular Medicine.
pGL3-Enhancer, a luciferase construct containing SV40 enhancer elements, was purchased from Promega.

2.4.2.2 Constructs

LYVE–1: Full-length human LYVE-1 cDNA cloned into pRcCMV is described in Banerji et al., (1999).

LYVE–1 Fc: The N-terminal leader and extracellular domain of human LYVE–1 (Met 1 – Gly 232) and mouse LYVE-1 (Met 1 – Gly 228) cloned into the pCDM7Ig vector as a fusion with the Fc domain of human IgG1 is described in Banerji et al., (1999) and Prevo et al., (2001) respectively.

Podoplanin Fc. Full length podoplanin was cloned into pCDM7Ig, as described in appendix II.

pBR-βactin-Luc, containing a chicken β-actin promoter and luciferase reporter gene on a pBR backbone was a kind gift from Dr. Katya Simon, MRC Human Immunology Unit, Weatherall Institute of Molecular Medicine.

pGL3-Basic and pGL3-Enhancer constructs containing either lengths of upstream human *LYVE-1* sequence or the chicken β-actin promoter from pBR-βactin-Luc were generated in this thesis (appendix I).

2.4.2.3 Agarose gel electrophoresis

Buffers

TBE (Tris-borate) EDTA buffer: 0.09 M Tris-borate, 0.002 M EDTA, pH 8.0 (stored at room temperature).

Loading buffer (6 x): 2.5 mg/ml bromophenol blue, 30% v/v glycerol (stored at room temperature).

Ethidium bromide: A 10 mg/ml stock solution was made in H_2O.

Procedure

Agarose gels (0.9 - 1.2% w/v) were made in TBE buffer supplemented with 0.5 µg/ml ethidium bromide. DNA samples were mixed with 1/6 vol of loading buffer and run under constant voltage (80 V to 110 V). Gels were visualised under UV illumination.

2.4.2.4 Digestion of DNA with restriction endonucleases

Typically 1 µg of plasmid or purified PCR product was digested with 10 – 20 units of the appropriate restriction enzyme supplemented with the appropriate buffer and BSA (100µg/ml) in a total volume of 50µl and incubated for at least 2.5 h at 37°C. Digests were loaded onto agarose gels for subsequent purification. Digests of PCR products were purified directly using GeneClean (see below).

2.4.2.5 Purification of DNA Fragments from Agarose Gels

DNA fragments were separated on agarose gels and bands were excised under brief UV illumination. DNA was then purified using the Bio 101 GeneClean II kit (Q-BIOgene) according to manufacturers' instructions. Briefly, 4.5 vol of 6 M NaI and 0.5 vol of TBE modifier was added to the gel fragment and heated at 55°C for 5 min to melt the gel. 10 µl of GLASSMILK® silica suspension was added and incubated for 1 min. The GLASSMILK® was washed three times with salt solution in 50% ethanol (NEW WASH) and DNA eluted in 20 µl H_2O in two successive steps, pooling eluants and centrifuging to remove any GLASSMILK carried over.

2.4.2.6 Ligation of digested DNA fragments

Ligations were carried out in a final volume of 10 µl containing approximately 0.2 µg of linearised plasmid, 50 ng of the appropriate purified insert and 200 U of T4 DNA ligase in 1x ligase buffer. Samples were incubated overnight at 15°C.

2.4.2.7 PCR (Polymerase Chain Reaction)

PCR was performed using either a Perkin Elmer Cetus DNA thermal cycler or a Hybaid PCR Express. *Taq* polymerase was used for large-scale screening of bacterial colonies or cDNA whilst *Pfu* polymerase or *Taq* Plus polymerase were used for amplification of DNA for protein expression. All solutions were prepared from freshly distilled de-ionised water. Primers were ordered from Invitrogen and their melting temperatures (T_m) were calculated according to their GC content: each A or T = 2°C, each G or C = 4°C. Annealing temperatures for PCR were set at 5°C below the calculated T_m.

2.4.2.8 Amplification with Taq Polymerase

Reactions were carried out in a total volume of 50µl in water with:

5 µl 10 x NH_4 buffer (supplied with Taq)
0.25 mM dNTP
1 mM $MgCl_2$

0.2 µM forward primer
0.2 µM reverse primer
0.5 µl Taq (2.5 U)
0.1µg of plasmid DNA (or 1 µl of cDNA), added last

25-30 cycles were carried out, each consisting of 1 min denaturing at 94°C, 1 min annealing at T_m–5°C and extension at 72°C for 1 min/kb target DNA

2.4.2.9 Amplification with Pfu Polymerase

Reactions were carried out in a total volume of 50µl in water with:

5 µl 10x *Pfu* buffer (1x = 10mM Tris pH 8.3, 50mM KCl, 2.5mM $MgCl_2$)
1 mM dNTP (0.25 mM of each dNTP)
0.2 µM forward primer
0.2 µM reverse primer
0.5 µl *Pfu* (2.5 U)
0.5 µg of plasmid DNA (or 1-2 µl of cDNA)

25 cycles were carried out, each consisting of 1 min denaturing at 94°C, 5 min annealing at T_m–5°C and extension at 68°C for 10 min

2.4.2.10 Amplification Using TaqPlus® Precision PCR System

This enzyme mixture (purchased from Stratagene) combines the proof-reading ability of *Pfu* with the faster polymerizing rate of *Taq* and was used to amplify longer DNA targets and generate higher yields of product for cloning. PCR was carried out according to the manufacturers instructions. Briefly, reactions were carried out in a total volume of 100µl in water, with *TaqPlus*® Precision 10 x buffer, 0.8 mM dNTP (0.2 mM of each dNTP), 2.5ng/µl of each primer, *TaqPlus*® Precision polymerase mixture, 5 U and 250 ng DNA template. The cycling parameters used were denaturing at 94°C for 1 min, followed by annealing at T_m–5°C for 1 min, then extension at 72°C for 1 min/kb target DNA.

2.4.2.11 Small-scale Preparation of Plasmid DNA (miniprep)

Plasmid DNA was prepared from overnight cultures grown in LB. Cultures were harvested by centrifuging at 472 g for 5 min in a Heraeus Megafuge 2.0. Plasmid DNA was extracted using the QIAprep Spin miniprep kit (Qiagen) according to the manufacturers' instructions. The integrity of the DNA was examined by agarose gel electrophoresis.

2.4.2.12 Large-scale Preparation of Plasmid DNA (maxiprep)

Solutions for maxiprep:

Resuspension buffer

25 mM Tris pH 8.0
10 mM EDTA

Lysis buffer

200 mM NaOH
1 % (w/v) SDS

Neutralisation buffer

3 M Potassium acetate
13.5% (v/v) Acetic acid

Procedure

A preculture was prepared using a single colony of the transformed bacteria of interest to inoculate 10 ml of LB supplemented with the appropriate antibiotics and grown overnight at 37°C with agitation. This was subsequently used to inoculate 1 litre of TB, again supplemented with antibiotics, which was agitated overnight at 37°C. The following day cells were pelleted by centrifugation at 2500 g for 15 min in 500 ml Heraeus Sepratech bottles in a bench-top centrifuge (Heraeus megafuge 2.0R). Cells were resuspended in 20 ml resuspension buffer and then lysed by adding 40 ml lysis buffer. Lysis was allowed to proceed for 5 min before the addition of 20 ml of ice-cold neutralisation buffer. The suspension was incubated on ice for 5 min prior to centrifugation at 2500 g for 20 min at 4°C. The supernatant was filtered and DNA precipitated by addition of 0.6x vol of isopropanol. The suspension was centrifuged at 2500 g for 20 min at 4°C and the DNA pellet

was washed in 75% ethanol and centrifuged as before. The pellet was air-dried, resuspended in 4-5 ml TE and 1.2 g/ml CsCl was added and warmed to 37°C to aid dissolving. Ethidium bromide was added at a final concentration of 0.8 mg/ml. This mixture was centrifuged at 2,500 g for 15 min at room temperature. The supernatant was transferred to thick-wall polycarbonate tubes (Beckman) and centrifuged in a TLA-100.3 rotor in a Beckman TL-100 ultracentrifuge at 270,000 g at 20°C overnight. The following day, the plasmid bands were extracted from the caesium gradient with a p1000 pipette and the ethidium bromide removed by repeated extraction with an equal volume of CsCl saturated isopropanol. The DNA was precipitated by addition of 10x vol of 50% (v/v) isopropanol and centrifuged at 3000 g for 15 min at 4°C. The pellet was washed in 75% ethanol, centrifuged as before and allowed to dry before finally dissolving in 1000 – 1500 µl of TE buffer. A typical yield was usually between 2-6 mg plasmid DNA/litre of bacterial culture.

2.4.2.13 Southern Blotting: Alkali Transfer by Upward Capillary Transfer

Following agarose-TBE gel electrophoresis and rinsing briefly in water, the gel was soaked in denaturation solution (NaOH 0.5 M and NaCl 1.5M) for 30 min with gentle agitation. Upward capillary transfer onto Hybond N+ was set up as for Northern blotting but using denaturation solution instead of SSC and allowing to transfer overnight. The membrane was then washed in 5x SSC.

2.4.2.14 Southern Hybridisation

The membrane containing the DNA from transfer was placed at 42°C in a hybridisation oven in hybridisation solution:

Formamide, (de-ionised) 50 % (v/v)
SSC, 5x
Na_2HPO_4, 0.05 M
SDS, 0.5 % (w/v)
Denhardt's reagent, 5x

Denhardt's reagent was made up as a 50x stock solution from Ficoll 400, polyvinylpyrrolidone and bovine serum albumin fraction V, all at 1 % (w/v) in water, filtered and stored in aliquots at –20°C

The membrane was incubated for 2h before the addition of denatured DNA probe (prepared as described earlier in "Preparation of ^{32}P-labelled DNA probes) and salmon testis DNA. Hybridisation was carried out overnight at 42°C. The following day the membrane was washed, as for Northern hybridisation and then submitted to autoradiography for 15 min 48h as appropriate.

2.4.2.15 Primer Extension Analysis

All reagents were prepared using DEPC-treated H_2O

Preparation of the Oligonucleotide Primers

Oligonucleotide primers were designed which were 90 oligonucleotides in length and would hybridise to target sequences located between 100 and 350 nucleotides downstream of the suspected 5′ terminus of the mRNA. Primers had a GC content of approximately 50% and had a G or C residue at the 3′ terminus. Five primers were used, designed to hybridise between 40 and 60 residues apart from each other in order that products would differ in size by an amount equivalent to the distance between the two primers and confirm results obtained from each primer.

Oligonucleotide primers were phosphorylated in a reaction containing:

Distilled deionized water	6.5µl
10X kinase buffer	1.5µl
oligonucleotide primer (5-7 pmoles or 60ng)	1.0µl
T7 polynucleotide kinase (~ 10 units)	1.0µl
[γ^{32}P]ATP (7000 Ci/mmole),(from Amersham)	2.0µl

Reactions were incubated at 37°C for 1h and then quenched by addition of 150 µl TE, pH 7.6. 25ng of carrier RNA (brewer's yeast tRNA) was added and nucleic acid was prepitated by addition of 0.1 x vol 3 M sodium acetate, pH 5.2 and 2.5 x vols 100 % ethanol and storage for at least 1h at –80 °C. The precipitated oligonucleotide was collected by centrifugation at 20,800 g for 15

min at 4°C. The radioactive supernatant was discarded and the pellet washed in 70 % ethanol prior to centrifuging again. The supernatant was discarded and the pellet air-dried and then dissolved in 500 µl TE. 2 µl of radiolabeled oligonucleotide primer was placed in 10ml scintillation fluid in a liquid scintillation counter. The specific activity of the radiolabeled primer was calculated to ensure that it ~2 x 10^6 cpm/pmole of primer.

Hybridization and Extension of the Oligonucleotide Primer

10^4 to 10^5 cpm (20-40 fmoles) of the DNA primer was added to 0.5-150µg of the RNA to be analyzed and 0.1 volume of 3M sodium acetate (pH 5.2) and 2.5 volumes of ethanol were added. The solution was stored for 1h at -80°C prior to recovery of nucleic acid by centrifugation at 20800 for 10 minutes at 4°C. The pellet was washed in 70% ethanol and centrifuged again. Following removal of ethanol, the pellet was air-dried and then resuspended in 8µl of TE (pH 7.6). Samples were re-dissolved by repeated pipetting, prior to adding 2.2µl of 1.25 M KCl and gently vortexing, then centrifuging for 2 seconds. The oligonucleotide/RNA mixture was placed in a heat block at 95 – 100°C for 5 min, followed by another heat block set to 60°C to allow annealing. The sample was incubated for 2h.

Meanwhile, a 300 µl aliquot of primer extension mix (20mM Tris-Cl (pH 8.4), 10mM $MgCl_2$, 1.6mM dNTP solution containing all four dNTPs and 50µg/ml actinomycin–D) was thawed on ice and supplemented with 3µl of 1M DTT and reverse transcriptase to a concentration of 2 units/µl. 0.1 unit/µl of RNasin was added, gently mixing by inverting the tube several times and then stored on ice.

The sample was removed from the water bath, centrifuged for 2 sec and then 48 µl of supplemented primer extension mix was added before mixing gently again and centrifuging for 2 seconds. The sample was incubated for 1.5h at 42°C to allow the primer extension reaction to proceed.

The reaction was quenched by addition of 200µl of TE (pH 7.6). Nucleic acids were precipitated by the addition of 50µl of 10M ammonium acetate and 700µl of ethanol. The sample was mixed well by vortexing and then

incubated for at least 1h at –80°C. The nucleic acid was pelleted by centrifugation at 20800 g for 10 min, then washed with 70% ethanol and centrifuged again, removing the supernatant.

Preparation of size markers

Two DNA ladders were radiolabelled and electrophoresed in parallel to primer extension products, to measure the size of the products.

pGEM4-MspI

The first ladder was prepared from pGEM-4, originally from Promega and kindly donated by Dr. Simon Brackenridge, MRC Human Immunology Unit, Weatherall Institute of Molecular Medicine. This plasmid was digested with *Msp*I to yield 18 fragments sized from 1bp to 242bp, in addition to three larger fragments of 404, 424 and 501bp. Following digestion of 20μg in 100μl, the reaction was quenched at 65°C for 20 min prior to the addition of DNA polymerase I, large (Klenow) fragment, 1 μl and [α^{32}P]dCTP (~3000 Ci/mmole) to a 20μl aliquot. As only one dNTP was present, the 3'→5' exonuclease activity of the enzyme degraded the double-stranded DNA from 3'OH until a base was exposed that was complementary to the dNTP present. Thus [α^{32}P]dCTP was incorporated into the 3' overhangs of fragments. The reaction was incubated for 30 minutes at 37°C before the addition of 100μl TE. DNA was precipitated by adding 12μl sodium acetate and 300μl ethanol, washed in 70% ethanol and resuspended in 10μl formamide loading buffer:

80% deionized formamide
10mM EDTA (pH8.0)
1mg/ml xylene cyanol F
1mg/ml bromophenol blue).

Approximately half of this was loaded onto the polyacrylamide gel.

ØX174-HaeIII

This ladder was purchased from New England Biolabs and radiolabelled in the following reaction mixture:

Distilled, deionised water	15.5µl
Polymerase buffer (supplied with the enzyme)	2.0µl
DNA (1µg/µl)	0.5µl
(Klenow) DNA polymerase I	1.0µl
[α^{32}P]dCTP (~3000 Ci/mmole)	1.0µl

The reaction was incubated for 30 minutes at 37°C and the DNA recovered as with pGEM4-*Msp*I ladder and loaded onto the gel in parallel with primer extension product to be analysed.

Analysis of the Primer Extension Products

The nucleic acid precipitate from a primer extension reaction was dissolved in 10µl formamide loading buffer (see above). The sample was re-dissolved by repeated pipetting and then heated for 8 minutes at 95°C before chilling rapidly on ice and analysing immediately by electrophoresis through a denaturing polyacrylamide gel.

Once the tracking dyes had migrated an appropriate distance through the gel, the gel was removed and transferred to a piece of Whatman 3MM filter paper for drying on a heat-assisted vacuum-driven gel dryer for 1 - 1.5h at 80°C. An image of the gel was established using autoradiography.

2.4.2.16 Preparation of genomic DNA

Buffers and solutions

Lysis buffer

20% (w/v) sucrose	27.5 ml
1M Tris-HCl, pH 7.4	0.5 ml
1M $MgCl_2$	0.25 ml
Triton X-100	0.5 ml
Water	21.25

SET buffer

1 M NaCl	7.5 ml
0.5M EDTA, pH 8.0	0.5 ml
1M Tris-HCl, pH 7.4	2.5 ml
Water	39.5 ml

Other reagents

Proteinase K was purchased from Boehringer Mannheim and a stock solution of 10 mg/ml was prepared in SET buffer. This was then stored in aliquots at -20°C.

Tris-HCl-saturated phenol (pH 8.0)

Phenol-chloroform, 1:1

4M sodium acetate, pH 5.0

SDS, 10% (w/v)

Tris-HCl, 10 mM (pH 8.0)

Procedure

Approximately 1 x 10^7 cells were centrifuged at 2000 RPM for 5 minutes and resuspended in 5 ml lysis buffer, prior to incubation on ice for 5 minutes to release the nuclei. Cells were then centrifuged at 3000 RPM for 20 minutes at 4°C and the nuclei resuspended in 5 ml SET buffer. Proteinase K was added to a final concentration of 200 µg/ml, as well as 500µl SDS. The suspension was gently mixed and incubated at 37°C overnight.

The following day, phenol extraction of genomic DNA was performed, with addition of an equal volume of phenol. An equal volume of phenol-chloroform was then added to the aqueous layer and a final extraction was performed with diethylether. DNA was precipitated by addition of 0.1 x volume sodium acetate and 2.5 x volume 100% ethanol and harvested by centrifugation at 4000 RPM to obtain a pellet. The DNA pellet was rinsed in 70% ethanol and air-dried briefly, then dissolved in 10 mM Tris-HCl.

2.5 Tissue Culture

2.5.1 Cell lines and transfectants

2.5.1.1 Transformed cell lines

293T cells: The transformed human primary embryonic kidney fibroblast cell line 293T was obtained from the Cancer Research UK cell bank.

Human LYVE–1 293T: stable transfectants of full-length human LYVE–1 in 293T were made by Dr. Suneale Banerji, MRC Human Immunology Unit, Oxford.

Mouse LYVE–1 293T: stable transfectants of full-length mouse LYVE–1 in 293T were made by Dr. Remko Prevo and Branwen Hide, MRC Human Immunology Unit, Oxford.

Y3 rat myeloma cells were kindly donated by Dr. Michael Puklavec, Dunn School of Pathology, University of Oxford

NS-1 mouse myeloma cells were kindly donated by Jackie Cordell at the Nuffield Department of Clinical Laboratory Sciences, University of Oxford, UK.

RAW 264.7 mouse monocyte-macrophage cells were kindly donated by Dr. Sigrid Heinsbroek, Dunn School of Pathology, University of Oxford.

2.5.1.2 Primary cell lines

HMVEC, primary human microvascular endothelial cells were purchased from Cambrex Bio Science as a cryopreserved stock

HDMEC, primary human dermal microvascular endothelial cells were purchased from PromoCell, Heidelberg, as a cryopreserved stock

HDMEC-derived immuno-selected primary lymphatic endothelial cells (LEC) were kindly donated by Dr. Ernst Kriehuber

HUVEC, human umbilical vein endothelial cells were purchased from Totem Biologicals

Primary mouse dermal LEC, lymphatic endothelial cells were prepared as described in section 2.5.8 of this chapter.

2.5.2 Culture conditions

All mammalian cells were grown at 37°C in humidified incubators with 5% CO_2.

293T, RAW 264.7, Y3 and NS-1 cells were grown in RPMI 1640 supplemented with 10% FCS (heat inactivated at 55°C for 20 min), 2 mM L-glutamine, IU/ml penicillin and 50 µg/ml streptomycin, hereafter referred as RPMI 10% FCS.

Stable LYVE–1 transfected 293T cells were grown in identical medium supplemented with 1.25 mg/ml G418.

Calcium phosphate transfections (see section 2.5.13.1) were carried out in DMEM medium with similar supplements (DMEM 10% FCS).

Hybridomas were grown in RPMI 1640 supplemented with 20% myeloma tested FBS, L-glutamine penicillin, streptomycin and 1 x HT, as described in section 2.1.4.

Endothelial cells were cultured in EGM–2 MV supplemented with the supplied SingleQuots (Hydrocortisone, EGF, FBS, VEGF, FGF-B, R3-IGF, ascorbic acid and gentamycin/amphotericin-B) prior to use. Primary human endothelial cells were cultured on gelatin-coated plasticware whilst mouse LEC were cultured on collagen-coated plasticware.

2.5.3 Collagen-coating of tissue culture dishes for mouse LEC

Type I collagen was dissolved in 20 mM acetic acid at 0.1 mg/ml and filter-sterilized. Sufficient solution was added to the culture dish or flask to cover the bottom and incubated at room temperature for 1h. The solution was then removed and the culture dish washed twice with PBS before being left for another hour to allow the dish to dry.

2.5.4 Gelatin-coating of tissue culture dishes for human endothelial cells

Sufficient gelatin, 0.1% in PBS was applied to the culture dish or flask to cover the bottom and incubated at 37°C for 2h before removing the gelatin solution for reuse and storing the tissue culture ware at 4°C until required

2.5.5 Passaging of cells

2.5.5.1 293T and RAW 264.7

Adherent cells were grown to confluence, washed with PBS and incubated in pre-warmed Trypsin/EDTA for 5 min at 37°C. Lifted cells were resuspended in 3-5 x the original volume of culture medium by gentle pipetting and divided over fresh culture dishes.

2.5.5.2 NS–1 and Y3

Fresh medium was added to cells which had grown to a high density in suspension and the cells were redistributed between new flasks, typically splitting 1:20. When cells were split for the final time before carrying out a fusion with splenocytes, NS-1 and Y3 were split more severely, typically 1:40.

2.5.5.3 Endothelial cells

Commercially available endothelial cells were cultured in EGM–2 MV according to the manufacturer's instructions. Other endothelial cells were cultured in the same manner. Human endothelial cell lines were cultured in gelatin-coated flasks whilst mouse endothelial cells were grown on collagen-coated flasks

2.5.6 Frozen storage of cells

Subconfluent cultures were detached in Trypsin/EDTA and 1 x vol of fresh medium added. Cells were centrifuged for 4 min at 1300 RPM in a bench top centrifuge. The pellet was then resuspended in freezing medium (90% FCS, 10% DMSO) and transferred to cryo-vials (1 ml per vial) for storage at –80°C or transferred to liquid nitrogen after 1-2 days at –80°C.

2.5.7 Recovery of frozen cells

The cryo-vial was warmed rapidly to 37°C and thawed cells were immediately transferred to culture medium. Endothelial cells were placed in flasks at a minimum density of 10000 cells/cm^2 and cultured overnight before applying fresh pre-warmed medium. All other cell types were suspended in

medium and centrifuged for 4 min at 1300 RPM before resuspending in fresh culture medium and transferring to a culture dish or flask.

2.5.8 Preparation of mouse LEC from skin

LECs were isolated from a litter of mouse pups, 3 and 4 days post partum. Between 8 and 12 pups were used for each preparation. Limbs and tail were discarded and the skin from the torso and head were removed, placing on ice in PBS supplemented with 5x penicillin-streptomycin for 30 min then transferring to Dispase (Gibco), 2 mg/ml in PBS, incubating dermis-side down overnight at 4°C

The following day, skin was rinsed in PBS and the epidermis removed. The dermal sheets were digested further with collagenase A, 2mg/ml; ovine testicular hyaluronidase, 0.2 mg/ml; DNase I, 50 µg/ml; and elastase, 50 µg/ml in 10 ml PBS, adding 20 ml more PBS before transferring to 37°C for 30 min incubation with agitation. The digest was then passed through a 70 µm filter, adding RPMI-10% FCS before centrifuging at 1700 RPM for 10 min. The pellet was resuspended in 20 ml RPMI-10% FCS prior to centrifuging again at 1500 RPM for 5 min. Cells were plated out in large (T225) gelatin-coated flasks for 4 h to allow adherence of endothelial cells, then washed with PBS before adding EGM-2, incubating overnight.

For selection of LEC, cells were first detached by incubation with accutase, prewarmed to 37°C. Cells were washed in MACS buffer (0.5 % BSA, 2 mM EDTA in PBS, maintained on ice throughout the procedure), centrifuging at 1500 RPM for 5 min and then resuspending in 10 ml MACS buffer and passed through a pre-wetted Miltenyi 30 µm filter, washing the filter with an extra 3 ml MACS buffer. Cells were centrifuged again and resuspended in 2 ml MACS buffer. Rat anti-mouse LYVE-1 monoclonal antibody, C1/8 (see chapter 3) was added to a final concentration of 5 µg/ml and the cells incubated at 5°C for 20 min on a rotating wheel. Cells were washed twice in 10 ml MACS buffer, then resuspended in 240 µl MACS buffer and 60 µl anti-rat MACS beads, incubating for 15 min at 5°C on a rotating wheel. Cells were then washed with MACS buffer, 5 ml and following centrifugation were

resuspended in 2 ml MACS buffer. Cells were passed through a pre-wetted Miltenyi 30 µm filter, washing with a further 1 ml MACS buffer. A Miltenyi LS MACS column with another 30 µm filter on a magnetic stand were pre-equibrated with 3 ml MACS buffer and the cells loaded onto the column through the filter. 1 ml of MACS buffer was added to the column and allowed to drain through, followed by a further 2 ml. The filter was discarded and 2 x 3ml buffer was run through the column. Cells bound to the column were eluted by removing the column from the magnetic stand, adding 5 ml MACS buffer and forcing it through using the plunger. Cells were pelleted by centrifugation at 1500 RPM for 5 min then resuspended in 2 ml buffer before passing though a second LS column as before but with no filters. Cells were collected by centrifugation and resuspended in 12 ml EGM-2, plating out in a medium-sized (T75) gelatin-coated flask.

The following day a second round of selection was carried out. Cells were lifted using accutase and following centrifugation and washing in 5 ml MACS buffer were resuspended in 1 ml MACS buffer. Cells were incubated and washed as before with rat anti-mouse LYVE–1, and MACS buffer then resuspended in 80 µl MACS buffer and 20 µl MACS beads. Following incubation as with the first selection, cells were washed in 5 ml MACS buffer and resuspended in 1 ml. A Miltenyi MS MACS column and 30 µm filter on a magnetic stand were pre-equilibrated with 1 ml buffer before application of the cell suspension. The column and filter were washed with 0.5 ml buffer; the filter was then discarded and the column washed a further 2 x 0.5 ml. Cells were eluted by removing the column from the magnetic stand, applying 2 ml of buffer and forcing it through the column using the plunger. Cells were pelleted by centrifugation and resuspended in 1 ml buffer for passage through a second MS column as before, then plated out in 5 ml EGM–2 in a collagen-coated small (T25) flask for expansion.

2.5.9 Derivation of primary HDLEC from HDMEC

Human dermal microvascular endothelial cells (HDMEC) were purchased from PromoCell, Heidelberg, Germany and cultured as described in sections 2.5.2 and 2.5.5.3 of this chapter, in medium (T75) flasks. At each passage, cells

were lifted with Accutase and half of the population were replated in a fresh flask whilst the other half were stained for expression of LYVE-1 (using the mAb 8C), podoplanin (with rabbit anti-sera) and CD34 (BD Pharmingen) and assayed by flow cytometry. The percentage of cells expressing the BEC marker CD34 was found to decrease with passaging whilst the number of cells expressing the LEC markers LYVE-1 and podoplanin increased, suggesting that the LEC outgrew the BEC. Thus at passage 12 and beyond, these cells were termed HDLEC.

2.5.10 Trypan blue dye exclusion assay

The viability of cultured cells was assessed by measuring the capacity to exclude trypan blue dye. Adherent cells were lifted with PBS-5mM EDTA, centrifuged at 1300 RPM for 4 min and resuspended in equal volumes of PBS and commercially prepared trypan blue dye solution (SIGMA). Following 10 min incubation at room temperature, cells were counted by haemocytometer and the number of cells excluding dye and thus appearing white expressed as a percentage of the total number of cells. Dead cells are unable to exclude the dye and therefore appear blue. A minimum of three cell counts were carried out per sample and the mean percentage viability expressed ± standard error.

2.5.11 MTT proliferation assay

The proliferation of cultured cells was measured by MTT (3-(4,5-dimethylthiazol-2-yl)-2,5-diphenyl tetrazolium bromide) colorimetric assay, originally described by Mosmann (1983). This assay measures the ability of mitochondrial enzymes to reduce the yellow MTT tetrazolium salt into blue crystals of MTT formaza. A stock solution of MTT (SIGMA) was prepared by dissolving 7.5 mg/ml in PBS pH 7.5 and filtering through a 0.22 μm filter (Gerlier and Thomasset, 1986). Cells were cultured in a monolayer in 24-well dishes (1.77cm2 per well) and to 200 μl medium, 40 μl MTT solution was applied per well. Following 1 h incubation at 37°C/5 % CO_2 in a humidified incubator, supernatant was removed and 200 μl of 0.04 M HCl in isopropanol was added to each well to dissolve the dark crystals of MTT formazan formed within cells. Cell debris was removed by centrifuging for 4 min at 1300 RPM.

Supernatants were transferred to a 96-well plate for quantitation in a microplate reader (BioRad) at 590 nm.

2.5.12 Tube-formation assay

24-well culture dishes were coated with Matrigel (BD), 0.5ml/well on ice and gels were allowed to solidify at 37°C for 1h. Cultured adherent HDLEC were lifted by trypsin-EDTA, seeded into Matrigel-coated wells at approximately 15000 cells/cm^2 and incubated for 24h at 37°C/5% CO_2 in a humidified atmosphere. Images were then captured using a Zeiss Axioskop microscope.

2.5.13 Transfection methods

2.5.13 1 Transient transfection of 293T cells by calcium phosphate precipitation

293T cells were grown in DMEM (10% FCS) until approximately 70% confluent. The transfection mixture was prepared by combining plasmid DNA (20 µg for a 14-cm dish or 5-10 µg for a 6-well dish) with 250 mM $CaCl_2$, 1 ml or 125 µl respectively. The same volume of HEPES buffer pH 6.95 (280 mM NaCl, 50 mM HEPES, 1.5 mM Na_2HPO_4) was then added drop by drop while vortexing. The mixture was incubated for 10 min on ice before adding to culture medium. Cells were incubated for 5-6 h at 37°C and the medium then changed to RPMI (10% FCS). Serum-free medium (UltraCHO) was used in place of RPMI 10% FCS when cells were transfected for production of soluble Fc fusion proteins, to avoid contamination of the fusion protein with bovine Ig.

2.5.13.2 Electroporation of HUVEC

HUVEC were passaged two days before transfection and cultured to approximately 90% confluency. The medium was removed and cells were washed with PBS prior to lifting using trypsin-EDTA. Fresh medium was applied to neutralise the trypsin and the cells were counted. 1 x 10^6 cells were used per nucleofection sample, centrifuging at 200 g for 10 minutes. The cell pellet was resuspended in HUVEC Nucleofector™ Solution (Amaxa

Biosystems), to which 5μg DNA (in up to 5μl distilled, deionised water) was added. The sample was then transferred to a cuvette (Amaxa Biosystems) and placed in the cuvette holder in the electroporator (also from Amaxa Biosystems), The sample was electroporated on programme U-01, before re-plating cells in pre-warmed medium within a gelatin-coated well of a six-well dish. Gene expression was assayed after 24h.

2.5.13.3 Lipofectin transfection of RAW 264.7

2 x 10^5 RAW 264.7 were seeded into a well of a six-well dish and cultured for approximately 24h until 60% confluent. The following solutions were prepared:

Solution A: 100 μl serum-free OptiMEM (Life Technologies)
2 μg DNA

Solution B: 5 μl LIPOFECTIN® reagent (Life Technologies)
100 μl serum-free OptiMEM

Solutions A and B were combined and incubated at room temperature for 12 minutes. Meanwhile, cells were lifted with trypsin-EDTA, neutralised with medium and then washed with 2 ml OptiMEM per well. 0.8 ml OptiMEM was added to the combined solutions, yielding a total volume of 1 ml which was used to resuspend the cell pellet. Cells were re-plated into 6-well dish wells and after 24h medium was replaced with normal growth medium (RPMI-10% FCS). Gene expression was assayed after a further 48h.

2.5.14 Expression and purification of soluble Fc fusion proteins

The fusion protein constructs (mouse LYVE–1 Fc, human LYVE–1 Fc and podoplanin Fc) were transfected into 293T cells by calcium phosphate precipitation. Transfected cells were grown in serum free UltraCHO for 3 days. Culture supernatants (300-400 ml) were harvested and the pH adjusted to pH 8 using 2M Tris pH 8.0 and passaged twice through protein A-Sepharose columns (1 ml), which were then washed with PBS and eluted with 0.1 M Glycine pH 2.5. Samples of effluent (0.5 ml) were neutralised by addition of 1/20 volume of 2 M Tris pH 8.0.

2.6 Protein Biochemical Methods

2.6.1 Measurement of protein concentration

Protein concentration was estimated by measuring the OD 280 nm using a UV spectrophotometer. An OD of 1.0 was assumed to be equivalent to 1 mg/ml protein.

2.6.2 SDS-Polyacrylamide gel electrophoresis (SDS-PAGE)

Gels were cast and run in a Hoefer gel caster and electrophoresis apparatus. The composition of a 10% gel, loading buffer and electrophoresis buffer is listed below. Typically 1 µg of sample protein was dissolved in 5-10 µl of SDS-PAGE loading buffer and boiled for 5 min. Gels were run at a constant current of 20 mA. Pre-stained molecular weight markers were purchased from Bio-Rad.

Buffers and solutions

<u>10% resolving gel (5 ml)</u>

2.3 ml H_2O	
1.3 ml 1.5 M Tris-HCl pH 8.8	(0.39 M)
1.3 ml 40% Acrylamide	(10.4 %)
50 µl 10% (w/v) SDS	(0.1 %)
50 µl 10% (w/v) ammonium persulphate	(0.1 %)
10 µl TEMED	(0.02 % v/v)

<u>5% stacking gel (2 ml)</u>

1.4 ml H_2O	
250 µl 1 Tris-HCl pH 6.8	(0.125 M)
250 µl 40 % Acrylamide	(5 %)
20 µl 10% SDS	(0.1 %)
20 µl 10% ammonium persulphate	(0.1 %)
5 µl TEMED	(0.03 %)

2 x Loading buffer

0.1 M Tris-HCl pH 8.0, 4% (w/v) SDS, 50 % (v/v) glycerol, 2 mg/ml bromophenolblue, +/- 0.36 M β-mercapto-ethanol.

Electrophoresis buffer

25 mM Tris, 250 mM glycine pH 8.3, 0.1% SDS.

2.6.3 Coomassie blue staining of protein gels

Gels were incubated in Coomassie blue stain solution (see below) for 30 min at room temperature and destained overnight. Gels were then dried for 1h at 80°C.

Coomassie stain solution

2.5 mg/ml coomassie blue
50% methanol
10% acetic acid

Destain solution

50% methanol
10% acetic acid

2.6.4 Western blotting

Following SDS-PAGE, gels were transferred to nitrocellulose membranes (Hybond C Extra; Amersham Life Sciences) using a semi-dry blotting apparatus (Hoefer). Three layers of Whatmann 3MM paper and the nitrocellulose membrane were soaked in blotting buffer (20% methanol, 20 mM Tris base, 150 mM glycine, 0.1% SDS). The membrane was laid on top of the Whatmann paper, with the gel and three additional Whatmann papers placed on top of the membrane. The gel was then transferred at constant current (1 h at 1.2 A or overnight at 0.2 A). After transfer, the membrane was washed in H_2O.

Membranes were blocked in incubation buffer (PBS, 0.2% (v/v) Tween, 5% (w/v) dried milk powder) for at least 1h and subsequently incubated with the primary antibody for 1h (see specific sections for details). After washing 4 times over a 30 min period in washing buffer, (PBS, 0.2% (v/v) Tween), membranes were incubated with HRP-conjugated secondary antibody (1 h), washed as before and developed using chemiluminescent detection (Supersignal chemiluminescent substrate, Pierce).

2.6.5 Enzyme-linked immunosorbant assay to quantitate chemokine concentrations

All ELISA kits for the quantitation of chemokines in cell culture supernatant were purchased from R and D systems and the manufacturer's instructions strictly adhered to. Briefly, appropriately diluted supernatant was applied in triplicate to pre-coated ELISA wells, alongside a negative control of medium alone and chemokines standards, applied in duplicate. Bound chemokine was detected using a secondary HRP-conjugated antibody and OPG, for measurement in a BioRad microplate reader at 490nm. Chemokine concentrations were calculated from a standard concentration curve and 4PL logistic plot.

2.6.6 Estimation of shed LYVE-1 in culture supernatant

HDLEC were passaged 48h prior to the experiment, to allow surface expression of LYVE-1 to have fully recovered from trypsin-EDTA-mediated loss. Cells were washed three times in PBS and once in unsupplemented endothelial cell basal medium EBM-2. Cells were then cultured for 24h in triplicate wells of either EBM-2 alone, or supplemented with TNFα or TNFβ.

96-well MaxiSorp™ (Nunc) ELISA plates were coated for 16h at room temperature with affinity-purified rabbit anti-human LYVE-1, 0.25 μg/well. Plates were rinsed and supernatant was applied. Dilutions of human LYVE-1 fusion protein (0-80 ng/ml) were applied in triplicate to permit quantitation of shed LYVE-1 in supernatants. Also, as a positive control, supernatant from PMA-stimulated 293T-human LYVE-1 tranfectants (20ng/ml PMA for 4h) was applied in triplicate. Following a 1h incubation, plates were washed and incubated with mouse anti-human LYVE-1 mAb for 1h before a secondary incubation of goat anti-mouse IgG (Pierce), 1:4000. Detection was performed using *O*-phenylenediamine substrate (OPD) substrate (Sigma) and the absorbance measured by Bio-Rad microplate reader at 490nm. Concentrations of shed LYVE-1 were calculated from the standard curve using a 4PL logistics plot.

2.7 Generation of Polyclonal Antisera

The general procedure for the generation of polyclonal antibodies is described below, whereas the production and purification of each immunogen is described in section 2.5.4.

2.7.1 Immunisation

For each individual antigen, two New Zealand White rabbits were immunised by staff at the Biomedical Services Unit of the John Radcliffe Hospital Oxford. Pre-immune bleeds (5 ml) were collected prior to the first injection. Rabbits were immunised with 100 µg of antigen suspended 1:1 (v/v) in complete Freund's adjuvant in a total volume of approximately 0.5 ml per rabbit. Two consecutive boosts were carried out at 4 weekly intervals with antigen mixed (1:1 v/v) in incomplete Freund's adjuvant. Test bleeds (5 ml) were carried out one week after each booster injection. Rabbits were bled out approximately one week after the last test bleed.
Blood collected in Falcon tubes was allowed to clot over night at 4°C. The following day, the samples were centrifuged at 2300 g for 10 min and the serum transferred to Eppendorf vials for another centrifugation step at 20,800 g for 5 min. Serum was then stored in aliquots at –20°C or at 4°C with 0.05 % azide as a preserving agent.

2.7.2 Assessment of antibody reactivity by ELISA

The specificity of antisera for the immunising antigen was tested by ELISA using immobilised antigen. ELISAs were performed in 96-well plates (Nunc Maxisorp) at room temperature. Plates were coated by overnight incubation with antigen and an irrelevant Fc fusion protein control as a negative control (to assess whether reactivity was against the required antigen as opposed to the human IgG1 Fc domain) dissolved in coating buffer (15 mM Na_2CO_3, 34 mM $NaHCO_3$ pH 9.3; 50 µl/well). The following day, wells were washed three times with PBS then once with washing buffer (PBS, 0.05% v/v Tween 20) before a final wash with PBS alone. Non-specific binding was blocked using blocking buffer (PBS, 1% w/v BSA. 0.05% Tween 20), 200µl per well, incubating for 2 h. Wells were washed as before then incubated with serial

dilutions of antiserum and preimmune serum in washing buffer, 50µl per well for 1 h. The plate was washed as before prior to detection of bound antibody using an HRP-conjugated secondary antibody, raised in goat against the primary species (1:4000), 50µl per well for 1 h. Wells were washed again prior to detection using 100µl per well O-phenylenediamine substrate (OPD). The reaction was quenched by addition of 2.5 M H_2SO_4 (100µl per well) after approximately 20 min and absorbance at 490nm measured in a BioRad microplate reader.

2.8 Generation of Monoclonal Antibodies Against Mouse LYVE–1

2.8.1 Testing of sera for myeloma culture

Test batches of foetal bovine serum (Australian origin) for myeloma culture were ordered from GIBCO in order to establish which serum was most efficient in supporting myeloma and hybridoma growth, permitting the growth of a colony from a single cell.

Mouse myeloma NS-1 and rat myeloma Y3 cells were diluted in RPMI supplemented with 10% test-serum and Glutamine/Penicillin/Streptomycin to theoretical densities of 1 cell/well and 5 cells/well of 96 well plate, 100µl per well. The FBS was deemed suitable if 100 % of wells at a density of 5 cells/well and over 90 % of wells at a density of 1 cell/well supported colonies after 12 days in culture. Sera from batches 3135881S and 3597502S were found to support myeloma growth at these cell densities and therefore used during the course of this thesis. Aliquots of sera were stored at -20°C until required. Medium supplemented with sera was stored at 4°C and any remaining after one week was discarded.

2.8.2 Immunisation

The antigen used for immunisation was a soluble fusion protein of mouse LYVE-1 and the Fc domain of human IgG_1 Female DA strain rats were immunised with purified LYVE-1 Fc fusion protein (100 µg) in complete Freund's adjuvant followed by two boosts in incomplete Freund's adjuvant. Test bleeds were taken by tail bleed one week after the booster injections and tested in ELISA as described below. A final boost without adjuvant in PBS alone was given three days before the sacrifice of the animal, to prepare the spleen for fusion.

2.8.3 Testing the titre of antisera

The reactivity of the antiserum with immunising antigen was tested by ELISA as described in detail in section 2.7.2. Briefly, plates were coated with 5 µg/ml LYVE-1 Fc or podoplanin-Fc as a negative control and were incubated with preimmune serum and serum from the immunized animals, followed by HRP-conjugated goat anti-rat IgG. (1:4000) and O-phenylenediamine (OPD) substrate.

2.8.4 Hybridoma fusions

One immunised animal was sacrificed by carbon dioxide and the spleen removed. Splenocytes were carefully drawn out using curved forceps and resuspended in GKN isotonic buffer (NaCl, 137 mM; KCl, 5.37 mM; Na_2HPO_4, 10 mM; $NaH_2PO_4.H_2O$, 5 mM, Glucose, 11 mM in water, filter sterilised) and passed through a cell strainer. Half of the splenocytes from a rat were used per fusion; the remainder were cryo-preserved in freezing solution, as described above. Splenocytes for the fusion were centrifuged at 100 g for 5 min in a Heraeus Labofuge 400 centrifuge and then counted (approximately 1.2×10^8). Cultures of the myeloma fusion partner (either NS-1 or Y3) which had been split 1:40 three days earlier were centrifuged twice in the same manner following a cell count, aspirating off the supernatant and resuspending the cells in GKN buffer between each centrifugation step. Typically 7×10^7 myeloma cells were used so that the ratio of spleen cells to myeloma cells was 1:2 in favour of splenocytes whilst using about 10 % more

myeloma cells than necessary (1.2:2.0) to compensate for losses incurred in the centifugation and aspiration steps. The splenocytes and NS-1 suspensions were combined and the mixture was incubated at 37 °C for 5 min before centrifuging (5 min at 100 g). The cell pellet was loosened by gentle tapping and 1 ml of pre-warmed Polyethylene Glycol (PEG) was added slowly for 1 min while stirring the cells with a pipette and then continuing stirring for a further minute. During this procedure the cells were kept warm by holding the tube in a beaker of water heated to 37°C. Subsequently, 1 ml of GKN buffer was added drop by drop over a period of 1 min, followed by another 1 ml GKN buffer for 1 min. Then 8 ml GKN buffer was added at a rate of 1 drop per sec, stirring after each minute. The cell suspension was topped up to 50 ml with GKN buffer and centrifuged at 50g for 5 min without braking. Cells were resuspended in RPMI supplemented with 20 % FBS and Pen/Strep. 1 ml of cell suspension was added to each well of a 24-well dish in a total of 4 dishes. Cells were grown for 4 h before the addition of 1 ml/well of 2x HAT in RPMI supplemented with 20 % FBS and Pen/Strep. Hybridomas were grown for two weeks before screening for positive clones.

2.8.5 Screening of hybridomas for production of antibodies against LYVE-1

Two different procedures were used to screen hybridoma supernatants for the presence of anti-LYVE-1 mAbs.

2.8.5.1 293T-mouse LYVE-1 transfectant assay

293T-Mouse LYVE–1 transient transfectants fixed on cytospin slides were used, prepared as described in section 2.9.2. Non-specific binding to cells was blocked by incubating with 10 % goat serum in PBS for 10 min. Supernatant from wells containing hybriomas was applied to each slide and incubated at room temperature for 30 min. In parallel one slide was incubated with rat IgG, 10 µg/ml in PBS-5% FCS as a negative control and another slide with rat anti-mouse LYVE-1 antiserum as a positive control, diluted 1:50 in PBS-5 % FCS. Slides were washed in PBS prior to application of the secondary antibody, goat anti-rat Alexa 488, 10 µg/ml in PBS-5 % FCS, for 30 min. Slides were washed in PBS and then fixed in formaldehyde, 2 % in PBS and covered with Vectashield with DAPI and a coverslip.

2.8.5.2 ELISA

The reactivity of the hybridoma supernatant against mouse LYVE-1 Fc fusion protein was tested by ELISA, in a similar manner to that in which reactivity of polyclonal antisera was assessed (section 2.7.2). Plates were coated with 5 µg/ml LYVE-1 Fc and incubated with undiluted hybrioma supernatant. A negative control of supernatant from a well with no hybridoma growing in it was included, as was a positive control of the rat serum, diluted 1:50 in RPMI-20 % FBS medium. Wells were then incubated with an HRP-conjugated goat anti-rat IgG. (1:4000) and O-phenylenediamine (OPD). Substrate absorbance at 490nm was measured in a BioRad microplate reader.

2.8.6 Re-cloning hybridomas

To ensure that a hybridoma was monoclonal, cells were diluted in supplemented medium to theoretical densities of 1 cell/well and 5 cells/well in 96-well plates, 100µl per well. Cells were cultured for one week prior to re-screening of supernatant for presence of LYVE-1 mAbs using both of the assays described above. Positive colonies were then re-cloned again in the same manner.

2.8.7 Ig subtyping of LYVE-1 monoclonal antibodies.

The subtype of the LYVE–1 mAbs was determined by ELISA using a commercial rat-hybridoma subtyping assay (BD Pharmingen), according to manufacturers' instructions. Briefly, ELISA plates were coated with mouse anti-rat subtype specific Ig, then incubated with hybridoma supernatant followed by HRP-conjugated mouse anti-rat antibodies and detected using *O*-phenylenediamine substrate (OPD).

2.8.8. Culture of hybridomas and purification of antibody

Hybridomas were cultured in RPMI-1640 supplemented with 20% FBS, 1x HT (see section 2.1.4), Penicillin/streptomycin and L-Glutamine in tissue culture flasks. For large-scale production of monoclonal antibodies, hybridoma supernatants were passed through 2 ml columns of protein G Sepharose. The columns were washed with PBS and bound mAb eluted with 0.1 M Glycine

pH 2.0 (500 µl fractions). Eluted fractions were neutralised with 100 µl 2 M Tris pH 8.0 and the purified antibody subsequently buffer exchanged into PBS by dialysis or by means of microcon concentrator tubes (Millipore) by Alastair Waugh, MRC Human Immunology Unit, WIMM. Antibody preparations were stored in aliquots at –80°C (long term) or 4°C (short term).

2.9 Immunohistochemistry and Immunofluorescence Antibody Staining

2.9.1 Source of tissue sections

2.9.1.1 Frozen human skin sections

Frozen sections of human squamous cell carcinoma were kindly donated by Graham Ogg, Weatherall Institute of Molecular Medicine, University of Oxford, UK.

2.9.1.2 Paraffin-embedded mouse tissues

Tissues from C57Bl/6 mice were kindly donated by Dr. Ian Dransfield, MRC Centre for Inflammation Research, University of Edinburgh, UK. Mouse tissues were fixed in PBS 4% paraformaldehyde. Tissues were embedded in paraffin wax and cut on silanized glass microscope slides, both manipulations being performed by Simon Bidolph, Department of Paediatric Pathology, John Radcliffe Hospital, Oxford.

2.9.1.3 Mouse frozen tissue sections

For frozen sections, tissues from Balb/c mice were snap-frozen on dry ice, cut into 8 µm sections using a cryotome and air-dried overnight before wrapping in aluminium foil for storage at –20°C.

2.9.2 Preparation of cytospin slides

Adherent cells were lifted with PBS- 5 mM EDTA, centrifuged at 1300 RPM for 4 min and then resuspended in PBS. Non-adherent cells were simply centrifuged and resuspended in PBS. Approximately 7 x 10^5 cells/ml suspension was placed on ice and three drops were applied to a cytospin bucket and centrifuged at 550 RPM for 5 min to transfer cells on to a Superfrost slide. Cells were fixed in acetone for 10 min and slides were stored wrapped in aluminium foil at – 80°C.

2.9.3 De-waxing and antigen retrieval of paraffin-embedded sections

Prior to staining, sections were dewaxed and rehydrated by successive incubation in Citroclear® (2 x 6 min), 100 % Ethanol (2 x 5 min), 50 % aqueous Ethanol (5 min) and water (5 min). Slides were then subjected to antigen retrieval by microwave treatment (95-100°C, 10 min) in DAKO Target Retrieval Solution pH 6.0. A glass staining jar was filled with sufficient quantity of buffer (approx. 400 ml) covered with SaranWrap and heated to 95-100°C in a microwave (4 min 750 W). The de-waxed slides were placed in buffer, briefly brought back to the boil by heating for 1 min at 750 W and then heated at 80 W for another 9 min. Slides were then transferred to PBS (at room temperature).

2.9.4 Single immunoperoxidase staining

Slides of paraffin-embedded sections of mouse tissues were de-waxed, rehydrated and subjected to antigen retrieval as described above. Slides were then washed in PBS and blocked in PBS 20% goat serum for at least 5 min. Endogenous peroxidase activity was blocked by a 5 min pre-incubation in a peroxidase quenching agent (DAKO, contains 0.03% H_2O_2) prior to incubation with the primary antibody, rat anti-mouse LYVE–1 monoclonal antibody in PBS 5% FCS for 30-45 min at room temperature. Controls included staining with rat IgG isotype control. After washing with PBS, slides were incubated with HRP-conjugated goat anti-rat Ig (DAKO Envision kit) for 30-35 min. After another wash step, slides were developed with diaminobenzidine (DAB; Envision kit) and counterstained with hematoxylin. Finally, slides

were mounted in Aquamount®, viewed under a Zeiss microscope and photographed using a ProgRes camera and software.

2.9.5 Flow cytometry

Adherent cells, either endothelial cells or 293T, were lifted in either PBS-5 mM EDTA by gentle pipetting following a 15-min incubation at 37°C or by Accutase, following a 5-min incubation at 37°C. Cells were transferred to 96 (U-shaped) well plates (≈ 2 x 10^5 cells/well). The cells were pelleted by centrifugation of the plate (380 g for 3 min), resuspended in FACS buffer (PBS, 5% FCS, 0.1% azide), 100 µl/well, and centrifuged again. Cell pellets were then resuspended in FACS buffer, 100 µl/well containing the appropriate primary antibody at 10 µg/ml and incubated for 30 min at 5°C with gentle shaking. Controls included staining with an isotype-matched antibody. Cells were centrifuged as before and washed by resuspension in 200 µl FACS buffer and centrifuged again. After centrifugation, cells were resuspended in 100 µl FACS buffer containing the secondary antibody, an AlexaFluor 488 conjugate at 1:200 and incubated for 30 min at 5°C with gentle shaking in the dark. After a final wash in 200 µl FACS buffer, cells were resuspended in 200 µl FACS fix (2% v/v formaldehyde in PBS) and transferred to FACS tubes. Samples were stored at 4°C until required and then analysed by flow cytometry using a Becton-Dickinson FacScan, FACscalibur.

2.9.6 Immunofluorescence staining of cells

For detection of cell surface proteins, adherent cells were grown in 24-well dishes or 8 well chamber slides and stained in situ. Wells were washed with PBS and then incubated with goat serum, 10 % in PBS for 10 min. Cells were incubated in FACS buffer (PBS, 5% FCS, 0.1% azide) containing the primary antibodies at 10 µg/ml and incubated for 30 min at room temperature. Controls included staining with an isotype matched antibody or pre-immune serum. Cells were subsequently washed with PBS and incubated with FACS buffer containing the secondary antibodies, AlexaFluor conjugates at a concentration at 1:200, for 30 min at room temperature in the dark. After a final wash, cells were fixed in 2% formaldehyde for 10 min. After removal of

the formaldehyde solution, cell were washed with PBS and then a drop of fluorescent mounting medium with DAPI (Vectashield®) was added and the cell layer was covered with a cover slip. When chamber slides were used, the plastic chamber walls were lifted from the slides by soaking in 80% methanol for 10 min. Slides were subsequently covered with fluorescence mounting medium and a cover slip. Cells were then viewed under a Zeiss Axioskop microscope equipped with epifluorescence illumination.

2.9.7 Staining of intracellular antigens

For detection of intracellular antigens, adherent cells were first permeabilised as follows. Cells were fixed by incubation in freshly prepared 4% (w/v) paraformaldehyde in PBS for at least 10 min at room temperature. Cells were then washed with PBS and incubated in permeabilisation buffer (PBS, 0.2 % saponin, 1% BSA, 10 % goat serum) for 20 min at room temperature. Cells were stained as normal, except that incubations with the primary and secondary antibodies were carried out for 45 min and all antibody incubations were performed in permeabilisation buffer.

For tracking TNFα-mediated LYVE-1 internalisation, cells in chamber slides were pre-incubated for 2h at 37°C with rabbit anti-human LYVE-1, 10μg/ml and TNFα, 10ng/ml. Cells were then permeabilised as detailed above and stained using the appropriate markers for subcellular compartments.

To stain nuclei for Prox-1, cells were fixed by incubation in freshly prepared 4% (w/v) paraformaldehyde in PBS for 20 min at room temperature, washed with PBS, permeabilised by incubation in 0.5% (v/v) Triton X100 in PBS for 5 min at room temperature and then washed in PBS again. Following a 5 min incubation in blocking buffer (4% (w/v) BSA and 5% goat serum in PBS) at room temperature, cells were incubated in the same buffer overnight at 4°C with rabbit anti-prox-1. The following day, cells were washed with PBS and incubated for 30 min in the presence of the secondary antibody (1:200) goat anti-rabbit AlexaFluor®594 in blocking buffer. Cells were washed in PBS and then fixed in 2% (v/v) formaldehyde in PBS for 10 min. After removal of the

formaldehyde solution, cell were washed with PBS and then a drop of fluorescent mounting medium with DAPI (Vectashield®) was added and the cell layer was covered with a cover slip. Cells were viewed under a Zeiss Axioskop microscope.

2.9.8 Whole mount staining of mouse ears

The ventral and dorsal surfaces of the ear were gently peeled apart to reveal the dermis and then laid dermal-side down in wells of a 24-well dish and fixed in 1 ml/well paraformaldehyde, 4 % (w/v) in PBS, pH 7.5, overnight at 5°C with gentle agitation. The following day, ears were washed in 0.3 % Triton X-100 in PBS for approximately 5 h at 5°C with gentle agitation, changing the buffer every hour after an initial brief wash. Tissue was washed briefly in blocking buffer (3 % skimmed milk powder in 0.3 % Triton X-100 in PBS) and then incubated for 2 h at room temperature in blocking buffer. The primary antibodies were then applied at 10 µg/ml in blocking buffer, 500 µl/well and tissue was incubated overnight at 5°C with gentle agitation. The following day, tissue was washed as before for about 5 h prior to a 2h incubation at room temperature in the dark in blocking buffer with secondary antibodies (1:200) conjugated with the appropriate AlexaFluor dye. Tissue was then washed as before and placed dermis side up on a Superfrost microscope slide, lowering on to a coverslip with Vectashield® and sealing using nail polish. Slides were stored at 4°C in the dark until viewed by confocal microscopy.

2.9.9 Confocal microscopy

Confocal microscopy was performed using a Bio-Rad Radiance 2000 laser scanning confocal microscope equipped with argon and green helium/neon lasers and analysed using LaserSharp2000 software. Cells were stained as for normal immunofluorescence microscopy and images taken in sequential scanning mode whereby each fluorophore is excited and analysed separately to prevent bleed-through of different fluorophores. Whole mount sections were visualised by XY scanning in LaserSharp2000 to create multiple layers, which were subsequently projected into one image.

2.10 Animal Procedures

2.10 1 Animals

All animals were maintained in the Biomedical Services Facility at the John Radcliffe Hospital, Headington, Oxford. The strains used were Balb/c mice, DA rats and New Zealand white rabbits.

2.10.2 Mouse ear explants

Male mice aged 8 weeks and older were euthanised by rising concentration of CO_2. Ears were then removed, incubated in 5X penicillin-streptomycin on ice for 30 min, split into dorsal and ventral halves and each floated split-side (dermis) down in RPMI 1640-10% FCS, penicillin-streptomycin and glutamine. Explants were cultured in a humidified atmosphere at 37°C in 5% CO_2, in either the presence or absence of recombinant murine TNFα, 100ng/ml.

2.10.3 Elicitation of oxazolone-induced contact hypersensitivity in mice

Balb/c male mice aged 8-10 weeks were sensitised by topical application of 3% (w/v) oxazolone (4-ethoxymethlene-2 phenyl-2-oxazoline-5-one, purchased from Sigma) in 95% ethanol to the shaved abdomen, 50µl per mouse. The following day a further 100µl of 2.5% (w/v) oxazolone was applied to each mouse. Five days later the outside of the left ears were challenged by topical application of 0.5% (w/v) oxazolone solution, 50 µl per ear, whilst the right ears were treated with vehicle alone.

CHAPTER 3

Generation of Monoclonal Antibodies against Mouse LYVE-1

3.1 Introduction.....140

3.2 Results.....144

3.3 Discussion.....167

3.1 Introduction

In 1975 Kohler and Milstein succeeded in maintaining an antibody-secreting cell in culture, exploiting the properties of transformed myeloma cells to confer immortalisation on primary spleen cells by somatic cell hybridisation or cell fusion. Thus hybrid clones or "hybridomas" were generated from individual B lymphocytes from a mouse immunised with a specific antigen, with each hybridoma producing a single monoclonal antibody against the predefined antigen.

Since the early 1970s the quest for isolating a homogeneous population of antibodies by creation of a hybridoma cell line sought to address three important technical difficulties. Firstly, an appropriate fusion partner was necessary. Myelomas (B-cell tumours) can be induced by intraperitoneal injection of mineral oil and once isolated may be immortalised to continue dividing *in vitro.* These cells may also be selected to yield a line which does not produce functional antibodies, as the transformation process that gives rise to these tumours results in cells secreting antibodies of unknown specificities, which could lead to the production of a hybridoma secreting more than one type of antibody. Secondly, the conditions for a successful fusion had to be determined. Initially SV40 was used to trigger fusion of the plasma membranes between two adjacent cells but this method has given way to the use of polyethylene glycol (Pontecorvo 1975). Thirdly, hybrid cells must be selected from a background of unfused cells. Spleen cells from the immunised animal are easily eliminated as they are not immortalised and cannot survive for more than one or two weeks in culture. However the myeloma cells will continue to divide, whether or not they have fused and due to their smaller karyon will rapidly out-compete the hybrid cells, which are in the minority. To achieve effective killing of unfused myeloma cells

these cells are selected to have a mutation in one of the enzymes of the salvage pathway of purine nucleotide biosynthesis (Littlefield 1964). If aminopterin, a folic acid antagonist that inhibits purine and pyrimidine nucleotide biosynthesis is added to the medium, *de novo* synthesis is blocked and these cells will die (figure 3.1). Such selected myeloma cells can only be rescued if they have successfully fused with a wild type spleen cell. The hybrid must then use the salvage pathway, which relies upon hypoxanthine and thymidine, supplied in the medium.

Monoclonal antibodies have three main advantages over polyclonal antibodies derived from the sera of immunised animals: they exhibit a single binding specificity, are biochemically homogeneous and are potentially in endless supply. Whilst immunisations of multiple animals are required to generate polyclonal antibodies, an established hybridoma cell line can go on producing antibodies against a specific epitope of the antigen for the lifetime of that cell line.

Previous studies into the expression of LYVE-1 in human have used both polyclonal antibodies raised in rabbit and monoclonal antibodies raised in mice. Antisera to mouse LYVE-1 have been raised in rabbits (Prevo et al, 2001) to demonstrate that mouse LYVE-1 antigen is an endocytic receptor for hyaluronan in 293T transfectants and a marker for lymphatic endothelium. However, a more extensive study into the physiological role of LYVE-1 *in vivo* and under various pathological conditions would benefit from the use of monoclonal antibodies to eliminate the possibility of cross-reactivity with apparently unrelated antigens, which can occur because polyclonal antiserum represents complex mixtures of antibodies of different specificities. One of the aims of this chapter was to generate a monoclonal antibody which could be used in tissue staining to detect changes in the expression of LYVE-1 during inflammation, as well as to permit

the isolation of murine primary dermal lymphatic endothelial cells from murine dermis. Such a reagent would prove invaluable to other studies detailed in this thesis and also for subsequent research.

In addition, another important requirement was to generate mAbs that could be used to investigate LYVE-1 function. Some antibodies block ligand binding, as was found to be the case with 3A, one of the human LYVE-1 mAbs generated by Dr. Remko Prevo in the same laboratory. The 3A mAb was found to block binding of HA and has been a valuable reagent for defining LYVE-1 function in transfected cells. Similiarly, in the case of CD44, numerous antibodies including BRIC 235, KM 81 and KM 201 have been shown to block HA-binding and these have proved invaluable in elucidating CD44 function (Lesley et al. 1993; Zheng et al., 1995). Additionally, Sherman et al. (1998) used an antibody to block the interaction of CD44 with FGF and thus demonstrated the role of CD44 in growth factor presentation and promoting limb outgrowth during development. Alternatively a mAb may induce ligand binding, as was found to be the case for IRAWB 14, dramatically inducing HA binding by some $CD44^+$ cell lines that did not constitutively bind HA (Lesley et al., 1992). Other mAbs may induce shedding of antigen, for example IM7.8.1 on CD44 (Zheng et al., 1995). An anti-mouse LYVE-1 function-blocking antibody could prove very useful in elucidating the role of LYVE-1 as an HA-binding protein under various physiological conditions and (in the case of a shedding-inducing antibody) the significance of membrane bound or soluble LYVE-1.

This chapter describes the generation of two mAbs against mouse LYVE-1 and a series of assays in which the various properties of these antibodies were explored.

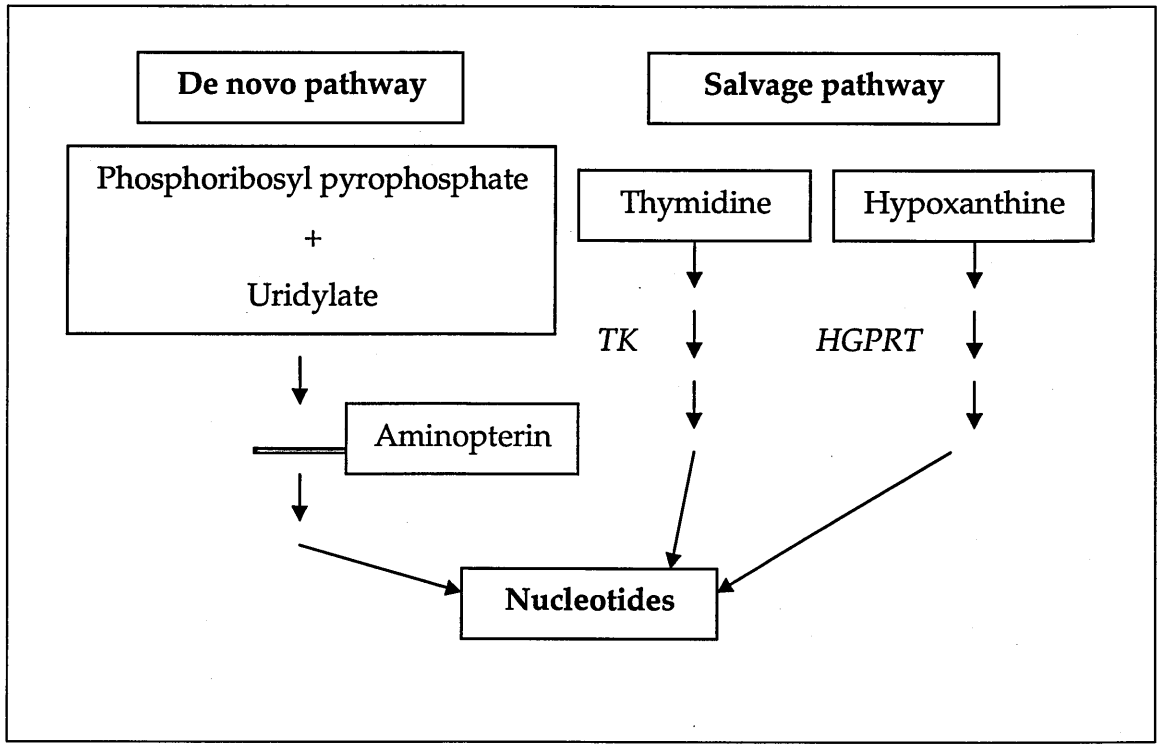

Figure 3.1 Selection of hybridomas through defects in nucleotide biosynthesis. Both the myeloma cells and splenocytes can synthesize purine nucleotides and thymidylate de novo from phosphoribosyl pyrophosphate and uridylate respectively in several steps. One of these steps involves the transfer of a methyl or formyl group from activated tetrahydrofolate. Aminopterin blocks the reactivation of tetrahydrofolate and thus inhibits the de novo pathway. Cells must then use the salvage pathway in which thymidylate is synthesized from thymidine using thymidine kinase (TK) and purine is synthesized from exogenously supplied hypoxanthine using the enzyme hypoxanthine-guanine phosphoribosyltransferase (HGPRT). Myeloma cells are defective in TK through selection in bromodeoxyuridine, which is metabolized by TK to form a toxic product. Similarly they are defective in HGPRT through selection in thioguanine or azaguanine, analogues of normal metabolites that function as substrates for HGPRT but give rise to non-functional purines. Thus such cells cannot grow in hypoxanthine-aminopterin-thymidine (HAT) medium unless "rescued" by their splenocyte fusion partner that possesses TK and HGPRT.

3.2 Results

3.2.1 Immunisation of rats and testing of antisera

Prior to the start of this PhD, a 694-bp LYVE-1 fragment encoding the cleavable NH_2 terminal leader and extracellular domain of mouse LYVE-1 was amplified from mouse stomach cDNA and cloned into the IgFc vector pCDM7Ig (Prevo et al., 2001). This yielded a construct encoding amino acid residues 1-228 of the LYVE-1 sequence, fused at the COOH terminus with the 234-residue hinge, CH2 and CH3 region of human IgG_1 (figure 3.2). This construct had proved immunogenic in rabbits and polyclonal antisera against LYVE-1 had been successfully raised. Hence it was used here in the immunisation of rats to generate monoclonal antibodies against mouse LYVE-1. The fusion protein was produced by transfecting the construct into human 293T cells using calcium phosphate and then purifying the secreted protein from the supernatant by protein A–Sepharose chromatography. 2 rats were immunised with the purified protein.

Antibody responses of the rats were monitored by ELISA. A microtitre plate was coated with either LYVE-1 Fc or podoplanin Fc, an irrelevant fusion protein generated by cloning cDNA encoding the extracellular domain of podoplanin into the same construct (see appendix II), to assess the proportion of immune response which had been raised against the Fc domain of the immunogen. Serum prepared from animals following immunisation and also from the same animals before the immunisation schedule had commenced (as preimmune controls), were applied to the microtitre plate. Bound antibody was detected by peroxidase-conjugated goat anti-rat IgG and *O*-phenylenediamine (OPD) substrate and quantitated by spectrophotometry at 490 nm. As shown in figure 3.3, the antiserum from both rats showed specific reactivity to LYVE-1.

A.

```
1                                                              50
MLQHTSLVFF LASIWTTRHP VQGADLVQDL SISTCRIMGV ALVGRNKNPQ

51                                                             100
MNFTEANEAC KMLGLTLASR DQVESAQKSG FETCSYGWVG EQFSVIPRIF

101                                                            150
SNPRCGKNGK GVLIWNAPSS QKFKAYCHNS SDTWVNSCIP EIVTTFYPVL

151                                                            200
DTQTPATEFS VSSSAYLASS PDSTTPVSAT TRAPPLTSMA RKTKKICITE

201                                                            250
VYTEPITMAT ETEAFVASGA AFKNEAAGFG GVPTALLVLA LLFFGAAAVL

251                                                            300
AVCYVKRYVK AFPFTTKNQQ KEMIETKVVK EEKADDVNAN EESKKTIKNP

301
EEAKSPPKTT VRCLEAEV
```

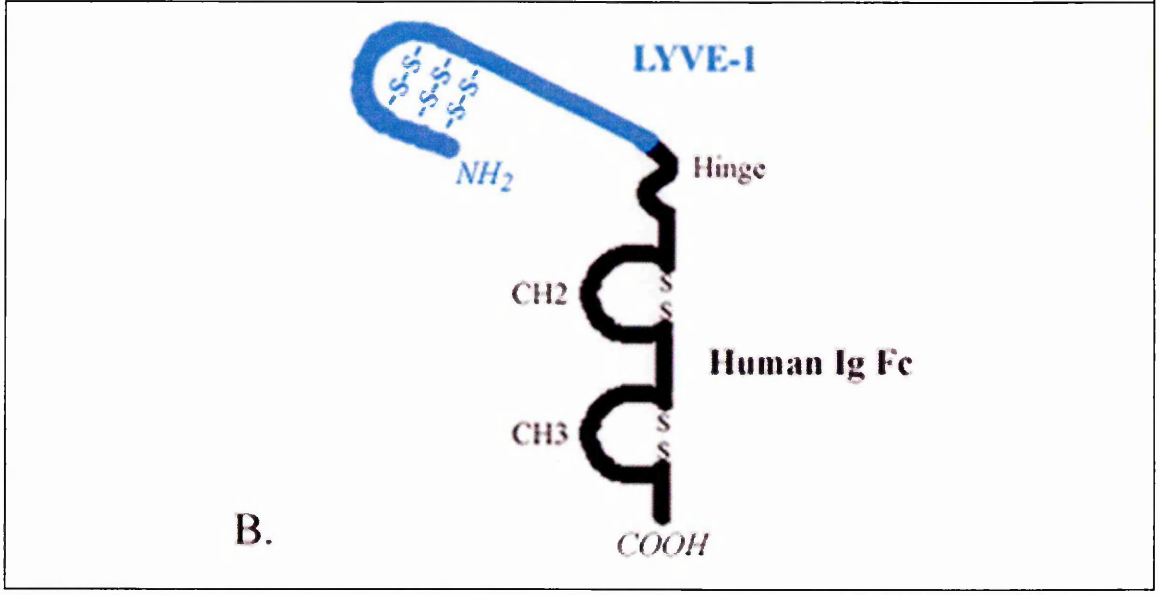

Figure 3.2 Schematic representation of the LYVE-1 Fc construct used for mAb production. Panel A shows the amino acid sequence for mouse LYVE-1. The N terminal leader and C-terminal transmembrane anchor are underlined and residues within the HA-binding Link module are shown in red. Amino acid residues 1-228 of the LYVE-1 sequence encoding the cleavable NH_2 terminal leader peptide and the extracellular domain are highlighted in yellow. Panel B shows the fusion protein resulting from cloning this 228-residue sequence into pCDM7 Ig. LYVE-1 sequence was fused at the COOH terminus with the 234-residue hinge, CH2 and CH3 region of human IgG_1, producing a soluble product when transfected into 293T fibroblasts.

In the case of rat 2, binding of the immune sera remained maximal even at a dilution of 1:10000, whereas binding of the pre-immune sera was negligible beyond 1:5000. Immune serum from rat 1 exhibited a much lower titre, apparent only at dilutions less than 1:2000. Hence rat 2 was chosen for hybridoma generation.

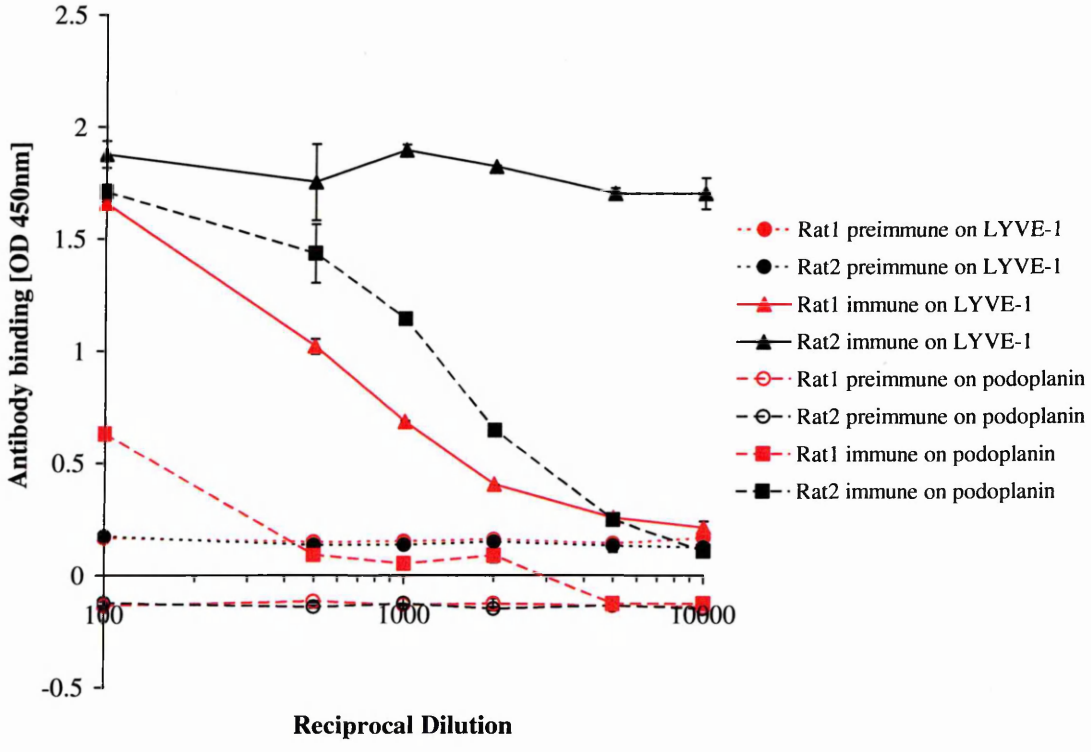

Figure 3.3 Test bleed of mouse LYVE-1Fc immunised rats. Sera from both rats, from either the preimmune test bleed (negative controls) or from the test bleed taken a week after the final immunisation, were serially diluted and applied to a microtitre plate precoated with either LYVE-1-Fc or podoplanin-Fc at 5 μg/ml. Bound antibody was detected with HRP-conjugated goat anti-rat antibody and OPD substrate, measuring the absorption at 490nm. Values are the mean ± standard deviation for triplicate wells.

3.2.2 Generation and screening of hybridomas

Two potential fusion partners for rat splenocytes were available, the mouse myeloma cell line NS-1 and the rat myeloma cell line Y3 (kindly provided by Dr. Mike Puklavec, Sir William Dunn School of Pathology, Oxford). To select the optimal fusion partner, mock fusions were carried out, using splenocytes from a naïve rat and either NS-1 or Y3. Cells from each fusion were plated out in four 24-well dishes and after 12 days the number of hybridomas was counted. From the NS-1 fusion, multiple hybridomas were visible in some wells, with 91% of wells containing a least one colony. In contrast only 9% of wells from the Y3 fusion contained hybridoma colonies. Therefore NS-1 was shown to be the optimal fusion partner with the respect to the number of successful fusion events and resulting colonies. However, as NS-1 are derived from murine myeloma, the fusion is cross species and whilst such a hybridoma is establishing a stable karyotype, a loss of chromosomes can occur which may result in the inability to secrete antibodies. Indeed before committing to a fusion the splenocytes from rat 2 with higher serum titre against LYVE-1, a fusion between splenocytes from rat 1 was performed with NS-1. 96% of wells in four 24-well plates contained one or more hybridomas and supernatants from the wells were assayed by ELISA in a microtitre plate coated with LYVE-1 Fc fusion protein. However no secretion of antibodies (either against LYVE-1 or the Fc portion) was detected (data not shown). Therefore Y3 were used as the fusion partner for rat 2 splenocytes for despite yielding a lower number of successful fusion events, this myeloma line was derived from the same species.

A final booster injection was administered to the rat three days before sacrifice. Half of the splenocytes were fused with Y3 cells as described in Methods and Materials; the remaining half were cryopreserved and then used for a second fusion at a later date. Cells from each fusion were plated out in four 24-well

plates and cultured for two weeks. From each fusion, seven wells from a total of 96 contained hybridomas. Supernatant was screened by immunofluorescence against human 293T fibroblasts transiently transfected with mouse LYVE-1. Cytospin slides of these cells were prepared and hybridoma supernatant was applied. Bound antibody was detected using the AlexaFluor® 488 goat anti-rat IgG, staining nuclei with DAPI to aid visualisation by fluorescence microscopy. This method had the advantage that hybridomas secreting antibodies against the Fc domain would not give a positive result in this assay. Figure 3.4 shows the staining of LYVE-1 transfectants by supernatant from an antibody-secreting hybridoma and also by the positive control of rat polyclonal antiserum, whilst a non-secreting hybridoma (the negative control) showed no staining.

An ELISA was also carried out, coating a microtitre plate with LYVE-1 Fc and applying the hybridoma supernatants. Bound antibody was detected by peroxidase-conjugated goat anti-rat IgG and *O*-phenylenediamine (OPD) substrate and quantitated by spectrophotometry at 490 nm. The comparative absorption values are shown in figure 3.5.

Two hybridomas from the first fusion and one hybridoma from the second showed reactivity against LYVE-1. Samples of these were cryopreserved; however unfortunately one of the hybridomas (A4) from the first fusion stopped growing, most probably due to chromosome instability and was abandoned. The remaining two hybridomas, B1/10 and C1/8 were cloned twice by limiting dilution and expanded. These were isotyped by ELISA and found to be IgG1 kappa and IgG2a kappa respectively (data not shown). Both hybridomas were grown in large scale culture and the antibodies purified from conditioned media by protein G-Sepharose chromatography.

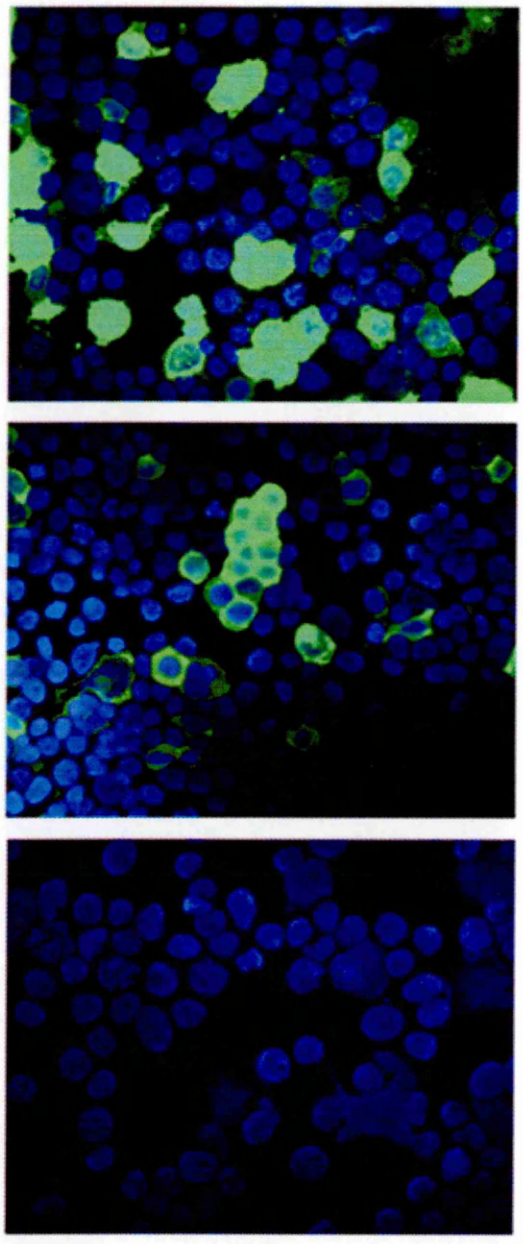

Figure 3.4 Screening hybridomas for binding to 293T-LYVE-1 transfectants by immunofluorescence microscopy. Positive transfectants were identified by supernatant from an anti-mouse LYVE-1 secreting hybridoma and goat anti-rat AlexaFluor 488 (upper panel) or by rat anti-mouse LYVE-1 polyclonal serum (positive control, middle panel). However, supernatant from a negative hybridoma failed to stain any cells (lower panel). Nuclei were stained with DAPI (blue).

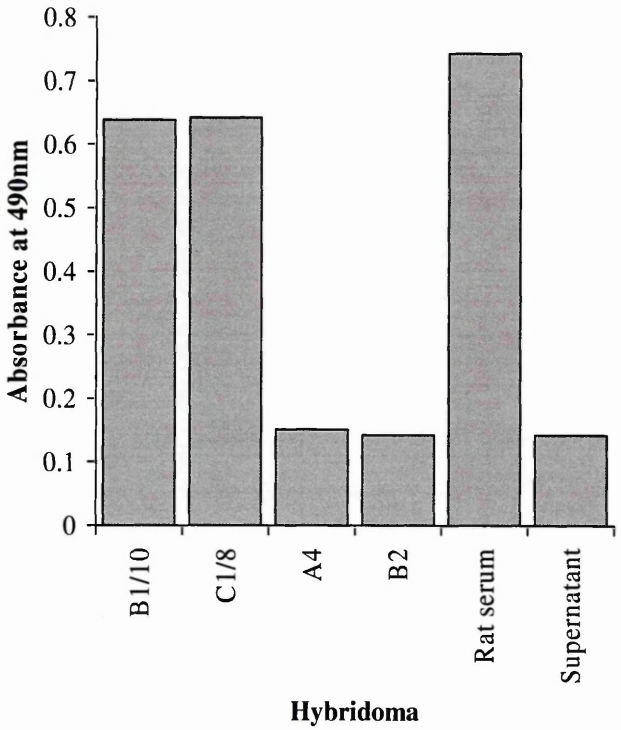

Figure 3.5 Screening hybridomas by ELISA. The supernatants from the anti-LYVE-1 secreting hybridomas B1/10 and C1/8 were applied to a microtitre plate precoated with LYVE-1Fc fusion protein, alongside supernatant from the A4 hybridoma which had ceased to secrete antibody and B2, a hybridoma which had tested negative in the transfectant assay. The positive control included in this assay was the rat serum from the final bleed out, diluted 1:50 in PBS-0.05% Tween20. The negative control was supernatant taken from a well where no hybridoma was growing. Values are the mean absorbances at 490nm, ± standard deviation for triplicate wells.

3.2.3 Assessing the LYVE-1 mAbs for immunoperoxidase staining of paraffin sections

The main purpose of generating mAbs against mouse LYVE-1 was to obtain a marker for detecting lymphatics in tissue sections which would avoid background non-specific binding artefacts associated with polyclonal antisera and permit greater flexibility when carrying out double-staining. The ability to survey LYVE-1 expression on lymphatics on paraffin sections would be particularly useful as embedding formalin-fixed sections in paraffin has been used extensively to preserve tissue structure even when stored for long periods of time at room temperature. Although some antigens have proved sensitive to the fixation procedure, human LYVE-1 proved to be still readily detected by both polyclonal sera and monoclonal antibodies and consequently it was predicted that the antibodies generated against mouse LYVE-1 would prove as effective.

To assess the reactivity of the mAbs against paraffin-fixed antigen, paraffin sections of mouse intestine and stomach were de-waxed and rehydrated, then heated treated with DAKO target retrieval solution pH 6.0. After treatment slides were stained with either B1/10, C1/8 or rat IgG isotype-matched control, followed by HRP-conjugated rabbit anti-rat Ig and DAB substrate to detect bound antibody. General tissue structure was stained using hematoxylin. As shown in figure 3.6 both B1/10 and C1/8 showed strong staining of vessels with collapsed lumens, the classic morphology of lymphatic vessels.

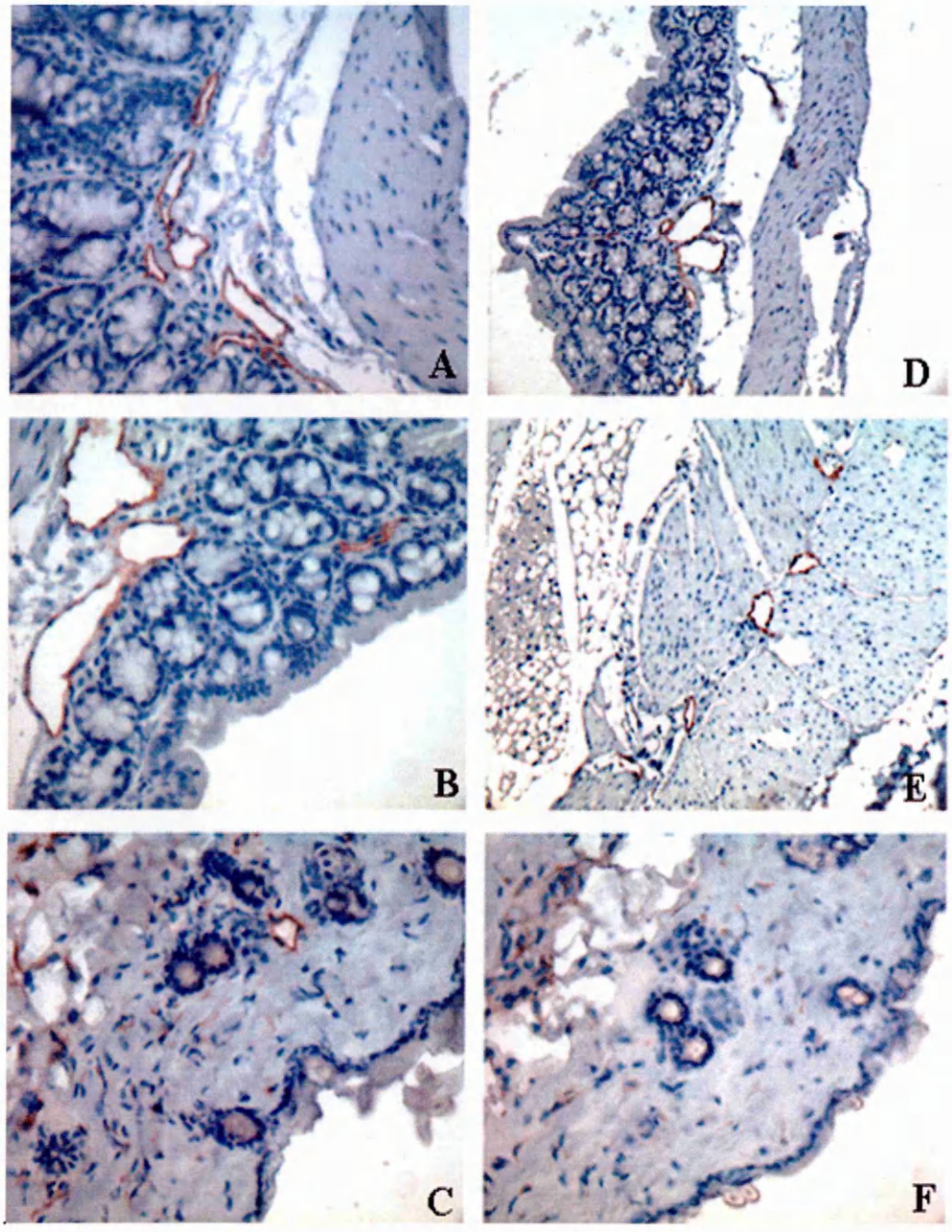

Figure 3.6 Specificity of mAbs B1/10 and C1/8 for immunohistochemical staining of LYVE-1 in paraffin sections. Mouse intestine and stomach tissue sections were dewaxed, rehydrated and retrieved prior to staining using either B1/10 (panels A, B and C), C1/8 (panels D and E) or an irrelevant rat IgG isotype control (panel F). Sections of intestine are shown in panels A, B and D; stomach sections are shown in panels C, E and F. Images were captured at either 200X magnification (panels A, D and E) or 400X (panels B, C and F).

3.2.4 Immunofluorescence staining using the newly generated mAbs

The ability of the mAbs to specifically stain lymphatic endothelium was confirmed by double staining with the lymphatic endothelium marker podoplanin. Frozen sections of 8μm thickness were prepared from mouse ear and stained with C1/8 and the hamster anti-mouse podoplanin monoclonal antibody 8.1.1. The AlexaFluor conjugates of goat anti-rat 488 and goat anti-hamster 568 were used to detect bound primary antibodies and revealed complete colocalisation of the C1/8 antigen with podoplanin (figure 3.7, panels A-C). Staining with the hamster anti-podoplanin antibody required fixation in paraformaldehyde (PFA) and therefore to investigate whether or not C1/8 was as effective on frozen tissue that had not been fixed, double staining with rabbit antisera against podoplanin was also performed (figure 3.7, panels D-F). Again clear colocalisation of C1/8 antigen with podoplanin was visible and C1/8 was shown to be of use on unfixed tissue.

3.2.5 The use of C1/8 for whole-mount staining of tissue lymphatics

In recent years the staining of whole mount sections of intact tissue has been used increasingly as a powerful way to visualise in three dimensions complete vessel structures. However this technique relies on fixing the tissue in paraformaldehyde (PFA), which is known to destroy some epitopes and render the monoclonal antibodies that recognise them completely useless. If one of these antibodies proved able to recognise tissue fixed in this manner, this would permit LYVE-1 expression to be surveyed on a greater number of vessels than is permitted by frozen sections and with different combinations of other antibodies. For example the rabbit antisera against podoplanin has proved a much more reliable antibody than the hamster mAb 8.1.1 and thus for double staining a LYVE-1 antibody other than that of rabbit antiserum is required.

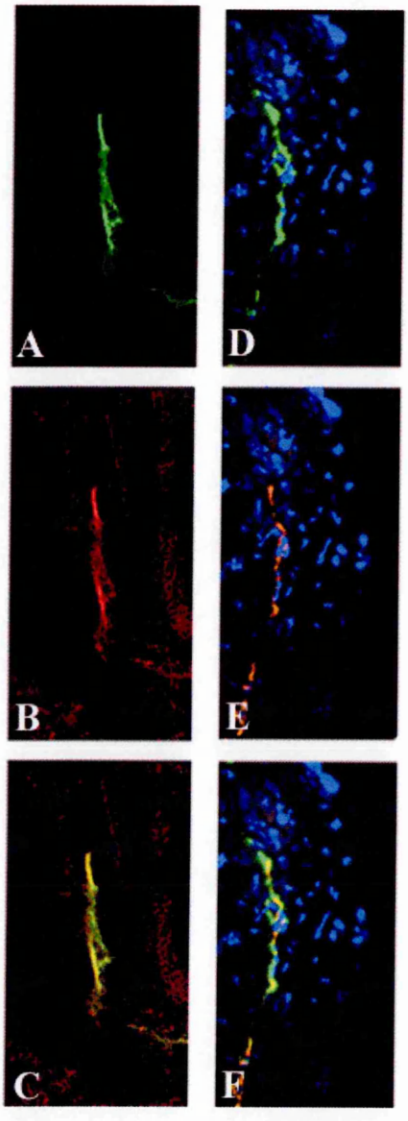

Figure 3.7 The use of C1/8 in immunofluorescence staining of frozen sections. Panels A-C: Frozen sections of mouse ear were fixed for 20 min at 4°C in PFA, blocked in 4% BSA and 5% goat serum, then stained using C1/8, 10μg/ml and the hamster anti-podoplanin mAb 8.1.1, 1:1000, detecting with the AlexaFluor® goat conjugates 488 (green) and 568 (red) respectively. Slides were then incubated in 10mM Tris-HCL for 10 min, before mounting in DAPI-Vectashield. Images were captured at 400X. C1/8 staining is shown in the top panel, 8.1.1 in the middle and a merge in the lower panel. Panels D-F: Frozen sections were stained using C1/8 and the rabbit antiserum against podoplanin, 1:800, detecting using the AlexaFluor® goat conjugates 488 (green) and 594 (red) respectively. Nuclei were stained with DAPI (blue) and images were captured by confocal microscopy at 600X.

As C1/8 had consistently shown greater binding to LYVE-1 on ELISA than B1/10 and was shown to work on PFA-fixed frozen sections (figure 3.7), whole mount staining using this mAb was attempted first as it was deemed more likely to be successful. Mouse ears were removed and immediately transferred to PFA, as described in detail in chapter 2. Tissue was permeabilised with PBS-0.3% Triton X-100 and C1/8 was applied at 10μg/ml in a blocking buffer of PBS-0.3% Triton X-100 with 3% skimmed milk powder. An AlexaFluor goat anti-rat 488 conjugate was used as the secondary detecting antibody and following mounting the tissue was viewed both with an inverted fluorescence microscope to capture images in one plane of focus only and subsequently with a confocal microscope, capturing multiple planes of focus to build up a three-dimensional image. C1/8 proved highly suitable for use in this technique, yielding strong staining of lymphatic vessels with very low background (figure 3.8, panel A). The staining pattern of C1/8 was identical to that obtained with rabbit anti-mouse LYVE-1 polyclonal antibody (figure 3.8 panel B), where the polyclonal antibody was used in double staining with a rat anti-mouse CD31 mAb and no LYVE-1 staining was visible on highly CD31-positive blood capillaries. (CD31 is expressed at higher levels by blood endothelial cells than lymphatic endothelium, (Hirakawa et al., 2003)). Thus it was shown that C1/8 is a suitable antibody for specifically staining LYVE-1 on lymphatic endothelium within whole mount ear sections. Further whole mount staining revealed that unlike most other antibodies tested, C1/8 was not sensitive to the length of fixation and still yielded clear staining in tissue fixed for as little as 3h to as long as 14 days. Hence double-staining with goat anti-ICAM-1 (which required a short fixation incubation of 3h, figure 3.8 panel C) was possible, as was staining with rabbit podoplanin antiserum (panel D), which required much longer fixation of at least 48h.

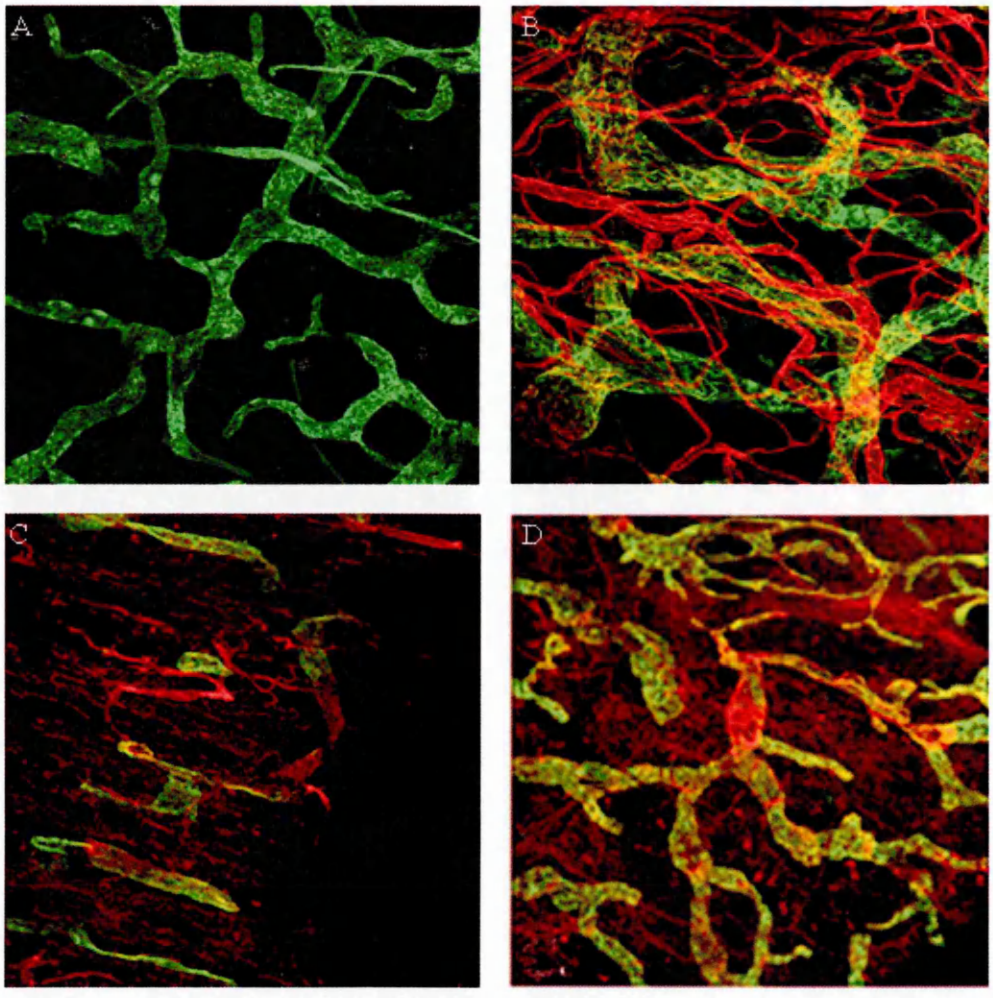

Figure 3.8 The specificity of C1/8 in whole-mount tissue staining. Mouse ear was fixed in PFA, permeabilised with Triton X-100 and stained with either C1/8 alone (panel A) or rabbit anti-LYVE-1 polyclonal antibody and anti-CD31 mAb (panel B), in combination with the AlexaFluor® conjugates 488 and 568. The LYVE-1-positive lymphatic vessels are shown in green whilst the CD31-positive blood vasculature is shown in red. Panel C shows tissue fixed for only 3h and stained with C1/8 (green) and goat anti-ICAM-1 (red) following inflammation induced by a delayed hypersensitivity reaction (detailed in chapter 6). Tissue in panel D was fixed for over 48h prior to staining with C1/8 (green) and podoplanin antisera (red). All images were captured by confocal microscopy at a magnification of 100X.

Whole mount staining of mouse ear tissue to detect LYVE-1 using C1/8 on SLC (Secondary lymphoid chemokine, 6Ckine or CCL21)-positive lymphatic vessels again reveals the specificity of C1/8, staining the individual lymphatic endothelial cells at cell-cell junctions whilst SLC appears to hold either an intracellular location or is membrane bound (figure 3.9).

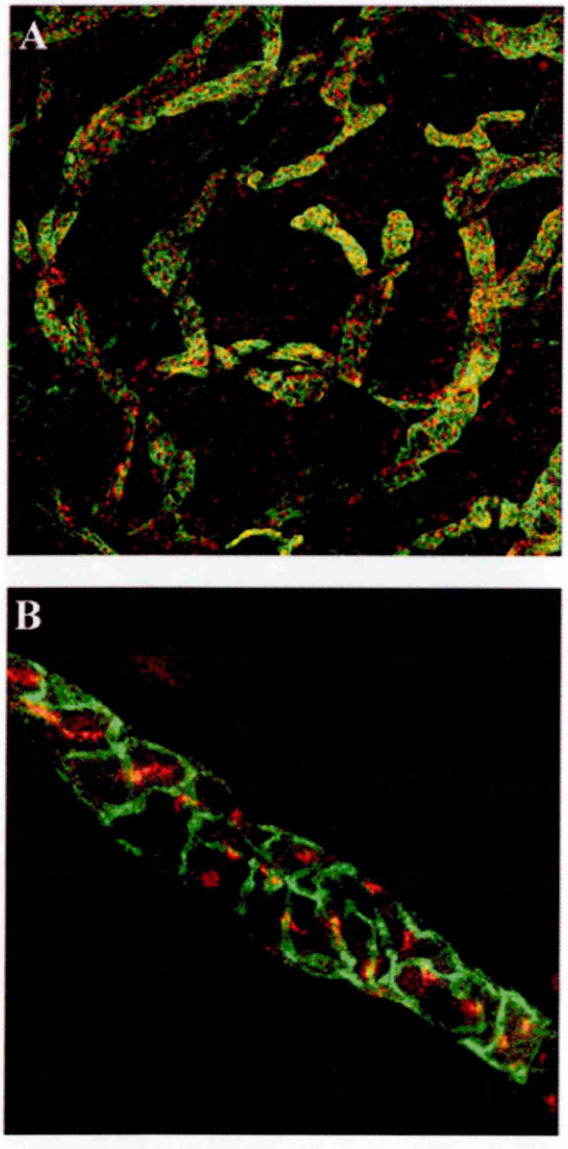

Figure 3.9 The specificity of C1/8 for SLC-positive lymphatic endothelium in whole mount tissue staining of mouse ear. Tissue was stained using goat anti-SLC (red) antisera and C1/8 (green), with the AlexaFluor® conjugates donkey anti-goat 568 and donkey anti-rat 488 respectively. Images were captured by confocal microscopy at 100X magnification (panel A) and 600X magnification (panel B), where an individual vessel can be seen.

3.2.6 Characterisation of the epitopes for LYVE-1 mAbs B1/10 and C1/8

In addition to the requirement for mAbs for use as markers for detecting lymphatics, it was of interest to carry out preliminary epitope mapping and functional assays. Mouse and human LYVE-1 share approximately 74% amino acid sequence homology and consequently it was possible that the mAbs generated here against the murine protein would cross-react with the human orthologue. An ELISA was used to test this, coating a microtitre plate with either human or mouse LYVE-1 Fc fusion proteins, then applying either B1/10 or C1/8 and detecting bound antibody using HRP-conjugated goat anti-rat antibody and *O*-phenylenediamine (OPD), quantitating by spectrophotometry at 490 nm. As shown in figure 3.10, both mAbs bound to mouse LYVE-1 in a concentration-dependent manner, attaining saturation binding at concentrations of 2.5 μg/ml and higher. However neither antibody bound to wells coated with human LYVE-1 even when tested at high concentrations (10μg/ml) and hence it was concluded that both were specific for the mouse and neither was reactive with the Fc portion. The maximum level of binding by C1/8 was consistently higher that that of B1/10, suggesting that these two mAbs recognise different epitopes. Also binding by C1/8 was approximately two-fold that of B1/10. There are several possible explanations for this. The first possibility is that the C1/8 epitope may be present as two copies per molecule and may include a post-translational modification with a repetitive structure. A second possible explanation may be that B1/10 recognises an epitope that represents a post-translational modification present only on a proportion of LYVE-1 molecules. A third alternative is that the B1/10 epitope may be masked on a proportion of LYVE-1 molecules, either due to self-association with other LYVE-1 molecules or glycosylation. The possibility that the epitopes consist solely of glycan chains is unlikely as no cross-reactivity with human LYVE-1 was observed.

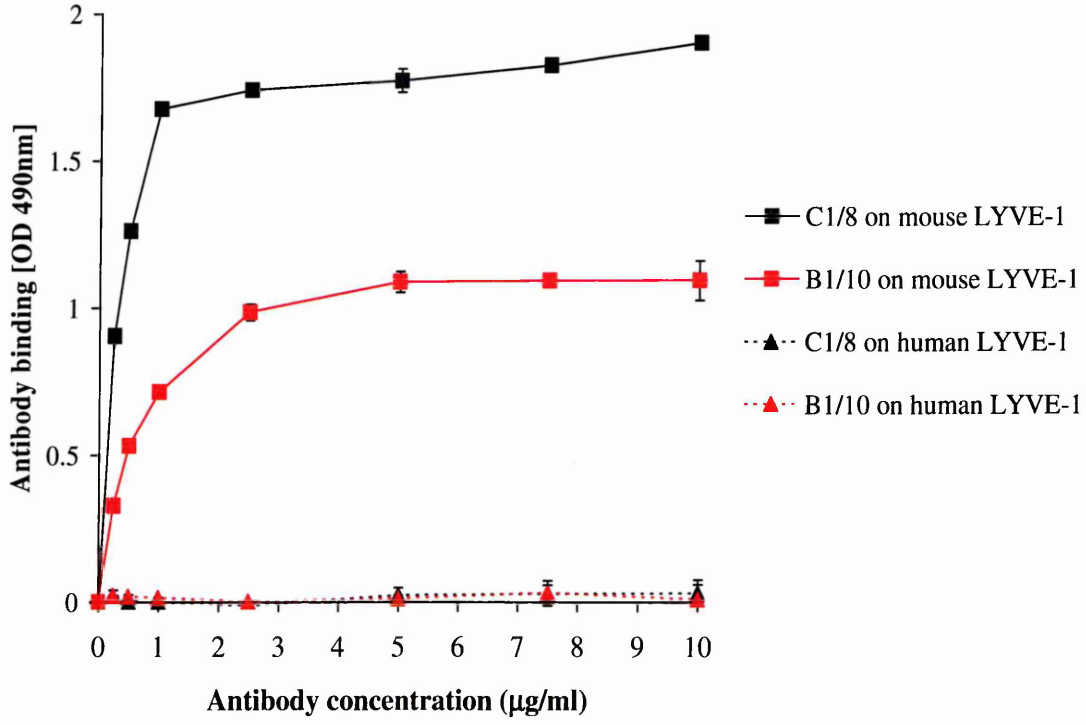

Figure 3.10 Titration of C1/8 and B1/10 and LYVE-1 species specificity. Affinity purified antibody was applied in triplicate at a series of concentrations to microtitre plates coated with either immobilised mouse or human LYVE-1 Fc fusion protein. Whilst both mAbs showed binding to the mouse protein, binding to human fusion protein was at background levels.

3.2.7 Determining the effect of the degree of LYVE-1 sialation on mAb binding

To explore the possibility that a post-translational modification was part of either B1/10 or C1/8 epitopes, the effect of desialation was explored. Experiments carried out by a fellow DPhil student in the same laboratory (Tom Nightingale) demonstrated that these N-glycans are sialated and that HA binding by LYVE-1 is tightly controlled by the degree of sialation. The effect of sialation on the ability of the mAbs to recognise and bind LYVE-1 was therefore investigated using an ELISA.

α 2-3, 6, 8-neuraminidase from *Vibrio cholerae* cleaves α2→3 and α2→6 linkages to Gal, GlcNAc and GalNAc residues. LYVE-1 is sialated at the N-glycosylation sites and possibly also on O-glycans but a more heavily sialated protein, fetuin was used as a positive control to ensure that the enzyme was effective, as observed by a decrease in the molecular weight (figure 3.11, panel A). Desialated LYVE-1 was used to coat a microtitre plate, alongside LYVE-1 which had been incubated in the same conditions but without neuraminidase (mock digestion) and LYVE-1 which was completely untreated (to ensure that the conditions of neuraminidase treatment alone were not sufficient to alter binding). B1/10 and C1/8 were applied to the plate and bound antibody was detected using HRP-conjugated goat anti-rat antibody and *O*-phenylenediamine (OPD), quantitating by spectrophotometry at 490 nm. Figure 3.11, panel B shows that binding of B1/10 decreased by approximately 37%. This suggests that a sialated glycan may lie close to or affect the conformation of the B1/10 epitope. This is not the case for C1/8, which showed little reduction in binding upon treatment with neuraminidase.

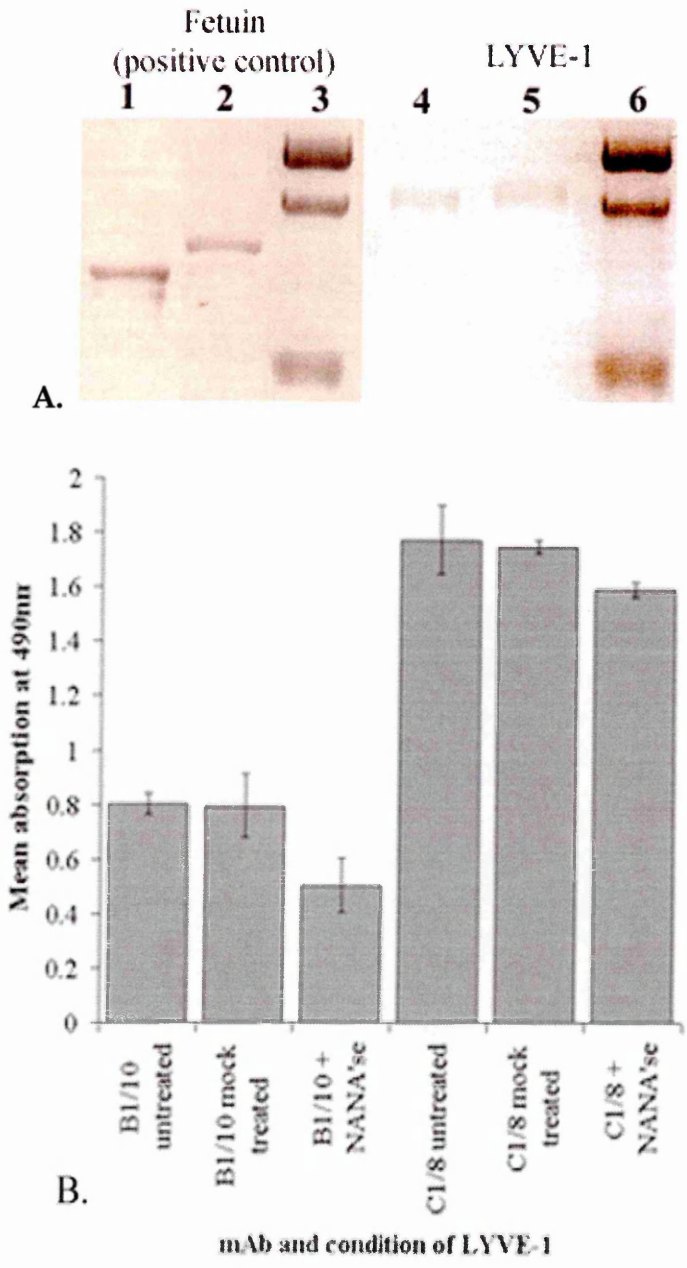

Figure 3.11 The effect of sialic acid removal on LYVE-1 mAb binding. Purified LYVE-1Fc was treated with neuraminidase in parallel to fetuin, a heavily sialated protein. Proteins were electrophoresed on a 10% polyacrylamide gel (panel A), showing de-sialated fetuin (lane 1), untreated fetuin (lane 2), de-sialated LYVE-1 (lane 4), untreated LYVE-1 (lane 5).and molecular weight markers in lanes 3 and 6, with bands of sizes 116, 80 and 51.8 kDa. A microtitre plate was precoated with LYVE-1Fc which was either untreated, mock-treated, or had been incubated with neuraminidase. mAbs were applied at 10μg/ml to triplicate wells and bound antibody was measured as mean absorption following detection with an HRP conjugate and substrate, ± standard error (panel B).

3.2.8 Preliminary epitope mapping using mouse/human LYVE-1 chimeras

The regions of the extracellular domain containing the B1/10 and C1/8 epitopes were further delineated using two mouse/human chimaeric LYVE-1 constructs, to establish whether the epitopes lay within the Link module and therefore may affect ligand binding. The chimaeras were kindly donated by a fellow DPhil student in the laboratory (Branwen Hide) and the compositions are illustrated in the schematic in the upper panel of figure 3.12. All transfectants were lifted with PBS-5mM EDTA prior to staining in triplicate with either of the mAbs and the AlexaFluor®488 conjugate. Both mAbs were found to recognise full length mouse LYVE-1 and chimaera C but not chimaera A. Therefore both epitopes are likely to lie in the region between residues 55 and 111.

3.2.9 Functional assays

3.2.9.1 Testing the ability of the mAbs to induce shedding of LYVE-1

The induction of shedding of antigen by certain antibodies has been well-documented, for example the shedding of CD44 by the mAb IM-7.8.1 (Zheng et al., 1995). Therefore it was of interest to determine whether or not either of the mAbs generated here could induce shedding of LYVE-1 from the cell surface in transfectants. 293T were transiently transfected with mouse LYVE-1 in pRcCMV and incubated for 24h at 37°C in the presence of either B1/10, C1/8 or rat IgG control, all in triplicate. Cells were then stained with rabbit anti-mouse LYVE-1 and AlexaFluor® 488-conjugated goat anti-rabbit to measure LYVE-1 surface expression by flow cytometry (figure 3.13). A decrease in LYVE-1 surface expression was observed after incubation with both B1/10 and C1/8 to 66% and 74% of that on cells incubated with the irrelevant isotype-matched control. However this could be due to suppression of polyclonal antibody binding to epitopes already occupied by mAbs rather than shedding of the antigen. Alternatively shedding may have occurred and to a more dramatic extent at an

earlier time point than that at which the experiment was carried out and by 24h expression had begun to recover. Antibody-induced shedding may also be temperature dependent and future experiments could explore whether or not this is the case. Also the loss of surface expression may be either due to internalisation or shedding and an ELISA or Western blot could be performed to detect shed LYVE-1 in the supernatant.

3.2.10 Determining ability of the mAbs to block HA binding

Certain antibodies have well-characterised abilities to block the binding of their antigen to its ligand and have thus proved invaluable reagents in functional studies, as outlined in the introduction to this chapter. To assess adhesion blockade of B1/10 and C1/8, 293T were transiently transfected with mouse LYVE-1 in pRcCMV and then incubated for 30 min in triplicate with either B1/10, C1/8 or rat IgG isotype-matched control at either 4°C or 37°C. FITC-HA was added and all cells were incubated at 4°C for 30 min to prevent endocytosis of HA. HA binding was assessed by flow cytometry, using untransfected cells incubated with FITC-HA as a control to demonstrate that no LYVE-1-independent or non-specific binding was occurring. Figure 3.14 shows that at 37°C B1/10 reduced HA binding by almost 70%, although such HA blocking did not occur at 4°C. This temperature dependence suggests that LYVE-1 was either internalised or shed at 37°C and the decrease in surface expression was responsible for a reduction in HA binding. It would be interesting to explore this possibility further, as outlined in the section above.

HA binding by mouse LYVE-1 in plate binding assays was found to only occur on very recently prepared protein (less than 12h following purification). However this approach could be used to assess the effect of the mAbs on ligand binding without the variables of internalisation or shedding.

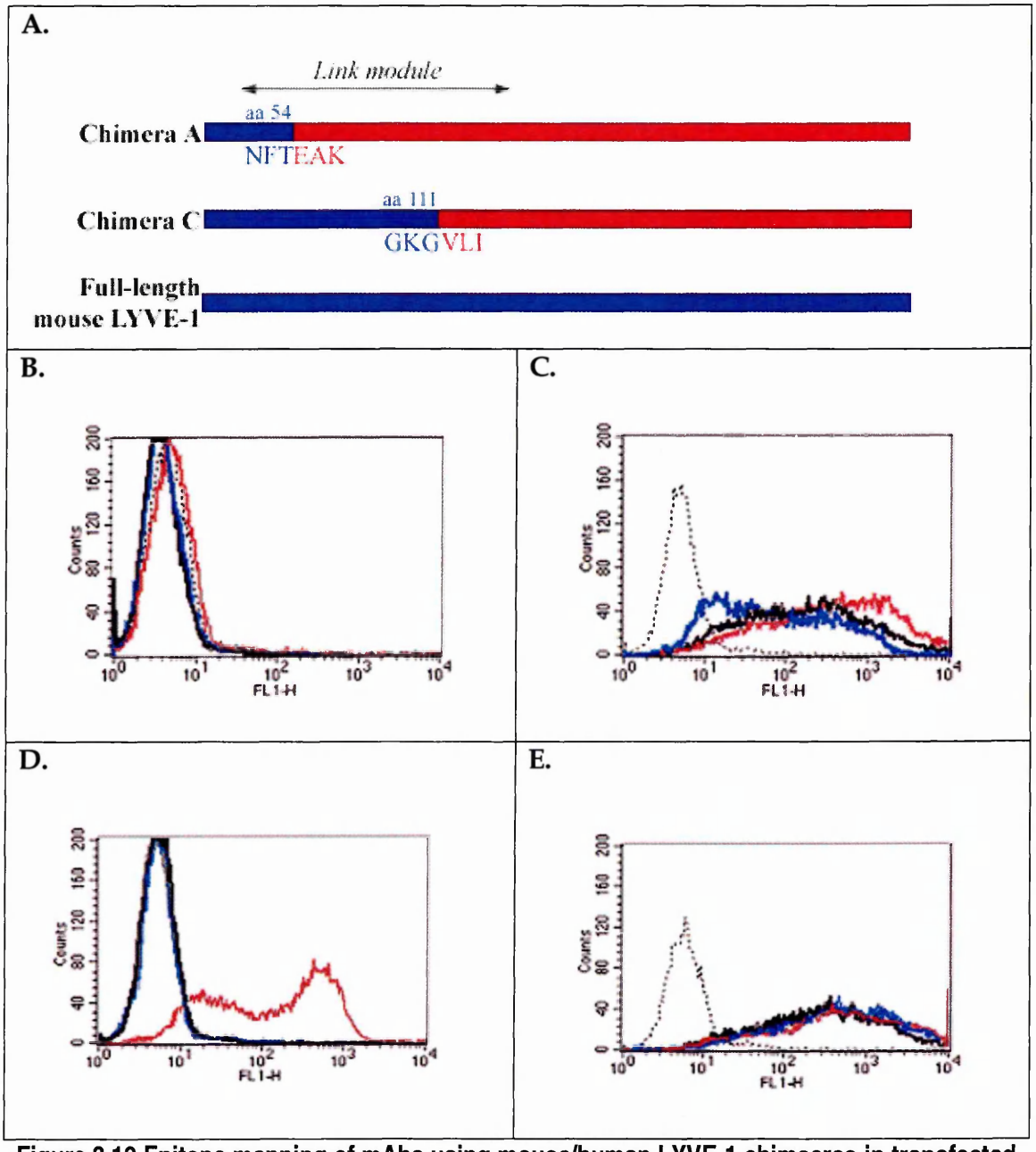

Figure 3.12 Epitope mapping of mAbs using mouse/human LYVE-1 chimaeras in transfected 293T cells. Panel A shows the LYVE-1 constructs used in 293T stable transfectants generated by Branwen Hide. Mouse sequence is shown in blue, with human sequence in red. The precise aa junctional regions are indicated. Lower panels show FACS histograms of 293T transfectants. Untransfected cells are shown in panel B. Panel C shows FACS of full length mouse LYVE-1 transfectants whilst chimera A and chimera C transfectants are shown in panels D and E respectively. Cells were stained with either C1/8 (blue), B1/10 (black), rabbit polyclonal anti-LYVE-1 (red) or an isotype-matched antibody (black dotted line) and AlexaFluor®488.

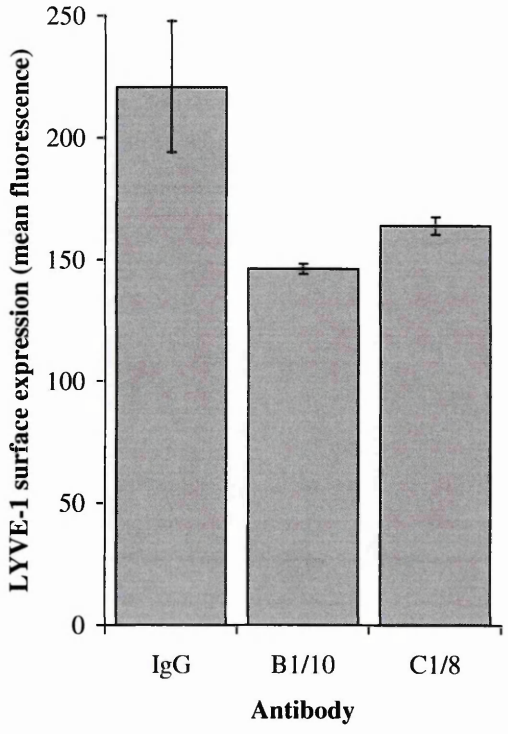

Figure 3.13 Testing for mAb-induced shedding of LYVE-1. Mouse LYVE-1 transfectants were incubated for 24h with antibodies at 50 μg/ml, either B1/10, C1/8 or an irrelevant isotype-matched antibody, IgG in triplicate. Cells were stained with rabbit anti-LYVE-1 and AlexaFluor 488 goat anti-rabbit in triplicate for each condition and LYVE-1 expression was measured by flow cytometry, ± standard error.

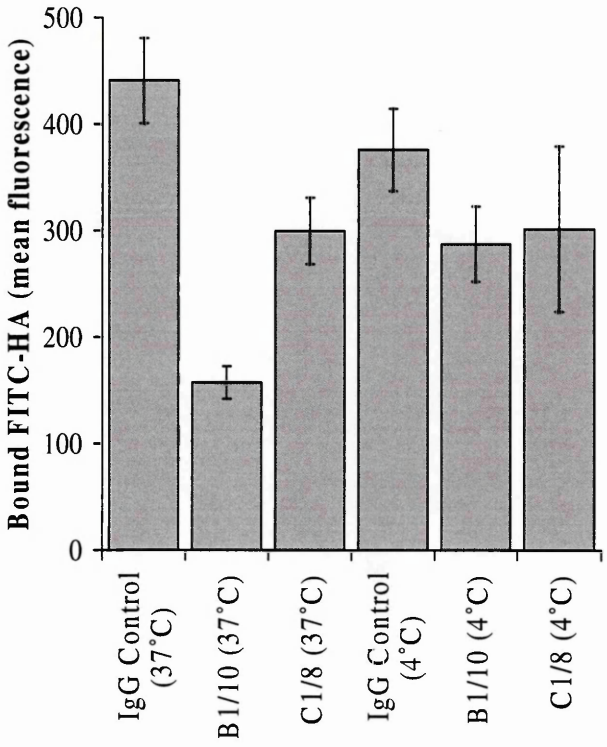

Figure 3.14 Assaying HA blocking ability of the LYVE-1 mAbs. The amount of FITC-HA bound to LYVE-1 transfectants after 30 min incubation at 4°C following pre-incubations with antibody at either 37°C or 4°C for 30 min was measured by flow cytometry, to quantitate the mean fluorescence of triplicate samples, ± standard error.

3.3 Discussion

This chapter has described the characterisation of two rat monoclonal antibodies generated against a fusion protein of mouse LYVE-1 and the Fc portion of human IgG. The two hybridomas were cloned and termed B1/10 and C1/8. Both mAbs were found to specifically bind mouse LYVE-1 and proved suitable antibodies for use in immunoperoxidase staining of paraffin-fixed sections as well as for immunofluorescence on cells and frozen sections, both fixed in PFA and unfixed. C1/8 was found to act as a specific marker for the detection of lymphatics in whole mounted mouse ear and was used extensively for this application (chapter 6), as it exhibited strong, specific binding which was not sensitive to the length of fixation. Thus C1/8 proved an invaluable reagent throughout this PhD, in the study of LYVE-1 expression, its variation both *in vitro* and *in vivo* and elucidating its possible functions. It also allowed greater flexibility in the choice of a second antibody when double staining. This was especially important as the most reliable podoplanin antibody was raised in rabbit and hence LYVE-1-podoplanin double staining could not be carried out if only polyclonal antisera against LYVE-1 existed. Another important application of these monoclonal antibodies was the positive selection of lymphatic endothelial cells when preparing a pure population from mouse dermal sheets (described in chapter 6). C1/8 yielded a purer population of LYVE-1-positive lymphatic endothelial cells (LEC) than either B1/10 or the rabbit polyclonal antibody (Dr. Steven Clasper, unpublished observation).

Both B1/10 and C1/8 were found to specifically recognise mouse LYVE-1 protein on both transfected cells and immobilised in plate-binding assays. No binding was observed to either immobilised human LYVE-1Fc in a plate-binding assay or to human LYVE-1 stable transfectants when measured by flow cytometry. This

demonstrated that the mAbs were not recognising the Fc portion of the protein or a novel epitope formed between the Fc domain and LYVE-1 and were specific for mouse LYVE-1, with no cross-reactivity towards the human orthologue. Partial epitope mapping using mouse-human LYVE-1 chimaeras showed that the epitopes of both B1/10 and C1/8 lie within the Link domain, between residues 55 and 111. As the maximum level of binding by C1/8 in microtitre plate assays was consistently higher that that of B1/10 by approximately two-fold, it is highly likely that these two mAbs recognise different epitopes. The C1/8 epitope may be present as two copies per molecule and may include a post-translational modification with a repetitive structure. Alternatively, the B1/10 epitope may represent a post-translational modification that is present only on a proportion of LYVE-1 molecules. Another possibility is that the B1/10 epitope is masked on a proportion of LYVE-1 molecules, either due to self-association with other LYVE-1 molecules or glycosylation. However, it is unlikely that the epitopes consist solely of glycan chains as no cross-reactivity with human LYVE-1 was observed. Mouse LYVE-1 contains sites for N-glycosylation at residues N52 and N129, i.e. adjacent to the 56-amino acid residue region to which the epitopes of B1/10 and C1/8 have been mapped. De-sialation of LYVE-1 resulted in a decrease in the binding of B1/10 by approximately 37%, which suggests that a sialated glycan may lie close to or affect the conformation of the B1/10 epitope. This is not the case for C1/8, which showed little reduction in binding upon treatment with neuraminidase.

Preliminary experiments into functional properties of the mAbs showed that B1/10 may induce loss of LYVE-1 expression from the surface of transfectants at 37°C. Thus the decrease observed in HA binding by these cells following incubation with B1/10 may be secondary to the reduction in LYVE-1 surface expression. However further experiments are required to assess the mechanism by which this occurs and to what extent over a time course.

CHAPTER 4

Effects of Inflammatory Cytokines on LYVE–1 Expression in Human Lymphatic Endothelial Cells

4.1 Introduction.....170
4.2 Results.....175
4.3 Discussion.....224

4.1 Introduction

4.1.1 Blood and lymphatic endothelial cells

The blood and lymphatic microvascular systems constitute discrete networks which perform very different but complementary functions. Whilst the blood vessels deliver dissolved proteins, fluids and cells to the interstitium, the lymphatics are responsible for draining excess fluid and returning protein to the circulation, thus maintaining homeostasis within the tissues. The two systems take on contrasting roles in antigen presentation too. Antigen presenting cells from the tissues travel to the lymph node via the lymphatics to be brought into contact with T-lymphocytes which have entered the lymph node via high endothelial venules (HEV) from the circulation. Although the morphology of isolated blood endothelial cells (BEC) does not permit them to be distinguished from isolated lymphatic endothelial cells (LEC), (Kriehuber et al., 2001), it would be fair to assume that their very different physiological roles would demand that they have distinct molecular phenotypic differences.

The first rigorous isolation and characterisation of dermal LEC and BEC was carried out by Kriehuber et al. (2001). These researchers isolated podoplanin-positive LEC and podoplanin-negative BEC from a dermal cell suspension obtained from adult patients undergoing breast reduction or abdominoplasty and sorted by flow cytometry. They showed that LEC and BEC constitute stable endothelial cell lineages which are specialized to carry out their diverse functions. Whilst both types of EC express VE-cadherin, CD31, vWF and secrete MIP-3β, LEC alone expressed LYVE-1, prox-1, podoplanin, VEGFR-3 and SLC. Also when the two EC types were plated in Matrigel™, they were found to assemble tubules in a strictly homotypic manner. In a more recent study, Hirakawa et al. (2003) showed that BEC and LEC are phenotypically distinct by

RNA array analysis, which permitted a much wider range of genes to be surveyed than studies with antibodies could allow. Transcription profiling studies revealed that BEC exhibit higher expression of several extracellular matrix and adhesion molecules in comparison to LEC, including versican, collagens, laminin, N-cadherin and CD34, as well as growth factor receptors endoglin and VEGFR-1. They also reported that LYVE-1 and prox-1 were not detected in BEC, as discussed previously in the general introduction. This present chapter details the investigations carried out into variations in LYVE-1 expression in cultured cells, shown by extensive phenotyping to be LEC.

4.1.2 Possible regulation of LYVE-1 expression in LEC

Previous examination of both mouse and human tissue by immunofluorescence microscopy revealed that even in apparently normal tissue, the expression of LYVE-1 varies much more dramatically than that of other lymphatic markers (unpublished observation). Such variation was also observed when primary human LEC were cultured *in vitro*. Both immunofluorescence microscopy and flow cytometry showed the differences in LYVE-1 expression between batches of cells in culture, even though no variation in the rate of proliferation or expression of other proteins was apparent. Throughout this PhD, primary endothelial cells were cultured in commercial Endothelial Growth Medium, EGM-2 purchased from Clonetics which was supplied as basal media requiring the addition of various supplements shortly before use. In addition to FBS, these included the recombinant growth factors acidic FGF, EGF and IGF; hydrocortisone; and ascorbic acid. LYVE-1 expression appeared particularly sensitive to the age of media: cells expressed higher levels of LYVE-1 when cultured in freshly supplemented medium, suggesting that LYVE-1 expression is influenced at least in part by the concentration and activity of a labile factor. Experiments carried out in this chapter sought to address the effects on LYVE-1 expression of such molecules, in particular growth factors and cytokines to which lymphatic

endothelium may be exposed in tissues. This was also driven by the knowledge that such factors are known to regulate expression of CD44, the closest homologue of LYVE-1. For example over-expression of EGF on tumour cells was found to be associated with *in vivo* tumour aggression due to increased proliferation, enhanced cell attachment and migration into the extracellular matrix (Zhang et al., 1996). EGF was found to induce CD44 expression both at the protein and mRNA levels in 3T3 mouse fibroblasts and enhanced cell attachment to HA. In a subsequent publication (1997), Zhang et al. identified a novel EGF-responsive element, ERE in the *CD44* promoter, to which an EGF-inducible nuclear protein binds. Clearly as growth factors can affect CD44 expression in such a specific manner, it was of interest to study the effects of EGF and other growth factors on lymphatic endothelium and expression of LYVE-1.

Experiments described in this chapter also sought to determine the effects of pro-inflammatory cytokines and chemokines on LYVE-1 expression. It is already widely accepted that inflammatory cytokines alter the expression of a variety of proteins in blood vascular endothelium, to enhance extravasation of leukocytes from the circulation (detailed in the general introduction). Thus it was considered likely that such a change in expression may also be induced in lymphatic endothelium, in response to the requirement for increased reverse migration of antigen presenting cells into the lymphatic vessels. It was of great interest to determine whether LYVE-1 was one such molecule that experienced a change in expression, in view of its possible involvement in facilitating leukocyte adhesion via HA-interactions (Jackson, 2004). In this respect it is noteworthy that other groups have demonstrated that CD44 on leukocytes was affected by pro-inflammatory agents. For example, expression of CD44 on monocytes was found to be elevated in inflamed tissue (Haynes et al., 1991) and the induction of CD44 on endothelial cells by IL-1α was demonstrated by Fitzgerald and O'Neill (1999). The functional role of CD44 in adhesion of leukocytes to inflamed vascular

endothelium is described in the general introduction to this thesis. As LYVE-1 is restricted to the lymphatic endothelium, experiments described in this chapter sought to determine whether its expression is up- or down-regulated during inflammation, signalling a role in regulating leukocyte adhesion or migration. Previous work in the Jackson laboratory (Tom Nightingale, DPhil thesis, University of Oxford, 2004) had shown that LYVE-1 is constitutively expressed in lymphatic endothelium in a sialated, non-binding form, thus suggesting that control of endogenous neuraminidase activity might regulate LYVE-1 function *in vivo*. Activation of such a LYVE-1-HA interaction might, for example, stimulate rearrangement of the endothelial cell cytoskeleton, to aid transmigration of APCs across the lymphatic endothelium. An interaction between CD44 on APCs and LYVE-1-bound HA could also occur. Alternatively LYVE-1 may play a role in sequestering smaller fragments of HA for degradation, to resolve acute inflammation. Thus the effect of pro-inflammatory mediators on LYVE-1 expression and HA binding could provide evidence for a physiological role for this lymphatic endothelium-restricted receptor.

Many human cancers are associated with pre-existing chronic inflammatory conditions (Schacter et al., 2002). A common feature of solid tumours is hypoxia, which is known to have radical effects on blood vessel endothelial cells, stimulating angiogenesis through the up-regulation of VEGF family receptors and ligands. It was therefore of interest to determine whether hypoxia might influence lymphatic endothelium in some way, initially focusing on LYVE-1 expression. If LYVE-1 did indeed possess a hypoxia responsive element, sensitivity to oxygen tension could explain variations observed in LYVE-1 expression *in vivo*. A dramatic change in expression could be of prognostic use, as has proved the case for carbonic anhydrase 9 (CA9), which is up-regulated by hypoxia in a number of cancers (Wykoff et al., 2000; Koukourakis et al., 2001; Olive et al., 2001).

Another agent which could affect LYVE-1 expression on LEC *in vitro* is the diacylglycerol analogue phorbol 12-myristate 13 acetate (PMA), a potent activator of mitogen activated kinases (MAPKs) through protein kinase C (PKC). Among the many proteins regulated by these intracellular molecular signals are matrix metalloproteinases, MMPs, which are capable of degrading extracellular matrix and play critical roles in endothelial cell migration (Park et al., 2003). Research carried out in the Jackson laboratory (S. Clasper and D. G. Jackson, unpublished; Tom Nightingale, DPhil thesis, University of Oxford, 2004) had found that PMA stimulated MMP-dependent shedding of LYVE-1 by 293T human fibroblast transfectants. In this chapter, further experiments were carried out to investigate whether this finding was borne out in human LEC which express endogenous LYVE-1, in order to assess whether regulation of LYVE-1 expression involves the MAPK pathway.

4.1.3 Aims

The experiments described in this chapter sought to determine factors and conditions responsible for regulating LYVE-1 expression in primary human LEC.

- A panel of growth factors, cytokines and chemokines, were used to stimulate LEC prior to quantitation of LYVE-1 expression.
- Extensive characterisation of the effect of TNFα on LYVE-1 expression and the mechanism of regulation were carried out
- The response of lymphatic endothelium to hypoxia was investigated in a preliminary study.
- Stimulation of LEC by PMA was carried out to determine the effect on LYVE-1 surface expression and the mechanism of regulation.

4.2 Results

4.2.1 Derivation of human lymphatic endothelial cells (LEC)

The study of LYVE-1 expression in response to various factors and conditions depended upon the availability of cultured primary lymphatic endothelial cells which endogenously expressed LYVE-1. Such cells had to be well adapted to culture and grow over a number of passages to allow for expansion of the population whilst retaining their molecular characteristics. Isolation of primary LEC from tissue was not possible due to the lack of availability of human tissue. Therefore primary LEC were obtained from commercially available human dermal microvascular endothelial cells (HDMEC), which contained both LEC and BEC. Such microvascular endothelial cells were purchased from two sources: PromoCell, Heidelberg and Clonetics, Cambrex Bioscience Inc, Walkersville, USA.

4.2.1.1 Human dermal endothelial cells from Clonetics, USA

HDMEC supplied by Clonetics had been isolated from dermal tissue from a 47 year old male and at early passages contained a mixed population of both LYVE-1-positive LEC and CD34-positive BEC in approximately equal numbers, as shown in figure 4.1A. However by passage 5 the number of LYVE-1 positive cells had diminished to approximately 10% (figure 4.1) and by passage 9 had entered senescence and ceased to proliferate. Attempts to derive a population of pure LEC through selection with mouse anti-human LYVE-1 mAb and anti-mouse magnetic cell sorting (MACS) beads failed to yield cells which would proliferate sufficiently to expand the population. Thus the unselected cells were used in preliminary experiments into regulation of LYVE-1 expression by growth factors, cytokines and chemokines. As BEC are LYVE-1 negative, the

contribution of such cells to total LYVE-1 expression was considered only important if one of the growth factors or cytokines induced a change in the transcriptional profile of BEC to resemble that of LEC and thus an indirect increase in LYVE-1 expression. However the advent of cells from PromoCell, Germany superseded the use of these cells.

4.2.1.2 Human dermal microvascular endothelial cells from PromoCell, Germany

HDMEC purchased from PromoCell had been derived from a 7 year old male donor and initially consisted of a mixed population of both LYVE-1-positive LEC and CD34-positive BEC. However unlike the HDMEC from Clonetics, these cells were found to proliferate beyond 20 passages. To investigate the expression of LEC markers LYVE-1 and podoplanin and the BEC marker CD34 with passaging, cells were continuously cultured and at each passage were lifted with PBS-5mM EDTA. Half of the population were re-plated for continued growth whilst the other half were stained with mouse anti-LYVE-1, mouse anti-CD34, rabbit anti-podoplanin or irrelevant isotype–matched controls and the appropriate AlexaFluor® 488 conjugated secondary antibody. Expression of each of these proteins at each passage was then assayed by flow cytometry (figure 4.2). The percentage of cells expressing the BEC marker CD34 was found to decrease with passaging whilst the number of cells expressing the LEC markers LYVE-1 and podoplanin increased, suggesting that the LEC outgrew the BEC. Hence all experiments were carried out on the same batch of PromoCell HDMEC, which were used at passage 12 or above.

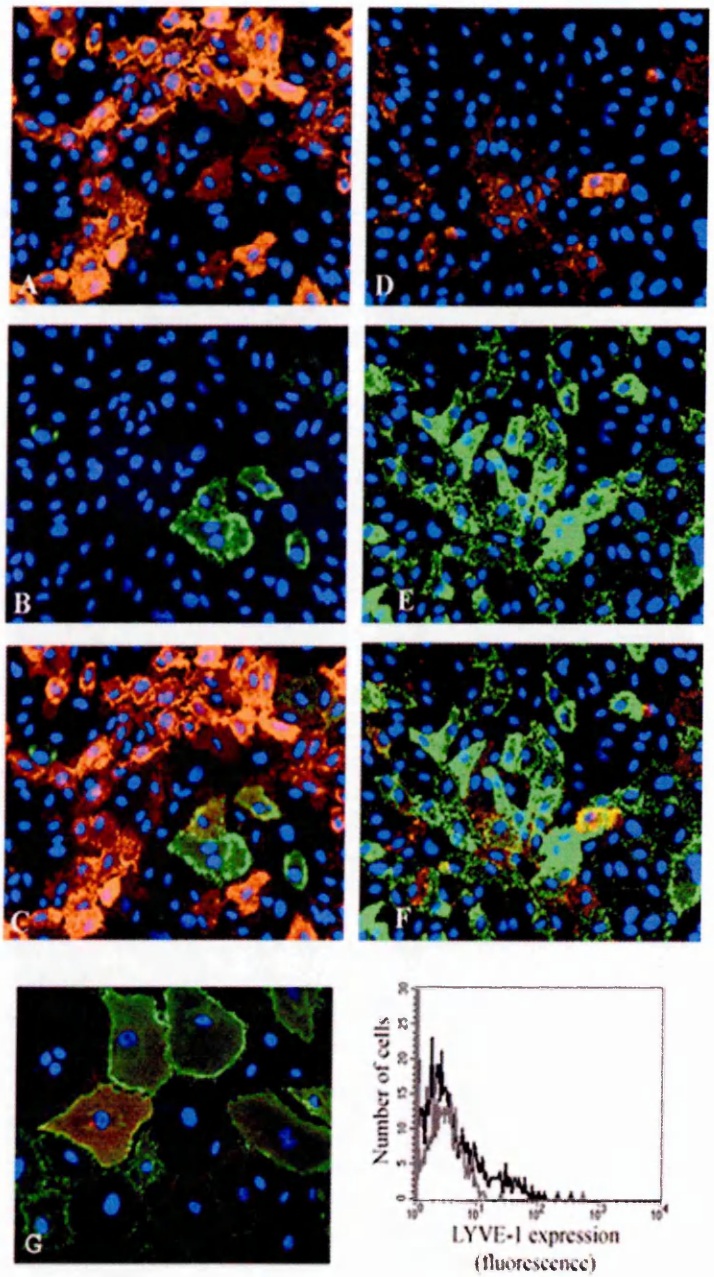

Figure 4.1 Mixed phenotype of commercial HDMEC (Clonetics). Early passage (typically passage 2-3) cells consisted of discrete islands of BEC (expressing CD34, red) and LEC (LYVE-1-positive). Panels A, B and C show a BEC-enriched region whilst panels D, E and F a LEC-enriched area. At later passage (passage 5 and after), expression of both LYVE-1 (panel G and FACS histogram) and CD34 (data not shown) had decreased markedly and cells ceased to proliferate.

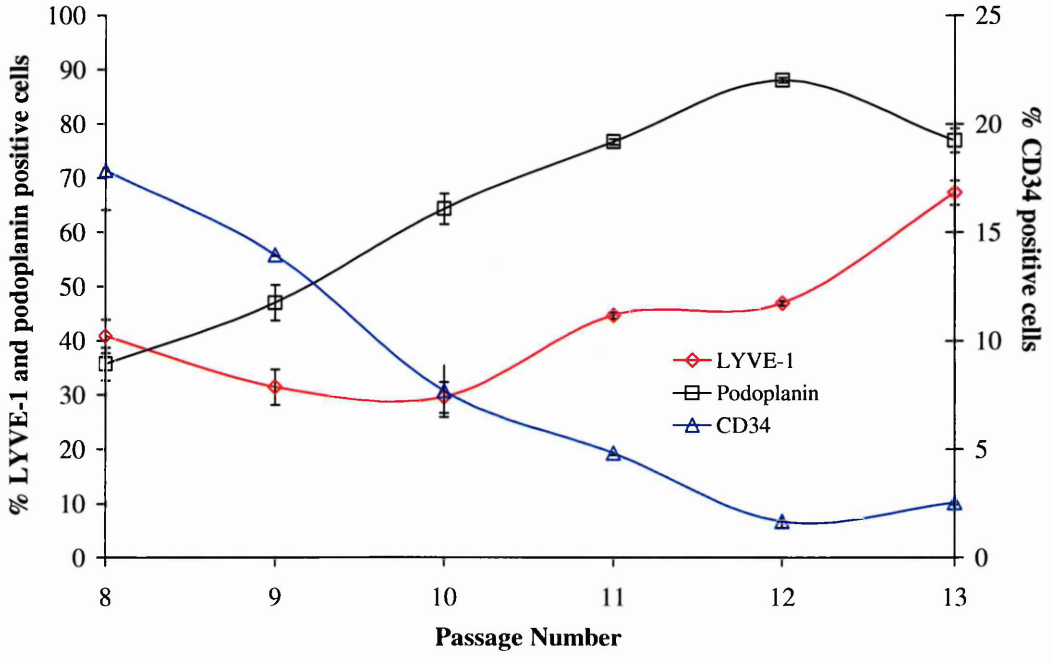

Figure 4.2 Derivation of a pure population of LEC by outgrowth from a mixed population of commercial HDMEC. PromoCell HDMEC were cultured continuously and at each passage a sample was stained in triplicate with either the anti-LYVE-1 mAb 8C, anti-CD34 or rabbit polyclonal anti-podoplanin. The appropriate AlexaFluor® 488 conjugated goat antibody was used for secondary detection and the percentage of positive cells (± standard error) assayed by flow cytometry. Staining using irrelevant isotype matched controls was also carried out at each passage.

4.2.1.3 Characterisation of PromoCell HDLEC

Immunofluorescence microscopy of the putative HDLECs showed that virtually all cells expressed the pan-endothelial cell marker CD31, podoplanin and the transcription factor prox-1 (seen within the nucleus, colocalising with DAPI, figure 4.3). In cells of passage 12 and above, over 99% of the population were podoplanin-positive, as shown by flow cytometry (figure 4.3, lower right panel) and no CD34 expression was observed (upper right panel). Due to their predominantly LEC phenotype these HDMEC-derived cells are hereafter termed human dermal lymphatic endothelial cells, HDLEC and prior to the availability of freshly immuno-isolated primary LEC for experimental work, served as a convenient cell line to study the regulation of LYVE-1 expression. Comprehensive analyses of adhesion molecule expression by HDLEC and of their changes in gene expression in response to inflammation are presented later in this thesis (chapter 5). Studies on primary LYVE-1 immuno-isolated murine LEC which became possible later during this thesis are also described in chapter 5.

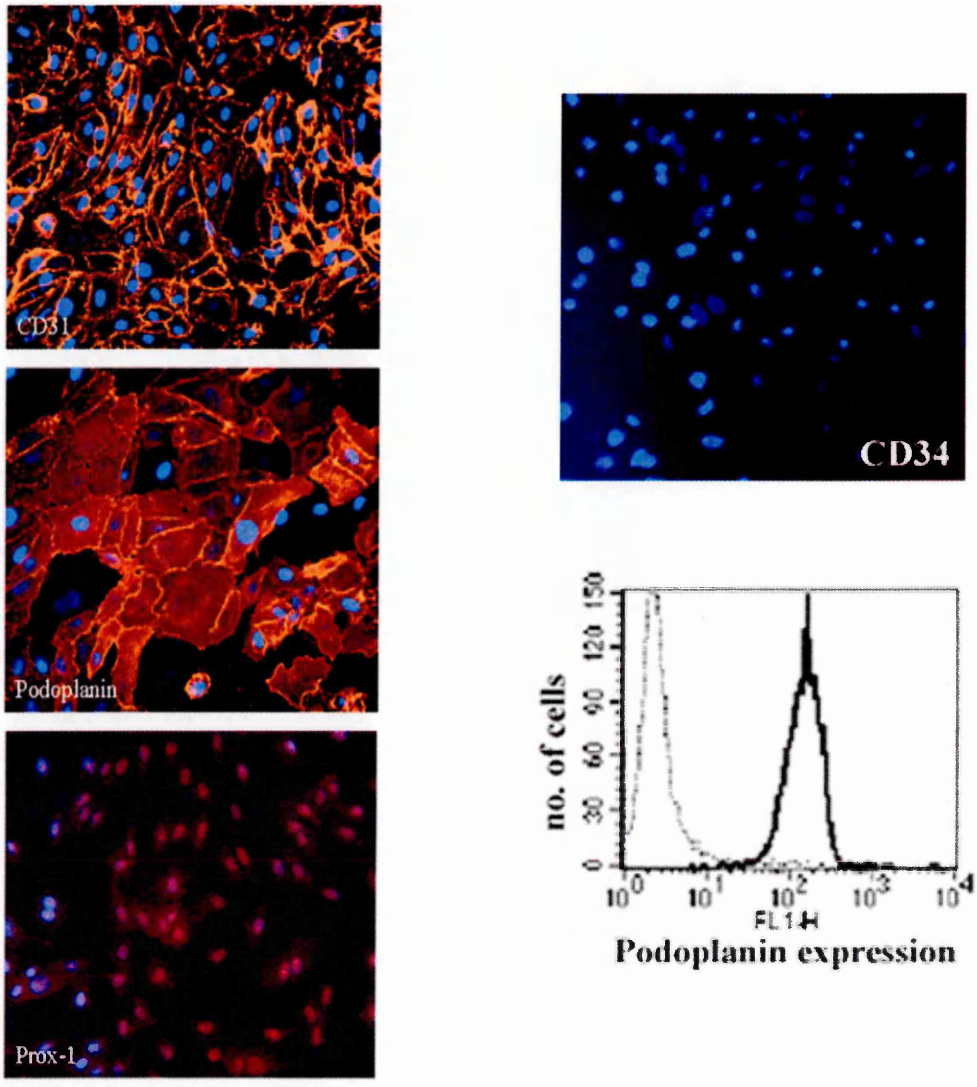

Figure 4.3 Characterisation of HDMEC-derived LEC (HDLEC). Immunofluorescence microscopy to show that the majority of cells express CD31, podoplanin and prox-1, whilst no cells express CD34. Cells were stained with either mouse anti-CD31, rabbit anti-podoplanin, mouse anti-prox-1 or mouse anti-CD34. The appropriate AlexaFluor® 568 goat secondary conjugates were used for detection and nuclei were counterstained using DAPI (left and upper right panels). Podoplanin expression was quantitated by flow cytometry, staining cells with the same polyclonal antibody and goat anti-rabbit AlexaFluor® 488 conjugate to demonstrate that over 99% of PromoCell HDLEC are podoplanin positive, (lower right panel). Microscopy images were captured at 200X magnification.

4.2.2 Changes in LYVE-1 surface expression in response to culture conditions

The effects of a panel of recombinant human cytokines, chemokines and growth factors on LYVE-1 expression were studied quantitatively using flow cytometry following incubation with individual factors for 72h of culture (figure 4.4). The inflammatory cytokine IL-6 induced an increase in LYVE-1 expression in the cells, as did Angiopoietin-2 and VEGF-C. A more marginal increase in expression was induced by the growth factors FGFacidic, G-CSF and GM-CSF, the cytokine IFNγ and chemokines MIP-3α and MIP-3β. However the most striking result obtained from this experiment was the abrogation of LYVE-1 surface expression following treatment with TNFα and TNFβ (figure 4.4).

The effects of cytokines and growth factors was next assessed on LEC present within commercial HDMEC obtained from Clonetics, USA. Although BEC are present in these populations, LYVE-1 expression has never been observed on such CD34-positive cells. However like the PromoCell HDLEC, these cells exhibited a similar loss of LYVE-1 following exposure to TNF (figure 4.5). Additionally a similar study on the effects of cytokines, chemokines and growth factors was also carried out on immunoselected primary human dermal LEC. These cells became available later in these studies and only in very limited quantities. They comprised a population isolated by immunoselection with podoplanin and were kindly donated by Dr. Ernst Kriehuber (laboratory of Prof. Donscho Kerjaschki, Vienna, Austria), the phenotype of which is described in detail in Kriehuber et al. (2001). TNF was found to precipitate the same loss of LYVE-1 from the cell surface (figure 4.6). Hence it can be concluded that down-regulation of LYVE-1 is likely to be an authentic response of LEC and the HDLEC derived from the initially mixed population of HDMEC have preserved the phenotype of primary LEC.

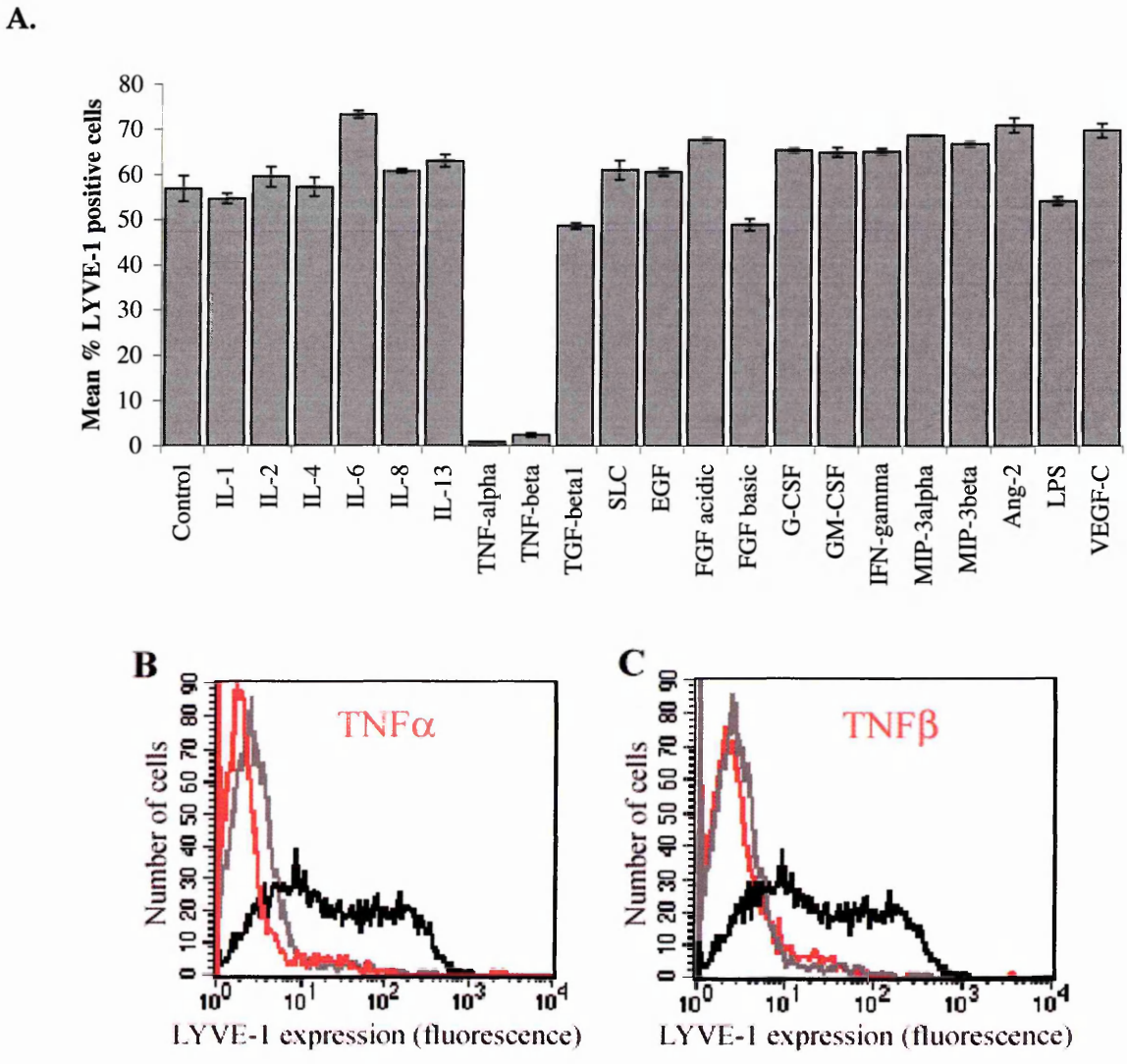

Figure 4.4A Effects of cytokines, chemokines and growth factors on LYVE-1 expression in primary HDLEC. Cells were cultured for 72h in the presence of one of the growth factors, chemokines or cytokines, then lifted with PBS-5mM EDTA and stained for LYVE-1 using the mAb 8C and AlexaFluor®488 goat anti-mouse. Cells were stained in triplicate alongside an isotype-matched control for quantitation by flow cytometry. Data shown are the mean percentage of LYVE-1-positive cells, ± standard error (panel A). Flow cytometry histograms to show the loss of LYVE-1 from PromoCell HDLEC following exposure to TNFα, 100ng/ml and TNFβ, 100ng/ml are shown in panels B and C respectively, where the black lines represent untreated (control) cells, red represents TNF-treated and grey the isotype-matched controls.

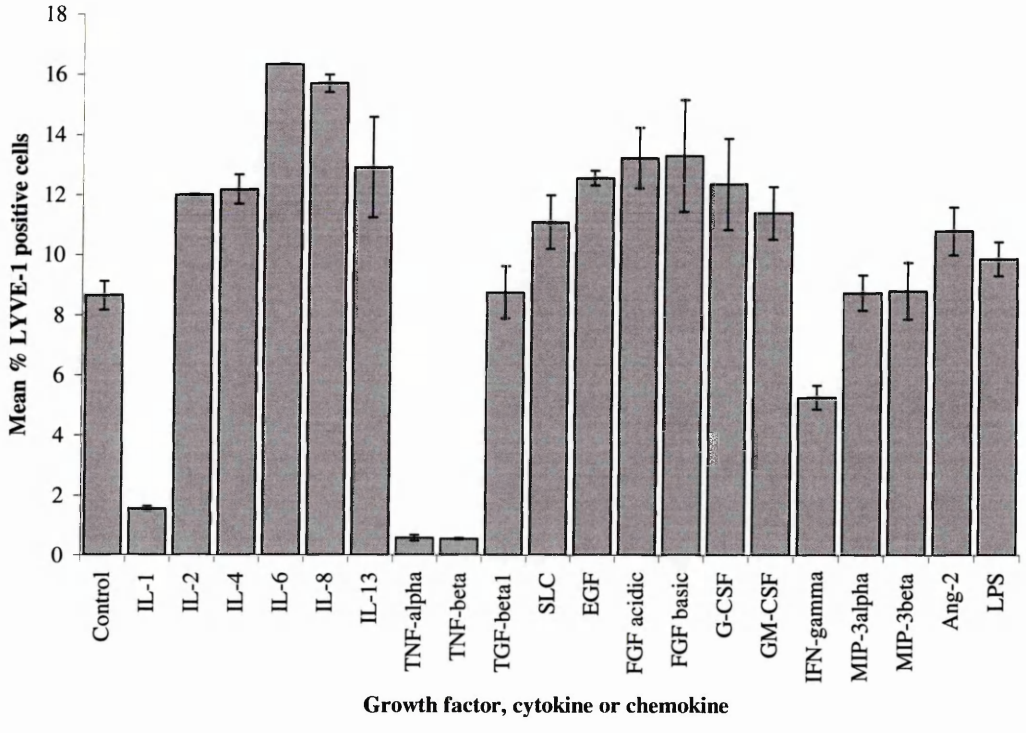

Figure 4.5 Effect of cytokines, chemokines and growth factors on LYVE-1 expression in LEC present within unselected commercial HDMEC (Clonetics). Cells were cultured following the same method as for PromoCell endothelial cells and assayed for surface expression in a similar manner but stained in duplicate (due to slower growth and hence fewer cells), with an isotype-matched control for each condition. Data shown are the mean percentage LYVE-1-positive cells, ± standard error.

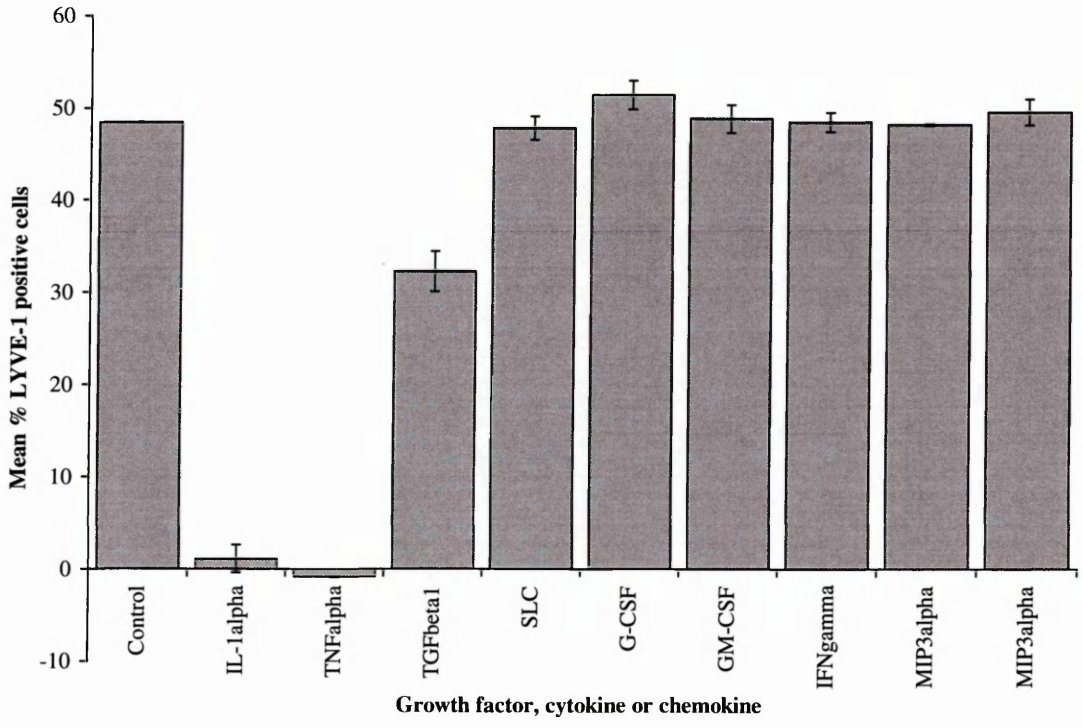

Figure 4.6 Effect of cytokines, chemokines and growth factors on LYVE-1 expression in immunoselected primary dermal human LEC. Primary LEC immuno-isolated for podoplanin expression (Kriehuber et al., 2001, see methods section for further details) were cultured following the same method as for PromoCell and Clonetics endothelial cells and assayed for surface expression in a similar manner in duplicate, with an isotype-matched control for each condition. As non-specific staining was higher on these cells than the other endothelial cells (typically 7% as opposed to less than 1%), the percentage of positive cells stained by the isotype-matched antibody for each condition were subtracted from the mean percentage of LYVE-1 positive cells. The corrected percentages of LYVE-1-positive cells are plotted ± standard error.

4.2.3 Effects of TNF on primary HDLEC

In view of the dramatic down-regulation of LYVE-1 in HDLEC induced by both TNFα and TNFβ, it was decided to characterise the response more fully in terms of the effects of these pro-inflammatory cytokines on HDLEC physiology and the fate of LYVE-1 upon down-regulation. HDLEC derived from PromoCell HDMEC were used for such experiments as they exhibited higher expression of LYVE-1 than the immunoselected LEC over a larger number of passages and had a shorter doubling time.

4.2.3.1 Effect on morphology

Following stimulation of primary HDLEC with TNFα or TNFβ, a striking change in morphology of the cells was observed, from rounded cobble-stone-like to elongated. Images were captured by phase contrast microscopy (figure 4.7). Such a change is indicative of cytoskeletal rearrangement induced by this pro-inflammatory cytokine and demonstrates that HDLEC undergo a much more dramatic change than simply a loss of LYVE-1 surface expression. However no increased propensity of cells to lose adhesion was observed.

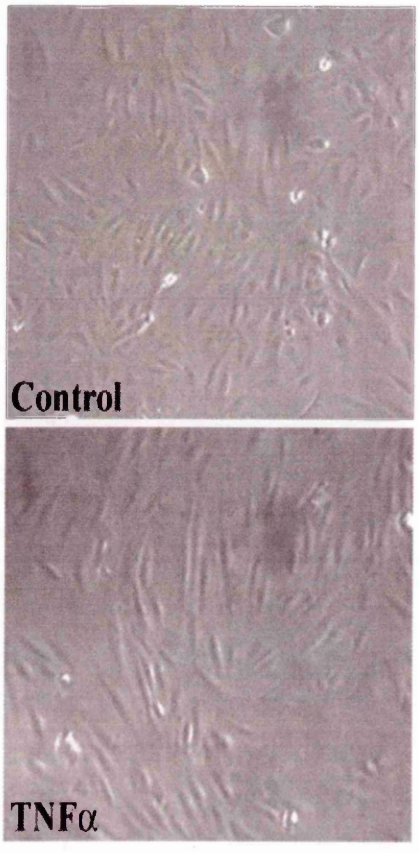

Figure 4.7 Effect of TNFα on the morphology of cultured primary HDLEC. Cells were cultured for 48h in either medium alone or supplemented with TNFα, 10ng/ml. Images were captured by phase contrast microscopy at 100x magnification. A similar elongated morphology was observed in cells following stimulation with TNFβ (data not shown).

4.2.3.2 Viability and proliferation

One possible explanation for the loss of surface expression of LYVE-1 by TNF-treated HDLEC might have been the induction of apoptosis or a loss of viability. TNFα was first isolated due to its ability to induce regression of tumours and is known to induce apoptosis in some transformed cell lines (detailed in the introduction to chapter 5). To assess a potential cytotoxic effect on HDLEC, a trypan blue dye-exclusion assay was performed. The results (table 4.1) showed that cells treated with TNFα or TNFβ excluded dye as effectively as untreated cells (table 4.1) and thus showed that TNF-treatment did not cause a reduction in viability in these cells. Viability was further confirmed by the continued expression of the lymphatic endothelium surface protein podoplanin (figure 4.8). Moreover, TNFα did not cause a significant reduction in the rate of proliferation of these cells when detected by the MTT dye-reduction assay (figure 4.9), as might have been expected if the cytokine were affecting cell integrity.

	% Viable cells	Standard error
Control	87.77	5.12
TNFα	87.51	2.37
TNFβ	92.98	0.68

Table 4.1 Viability of TNF-stimulated HDLEC. A trypan blue dye exclusion assay was performed on cells cultured for 48h in the presence of either TNFα (100ng/ml), TNFβ (100ng/ml), or in medium alone and then lifted with PBS-5mM EDTA (as for analysis by flow cytometry) and incubated on ice for 30min. Data represent cells counted from five replicates.

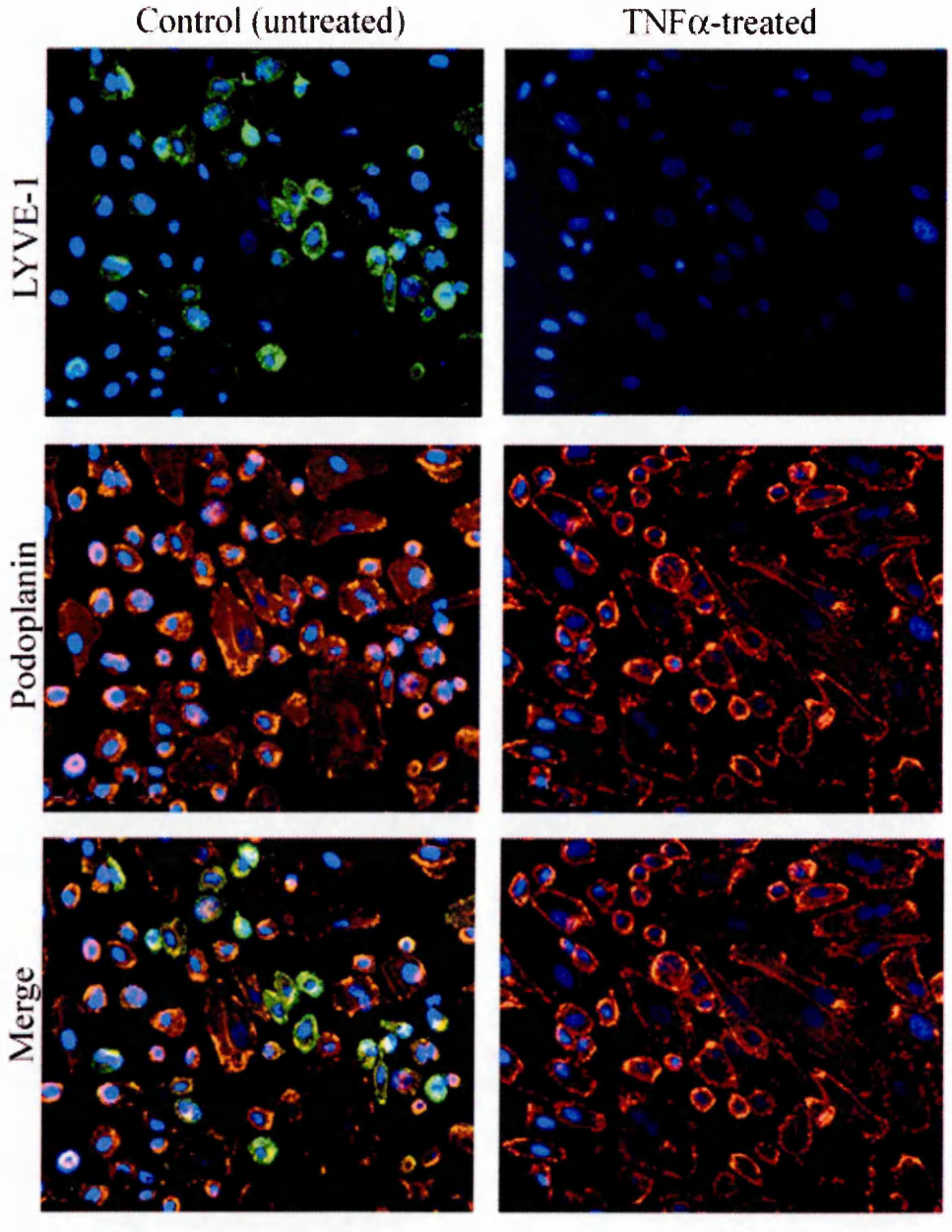

Figure 4.8 Loss of surface LYVE-1 in TNFα treated HDLEC, as assessed by immunofluorescence microscopy. Cells were cultured for 48h with or without TNFα, (100ng/ml), and then double-stained using the mAb 8C and rabbit anti-podoplanin serum, with AlexaFluor® conjugates 488 (green) and 594 (red) respectively. Fluorescence is shown both as the LYVE-1 and podoplanin channels alone and as both channels merged. Double positive cells appear yellow.

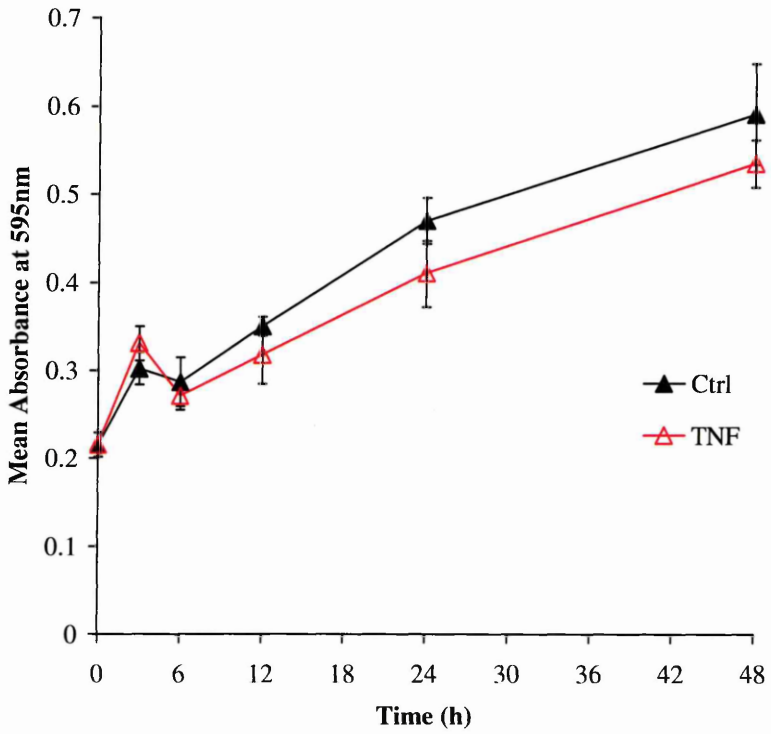

Figure 4.9 Effect of TNFα on the rate of HDLEC proliferation *in vitro*. Cells were cultured with or without TNFα and MTT was applied at several time points to triplicate wells for 1 h incubation. The absorbance of the cell lysate was measured at 490nm and the mean absorbance plotted at each time point ± standard error.

4.2.3.3 Effect of TNFα on tube formation by HDLEC in Matrigel™

To address the possibility that TNFα might affect the ability of HDLEC to form tubules, cells were plated out on Matrigel™, a solubilized basement membrane preparation isolated from Engelbreth-Holm-Swarm (EHS) mouse sarcoma which is rich in extracellular matrix proteins. HDLEC were plated out on Matrigel™ in either the presence or absence of TNFα. After 24h cells had formed extensive tubules and images were captured from phase contrast microscopy. Representative fields of view are shown in figure 4.10. However no difference in overall tubule density or individual tubule branching was observed between untreated and TNFα-stimulated. This correlates with the proliferation assay and thus these experiments show that TNFα does not have a significant effect on lymphangiogenesis or HDLEC proliferation.

4.2.3.4 Time course

A time course to follow the effect of TNFα on surface expression of LYVE-1 was carried out, measuring the percentage of LYVE-1-positive cells by flow cytometry at 0, 6, 12, 24, 48 and 72h following exposure to the cytokine (figure 4.11). A reduction in expression was apparent within the first 6h of treatment, during which time the level (measured as percentage of LYVE-1 positive cells) decreased by over 50% of the initial value; however, total abrogation of surface expression was only complete after 48h.

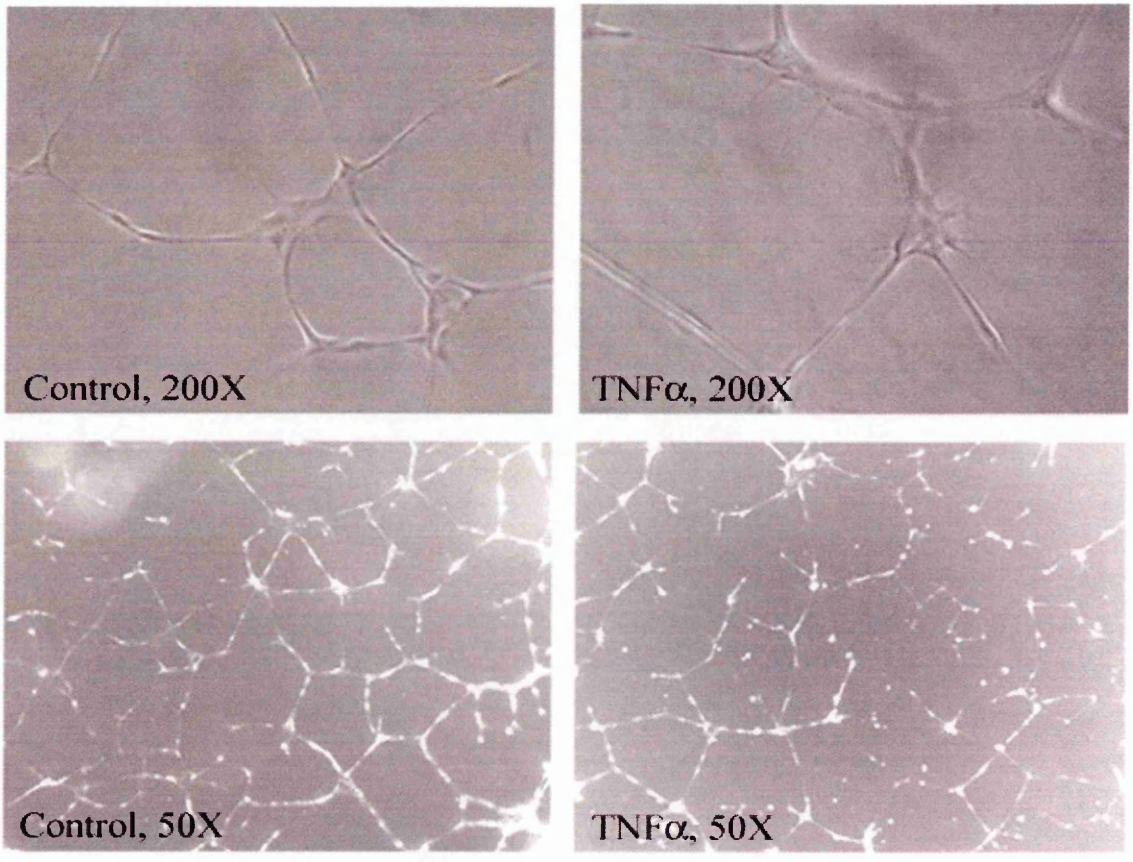

Figure 4.10 Effect of TNFα on HDLEC tubule formation *in vitro*. Cells were plated out at a density of 15000/cm^2 on 0.5cm-thick Matrigel™ either in EGM-2 alone or supplemented with TNFα, 10ng/ml. After 24h, images were captured at 50x and 200x by phase contrast microscopy.

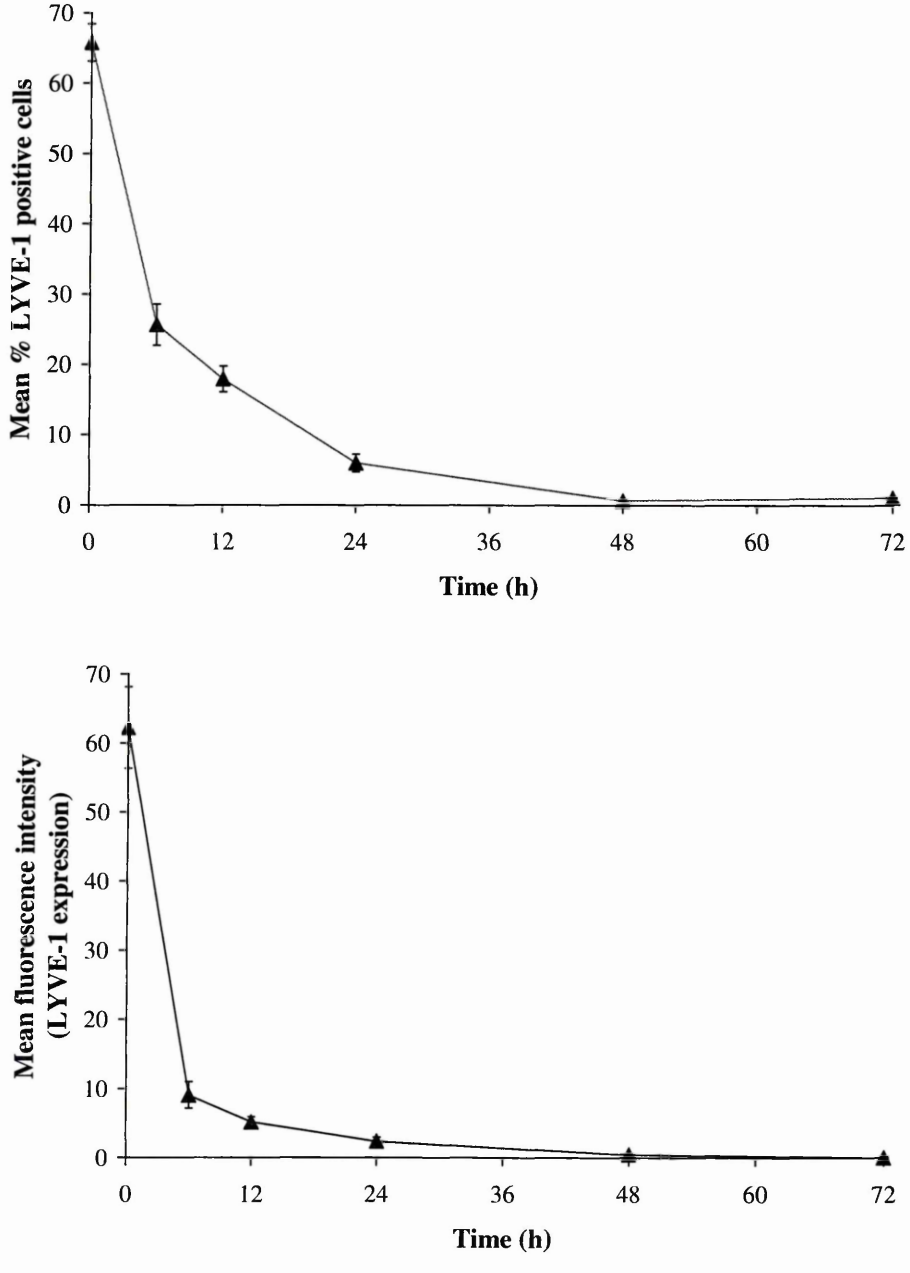

Figure 4.11 Time course of TNFα-induced LYVE-1 down-regulation in primary HDLEC. Cells were cultured for between 0 and 72h in quadruplicate in the presence of TNFα, then lifted and stained with the anti-LYVE-1 mAb 8C and goat anti-mouse AlexaFluor®488 for analysis by flow cytometry. The mean percentage of LYVE-1 positive cells (upper graph) and mean fluorescence intensity (lower graph) are plotted at each time point, ± standard error.

4.2.3.5 Concentration dependence

Soluble TNFα binds TNFRI with a K_d of 20-60 pM whilst TNFβ displays a slightly lower affinity, with a K_d of 650 pM (Marsters et al., 1992). Initial experiments carried out in this thesis used a concentration of TNF of 100ng/ml (approximately 6nM and 100 x Kd). Therefore LEC were treated with lower concentrations of the cytokine and LYVE-1 expression assayed by flow cytometry, to investigate whether the effect was as pronounced at concentrations closer to the Kd of TNF are used. Surface expression was measured by flow cytometry after 48h following exposure of cells to TNFα in the range of 0.1 to 100ng/ml (6pM-6nM) of TNF. As shown in figure 4.12, concentrations of TNFα at or just above the Kd value (5ng/ml; 160pM) were sufficient to result in total loss of surface expression of LYVE-1, whilst even the lowest concentration of 0.1ng/ml (10x fold below the Kd value) still induced approximately 50% loss.

4.2.3.6 Recovery

The next question posed was whether the effect of TNFα on LYVE-1 expression was reversible upon removal of the cytokine. To investigate the phenomenon, HDLEC were cultured for 48h in either the presence or absence of TNFα followed by withdrawal and replacement of the medium with cytokine-free EGM-2 and measurement of LYVE-1 surface expression by flow cytometry. The results (figure 4.13) showed that the effects of TNFα were fully reversible with full recovery of LYVE-1 within 48h.

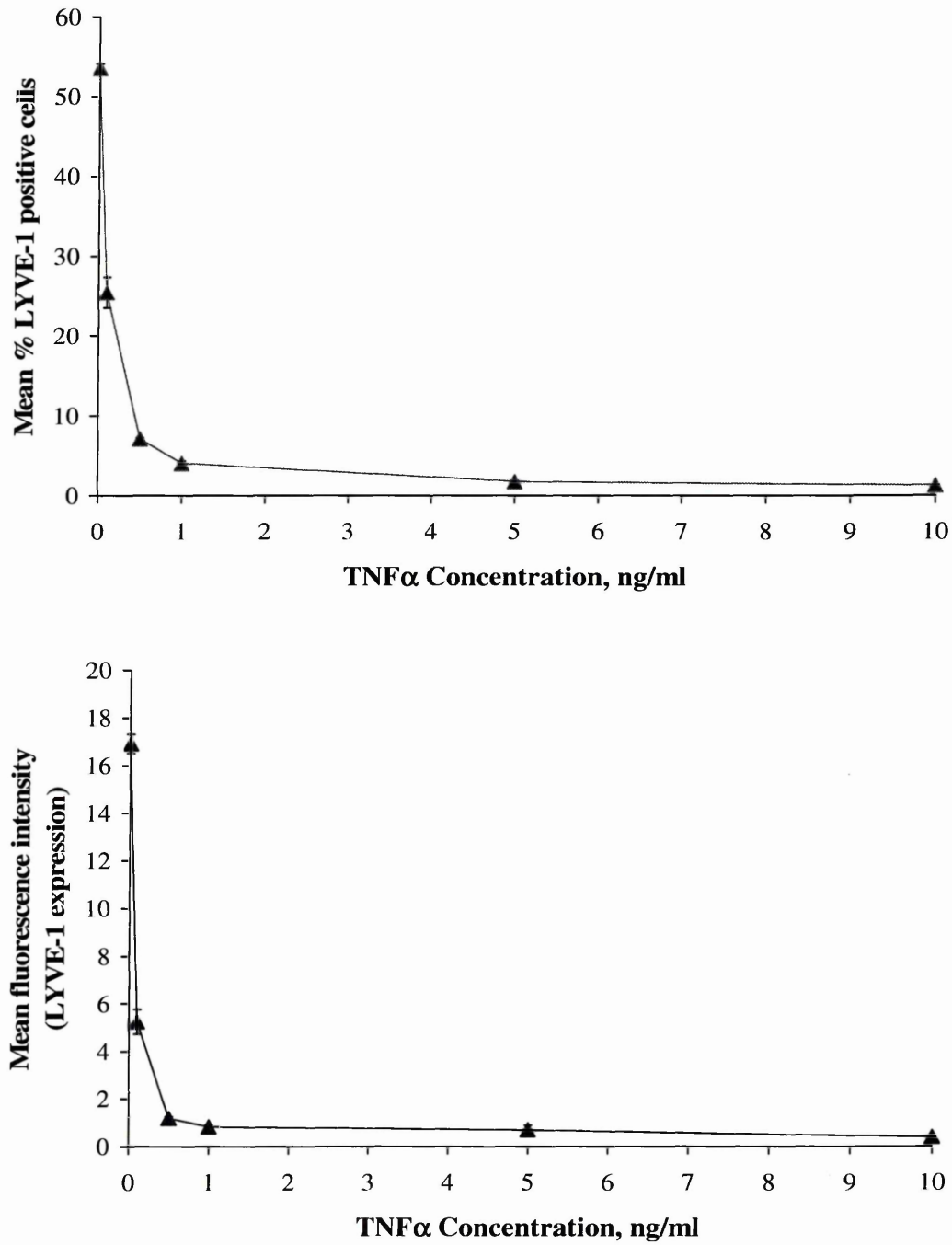

Figure 4.12 Concentration dependence of TNFα. Cells were cultured for 48h in triplicate in the presence of TNFα at concentrations between 0 and 10 ng/ml, then lifted and stained with the anti-LYVE-1 mAb 8C and goat anti-mouse AlexaFluor®488 for analysis by flow cytometry. Data are plotted as the mean percentage of positive cells (upper graph) and mean fluorescence intensity (lower graph) ± standard error.

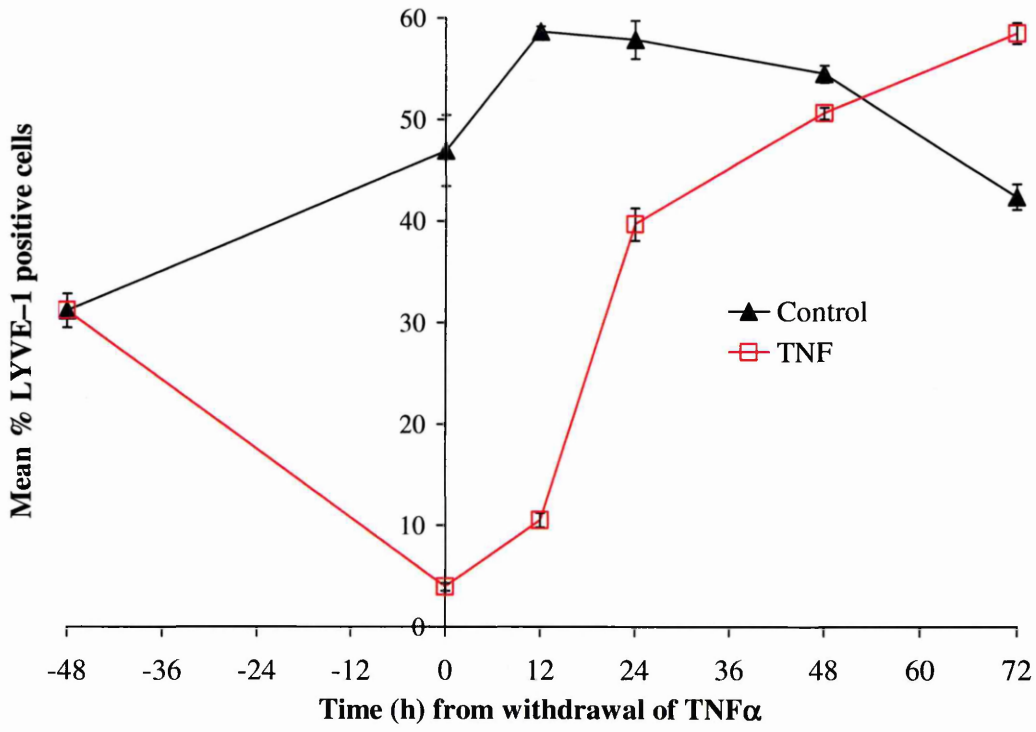

Figure 4.13 Reversibility of TNF-induced down-regulation of LYVE-1 in cultured HDLEC. Cells were cultured for 48h in the presence of TNFα, 10 ng/ml, then washed twice with PBS and once with fresh EGM-2 medium before continued culture in media with no additions of cytokine. At 12h, 24h, 48h and 72h after the change of medium, cells from triplicate wells were lifted and stained with the anti-LYVE-1 mAb 8C and goat anti-mouse AlexaFluor®488 for analysis by flow cytometry. The graph shows the mean percentage of LYVE-1 positive cells, ± standard error at each time point.

4.2.4 The fate of LYVE-1 following exposure to TNF

4.2.4.1 Effects of TNFα stimulation on LYVE-1 protein

TNFα-induced down-modulation of LYVE-1 could be mediated by either shedding or internalisation of the receptor. The following experiments were designed to determine which of these two mechanisms was involved.

During the course of this thesis, studies carried out by a fellow DPhil. student Tom Nightingale on 293T stable transfectants had shown that phorbol 12-myristate 13 acetate (PMA), an analogue of diacylclycerol that signals via protein kinase-C (PKC) induced shedding of LYVE-1 from the cell surface. To investigate whether such shedding also occurred following stimulation with TNFα or TNFβ, cells were cultured for 24h in the presence or absence of these cytokines and the loss of cell surface LYVE-1 assessed by immunofluorescence microscopy (figure 4.8). In addition, the supernatants were removed and assayed for shed LYVE-1 using a quantitative enzyme-linked immunosorbent assay (ELISA) calibrated with purified soluble LYVE-1 Fc and detected with the LYVE-1 mAb 8C. Culture media from LYVE-1 transfected 293T cells which shed receptor in response to PMA were used as a positive control. The results revealed that untreated HDLEC shed low but appreciable levels of LYVE-1 into the culture media, (approximately 10ng/ml). Surprisingly however, shedding was suppressed following TNFα treatment (figure 4.14).

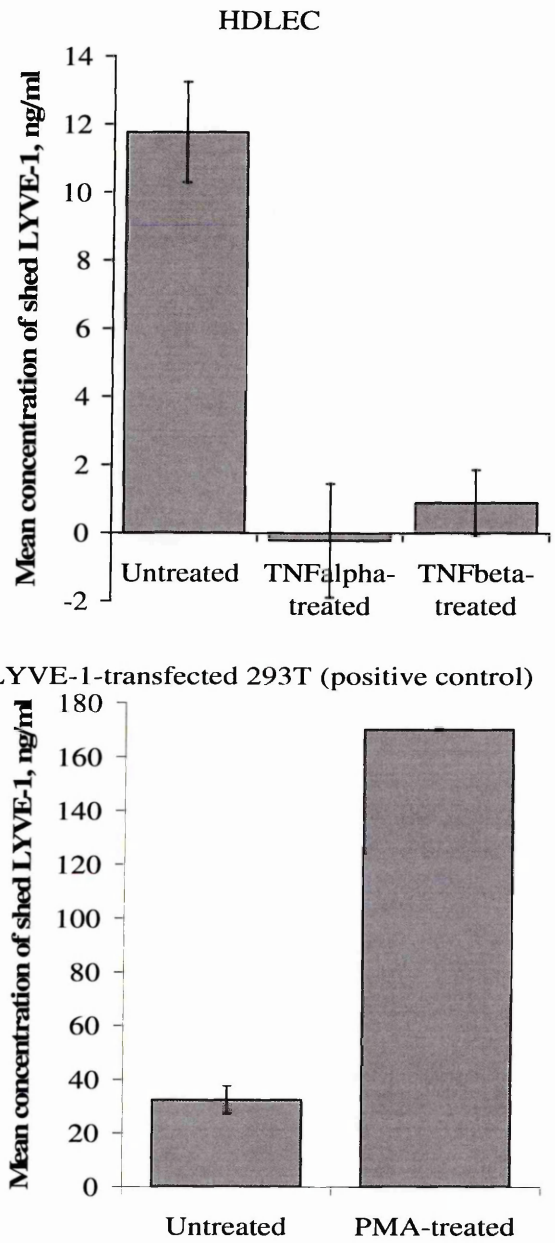

Figure 4.14 Shedding of LYVE-1 by cultured primary HDLEC in response to TNF. HDLEC were cultured for 24h in the presence of either TNFα, TNFβ or with no additions. The supernatants were then applied to a microtitre plate, precoated with rabbit anti-human LYVE-1. The ELISA was calibrated with purified soluble LYVE-1 Fc fusion protein and supernatants from 293T human LYVE-1 transfectants stimulated for 4h with PMA, (20ng/ml) were used as a positive control. Bound protein was detected using the LYVE-1 mAb 8C and an HRP-conjugated goat antibody with OPG and the mean concentration of LYVE-1 ± standard error was calculated.

It should be noted however that although no shed LYVE-1 could be detected in the supernatant following TNFα stimulation, the mechanism of shedding may have destroyed epitopes which could be recognised by the mAb employed in the above ELISA. PMA-induced shedding of LYVE-1 by transfectants had previously been shown to be mediated by matrix metalloproteinases (MMPs) and hence could be inhibited by the broad spectrum MMP inhibitor Ilomastat. To investigate whether the same mechanism was responsible for TNFα–induced loss of surface expression, cells were treated for 1h with Ilomastat prior to incubation for 24h in either EGM-2 alone or with TNFα. Surface expression of LYVE-1 was then assayed by flow cytometry. Ilomastat was found to have no effect on loss of cell surface LYVE-1 following stimulation with TNFα (figure 4.15) and thus it was concluded that TNFα-induced LYVE-1 down-regulation was not mediated by MMPs.

These data suggested that LYVE-1 was being internalised rather than shed. To investigate this latter possibility, confocal microscopy was used. HDLEC were cultured for 3h, 6h, 12h, 24h and 48h in the presence or absence of TNFα then either permeabilised with saponin or left intact prior to staining for LYVE-1 and podoplanin. The results confirmed initial co-localisation of LYVE-1 with podoplanin at the cell surface (figure 4.16). However as early as 3h after TNFα addition, only podoplanin remained in this location and LYVE-1 was completely lost. Permeabilisation of the cells revealed that LYVE-1 was present intracellularly, consistent with TNF-induced internalisation. By 48h the intracellular LYVE-1 had also disappeared, indicative of degradation.

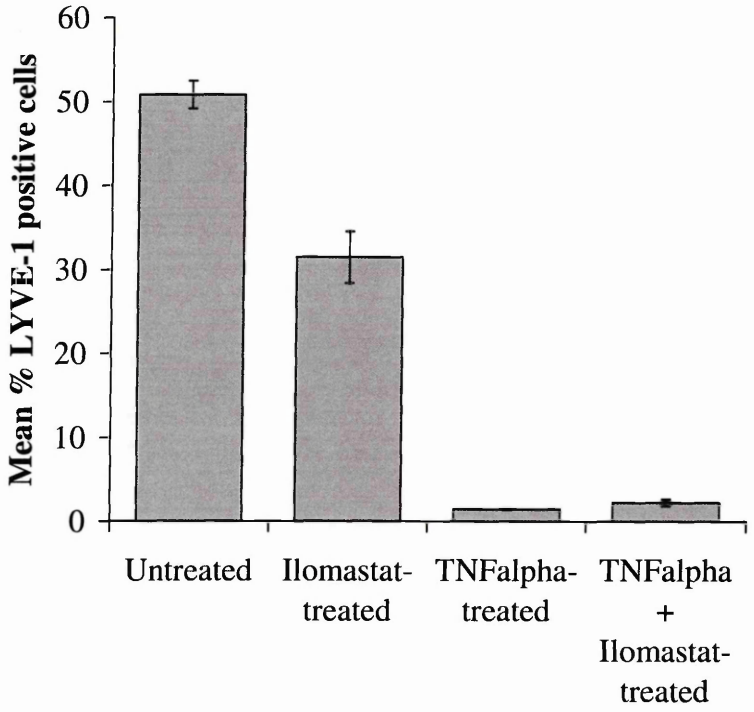

Figure 4.15 Effect of Ilomastat on TNF-induced loss of surface LYVE-1 by cultured primary HDLEC. Cells were cultured in triplicate for 1h in the presence of Ilomastat, (25 μM) prior to the addition of TNFα, 10 ng/ml and incubation for 24h. Cells were then lifted and stained in triplicate with the LYVE-1 mAb 8C and goat anti-mouse AlexaFluor®488 for analysis by FACS. The mean percentage of LYVE-1 positive cells was calculated for each condition ± standard error.

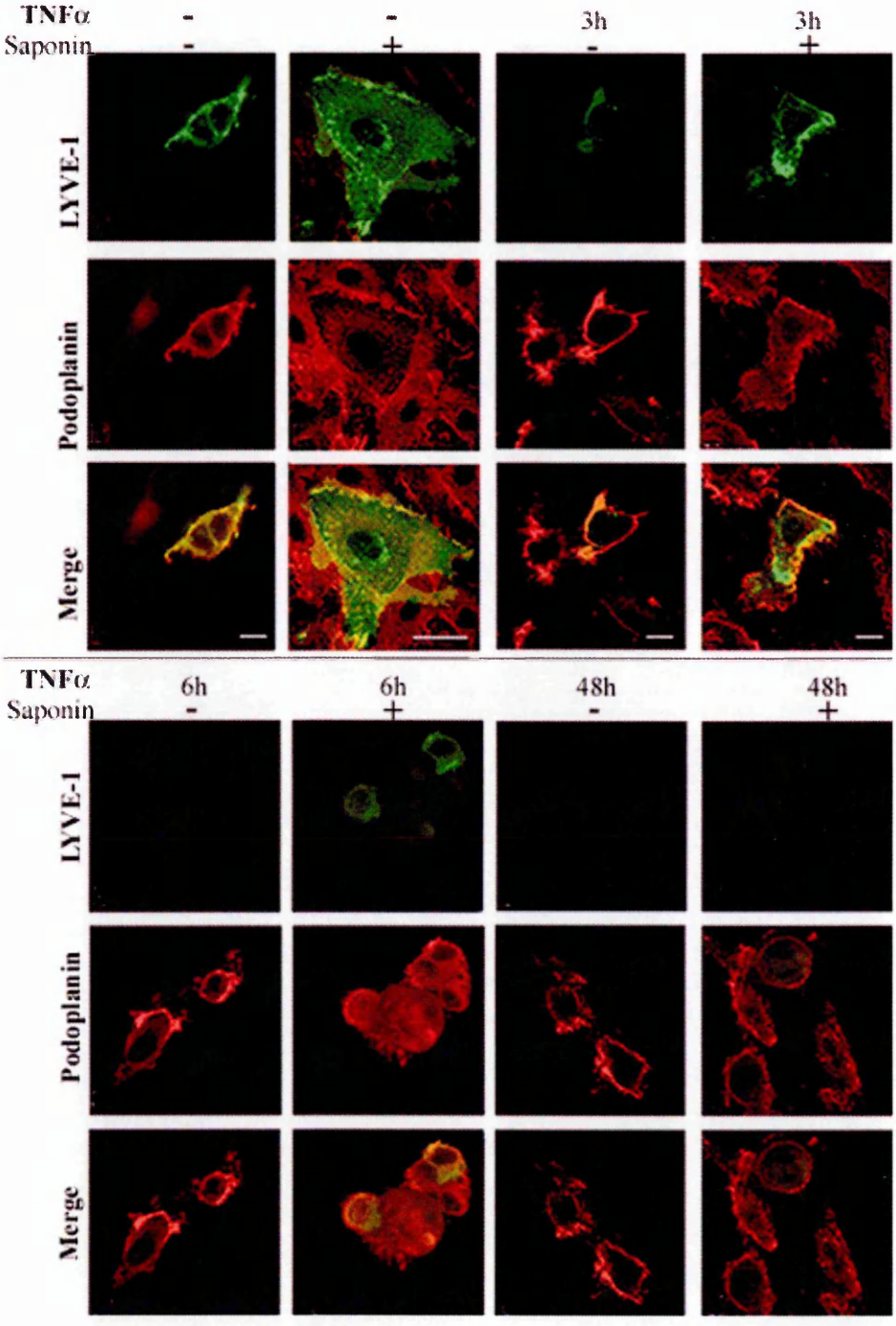

Figure 4.16 Analysis of TNFα-induced LYVE-1 internalisation by confocal microscopy (following page). HDLEC were stimulated with TNFα, (10ng/ml) and at each time point cells were either permeabilised with saponin or left intact. LYVE-1 was detected using 8C and goat anti-mouse AlexaFluor®488 (shown in green) whilst podoplanin was detected using rabbit antisera and goat anti-rabbit AlexaFluor®594 (red). Bars represent 10μm.

To identify the intracellular compartment with which LYVE-1 was associated, a series of markers were employed. These included CD63, an integral membrane protein with four transmembrane regions and the putative lysosomal targeting signal Gly-Tyr in its short cytoplasmic tail, found in lysosomes and late endosomes (Metzelaar et al, 1991) and early endosome antigen 1 (EEA-1), a hydrophilic peripheral membrane protein believed to be required for vesicular transport of proteins (Mu et al, 1995). Other markers were protein disulphide isomerase (PDI), a highly active and abundant protein chaperone found on the endoplasmic reticulum (Narindrasorasak et al, 2003), TGN46, a glycoprotein implicated in the recruitment of cytosolic factors and vesicle formation on the trans-Golgi network (Prescott et al, 1997; Hickinson et al, 1997) and cytochrome c, the mitochondrial marker. Following 3h of TNF stimulation, LYVE-1 was found to colocalise less with PDI and TGN46, suggesting a decrease in *de novo* synthesis (figure 4.17). To study newly internalised LYVE-1, cells were incubated with rabbit anti-human LYVE-1 in either the presence or absence of TNFα, then permeabilised and stained for either CD63 or with EEA-1. After 3h of TNFα stimulation, cells showed colocalisation of LYVE-1 with both the lysosomal and early endosomal markers. However, more cells showed a greater abundance of LYVE-1 within the lysosomal compartment at this time point. As expected no colocalisation of LYVE-1 was observed with cytochrome c, the mitochondrial marker. Thus it was concluded that TNFα stimulation induces internalisation of LYVE-1 and degradation within lysosomes, concomitant with a rapid decrease in *de novo* synthesis.

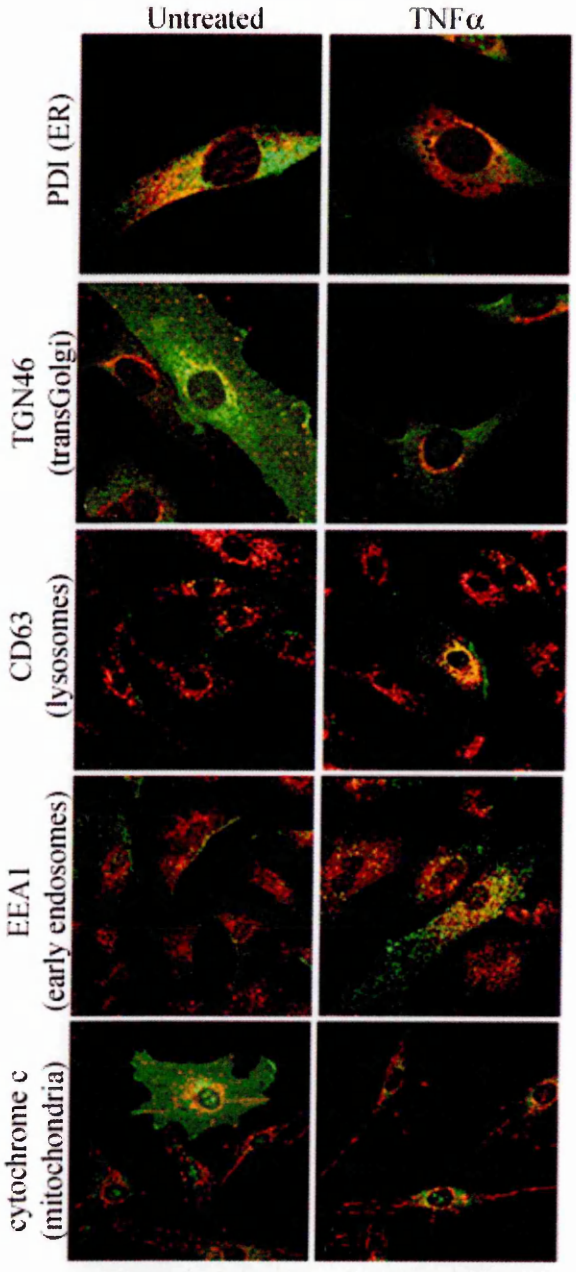

Figure 4.17 Intracellular localisation of LYVE-1 in primary HDLEC following TNFα stimulation. To study location of intracellular LYVE-1, cells were cultured for 3h either with or without TNFα then permeabilised with saponin and stained with rabbit anti-human LYVE-1 (green) and for intracellular vesicle markers PDI or TGN46 in red, with secondary antibodies goat anti-rabbit AlexaFluor®488 and anti-mouse AlexaFluor®568 respectively. To study location of internalised LYVE-1, cells were incubated for 3h with rabbit anti-LYVE-1 (green) +/- TNFα, then permeabilised and stained with either anti-CD63, anti-EEA-1 or anti-cytochrome c (red), with secondary antibodies goat anti-rabbit AlexaFluor®488 and anti-mouse AlexaFluor®568 respectively. Images were captured at magnification: 600X.

4.2.4.2 Effects of TNFα stimulation on LYVE-1 mRNA levels

The preceding sections describe how exposure to TNF led to internalisation and degradation of cell surface LYVE-1 by HDLEC. Confocal microscopy had revealed a decrease in LYVE-1 localised to the endoplasmic reticulum and Golgi apparatus, suggesting a decrease in synthesis. It was next determined whether the putative inhibition by TNFα of *de novo* synthesis of LYVE-1 was manifest at the level of transcription or translation.

HDLEC were cultured for 72h in either medium alone or with TNFα (10 ng/ml). Total RNA was prepared and subjected to agarose-formaldehyde gel electrophoresis, then transferred onto charged membrane and probed with [α-^{32}P] labelled *LYVE-1* for Northern hybridisation. Figure 4.18 shows that although the 1.8kb LYVE-1 mRNA was clearly observed in untreated cells, no message was detected after TNFα treatment, despite equal loading of RNA, as shown by the β-actin controls.

To investigate the rate of LYVE-1 mRNA loss, total RNA was isolated from HDLEC cultured for 12, 24, 48 or 72h in the presence or absence of TNFα. Reverse transciptase-PCR was then carried out on this RNA using either LYVE–1 or β-actin primers for 10-30 cycles. Products were run on an agarose gel and then transferred to nylon membrane for Southern blotting using LYVE-1 or β-actin radiolabelled probes (figure 4.19). This revealed that loss of LYVE-1 mRNA was already complete by 12h of TNF treatment, consistent with the findings from confocal microscopy which revealed a loss of LYVE-1 surface expression and detection of less nascent protein in association with the biosynthetic machinery of the endoplasmic reticulum and Golgi after only 3h (see figure 4.17). Similarly, surface LYVE-1 protein was internalised within 3h and had undergone substantial degradation by 12h. Thus the down-regulation of both LYVE-1 mRNA and protein occur concurrently.

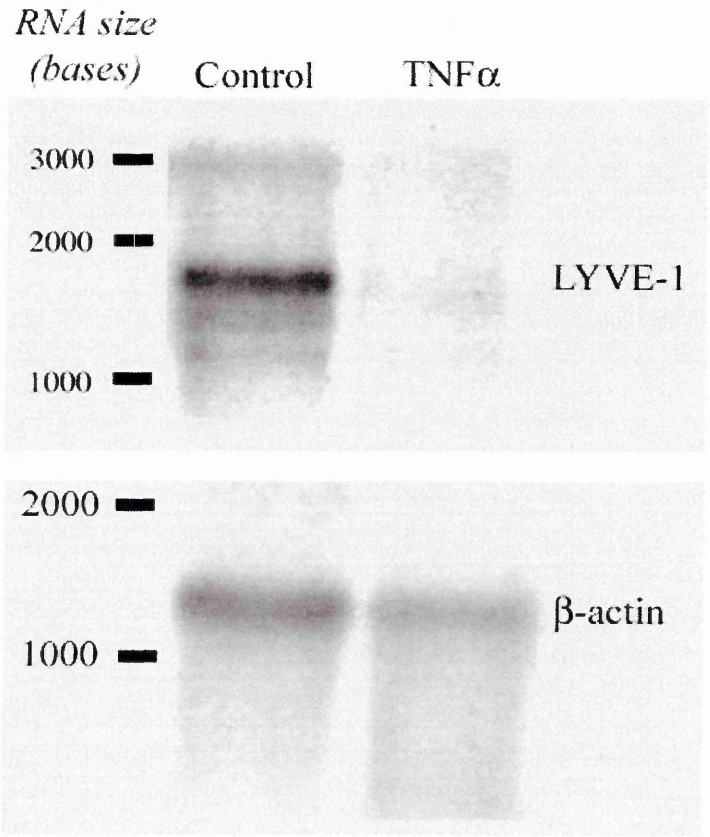

Figure 4.18 Effect of TNFα on LYVE-1 mRNA in primary HDLEC. A Northern blot of total RNA isolated from HDLEC cultured for 72h +/- TNFα, (10ng/ml) was probed with either LYVE-1 or β-actin ^{32}P-labelled cDNAs, followed by autoradiography. An RNA ladder was electrophoresed in parallel and size markers in bases are indicated on the left.

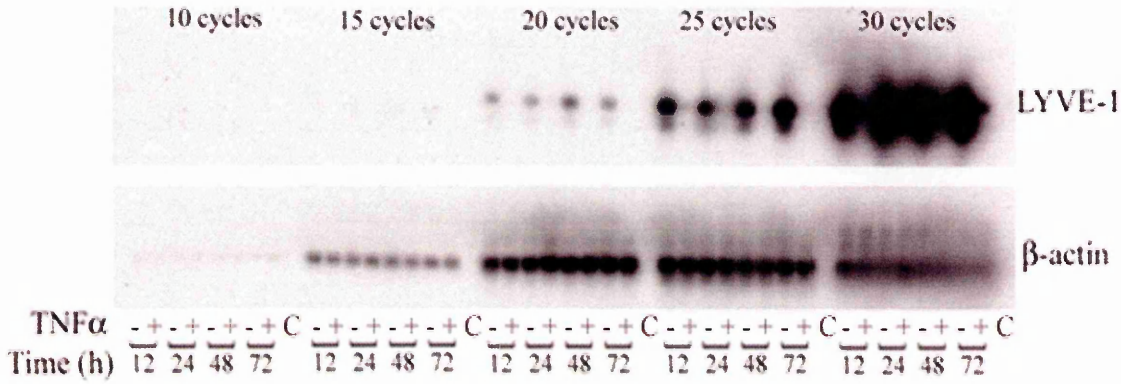

Figure 4.19 Effect of TNFα on LYVE-1 mRNA levels in primary HDLEC, assessed by semi-quantitative PCR. First strand cDNA prepared from primary HDLEC cultured for varying time periods (12-72h) with or without TNFα were subjected to RT-PCR using LYVE-1 primers 269F and 764R or β-actin primers from 10-30 cycles prior to electrophoresis, transfer to nitrocellulose and hybridisation to LYVE-1 or β-actin probes (see methods, chapter 2). Samples in which the cDNA was omitted (C) were included as negative controls.

4.2.5 Investigating possible involvement of NFkB in TNFα-induced down-regulation of LYVE-1

TNF is one of many inducers of NFκB, the inducible eukaryotic transcription factor (Bowie and O'Neill, 1999). Other activators of NFκB include viral and bacterial products, T- and B-cell mitogens, agents of cellular stress such as endoplasmic reticulum protein overload, UV light, oxidizing agents, cigarette smoke and asbestos fibres, to mention only a few on an ever expanding list. Within unstimulated cells NFκB exists in the cytoplasm in an inactive form, comprising the transcriptionally active dimer bound to an inhibitor protein, IκB. Although NFκB can be composed of a variety of different subunits, the majority of work has focused on the p50/p65 dimer and its association with IκBα (Bowie and O'Neill, 1999). Upon stimulation, IκBα is rapidly phosphorylated on two serine residues, thus targeting the inhibitor protein for ubiquitination and degradation by proteasome. The NFκB dimer is then released and can translocate to the nucleus to activate target genes by binding to κB elements within their promoters. NFκB may act as either an inducer or repressor of transcription. To explore the possibility that LYVE-1 down modulation was via an NFκB-dependent pathway, preliminary experiments into the effect of inhibitors were carried out.

Among many different inhibitors of NFκB, the compound BAY 11-7082 which blocks the phosphorylation of IκB-α was shown to inhibit NFκB-mediated induction of ICAM-1, VCAM-1 and E-Selectin in HUVEC (Pierce et al., 1999). Therefore BAY 11-7082 was used in preliminiary experiments to investigate the involvement of NFκB in TNFα-induced down-regulation of LYVE-1. To establish the optimal concentration of BAY 11-7082, the effects were first tested by cell viability. Primary HDLEC were treated for 24h and then their viability assessed

by a trypan blue dye-exclusion assay in which dead cells were distinguished by their failure to exclude dye and distinct morphology (figure 4.20). BAY 11-7082 was found to be very toxic to HDLEC at concentrations of 5μM and above, which were used in the paper by Pierce et al. (1999). A titration of BAY 11-7082 concentration and dye exclusion assay was also performed on 293T cells. These cells also failed to exclude dye and lost adherence at concentrations of BAY-11-7082 of 10 μM and higher (data not shown). Therefore a concentration of 2 μM of BAY 11-7082 was used for subsequent experiments. Cells were pre-incubated with BAY 11-7082 for 1h before the addition of TNFα. 24h later cells were lifted and stained for LYVE-1 expression for quantitation by flow cytometry (figure 4.21). Although TNF-induced loss of LYVE-1 was not prevented by preincubation with BAY 11-7082, the inhibitor reduced the loss of LYVE-1 by TNFα and TNFβ by 21% and 25% respectively.

While these results provided suggestive evidence to support the hypothesis that TNF-induced loss of LYVE-1 was mediated by NFκB, this could not be demonstrated conclusively by this experiment due to the toxicity of BAY 11-7082. An alternative, less toxic inhibitor of NFκB was therefore employed, prostaglandin A1, PGA1 (Rossi et al., 2000). Cells were treated with PGA1 prior to stimulation with TNFα and after 5h, LYVE-1 surface expression was measured by flow cytometry. It was found that PGA1 itself caused loss of surface expression (figure 4.22).

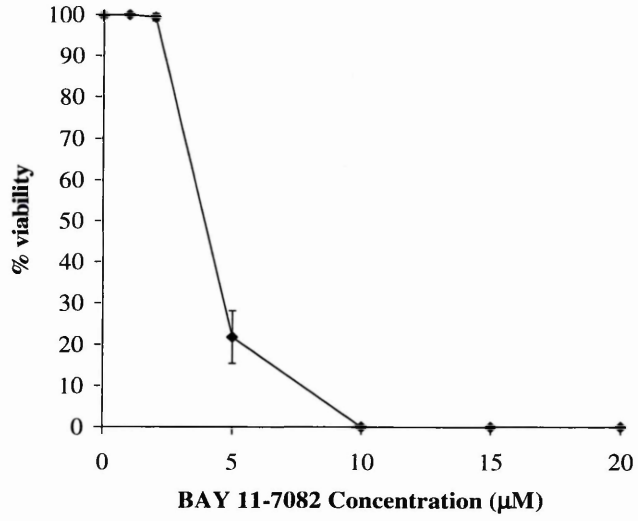

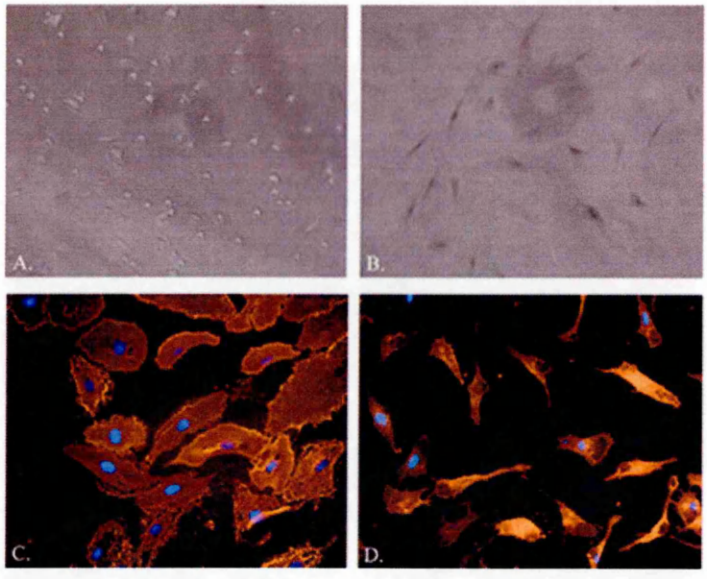

Figure 4.20 Effect of BAY 11-7082 on HDLEC viability. Cells were cultured for 24h in EGM-2 medium supplemented with BAY 11-7082, 0 – 20 μM. Supernatants were then removed and trypan blue applied. After 10 minutes the percentage of live cells was assayed in triplicate at each concentration of BAY 11-7082 ± standard error (upper graph). Untreated cells (panel A) excluded dye whilst cells treated with 10 μM or higher concentrations of BAY 11-7082 failed to exclude dye (panel B). Immunofluorescence staining with rabbit anti-podoplanin and goat anti-rabbit AlexaFluor® 594 with nuclei counterstained with DAPI revealed that unlike the untreated cells (panel C), cells which had been exposed to BAY 11-7082 became largely de-nucleated and permeable to antibody (panel D). Magnification: X100.

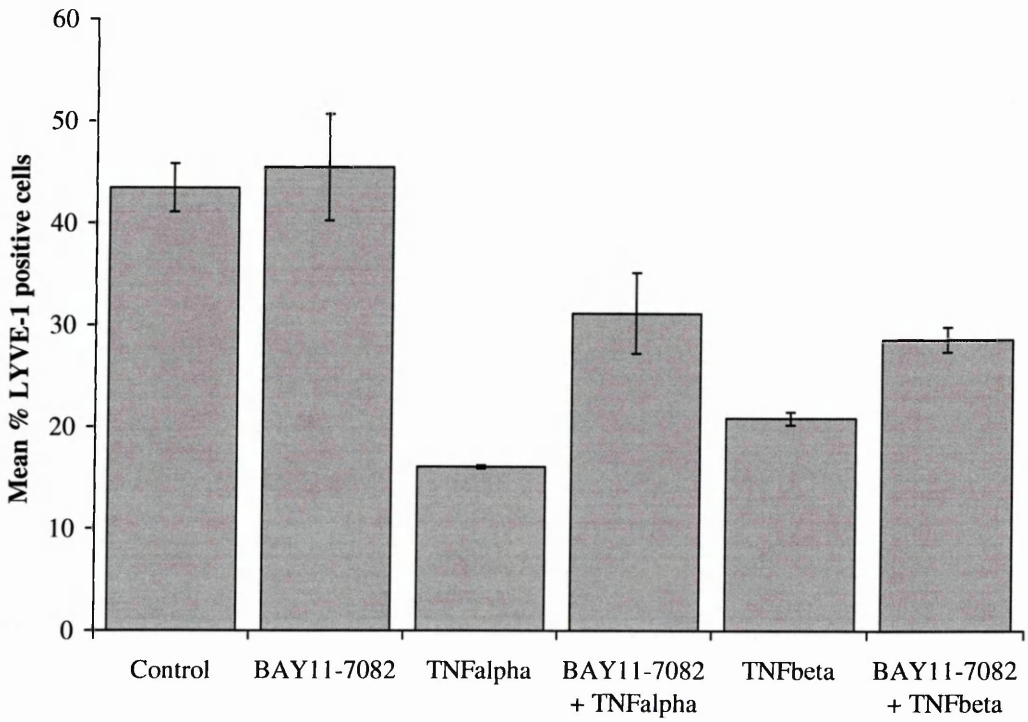

Figure 4.21 Effects of BAY 11-7082 on TNF-induced shedding of LYVE-1 in HDLEC. Cells were incubated for 1h with BAY 11-7082, 2 μM prior to addition of either TNFα, (10 ng/ml) or TNFβ, (100 ng/ml). Cells were incubated for 24h, then lifted and stained with the LYVE-1 mAb 8C and goat anti-mouse AlexaFluor®488 for quantitation of LYVE-1 surface expression by flow cytometry. The bar chart shows the mean percentage of LYVE-1 positive cells ± standard error for cells under each condition.

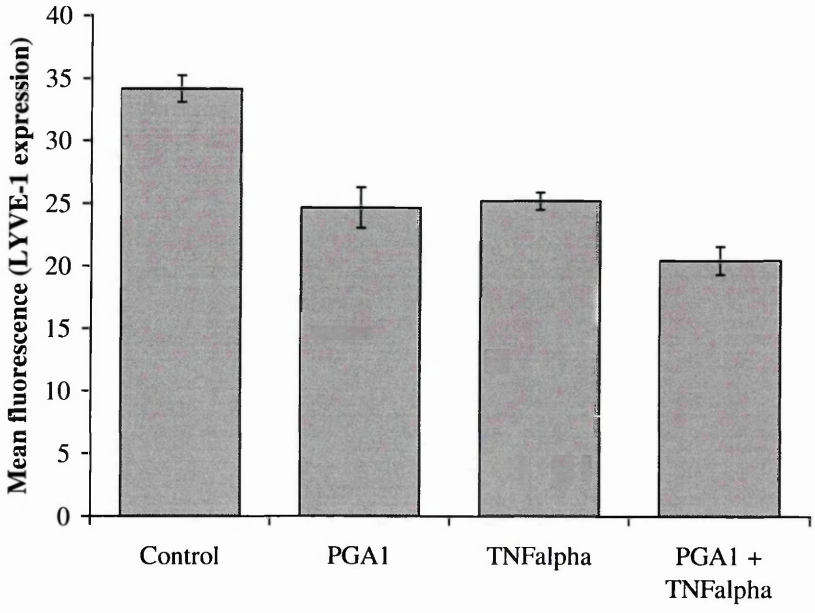

Figure 4.22 Effect of PGA1 on surface expression of LYVE-1 in HDLEC. Cells were preincubated with PGA1, 100μM for 1h prior to the addition of TNFα. Following a 5h incubation, cells were lifted and stained with 8C and goat anti-mouse AlexaFluor®488 to measure LYVE-1 expression by flow cytometry, ± standard error.

4.2.6 Possible effects of LYVE-1 down-regulation on HA binding

In view of the finding that inflammatory mediators down-regulate LYVE-1 in primary HDLEC, it was interesting to consider the possible physiological consequences. As described in the general introduction to this thesis (chapter 1), LYVE-1 expressed on primary HDLEC does not constitutively bind HA. Therefore subsequent experiments focused on whether LYVE-1 becomes functionally activated during TNFα-induced internalisation, leading to uptake and/or degradation of its ligand, HA.

4.2.6.1 Effects of TNFα on HA binding by LYVE-1 in HDLEC

To test this hypothesis, confocal microscopy was used to detect HA colocalisation with internalised LYVE-1 2h following stimulation with TNFα, as at this time LYVE-1 had been internalised but not degraded. As HDLEC also express CD44 (chapter 5) which might interfere with interpretation of the results, cells were pre-incubated with the mAb BRIC235 which blocks HA binding by CD44 (Lesley et al., 1993). Following a 40-minute incubation with BRIC235 and rabbit anti-human LYVE-1, biotinylated high molecular weight HA, > 1 MDa (prepared by Dr. David Mahoney, Department of Biochemistry, Oxford) and TNFα were added. Cells were permeabilised with saponin after 2h and HA and LYVE-1 detected with the conjugates streptavidin-AlexaFluor®568 and AlexaFluor®488 respectively (figure 4.23).

Internalised HA was detected in both untreated and TNFα-stimulated HDLEC. However, following 2h incubation in the presence of TNFα, a marginal increase in the amount of intracellular HA was observed, a proportion of which appeared to colocalise with the newly internalised LYVE-1 (figure 4.23).

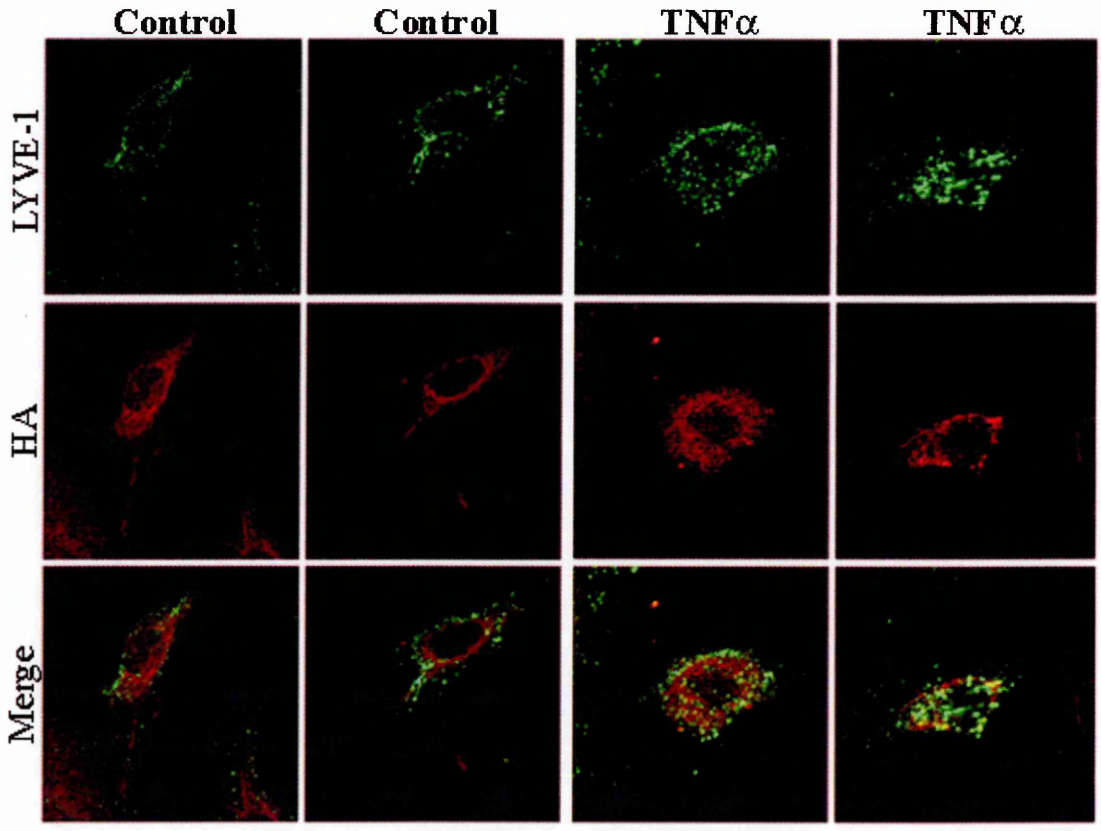

Figure 4.23 Effect of TNFα on HA internalisation by primary HDLEC. Cells were pre-incubated with rabbit anti-LYVE-1 and BRIC235 prior to the addition of either biotinylated HA alone (~175 μg/ml) or with TNFα (10ng/ml). Following a 2h incubation, cells were fixed with PFA and permeabilised with saponin. Bound rabbit anti-LYVE-1 was detected by goat anti-rabbit AlexaFluor®488 (green) and biotinylated HA by streptavidin-conjugated AlexaFluor®568 (red).

4.2.6.2 Effects of TNFα on HA binding by LYVE-1 in primary mouse dermal LEC

The previous experiment indicated that HDLEC internalise HA and that the extent of uptake was marginally increased in response to TNFα, perhaps via LYVE-1. To further investigate this, primary mouse dermal LEC were used (described more fully in chapter 5). These cells were fresh isolates at a much earlier passage than HDLEC and consequently did not express CD44. Resting and TNFα-treated mouse LEC were assayed for their capacity to internalise fluorescent high molecular weight (> 1MDa) HA using both flow cytometry (figure 4.24) and confocal microscopy (figure 4.25).

Figure 4.24 shows that a small but significant number of cells (5.4%) either bound or internalised fluorescent HA and this number increased (11.6%) following stimulation for 2h with TNFα. To assess whether this fluorescence represented internalised HA, confocal microscopy was used and revealed that fluorescent HA was internalised by LYVE-1-positive mouse LEC, both in the resting state and following TNFα stimulation (figure 4.25). As with the human cells, some colocalisation between LYVE-1 and HA was visible, although no dramatic increase in intracellular HA was apparent following incubation with TNFα. In summary, the internalisation of HA by LYVE-1-positive primary mouse dermal LEC has been shown and future experiments to address the mechanism of this and possible involvement by LYVE-1 and TNFα–induced activation could seek to explore this phenomenon more fully.

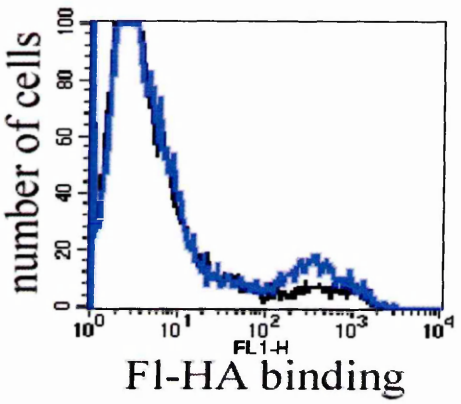

Figure 4.24 Binding of fluorescent HA by primary mouse dermal LEC. Cells were cultured in the presence of fluorescent HA, (10μg/ml), prior to lifting with PBS-5mM EDTA and assaying either bound or internalised HA by flow cytometry. Resting cells are shown in black and TNFα-stimulated (10ng/ml) cells in blue. 5.4% of resting cells bound fluorescent HA whereas 11.6% of cells bound HA following 2h of stimulation with TNFα.

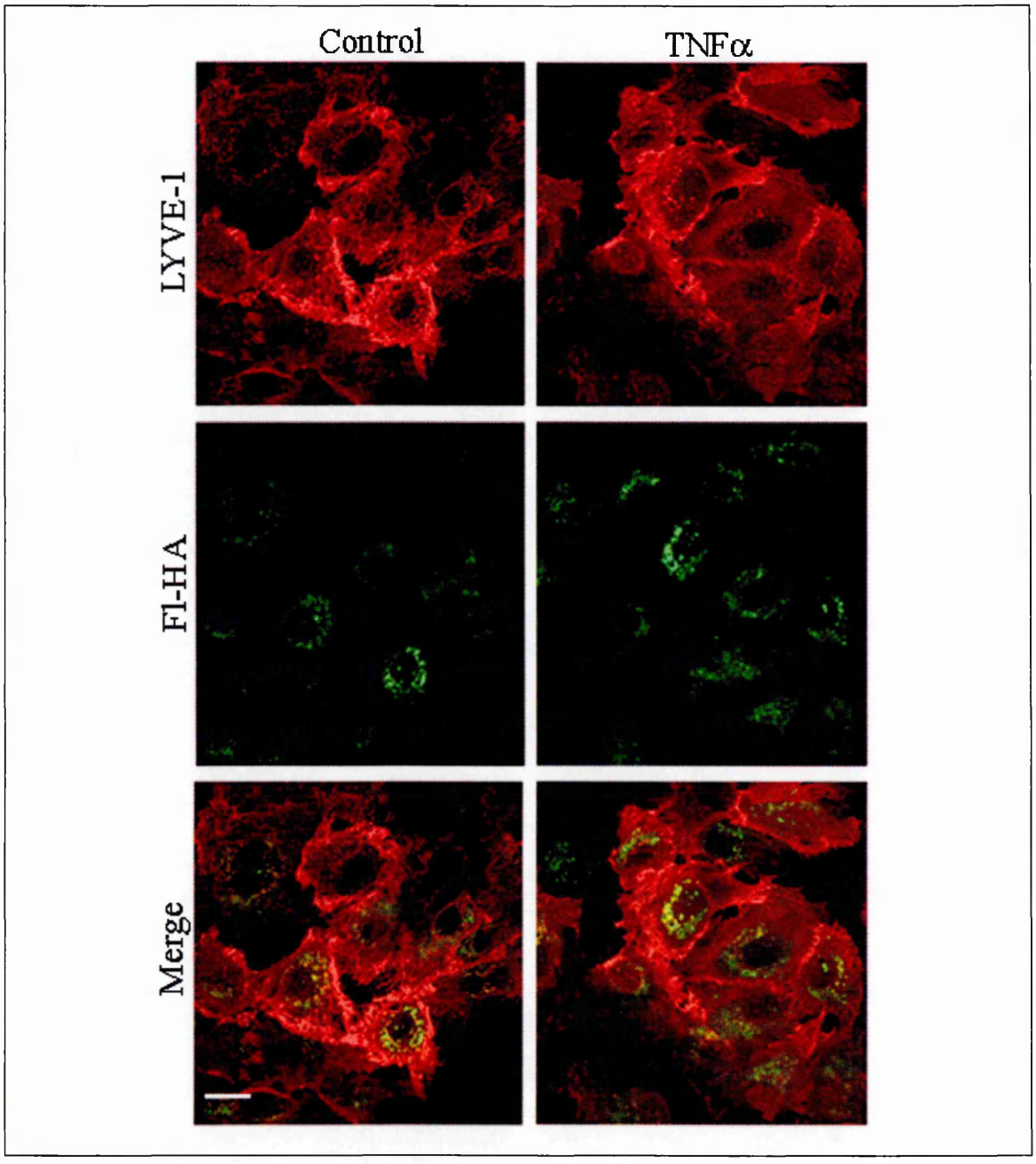

Figure 4.25 Immunofluorescence microscopy to demonstrate that fluorescent-HA is internalised by primary dermal mouse LEC. Cells were pre-incubated with fluorescent-HA and the anti-LYVE-1 mAb C1/8 prior to culturing in either the presence or absence of mouse recombinant TNFα, 100ng/ml. Cells were then fixed with PFA, permeabilised with saponin and LYVE-1 was detected using AlexaFluor®568 (red) goat anti-rat secondary antibody. Representative images were captured at a magnification of X 600. Bar = 72μm.

4.2.7 Effect of IL-6 on LYVE-1 expression on HDLEC

Earlier experiments had shown a marginal increase of LYVE-1 expression on HDLEC following exposure to IL-6. LYVE-1 surface expression was found to increase on both PromoCell HDLEC (figure 4.4) and Clonetics HMVEC (figure 4.5). To assess the possible significance, this was characterised further using PromoCell HDLEC.

4.2.7.1 Concentration dependence

HDLEC were cultured for 48h in varying concentrations of IL-6, from 0-20 ng/ml. Cells were then lifted and stained for LYVE-1 expression for quantitation by flow cytometry. Figure 4.26A shows the IL-6 concentration-dependent increase in the number of LYVE-1 positive cells, with the maximal increase occurring at 10-20 ng/ml. The FACS histograms are displayed in figure 4.26B and show the marginal increase in both the number of LYVE-1 positive cells and the amount of protein expressed.

4.2.7.2 Time-course

The effect of IL-6, 20ng/ml, on surface expression was quantitated using flow cytometry after 0, 6, 12, 24, 48 and 72h of exposure. Figure 4.27 shows that LYVE-1 surface expression steadily increased up to 72h after exposure. These results further strengthen the evidence that IL-6 induces or otherwise stabilises LYVE-1 expression in HDLEC. Although not pursued further in this present thesis, the potential significance or these findings are discussed later in the chapter (section 4.3).

A.

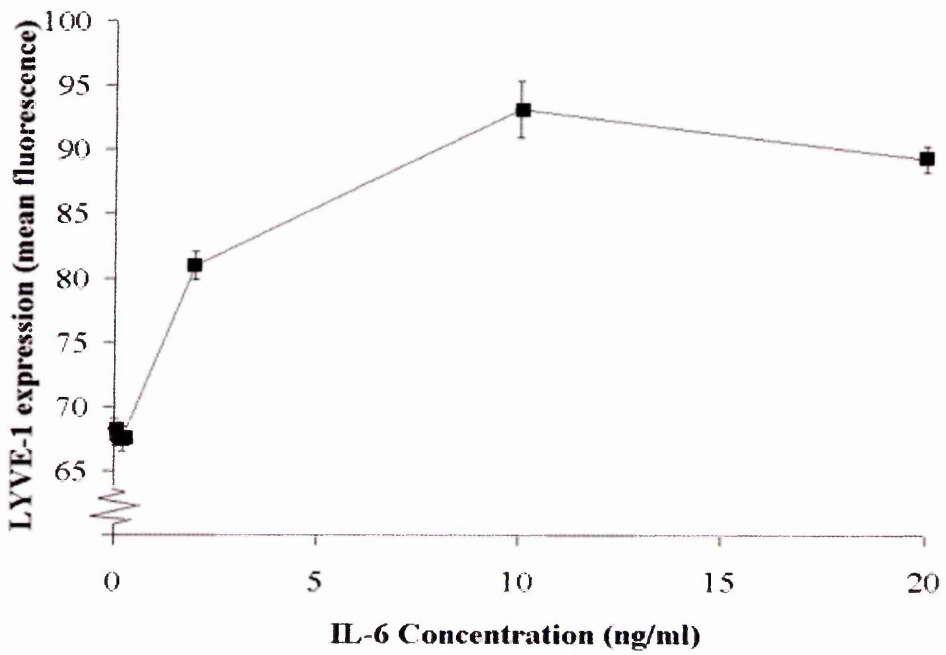

B.

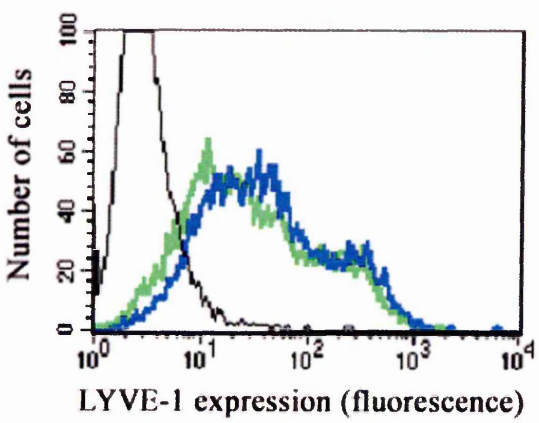

Figure 4.26 Effect of IL-6 on LYVE-1 surface expression in HDLEC. A. Cells were cultured in the presence of recombinant human IL-6 at concentrations between 0 and 20 ng/ml for 48h in triplicate. Cells were then lifted and stained with 8C and goat anti-mouse AlexaFluor®488. LYVE-1 expression as represented by mean fluorescence was assayed by flow cytometry and the mean of triplicate samples is expressed ± standard error. B. Flow cytometry plots of LYVE-1 expression. Untreated cells are represented by a green line; cells treated with IL-6, 20 ng/ml are shown in blue. Staining using isotype-matched control antibody is shown in black.

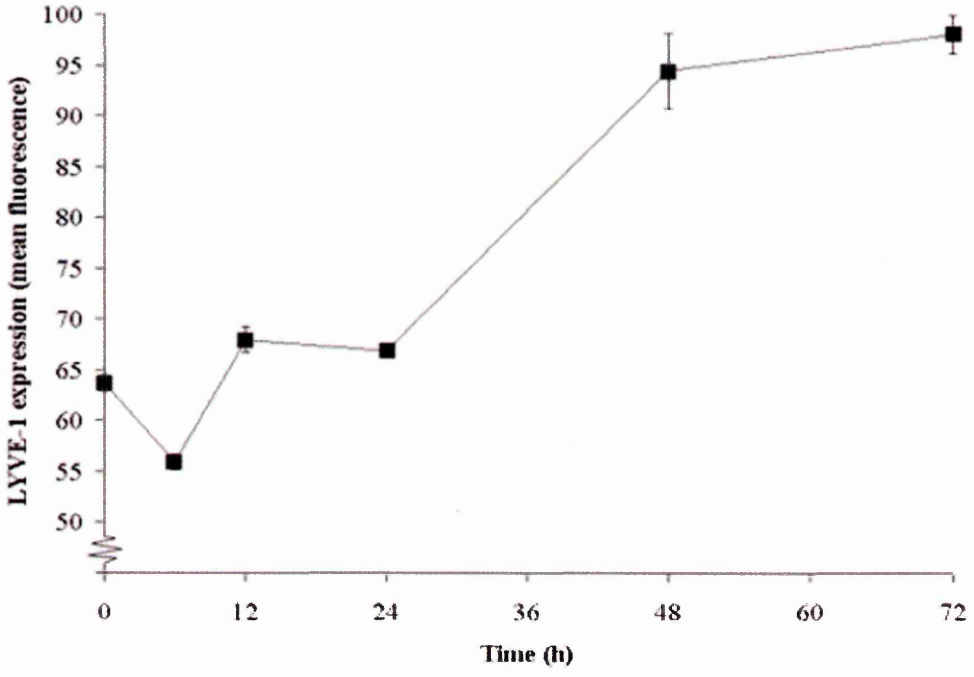

Figure 4.27 Time course of effect of IL-6 on LYVE-1 expression on HDLEC. Cells were treated with IL-6, 20 ng/ml, in triplicate for between 6 and 72h; some cells were left untreated. Cells were then lifted and stained with 8C and goat anti-mouse AlexaFluor®488. LYVE-1 expression as represented by mean fluorescence was assayed by flow cytometry and the mean of triplicate samples is expressed ± standard error.

4.2.8 Effect of hypoxia on HDLEC

Hypoxia is known to have a dramatic effect on protein expression and cell biology in blood vascular endothelial cells. To determine whether hypoxia might influence HDLEC in some manner, preliminary experiments sought to address the effect of hypoxia on LYVE-1 expression. HDLEC were cultured for 14h in either normoxic conditions or hypoxic conditions (0.1% oxygen). Cells were lifted and stained for LYVE-1, podoplanin or carbonic anhydrase-9, CA9 (an indicator of hypoxic shock on endothelial cells) and surveyed by flow cytometry (figure 4.28). CA9 was induced following hypoxic shock as expected. Interestingly, the levels of LYVE-1 expression were decreased by 40% under hypoxic conditions, whereas the levels of podoplanin (included as a control) remained unchanged.

4.2.9 Effect of PMA on LYVE-1 expression.

In addition to the pro-inflammatory down-regulation of LYVE-1 expression on HDLEC, LYVE-1 expression might also be altered through a different signal cascade, the MAPK pathway, by the diacylglycerol analogue PMA (detailed in the introduction to this chapter). It was of interest to determine whether the phenomenon of PMA-induced MMP-dependent shedding of LYVE-1 by 293T human fibroblast transfectants (S. Clasper and D. G. Jackson, unpublished; Tom Nightingale, DPhil thesis, University of Oxford, 2004) also occurred in human LEC which expressed endogenous LYVE-1 and whether it was via the same mechanism.

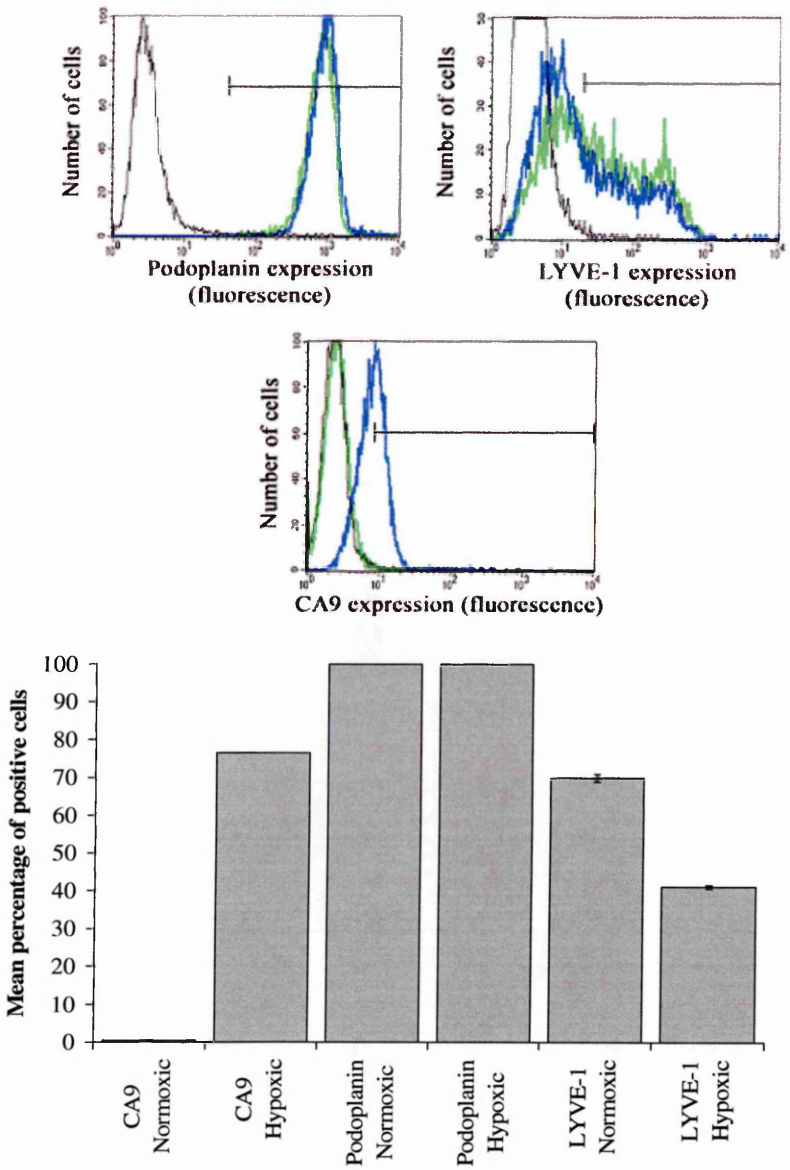

Figure 4.28 Effect of hypoxia on LYVE-1 expression in primary HDLEC. Cells were cultured for 14h either under normal conditions, i.e. 20% O_2, 5% CO_2 at 37°C in a humidified incubator, or at 0.1% O_2, 5% CO_2 at 37°C in a humidified incubator. Cells were then lifted and stained in triplicate using either mouse anti-CA9, rabbit anti-podoplanin or 8C and the appropriate goat AlexaFluor®488 conjugate for quantitation by flow cytometry. Normoxic expression is shown in green, hypoxic in blue and isotype-matched controls in black. Representative histograms for each are shown in the upper panel. The percentage positive cells were calculated from the gates indicated by a black horizontal line on the histograms, discounting cells stained by the isotype control antibodies. The mean percentage of positive cells for each protein ± standard error is plotted in the lower panel.

4.2.9.1 The effect of PMA on LYVE-1 shedding in HDLEC

To investigate the whether or not any shedding of LYVE-1 occurred upon stimulation of PKC, HDLEC were treated with PMA for 4h prior to the removal of supernatant. The presence of shed LYVE-1 in the supernatant was assayed by an ELISA calibrated by soluble LYVE-1 Fc. Supernatant samples were applied in triplicate to a microtitre plate pre-coated with rabbit anti-human LYVE-1. Bound antigen was detected by the mouse anti-human LYVE-1 mAb 8C and goat anti-mouse HRP-conjugate with OPG substrate. As shown in figure 4.29, LYVE–1 was shed upon stimulation with PMA and soluble LYVE-1 was detected in medium. Less shed LYVE-1 was detected in the supernatant from HDLEC than from 293T transfectants largely because 293T grow to greater densities and the transfectants expressed elevated levels of LYVE-1 in comparison to those endogenously expressed in HDLEC.

4.2.9.2 Involvement of matrix metalloproteases

The previous experiment had shown that PMA stimulated shedding of LYVE-1 from HDLEC as had been found originally on 293T transfectants. Therefore it was deemed likely that shedding was occurring through a very similar process, namely by matrix metalloproteinases. To test this hypothesis, HDLEC were preincubated for 2h with the MMP inhibitor Ilomastat and then incubated with PMA, prior to lifting and staining for LYVE-1, for quantitation by flow cytometry (figure 4.30). The results revealed that Ilomastat blocked shedding by 47%. Hence it was concluded that PMA-stimulated shedding is mediated by MMPs and is distinct from the mechanism that down-regulates LYVE-1 surface expression in response to TNFα.

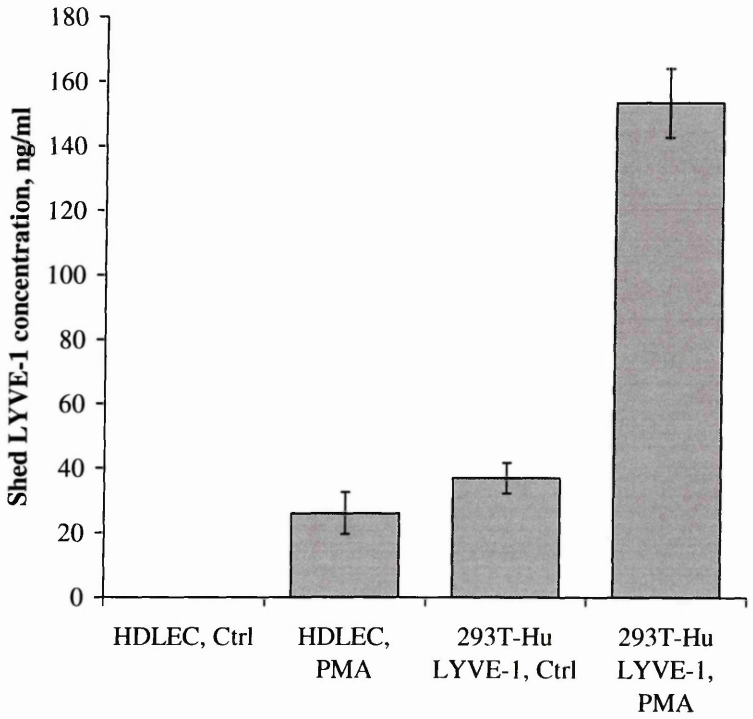

Figure 4.29 Effect of PMA on LYVE-1 shedding. HDLEC and 293T human LYVE-1 transfectants were cultured in triplicate for 4 h in either the presence or absence of PMA, 20ng/ml; supernatants were harvested and applied to a microtitre plate which was precoated with rabbit anti-human LYVE-1. Bound protein was detected using 8C and an HRP-conjugated goat antibody with OPG substrate. Protein was quantitated using soluble LYVE-1 Fc at known dilutions and the values are expressed ± standard error.

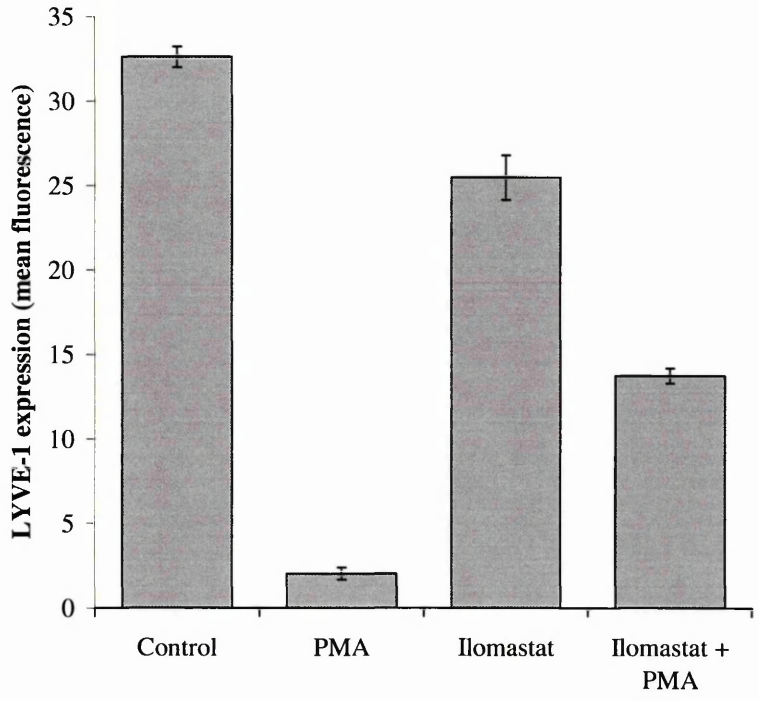

Figure 4.30 Effect of Ilomastat on PMA-induced shedding of LYVE-1 from HDLEC. Cells were preincubated with Ilomastat, 25 μM, for 2 h prior to the addition of PMA, 20ng/ml. Following a 4h incubation, cells were lifted and stained in triplicate with 8C and goat anti-mouse AlexaFluor®488 to measure LYVE-1 surface expression by flow cytometry. The mean fluorescence of cells from each condition was plotted ± standard error.

4.3 Discussion

4.3.1 Preliminary phenotyping of HDLEC

The primary aim of this chapter was to determine factors which regulated expression of LYVE-1 on primary human dermal lymphatic endothelial cells, (HDLEC) in culture. The cells upon which the majority of these studies were carried out were derived from commercial human dermal microvascular endothelial cells (HDMEC) that contained a mixture of both lymphatic (LEC) and blood vascular endothelial cells (BEC). These cells gave rise to a predominantly LEC phenotype with continuous culture and thus at later passages of 12 and above, virtually all cells expressed the LEC markers podoplanin, prox-1, the pan-endothelial cell marker CD31 and retained expression of LYVE-1. A loss of LYVE-1 expression was observed in other primary endothelial cell lines at higher passage numbers.

The outgrowth of BEC by LEC described in this thesis is similar to that reported by Nisato et al. (2004), in a manuscript published during the later stages of this PhD. These researchers also investigated the phenotype of commercially available HDMEC and demonstrated outgrowth by LEC, resulting in a pure LEC population at later passages, defined by expression of podoplanin. However, in contrast to the finding described in this thesis, Nisato et al. reported optimal yields of LEC from HDMEC purchased from Clonetics rather than PromoCell. The likely explanation for the differences in results is batch to batch variation between commercial HDMEC preparations in terms of initial LEC/BEC ratios and that LEC can in fact be isolated from either source.

The molecular basis to explain the phenomenon of outgrowth by one cell population over another was very recently partially elucidated by Gröger et al.,

2004. They demonstrated that podoplanin-selected LEC constitutively express IL-3, a broadly acting cytokine which regulates haematopoietic cell differentiation. The endogenous supply of cytokine was found to be responsible for maintaining a LEC phenotype in culture and regulated both expression of prox-1 and podoplanin. BEC were not found to express IL-3 but addition of IL-3 to the medium induced transdifferentiation of BEC into LEC. Thus the LEC are not truly outgrowing the BEC but secreting IL-3 to induce a predominantly LEC phenotype.

The paper by Gröger et al., 2004 raises the question of how phenotypically similar BEC-derived LEC are to LEC which have undergone no such transdifferentiation. However, data obtained from experiments using PromoCell HDLEC showing the down-regulation of LYVE-1 by TNFα has been confirmed by two other human cell lines: HDMEC from Clonetics and LEC isolated by immunoselection with podoplanin from Dr. Ernst Kriehuber (detailed in this chapter), as well as in mouse primary LEC and in a murine model (described in chapter 5). Therefore the PromoCell HDLEC have been shown to be suitable for use in the *in vitro* characterisation of factors affecting the variability of LYVE-1 expression on human LEC.

4.3.2 Factors affecting variability of LYVE-1 expression in cultured cells

Although PromoCell HDLEC retained expression of podoplanin and prox-1 at consistent levels beyond passage 12, LYVE-1 expression was found to be highly variable, with between 55% and 80% of cells LYVE-1 positive. This reflected the observation of variable LYVE-1 expression in tissues and suggests that LYVE-1 on cultured cells may be regulated by labile factors within the medium which are also present *in vivo*. To address this observation of variability, LYVE-1 expression on PromoCell HDLEC was measured by flow cytometry following culture in media supplemented with a panel of recombinant human growth

factors, cytokines and chemokines. These were selected on the basis that they may come into contact with lymphatic endothelium *in vivo*, both under normal physiological conditions and also in inflammation, as the response of lymphatic endothelium to inflammatory stimuli had not previously been characterised. The growth factors FGF acidic, VEGF-C and angiopoietin-2 promoted a marginal increase in LYVE-1 expression, typically from 57% to 70%. However most strikingly, the inflammatory cytokines TNFα and TNFβ precipitated a loss of LYVE-1 surface expression, to less than 1% and 2% respectively of the starting level. This result was confirmed by similar studies detailed in this chapter, which were carried out using HDMEC from Clonetics and LEC isolated by immunoselection with podoplanin from Dr. Ernst Kriehuber: both cell lines experienced a total loss of LYVE-1 upon stimulation with TNFα, which was quantitated by flow cytometry. Such a dramatic effect demanded follow-up experiments to characterise it fully.

4.3.3 Characterisation of TNFα-induced down-regulation of LYVE-1

Neither TNFα nor TNFβ induced an apoptotic, necrotic or autophagic response in HDLEC. Cell viability was confirmed by the ability to exclude dye and by sustained expression of the lymphatic endothelial cell surface glycoprotein podoplanin. Moreover the rate of proliferation was unaffected and cells showed no greater or lesser propensity to form tubules in Matrigel™ when exposed to TNFα. Thus TNFα did not appear to induce lymphangiogenesis in acute stimulation (up to 72h) of LEC. Chronic inflammation in tissues is known to induce both angiogenesis and lymphangiogenesis (Fogt et al., 2004; Kaiserling et al., 2003; Baluk et al., 2005) and therefore stimulation of LEC by the pro-inflammatory cytokine TNFα might have been expected to increase proliferation and tubule formation. However, it is likely that other factors such as VEGF-C release by infiltrating macrophages induce lymphangiogenesis during chronic inflammation. Equally, it is not clear whether chronically inflamed lymphatics

shown the same down-regulation of LYVE-1 as in acute inflammation. Clearly those issues warrant further investigation in future studies.

TNFα was found to induce a very striking change in the morphology of HDLEC, with confluent cultures assuming an elongated shape very distinct from the more rounded cobble-stone appearance of untreated cells. Other studies have shown that vascular endothelial cells in inflamed tissue also undergo a change in shape and basement membrane remodelling to aid extravasation of leukocytes but maintain vascular integrity, with no increase in the permeability of the endothelial cell monolayer or decrease in electrical resistance, (reviewed by Muller, 2003). The change in morphology of HDLEC suggested that the cells were undergoing major rearrangements in the cytoskeleton and it is tempting to speculate that these might facilitate leukocyte reverse transmigration in a similar manner to the forward transmigration seen in vascular endothelium, a phenomenon investigated further in chapters 5 and 6.

The dependence of down-regulation of LYVE-1 on TNFα concentration was demonstrated by titration: a maximal effect was attained by 5 ng/ml TNFα, although the loss of 50% of LYVE-1 surface expression occurred at less than 0.1 ng/ml. Although normal plasma concentrations of TNFα are much lower than this, typically 5.6 pg/ml (Zinman et al. 1999), this cytokine can reach much higher concentrations within the tissues in disease. For example, a study by Calabresi et al. (2003) measured ischemia-induced cardiac TNFα in rats as 80 pg/mg protein, as opposed to the normal cardiac TNFα concentration of 50 pg/mg protein.

The effect of TNFα was also found to be completely reversible, thus supporting earlier findings that the cytokine was not inducing cell death. Cells were stimulated with TNFα for 48h before thorough washing and application of fresh

medium. Expression recovered to the level measured in untreated cells by 48h, with a rapid increase in LYVE-1 surface expression measured by flow cytometry between 12 and 24h after replacement with fresh medium. Hence this would suggest that *in vivo*, LYVE-1 expression recovered once TNF was down-regulated and the acute phase of inflammation was over. Experiments carried out in this chapter may also implicate IL-6 in this recovery of expression.

IL-6 induced a marginal increase in LYVE-1 expression on HDLEC from PromoCell (from 57% to 73% of cells) and HDMEC from Clonetics (from 9% to 16%). This increase in expression was found to be dependent upon the concentration of the cytokine, with maximal effects observed at 10-20ng/ml at 48h. This increase was shown in both the percentage of LYVE-1 positive cells and the mean and median fluorescence but was not nearly as striking as the TNF-induced loss of expression. However, the effect of IL-6 on increasing LYVE-1 expression on HDLEC may play an important role in inflammation. Other studies have shown that a variety of peptide factors including IL-1 and TNFα enhance IL-6 production in fibroblasts (reviewed by Akira and Kishimoto, 1992). However, IL-6 suppresses LPS-induced IL-1 and TNFα production. Hence the concentrations of these cytokines fall in the later stages of acute inflammation, whilst the concentration of IL-6 rises. Therefore IL-6 may play a role in stimulating the recovery of LYVE-1 surface expression. IL-6 may also serve as an autocrine or paracrine factor for LEC differentiation, in a similar manner to IL-3 (Gröger et al., 2004). Future experiments will seek to investigate this further.

4.3.4 The mechanism for TNFα-mediated LYVE-1 down-regulation

The loss of LYVE-1 surface expression following TNFα stimulation was found to be due to internalisation and degradation rather than through MMP-mediated shedding. Untreated HDLEC were shown by ELISA to shed low levels of LYVE-1 constitutively; however no soluble LYVE-1 was detected in the supernatant

following stimulation with either TNFα or TNFβ and even constitutive shedding was abolished. Furthermore, the loss of LYVE-1 could not be prevented by incubation with the MMP inhibitor, Ilomastat. This contrasts with the mechanism of PMA-induced loss of LYVE-1 surface expression. Previous work in the Jackson laboratory had shown that PMA stimulated PKC and induced MMP-dependent shedding of LYVE-1 in 293T human fibroblast transfectants through MAPK signal transduction (S. Clasper and D. G. Jackson, unpublished; Tom Nightingale, DPhil thesis, University of Oxford, 2004). Experiments detailed in this chapter demonstrated that MMP-mediated shedding also occurred in primary HDLEC, which endogenously express LYVE-1. Thus TNFα-induced down-regulation is via a very different mechanism to that of PMA-mediated shedding and LYVE-1 expression is regulated by multiple signal cascades. It will be very interesting to explore the pathway involved in IL-6-mediated up-regulation of LYVE-1 in future experiments, as well as the mechanism whereby LYVE-1 is partially down-regulated in hypoxia, discussed later in this thesis section.

The internalisation of LYVE-1 was followed using confocal microscopy. In untreated cells LYVE-1 colocalised with podoplanin and was almost entirely restricted to the surface. After 3h of stimulation with TNFα, LYVE-1 appeared to be intracellular and colocalised with EEA-1, an early endosome marker and CD63, a lysosomal marker. More colocalisation of LYVE-1 with CD63 than EAA-1 was observed at this time point, suggesting a rapid internalisation and incipient degradation within 3h. By 48h no LYVE-1 was detected but podoplanin expression was retained at the cell surface. These results imply that the down-modulation of LYVE-1 by TNFα occurs by internalisation and transport through the endosomal pathway, most likely culminating in degradation within a lysosome (figure 4.31).

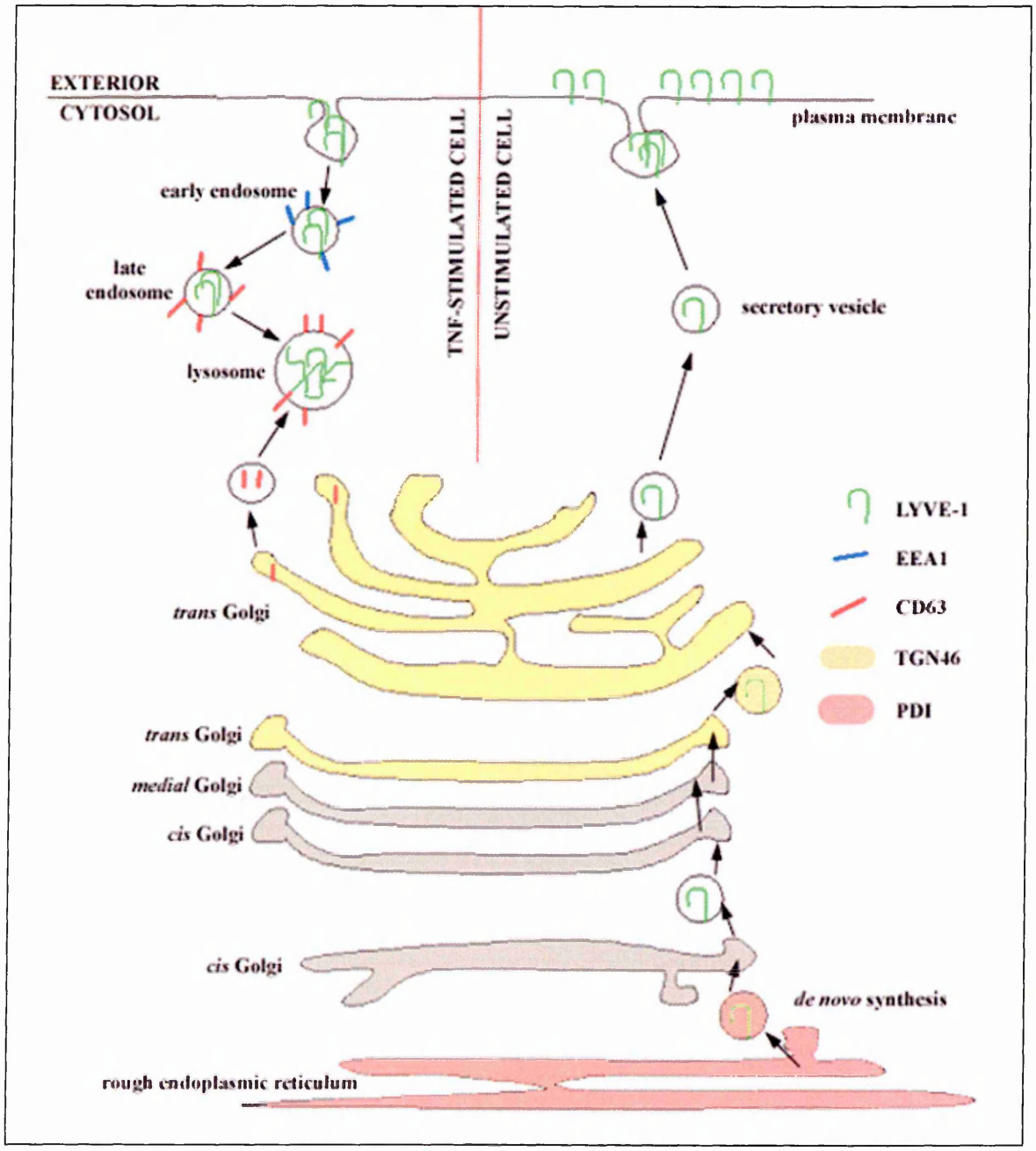

Figure 4.31 Intracellular localisation of LYVE-1 in a resting lymphatic endothelial cell (right) and following TNFα stimulation (left). In an unstimulated cell, de novo synthesis of LYVE-1 is carried out at the endoplasmic reticulum and the protein undergoes post-translational modifications within the Golgi, prior to vesicular transport to the plasma membrane and expression at the cell surface. Following TNFα stimulation, this synthesis stops and cell surface LYVE-1 is internalised and transported via endosomes to a lysosome, where it is degraded.

After stimulation with TNFα, there was a reduction in the amount of LYVE-1 associated with the endoplasmic reticulum and the trans-Golgi network, suggesting a decrease in *de novo* synthesis. A Northern blot of total RNA isolated from LEC cultured for 72h either in the presence or absence of TNFα revealed that the major 1.8kb LYVE-1 mRNA species was only detected in RNA from untreated cells. Semi-quantitative PCR was used to analyse mRNA levels at earlier time points and revealed that the loss of LYVE-1 mRNA had occurred within 12h. Clearly the internalisation and degradation of LYVE-1 was coupled with transcriptional down-regulation, either at the level of mRNA synthesis or turnover. A time course to follow the loss of LYVE-1 from the cell surface revealed that more than half of this protein was lost within 6h and by 48h no LYVE-1 remained. Thus the abundance of LYVE-1 mRNA is reduced concurrent with the internalisation and degradation of LYVE-1. Colocalisation studies using the ER and Golgi markers would suggest that the down-regulation of message has occurred by 3h following stimulation.

4.3.5 Putative down-modulation of LYVE-1 via NFκB

Preliminary experiments to investigate the involvement of the transcription factor NFκB in TNF-induced down-regulation of LYVE-1 found that pre-incubation with the NFκB inhibitor BAY 11-7082 reduced TNFα- and TNFβ-induced loss of LYVE-1 surface expression by 21% and 25% respectively. This provided strong evidence that TNF down-modulated LYVE-1 through NFκB, although further experiments using gel shift assays will be required to prove the involvement of this transcription factor. The NFκB pathway is known to initiate a new transcription profile in a cell in response to pro-inflammatory stimulation. Therefore the involvement of this transcription factor following TNF stimulation of HDLEC would suggest a change in expression of other proteins in addition to LYVE-1. The nature of these changes is detailed in the next chapter of this thesis.

The apparent cytotoxicity of BAY 11-7082 to both HDLEC and 293T was not found in HUVEC by Pierce et al., 1997, in the paper where the effects of BAY 11-7082 were originally characterised. These researchers claim that BAY 11-7082 had no effect on the rate of proliferation of HUVEC when used at concentrations which in this PhD were found to be cytotoxic to HDLEC and 293T. The resistance of HUVEC to cytotoxicity is surprising and it would be interesting to carry out a trypan blue exclusion assay on such cells treated with BAY 11-7082, to validate the results of the proliferation assay carried out in the original study.

In several of the experiments detailed in this chapter, TNFα appeared to have a more dramatic effect of LYVE-1 expression than TNFβ. An example of this is shown in the experiment involving BAY 11-7082, where following 24h of stimulation, TNFα had precipitated a 76% loss of LYVE-1 expression whereas TNFβ had only induced a 55% loss. This finding is corroborated by numerous studies, including that carried out by Desch et al (1990) who found that the adhesion of neutrophils to HUVEC was more pronounce when the endothelial cells were stimulated with TNFα rather than TNFβ. The recombinant proteins were both expressed in mammalian systems to allow the appropriate post-translational modifications and both were equipotent on a molar basis in producing cytotoxicity in L929 fibroblast cells. The researchers concluded that the difference in pro-inflammatory activity was due to primary sequence differences.

4.3.6 Does TNFα activate LYVE-1 to bind HA?

The physiological consequences of the TNFα-mediated internalisation and degradation of LYVE-1 were explored in some preliminary experiments to address the intriguing possibility that TNFα transiently activates HA binding and uptake. As discussed in chapter 1 of this thesis, LYVE-1 expressed on LEC does not bind HA. However, TNFα may activate LYVE-1 to precipitate binding

and transient uptake of HA in the primary stages of inflammation. LYVE-1 has previously been shown to promote binding and internalisation of HA through receptor-mediated endocytosis in 293T transfectants (Prevo et al., 2001). As it has been shown in this chapter that LYVE-1 is degraded following TNFα-induced internalisation, TNFα-stimulated cells were examined by confocal microscopy after 2h, before degradation had occurred. Internalisation of HA by both primary human dermal LEC and primary mouse dermal LEC was shown and some colocalisation of HA with LYVE-1 was visible, particularly in the case of the human cells. However this colocalisation may be due to intracellular transport to the same subcellular compartment, namely the lysosomes. Uptake of fluorescent HA was also quantitated by FACS, which showed that a small but significant (approximately 5%) portion of mouse LEC were either binding or had internalised HA. This increased to over 11% following stimulation with TNFα, although expression of CD44 was also up-regulated on some cells, which may be responsible for some or all of the increased binding. Also, although LEC appear capable of internalising HA, the mechanism by which this occurs and the involvement, if any, of LYVE-1 remains to be determined. Future experiments will employ the human LYVE-1 blocking antibody 3A, to investigate whether incubation with these antibodies reduces HA uptake. Also it would be interesting to incubate HA with primary LEC isolated from the LYVE-1$^{-/-}$ knock-out mouse, to determine by microscopy whether they are capable of internalisation of HA. This would test whether a LYVE-1 dependent mechanism is responsible, or either a LYVE-1 independent mechanism or a second compensatory mechanism is employed.

A role for LYVE-1 in the transport of HA across lymphatic endothelium has previously been suggested, as HA is transported from the tissues to the regional lymph node through lymphatic vessels and LYVE-1 was shown to mediate HA-internalisation in LYVE-1 293T transfectants (Prevo et al., 2001). As LYVE-1 is

expressed on both the luminal and abluminal faces of the lymphatic endothelium, it was suggested that this lymphatic-specific receptor for HA may act as a shuttle for transcytosis of the ligand, binding it at the abluminal face and releasing it into the lumen of the vessel. Uptake from the abluminal face, particularly in response to inflammation may be to remove low molecular weight fragments of HA from the interstitium to aid clearance of potentially pro-inflammatory signals and precipitate the resolution of acute inflammation. Cultured cells have their basal surface in contact with the substrate and therefore uptake may be more pronounced if the cells are cultured in Matrigel and permitted to form tubules prior to the addition of HA.

4.3.7 Investigating the response of LYVE-1 expression to hypoxia

Hypoxia is a common feature in solid tumours and is associated with aggressive growth, metastasis and poor response to treatment (Höckel et al., 1996; Brizel et al., 1996). Moreover, many human cancers are associated with pre-existing chronic infectious or inflammatory conditions (Schacter et al., 2002). Given that the data reported in this chapter has consistently shown that LYVE-1 is down-regulated by the pro-inflammatory cytokines TNFα and TNFβ, it was of also of interest to examine LYVE-1 expression under hypoxic conditions. Preliminary studies to address this on HDLEC found that following culture for 14h under hypoxic conditions, a marginal decrease in LYVE-1 expression was measured, whilst no change in the amount of surface expression of podoplanin was observed. Therefore expression of LYVE-1 by HDLEC was shown to be sensitive to oxygen tension and future experiments will address the mechanism by which this occurs and whether down-regulation is more pronounced at other time points. LYVE-1 does not appear to possess a hypoxic response element, as if this were the case a more dramatic change in expression such as that seen in the positive control, carbonic anhydrase 9 (CA-9),would have occurred. A possible mechanism by which LYVE-1 is down-regulated could be via IL-1α, which has

been shown to be induced in vascular endothelium following hypoxia and up-regulated the adhesion molecules E-selectin and ICAM-1 upon reoxygenation, thus potentially altering endothelium-leukocyte adherence. Therefore it would be interesting to measure LYVE-1 expression in HDLEC undergoing reoxygenation following hypoxic shock. Studies described in chapter 5 and 6 of this thesis found that the adhesion molecules VCAM-1, ICAM-1 and E-selectin are up-regulated on lymphatic endothelium following stimulation with TNFα and it would also be interesting to examine the expression of these receptors on lymphatic endothelium following hypoxic shock.

4.3.8 Conclusion

Experiments detailed in this chapter have identified LYVE-1 as a tightly regulated cell surface protein on HDLEC cultured *in vitro*, with a putative role in the acute phase of inflammatory events within the lymphatics. The internalisation of LYVE-1 following TNFα stimulation may serve as a mechanism by which LYVE-1 is activated to bind HA and thus HA uptake by lymphatic endothelium is accomplished under pro-inflammatory conditions. Alternatively LYVE-1 may serve another function in addition to that of an HA receptor and require down-regulation in order for the inflammatory reaction of lymphatic endothelium to proceed. The role of LYVE-1 in inflammation was further explored in the experiments described in chapter 5.

CHAPTER 5

An Inflammation-induced Expression Programme in Lymphatic Endothelial Cells

5.1 Introduction.....237

5.2 Results.....240

5.3 Discussion.....282

Introduction

The dramatic and specific down-regulation of LYVE-1 expression by TNFα and TNFβ described in the previous chapter illustrates the potent effects that such pro-inflammatory cytokines may have on lymphatic endothelium. In this chapter these effects are explored further, assessing the effects of TNFα on the expression of other proteins relevant to cell adhesion and migration in the lymphatics.

5.1.1 Inflammation-induced changes in gene expression on blood vascular endothelium

Recruitment of leukocytes such as macrophages and dendritic cells (DCs) from the blood to tissues occurs in the absence of inflammation, as detailed in the general introduction to this thesis in chapter 1. However in the presence of pro-inflammatory stimuli, the vascular endothelium becomes activated to recruit an increased number of leukocytes from the blood, which extravasate into the tissues to the site of inflammation.

The response of blood vascular endothelial cells to pro-inflammatory mediators such as TNFα, particularly with respect to the adhesion molecules induced, has been extensively characterised and is detailed in chapter 1 of this thesis. Blood vascular endothelium is known to up-regulate the adhesion molecules E-selectin, which binds to complex sialylated carbohydrate groups related to the Lewis-X or Lewis-A family on a variety of leukocytes (reviewed by Albelda et al., 1994); vascular cell adhesion molecule-1 (VCAM-1), binding the integrin ligand VLA-4 (α4β1), (Staunton et al., 1988; Springer, 1990); and intercellular adhesion molecule-1 (ICAM-1), binding to its integrin ligand LFA-1 (αLβ2), (Rothlein et al.,

1986). However no comprehensive study has been carried out, to date, to examine the expression of these adhesion molecules on lymphatic endothelium.

The increased chemokine secretion by blood vascular endothelium in response to pro-inflammatory stimuli has also been extensively documented, for example RANTES (regulated upon activation, normal T-cell expressed and secreted, CCL5), IL-8 (interleukin-8, CXCL8) and MCP-1 (monocyte chemotactic protein-1, CCL2), which may enhance the arrest of rolling monocytes on HUVEC (Gerszten et al., 1999). Also, in addition to enhanced adhesion of T-cells, secretion of MIP-1β (macrophage inflammatory protein-1β, CCL3/4) by vascular endothelium was found to induce chemotaxis and further recruit circulating leukocytes from the blood (Tanaka et al., 1993).

To aid the extravasation of leukocytes from the blood, vascular endothelial cells undergo a change in shape but without compromising vascular integrity (reviewed by Muller, 2003). These endothelial cells also undergo extensive remodelling of cell-cell junction to control leukocyte diapedesis. For example the transmembrane immunoglobulin superfamily member CD31 is redistributed from the intercellular junctions, perhaps as a means of regulating the transmigration of leukocytes (Romer et al., 1995). Furthermore anti-CD31 antibodies have been shown to block transmigration (Muller et al., 1993), as have antibodies against CD99, a transmembrane glycoprotein also found at endothelial cell-cell junctions (Schenkel et al., 2002).

5.1.2 Aims

The active role played by blood vascular endothelium in recruiting increased number of leukocytes to inflamed tissue has been shown extensively in previous studies. However the mechanisms whereby these newly recruited cells, (such as those which have differentiated from monocytes into professional antigen presenting cells), leave the tissue via lymphatic capillaries to travel to the lymph nodes remain to be characterised. Data from the previous chapter of this thesis had indicated that lymphatic endothelial cells respond to the pro-inflammatory TNFα with a marked change in morphology, indicative of cytoskeletal rearrangement, as well as a dramatic down-modulation of LYVE-1, the lymphatic endothelial specific HA receptor. Experiments detailed in this chapter examined the inflammation-induced change in expression of molecules in primary lymphatic endothelial cells *in vitro*, which may be involved in reverse-transmigration of leukocytes across lymphatic endothelium from inflamed tissue.

Results

5.2.1 Effect of proinflammatory cytokines and chemokines on expression of leukocyte adhesion molecules in primary HDLEC

The previous chapter describes the derivation of a pure population of LEC from a mixed population of human dermal microvascular cells purchased from PromoCell. These cells proved to be well adapted to culture and retained expression of the lymphatic markers LYVE-1, podoplanin and prox-1. It was also found that when stimulated with TNFα and TNFβ, LYVE-1 was dramatically down-regulated. However, there is comparatively little known about the identities of other cell surface receptors or adhesion molecules expressed by lymphatic endothelial cells, or how their levels might be affected by inflammatory mediators.

To initiate such a study, the expression of key leukocyte adhesion molecules ICAM-1 and VCAM-1 on resting and cytokine-treated primary HDLEC in culture was investigated. The expression of these receptors is known to be regulated by inflammatory cytokines in blood vascular endothelium and it was of interest to examine whether their expression was similarly regulated on primary HDLEC.

HDLEC were cultured for 24h in either unsupplemented medium or in the presence of one of the following cytokines or chemokines: IL-1α, IL-2, IL-6, IL-8, TNFα, TNFβ, IFNγ, MIP-3α or LPS. Cells were then assayed by flow cytometry for the expression of VCAM-1 and ICAM-1 (figures 5.1 and 5.2).

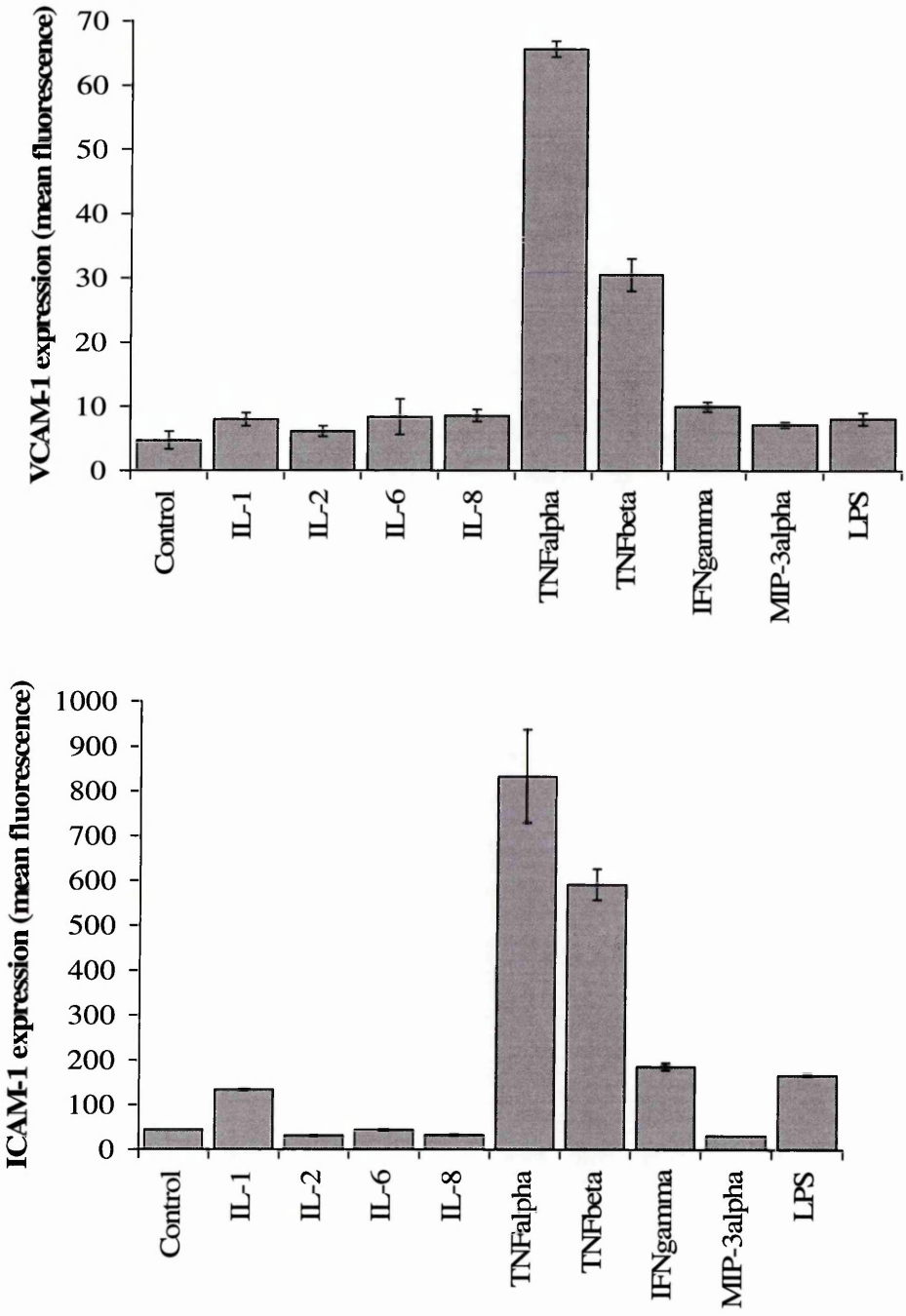

Figure 5.1 Effects of inflammatory cytokines on VCAM-1 and ICAM-1 expression in cultured primary HDLEC. Cells were cultured for 24h with individual cytokines or LPS as indicated (see methods), then lifted with PBS-5mM EDTA and stained using either mouse anti-VCAM-1 (BD Pharmingen, mAb: 51-10C9, upper graph) or anti-ICAM-1 (Serotec, lower graph) or a mouse IgG1 isotype-matched control, with AlexaFluor®488 goat anti-mouse conjugate to permit detection by flow cytometry. Samples were cultured and stained in triplicate, with an isotype-matched control for each cytokine/chemokine which exhibited a mean fluorescence $\leq$1.0. Data plotted represent the mean fluorescence, ± standard error.

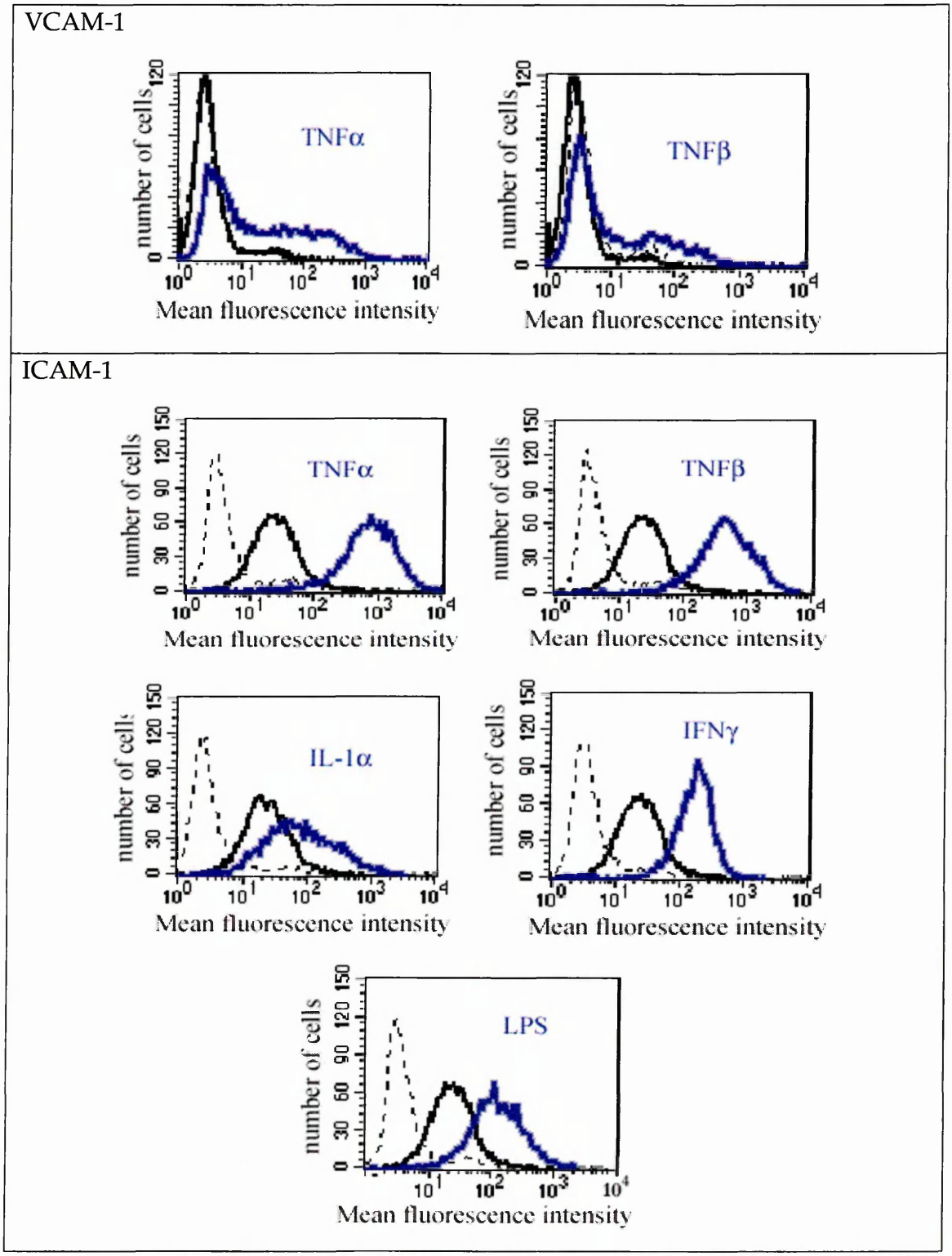

Figure 5.2 Representative FACS histogram plots to show up-regulation of VCAM-1 and ICAM-1 on HDLEC following stimulation under pro-inflammatory conditions. Expression on untreated cells is shown in black, cytokine/chemokine-treated cells in blue and the isotype-matched control as a dotted black line.

Virtually no VCAM-1 was detected on untreated cells but following stimulation with TNFα and TNFβ, expression was induced 19 fold and 13 fold respectively. In contrast, low to intermediate levels of ICAM-1 were detected even on unstimulated cells. However treatment with TNFα or TNFβ resulted in a 14 fold and 6 fold up-regulation of ICAM-1 expression, which also increased in response to IL-1α, IFNγ and LPS, albeit to a lesser extent (3-4 fold). No such effects on expression of either molecule were observed in response to IL-2, IL-6 or the inflammatory chemokines IL-8 and MIP-3α (CCL20). As TNFα was the most potent inducer of both VCAM-1 and ICAM-1 expression, as well as inducing the down-modulation of LYVE-1 characterised in chapter 4, all subsequent experiments involved this pro-inflammatory cytokine.

5.2.2 Kinetics of adhesion molecule up-regulation in primary HDLEC

To establish the kinetics of adhesion molecule expression induction in primary HDLEC by TNFα, surface expression of VCAM-1 and ICAM-1 was assessed by flow cytometry between 0 and 48h following TNFα stimulation. Expression of E-selectin was also measured, as this molecule is known to be involved in the preliminary attachment of leukocytes to inflamed vascular endothelium prior to VCAM-1- and ICAM-1-mediated interactions.

Results (figure 5.3) show that E-selectin had undergone a considerable (6-7 fold) induction by 6-12h but was much more transient than either ICAM-1 (reaching maximal expression at 12h) or VCAM-1 (peaking at around 24h), both of which are more sustained. The gradual increase in the expression of adhesion molecules following exposure TNFα suggests new protein synthesis rather than translocation of existing protein to the cell surface. This response of de novo synthesis supports the array analysis data indicating a new expression program in lymphatic endothelium induced by inflammation.

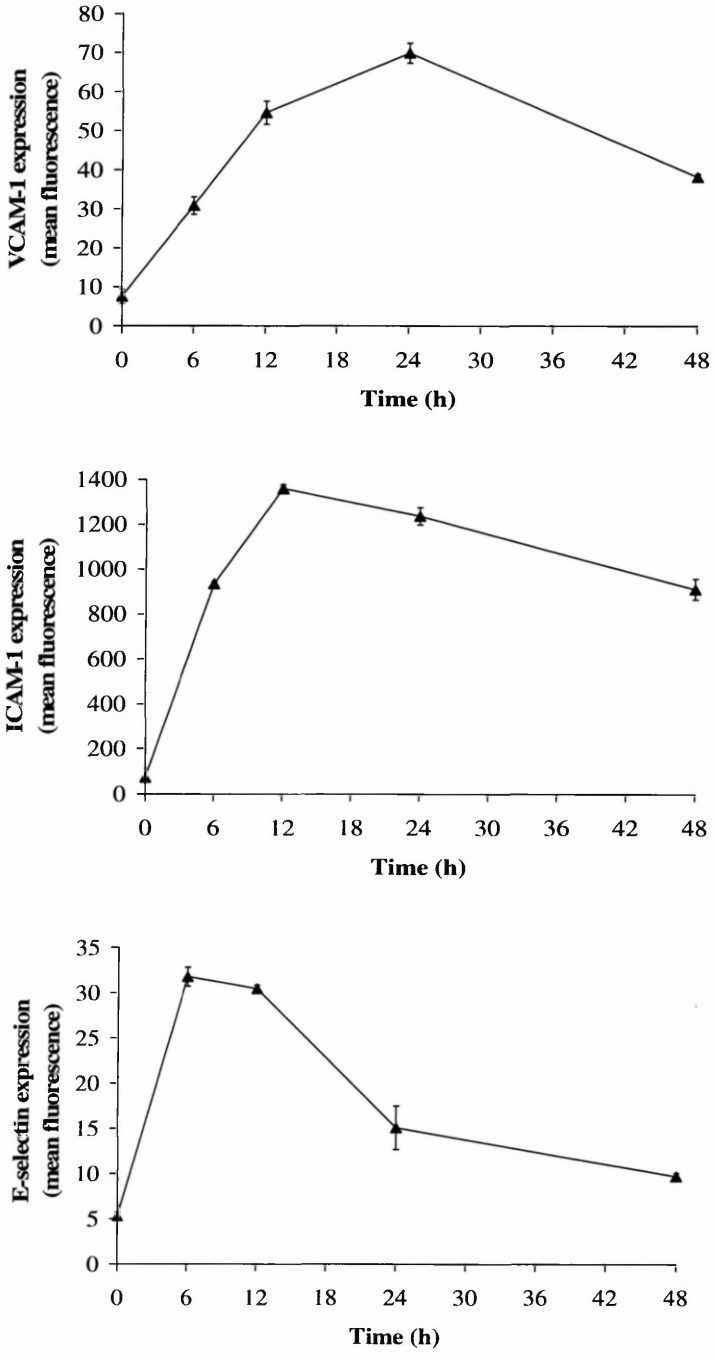

Figure 5.3 Time course to follow the up-regulation of VCAM-1, ICAM-1 and E-Selectin on primary HDLEC. Samples of HDLEC were cultured in triplicate for between 0 and 48h in TNFα (10ng/ml)-supplemented medium, then lifted with PBS-5mM EDTA and stained with either anti-VCAM-1 (mAb: 51-10C9), anti-ICAM-1 (mAb: PIW16), anti-E-selectin (BIIG-E4) or an isotype-matched control. Goat anti-mouse AlexaFluor 488 was used to detect bound antibody for quantitation of protein by flow cytometry. Irrelevant isotype-matched controls were included at each time point, with mean fluorescence $\leq$1.0. Data shown represent mean fluorescence, ± standard error.

5.2.3 Effects of TNFα on other key leukocyte adhesion molecules

Given the dramatic response to TNFα of ICAM-1 and VCAM-1 expression on HDLEC, it was of interest to establish whether other adhesion molecules involved in leukocyte adhesion and transmigration were also expressed on HDLEC and whether their expression level was altered by cytokine treatment. To achieve this, HDLEC were screened with a large panel of mAbs to a variety of proteins including the Ig superfamily receptors ICAM-2 and ICAM-3, the integrins α3, α4, α6 and β1, as well as the junctional adhesion molecule JAM-1 (table 5.1). For some adhesion molecules, more than one antibody was used, to ensure that an antibody suitable for use in flow cytometry was employed. Representative FACS histogram profiles are shown in figure 5.4. A summary of proteins detected and the antibodies used is shown in table 5.1.

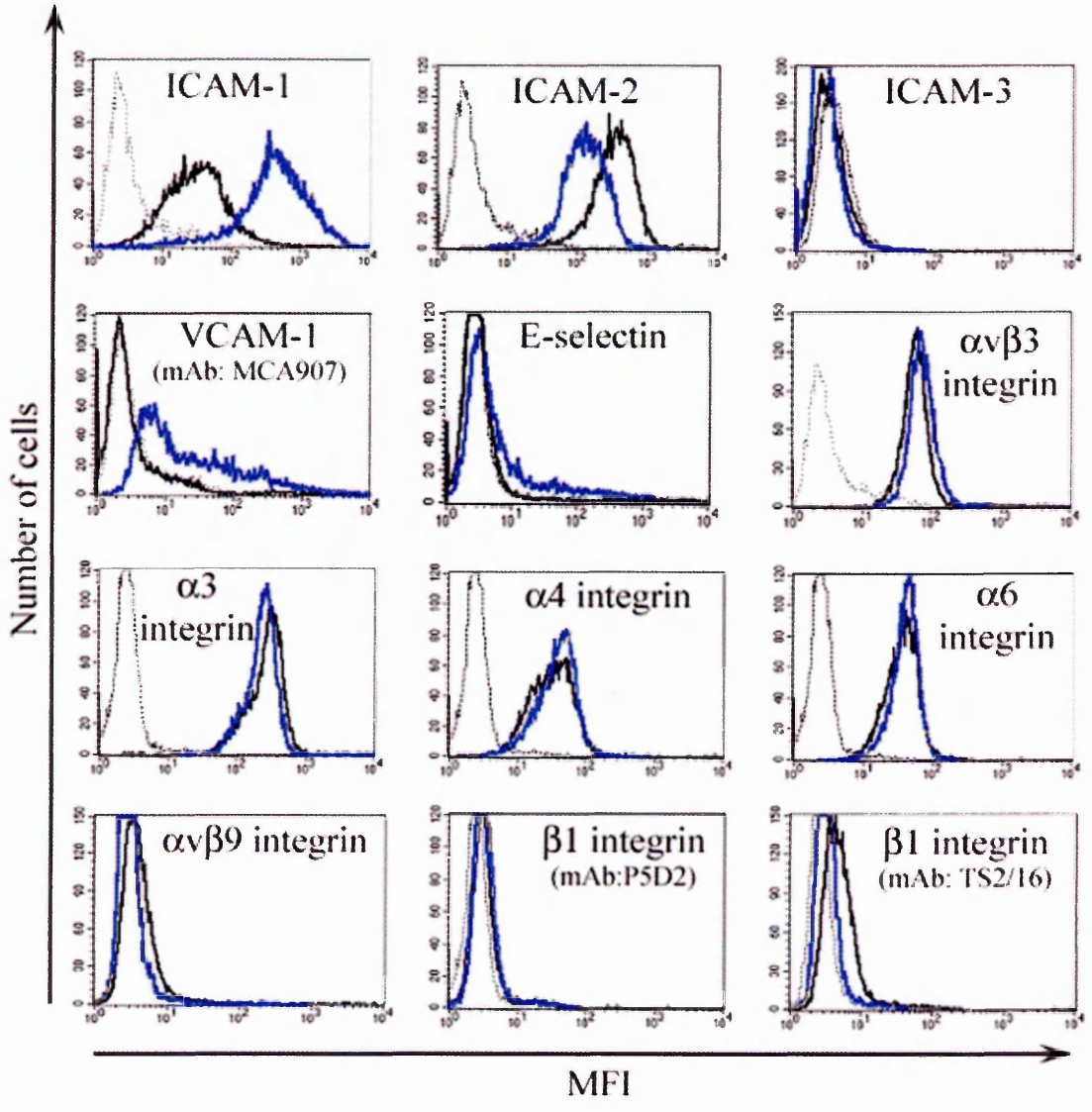

Figure 5.4 Effect of TNFα on expression of adhesion molecules in primary HDLEC. Cells were cultured in triplicate in either medium alone (black line) or in the presence of TNFα, 10ng/ml (blue line) for 48h prior to lifting with PBS-5mM EDTA and staining with the antibodies as indicated in the figure (see also table 5.1). Irrelevant isotype-matched antibodies were included as controls (dotted lines). AlexaFluor®488 conjugates were used for detection and representative histograms are shown (MFI = mean fluorescence intensity). Where more than one antibody was used, the hybridoma name is shown in brackets. Cells stained using D2/40 were fixed in formaldehyde prior to staining, as detailed in the methods. As positive controls for the efficacy of stimulation by TNFα, some cells were also stained for LYVE-1 using 8C , as well as VCAM-1 and ICAM-1. (Histograms continued on following page)

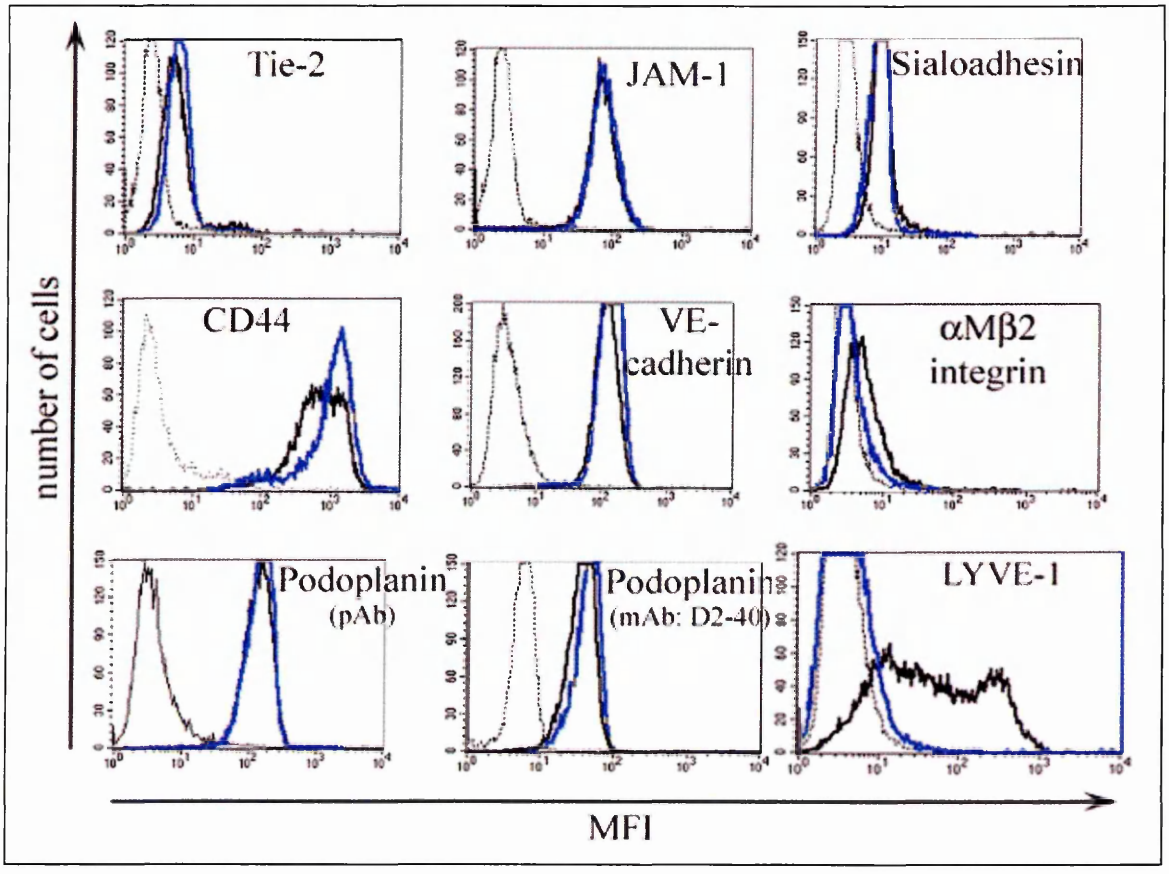
Tie-2
JAM-1
Sialoadhesin
CD44
VE-cadherin
αMβ2 integrin
Podoplanin (pAb)
Podoplanin (mAb: D2-40)
LYVE-1
number of cells
MFI

Adhesion molecule	Antibody name	Expression level in primary HDLEC (mean fluorescence)		
		Control	+TNFα	X fold change
α3 Integrin	1A3	238.41	218.74	- 0.92
α4 Integrin	7.2	28.76	36.86	+ 1.28
α6 Integrin	MP4F10	33.51	38.32	+1.14
α9β1 Integrin	Y9A2	3.36	2.51	- 1.34
αVβ3 Integrin	23C6	57.13	71.69	+ 1.24
αMβ2 Integrin	24	3.54	3.08	- 1.15
αMβ2 Integrin	TS2/4.1.1	4.41	2.98	- 1.48
CD44	E1/2.8	683.64	1083.92	+ 1.59
E-Selectin	BIIG-E4	2.94	4.51	+ 1.53
ICAM-1	PIW16	35.8	561.34	15.68
ICAM-2	B-T1	371.86	150.62	- 2.47
ICAM-3	ICAM3.2	2.41	2.07	-
JAM-1	3b8	62.09	69.38	+ 1.12
LYVE-1	8C	29.88	2.97	- 10.01
Podoplanin	polyclonal	135.65	141.73	+ 1.04
Podoplanin	D2-40	36.09	38.8	+ 1.08
Sialoadherin	HSn 7D2	8.43	7.24	- 1.16
β1 Integrin	P5D2	2.57	2.78	-
β1 Integrin	TS2/16	4.01	2.81	- 1.43
Tie-2	4g8	5.18	5.82	+ 1.12
VCAM-1	MCA 907	1.94	10.4	+ 5.36
VCAM-1	51-10C9	2.58	14.75	+ 5.72
VE-Cadherin	CAD-5	104.3	119.77	+ 1.15

Table 5.1 Quantitative analysis of adhesion molecule expression in primary HDLEC. Values of mean fluorescence obtained by flow cytometry from the histogram plots shown in figure 5.4. Isotype-matched antibodies gave values of mean fluorescence of 2.0 or less.

Results from these experiments show that in addition to the marked up-regulation of the leukocyte adhesion molecules VCAM-1 and ICAM-1, E-selectin (involved in leukocyte tethering in vascular endothelium) was also up-regulated 1.5 fold. The data also show that ICAM-2, an alternative receptor to ICAM-1 for the integrin LFA-1 (αLβ2), is expressed. ICAM-2 is implicated in constitutive trafficking across blood vascular endothelium. Intriguingly ICAM-2 is down-modulated (2.5 fold) following stimulation with TNFα, as has been reported on vascular endothelium (McLaughlin et al., 1998). No ICAM-3 expression was detected in primary HDLEC, confirming an earlier study by Doussis-Anagnostopoulou et al. (1993), which found that ICAM-3 expression rarely occurs on endothelium but may be induced by an unidentified cytokine-mediated mechanism in lymphoid neoplasms. The experiment detailed in this thesis has shown that TNFα is not involved in the *in vitro* induction of ICAM-3 in primary lymphatic endothelial cells.

Expression of the integrins α3, α4, α6 and αVβ3 was also detected, particularly α3 integrin, which exhibited very high levels of expression, typically 10 fold high than those of other integrins. The known ligands of α3 integrin include fibronectin, laminin and collagens, whilst α4 integrin interacts with fibronectin, α6 integrin with laminin and αVβ3 with vitronectin, fibrinogen, von Willebrande factor, thrombospondin, fibronectin, osteopontin and collagen (Lodish et al., 1995). Thus these integrins connect cells with the extracellular matrix. Curiously only very low levels of β1 integrin were detected, suggesting that the antibodies used do not detect the particular splice variants of β1 integrin expressed by primary HDLEC. Alternatively the α integrins detected may form heterodimers with integrins other than β1 in primary HDLEC, for example α6β4 and α4β7. Integrin α4 (with β1 or β7) may also play a role in leukocyte adhesion through interactions with VCAM-1. However no significant change in expression occurred following stimulation with TNFα.

High expression of the junctional molecules JAM-1 (also known as JAM-A) and vascular endothelial-cadherin (VE-cadherin, or cadherin-5) were detected in primary HDLEC. JAM-1 and VE-cadherin are known to be associated with tight junctions and adherens junctions respectively. However no significant change in the level of surface expression was detected. Low levels of expression of the angiopoietin receptor Tie-2 were detected on primary HDLEC, confirming an earlier study by Kriehuber et al. (2001), in which Tie-2 was detected by both Northern and Western analyses in primary LEC and BEC. Similarly low levels of sialoadhesin (siglec-1), a sialic acid-binding immunoglobulin-like lectin were also detected and underwent no significant change in response to TNFα.

5.2.4 Gene array analysis

To assess the effects of TNFα on LEC gene expression more comprehensively, a gene array analysis of LEC cultured in either the presence or absence of TNFα was carried out. Thus virtually the entire human genome could be surveyed for genes responsive to TNFα. Clearly changes in expression of other adhesion molecules were of particular interest and this approach was not limited by availability and expense of antibodies, as such analysis at the protein level would be. Also the array analysis allows read-out for other molecules relevant to inflammation, such as chemokines, cytokines and matrix metalloproteinases, that would be difficult to survey in large numbers by antibodies.

LEC were cultured for 72h in either the presence or absence of TNFα. Total RNA was prepared by RNeasy (Qiagen), figure 5.5A and double-stranded DNA synthesized using the Ambion aRNA kit. The same kit was used to perform *in vitro* transcription to amplify the number of original transcripts and obtain biotin-labelled complementary RNA (figure 5.5B), which was subsequently

fragmented by metal-induced hydrolysis to obtain suitably sized RNA oligonucleotides (figure 5.5C) for application to the array.

Hybridisation to the Affymetrix® gene-chip (GeneChip® Human Genome U133 Plus 2.0) was performed by the CR-UK microarray facility at the Paterson Institute for Cancer Research. The probe sets represented on the array were derived from sequences selected from GenBank®, dbEST and RefSeq. This single array provided comprehensive coverage of the transcribed human genome and permitted the analysis of the expression level of over 47,000 transcripts and variants, including 38,500 well-characterised human genes.

Each GeneChip® probe array consisted of many probe cells, each containing millions of copies of oligonucleotide probes. The biotinylated, fragmented target RNA was applied to the probe array in a hybridization cocktail containing blocking agents BSA and herring sperm DNA, along with probe array controls. The controls consisted of known amounts of biotinylated prokaryotic genes and permitted assessment of the performance of hybridisation, washing and labelling procedures. Following a 16h incubation, the probe array underwent automated washing with non-stringent and then stringent wash buffers on a Fluidics station operated by Affymetrix® Microarray Suite software. Targets were labelled using streptavidin phycoerythrin (SAPE) and washed, all on the Fluidics station with Microarray Suite. The probe array was then scanned using a laser. The amount of light emitted at 570nm is proportional to the bound target and the software defined the probe cells whilst measuring the intensity of each. Data was normalised and scaled according to the intensity of signals from the house-keeping genes GAPDH, β-actin and ISGF-3 (STAT1), which show consistent levels of expression over a diverse set of tissues.

Duplicate sets of complementary RNAs (cRNA) were prepared and the quality of each probe cRNA was assessed by comparing the ratio of 5′ to 3′ ends: ratios

greater than 1.0 indicate degradation of probe RNA. Researchers at the Paterson Institute found that the quality of RNA yielded by the Ambion kit was highly variable and thus this method was replaced by preparation of complementary RNA at the Institute from total RNA supplied. Thus, RNA was prepared as before from HDLEC cultured either in EGM-2 alone or supplemented with TNFα and cRNA was synthesized at the Patterson Institute. Triplicate sets of data were obtained and are summarized in table 5.2.

Analysis of the data confirmed findings obtained from earlier FACS analyses which had shown induction of VCAM-1, ICAM-1 and E-selectin expression. The abundance of these transcripts increased 4-177 fold following stimulation with TNFα. Similarly down-regulation of LYVE-1 was also borne out in this experiment, confirming the Northern blot analysis and semi-quantitative reverse-transcriptase PCR experiment described in chapter 4. Interestingly, the array analysis also showed that LYVE-1 underwent the most dramatic down-regulation of all the transcripts surveyed on this array. No significant change was observed in integrins α3, α4, α5, α9 or β1 transcripts, although these were detected in both untreated and TNFα-treated cells. αV integrin transcript was found to be induced almost 3 fold, although only a 1.2 fold increase in expression was detected by FACS.

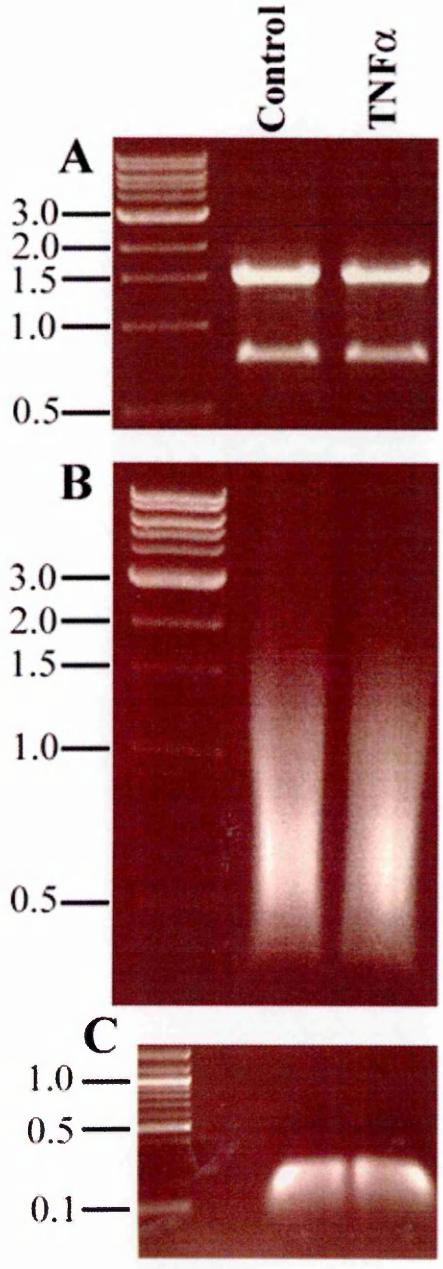

Figure 5.5 Preparation of RNA for hybridisation to the Affymetrix® gene-chip. RNA from HDLEC cultured for 72h in either the presence or absence of TNFα was prepared (RNeasy, Qiagen), panel A. Synthesis of double-stranded cDNA and *in vitro* transcription was performed using the Ambion aRNA kit, to obtain biotin-labelled complementary RNA (panel B), which was fragmented to obtain RNA oligonucleotides (panel C) for application to the array. Approximately 3 µg of RNA at each step was subjected to electrophoresis on a 1% agarose-TBE gel in 70% formamide buffer. DNA ladders were electrophoresed on the same gels and the size (kb) of bands are indicated.

Genes up-regulated

Adhesion Molecules	Fold change
VCAM-1	177.17
ICAM-1	16.99
Claudin-1	5.30
E-Selectin	4.03
Integrin αV	2.72
Claudin-14	2.34
Desmoplakin	1.91
Chemokines, Growth Factors and Cytokines	
MCP-1 (CCL2)	131.03
GCP-2 (CXCL6)	48.84
ENA-78 (CXCL5)	44.58
RANTES (CCL5)	44.46
MIP3α (CCL20)	28.91
IL-8 (CXCL8)	21.87
I-TAC (CXCL11)	11.79
Fractalkine (CX_3CL1)	10.55
IL-1α	9.05
GM-CSF (CSF-2)	7.72
IP-10 (CXCL10)	5.64
IL-15	4.80
VEGF-C	4.37
TNFS6	3.88
IL-1β	3.26
M-CSF (CSF-1)	3.21
TNFS13	3.19
TNFS4	2.15
TNFS18	2.15
CXCL16	2.13
FGF-5	2.05

Extracellular Matrix Molecules	Fold change
Reelin	2.77
Syndecan-4	1.82
Matrix Metalloproteases	**Fold change**
MMP10	5.65
MMP19	2.93
ADAM8	2.16
MMP9	2.13
ADAM9	1.43
ADAM17	1.42
Receptors	
CD69	5.18
TNFRS4	4.67
C-type lectin-like receptor-1	3.21
IL-7R	3.16
Miscellaneous	
Diubiquitin	122.36
TRAF-1	10.46
TNFAIP3	10.41
NFκB2	5.23
NFκB3	3.49
TNFAIP2	3.46
TNFAIP1	2.58
TANK	2.22
TNFAIP6	2.13
NFκB1	2.09
Podoplanin	1.42

Genes down-regulated

Adhesion Molecules	Fold change
LYVE-1	94.65
Endomucin-2	18.32
Multimerin	18.12
Integrin β5	2.31
ICAM-2	2.23
Integrin α8	1.04
CD31	1.98
Integrin β4	1.83
Integrin αE	1.67
Plakoglobin	1.63
Connexin-37	1.58
Integrin α10	1.48
Integrin α6	1.44
Chemokines and Growth Factors	
HCC-1 (CCL14)	2.73
FGF basic	1.56
FGF acidic	1.49

Extracellular Matrix Molecules	Fold change
Semaphorin sem2	4.58
Syndecan-2	3.07
Versican	2.16
Tensin	1.97
Glypican	1.95
Matrix Metalloproteases	
ADAMTS-1	4.06
METH1	3.24
MMP16	1.78
Receptors	
CXCR4 (Fusin)	6.61
Endoglin	1.90
Flt4	1.63
IL1R1	0.68
Mannose receptor, C type 1	1.44
Miscellaneous	
Prox-1	5.28
vWf	3.51

Table 5.2 Representative data from Affymetrix® array analysis in HDLEC. Cells were cultured in triplicate +/- TNFα, 10ng/ml for 72h. Total RNA was prepared from each sample and complementary, biotinylated RNA synthesised at the Patterson Institute, for application to the gene-chip. Data was normalised and mean values of expression for each transcript calculated from the triplicate samples. Fold changes in expression induced by TNFα are shown for each transcript.

The dramatic up-regulation of transcripts encoding the leukocyte inflammatory chemokines MCP-1, RANTES and MIP-3α suggested lymphatic endothelial cells may play a role in promoting migration of leukocytes during inflammation. Kriehuber et al. (2001) had detected TNFα-stimulated induction of MIP-3α and MCP-1 in LEC at the protein level. However, data from the microarrays in this current thesis indicate that a wide range of other chemokines were also induced (2-50x fold) including the CXC chemokines GCP-2, ENA-78, IL-8, I-TAC, IP-10 and CXCL16, as well as the CX_3C chemokine fractalkine and the monocyte/macrophage chemoattractant CSF-1. No significant changes in transcript levels were seen for SLC, the main constitutive chemokine thought to regulate trafficking of CCR7-positive dendritic cells to the lymph nodes through afferent lymphatics (and also implicated in recruitment of naïve T cells across HEVs). In addition to chemokines, the matrix metalloproteinases MMP9 (gelatinase B), MMP10 (stromelysin-2), MMP19 and the enzyme ADAM8 were significantly induced (2-5 fold) by TNFα. These molecules are associated with many diverse functions including leukocyte trafficking and regulation of chemokine activity. Numerous TNF receptor associated proteins such as TNF receptor-associated factor-1 (TRAF-1) and TNF associated proteins-1, -2 and -3 (TNFAIP-1, -2 and -3), involved in signal transduction are also up-regulated, which have never been characterised in lymphatic endothelium before to date. NFκB transcripts also increased.

In addition to LYVE-1, other genes downregulated by TNFα included the secretory granule protein multimerin, the L-selectin ligand endomucin, the type I mannose receptor and β5 integrin. Transcripts of the adherens junction components plakoglobin and CD31 also decreased in abundance, as did the gap junction molecule connexin-37, suggestive of a loosening of cell-cell junctions prior to leukocyte transmigration. Intriguingly the transcription factor Prox-1 underwent down-regulation by over 5 fold. This result was unexpected as this

protein has never been implicated in inflammation but rather is more commonly associated with establishing a lymphatic endothelial lineage, triggering embryonic lymph bud development and lymphatic endothelial cell differentiation.

Data from this array analysis demonstrate that lymphatic endothelial cells respond to the pro-inflammatory cytokine TNFα with major changes in the expression of genes associated with leukocyte adhesion and trafficking. In this way lymphatic endothelium possesses an inflammation-induced expression program similar to that seen in the blood vasculature.

5.2.5 Kinetics of induction of chemokine synthesis in primary HDLEC

The Affymetrix array analysis had demonstrated that synthesis of chemokines transcripts such as those for MCP-1, RANTES and MIP-3α increase dramatically following stimulation with TNF. To determine whether these chemokines were expressed at the protein level and secreted, ELISAs were carried out to detect presence of chemokines in the supernatant of HDLEC after stimulation with TNFα for 6h to 48h as a time course. Another group of cells was left untreated, to assay for chemokine production in unstimulated cells. A negative control of tissue culture medium (EGM-2) alone was used, to ensure that there was no cross-reactivity between the antibodies used to detect the chemokines and components in the medium. Time courses for each chemokine are shown in figure 5.6.

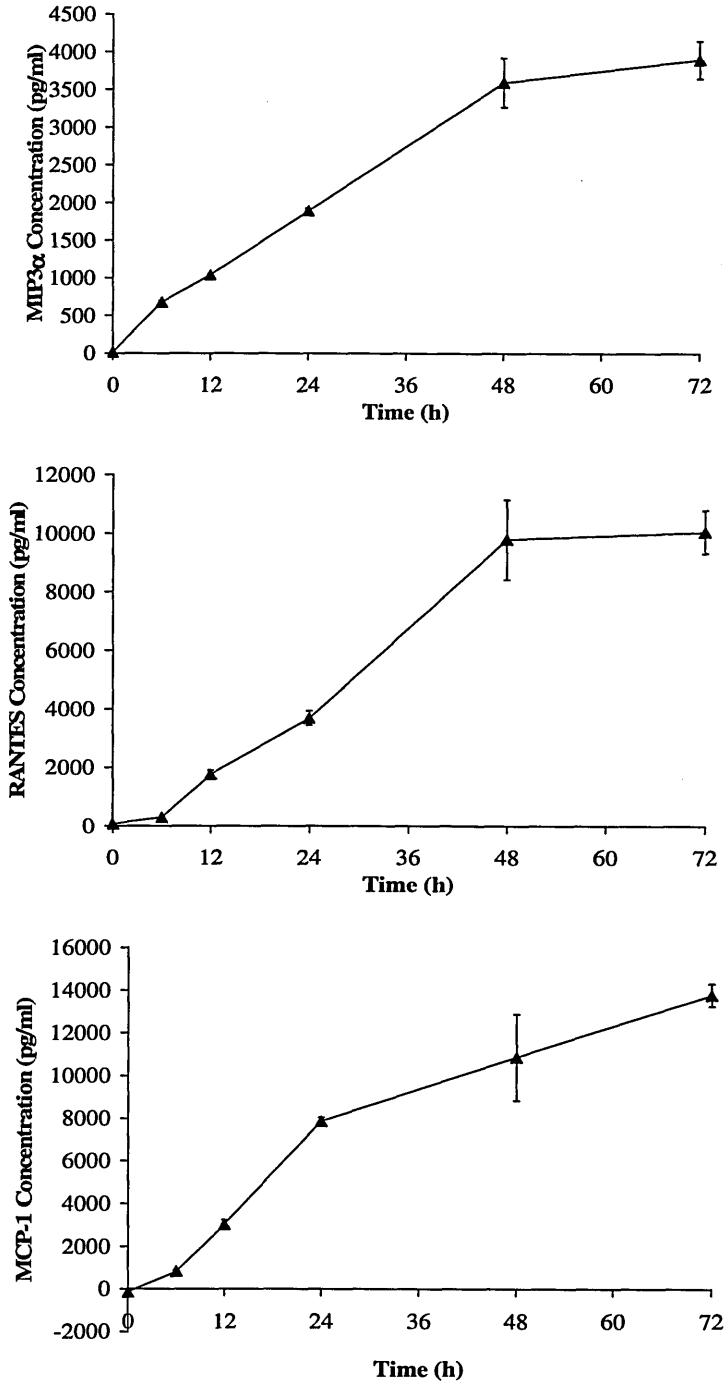

Figure 5.6 Time course of chemokine production by primary HDLEC treated with TNFα. Supernatant from cells cultured in TNFα, 10ng/ml was assayed in triplicate by ELISA for MIP3α (first graph), RANTES (second graph) and MCP-1 (third graph), (R and D systems) according to the manufacturer's instructions. Data shown are mean concentrations calculated from chemokine standard concentration curves, ± standard error.

The results show that untreated HDLEC secrete very low levels of RANTES and MIP-3α (64 pg/ml and 12 pg/ml respectively) and no MCP-1. TNFα induced secretion of all three chemokines (up to 4-14 ng/ml by 72h) and secretion was found to be maximal between 6 and 48h. Thus the fold increases in transcript levels shown by the array analysis were confirmed at the protein level, where TNFα was shown to induce physiological concentrations of these pro-inflammatory chemokines.

5.2.6 Effects of TNFα on mouse LEC

The previous sections of this chapter have described the dramatic effects of TNFα on primary cultured human LEC derived from commercial HDMEC. Although these cells have many if not all the phenotypic characteristics of authentic tissue LEC, it was nevertheless important to confirm the findings with freshly isolated, early passage LEC from a different source.

5.2.6.1 Isolation of mouse LEC

Primary mouse LEC were isolated from neonatal dermal skin, according to a protocol established by Dr. Steven Clasper in the same laboratory (Clasper and Jackson, unpublished). In this procedure, which used 3-4 day post-partum mice, the skins were removed and incubated overnight in dispase to separate the epidermis from the dermal sheets. The dermal sheets were disrupted by a cocktail of enzymes (collagenase, hyaluronidase, elastase and DNase I) and passed through a 70 μm filter to remove cell clumps from the suspension, prior to plating out on gelatine-coated flasks. Endothelial cells adhered more rapidly than other dermal cells such as fibroblasts, which form the majority and have a more rapid doubling time in culture. Therefore approximately four hours after plating, flasks were vigorously tapped to remove and discard non-adherent or weakly attached cells, prior to culture of remaining cells overnight, thus avoiding immediate overgrowth of LEC by fibroblasts. The following day, lymphatic

endothelial cells were clearly visible as small "islands" of cobble-stoned morphology, between other cells, predomainantly fibroblasts. Cells were lifted with a commercial protease preparation, accutase, which unlike trypsin does not proteolytically cleave LYVE-1 and is more efficient than EDTA at breaking cell contacts with the substratum. LYVE-1-positive LEC were then isolated by magnetic bead immuno-selection using the LYVE-1 mAb, C1/8 (generated as described in chapter 3). The resulting cells displayed abundant expression of LYVE-1 and Prox-1 (figure 5.7). Detection of the other lymphatic markers podoplanin (with the mAb 8.1.1) and VEGFR3 (with polyclonal goat antiserum) was also performed but these antibodies proved unsuitable for use in immunofluorescence microscopy.

5.2.6.2 Effects of TNFα on mouse LEC morphology

To investigate whether the TNFα-induced change in morphology of the primary HDLEC (chapter 4) was also precipitated by mouse recombinant TNFα on primary mouse LEC, cells were cultured for 24h in either EGM-2 medium alone or in media supplemented with mouse recombinant TNFα. Mouse LEC were then visualised by phase contrast microscopy. The results (figure 5.8) showed that in response to TNFα, the mouse LEC were found to elongate in a very similar manner to that of the human LEC, described in chapter 4. TNFα appears to induce cytoskeletal rearrangement of the primary mouse LEC, indicating that these cells are responsive to this pro-inflammatory cytokine.

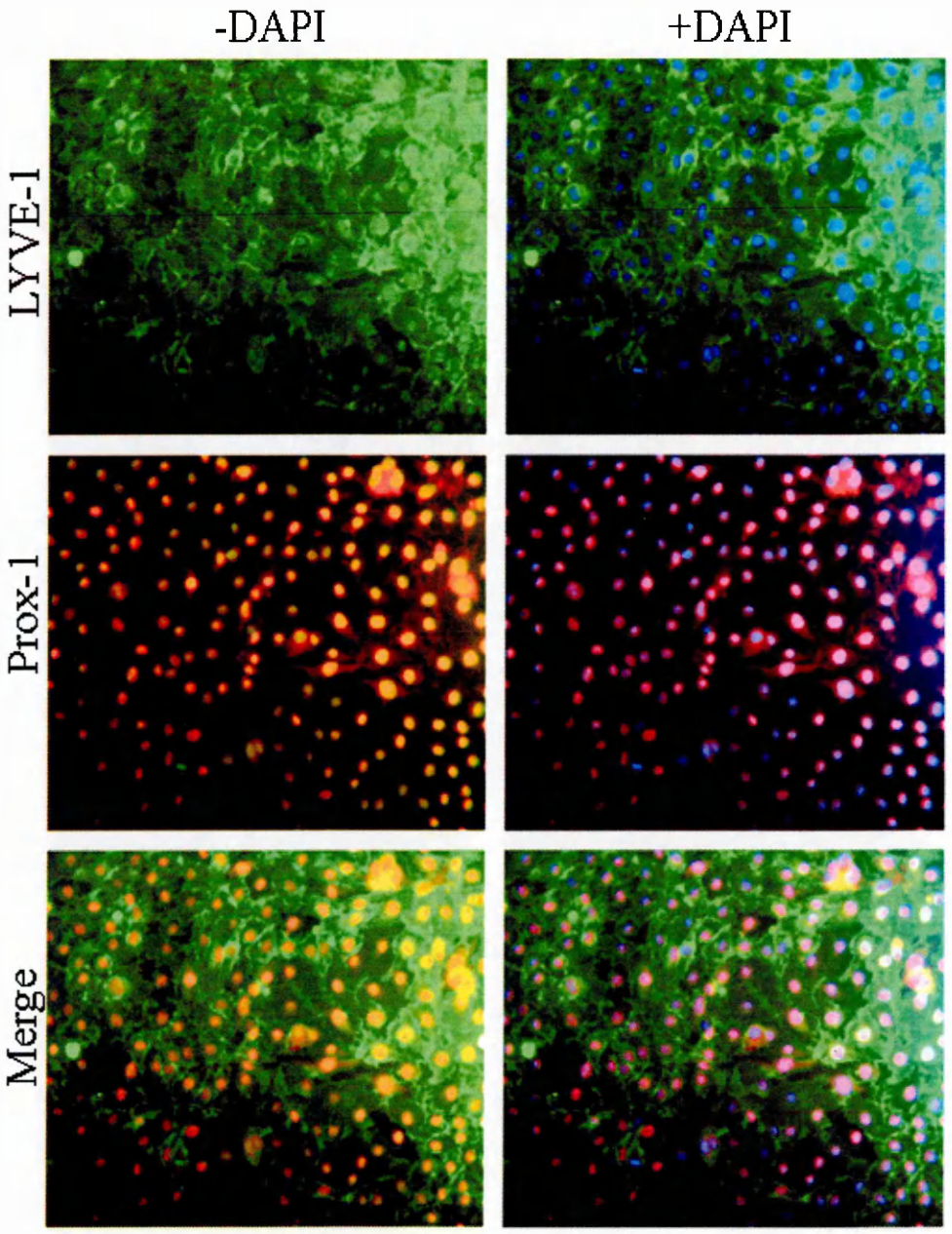

Figure 5.7 Characterisation of primary mouse dermal LEC by immunofluorescence microscopy. Immuno-isolated cells were stained with rat anti-mouse LYVE-1 and rabbit anti-prox-1, detecting with the appropriate AlexaFluor® conjugates, 488 and 568 respectively and counterstaining with the blue nuclei stain DAPI. Cells express both LYVE-1 (green) and prox-1 (red, but colocalising with DAPI in the nuclei and thus appearing pink).

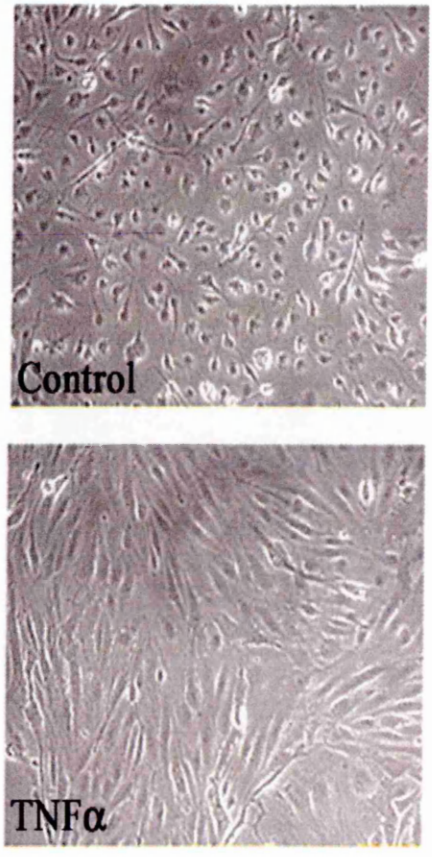

Figure 5.8 Phase contrast microscopy of mouse LEC to show the TNFα-induced change in morphology. Untreated cells exhibit a cobble-stone-like morphology (upper panel) which contrasts with the elongation observed following 24h of stimulation with TNFα, (100ng/ml), shown in the lower panel. Images were captured at 100X magnification.

5.2.6.3 Effect of TNFα on LYVE-1 expression

To determine whether expression of LYVE-1 in primary mouse LEC is affected by TNFα in a similar manner to as in HDLEC, early passage (passage four) cells were stimulated with TNFα for 12, 24 and 48h, then assayed for LYVE-1 expression by flow cytometry. The results (figure 5.9) showed that LYVE-1 surface expression decreased over a period of 48h. However, unlike their human counterparts, mouse LEC showed only a 55% loss of LYVE-1 surface expression, rather than complete loss of the receptor. Maximal loss of LYVE-1 was observed at 12h, after which time expression recovered, even when the cells were maintained in the presence of TNFα throughout the experiment. To address the possibility that mouse TNFα is more labile at 37°C, the experiment was repeated using human TNFα, as TNFRI from both species binds human and mouse TNFα with equal affinity (Barrett et al., 1991). However TNFα from both species was found to precipitate similar decreases in the expression of LYVE-1 (figure 5.10).

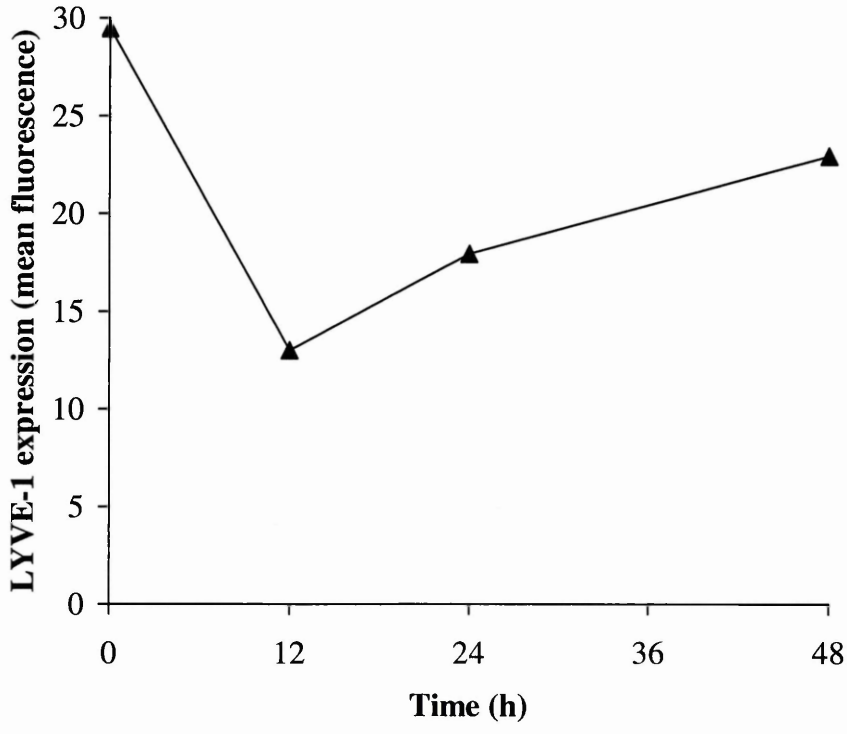

Figure 5.9 Time course of LYVE-1 down-regulation in primary mouse LEC treated with TNFα. Cells were cultured for 0h, 12h, 24h and 48h in the presence of TNFα, 100ng/ml then lifted with accutase and stained for LYVE-1 using the mAb C1/8 and goat anti-rat AlexaFluor®488 prior to analysis by flow cytometry. Values shown are the mean fluorescence of C1/8 staining, with values for mean fluorescence of staining by an irrelevant rat IgG control subtracted at each time point.

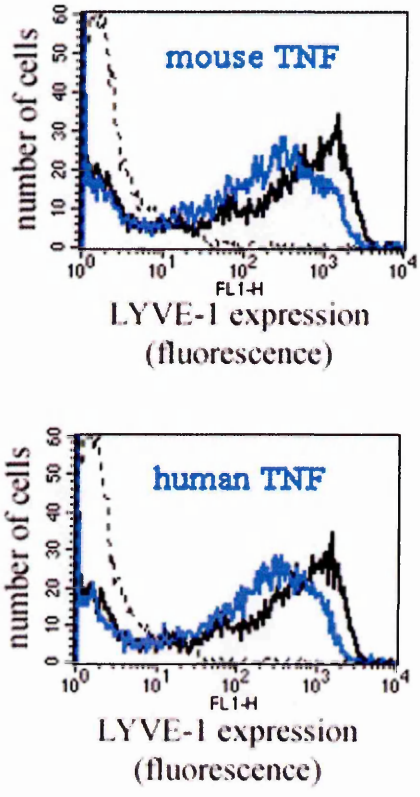

Figure 5.10 Comparative effects of human and murine TNFα on LYVE-1 down-regulation in primary mouse LEC. Cells were cultured 12h in the presence or absence of either human or murine recombinant TNFα (100ng/ml), then lifted with accutase and stained for LYVE-1 using the mAb C1/8 and goat anti-rat AlexaFluor®488 prior to analysis by flow cytometry. Untreated cells are shown in black, cells treated with TNFα are in blue and those stained with an isotype matched control as a dotted black line.

One possible explanation for the reduced response of these cells is that the murine LEC were isolated from post-partum dermis, whereas human LEC were isolated from young adult dermis. Delayed up-regulation of blood vascular endothelial adhesion molecules due to depressed endogenous TNFα production in the lungs of neonatal mice following elicitation of inflammation has been reported by Qureshi et al., (2003). However in the present case, exogenous TNFα was administered and therefore this cannot be the explanation here. Nevertheless, expression of TNF receptors has not been measured on these cells and a low expression may account for why these cells are less responsive than the HDLEC.

To address this issue, mouse dermal LEC were isolated from adult nude mice and tested for their responses to TNFα. Immuno-competent mice could not be used for such studies as the depilatory cream employed to remove the fur was found to substantially reduce the yield and viability of the isolated cells (S. Clasper, unpublished observation). The results (figure 5.11) showed that these cells displayed the same degree of response to TNFα as those cells isolated from neonates. Although it is possible that LEC from the nude, athymic mice also exhibit reduced responsiveness to TNFα, there may be species differences in TNFα response of lymphatic endothelial cells. Data from HDLEC derived from PromoCell HDMEC have been validated in chapter 4 by identical responses to TNFα of both HDMEC from Cambrex and podoplanin-positive immuno-selected HDLEC from the laboratory of Prof. Dontscho Kerjaschki. Hence the results appear to reveal an inherent difference between human and murine LEC in terms of their response to an inflammatory stimulus.

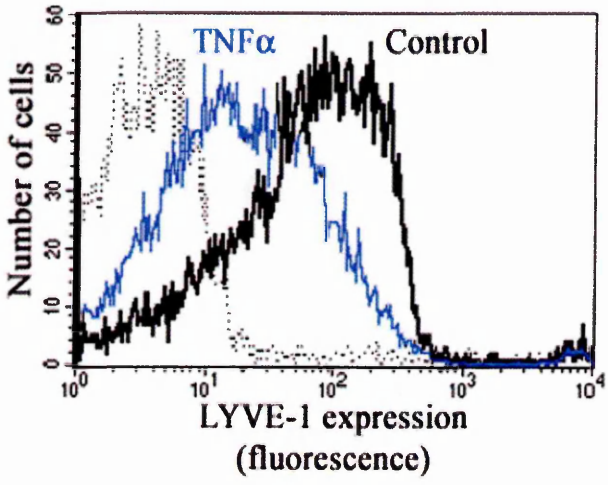

Figure 5.11 Response to TNFα of primary LEC isolated from adult nude mice. Cells were cultured for 48h in either the absence (black line) or presence (blue line) of mouse recombinant TNFα, 100ng/ml. Cells were stained for LYVE-1 expression with the mAb C1/8 or an isotype-matched control (dotted line) and goat anti-rat AlexaFluor®488 prior to analysis by flow cytometry.

5.2.6.4 Effects of TNFα on expression of key leukocyte adhesion molecules

Earlier experiments detailed in this chapter had shown that low levels of ICAM-1 were expressed on unstimulated HDLEC but following stimulation with pro-inflammatory cytokines, expression of both ICAM-1 and VCAM-1 were up-regulated. To investigate whether similar up-regulation of leukocyte adhesion receptors occurred in primary mouse LEC, cells were cultured for 12h in either EGM-1 medium alone or in media supplemented with TNFα, prior to immunofluorescence microscopy to detect LYVE-1 with either VCAM-1 or ICAM-1 expression (figure 5.12).

Results showed that unstimulated cells expressed virtually no VCAM-1 and low levels of ICAM-1, whilst retaining high levels of expression of LYVE-1. However following stimulation with TNFα, cells exhibited clear up-regulation of both VCAM-1 and ICAM-1. The increased expression of VCAM-1 was also quantitated by flow cytometry (figure 5.13).

To study expression of other adhesion molecules, further immunofluorescence microscopy was performed using antibodies against the junctional molecules CD31 and VE-cadherin. Experiments presented earlier in this chapter had shown that both of these molecules were expressed by primary HDLEC but neither underwent marked changes in expression following stimulation with TNFα. As shown in figure 5.14, expression of both CD31 and VE-cadherin was detected on primary mouse LEC. No change in expression was induced by TNFα, despite the decrease in LYVE-1 expression which indicated that the cells in the representative fields of view were responsive to the cytokine (figure 5.14). Thus the early passage mouse LEC confirmed the results obtained with late passage HDLEC.

Figure 5.12 Effect of TNFα on expression of VCAM-1 and ICAM-1 in primary mouse dermal LEC *(following page).* Cells were cultured for 12h in either medium alone or supplemented with TNFα, (100ng/ml). Cells were then stained with rabbit anti-LYVE-1 (green) and either rat anti-VCAM-1 (red) or rat anti-ICAM-1 (red) as indicated, detecting using the appropriate AlexaFluor®488 and 568 conjugates and counterstaining nuclei with DAPI. Representative images were captured at magnification: x 100.

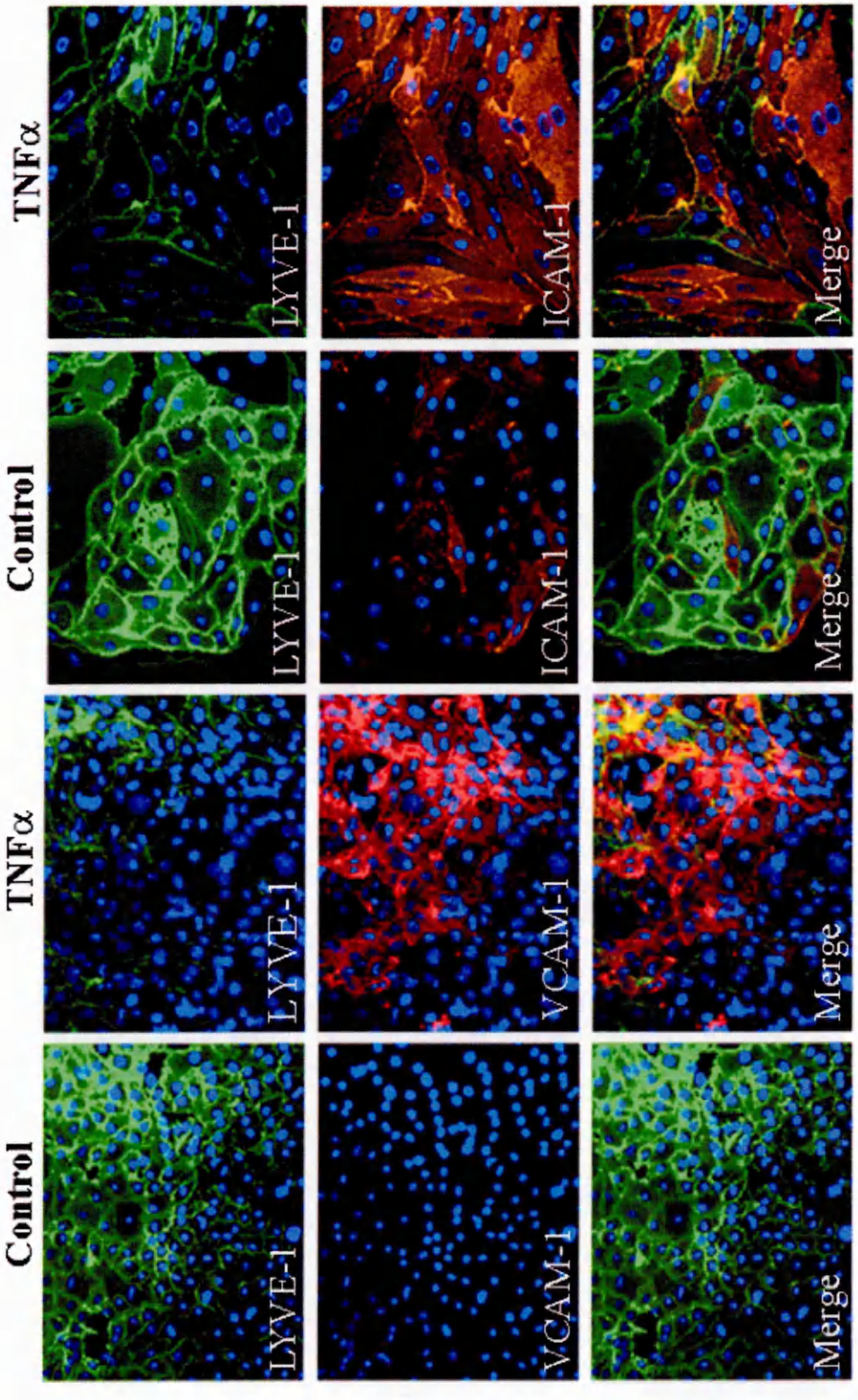
Control
TNFα
Control
TNFα
LYVE-1
VCAM-1
Merge
LYVE-1
ICAM-1
Merge

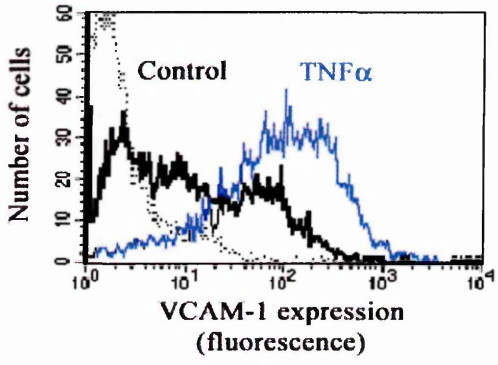

Figure 5.13 Quantitation of the increase in VCAM-1 expression in TNFα-stimulated mouse LEC. Cells were cultured for 12h in either the presence or absence of recombinant mouse TNFα, 100ng/ml, then lifted with accutase and stained for VCAM-1, detecting using the AlexaFluor®488 goat anti-rat conjugate and flow cytometry. Untreated cells are represented by a black line, TNFα-stimulated cells in blue and cells stained with an irrelevant isotype matched control shown by the dotted line.

Figure 5.14 Effects of TNFα on expression of CD31 and VE-cadherin in primary mouse dermal LEC (*following page).* Cells were cultured for 12h in either medium alone or supplemented with TNFα, (100ng/ml). Cells were then stained with rabbit anti-LYVE-1 (green) and either rat anti-CD31 (red) or rat anti-VE-cadherin (red) as indicated, detecting using the appropriate AlexaFluor®488 and 568 conjugates and counterstaining nuclei with DAPI. Images were captured at 100X.

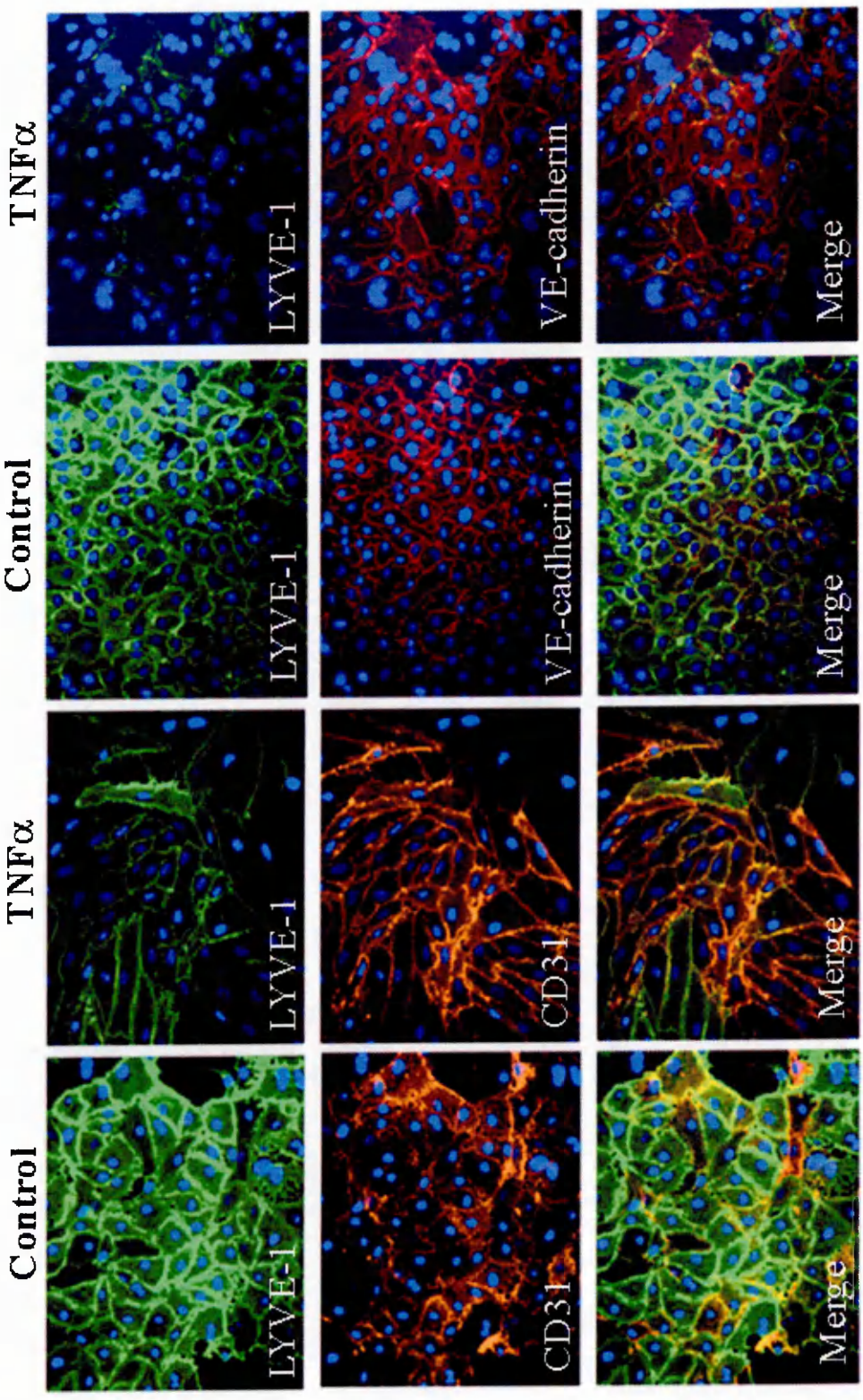
Control
TNFα
Control
TNFα
LYVE-1
CD31
Merge
LYVE-1
VE-cadherin
Merge

To detect whether the primary mouse LEC expressed CD44, as had been found in HDLEC, immunofluorescence microscopy was performed on mouse LEC, cultured either in the presence or absence of TNFα. All early passage cells were CD44-negative but at later passages (six and beyond) a minority of cells were found to express CD44 following stimulation with TNFα. This suggested de-differentiation at higher passage number (figure 5.15).

5.2.6.5 Microarray analysis of resting and TNFα-stimulated mouse LEC

As with primary HDLEC, total RNA was prepared from primary murine LEC cultured in either the presence or absence of TNFα and complementary RNA was prepared at the Cancer Research UK Patterson Institute, Manchester, where it was applied to the GeneChip® Mouse Expression Set 430 array. This two array set allows analysis of the expression levels for over 39,000 transcripts and variants, including 34,000 confirmed mouse genes and was carried out in a similar manner to that of the human gene array analysis. It was imperative to use cells which had been cultured for the shortest possible time and therefore rather than the triplicate analyses used in the HDLEC samples, this assay was carried out using a single set of RNA samples. Data are summarised in table 5.3.

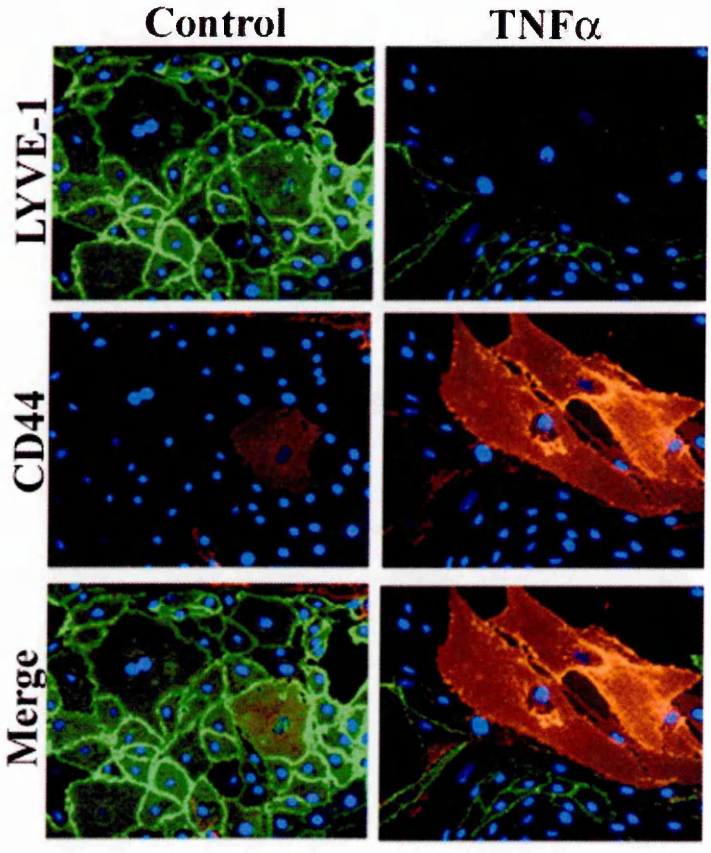

Figure 5.15 Evidence for de-differentiation in later-passage primary mouse dermal LEC. Later passage cells (passage seven) were cultured for 12h in either medium alone or supplemented with TNFα, (100ng/ml). Cells were then stained with rabbit anti-LYVE-1 (green) and the rat anti-CD44 mAb, IM7 (red). The appropriate AlexaFluor®488 and 568 conjugates were used for detection and nuclei were counterstained using DAPI. Images were captured at 100X

Genes up-regulated

Adhesion molecules	**Fold change**
ICAM-1	8.39
E-Selectin	5.85
VCAM-1	4.81
Integrin α3	2.49
Integrin α5	2.17
Claudin-12 orthologue	2.18
Integrin β3	1.71
Chemokines, cytokines and growth factors	
MCP-3 (CCL1)	20.76
GROβ (CXCL2)	9.94
VEGF-C	5.68
IP-10 (CXCL10)	5.30
JE/MCP-1 (CCL2)	4.92
M-CSF (CSF-1)	4.20
RANTES (CCL5)	3.97
MIP3α (CCL20)	3.52
MIP1γ (CCL9/10)	2.78
IL-6	2.19
ENA-78 (CXCL5)	2.06
PDGFα	1.97
MIP1β (CCL3)	1.95
IGF-7	1.75
I-TAC (CXCL11)	1.62

Extracellular matrix molecules	
Fibronectin	1.71
Matrix metalloproteinases	
MMP13	39.61
MMP10	13.94
MMP3	12.18
MMP2	2.34
Receptors	
EGF receptor	5.25
Miscellaneous	
TNFAIP3	2.77
vWf	2.31
TNFRS6	2.21
TRAF-1	2.14
TANK	2.14
NFκB2	2.12
TRAF-3	2.11
TNFAIP1	2.08
Endothelial cell specific molecule 1	2.07
Podoplanin	1.25

Genes down-regulated

Adhesion molecules	**Fold change**
Occludin	7.13
Claudin-5	3.48
Integrin α8	2.76
Multimerin	2.47
Cadherin-5 (VE-cadherin)	2.35
Connexin 34	2.20
Integrin α9	1.77
LYVE-1	1.51
Integrin α6	1.37
CD31	1.36
ICAM-2	1.27
Chemokines, cytokines and growth factors	
IGF-2	5.39
IGF-1	3.98
Angiopoietin	3.88
IL-7	2.25
BCA-1 (CXCL13)	1.23
Extracellular matrix molecules	
Reelin	8.45
Matrix metalloproteinases and inhibitors	
ADAMTS5	8.10
Timp-3	4.48
ADAM10	2.40
Receptors	
Mannose receptor, C type 1	4.39
VEGFR-3	1.83
Miscellaneous	
Prox-1	4.39

Table 5.3 Representative data from Affymetrix® microarray analysis in primary mouse dermal LEC. Cells were cultured in either the presence or absence of TNFα, (100ng/ml) for 12h. Total RNA was prepared and complementary, biotinylated RNA synthesised at the Patterson Institute, for application to the gene-chip. Data was normalised and fold changes in expression induced by TNFα are shown for each transcript.

The results show TNFα-induced up-regulation of the transcripts encoding ICAM-1 and VCAM-1, as was also seen in the human LEC. However the magnitude of changes are more moderate in the mouse primary dermal LEC, with increases of 8.4 fold and 4.8 fold for the respective molecules as opposed to 177 fold and 17 fold recorded in the human LEC. E-selectin transcript exhibited up-regulation by 5.9 fold, which is more comparable to that found in the human LEC (4 fold).

Up-regulation of transcripts encoding the chemokines IP-10, RANTES, MIP-3α, ENA-78, I-TAC and JE, the mouse orthologue of human MCP-1, were recorded in TNFα-stimulated murine LEC as well as in the stimulated human LEC described earlier in this chapter. However as with the adhesion molecules transcripts the extent of up-regulation of chemokines was not as dramatic as in the human LEC. The two species also exhibited some differences in the chemokines induced. For example MCP-and GROβ were up-regulated in mouse LEC alone whereas GCP-2 was only induced in human LEC.

The data also show up-regulation of matrix metalloproteinases in primary mouse dermal LEC. Induction of MMP10 (stromelysin-2) was detected in both mouse and human LEC following TNFα stimulation, although the identities of other MMPs induced differed between the species. Curiously the MMPs detected in the murine LEC underwent a more marked up-regulation of transcript abundance (up to 39.6 fold) than the human LEC (less than 5.7 fold).

Transcripts of the integrins α4, αV and α1 were detected but did not change significantly upon TNFα stimulation. Interestingly, unlike human LEC, the mouse cells showed up-regulation in IL-6 mRNA following TNF stimulation. This could account for the recovery of expression of LYVE-1 on these cells without the removal of the TNF-supplemented medium, as suggested in chapter 4. The lack of IL-6 synthesis following TNFα stimulation (Abbas et al., 1997) in

the human LEC studied may be involved in the failure to re-express LYVE-1. Whether this is unique to the human lymphatic endothelial cell line or whether it is true in human lymphatic endothelium in general remains to be determined. The former hypothesis is more likely correct; otherwise another mechanism would have to be responsible for the resolution of the early stages of acute inflammation.

As in the data obtained from TNFα-stimulated human LEC, the mouse LEC underwent up-regulation of transcript abundance of various TNF receptor associated proteins such as TNF receptor-associated factor-1 (TRAF-1) and TNF associated proteins-1 and -3 (TNFAIP-1 and -3), as well as NFκB2. However again the increase in abundance (2-3 fold) was not as dramatic as that measured in the human LEC (2-10 fold).

5.2.6.6 Effect of TNF on chemokine production by mouse LEC

As with HDLEC, the Affymetrix array analysis on mouse LEC demonstrated that synthesis of chemokines such as RANTES (CCL5), MIP3α (CCL20) and JE, the mouse homologue of MCP-1 (CCL2) increase dramatically following stimulation with TNFα. Chemokine production by mouse LEC was assayed at the protein level in a similar manner to the human LEC, using R and D Systems ELISA kits. However, only assays for JE and RANTES were available. Mouse LEC were stimulated with TNF for 6h to 48h as a time course and as before some cells in each case were left untreated, to assay for chemokine production in unstimulated cells. A negative control of EGM-2 medium alone was used, to ensure that there was no cross-reactivity between the antibodies used to detect the chemokines and components in the medium.

Mouse LEC were found to secrete concentrations of JE and RANTES of 100 ng/ml and 1.6 ng/ml respectively over 72h (figure 5.16). The concentration of JE

is approximately 10 fold higher than that of the supernatant from stimulated HDLEC, whilst the concentration of RANTES is approximately 10 fold less than that of the HDLEC. Clearly, direct comparison of these chemokine concentrations to those in inflamed tissue *in vivo* is not possible as the values from *in vitro* experiments are dependent largely on cell density and volume of the medium. However, concentrations of the order of ng/ml are detected in serum following inflammatory stimuli in animals. For example, after intraperitoneal injection of LPS in mice, serum concentrations of MCP-1 of up to 9 ng/ml were recorded (Marino et al., 1997). Therefore the secretion of these pro-inflammatory chemokines in lymphatic endothelial cells could be expected to have a significant biological effect *in vivo*.

The kinetics of chemokine secretion by primary mouse dermal LEC are similar to those of the HDLEC. Mouse LEC continue to secrete JE/MCP-1 at a steady rate from 6h after stimulation to 72h. RANTES secretion reaches a plateau after 48h followed by an apparent decrease, indicating possible uptake and perhaps degradation of the chemokine between 48-72h, which may be to prevent a prolonged effect.

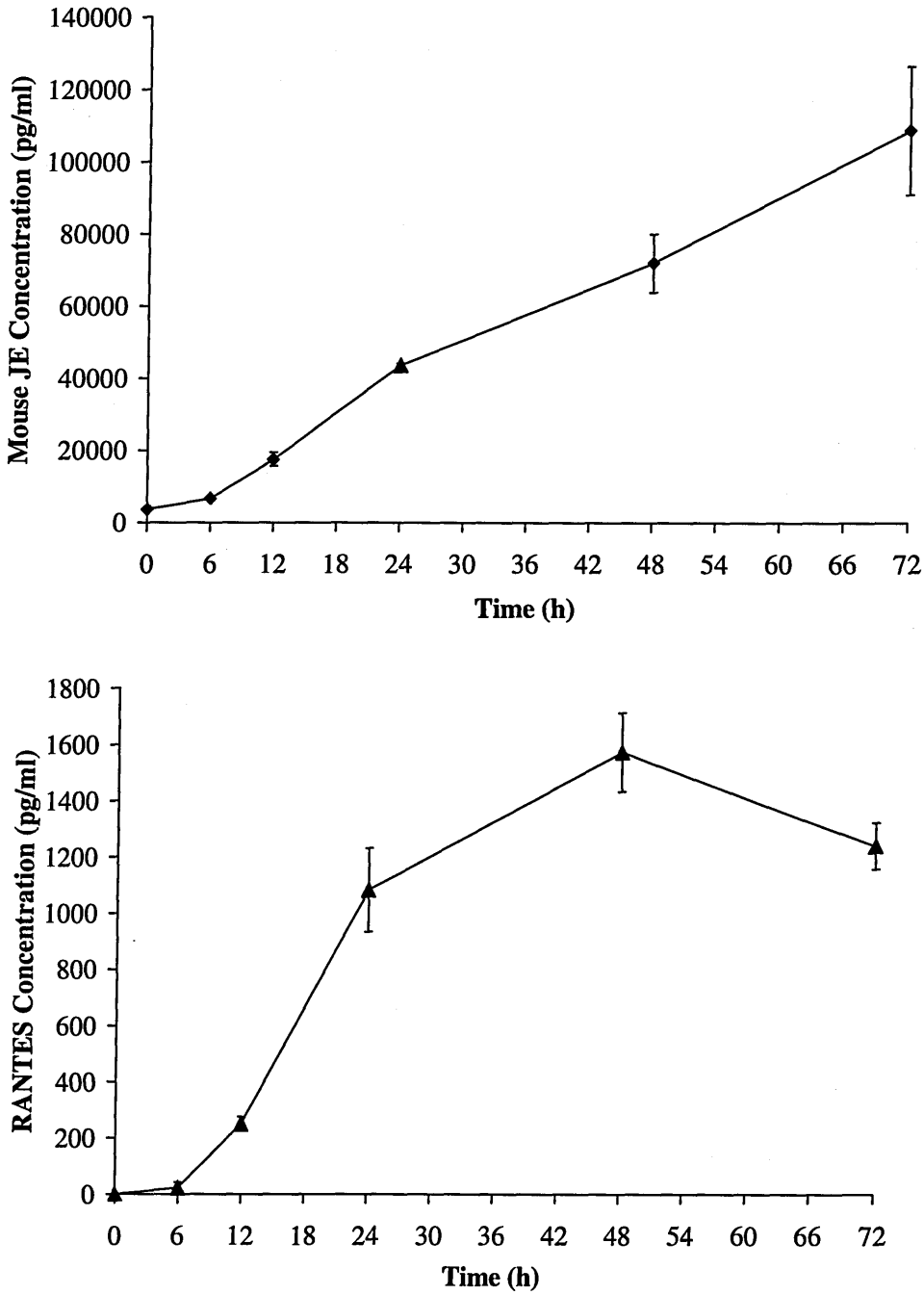

Figure 5.16 Time courses of chemokine production by LEC treated with TNFα. Cells were cultured in triplicate +/- TNFα, 100ng/ml for each time point and diluted supernatants applied to ELISAs (R and D systems) to detect JE (upper panel) and RANTES (lower panel). Data shown are mean concentrations calculated from chemokine standard concentration curves, ± standard error.

5.3 Discussion

The results in this chapter have presented new evidence that primary LEC respond to pro-inflammatory cytokines by adopting a programme of gene expression that suggests an active role in co-ordinating leukocyte trafficking. Primary HDLEC, initially described in chapter 4, were phenotyped more extensively as were primary mouse dermal LEC isolated from neonates, both when untreated and following stimulation with TNFα, by flow cytometry, ELISA and microarray analysis.

5.3.1 Expression of adhesion molecules on LEC

Cultured HDLEC and freshly immuno-isolated low-passage mouse LEC displayed marked up-regulation of key leukocyte-endothelial adhesion molecules ICAM-1, VCAM-1 and E-selectin in response to TNFα. In both cases, there was a concomitant down-modulation of LYVE-1, described in chapter 4. Flow cytometry studies revealed that both E-selectin and VCAM-1 were absent from unstimulated LEC but were induced following exposure to TNFα or TNFβ. ICAM-1 was expressed at low levels on LEC but markedly up-regulated following exposure to TNFα, TNFβ, IL-1α, IFNγ and LPS. These data were confirmed by microarray analysis, which revealed that up-regulation of these adhesion receptors occurs also at the level of mRNA in both the human and mouse. Results described in this chapter show that TNFα has a more potent inflammatory effect on LEC that TNFβ, confirming an earlier study by Desch et al., 1990, who found that TNFα was more effective than TNFβ in promoting adhesion of neutrophils to cytokine-activated HUVEC.

Historically, leukocyte transmigration across blood vascular endothelium has been studied much more thoroughly than that across the lymphatics, as outlined

in detail in the introduction to this thesis. In the case of non-inflamed blood vessel endothelium, the multi-step process of transmigration involves initial weak interactions between leukocyte selectins and endothelial mucins, followed by chemokine-induced firm adhesion between the leukocyte integrins αLβ2, αMβ2, α4β7 and their endothelial ligands ICAM-1, ICAM-2 and MAdCAM-1 (reviewed by von Andrian and Mackay, 2000). During tissue inflammation, cytokines including TNFα, IL-1 and INFγ induce peripheral vascular expression of VCAM-1, promoting adherence of memory T cells and monocytes bearing the VCAM-1 ligand α4β1 (Alon et al., 1995; Van Dinther-Janssen et al., 1991). ICAM-1 is also up-regulated on endothelium of the blood vasculature and engages with leukocyte integrins LFA-1 and Mac-1 both to permit firm adhesion and initiate transmigration (Dustin and Springer., 1988). ICAM-1 has also been implicated in assisting transmigration of Langerhans cells into afferent lymphatic vessels and trafficking to lymph. For example Sligh et al. (1993) demonstrated that ICAM-1 deficient mice have defective hapten-induced contact hypersensitivity responses in the skin. Also Xu et al. (2001) showed that disruption of the *ICAM-1* gene blocked trafficking of hapten-presenting LC to the lymph node from allergen-sensitised skin. However, expression of ICAM-1 by the lymphatics was not conclusively demonstrated and it was not known whether it played a role in the entry of DCs to afferent lymphatics, migration through the lymphatics or transmigration across the lymph node sinus endothelium to enter the lymph node paracortex. The data shown in this chapter constitute the first direct evidence that ICAM-1 is a significant and highly inducible component of lymphatic endothelial cells and supports the earlier research by other groups in suggesting a role for ICAM-1 in leukocyte migration in the lymphatics. As both the mouse and human LEC used in this chapter are of dermal origin, this would suggest that the adhesion molecules are up-regulated in the initial lymphatic capillaries and thus may play a role in the initial entry of DCs into the

lymphatics. Experiments detailed in the following chapter will explore this more fully *in vivo*.

HDLEC were also found to express ICAM-2, which is expressed constitutively in blood vascular endothelium (Staunton et al., 1989). Both ICAM-1 and ICAM-2 are receptors for LFA-1 (CD11a/CD18 or αLβ2, Makgoba et al., 1988) but ICAM-2 can also interact with DC-SIGN (CD209), a C-type lectin expressed on DCs. As on blood endothelium (McLaughlin et al., 1998), ICAM-2 in primary HDLEC underwent a marginal but significant down-regulation in response to TNFα. This would suggest that lymphatic endothelial ICAM-2 does not have a role in inflammation but rather is constitutively expressed in normal tissue. Blood endothelial ICAM-1 and ICAM-2 have been shown by Lehmann et al. (2003) to have redundant roles in lymphocyte recirculation through lymph nodes but ICAM-1 alone was shown to be involved in T cell migration into inflamed skin. Geijtenbeek et al. (2000a) demonstrated that ICAM-2 also interacts with DC-SIGN to mediate the extravasation of DC precursors from the blood into the tissue. Therefore expression of ICAM-2 on lymphatic endothelium may play a role in migration of DCs across the lymphatic endothelium. Alternatively it may aid constitutive leukocyte transmigration through the afferent lymphatics. Electron microscopy experiments to address whether ICAM-2 is expressed on the luminal or abluminal side of endothelium could provide further evidence to suggest if ICAM-2 interactions occur with leukocytes entering the lymphatics or cells already within the lumen. DC-SIGN can also bind ICAM-3 to enable transient high affinity interactions between DCs and T cells to support primary immune responses (Geijtenbeek et al., 2000b). Therefore as anticipated no ICAM-3 was detected on primary HDLEC.

5.3.2 Chemokines

The microarray analysis of resting and TNFα-treated LEC not only bore out what had been observed at the protein level for the adhesion molecules in terms of comparative message abundance but also illustrated the vast range of chemokines newly transcribed by LEC.

Stimulation of LEC with TNFα induced the synthesis of chemokines such as RANTES, MCP-1, MIP-3α, MCP-3, Fractalkine and IL-8, which act through the receptors CCR1 and CCR5; CCR2; CCR6; CCR1, CCR2 and CCR3; CX_3CR1; and CXCR8 respectively to promote migration of DCs to sites of inflammation and recruitment of monocytes and T cells (reviewed by von Andrian and Mackay, 2000). Neutrophil chemokines such as ENA-78, IL-8 and GROβ were also induced, acting via the receptors CXCR1 and CXCR2. Expression of RANTES, MCP-1 and MIP-3α was confirmed by ELISA, whereby these secreted chemokines were detected in culture supernatant. Thus the results described in this chapter indicate that the lymphatics have the capacity to actively guide migrating cells towards themselves. As blood and lymphatic capillaries are so closely apposed within the dermis, it is also possible that these chemokines act in a paracrine fashion to recruit more monocytes from the blood after transfer to the luminal face of blood vascular endothelium, (Middleton et al., 1997).

Microarray analysis data detailed in this chapter show that the CXC chemokine IP-10 transcript was up-regulated in both mouse and human LEC following stimulation with TNFα. IP-10 is known to act through CXCR3 to promote the migration of effector type I helper T cells (reviewed by von Andrian and Mackay, 2000). Recently Nakae et al. (2002) found that this chemokine is up-regulated in mouse skin in a model of delayed hypersensitivity, through a TNFα-dependent pathway. However, the cells producing IP-10 were not identified in that study.

The data from the gene array analyses performed here in this thesis suggest that the lymphatic endothelium is at least partly responsible for the increased expression of IP-10 in mouse skin challenged with a sensitising agent. Indeed IP-10 is but one of several chemokines up-regulated following TNFα stimulation of lymphatic endothelium.

The results described in this chapter also confirm the finding of Mancardi et al, 2003, in their study on secretion of chemokines from cells derived from experimentally induced lymphangioma, where they found high levels of JE/MCP-1 and RANTES; the cells they isolated were podoplanin positive and were thus deemed mouse LEC. However unlike the present study, that of Mancardi et al. did not detect MIP-1β or MIP-1γ message. Also the expression of C10, classically found on haematopoietic cells was detected in the 2003 publication but not by array analysis. These differences in expression may be accounted for by the source from which the LEC are derived.

The down-modulation of HCC-1 in TNFα-treated HDLEC was surprising as this chemokine is associated with migration of dendritic cells and monocytes in inflammation through CCR1. It is possible that HCC1 is up-regulated at an earlier time point (less than 72h following TNFα stimulation) than the other chemokines. There is a marginal reduction in abundance of BCA-1 mRNA in the mouse LEC but this is less surprising than HCC-1 as it is primarily involved in migration of B cells (through CXCR5), rather than possible recruitment of antigen presenting cells towards lymphatic endothelium for transmigration into the lymphatics (von Andrian and Mackay, 2000).

Although the chemokines MCP-1, MIP-3α, RANTES, ENA78, IP10 and CSF-1 are induced in both mouse and human LEC, up-regulation of other chemokines was restricted to only one of the two species. There is no known mouse homologue

of IL-8 and therefore the up-regulation of other chemokines such as GROβ (which is not up-regulated in the human), may play a compensatory role in the mouse in the recruitment of neutrophils, in addition to ENA-78. Other species differences indicated from the array analysis include the induction of GCP-2 in human LEC but not in mouse, and up-regulation of MCP-3 in mouse but not human.

5.3.4 Matrix metalloproteinases

The induction of matrix metalloproteinases such as MMP-3, -6, -9, -10 and -19 was a striking observation from the microarray data. It is tempting to speculate that such molecules could potentially facilitate extravasation of monocytes from the blood by degrading basement membrane structures on interendothelial tight junctions of juxtaposed blood capillaries. It is also possible that they contribute to the establishment of chemokine gradients by releasing immobilised chemokines from their heparan sulphate proteoglycan binding sites within the extracellular matrix (Parks et al., 2004) and, through cleavage of the chemokine, activate chemotactic activity. A prime example of this is the neutrophil chemokine IL-8, (Van Den Steen et al., 2000), which stimulates the release of MMP-9 (gelatinase B) from neutrophils, which was then shown to specifically process IL-8 at the amino-terminus, increasing the specific activity and altering receptor usage. MMP-9 was later shown to also regulate the other CXC chemokines GCP-2 and ENA-78, again at the amino-terminus, inactivating ENA-78 (Van den Steen et al., 2003a). MMP-9 was also shown to negatively regulate MIG and IP-10 through carboxy-terminal cleavage (Van den Steen et al., 2003b).

The negative regulation of chemokine activity by MMPs is not restricted to MMP-9 and ENA78: cleavage of MCP-1, MCP-3 and GCP-2 by MMP-2, -3 or -9 can also destroy chemotactic activity (McQuibban et al., 2001; McQuibban et al., 2002; reviewed by Parks et al., 2004). Such modification may even result in these

chemokines being converted into antagonistic agents. Thus, by modulation of chemokine activity, MMPs may be involved in the recruitment of specific inflammatory cells into the dermis in response to a particular antigen. The establishment of a chemokine gradient and modifications to extracellular matrix by MMPs also regulate migration of antigen presenting cells towards the lymphatics. Evidence from the microarray data suggests that this carefully orchestrated process is regulated at least in part by lymphatic endothelial cells, which may instigate both the initiation and resolution of inflammation.

5.3.5 TNF superfamily members

Both the human and mouse microarray data showed that numerous TNF receptor associated proteins and NFκB transcripts increased following stimulation with TNFα. Intriguingly, the human microarray data also showed that TNFα induces expression of the TNF superfamily receptor OX40 (also known as CD134, or by the systematic name TNFRSF4) and its ligand OX40L (CD134L or TNFSF4). This receptor is a T cell activation marker with limited expression which is believed to promote the survival and perhaps prolong the immune response of $CD4^+$ T cells at sites of inflammation (Godfrey et al., 1994). Expression of the ligand has been reported on vascular endothelial cells (Imura et al., 1996) but the receptor was believed to be restricted to activated $CD4^+$ and $CD8^+$ cells. An increase in transcript abundance was also detected for CD137 (TNFRSF9), another activation-induced glycoprotein which had not been found on endothelial cells before. Ligation of this receptor is reported to interrupt T cell apoptotic programs associated with activation-induced cell death (Hurtado et al., 1997). Data from the array analysis could suggest that lymphatic endothelial cells are capable of protecting themselves from apoptotic signals during inflammation, as well as synthesising ligands to ensure the survival of neighbouring T cells. GITR ligand (glucocorticoid-induced TNFR family-related ligand, TNFSF18) is another transcript up-regulated in TNFα-treated LEC, which

has been shown to interrupt apoptosis in T cells when binding to its receptor, expressed on normal T lymphocytes from lymphoid tissue (Nocentini et al., 1997). Interestingly, Fas ligand (TNFSF6) is also transcribed by TNFα-treated LEC and this may induce either apoptosis or proliferation of Fas (CD95, TNFRSF6) positive cells, depending upon the relative number of expressed Fas molecules (Freiberg et al., 1997). While it must be stressed that the consequences of these changes in transcription levels remain to be explored *in vivo*, the data are at least suggestive of a role for the lymphatic endothelium in influencing the fate of neighbouring leukocytes as well as their own survival.

5.3.6 LYVE-1

The dramatic down-modulation of LYVE-1 in HDLEC first described in chapter 4 was confirmed again in this chapter in the microarray analyses, where LYVE-1 mRNA underwent the most dramatic reduction of abundance of all the genes surveyed by the human microarray, consisting of over 47 000 transcripts and variants. Curiously, mouse LEC did not exhibit the same striking down-regulation. Whether the reason for this lies in the developmental stage at which the cells were isolated (as discussed earlier in this chapter) or the species from which they were derived is unclear, although none of the mouse LEC transcripts underwent such dramatic changes as those in the HDLEC.

Another intriguing difference between the mouse and human LEC was the recovery of expression of LYVE-1 by mouse LEC that was observed even in the presence of TNFα. Experiments described in chapter 4 showed that stimulation of HDLEC with IL-6 induced a marginal increase in LYVE-1 surface expression and as the microarray analyses carried out in this chapter indicate that IL-6 mRNA is up-regulated following TNFα stimulation, one could speculate that this may be a mechanism whereby the cells recover LYVE-1 expression spontaneously. Experiments detailed in this chapter have shown that IL-6

induces an increase in LYVE-1 surface expression and TNFα is known to up-regulate IL-6, which subsequently suppresses TNFα production (Akira and Kishimoto, 1992). However why the HDLEC fail to up-regulate IL-6 mRNA in response to TNFα and spontaneously recover LYVE-1 expression is unknown.

The down-regulation of LYVE-1 in mouse lymphatic endothelial cells has been shown in this chapter and experiments on a mouse model of inflammation in the following chapter were devised to ascertain whether this also occurs *in vivo*. These subsequent experiments also sought to address the possible physiological role for LYVE-1.

5.3.7 Conclusion

The experiments described in this chapter provide the first direct evidence to suggest that lymphatic endothelial cells play an active role in inflammation. Much of the data described in this chapter has illustrated that lymphatic vessel endothelium behaves in a similar manner to that of blood endothelium during inflammation, despite the fact that lymphatic vessels experience reverse transmigration, with leukocytes crossing from the abluminal rather than luminal surface. Thus these two distinct circulatory systems share parts of the same address code for specific vascular targeting.

CHAPTER 6

The Effects of Inflammation on Lymphatic Endothelium in Whole Tissue

6.1 Introduction.....292
6.2 Results.....295
6.3 Discussion.....323

6.1 Introduction

6.1.1 The effects of TNF in the skin

The skin, or integumentary system represents the boundary between an organism and its environment, and thus it must play a vital role in protecting the body from mechanical injury, water loss and the entry of harmful agents. Langerhans cells (LC) are dendritic cells found within the basal and suprabasal layers of the epidermis. These highly specialised antigen-presenting cells (APCs) constitute the first line of immune defence. These cells aggregate to form a continuous network and may ingest intruding microbes and other environmental components. Such complex antigens are loaded onto MHC class II molecules within the cell for presentation at the cell surface to T cells within a regional lymph node. Thus LC are responsible for initiating systemic immune responses and all migratory events of these cells must be tightly regulated, from the initial recruitment of their precursors from the circulation to their mobilisation via the lymphatics to regional lymph nodes.

LC are retained within the epidermis by E-cadherin-mediated homophilic attachments with keratinocytes (Jakob et al., 1999). Transforming growth factor-β (TGF-β) is also believed to play a role in retaining LC by up-regulating E-cadherin on these cells and blocking TNFα-induced up-regulation of CCR7, which is critical in the migration of LC to the lymphatics (reviewed by Jakob et al., 2001).

The well-characterised murine contact hypersensitivity (CHS) model has been used extensively to study the migration of antigen-presenting cells from the skin in response to antigenic challenge. In this model (detailed in chapter 1), a skin sensitising agent is applied to an area of mouse skin and is captured by LC or

dermal DC, which migrate to lymph nodes (Cumberbatch et al., 2002) and elicit hapten-specific T cell activation (Nakae et al., 2002). Once the mouse has been sensitised and memory T cells are resident throughout the body, a challenge by cutaneous application of the same antigen, typically to the ear, results in local inflammation and oedema. The sensitisation phase of CHS has been extensively studied to determine the molecular mechanism whereby LC are mobilised. Topical application of skin sensitising agents induces an increase in the expression of MHC class II molecules on LC and a decrease in LC density in the epidermis (Aiba and Katz, 1990). mRNAs of TNFα and IL-1 are rapidly up-regulated within minutes of application (Enk and Katz, 1992) and blocking of these pro-inflammatory cytokines with neutralising antibodies can prevent the induction of contact hypersensitivity (Cumberbatch and Kimber, 1992). IL-1 and TNFα down-regulate E-cadherin mRNA, leading to a reduction in E-cadherin surface expression and loss of cellular adhesion between LC and keratinocytes (Jakob and Udey, 1998). The maturing LC leave the epidermis and then must migrate through the extracellular matrix of the dermis towards the lymphatics.

Proteolytic enzymes such as the matrix metalloproteinases (MMPs) are believed to play a role in LC and dendritic cell (DC) migration through the extracellular matrix. For example MMP-9 has been detected in LC *in situ* under conditions that induce LC migration and emigration of LC from tissue explants may be blocked by MMP inhibitors (reviewed by Jakob et al., 2001). Also chemokines and their receptors play critical roles in migration. Expression of chemokine receptors on DC and LC alters as these cells mature and migrate. Maturing DCs up-regulate receptors for constitutively expressed chemokines such as CCR7, which permits chemoattraction towards lymphatic endothelium, which expressed the ligand for this receptor, SLC. CCR7 has recently been shown to play a vital role in both constitutive DC migration and in increased trafficking which occurs in inflammation (Ohl et al., 2004).

Immature DCs express a number of chemokines receptors such as CCR1, CCR2, CCR5 and CXCR1 for the inducible chemokines RANTES (CCL5), MIP-1α (CCL3), MCP-3 (CCL7) and IL-8 (CXCL8). Upon inflammation and activation of DCs, these receptors are down-regulated to permit the cells to leave the inflammatory site which has the highest chemokine concentration (von Andrian and Mackay). Inflammation also stimulates recruitment of additional monocytes from the blood, which differentiate into dendritic cells and contribute to the increased trafficking of antigen presenting cells from the dermis to the lymph node (Randolph et al., 1998).

Once the DCs have migrated through the extracellular matrix, they must gain entry to the lymphatic capillary and traffick through the lymphatics to the regional lymph node. However, the roles that the lymphatic endothelium play in migration of DCs, both constitutive and in inflammation, have yet to be identified. The *in vitro* studies detailed in chapters 4 and 5 of this thesis document a change in transcription and protein profiles in LEC specifically in response to pro-inflammatory conditions. One interpretation of this "re-programming" is that lymphatic endothelium is required to perform vital functions in the onset of inflammation, including attracting leukocytes from the tissues by the secretion of chemokines, tethering them at the surface through the newly expressed adhesion molecules and then allowing transmigration by remodeling of cell-cell junctions. To substantiate this hypothesis, experiments detailed in this chapter sought to confirm whether or not these changes were also observed within intact lymphatic vessels *in vivo* and are concurrent with the massive up-regulation of trafficking which occurs in inflammation.

6.2 Results

6.2.1 Cultured mouse ear tissue

Experiments detailed in the previous two chapters had shown LYVE-1 down-modulation by TNFα in three human primary lymphatic endothelial cell lines and two primary mouse cell lines. Similar studies also showed up-regulation of ICAM-1 in both mouse and human LEC. To investigate the responsiveness of lymphatic endothelium to this pro-inflammatory cytokine within intact tissue, mouse ear explants were used and lymphatic endothelium surveyed for LYVE-1 and ICAM-1 expression by whole mount tissue staining.

Ear explants were cultured in either medium alone (described in chapter 2) or supplemented with recombinant mouse TNFα, 100ng/ml. Whole mount tissue samples were then prepared, staining for LYVE-1 or ICAM-1.

The images captured of whole mount sections show the branched network of blind-ended lymphatic vessels spread throughout the tissue. Strong staining of these LYVE-1-positive vessels was observed in tissue cultured in medium alone. However a clear reduction in expression of LYVE-1 was observed following culturing of explanted tissue in the presence of TNFα. Representative fields of view are shown in figure 6.1.

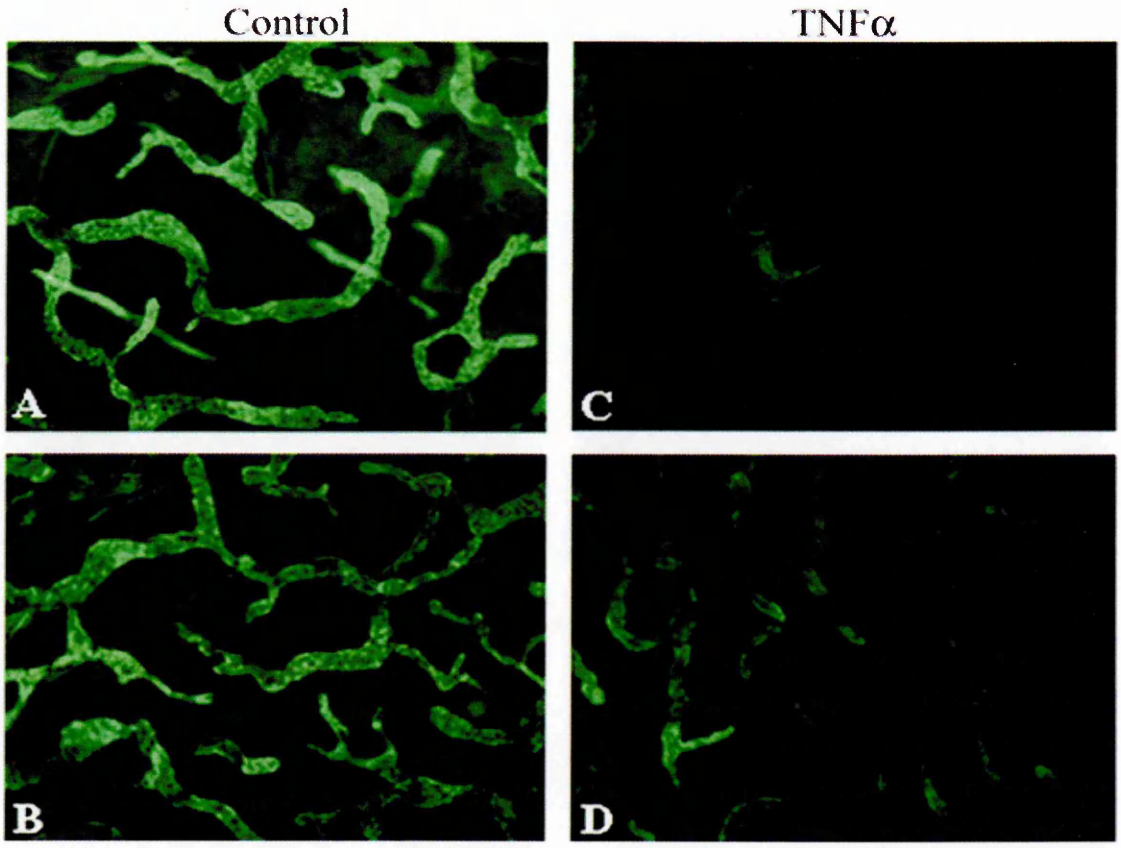

Figure 6.1 Effect of TNFα on LYVE-1 expression in intact dermal lymphatic vessels. Mouse dermal explants were cultured for 24h in either medium alone (panels A and B) or in medium supplemented with TNF, 100ng/ml (C and D), prior to whole mount staining using the LYVE-1 mAb C1/8 and goat anti-rat AlexaFluor®488. The fluorescence microscope images shown in panels A and C were captured at the same exposure and gain settings, as were B and D, at magnification: X 100.

To quantitate the reduction in expression of LYVE-1, 10 LYVE-1-stained images of control and TNFα-treated tissue were captured and converted to grey scale to measure the mean fluorescence of each image by OpenLab software, subtracting the background staining from each image captured. The Mann-Whitney statistical test was performed on data sets from each pair of ears, to compare the difference between the two means. This test was chosen as it makes no assumptions that the data is normally distributed, unlike a two-sample t-test. The results of analyses show that the majority of pairs demonstrate a statistically significant difference at the 0.1% level (figure 6.2). However, it should be noted that there was considerable variation between individual ear preparations in the expression of LYVE-1, efficiency of staining and responsiveness to TNFα, even when manipulations were performed in parallel. In some cases TNFα-treatment resulted in a reduction in LYVE-1 expression which was only significant at the 10% level. In addition, the level of LYVE-1 expression varied between samples of untreated tissues and even within different areas of the same ear, as has been observed before in both cultured cells and in tissue samples. This variation is most probably due to the preparation of ear tissue to expose the dermis, which itself acts as a stimulus to induce migration of Langerhans cells from the epidermis through up-regulating the production of endogenous pro-inflammatory cytokines. Nevertheless, stimulation with TNFα induced a significant reduction in LYVE-1 expression on the intact lymphatic vessels within cultured mouse ear tissue.

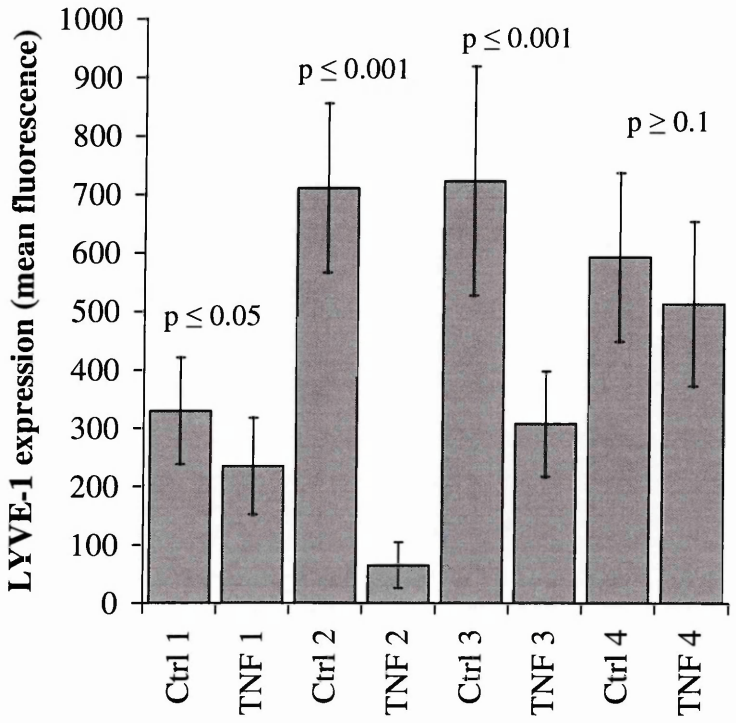

Figure 6.2 Quantitation of LYVE-1 down-regulation in intact lymphatic vessels. Mouse ear tissue was cultured for 24h in either medium alone or in media supplemented with TNFα, (100ng/ml), prior to whole mount staining using the LYVE-1 mAb C1/8 and goat anti-rat AlexaFluor®488. 10 images were captured of each ear section by fluorescence microscopy and the mean fluorescence of each field of view measured by Open Lab software. Representative pairs of data are shown on the graph, ± standard error. The Mann-Whitney test was performed to assess the statistic significance between each pair of data.

Parellel whole mount staining of the same dermal explants to detect ICAM-1 expression showed clear up-regulation of ICAM-1 throughout the tissue following TNFα-treatment (figure 6.3). However many of these structures were much thinner than lymphatic vessels and likely to represent inflamed blood vessel endothelium which characteristically shows an increase in ICAM-1 expression upon stimulation with TNFα (Springer, 1990). Initial attempts to measure ICAM-1 up-regulation on lymphatic endothelium by double-staining whole mount tissue with ICAM-1 and the lymphatic marker podoplanin were unsuccessful as the antibodies require short (3h) and long (48h) fixation times respectively and therefore could not be used in the same staining procedure. Also anti-CD34 antibody (to distinguish blood vessels) proved unsuitable for use on these tissue sections, probably due to the inability of the antibody to recognise paraformalehyde-fixed antigen.

To quantitate ICAM-1 expression in ear tissue cultured in either the presence or absence of TNFα, 10 images in grey-scale were captured of each ear section stained and the mean fluorescence of each image measured by OpenLab software, as had been performed for the quantitation of LYVE-1 expression. The results (figure 6.4) show that the mean fluorescence from ICAM-1 staining was higher in TNFα-stimulated tissue. However, the large variations in intensity of staining in untreated tissue meant that the differences in expression were only statistically significant at the 5% level. Also any increase in expression cannot be attributed to that on lymphatic endothelium alone.

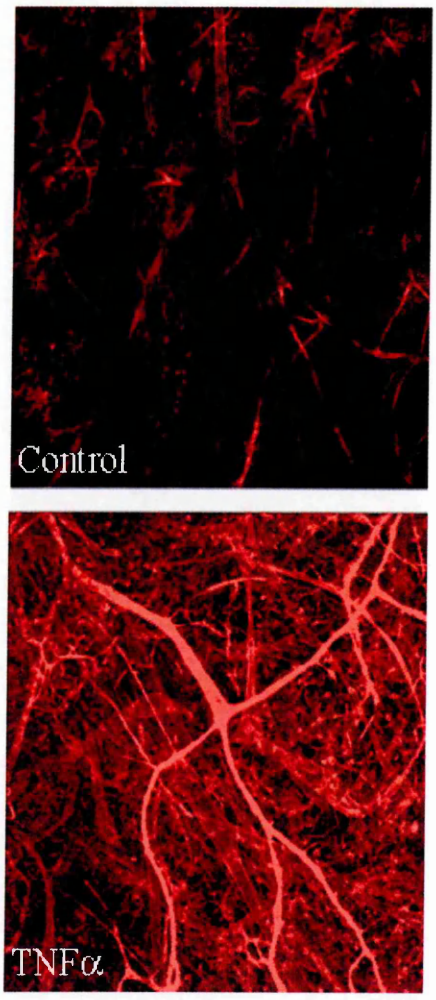

Figure 6.3 Effect of TNFα on ICAM-1 expression in mouse dermal explants. Tissue was cultured for 24h in either medium alone or in media supplemented with TNFα, (100ng/ml), prior to whole mount staining using the goat anti-ICAM-1 (R and D Systems) and donkey anti-goat AlexaFluor®568. Images were captured by fluorescence microscope, at magnification: X 100.

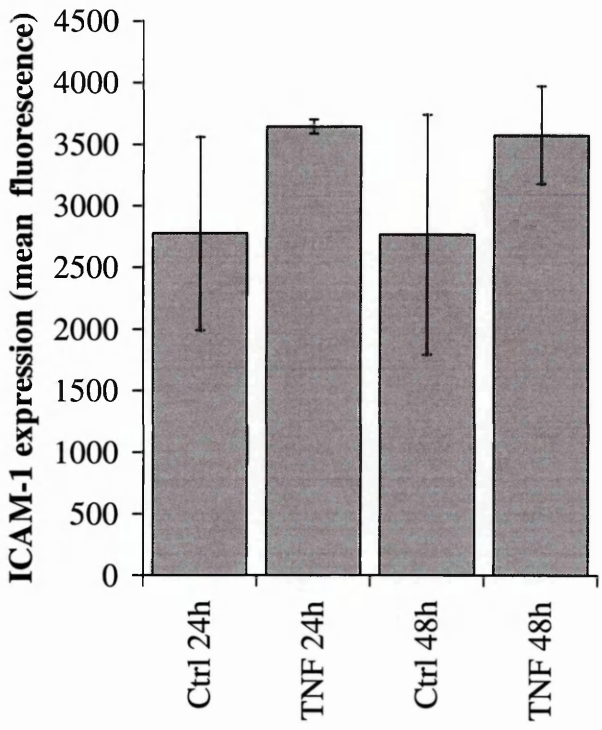

Figure 6.4 Quantitation of ICAM-1 up-regulation in mouse dermis. Mouse ear tissue was cultured for 24h in either medium alone or in media supplemented with TNFα, (100ng/ml), prior to whole mount staining with goat anti-mouse ICAM-1 and an AlexaFluor®568 donkey anti-goat conjugate. 10 images were captured of each ear section by fluorescence microscopy and the mean fluorescence of each field of view measured by Open Lab software. Representative pairs of data are shown on the bar chart, ± standard error. The Mann-Whitney test was performed to assess the statistic significance between each pair of data.

6.2.2 TNFα-mediated contact hypersensitivity in mice

The well-characterised model of oxazolone-induced contact hypersensitivity (CHS) was used to study acute inflammation in mice. It held the advantage over the use of explant tissue culture of being a more physiological setting for inflammation, with endogenously produced pro-inflammatory cytokines eliciting the reaction. The model is described in more depth in the introduction to this chapter and in chapter 1. The whole animal studies permitted tracking of leukocyte migration in relation to any changes in lymphatic vessel receptor expression during the elicitation phase, where the sensitised animal is challenged with the same antigen.

6.2.2.1 Expression of LYVE-1 following challenge

To assess whether LYVE-1 is down-modulated in TNFα-mediated inflammation within mouse dermis, male Balb/c mice were sensitised by application of oxazolone to their shaved abdomens. Five days later the left ear of each mouse was challenged by painting oxazolone on to the dorsal surface, whilst 95% ethanol carrier alone was applied to the right ears as a mock-treated control. The mice were sacrificed 24h post-challenge and the increase in ear mass due to oedema was used as a parameter for the extent of inflammation (figure 6.5). Oxazolone treatment was found to induce a mean gain in mass of mouse ear tissue of 2.28 x fold, in comparison to the mass of the contra lateral mock-treated ear (± 0.41). Whole-mount tissue sections were prepared of the dorsal and ventral aspects. Double-immunofluorescence staining for LYVE-1 and podoplanin (figure 6.6) showed that LYVE-1 is indeed down-regulated relative to the more stably expressed podoplanin-marker.

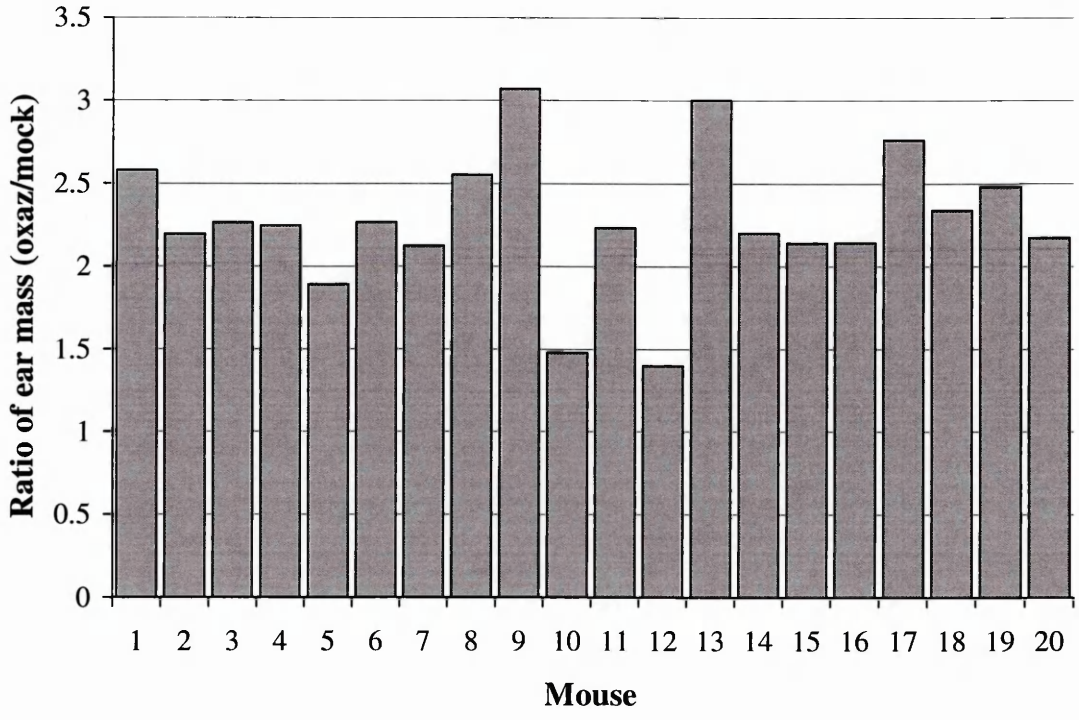

Figure 6.5 Increased ear mass elicited by oxazolone in CHS reactions in mice. Oxazolone-sensitised male balb/c mice were challenged with the agent on one ear and with ethanol alone to the contra-lateral as a mock-treated control. 24h following challenge, mice were sacrificed and ears removed and weighed. Ratios of ear masses (oxazolone-treated / mock-treated) of 20 mice are shown in the graph above.

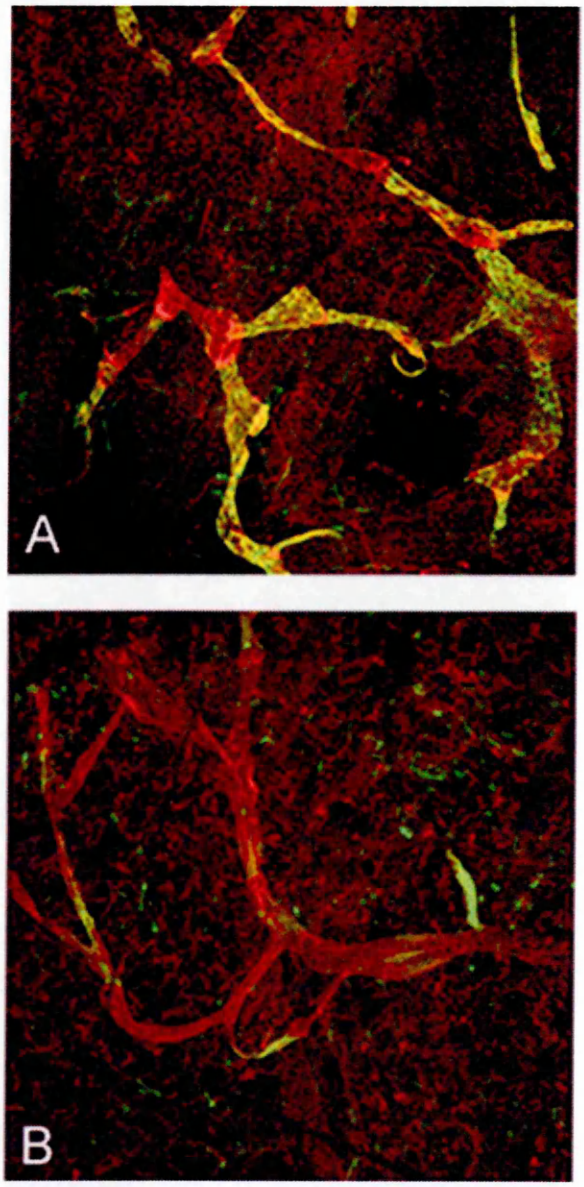

Figure 6.6 Down-modulation of LYVE-1 in mouse dermis following CHS. Ears from a sensitised mouse were painted with either ethanol alone (panel A) or with oxazolone in ethanol (panel B). 24h following the challenge, whole mount dermal tissue sections were prepared and stained for LYVE-1 using C1/8 and polyclonal antibodies to podoplanin. AlexaFluor® conjugates 488 (green) and 594 (red) were used respectively. Images were captured at 100X by confocal microscopy.

LYVE-1 expression before and after oxazolone treatment was quantitated using the same procedure as for the explant studies. A statistically significant decrease in LYVE-1 expression was measured in most ears from mice sacrificed 24h following oxazolone challenge (figure 6.7, upper panel). Interestingly, ventral aspects of mouse ear tissue showed less significant difference in LYVE-1 expression and in some cases no difference at all. One possible explanation for this is because oxazolone was applied to the dorsal aspect of the ear and thus the ventral side would not receive such high levels of stimulation.

Although LYVE-1-negative lymphatic vessels were observed in tissue prepared from mice sacrificed 12h post challenge, the difference in expression was not statistically significant., (figure 6.7, lower panel).

6.2.2.2 Kinetics of LYVE-1 down-regulation in inflamed dermal tissue

To investigate the kinetics of LYVE-1 down-regulation during the early stages of the elicitation phase of oxazolone induced CHS, frozen sections of ears were prepared from sensitised mice which had been sacrificed 3h, 6h, 12h, 18h and 24h following challenge. As before, the increase in ear mass was used as a parameter for the extent of inflammation over this time course (figure 6.8). Double-immunofluorescence staining for podoplanin and LYVE-1 was performed on each tissue section (figure 6.9) and the number of podoplanin-positive vessels expressing LYVE-1 recorded (table 6.1). Although lymphatic vessels expressing depressed levels of LYVE-1 could be observed, in the mock challenged ear as well as at 3h following elicitation, such vessels were rare, accounting for approximately less than 5% of podoplanin-positive vessels observed. At 12h LYVE-1-negative vessels became more frequently observed, accounting for 71% of the vessels examined and by 18h and 24h, only 30% of lymphatic vessels had retained LYVE-1 expression.

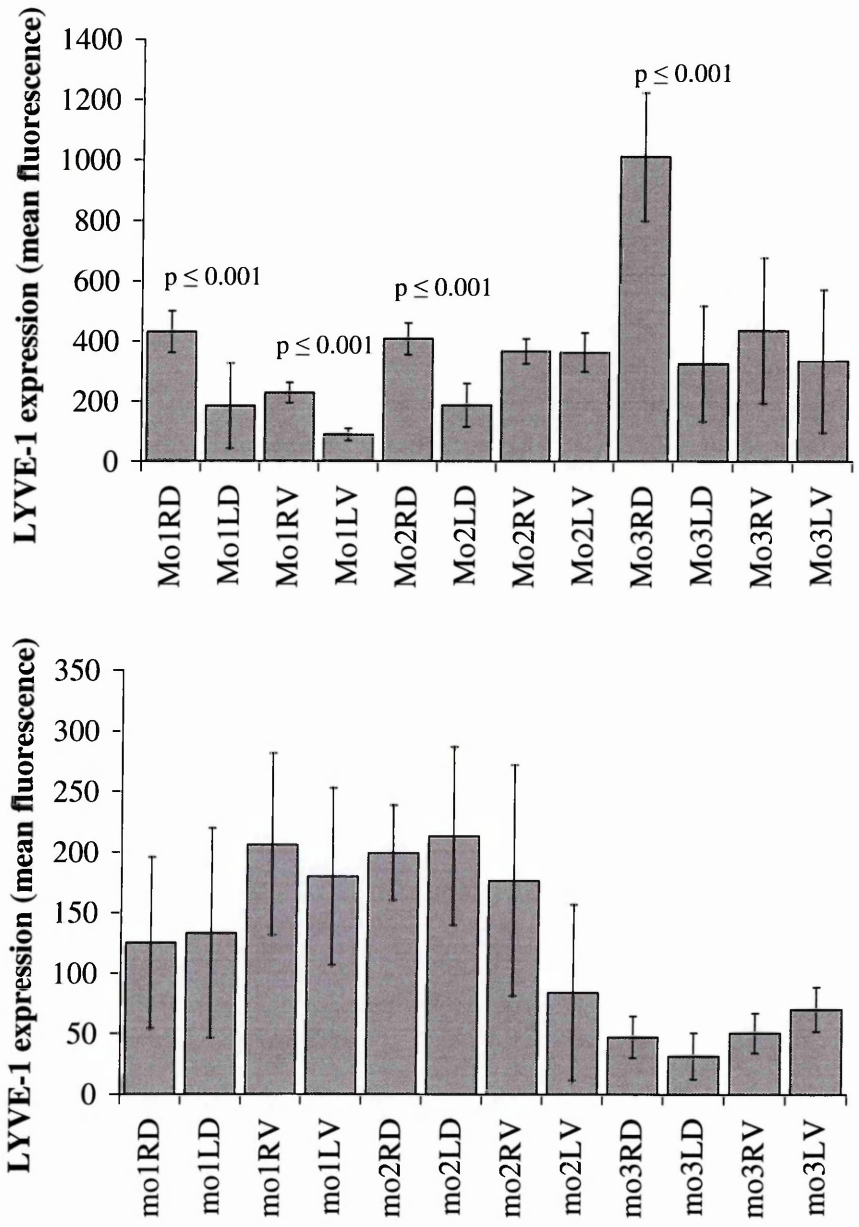

Figure 6.7 Quantitation of LYVE-1 expression detected by immunofluorescence microscopy of whole mount mouse ear sections. Ears from sensitised mice were painted with either ethanol alone or with oxazolone in ethanol and then sacrificed either 12h (lower graph) or 24h (upper graph) following the challenge. Whole-mount dermal tissue sections were prepared of the dorsal (D) and ventral (V) aspects and stained for LYVE-1 using C1/8 and goat anti-rat AlexaFluor®488. Fluorescence was quantitated by Open Lab software, capturing 10 images of each ear at x 100 magnification, both left (L, challenged) and right (R, unchallenged). Exposure and gain settings of the camera were unaltered between collecting data of each pair. Background fluorescence was subtracted from each image prior to quantitation.

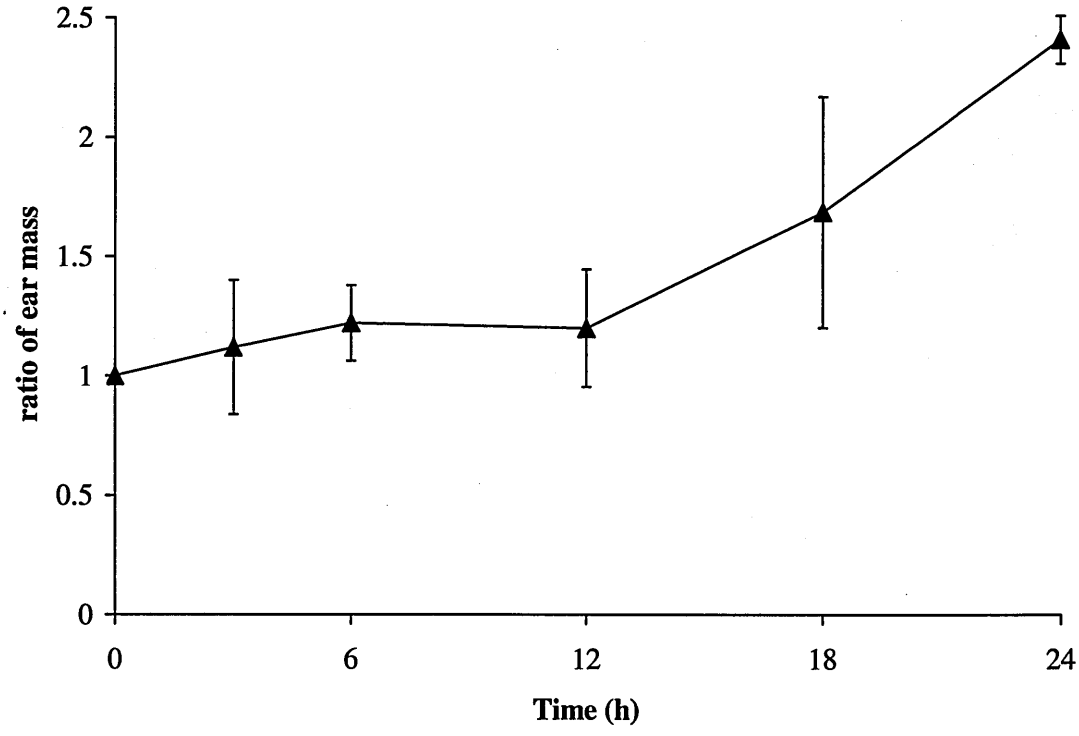

Figure 6.8 Kinetics of the increase in ear mass elicited by oxazolone in CHS reactions in mice. Oxazolone-sensitised male balb/c mice were challenged with the agent on one ear and with ethanol alone to the other as a mock-treated control. 3-24h following challenge, mice were sacrificed in triplicate at each time point and ears removed and weighed. Ratios of unchallenged ear mass to challenged ear mass were calculated and are plotted ± standard error.

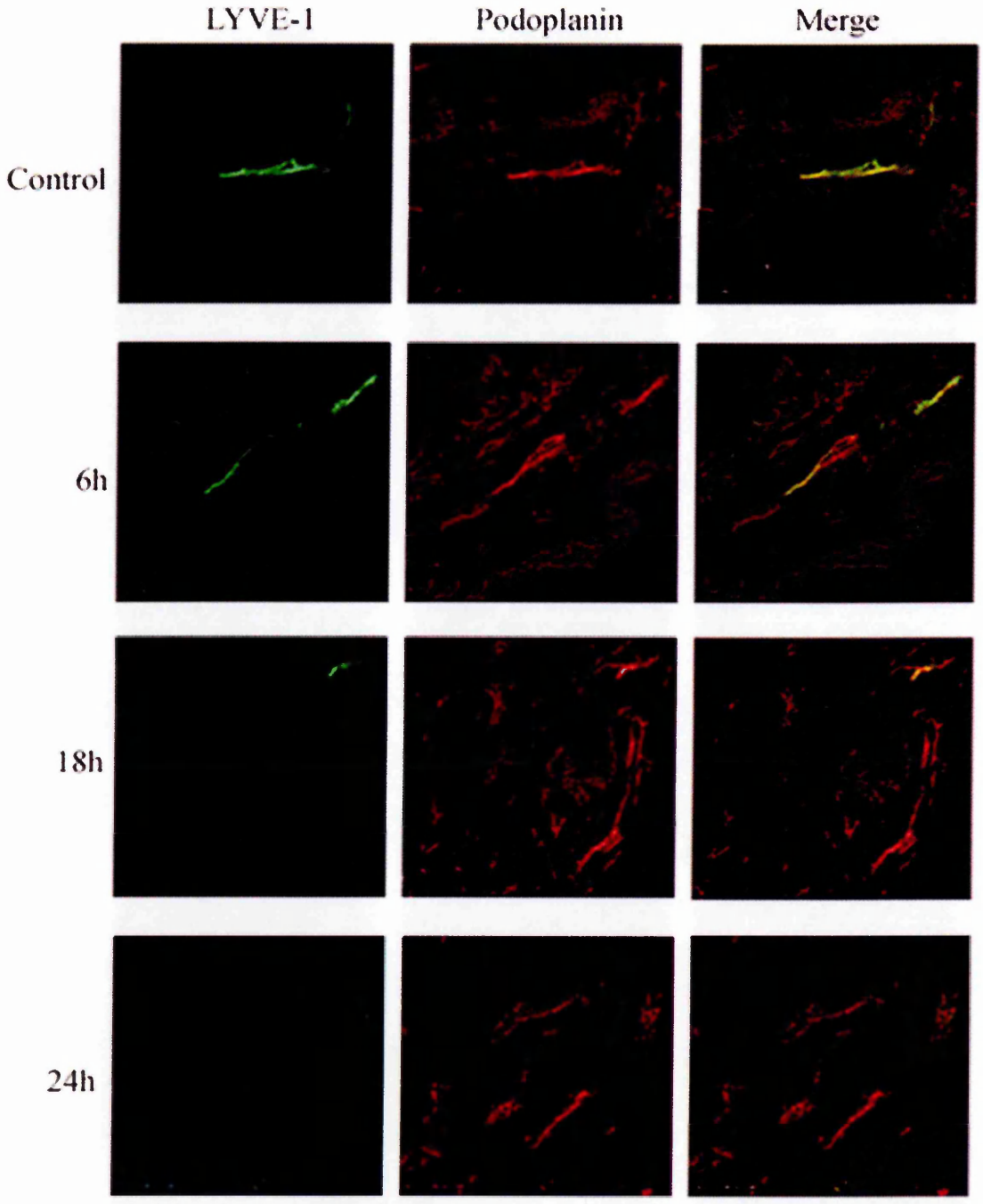

Figure 6.9 Time course to follow the down-modulation of LYVE-1 on mouse ears in the elicitation of DCH. Frozen sections of ears from unchallenged mouse ear (control) and from mice sacrificed at 6h, 18h and 24h post-oxazolone challenge were stained for LYVE-1 (green) and podoplanin (red) with the appropriate AlexaFluor® conjugates. Images were captured at 600X magnification by confocal microscopy.

Time (h)	Number of podoplanin-positive vessels	Number of LYVE-1-positive vessels	Percentage of LYVE-1-positive vessels (%)
0	24	23	96
3	23	22	96
6	23	22	96
12	24	17	71
18	25	8	32
24	26	8	31

Table 6.1 Quantitation of the percentage of LYVE-1 positive lymphatic vessels in mouse dermis following elicitation of inflammation by CHS. The numbers of podoplanin-positive vessels visible in 8μm frozen sections were counted and expression of LYVE-1 by these vessels was recorded and expressed as a percentage of the number of podoplanin-lymphatic vessels.

6.2.2.3 Expression of leukocyte adhesion molecules by dermal lymphatic vessel endothelia following oxazolone challenge

To follow the expression of the adhesion molecules VCAM-1 and ICAM-1 in DCH, frozen sections prepared at 3h, 6h, 12h, 18h and 24h post-challenge were double stained for podoplanin and either VCAM-1 or ICAM-1 (figures 6.10 and 6.11) and the number of podoplanin-positive vessels expressing these proteins recorded (tables 6.2). The results show that expression of neither receptor was evident on lymphatic vessels in untreated tissues but 3h following the elicitation of inflammation, a minority of vessels (5-10%) was found to be positive for these molecules. By 18h, approximately 50% of the lymphatic vessels observed expressed these receptors, concurrent with the down-regulation of LYVE-1 (figure 6.9 and table 6.1). Many of these vessels had adopted an unusual morphology: instead of the characteristic collapsed lumen apparent in uninflamed tissue, the lumens of many vessels (for example, in figure 6.11 at the 18h time point) appeared distended. This was most probably due to the increased interstitial pressure induced by the oedema associated with the elicitation phase of CHS. The increased interstitial pressure stretches the collagen and elastin fibres which anchor lymphatic endothelium in the tissues and expands the lumen of the vessel, opening intercellular junctions between overlapping endothelial cells to allowing passage of fluid and macromolecules into the vessel.

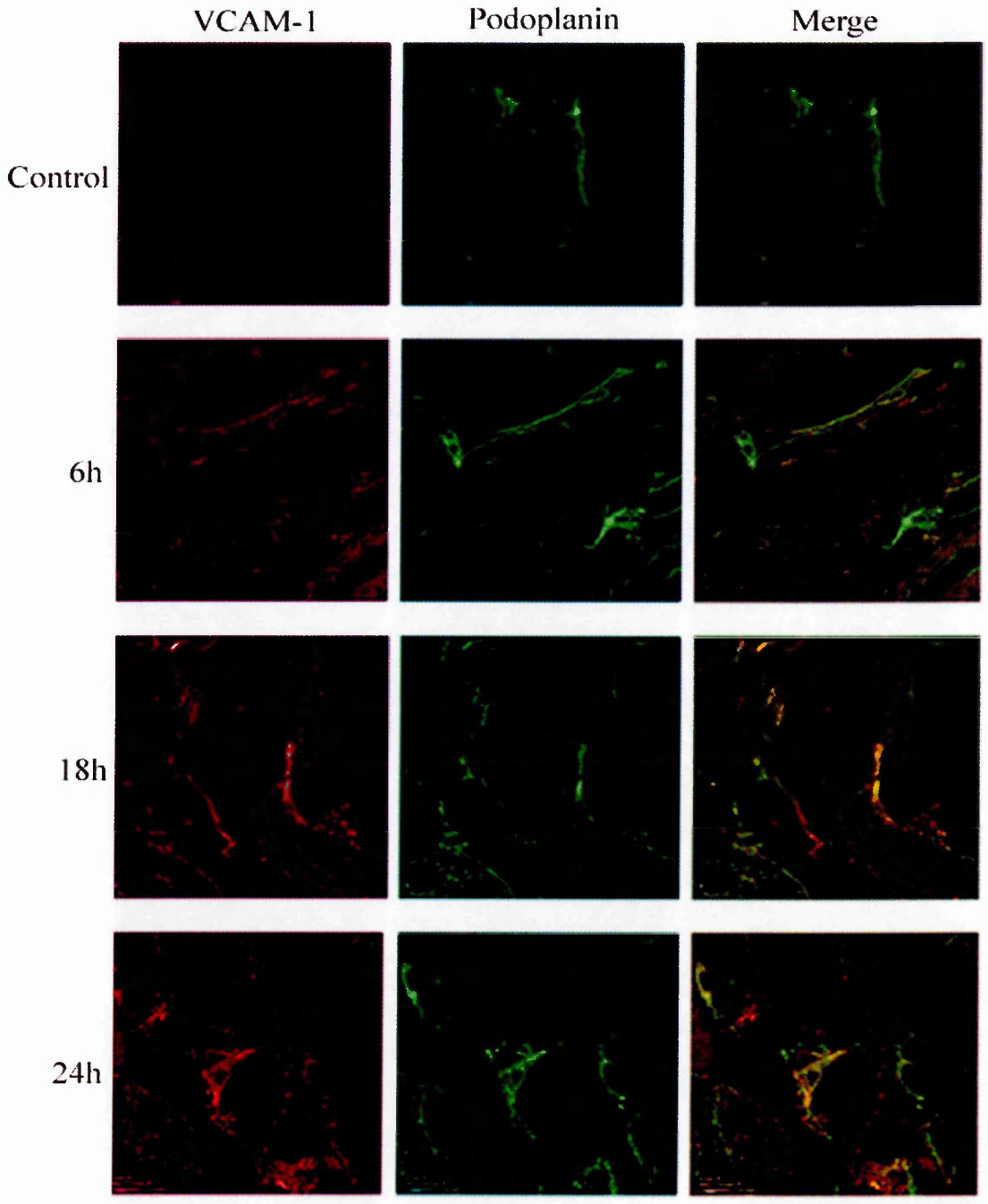

Figure 6.10 Time-course of VCAM-1 expression on mouse dermal lymphatics in the elicitation of CHS. Frozen sections of ears from unchallenged mouse ear (control) and from mice sacrificed at 6h, 18h and 24h post-oxazolone challenge were stained for VCAM-1 (red) and podoplanin (green), with the appropriate AlexaFluor® conjugates. Images were captured at 600X magnification by confocal microscopy.

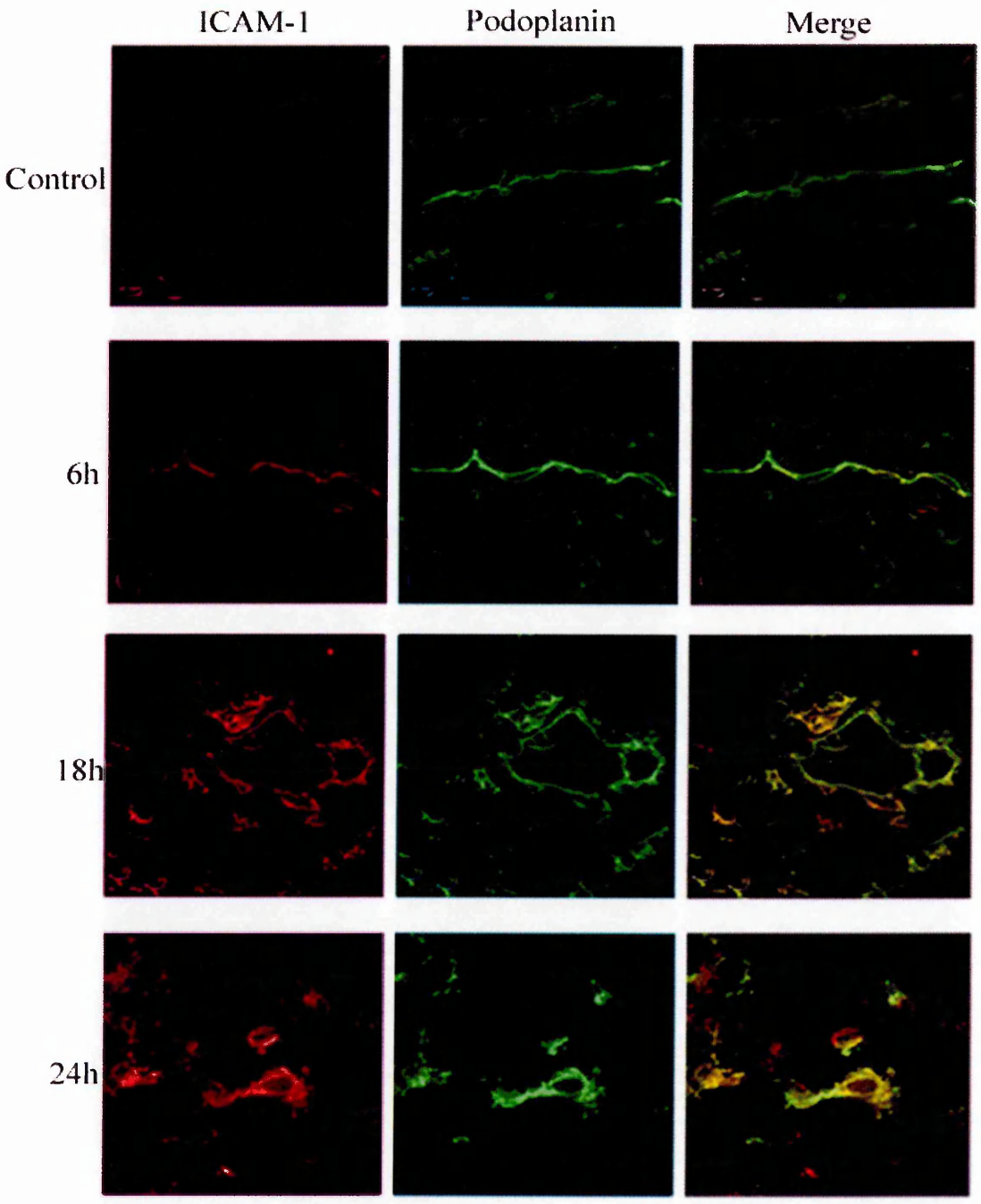

Figure 6.11 Time course of ICAM-1 expression on mouse dermal lymphatics in the elicitation of CHS. Frozen sections of ears from unchallenged mouse ear (control) and from mice sacrificed at 6h, 18h and 24h post-oxazolone challenge were stained for ICAM-1 (red) and podoplanin (green), with the appropriate AlexaFluor® conjugates. Images were captured at 600X magnification by confocal microscopy.

Time (h)	Number of podoplanin-positive vessels	Number of VCAM-1-positive vessels	Percentage of VCAM-1-positive vessels (%)	Number of podoplanin-positive vessels	Number of ICAM-1-positive vessels	Percentage of ICAM-1-positive vessels (%)
0	19	0	0	20	0	0
3	24	2	8	21	1	5
6	31	4	13	32	6	19
12	24	4	17	24	4	17
18	24	12	50	23	11	48
24	23	12	52	20	14	70

Table 6.2 Quantitation of the percentage of VCAM-1- and ICAM-1-positive lymphatic vessels in mouse dermis following elicitation of inflammation by CHS. The numbers of podoplanin-positive vessels visible in 8μm frozen sections were counted from 7 fields of view and expression of the leukocyte adhesion molecules by these vessels was recorded and expressed as a percentage of the number of podoplanin-lymphatic vessels.

6.2.2.4 Effects of inflammation on dermal leukocyte trafficking

The up-regulation of VCAM-1 and ICAM-1 in inflamed lymphatic endothelium, coupled with the decreased expression of LYVE-1 is likely to have implications for the trafficking of leukocytes such as antigen presenting cells (APCs) *en route* from the dermis to the lymph nodes. To test the hypothesis that APC trafficking occurs concurrently with the changes in expression of these receptors, frozen sections of mouse ear from the same time points following elicitation of the CHS response were again analysed by immunofluorescence, using MHC class II as a marker for DCs, monocytes and macrophages. The MHC class II-positive cells were closely associated with the lymphatic endothelium, and most likely in the process of reverse transmigration. These vessels frequently exhibited a distended lumen, suggestive of high interstitial pressure and inflammation as described earlier. This apparent reverse transmigration was observed at 18h and 24h following stimulation, time points at which double-immunofluorescence staining detailed in figures 6.10 and 6.11 had shown the up-regulation of VCAM-1 and ICAM-1 and down-modulation of LYVE-1 (figure 6.9). Thus it is likely that the change in expression of surface molecules is a necessary pre-requisite for the increase in DC trafficking which occurs in inflammation. Some transmigration of MHC class II positive cells occurred at earlier time points, for example 3h following elicitation of inflammation (figure 6.12). These may represent constitutive trafficking events as it is known that DC circulate from the dermis to the lymph nodes even in the absence of inflammatory stimuli, as described in the general introduction (chapter 1), by a mechanism which may not require high expression of adhesion molecules such as ICAM-1 and VCAM-1.

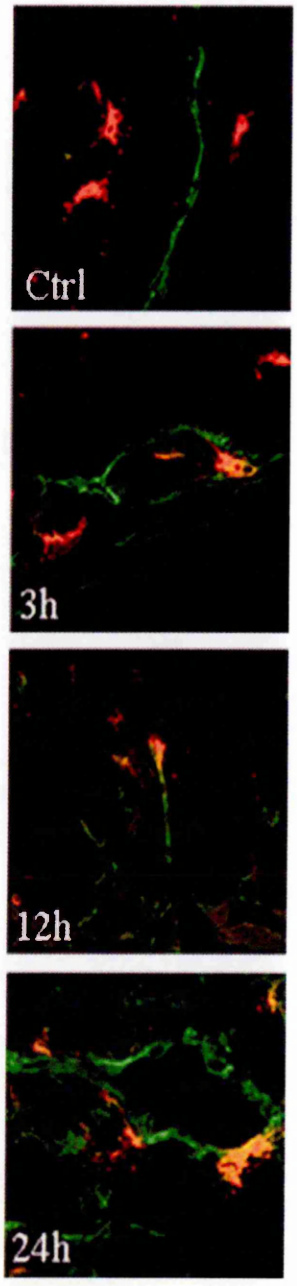

Figure 6.12 Reverse transmigration of MHC class II-positive APCs into the lymphatics over a 24h period following elicitation of DCH in mouse ear. Frozen sections were prepared from unchallenged tissue (Ctrl) and challenged tissue harvested at 3h, 12h, and 24h post-challenge, then stained for podoplanin (green) and MHC class II (red) using the appropriate secondary conjugates. Images were captured by confocal microscopy at 600X magnification.

To gain a three-dimensional perspective of MHC class II-positive cells during reverse transmigration, whole mount staining was performed using this marker in combination with either LYVE-1 or podoplanin antibodies (figure 6.13). In the unstimulated dermis, these APCs appear randomly dispersed between the large branched lymphatic vessels and probably constitute immature DCs and LCs resident in the tissue (figure 6.13 panel A). Following elicitation of inflammation, extensive infiltration of the tissue by inflammatory cells was observed, which can be seen surrounding podoplanin-negative dermal capillaries (figure 6.13 panel B). These are likely to constitute newly recruited monocytes transmigrating from the blood circulation, which subsequently differentiate into DCs and migrate into the lymphatics or will remain in the tissue as macrophages (Randolph et al., 1998). In inflamed dermis, MHC class II-positive cells could be seen surrounding podoplanin-positive lymphatic endothelium, probably prior to reverse transmigration. The majority of the vessels in contact with these putative APCs commonly had a loop-like structure (figure 6.13 panel D), typical of lymphatics in association with sweat glands (Prof. Francesco Pezzella, personal communication). Such regions of the dermis might be expected to receive higher doses of oxazolone, through entry via the sweat gland pore, which could explain why more trafficking events occurred across these looped lymphatic capillaries. Interestingly, the APCs observed also appeared to associate preferentially with LYVE-1-low lymphatic vessels rather than those vessels which retained higher expression (figure 6.13 panel C). Whether the down-regulation of LYVE-1 and the reverse transmigration of DCs are independent events or whether LYVE-1 down-regulation is a pre-requisite of DC migration remains to be determined.

Figure 6.13 Whole mount staining to illustrate the migration of APCs to lymphatic vessels. Tissue was stained with either rabbit anti-LYVE-1 and rat anti-MHC class II (panels A and C) or rabbit anti-podoplanin and rat anti-MHC class II (panels B and D). In naïve ear tissue (panel A and below), MHC II positive cells appear scattered throughout the tissue. 24h following challenge of sensitised tissue with oxazolone, MHCII positive cells are visible lining up alongside podoplanin-negative vessels (B) and migrating towards lymphatic vessels expressing LYVE-1 (C) and podoplanin (D). Images were captured by confocal microscopy at magnification x 100.

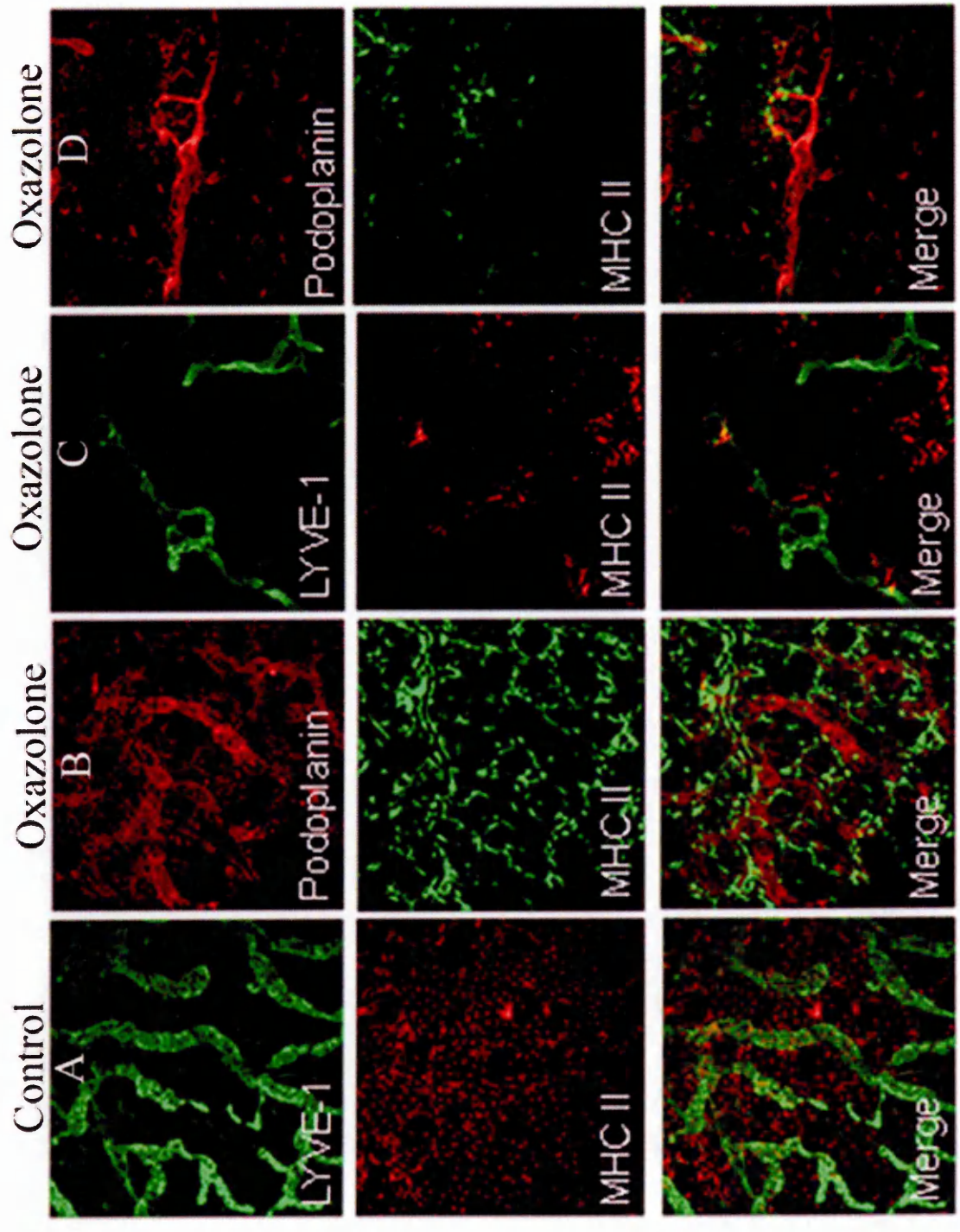
Control
Oxazolone
Oxazolone
Oxazolone
A
B
C
D
LYVE-1
Podoplanin
LYVE-1
Podoplanin
MHC II
MHC II
MHC II
MHC II
Merge
Merge
Merge
Merge

6.2.2.5 Effects of inflammation on dermal chemokines expression

The results in chapter 5 showed that the expression and secretion of inflammatory leukocyte chemokines including JE, a homologue of human MCP-1 (CCL2) were strongly up-regulated on TNFα-stimulated primary mouse LEC during *in vitro* culture. To investigate whether this is borne out in inflamed tissue, whole-mount tissue sections of oxazolone challenged mouse ear were prepared and stained for expression of JE, as well as SLC (CCL21), a chemokine reported to be constitutively expressed in lymphatic endothelium (Kriehuber et al., 2001), (figure 6.14). In unstimulated dermis, virtually no JE was detected. However, 24h following administration of oxazolone to a sensitised mouse, JE expression increased dramatically. Curiously, JE was not closely associated with lymphatic vessels but scattered throughout the tissue. However, as the sections were not double-stained for a lymphatic marker it is possible that some co-localisation occurs with the lymphatics but is not clearly visible due to the high concentration of chemokine secreted from other cells in the tissue. In addition, the possibility could not be excluded that the source of JE was indeed the inflamed lymphatic endothelium, but that the chemokine was secreted and bound to low-affinity sites (such as heparin sulphate proteoglycans) in the matrix.

Unlike JE, expression of SLC did not appear to increase in response to oxazolone, rather a slight decrease in staining intensity was observed, confirming the findings of Kriehuber et al. (2001) from *in vitro* studies and the results from the microarray analyses described in chapter 5 of this thesis. Also SLC appeared restricted to the lymphatic endothelium, in contrast to JE. Expression of SLC with LYVE-1 on lymphatic endothelium of normal mouse ear tissue is shown in figure 6.15. SLC does not co-localise with LYVE-1, which is expressed primarily at cell-cell junctions, as has been observed in confluent lymphatic endothelial

cells in culture (chapter 5). Instead, SLC occupies either an intracellular location or is displayed at the surface, bound to heparin sulphate proteoglycan.

Goat polyclonal antisera against RANTES and MCP-1 yielded no staining in either normal or inflamed mouse ear tissue (data not shown). This was probably due to the failure of these antibodies to recognise formaldehyde-fixed antigen, rather than a lack of expression of these chemokines, which are known to be expressed by a variety of cell types under inflammatory conditions, including keratinocytes and blood vascular endothelium. Therefore further experiments would be required to optimize conditions for staining, for example the length of paraformaldehyde fixation (which proved to be critical for podoplanin staining using the rabbit polyclonal antibody). Immunofluorescence staining of frozen sections with chemokines yielded images upon which it was impossible to distinguish background staining from expression dispersed throughout the tissue. Therefore the key chemoattractants of APCs for lymphatic capillaries remain to be identified but the close association of these cells with the lymphatic vessels is highly suggestive of reverse transmigration, which is likely to be promoted by chemokine secretion from lymphatic endothelial cells, as suggested from *in vitro* studies described in chapter 5.

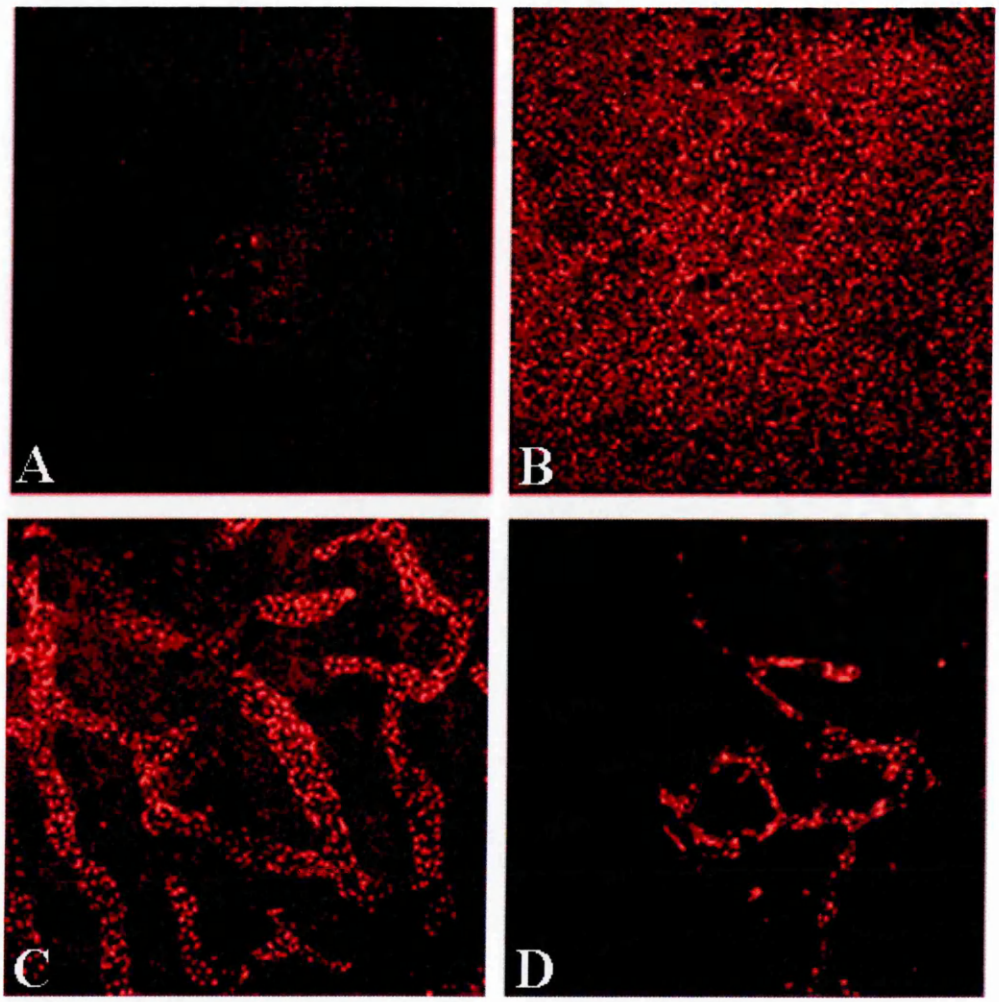

Figure 6.12 Whole mount staining of chemokines in inflamed dermis. Paired lateral and contra-lateral ears from mice which had either remained unchallenged (panels A and C) or had undergone challenge with oxazolone (panels B and D) were stained with either goat anti-JE (panels A and B) or goat anti-SLC (panels C and D), detecting with AlexaFluor®568 donkey anti-goat conjugate. Images were captured by confocal microscopy at X 100.

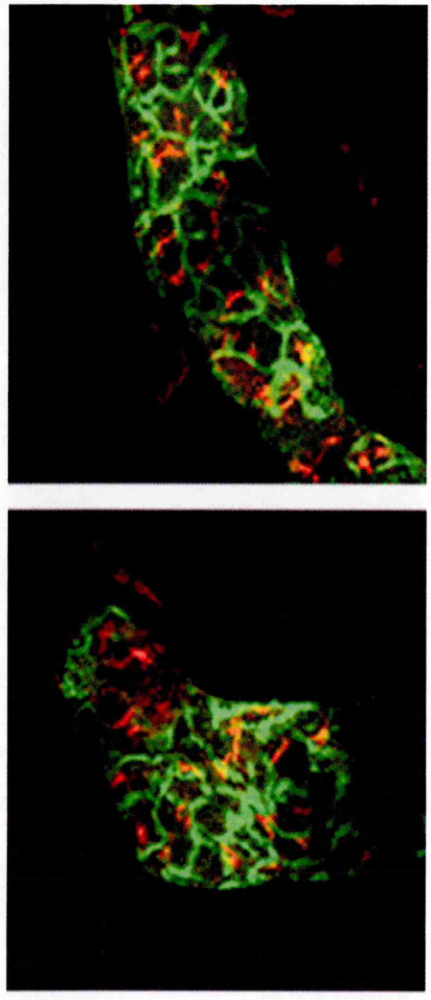

Figure 6.13 Expression of SLC by lymphatic endothelium in normal mouse ear. Tissue was stained using goat anti-SLC and the LYVE-1 mAb C1/8, detecting using the AlexaFluor® conjugates 568 (red) and 488 (green) raised in donkey. Images were captured by confocal microscopy at magnification X 600.

6.3 Discussion

6.3.1 Expression of adhesion receptors in inflammation

The findings in this chapter have confirmed that the down-modulation of LYVE-1 which was characterized *in vitro* in both human and mouse LEC (chapters 4 and 5) also occurs in intact lymphatic vessels. Mouse dermal explants cultured in the presence of TNFα showed a statistically significant lower expression of LYVE-1 than tissue cultured in media alone. Moreover, down-regulation of LYVE-1 was also observed and quantitated in oxazolone-induced delayed contact hypersensitivity, a well-characterised TNFα-mediated model of inflammation in the skin. Following 12h of elicitation of inflammation, over 50% of lymphatic vessels exhibited a loss of LYVE-1, concurrent with the up-regulation of the leukocyte adhesion molecules VCAM-1 and ICAM-1 on lymphatic vessels. This confirmed the results described in chapter 5, where induction of these receptors by TNFα and TNFβ was detected in cultured primary mouse and human LEC. An earlier study by McHale et al. (1999) had detected an increase in expression of ICAM-1 and VCAM-1 in endothelium during the elicitation phase of contact hypersensitivity in mice, mediated by TNFα. However the immunohistochemical studies carried out had not used either blood vascular or lymphatic endothelial markers and thus the identity of adhesion molecule-positive vessels could not be determined. Other studies had presented limited evidence for ICAM-1 and VCAM-1 expression in human and ovine lymph node sinuses (Sawa et al., 1999; Young et al., 2000) but these were not substantiated by co-localization with lymphatic vessel specific markers. Therefore the study described in this chapter is the first to convincingly demonstrate expression of VCAM-1 and ICAM-1 in tissue lymphatics and to show their up-regulation during inflammation.

In oxazolone-induced contact hypersensitivity in mice, the up-regulation of ICAM-1 and VCAM-1 were concurrent with the down-modulation of LYVE-1 and the massive increase in the number of APC trafficking events across lymphatic endothelium which occurs with the onset of inflammation. 12h following elicitation of inflammation, extravasation of newly recruited MHC class II-positive cells, most likely monocytes, from blood capillaries were observed. These differentiate in the dermis into either macrophages which stay resident in the peripheral tissue or DCs, which reverse transmigrate into the lymphatics to present their newly acquired antigen within the T cell-rich paracortical area of a regional lymph node (Randolph et al., 1998). Data presented both in this chapter and in chapter 5 suggest that the lymphatic endothelium plays an active role in the regulation of these trafficking events and up-regulation of the adhesion receptors ICAM-1 and VCAM-1 may be necessary to support the increased number of APC trafficking events of reverse migration into afferent lymphatic vessels which occur during inflammation.

6.3.2 The role of chemokines and their receptors in leukocyte trafficking into lymphatic endothelium

In recent studies by other workers, constitutive trafficking of DCs was reported to occur through a mechanism which involves (among other interactions yet to be elucidated) binding of SLC (CCL21) to its receptor CCR7 on the DC surface. (Ohl et al., 2004). A role for CCR8 in migration of monocyte-derived DC from the dermis to the lymph node under mild inflammatory conditions has also been suggested (Qu et al., 2004). However studies of knock-out mice which lack several genes encoding CCR7 ligands revealed a reduction in Langerhans cell recruitment to the lymph node and thus suggested that CCR8 does not replace a need for CCR7 ligands and the two receptors function at different points in a common pathway downstream of recruitment into the skin. Qu et al. (2004) also showed that CCR8 knock-out mice showed decreased accumulation of

phagocytic DC within the lymph node. They then went on to demonstrate that CCL1, the ligand of CCR8, was not expressed in LYVE-1-positive dermal lymphatic vessels. This is confirmed by data from the microarray analyses (detailed in chapter 5 of this thesis) which found that the transcript for CCL1 (TCA-3 in mouse, I-309 in human) was virtually absent in both the mouse and human LEC surveyed. However, Qu et al. (2004) detected CCL1 in the subcapsule of the lymph node and paracortical vessels that were thought to be HEVs and therefore the CCL1/CCR8 interaction may act down-stream of entry into the afferent lymphatics, perhaps in regulating entry in the subcapsular sinus of the regional lymph node. Whether another ligand for CCR8 is expressed on the endothelium of initial lymphatics to mediate reverse transmigration in addition to the CCL21/CCR7 interactions or whether CCR8 plays a role in the transition between human monocyte subsets and thus indirectly affects trafficking across the lymphatic endothelium remains to be determined.

Neither CCR2 nor CX_3CR1 (mediating inflammatory monocyte recruitment into tissue, reviewed by von Andrian and Mackay, 2000) were found to be essential for accumulation of Gr-$1^{intermediate}$ monocytic DC precursors in skin or lymph nodes under the mildly inflammatory conditions assessed (Qu et al., 2004). Whole mount staining shown in this chapter revealed that expression of JE/MCP-1 (CCL2), one of the ligands for CCR2, was dramatically induced in inflamed mouse dermis. However, although experiments in chapter 5 had shown this chemokine is up-regulated by TNFα on both mouse and human primary LEC, no clear association with any vessel-like structure could be observed *in vivo*. Instead expression was high throughout the tissue. Thus lymphatic endothelium may play a general role in inflammatory cell recruitment to the tissues and the chief role of MCP-1 secreted by lymphatic endothelium may be in recruiting monocytes from the blood circulation rather than in reverse transmigration into the lymphatics, as blood capillaries and initial lymphatics are

frequently juxtaposed within the dermis. In addition, the chemokines secreted by the lymphatic endothelium may exert a more distant effect. An earlier study by Palframan et al. (2001) had shown that MCP-1 underwent dramatic induction during inflammation in the skin and was transported through the afferent lymph to the lymph node cortex from where it was conveyed to the luminal surface of HEVs by reticular network fibres, triggering integrin-dependent arrest of rolling monocytes and thus enhanced recruitment to the lymph node. The researchers concluded that inflamed peripheral tissues could exert "remote control" over the composition of leukocyte populations homing to the draining lymph nodes through the projection of their local chemokine profile. Results from this chapter and chapter 5 suggest that afferent lymphatic endothelial cells may be the source of MCP-1 detected by Palframan et al. (2001) and possibly other additional chemokines. Thus the lymphatic endothelium may be involved in this one-way line of communication and not only influence leukocyte migration and fate in the vicinity but also at other more distant locations. It would be of interest to investigate whether LEC secrete chemokines into the surrounding extracellular matrix and or in the basolateral direction, for transport to the peripheral draining lymph node. Transwell™ assays could be employed to test this and determine which chemokines are secreted from which surface.

Expression of the constitutive lymphatic vessel chemokine SLC by oxazolone-induced inflammation in dermal vessels did not change significantly. Similarly, expression of SLC by LEC did not change significantly following stimulation with TNFα in the array analysis (chapter 5). Data from the human array revealed a very marginal increase (1.1 fold) in expression whereas the mouse transcipt showed a very marginal decrease (0.8 fold). This is in agreement with the work of Kriehuber et al. (2001), who found that SLC was expressed in an activation-independent manner by isolated primary LEC. However Sallusto et al. (1994) and Martin-Fontecha et al. (2003) reported an increase in SLC in inflammation

based on immunohistochemical staining of tissue sections. It should be noted in those latter studies that no attempt was made to identify the SLC-positive vessels as lymphatic endothelium using specific markers, whereas studies by Kriehuber et al. drew their conclusions from cells which had been extensively phenotyped as LEC on the basis of their expression of the lymphatic markers LYVE-1, prox-1, podoplanin and VEGFR-3.

6.3.3 LYVE-1

The dramatic down-modulation of LYVE-1 by LEC has been shown throughout this chapter as well as in chapters 4 and 5 of this thesis. This begs the question why, upon stimulation with TNF are LEC so keen to remove this receptor from their surface and from the surrounding medium? Observations from the whole mount tissue sections of oxazolone-challenged mouse dermis may hold a clue. Many of the sections examined appeared to show a preference of transmigrating MHC class II-positive leukocytes for LYVE-1-low lymphatic vessels, on which LYVE-1 had been partially or fully down-regulated. Thus it is tempting to speculate that in normal uninflamed tissue LYVE-1 plays a role in maintaining lymphatic permeability and the stabilisation of cell-cell junctions, regulating accessibility of the vessel to migrating antigen presenting cells. Clearly some constitutive migration must be permitted but the bulk of DCs are known to remain in the dermis and epidermis, always on guard against an antigen challenge and only exiting after inflammation-induced maturation. The microarray analyses in chapter 5 indicated that certain claudins and occludins, known players in cell-cell junctions were also down-regulated. Whole-mount staining of intact lymphatic vessels shown in this chapter, as well as immunofluorescence images of lymphatic endothelial cells in culture in chapter 5, have shown that LYVE-1 tends to be expressed preferentially at the cell-cell junctions. Also, recent research by Poritz et al (2004) has shown that TNFα disrupts tight junction assembly. Perhaps in the absence of LYVE-1, the vessel

may permit more transmigration between endothelial cells and entry into the lymphatics, to cope with the increased trafficking of newly extravasated monocytes. Peripheral blood monocytes entering the tissues must first differentiate into DCs before exiting via the lymphatics following oxazolone challenge and evidence from *in vitro* and *in vivo* studies have shown that this process may take up to two days to complete (Randolph et al., 1998; Rotta et al., 2003). Experiments described in this chapter have shown that the onset of loss of LYVE-1 does not occur instantaneously following the elicitation of inflammation but rather at 12h and later time points following challenge, which would be more concurrent with the reverse transmigration of monocyte-derived DC. To establish whether the down-modulation of LYVE-1 is a necessary pre-requisite for increased leukocyte trafficking, transmigration assays of monocyte-derived DCs through monolayers of LEC could be used, removing LYVE-1 expression by the use of siRNA. Such a model could also be used to examine the roles of adhesion molecules, by inducing up-regulation of expression by TNFα and using blocking antibodies against these receptors to assess their individual contributions to trafficking.

If LYVE-1 does indeed play the role of a "gate keeper" in normal healthy tissue, the phenotype of the recently generated LYVE-1 knock-out mouse would be expected to show increased trafficking of antigen-presenting cells to the lymph nodes, even in the absence of pro-inflammatory stimulus. Recent research by Cera et al. (2004) into the functions of the junctional adhesion molecule JAM-A demonstrated that DCs from *Jam-A*$^{-/-}$ mice exhibit an increase in random migration and transmigration across lymphatic endothelial cells. Such mice also showed increased localisation of skin DCs to lymph nodes and an enhanced reaction to contact hypersensitivity. Earlier work had found that JAM-A on blood vascular endothelial cells enhanced transmigration and therefore it would appear that endothelial JAM-A has a positive role in promoting cell

extravasation. However JAM-A expressed on DC was found to play a role in limiting cell motility. It will be fascinating to discover how the LYVE-1 $^{-/-}$ mouse responds in the delayed hypersensitivity reaction and whether increased trafficking is observed. However the mechanism by which LYVE-1 could act as such a barrier remains purely speculative at this stage. The fact that LYVE-1 is abundantly expressed on lymphatic endothelium *in vivo* and in primary cultured LEC *in vitro* despite being functionally silent with respect to HA-binding is perhaps indicative that LYVE-1 can bind other ligands, either in LEC themselves or in the surrounding medium. Such interactions could contribute to the barrier function. Another possibility is that LYVE-1 may engage in homophilic interactions in a similar manner to CD31. Unlike CD31, LYVE-1 does not possess Ig domains or any similar structures which might mediate such an interaction. However LYVE-1 can form homo-dimers via the unpaired cysteine residue (Cys257) in the transmembrane proximal domain (Tom Nightingale, DPhil thesis, University of Oxford, 2004). The formation of dimers may give rise to a novel domain between the link modules of the adjacent units, which could interact with such a dimer on an adjacent cell. The lack of constitutive binding by LYVE-1 of its glycosaminoglycan ligand, HA is clearly suggestive of another function, yet to be elucidated, in addition to that of an HA receptor.

6.3.4 Conclusion

Results described in this chapter have shown that the up-regulation of the leukocyte adhesion molecules VCAM-1 and ICAM-1 that had been extensively characterised *in vitro* (chapter 5) also occurs in a mouse model of TNFα-mediated inflammation. Additionally, the TNFα-mediated down-regulation of LYVE-1 in intact lymphatic vessels in dermal tissue explants and in the mouse model of inflammation was also shown, confirming data from three primary human LEC and two mouse LEC lines described in chapters 4 and 5. Finally the up-regulation of JE/MCP-1 was also detected in inflamed mouse dermis. Thus, data

from the *in vivo* studies in this chapter has confirmed many of the *in vitro* findings, which suggest that the lymphatic endothelium responds to inflammatory cytokines with an expression programme to promote leukocyte migration into the lymphatics.

CHAPTER 7

General Discussion

7.1 LYVE-1.....333

7.2 Effects of TNFα on lymphatic endothelium.....339

7.3 Conclusion.....347

The lymphatic system constitutes a network of highly permeable absorbing vessels that is structurally distinct from the blood vasculature but functionally connected. Together these two circulatory systems act in concert to maintain homeostasis within the tissues, cell nutrition and removal of metabolic by-products (reviewed by Mortimer, 1997). The initial lymphatic capillaries within the skin originate as blind-ended endothelial-lined tubes and drain through a series of enlarging vessels, diminishing in number until they reach the thoracic duct, where the lymph fluid is returned to the vasculature. Impaired lymphatic function can lead to the debilitating disease of oedema (Berne et al., 1998) and cessation in lymphatic flow will result in death (Adair and Guyton, 1985).

The lymphatics provide a major exit route from the skin for circulating cells such as T-lymphocytes and macrophages, as well as professional antigen presenting cells (APCs) such as dendritic cells (DCs). Antigens are transported to the regional lymph node and a primary immune response is initiated as naïve lymphocytes are brought into contact with APCs. Thus the lymphatics play critical roles in immune surveillance and in the trafficking of APCs to the lymph nodes, both constitutively and during inflammation, where a dramatic increase in the number of trafficking events occurs (reviewed by Randalph, 2001).

The elucidation of the molecular mechanisms behind lymphatic functioning relies upon the use of specific markers to discriminate between lymphatic vessels and blood vasculature in tissue sections and in cultured cells. One of the specific markers for the lymphatics is LYVE-1 (Banerji et al., 1999), the lymphatic HA receptor that forms the major subject of this thesis. Despite the wide use of this protein as a marker, its functions and the mechanisms by which expression is regulated have remained unknown. This PhD has sought to characterise the regulation of expression of LYVE-1 and to examine the response of the lymphatic endothelium to inflammation.

7.1 LYVE-1

7.1.1 Generation of monoclonal antibodies against mouse LYVE-1

To permit investigations into mouse tissue and complement studies carried out using the human monoclonal antibodies against LYVE-1 already raised by Dr. Remko Prevo in the same laboratory, two monoclonal antibodies (mAbs) against mouse LYVE-1 Fc fusion protein were generated and characterised (chapter 3). The epitopes of both antibodies were shown to lie within the extracellular domain, in close proximity to the Link module, the HA-binding domain. One of the mAbs, (C1/8) proved a powerful tool for detecting lymphatics within mouse tissue, particularly in whole-mount staining which permitted a three-dimensional perspective of lymphatic vessels and surrounding APCs (chapter 6). C1/8 was also used extensively in the immuno-selection of primary mouse dermal LEC (chapter 5), where it was found to have a greater specificity for LYVE-1-positive LEC than rabbit polyclonal antisera and thus yielded a purer population of LEC.

Preliminary experiments were carried out to establish whether either mAb induced functional effects on the LYVE-1 antigen. Curiously, the second mAb (B1/10) was found to reduce HA-binding by almost 70% in 293T-LYVE-1 transfectants but only when cells were exposed to the antibody during an incubation at 37°C: no such effect was observed at 4°C. Furthermore a 33% loss of LYVE-1 surface expression was detected by flow cytometry following incubation of transfectants in the presence of B1/10 for 24h at 37°C. This most likely indicates that B1/10 mediates loss of LYVE-1 surface expression through either shedding or internalisation. Further characterisation of this mAb could include a time course to measure the kinetics of the disappearance of LYVE-1 surface expression from transfectants by flow cytometry. To detect B1/10-

mediated shedding, an ELISA could be employed to detect shed LYVE-1 in the supernatant. The possibility of internalisation could be addressed using confocal microscopy, double-staining with polyclonal antisera to LYVE-1 and markers for the cell surface and subcellular compartments, to determine the intracellular location of LYVE-1.

7.1.2 Factors regulating LYVE-1 expression

In order to define the limitations that LYVE-1 may have as a lymphatic marker, as well as shedding light on the roles it may play under physiological and pathological conditions, factors regulating LYVE-1 expression were investigated extensively, using commercially available primary human dermal LEC (chapter 4). Following incubation with a panel of growth factors, cytokines and chemokines, LYVE-1 expression was assayed by flow cytometry. Whereas the majority of factors did not significantly affect LYVE-1 surface expression, the pro-inflammatory cytokines TNFα and TNFβ precipitated a dramatic loss of expression. This result was confirmed by two similar studies in this thesis, firstly using immuno-selected podoplanin-positive human LEC which were a kind gift from Dr. Ernst Kriehuber and secondly, a mixed population of commercially available primary HDMEC. Furthermore, initial analysis of human tissue sections from squamous cell carcinomas provides preliminary evidence to suggest that LYVE-1 is down-regulated *in vivo* under pro-inflammatory conditions (appendix III). The development of this skin carcinoma is known to by driven by inflammation, up-regulation of TNFα and TNFR1-mediated signalling (Lind et al., 2004). These observations, though based on a very limited number of tissue samples, raise the possibility that LYVE-1 down-regulation may play a role in the pathology of some human cancers. Further substantial studies to pursue this observation will require staining of squamous cell carcinoma tissue samples from many more patients, to investigate the percentage of samples in which LYVE-1 is down-regulated and explore any correlation

between the loss of LYVE-1 expression and other characteristics of the lesion, for example invasiveness.

As LYVE-1 can be so dramatically down-regulated under pro-inflammatory conditions, the use of this marker alone could have lead to an underestimation of tumour lymphatic vessel density in other previous studies.

7.1.3 The effect of TNFα on LYVE-1 expression in primary LEC

TNFα and TNFβ were both found to induce total loss of surface expression of LYVE-1 in the three sources of human LEC examined. Curiously, following stimulation of primary mouse LEC with TNFα, LYVE-1 surface expression was significantly reduced but loss was not absolute (chapter 5). Moreover, expression recovered without the need to remove the cytokine-supplemented medium. Whether this discrepancy is due to differences between the species or between the cell lines remains unclear. The murine LEC were isolated from post-partum dermis and such cells from neonates may not have developed a full inflammatory response, whereas human LEC were isolated from young adult dermis. The primary cell lines also differ in passage number at which the experiments were carried, as human LEC could be cultured to much later passages than mouse LEC. However a loss of LYVE-1 was observed in intact lymphatic endothelium in mouse tissue, both in ear tissue which had been cultured in the presence of TNFα and in TNFα-mediated inflammation within the ears of mice in contact hypersensitivity (chapter 6), in which a loss of LYVE-1 expression was recorded from almost 70% of vessels following 18h of elicitation of inflammation. Down-modulation of LYVE-1 has not been reported during chronic inflammation, such as that occurring following bacterial infection (Baluk et al., 2005) and therefore would appear to be only a feature of acute inflammation.

The TNFα-induced loss of LYVE-1 surface expression was further characterised *in vitro* in primary HDLEC (chapter 4). The cytokine did not induce any apoptotic or necrotic response in primary HDLEC and upon removal of cytokine from the medium, LYVE-1 expression completely recovered within 72h. Subsequent experiments revealed that the cells had commenced internalising LYVE-1 within 3h of TNFα stimulation and it was associated with the lysosomal compartment, accompanied by a decrease in the abundance of LYVE-1 mRNA within 12h of stimulation and abolition of constitutive shedding, which had been found to occur in unstimulated cells. The meticulous avoidance of the cells to shed any LYVE-1 could suggest potential biological activity of soluble LYVE-1. For example, this mechanism of removal of cell surface LYVE-1 was in stark contrast to that mediated by the phorbol ester, PMA which has been shown in previous studies to induce MMP-dependent shedding via activation of the PKC pathway in 293T LYVE-1 transfectants and also in this study in primary HDLEC, which endogenously express LYVE-1. Whether this soluble LYVE-1 binds its glycosaminoglycan ligand, HA (discussed in section 7.1.4) or whether it binds another as yet unidentified ligand remains to be identified. The development of arrays of immobilized oligosaccharides could enable broad screening for potential sugar ligands and comparison of specificities of LYVE-1 binding, similar to the study recently carried out by Guo et al. (2004), into ligand binding of DC-SIGN and L-SIGN.

TNFα-stimulated internalisation of LYVE-1 in human LEC, and cessation of constitutive shedding, were detected by the mAb 8C and LYVE-1 polyclonal antisera, all raised against the extracellular domain of LYVE-1. Thus, whilst the degradation of the extracellular domain was shown conclusively by experiments in this thesis, the fate of the transmembrane and cytoplasmic domains remain to be explored. As this domain is highly conserved, it may not prove sufficiently immunogenic in rabbits if cloned into the pCDM7Ig plasmid to yield a fusion

protein with human Fc (as was found with podoplanin Fc, described in appendix II). An alternative approach to raise polyclonal antisera in rabbits may be to generate a rabbit IgG Fc-LYVE-1-cytoplasmic tail construct. Such a reagent would permit the subcellular localisation of the LYVE-1 intracellular domain to be determined following TNFα-stimulation. It is possible that this domain may be cleaved from the internalised protein, and translocate to another part of the cell concurrent with the degradation of the extracellular domain. For example, the cytoplasmic domain of CD44, the more widely expressed homologue of LYVE-1, was shown by Okamoto et al. (2001) to be involved in signal transduction following phorbol ester-induced proteolytic release from the ectodomain of the molecule by membrane type 1 matrix metalloproteinase. This intracellular domain (ICD) was found to translocate to the nucleus and activate transcription through phorbol ester-responsive elements, found in numerous genes involved in diverse cellular processes, including CD44. The intriguing prospect that the cytoplasmic domain of LYVE-1 could exhibit similar biological activity will be addressed in future experiments. Confocal microscopy could be used to identify whether the cytoplasmic domain of LYVE-1 may translocate to the nucleus of human LEC following stimulation with PMA or TNFα and membrane/cytosol and nuclear fractions could be analysed by Western blotting with antisera against the LYVE-1 cytoplasmic domain.

7.1.4 HA binding by LYVE-1

Previous work by Tom Nightingale in the Jackson laboratory (DPhil thesis, University of Oxford, 2004) has shown that LYVE-1 expressed on primary human and murine LEC does not constitutively bind HA. However, confocal microscopy and flow cytometry carried out in chapter 4 of this thesis provided some evidence that HA is internalised by lymphatic endothelial cells and a marginal increase in binding of HA by these cells occurs following TNFα stimulation. That raises the question as to whether LYVE-1 becomes activated to

bind HA simultaneous with its internalisation or whether some other receptor is involved. Future experiments could distinguish between these possibilities. The human LYVE-1 blocking antibody 3A could be employed to investigate whether this mAb reduces HA uptake in primary HDLEC. Also if the mouse mAb B1/10 generated in this PhD proves to induce loss of LYVE-1 surface expression, it could be used to establish a role for LYVE-1 in HA internalisation in primary mouse LEC. Additionally it would be interesting to incubate HA with primary LEC isolated from the LYVE-1$^{-/-}$ knock-out mouse, to determine by microscopy whether they are capable of internalisation of HA. These experiments would test whether a LYVE-1-dependent mechanism is responsible, or either a LYVE-1-independent mechanism or a second compensatory mechanism is employed.

7.1.5 A putative role for LYVE-1 in regulating reverse transmigration

Observations from the whole-mount tissue sections of mouse dermis following elicitation of inflammation in a model of delayed contact hypersensitivity (CHS), (described in chapter 6) suggest that LYVE-1 may have another function besides that of an HA receptor. Significant down-regulation of LYVE-1 was observed in lymphatic vessels within inflamed tissue. Moreover, MHC class II-positive APCs could be seen preferentially surrounding and presumably reverse-transmigrating across lymphatic vessels upon which LYVE-1 had been either partially or fully down-regulated. Additionally, both whole-mount staining of intact vessels and immunofluorescence microscopy has shown that LYVE-1 is expressed preferentially at the cell-cell junctions. One possibility is that in normal non-inflamed tissue LYVE-1 may play a role in the maintenance of cell-cell junctions, permitting only a low level of constitutive migration. The microarrays performed in this PhD showed that upon activation of the lymphatic endothelium, junctional molecules such as claudins and occludin are down-regulated as well as LYVE-1. This permits the increased number of transmigration events resulting from increased trafficking of newly extravasated

monocytes, which must gain entry into the lymphatics. To establish whether the down-modulation of LYVE-1 is a necessary pre-requisite for increased leukocyte trafficking, future experiments could include transmigration assays of human monocyte-derived DCs through monolayers of primary HDLEC, removing LYVE-1 expression by the use of siRNA. Alternatively (depending upon the efficacy of removal of surface expression induced by the mouse mAb B1/10), a mouse *in vitro* model of transmigration could be used, using B1/10 to remove LYVE-1 expression in place of small interfering RNAs (siRNA). Also, the number of constitutive trafficking events in the LYVE-1$^{-/-}$ knock-out mouse could be assessed. If LYVE-1 does indeed play the role of a "gate keeper", increased constitutive trafficking would be expected in the knock-out mouse, which may exhibit higher numbers of DCs within the lymph nodes that would be apparent in FACS analysis of lymph node cell populations. This might also be manifest as fewer DC resident within the dermis and perhaps a delay in the onset of inflammation following elicitation of delayed contact hypersensitivity.

7.2 The effects of TNFα on lymphatic endothelial cells *in vitro* and in intact tissue

7.2.1 TNFα-mediated induction of key leukocyte adhesion molecules

Another major finding in this PhD was the induction by TNFα and TNFβ of key adhesion molecules, previously associated with inflamed blood vascular endothelium. Both cultured HDLEC and newly derived isolates of mouse LEC displayed marked up-regulation of ICAM-1, VCAM-1 and E-selectin. Flow cytometry studies revealed that both E-selectin and VCAM-1 were absent from unstimulated LEC but were induced following exposure to TNFα or TNFβ. HDLEC were found to constitutively express ICAM-2, which was down-modulated following stimulation with TNFα, although not to the same pronounced extent as LYVE-1.

In the TNFα-mediated CHS model in mice, over 50% of lymphatic vessels expressed VCAM-1 and ICAM-1 within 18h of the elicitation of inflammation, and concurrent with the loss of LYVE-1 from almost 70% of vessels (chapter 6). Furthermore, the change in expression of these receptors was concomitant with the observation of MHC class II-positive APCs surrounding the lymphatics, apparently in preparation for reverse transmigration. 12h following elicitation of inflammation, extravasation of newly recruited monocytes from blood capillaries was observed. These differentiate in the dermis into either macrophages which stay resident in the peripheral tissue or DCs, which transmigrate into the lymphatics to present their newly acquired antigen within the T cell-rich paracortical area of a regional lymph node (Randolph et al., 1998). Thus the onset of inflammation heralds a massive increase in the number of trafficking events and the up-regulation of known leukocyte adhesion molecules may be a necessary pre-requisite. Future experiments should include triple immunofluorescence staining of tissue with antibodies against podoplanin, MHC class II and either VCAM-1 or ICAM-1, to establish whether transmigrating cells are associated with lymphatic vessel expression these leukocyte adhesion molecules. Also, future studies could use specific markers to distinguish subsets of MHC class II-positive APCs. A recent study by Qu et al. (2004) has shown that CCR8 can serve as a marker for monocyte-derived DCs and therefore future experiments could use this to distinguish constitutive trafficking from the increased trafficking of DCs derived from newly recruited monocytes from the blood.

The involvement of VCAM-1 and ICAM-1 in leukocyte transmigration across lymphatic endothelium which is suggested by the data in chapters 5 and 6 of this thesis could also be elucidated more fully by further experiments *in vitro*. Effects of receptor neutralising antibodies on migration of monocyte-derived DCs could

be investigated in transmigration assays across an endothelial monolayer. Randolph and Furie (1996) have previously shown that ICAM-1 neutralising antibodies totally block transmigration of mononuclear phagocytes (which were in the process of differentiating towards DC-like cells), from basal to apical surfaces of a HUVEC monolayer. It would be interesting to investigate whether such antibodies have a similar effect on monocyte-derived DC migration across a primary LEC monolayer. To observe the localization of adhesion molecules on lymphatic endothelium during transmigration events, electron microscopy with immuno-gold labeling could be used. If expression of the adhesion molecules on the abluminal or luminal surface of the endothelium could be determined, this could provide evidence as to whether these receptors are involved in the initial transmigration into the vessel or during migration of the leukocyte through the lymphatics. Earlier studies have shown that ICAM-1 is expressed on both surfaces of HUVEC whereas VCAM-1 expression is restricted to the apical surface (Oppenheimer Marks et al., 1991; Randolph and Furie, 1996), as VCAM-1 is only involved in adhesion whereas ICAM-1 also plays a role in transmigration. A previous study by Xu et al. (2001) showed that ICAM-1 deficiency on lymphatic endothelium resulted in reduced migration of Langerhans cells from the skin into draining lymph nodes. However, no accumulation of DC around lymph vessels in the dermis of ICAM-1-deficient mice was observed, arguing that ICAM-1 is not required for DC entry to the lymphatic vessels in the skin. This suggests that ICAM-1 may play a role in events down-stream of reverse transmigration, such as the trafficking of leukocytes through the afferent lymphatics. Nevertheless, a role for ICAM-1 in reverse transmigration cannot be dismissed as it is possible that in the ICAM-1-deficient mouse, other compensatory mechanisms are involved, for example ICAM-2 which is an alternative ligand for LFA-1 (CD11a/CD18 or αLβ2, (Makgoba et al., 1988). Moreover, blood endothelial ICAM-1 and ICAM-2 have been shown to have redundant roles in lymphocyte recirculation through lymph nodes (Lehmann et

al., 2003). As on blood endothelium (McLaughlin et al., 1998), ICAM-2 in primary HDLEC underwent a marginal but significant down-regulation in response to TNFα, suggesting that lymphatic endothelial ICAM-2 does not have a role in inflammation but rather is constitutively expressed in normal tissue. However ICAM-2 on lymphatic endothelium may play a role in constitutive leukocyte migration across the lymphatic endothelium and may compensate for ICAM-1 deficiency during inflammation.

7.2.2 TNFα-induced change in morphology of lymphatic endothelial cells

A striking change in cell morphology was observed in both primary HDLEC and mouse LEC following TNFα-stimulation, from rounded to elongated. This suggests rearrangement of cytoskeletal elements, which could be assessed by confocal microscopy. It is tempting to speculate that such reorganisation might facilitate leukocyte reverse transmigration across lymphatic endothelium during inflammation.

7.2.3 Synthesis of pro-inflammatory chemokines by lymphatic endothelial cells

Both the microarray analyses and ELISA data revealed that in addition to affecting expression of adhesion molecules, TNFα induces synthesis of a vast range of pro-inflammatory chemokines including RANTES, MCP-1, MIP-3α, MCP-3, Fractalkine, IL-8, ENA-78 and GROβ which are chemotactic for monocytes, DCs, T-cells and neutrophils (von Andrian and Mackay, 2000). This indicates that the lymphatics have the capacity to play an active role in recruitment of leukocytes from the tissues to the draining lymph node. Alternatively, as lymphatic vessels lie close to blood capillaries, these chemokines could be to aid extravasation of newly recruited inflammatory cells from the blood. Another interesting possibility is these chemokines might be released into the lumen of the lymphatic vessel and transported through the afferent lymph to the lymph node cortex for presentation on the luminal face of

HEVs. Such a process has been described in a study by Palframan et al. (2001), which followed the path of MCP-1 secreted by unspecified cells within the dermis to the luminal surface of HEVs by reticular network fibres, triggering integrin-dependent arrest of rolling monocytes and thus enhanced recruitment to the lymph node. To investigate which chemokines are secreted from the abluminal surface into the surrounding extracellular matrix, and which in the basolateral direction for transport to the peripheral draining lymph node, LEC could be cultured in Transwell™ assays and stimulated with TNFα. Supernatant from both the upper and lower chambers would then be harvested and chemokine secretion detected by ELISA.

7.2.4 Induction of MMPs by lymphatic endothelial cells

The microarray data also indicated the induction of transcripts of matrix metalloproteinases (MMPs) such as MMP-3 (Stromelysin-1), MMP-6, MMP-9 (Gelatinase B), MMP-10 (Stromelysin-2) and MMP-19. The substrates of MMP-3 include E-cadherin and TGF-β1 (reviewed by Parks et al., 2004). Therefore it is possible that MMP-3 may enhance mobilisation of Langerhans cells from the epidermis by breaking E-cadherin-mediated homophilic interactions with keratinocytes (Jakob et al., 1999) and inactivating TGFβ1, which mediates retention of Langerhans cells by up-regulating E-cadherin and blocking TNFα-induced up-regulation of CCR7, which is critical in the migration of LC to the lymphatics (reviewed by Jakob et al., 2001). MMPs such as MMP-9 may also contribute to the establishment of chemokine gradients by releasing immobilised chemokines from their heparan sulphate proteoglycan binding sites within the extracellular matrix and regulate chemotactic activity through proteolytic cleavage of chemokines (Parks et al., 2004; Van den Steen et al., 2003a; and Van den Steen et al., 2003b). MMP-9 has also been shown to regulate chemotactic activity of ENA-78, GCP-2, IL-8, MIG and IP-10 through proteolytic cleavage of these chemokines (Van den Steen et al., 2003). These chemokines were all shown

to be induced in LEC following stimulation with TNFα by the microarray analyses performed in this PhD. MMPs are known to be responsible for the turnover and degradation of the extracellular matrix and therefore may facilitate extravasation of monocytes from the blood by degrading basement membrane structures on inter-endothelial tight junctions of juxtaposed blood capillaries. Clearly expression of all of these transcripts must be confirmed at the protein level in TNFα-stimulated primary LEC and in inflamed tissue.

7.2.5 Synthesis of TNF superfamily members by lymphatic endothelial cells

The microarray data from primary HDLEC further suggests an influence by the lymphatic endothelium on other cells within its environs by expression of TNF superfamily members and their receptors. TNFα was found to induce expression of OX40 (also known as CD134, or by the systematic name TNFRSF4) and its ligand OX40L (CD134L or TNFSF4), as well as GITR ligand (glucocorticoid-induced TNFR family-related ligand, TNFSF18). These receptors and ligands promote the survival and perhaps prolong the immune response of $CD4^+$ T cells at sites of inflammation (Godfrey et al., 1994) and interrupt apoptosis in T cells (Nocentini et al., 1997). The effect of LEC in promoting T cell survival could be assessed *in vitro* by inducing apoptosis on T cells artificially and then incubating these cells in the presence of a TNFα-stimulated LEC monolayer. Annexin V could be used as a marker for apoptosis to compare the number of apoptosing T cells incubated with unstimulated LEC with that of T cells incubated with the TNFα-stimulated monolayer. An increase in transcript abundance of CD137 (TNFRSF9) was also observed in the data generated by the microarray and as ligation of this receptor is reported to interrupt T cell apoptotic programs associated with activation-induced cell death (Hurtado et al., 1997), this would suggest that the lymphatic endothelial cells are also capable of protecting themselves from apoptotic signals during inflammation, as well as synthesising ligands to ensure the survival of neighbouring T cells.

7.2.6 A model for the inflammation-induced expression programme in lymphatic endothelium

Experiments detailed in chapters 4, 5 and 6 have shown that the lymphatic endothelium responds to inflammatory cytokines with an expression programme which would suggest that it is responsible for actively promoting leukocyte migration into the lymphatics. The following model is proposed (figure 7.1), although clearly *in vitro* studies are required to establish the roles of individual molecular interactions between migrating leukocyte and endothelium.

In normal non-inflamed lymphatic endothelium, ICAM-2 and low levels of ICAM-1 are expressed to permit low levels of constitutive migration and LYVE-1 is localised primarily at cell-cell junctions (figure 7.1). Following the activation of endothelium by stimulation with TNFα or TNFβ, LYVE-1 is internalised and degraded concurrent with the up-regulation of E-selectin, which it is tempting to speculate, could permit the initial loose capture of neighbouring leukocytes. Increased expression of ICAM-1 and VCAM-1 would permit more high affinity interactions to form between the endothelium and leukocyte via counter receptors, whilst the secretion of newly synthesised chemokines from basolateral and luminal faces of the endothelium would chemoattract leukocytes, not only from the immediate vicinity but also across distant lymph node HEV, by a mechanism of remote control. Increased synthesis of MMPs contributes by modulating chemokine activity, mobilising Langerhans cells and degrading basement membranes to enhance extravasation of more inflammatory cells from the blood. Thus lymphatic endothelial cells play dynamic roles in influencing both neighbouring leukocytes and the biology of the interstitium surrounding them.

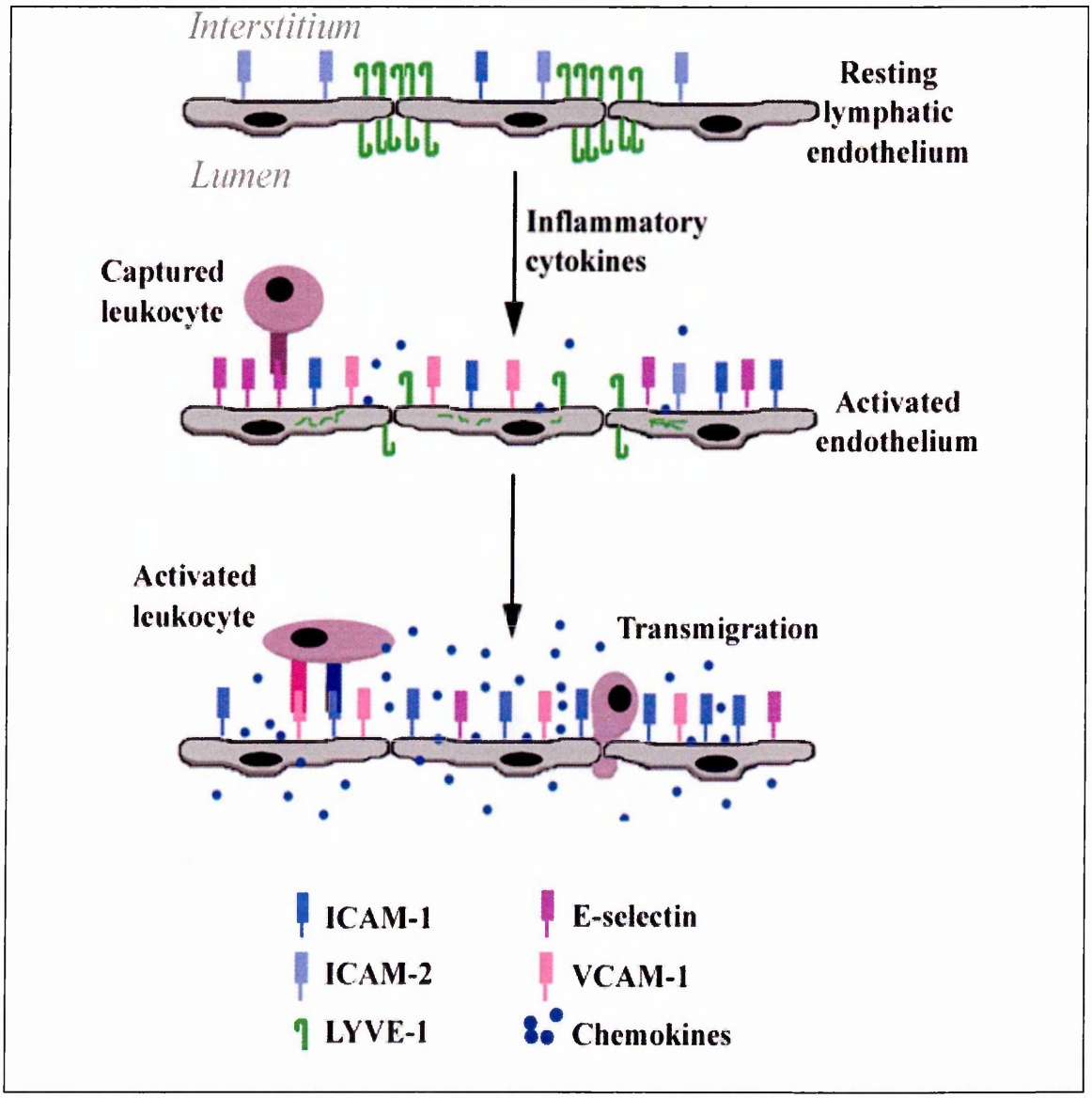

Figure 7.1 Schematic representation of lymphatic endothelium during inflammation. This figure depicts a model in which resting lymphatic endothelium expresses abundant LYVE-1 at cell-cell junctions as well as ICAM-2 and low levels of ICAM-1 which may participate in constitutive trafficking of leukocytes. Upon activation by pro-inflammatory cytokines, E-selectin, VCAM-1 and ICAM-1 are up-regulated, bringing about capture, activation and ultimately transmigration of leukocytes through interactions with their counter receptors. The up-regulation of these adhesion molecules may be necessary to support the increased number of trafficking events which occur during inflammation. ICAM-2, involved only in constitutive migration, is down-regulated and LYVE-1 is internalised, degraded and thus removed from the cell-cell junctions. The endothelium secretes high levels of inflammatory chemokines as well as other soluble factors, thus radically affecting its environment to promote further leukocyte transmigration into the lumen of the lymphatic vessels for transport to a regional lymph node.

7.3 Conclusion

The data presented in this thesis have shown that the expression of the lymphatic vessel HA receptor LYVE-1 on lymphatic endothelium is tightly regulated and radically down-modulated following stimulation with the pro-inflammatory cytokine TNF, both in cultured primary dermal LEC and in an allergen-induced mouse model of skin inflammation. This thesis has also shown that lymphatic endothelium responds to key inflammatory cytokines by instigating a distinct expression programme characterised by up-regulation of the key leukocyte adhesion receptors ICAM-1, VCAM-1 and E-selectin, chemokines and other potential regulators of leukocyte entry. The major components of this program were found to be induced in dermal lymphatic vessels in vivo, simultaneous with the transmigration of leukocytes into the lymphatic lumen. Thus these results provide the first evidence that lymphatic endothelial cells play an active role in inflammation and indicate that parts of the same address code for specific vascular targeting are found in both the lymphatics and blood vascular system.

Bibliography

Abbas AK, Lichtman AH and Pober JS (1997) *Cellular and Molecular Immunology.* W. B. Saunders Company, Philadelphia.

Abtahian F, Guerriero A, Sebzda E, Lu M-M, Zhou R, Mocsai A, Myers EE, Huang B, Jackson DG, Ferrari VA, Tybulewicz V, Lowell CA, Lepore JJ, Koretzky GA and Kahn ML (2003) Regulation of blood and lymphatic vascular separation by signaling proteins SLP-76 and Syk. *Science* **299**:247-251.

Achen MG, Jeltsch M, Kukk E, Makinen T, Vitali A, Wilks AF, Alitalo K and Stacker SA (1998) Vascular endothelial growth factor D (VEGF-D) is a ligand for the tyrosine kinases VEGF receptor 2 (Flk1) and VEGF receptor 3 (Flt4). *Proceedings by the National Academy of Sciences of the USA* **95**:548-553.

Adair TH and Guyton AC (1985) Lymph formation and its modification in the lymphatic system., in *Experimental Biology of the Lymphatic Circulation.* (Johnston MG ed) pp 13-44, Elsevier, Amsterdam.

Aiba S and Katz SI (1990) Phenotypic and functional characteristics of in vivo-activated Langerhans cells. *Journal of Immunlogy* **145**:2791-2796.

Akira S and Kishimoto T (1992) IL-6 and NF-IL6 in acute-phase response and viral infection. *Immunological Reviews* **127**:25-50.

Allan L (1967) Lymphatics and lymphoid tissues. *Annual Reviews in Physiology* **29**:197-224.

Anagnostopoulou I, Kaklamanis L, Cordell J, Jones M, Turley H, Pulford K, Simmons D, Mason D and Gatter K (1993) ICAM-3 expression on endothelium in lymphoid malignancy. *American Journal of Pathology* **143**:1040-1043.

Anderson AO and Anderson ND (1976) Lymphocyte emigration from high endothelial venules in rat lymph nodes. *Immunology* **31**:772-778.

Anderson ND, Anderson AO and Wyllie RG (1976) Specialized structure and metabolic activities of high endothelial venules in rat lymphatic tissues. *Immunology* **31**:455-473.

Aprelikova O, Pajusola K, Partanen J, Armstrong E, Alitalo R, Bailey SK, McMahon J, Wasmuth J, Huebner K and Alitalo K (1992) FLT4, a novel class III receptor tyrosine kinase in chromosome 5q33-qter. *Cancer Research* **52**:746-748.

Aukland K and Reed RK (1993) Interstitial-lymphatic mechanisms in the control of extracellular fluid volume. *Physiology Reviews* **73**.

Baker SJ and Reddy EP (1996) Transducers of life and death: TNF receptor superfamily and associated proteins. *Oncogene* **12**:1-9.

Baker SJ and Reddy EP (1998) Modulation of life and death by the TNF receptor superfamily. *Oncogene* **17**:3261-3270.

Balazs EA, Laurent TC and Jeanloz RW (1986) Nomenclature of hyaluronic acid. *Biochemical Journal* **235**:903.

Baluk P, Tammela T, Ator E, Lyubynska N, Achen MG, Hicklin DJ, Jeltsch M, Petrova TV, Pytowski B, Stacker SA, Yla-Herttuala S, Jackson DG, Alitalo K and McDonald DM (2005) Pathogenesis of persistent lymphatic vessel hyperplasia in chronic airway inflammation. *Journal of Clinical Investigation* **115**:247-257.

Banerji S, Ni J, Wang S-X, Clasper S, Su S, Tammi R, Jones M and Jackson DG (1999) LYVE-1, a new homologue of the CD44 glycoprotein, is a lymph-specific receptor for hyaluronan. *Journal of Cell Biology* **144**:789-801.

Barreiro O, Yanez-Mo M, Serrador JM, Montoya MC, Vincente-Manzanares M, Teyedor R, Furthmayr H and Sanchez-Madrid F (2002) Dynamic interaction of VCAM-1 and ICAM-1 with moesin and ezrin in a novel endothelial docking structure for adherent leukocytes. *Journal of Cell Biology* **157**:1233-1245.

Barrett K, Taylor-Fishwick DA, Cope AP, Kissonerghis AM, Gray PW, Feldmann M and Foxwell BM (1991) Cloning, expression and cross-linking analysis of the murine p55 tumor necrosis factor receptor. *European Journal of Immunology* **21**:1649-1656.

Bauman H and Gauldie J (1994) The acute phase response. *Immunology Today* **15**:74-80.

Baumhueter S, Dybdal N, Kyle C and Lasky LA (1994) Global vascular expression of murine CD34, a sialomucin-like endothelial ligand for L-selectin. *Blood* **84**:2554-2565.

Baumhueter S, Singer MS, Henzel W, Hemmerich S, Renz M, Rosen SD and Lasky LA (1993) Binding to L-selectin to the vascular sialomucin CD34. *Science* **262**:436.

BD Biosciences C (2002) Matrigel Basement Membrane Matrix - product specification sheet.

Berman ME and Muller WA (1995) Ligation of platelet/endothelial cell adhesion molecule 1 (PECAM-1/CD31) on monocytes and neutrophils increases binding capacity of leukocyte CR3 (CD11b/CD18). *Journal of Immunology* **154**:299-307.

Berne RM, Levy MN, Koeppen BM and Stanton BA (eds) (1998) *Physiology.* Mosby, Inc, St. Louis.

Bevilacqua MP, Stengelin S, Gimbrone MAJ and Seed B (1989) Endothelial leukocyte adhesion molecule 1: an inducible receptor for neutrophils related to complement regulatory proteins and lectins. *Science* **243**:1160-1165.

Beyer EC (1993) Gap junctions. *International Reviews in Cytology* **137C**:1-37.

Bird IN, Taylor V, Newton JP, Spragg JH, Simmons DL, Salmon M and Buckley CD (1999) Homophilic PECAM-1 (CD31) interactions prevent endothelial cell apoptosis but do not support cell spreading or migration. *Journal of Cell Science* **112**:1989-1997.

Bissonnette EY, Chin B and Befus AD (1995) Interferons differentially regulate histamine and TNF-alpha in rat intestinal mucosal mast cells. *Immunology* **86**:12-17

Black RA, Rauch CT, Kozlosky CJ, Peschon JJ, Slack JL, Wolfson MF, Castner BJ, Stocking KL, Reddy P, Srinivasan S, Nelson N, Boiani N, Schooley KA, Gerhart M, Davis R, Fitzner JN, Johnson RS, Paxton RJ, March CJ and Cerretti DP (1997) A metalloproteinase disintegrin that releases tumour-necrosis factor-alpha from cells. *Nature* **385**:729-733.

Bogen SA, Baldwin HS, Watkins SC, Albelda SM and Abbas AK (1992) Association of murine CD31 with transmigrating lymphocytes following antigenic stimulation. *American Journal of Pathology* **141**:843-854.

Borg JP, deLapeyriere O, Hoguchi T, Rottapel R, Dubreuil P and Birnbaum D (1995) Biochemical characterization of two isoforms of FLT4, a VEGF receptor-related tyrosine kinase. *Oncogene* **10**:973-984.

Borghaei RC, Rawlings PLJ, Javadi M and Woloshin J (2004) NFkB binds to a polymorphic repressor element in the MMP-3 promoter. *Biochemistry and Biophysics Research Communications* **316**:182-188.

Bourguignon LYW, Lokeshwar VB, Chen X and Kerrick WBL (1993) Hyaluronic acid-induced lymphocyte signal transduction and HA receptor (GP85/CD44)-cytoskeleton interaction. *Journal of Immunlogy* **151**:6634-6644.

Bowie A and O'Neill LAJ (2000) Oxidative stress and nuclear factor-kB activation. A reassessment of the evidence in the light of recent discoveries. *Biochemical Pharmacology* **59**:13-23.

Breiteneder-Geleff S, Matsui K, Soleiman A, Meraner P, Poczewski H, Kalt R, Schaffner G and Kerjaschki D (1997) Podoplanin, novel 43-kd membrane protein of glomerular epithelial cells, is down-regulated in puromycin nephrosis. *American Journal of Pathology* **154**:1141-1152.

Bretscher A and Berryman M (1999) ERM proteins:ezrin, radixin and moesin., in *Guidebook to the cytoskeletal and motor proteins.* (Kreis T and Vale R eds) pp 88-91, Sambrook and Tooze, Oxford University Press, Oxford.

Brizel DM, Scully SP, Harrelson JM, Layfield LJ, Bean JM, Prosnitz LR and Dewhirst MW (1996) Tumor oxygenation predicts for the likelihood of distant metastases in human soft tissue sarcoma. *Cancer Research* **56**:941-943.

Brocke S, Piercy C, Steinman L, Weissman IL and Veromaa T (1999) Antibodies to CD44 and integrin alpha4, but not L-selectin, prevent central nervous system inflammation and experimental encephalomyelitis by blocking secondary leukocyte recruitment. *Proceedings of the National Academy of Sciences of the USA* **96**:6896-6901.

Brown J, Greaves MF and Molgaard HV (1991) The gene encoding the stem cell antigen CD34 is conserved in mouse and expressed in haematopoietic progenitor cell lines, brain and embryonic fibroblasts. *International Immunology* **3**:175.

Browning JL, Ngam-ek A, Lawton P, DeMarinis J, Tizard R, Chow EP, Hession C, O'Brine-Greco B, Foley SF and Ware CF (1993) Lymphotoxin beta, a novel member of the TNF family that forms a heteromeric complex with lymphotoxin on the cell surface. *Cell* **72**:847-856.

Buckley CD, Doyonnas R, Newton JP, Blystone SD, Brown EJ, Watt SM and Simmons DL (1996) Identification of alpha v beta 3 as a heterotypic ligand for CD31/PECAM-1. *Journal of Cell Science* **109**:437-445.

Calabresi L, Rossoni G, Gomaraschi M, Sisto F, Berti F and Franceschini G (2003) High-density lipoproteins protect isolated rat hearts from ischemia-reperfusion injury by reducing cardiac tumor necrosis factor-alpha content and enhancing prostaglandin release. *Circulation Research* **92**:330-337.

Camenisch TD, Spicer AP, Brehm-Gibson T, Biesterfeldt J, Augustine ML, Calbro AJ, Kubalak S, Klewer SE and McDonald JA (2000) Disruption of hyaluronan synthase-2 abrogates normal cardiac morphogenesis and hyaluronan-mediated transformation of epithelium to mesenchyme. *Journal of Clinical Investigation* **106**:349-360.

Carman CV, Jun C-D, Salas A and Springer TA (2003) Endothelial cells proactively form microvilli-like membrane projections upon intercellular adhesion molecule 1 engagement of leukocyte LFA-1. *Journal of Immunology* **171**:6135-6144.

Carman CV and Springer TA (2004) A transmigratory cup in leukocyte diapedesis both through individual vascular endothelial cells and between them. *Journal of Cell Biology* **167**:377-388.

Carswell EA, Old LJ, Kassel RL, Green S, Fiore N and Williamson B (1975) An endotoxin-induced serum factor that causes necrosis of tumors. *Proceedings of the National Academy of Sciences of the USA* **72**:3666-3670.

Cera MR, Del Prete A, Vecchi A, Corada M, Martin-Padura I, Motoike T, Tonetti P, Bazzoni G, Vermi W, Gentili F, Bernasconi S, Sato T, Mantovani A and Dejana E (2004) Increased DC trafficking to lymph nodes and contact hypersensitivity in junctional adhesion molecule-A-deficient mice. *Journal of Clinical Investigation* **114**:729-738.

Civin CI, Strauss LC, Brovall C, Fackler MJ, Schwartz JF and Shaper JH (1984) Antigenic analysis of hematopoiesis III. A hematopoietic progenitor cell surface antigen defined by a monoclonal antibody raised against KG1a cells. *Journal of Immunology* **133**:157.

Clark EA, Alon R and Springer T (1996) CD44 and hyaluronan-dependent rolling interactions of lymphocytes on tonsillar stroma. *Journal of Cell Biology* **134**:1075-1087.

Corredor J, Yan F, Shen CC, Tong W, John SK, Wilson G, Whitehead R and Brent Polk D (2003) Tumour necrosis factor regulates intestinal epithelial cell migration by receptor-dependent mechanisms. *Americal Journal of Physiology: Cell Physiology* **284**:C953-C961.

Csoka A, B, Frost GI and Stern R (2001) The six hyaluronidase-like genes in the human and mouse genomes. *Matrix Biology* **20**:499-508.

Culty M, Nguyen HA and Underhill CB (1992) The hyaluronan receptor (CD44) participates in the uptake and degradation of hyaluronan. *Journal of Cell Biology* **116**:1055-1062.

Cumberbatch M, Dearman RJ, Groves RW, Antonopoulos C and Kimber I (2002) Differential regulation of epidermal Langerhans cell migration by interleukins (IL)-1alpha and IL-1beta during irritant- and allergen-induced cutaneous immune responses. *Toxicology and Applied Pharmacology* **182**:126-135.

Cumberbatch M and Kimber I (1992) Dermal tumour necrosis factor-alpha induces dendritic cell migration to draining lymph nodes and possibly provides one stimulus for Langerhans cell migration. *Immunology* **75**:257-263.

Cupedo T, Vondenhoff MFR, Heeregrave EJ, de Weerd AE, Jansen W, Jackson DG, Kraal G and Mebius RE (2004) Presumptive lymph node organizers are differentially represented in developing mesenteric and peripheral nodes. *Journal of Immunology* **173**:2968-2975.

Dadras SS, Paul T, Bertoncini J, Brown LF, Muzikansky A, Jackson DG, Ellwanger U, Garbe C, Mihm MC and Detmar M (2003) Tumour lymphangiogenesis. A novel prognostic indicator for cutaneous melanoma metastasis and survival. *American Journal of Pathology* **162**:1951-1960.

Dalchau R, Kirkley J and Fabre JW (1980) Monoclonal antibody to a human brain-granulocyte-T lymphocyte antigen probably homologous to the W 3/13 antigen of the rat. *European Journal of Immunology* **10**:745-749.

Dangerfield J, Larbi KY, Huang M-T, Dewar A and Nourshargh S (2002) PECAM-1 (CD31) homophilic interaction up-regulates alpha 6 beta 1 on transmigrated neutrophils in vivo and plays a functional role in the ability of alpha 6 integrins to mediate leukocyte migration through the perivascular basement membrane. *Journal of Experimental Medicine* **196**:1201-1211.

Day AJ and Prestwich GD (2002) Hyaluronan-binding proteins:tying up the giant. *Journal of Biological Chemistry* **277**:4585-4588.

Decoster E, Vanhaesebroeck B, Vanhaesebroeck P, Grooten J and Fiers W (1995) Generation and biological characterization of membrane-bound, uncleavable murine tumor necrosis factor. *Journal of Biological Chemistry* **270**:18473-18478.

DeGrendele HC, Estess P, Picker LJ and Siegelman MH (1996) CD44 and its ligand hyaluronate mediate rolling under physiologic flow: a novel lymphocyte-endothelial cell primary adhesion pathway. *Journal of Experimental Medicine* **183**:1119-1130.

DeGrendele HC, Estess P and Siegelman MH (1997b) Requirement for CD44 in activated T cell extravasation into an inflammatory site. *Science* **278**:672-675.

DeGrendele HC, Kosfiszer M, Estess P and Siegelman MH (1997a) CD44 activation and associated primary adhesion is inducible via T cell receptor stimulation. *Journal of Immunlogy* **159**:2549-2553.

Del Maschio A, de Luigi A, Martin-Padura I, Brockhaus M, Bartfai T, Fruscella P, Adorini L, Martino GV, Furlan R, de Simoni MG and Dejana E (1999) Leukocyte recruitment in the cerebrospinal fluid of mice with experimental meningitis is inhibited by an antibody to junctional adhesion molecule (JAM). *Journal of Experimental Medicine* **190**:1351-1356.

Delia D, Lampugnani MG, Resnati M, Dejano E, Aiello A, Fontanella E, Soligo D, Pierotti MA and Greaves MF (1993) CD34 expression is regulated reciprocally with adhesion molecules in vascular endothelial cells in vitro. *Blood* **81**:1001-1008.

Desch CE, Dobrina A, Aggarwal BB and Harlan JM (1990) Tumour necrosis factor-alpha exhibits greater proinflammatory activity than lymphotoxin in vitro. *Blood* **75**:2030-2034.

Dobbs LG, Williams MC and Gonzalez R (1988) Monoclonal antibodies specific to apical surfaces of rat alveloar type I cells bind to surfaces of cultured, but not freshly isolated, type II cells. *Biochemica et Biophysica Acta* **970**:146-156.

Drillenburg P and Pals ST (2000) Cell adhesion receptors in lymphoma dissemination. *Blood* **95**:1900-1910.

Dumont DJ, Jussila L, Taipale J, Lymboussaki A, Mustonen T, Pajusola K, Breitman M and Alitalo K (1998) Cardiovascular failure in mouse embryos deficient in VEGF receptor-3. *Science* **282**:946-949.

Dustin ML and Springer TA (1988) Lymphocyte function-associated antigen-1 (LFA-1) interaction with intercellular adhesion molecule-1 (ICAM-1) is one of at least three mechanisms for lymphocyte adhesion to cultured endothelial cells. *Journal of Cell Biology* **107**:321-331.

Ebnet K, Aurrand-Lions M, Kuhn A, Kiefer F, Butz S, Zander K, Meyer zu Brickwedde M-K, Suzuki A, Imhof BA and Vestweber D (2003) The junctional adhesion molecule (JAM) family members JAM-2 and JAM-3 associate with the cell polarity protein PAR-3: a possible role for JAMs in endothelial cell polarity. *Journal of Cell Science* **116**:3879-3891.

Eck MJ, Ultsch M, Rinderknecht E, de Vos AM and Sprang SR (1992) The structure of human lymphotoxin (tumor necrosis factor-beta) at 1.9-A resolution. *Journal of Biological Chemistry* **267**:2119-2122.

Enholm B, Karpanen T, Jeltsch M, Kubo H, Stenbach F, Prevo R, Jackson DG, Yla-Herttuala S and Alitalo K (2001) Adenoviral expression of vascular endothelial growth factor-C induces lymphangiogenesis in the skin. *Circulation Research* **88**:623-629.

Enk AH and Katz SI (1992) Early molecular events in the induction phase of contact sensitivity. *Proceedings of the National Academy of Sciences of the USA* **89**:1398-1402.

Estess P, DeGrendele HC, Pascual V and Siegelman MH (1998) Functional activation of lymphocyte CD44 in peripheral blood is a marker of autoimmune disease activity. *Journal of Clinical Investigation* **102**:1173-1182.

Evanko SP, Angello JC and Wight TN (1999) Formation of hyaluronan- and versican-rich pericellular matrix is required for proliferation and migration of vascular muscle cells. *Arteriosclerosis, Thrombosis, and Vascular Biology* **19**:1004-1013.

Fackler MJ, Krause D, Smith O, Civin CI and May W (1995) Full length but not truncated CD34 inhibits haematopoietic cell differentiation of M1 cells. *Blood* **85**:3040.

Famiglietti J, Sun J, DeLisser HM and Albelda SM (1997) Tyrosine residue in exon 14 of the cytoplasmic domain of platelet endothelial cell adhesion molecule-1 (PECAM-1/CD31) regulates ligand binding specificity. *Journal of Cell Biology* **138**:1425-1435.

Fawcett DW (1986) *A textbook of histology*. W.B. Saunders, Philadelphia.

Feng D, Nagy JA, Pyne K, Dvorak HF and Dvorak AM (1998) Neutrophils emigrate from venules by a transendothelial cell pathway in response to FMLP. *Journal of Experimental Medicine* **187**:903-915.

Fina L, Molgaard HV, Robertson D, Bradley NJ, Monaghan P, Delia D, Sutherland DR, Baker MA and Greaves MF (1990) Expression of the CD34 gene in vascular endothelial cells. *Blood* **75**:2417-2426.

Fitzgerald KA and O'Neill LAJ (1999) Characterization of CD44 induction by IL-1: a critical role for Egr-1. *Journal of Immunology* **162**:4920-4927.

Fogt F, Zimmerman RL, Daly T and Gausas RE (2004) Observation of lymphatic vessels in orbital fat of patients with inflammatory conditions: a form fruste of lymphangiogenesis? *International Journal of Molecular Medicine* **13**:681-683.

Forster R, Schubel A, Breitfeld D, Kremmer E, Renner-Muller I, Wolf E and Lipp M (1999) CCR7 coordinates the primary immune response by establishing functional microenvironments in secondary lymphoid organs. *Cell* **99**:23-33.

Frankenberger M, Sternsdorf T, Pechumer H, Pforte A and Ziegler-Heitbrock HW (1996) Differential cytokine expression in human blood monocyte subpopulations: a polymerase chain reaction analysis. *Blood* **87**:373-377.

Fransen L, Muller R, Marmenout A, Tavernier J, van der heyden J, Kawashima E, Chollet A, Tizard R, van Heuverswyn H, van Vliet A, Ruysschaert M-R and Fiers W (1985) Molecular cloning of mouse tumour necrosis factor cDNA and its eukaryotic expression. *Nucleic Acids Research* **13**:4417-4429.

Fraser JR, Laurent TC and Laurent UBG (1997) Hyaluronan: its nature, distribution, functions and turnover. *Journal of Internal Medicine* **242**:27-33.

Freiberg RA, Spencer D, M., Choate KA, Duh HJ, Schreiber SL, Crabtree GR and Khavari PA (1997) Fas signal transduction triggers either proliferation or apoptosis in human fibroblasts. *Journal of Investigative Dermatology* **108**:215-219.

Furuse M, Fujita K, Kiiragi T, Fujimoto K and Tsukita S (1998) Claudin-1 and -2: novel integral membrane proteins localizing at tight junctions with no sequence similarity to occludin. *Journal of Cell Biology* **141**:1539-1550.

Galland F, Karamysheva A, Pebusque MJ, Borg JP, Rottapel R, Dubreuil P, Rosnet O and Birnbaum D (1993) The FLT4 gene encodes a transmembrane tyrosine kinase related to the vascular endothelial growth factor receptor. *Oncogene* **8**:1233-1240.

Gee K, Kozlowski M and Kumar A (2003) Tumour necrosis factor-alpha induces functionally active hyaluronan-adhesive CD44 by activating sialidase through p38 mitogen-activated protein kinase in lipopolysaccharide-stimulated human monocytic cells. *Journal of Biological Chemistry* **278**:37275-37287.

Geijtenbeek TB, Torensma R, van Vliet SJ, van Duijnhoven GC, Adema GJ, van Kooyk Y and Figdor CG (2000a) Identification of DC-SIGN, a novel dendritic cell-specific ICAM-3 receptor that supports primary immune responses. *Cell* **100**:575-585.

Geijtenbeek TBH, Krooshoop DJEB, Bleijs DA, van Vliet SJ, van Duijnhoven GCF, Grabovsky V, Alon R, Figdor CG and van Kooyk Y (2000b) DC-SIGN-ICAM-2 interaction mediates dendritic cell trafficking. *Nature Immunology* **1**:353-357.

Gerlier D and Thomasset N (1986) Use of MTT colorimetric assay to measure cell activation. *Journal of Immunological Methods* **94**:57-63.

Gerszten RE, Garcia-Zepeda EA, Lim Y-C, Yoshida M, Ding HA, Gimbrone MAJ, Luster AD, Luscinskas FW and Rosenzweig A (1999) MCP-1 and IL-8 trigger firm adhesion of monocytes to vascular endothelium under flow conditions. *Nature* **398**:718-723.

Goldstein LA, Zhou DFH, Picker LJ, Minty CN, Bargatze RF, Ding JF and Butcher EC (1989) A human lymphocyte homing receptor, the Hermes antigen, is related to cartilage proteoglycan core and link proteins. *Cell* **56**:1063-1072.

Gonzalez-Hernandez JA, Ehrhart-Bornstein M, Spath-Schwalbe E, Scherbaum WA and Bornstein SR (1996) Human adrenal cells express tumor necrosis factor-alpha messenger ribonucleic acid: evidence for paracrine control of adrenal function. *Journal of Clinical Endocrinology and Metabolism* **81**:807-813.

Graesser D, Solowiej A, Bruckner M, Osterweil E, Juedes A, Davis S, Ruddle NH, Engelhardt B and Madri JA (2002) Altered vascular permeability and early onset of experimental autoimmune encephalomyelitis in PECAM-1-deficient mice. *Journal of Clinical Investigation* **109**:383-392.

Gray PW, Aggarwal BB, Benton CV, Bringman TS, Henzel WJ, Jarrett JA, Leung DW, Moffat B, Ng P and Svedersky LP (1984) Cloning and expression of cDNA for human lymphotoxin, a lymphokine with tumour necrosis activity. *Nature* **312**:721-724.

Gray PW, Barrett K, Chantry D, Turner M and Feldmann M (1990) Cloning of human tumor necrosis factor (TNF) receptor cDNA and expression of recombinatn soluble TNF-binding protein. *Proceedings of the National Academy of Sciences of the USA* **87**:7380-7384.

Greenspan FS and Strewler GJ (eds) (1997) *Basic and clinical endocrinology*. Appleton and Lange, Stamford.

Greenwood J, Wang Y and Calder VL (1995) Lymphocyte adhesion and transendothelial migration in the central nervous system: the role of LFA-1, ICAM-1, VLA-4 and VCAM-1. *Immunology* **86**:408-415.

Grell M (1995) Tumor necrosis factor (TNF) receptors in cellular signaling of soluble and membrane-expressed TNF. *Journal of Inflammation* **47**:8-17.

Gretz JE, Anderson AO and Shaw S (1997) Cords, channels, corridors and conduits: critical architectural elements facilitating cell interactions in the lymph node cortex. *Immunology Reviews* **156**:11-24.

Gretz JE, Norbury CC, Anderson AO, Proudfoot AEI and Shaw S (2000) Lymph-borne chemokines and other low molecular weight molecules reach high endothelial venules via specialized conduits while a functional barrier limits access to the lymphocyte microenvironments in lymph node cortex. *Journal of Experimental Medicine* **192**:1425-1439.

Gröger M, Loewe R, Holnthoner W, Embacher R, Pillinger M, Herron GS, Wolff K and Petzelbauer P (2004) IL-3 induces expression of lymphatic markers prox-1 and podoplanin in human endothelial cells. *Journal of Immunlogy* **173**:7161-7169.

Gumina RJ, Kirschbaum NE, Rao PN, VanTuinen P and Newman PJ (1996) The human PECAM1 gene maps to 17q23. *Genomics* **34**:229-232.

Gunn MD, Kyuwa S, Tam C, Kakiuchi T, Matsuzawa A, Williams LT and Nakano H (1999) Mice lacking expression of secondary lymphoid organ chemokine have defects in lymphocyte homing and dendritic cell localization. *Journal of Experimental Medicine* **189**:451-460.

Guo Y, Feinberg H, Conroy E, Mitchell DA, Alvarez R, Blixt O, Taylor ME, Weis WI and Drickamer K (2004) Structural basis for distinct ligand-binding and targeting properties of the receptors DC-SIGN and DC-SIGNR. *Nature Structural and Molecular Biology* **11**:591-598.

Halden Y, Rek A, Atzenhofer W, Szilak L, Wabnig A and Kungl AJ (2004) Interleukin-8 binds to syndecan-2 on human endothelial cells. *Biochemistry Journal* **377**:533-538.

Hardingham TE and Muir H (1972) The specific interaction of hyaluronic acid with cartilage proteoglycans. *Biochemica et Biophysica Acta* **279**:401-405.

Haynes BF, Hale LP, Patton KL, Martin ME and McCallum RM (1991) Measurement of an adhesion molecule as an indicator of inflammatory disease activity. Upregulation of the receptor for hyaluronate (CD44) in rheumatoid arthritis. *Arthritis and Rheumatism* **34**:1434-1443.

Haynes BF, Telen MJ, Hale LP and Denning SM (1989) CD44 - a molecule involved in leukocyte adherence and T cell activation. *Immunology Today* **10**:423-428.

Hickinson DM, Lucocq JM, Towler MC, Clough S, James J, James SR, Downes CP and Ponnambalam S (1997) Association of a phosphatidylinositol-specific 3-kinase with a human trans-Golgi network resident protein. *Current Biology* **7**:987-990.

Hirakawa S, Hong Y-K, Harvey N, Schacht V, Matsuda K, Libermann T and Detmar M (2003) Identification of vascular lineage-specific genes by transcriptional profiling of isolated blood vascular and lymphatic endothelial cells. *American Journal of Pathology* **162**:575-586.

Hochman PS, Majeau GR, Mackay F and Browning JL (1995) Proinflammatory responses are efficiently induced by homotrimeric but not heterotrimeric lymphotoxin ligands. *Journal of Inflammation* **46**:220-234.

Höckel M, Schlenger K, Aral B, Mitze M, Schaffer U and Vaupel P (1996) Association between tumour hypoxia and malignant progression in advanced cancer of the uterine cervix. *Cancer Research* **56**:4509-4515.

Hong Y-K, Harvey N, Noh Y-H, Schacht V, Hirakawa S, Detmar M and Oliver G (2002) Prox1 is a master control gene in the program specifying lymphatic endothelial cell fate. *Developmental Dynamics* **225**:351-357.

Hua Q, Knudson CB and Knudson W (1993) Internalization of hyaluronan by chondrocytes occurs via receptor-mediated endocytosis. *Journal of Cell Science* **106**:365-375.

Huang F-P, Platt N, Wykes M, Major JR, Powell TJ, Jenkins CD and MacPherson GG (2000) A discrete subpopulation of dendritic cells transports apoptotic intestinal epithelial cells to T cell areas of mesenteric lymph nodes. *Journal of Experimental Medicine* **191**:435-443.

Huntington GS and McClure CFW (1910) The anatomy and development of the jugular lymph sac in the domestic cat (Felis domestica). *American Journal of Anatomy* **10**:177-311.

Hurtado JC, Kim Y-J and Kwon BS (1997) Signals through 4-1BB are costimulatory to previously activated splenic T cells and inhibit activation-induced cell death. *Journal of Immunlogy* **158**:2600-2609.

Imhof BA and Aurrand-Lions M (2004) Adhesion mechanisms regulating the migration of monocytes. *Nature Reviews Immunology* **4**:423-444.

Imura A and al. e (1996) *Journal of Experimental Medicine* **183**:2185-2194.

Irjala H, Johansson E-L, Grenman R, Alanen K, Salmi M and Jalkanen S (2001) Mannose receptor is a novel ligand for L-selectin and mediates lymphocyte binding to lymphatic endothelium. *Journal of Experimental Medicine* **194**:1033-1041.

Irrthum A, Karkkainen MJ, Devriendt K, Alitalo K and Vikkula M (2000) Congenital hereditary lymphedema caused by a mutation that inactivates VEGFR3 tyrosine kinase. *Americal Journal of Human Genetics* **67**:295-301.

Jackson DE (2003) The unfolding tale of PECAM-1. *Federation of European Biochemical Societies Letters* **540**:7-14.

Jackson DG (2004) Biology of the lymphatic marker LYVE-1 and applications in research into lymphatic trafficking and lymphangiogenesis. *Acta Pathologica, Microbiologica et Immunologica Scandinavica.* **112:** 526-538

Jakob T, Brown MJ and Udey MC (1999) Characterization of E-cadherin-containing junctions involving skin-derived dendritic cells. *Journal of Investigative Dermatology* **112**:102-108.

Jakob T, Ring J and Udey MC (2001) Multistep navigation of Langerhans/dendritic cells in and out of the skin. *Journal of Allergy and Clinical Immunology* **108**:688-696.

Jakob T and Udey MC (1998) Regulation of E-cadherin-mediated adhesion in Langerhans cell-like dendritic cells by inflammatory mediators that mobilize Langerhans cells in vivo. *Journal of Immunlogy* **160**:4067-4073.

Jalkanen S, Jalkanen M, Bargatze R, Tammi M and Butcher EC (1988) Biochemical properties of glycoproteins involved in lymphocyte recognition of high endothelial venules in man. *Journal of Immunlogy* **141**:1615-1623.

Jeltsch M, Kaipainen A, Joukov V, Meng X, Lakso M, Rauvala H, Swartz M, Fukumura D, Jain RK and Alitalo K (1997) Hyperplasia of lymphatic vessels in VEGF-C transgenic mice. *Science* **276**:1423-1428.

Johnson-Leger C, Aurrand-Lions M, Beltraminelli N, Fasel N and Imhof BA (2002) Junctional adhesion molecule-2 (JAM-2) promotes lymphocyte transendothelial migration. *Blood* **100**:2479-2486.

Johnson-Leger C, Aurrand-Lions M and Imhof BA (2000) The parting of the endothelium: miracle, or simply a junctional affair? *Journal of Cell Science* **113**:921-933.

Joukov V, Pajusola K, Kaipainen A, Chilov D, Lahtinen I, Kukk E, Saksela O, Kalkkinen N and Alitalo K (1996) A novel vascular endothelial growth factor, VEGF-C, is a ligand for the FLT4 (VEGFR-3) and KDR (VEGFR-2) receptor tyrosine kinases. *EMBO Journal* **15**:290-298.

Kaiserling E, Krober S and Geleff S (2003) Lymphatic vessels in the colonic mucosa in ulcerative colitis. *Lymphology* **36**:52-61.

Karkkainen MJ, Haiko P, Sainio K, Partanen J, Taipale J, Petrova TV, Jeltsch M, Jackson DG, Talikka M, Rauvala H, Betsholtz C and Alitalo K (2003) Vascular endothelial growth factor C is required for sprouting of the first lymphatic vessels from embryonic veins. *Nature Immunology* **5**:74-80.

Karpanen T, Egeblad M, Karkkainen MJ, Kubo H, Yla-Herttuala S, Jaattela M and Alitalo K (2001) Vascular endothelial growth factor C promotes tumour lymphangiogenesis and intralymphatic tumour growth. *Cancer Research* **61**:1786-1790.

Kaufman MH (1999) Observations of some of the plates used to illustrate the lymphatics sections of Andrew Fyfe's Compendium of the Anatomy of the Human Body, published in 1800. *Clinical Anatomy* **12**:27-34.

Kavanaugh AF, Lightfoot E, Lipsky PE and Oppenheimer-Marks N (1991) Role of CD11/CD18 in adhesion and transendothelial migration of T cells. *Journal of Immunology* **146**:4149-4156.

Kaya G, Rodriguez I, Jorcano JL, Vassalli P and Stamenkovic I (1997) Selective suppression of CD44 in keratinocytes of mice bearing an antisense CD44 transgene driven by a tissue-specific promoter disrupts hyaluronate metabolism in the skin and impairs keratinocyte proliferation. *Genes and Development* **11**:996-1007.

Kelm S, Schauer R and Crocker PR (1996) The sialoadhesins - a family of sialic acid-dependent cellular recognition molecules within the immunologlobulin superfamily. *Glycoconj J.* **13**:913-926.

Kern PA, Saghizadeh M, Ong JM, Bosch RJ, Deem R and Simsolo RB (1995) The expression of tumor nectorsis factor in human adipose tissue. Regulation by obseity, weight loss, and relationship to lipoprotein lipase. *Journal of Clinical Investigation* **95**:2111-2119.

Kirschbaum NE, Gumina RJ and Newman PJ (1994) Organization of the gene for human platelet/endothelial cell adhesion molecule-1 shows alternatively spliced isoforms and a functionally complex cytoplasmic domain. *Blood* **84**:4028-4037.

Kleinman HK, McGarvey ML, Liotta LA, Robey PG, Tryggvason K and Martin GR (1982) Isolation and characterization of type IV procollagen, laminin, and heparan sulfate proteoglycan from the EHS sarcoma. *Biochemistry* **21**:6188-6193.

Knudson CB and Knudson W (1993) Hyaluronan-binding proteins in development, tissue homeostasis, and disease. *FASEB Journal* **7**:1233-1241.

Knudson W, Bartnik E and Knudson CB (1993) Assembly of pericellular matrices by COS-7 cells transfected with CD44 homing receptor genes. *Proceedings of the National Academy of Sciences of the USA* **90**:4003-4007.

Kohda D, Morton CJ, Parkar AA, Hatanaka H, Inagaki FM, Campbell ID and Day AJ (1996) Solution structure of the link module: a hyaluronan binding domain involved in extracellular matrix stability and cell migration. *Cell* **86**:767-775.

Koukourakis MI, Giatromanolaki A, Sivridis E, Simopoulos K, Pastorek J, Wykoff CC, Gatter KC and Harris AL (2001) Hypoxia-regulated carbonic anhydrase-9 (CA9) relates to poor vascularization and resistance of squamous cell head and neck cancer to chemoradiotherapy. *Clinical Cancer Research* **7**:339-3403.

Krause DS, Fackler MJ, Civin CI and May WS (1996) CD34: Structure, biology and clinical utility. *Blood* **87**:1-13.

Kriehuber E, Breiteneder-Geleff S, Groeger M, Soleiman A, Schoppmann SF, Stingl G, Kerjaschki D and Maurer D (2001) Isolation and characterization of dermal lymphatic and blood endothelial cells reveal stable and functionally specialized cell lineages. *Journal of Experimental Medicine* **194**:797-808.

Kubo H, Fujiwara K, Jussila L, Hashi H, Ogawa M, Shimizu K, Awane M, Sakai Y, Takabayashi A, Alitalo K, Yamaoka Y and Nishikawa S-I (2000) Involvement of vascular endothelial growth factor receptor-3 in maintenance of integrity of endothelial cell lining during tumor angiogenesis. *Blood* **96**:546-553.

Kukk E, Wartiovaara U, Gunji Y, Kaukonen J, Buhring HJ, Rappold I, Matikainen MT, Vinko P, Partanen J, Palotie A, Alitalo K and Alitalo R (1997) Analysis of Tie receptor tyrosine kinase in haemopoietic progenitor and leukaemia cells. *British Journal of Haematology* **98**:195-203.

Kurth I, Willimann K, Schaerli P, Hunziker T, Clark-Lewis I and Moser B (2001) Monocyte selectivity and tissue localization suggests a role for breast and kidney-expressed chemokine (BRAK) in macrophage development. *Journal of Experimental Medicine* **194**:855-861.

Latchman D (1995) *Gene Regulation: A eukaryotic perspective.* Chapman and Hall, London.

Laurent TC and Fraser JR (1992) Hyaluronan. *FASEB Journal* **6**:2397-2404.

Leak LV and Burke JF (1966) Fine structure of the lymphatic capillary and the adjoining connective tissue area. *American Journal of Anatomy* **118**:785-809.

Lee SC, Liu W, Dickson DW, Brosnan CF and Berman JW (1993) Cytokine production by human fetal microglia and astrocytes. Differential induction by lipopolysaccharide and IL-1 beta. *Journal of Immunology* **150**:2659-2667.

Legg JW and Isacke C (1998) Identification and functional analysis of the exrin-binding site in the hyaluronan receptor, CD44. *Current Biology* **8**:705-708.

Lehmann JCU, Jablonski-Westrich D, Haubold U, Gutierrez-Ramos J-C, Springer T and Hamann A (2003) Overlapping and selective roles of endothelial intercellular adhesion molecule-1 (ICAM-1) and ICAM-2 in lymphocyte trafficking. *Journal of immunology* **171**:2588-2593.

Lesley J, He Q, Miyake K, Hamann A, Hyman R and Kincade PW (1992) Requirements for hyaluronic acid binding by CD44: a role for the cytoplasmic domain and activation by antibody. *Journal of Experimental Medicine* **175**:257-266.

Lesley J, Howes N, Perschl A and Hyman R (1994) Hyaluronan binding function of CD44 is transiently activated on T cells during an in vivo immune response. *Journal of Experimental Medicine* **180**:383-387.

Lesley J, Hyman R and Kincade PW (1993) CD44 and its interaction with extracellular matrix. *Advances in Immunology* **54**:271-335.

Leu AJ, Berk DA, Lymboussaki A, Alitalo K and Jain RK (2000) Absence of functional lymphatics within a murine sarcoma: a molecular and functional evaluation. *Cancer Research* **60**:4324-4327.

Levesque MC and Haynes BF (1996) In vitro culture of human peripheral blood monocytes induces hyaluronan binding and up-regulates monocyte variant CD44 isoform expression. *Journal of Immunology* **156**:1557-1565.

Levesque MC and Haynes BF (1997) Cytokine induction of the ability of human monocytes CD44 to bind hyaluronan is mediated primarily by TNFalpha and is inhibited by IL-4 and IL-13. *Journal of Immunology* **159**:6184-6194.

Lewthwaite J, Blake S, Hardingham T, Foulkes R, Stephens S, Chaplin L, Emtage S, Catterall C, Short S and Nesbitt A (1995) Role of TNF alpha in the induction of antigen induced arthritis in the rabbit and the anti-arthritic effect of species specific TNF alpha neutralising monoclonal antibodies. *Annals of Rheumatic Disease* **54**:366-374.

Li C-B, Gray PW, Lin P-F, McGrath KM, Ruddle FH and Ruddle NH (1987) Cloning and expression of murine lymphotoxin cDNA. *Journal of Immunlogy* **138**:4496-4501.

Liao HX, Lee DM, Levesque MC and Haynes BF (1995) N-terminal and central regions of the human CD44 extracellular domain participate in cell surface hyaluronan binding. *Journal of Immunology* **155**:3938-45.

Lind MH, Rozell B, Wallin RPA, van Hogerlinden M, Ljunggren H-G, Toftgård R and Sur I (2004) Tumor necrosis factor receptor 1- mediated signaling is required for skin cancer development induced by NF-kB inhibition. *Proceedings of the National Academy of Sciences of the USA* **101**:4972-4977.

Lisby S, Muller KM, Jongeneel CV, Saurat JH and Hauser C (1995) Nickel and skin irritants up-regulate tumor necrosis factor-alpha mRNA in keratinocytes by different but potentialily synergistic mechanisms. *International Immunology* 7:343-352.

Liu D and Sy MS (1997) Phorbol myristate acetate stimulates the dimerization of CD44 involving a cysteine in the transmembrane domain. *Journal of Immunology* **159**:2702-2711.

Lodish H, Baltimore D, Berk A, Zipursky SL, Matsudaira P and Darnell J (1995) *Molecular Cell Biology.* Scientific American Books, Inc.

Loetscher H, Pan YC, Lahm HW, Gentz R, Brockhaus M, Tabuchi H and Lesslauer W (1990) Molecular cloning and expression of the human 55 kd tumor necrosis factor receptor. *Cell* **61**:351-359.

Lou W, Krill D, Dhir R, Becich MJ, Dong J-T, Frierson HFJ, Isaacs WB, Isaacs JT and Gao A (1999) Methylation of the CD44 metastasis suppressor gene in human prostate cancer. *Cancer Research* **59**:2329-2331.

Luscinskas FW, Ma S, Nusrat A, Parkos CA and Shaw SK (2002) The role of endothelial cell lateral junctions during leukocyte trafficking. *Immunological Reviews* **186**:57-67.

Luther SA, Tang HL, Hyman PL, Farr AG and Cyster JG (2000) Coexpression of the chemokines ELC and SLC by T zone stromal cells and deletion of the ELC gene in the plt/plt mouse. *Proceedings of the National Academy of Sciences of the USA* **97**:12694-12699.

Lymboussaki A, Partanen TA, Olofsson B, Thomas-Crusells J, Fletcher CDM, de Waal RMW, Kaipainen A and Alitalo K (1998) Expression of the vascular endothelial growth factor C receptor VEGFR-3 in lymphatic endothelium of the skin and in vascular tumors. *Americal Journal of Pathology* **153**:395-403.

Madriota SJ, Jussila L, Jeltsch M, Compagni A, Baetens D, Prevo R, Banerji S, Huarte J, Montesano R, Jackson DG, Orci L, Alitalo K, Christofori G and Pepper MS (2001) Vascular endothelial growth factor-C mediated lymphangiogenesis promotes tumour metastasis. *EMBO Journal* **20**:672-682.

Makgoba MW, Sanders ME, Ginther Luce GE, Dustin ML, Springer TA, Clark EA, Mannoni P and Shaw S (1988) ICAM-1 a ligand for LFA-A-dependent adhesion of B, T and myeloid cells. *Nature* **6151**:86-88.

Mäkinen T, Jussila L, Veikkola T, Karpanen T, Kettunen M, Pulkkanen KJ, Kauppinen R, Jackson DG, Kubo H, Nishikawa S-I, Ylä-Herttuala S and Alitalo K (2001a) Inhibition of lymphangiogenesis with resulting lymphoedema in transgenic mice expressing soluble VEGF receptor-3. *Nature Medicine* 7:199-205.

Mäkinen T, Veikkola T, Mustjoki S, Karpanen T, Catimel B, Nice EC, Wise L, Mercer A, Kowalski H, Kerjaschki D, Stacker SA, Achen MG and Alitalo K (2001b) Isolated lymphatic endothelial cells transduce growth, survival and migratory signals via the VEGF-C/D receptor VEGFR-3. *EMBO Journal* **20**:4762-4773.

Mancardi S, Vecile E, Dusetti N, Calvo E, Stanta G, Burrone OR and Dobrina A (2003) Evidence of CXC, CC and C chemokine production by lymphatic endothelial cells. *Immunology* **108**:523-530.

Marchesi VT and Gowans JL (1964) The migration of lymphocytes through the endothelium of venules in lymph nodes: an electron microscope study. *Proc. R. Soc. Lon. Ser. B.* **159**:283-290.

Marino MW, Dunn A, Grail D, Inglese M, Noguchi Y, Richards E, Jungbluth A, Wada H, Moore M, Williamson B, Basu S and Old LJ (1997) Characterization of tumor necrosis factor-deficient mice. *Proceedings of the National Academy of Sciences of the USA* **94**:8093-8098.

Marsters SA, Frutkin AD, Simpson NJ, Fendly BM and Ashkenazi A (1992) Identification of cysteine-rich domains of the type I tumor necrosis factor receptor involved in ligand binding. *Journal of Biological Chemistry* **267**:5747-5750.

Martin-Fontecha A, Sebastiani S, Hopken UE, Uguccinoni M, Lipp M, Lanzavecchia A and Sallusto F (2003) Regulation of dendritic cell migration to the draining lymph node: impact on T lymphocyte traffic and priming. *Journal of Experimental Medicine* **198**:615-621.

Mattila MM-T, Ruohola JK, Karpanen T, Jackson DG, Alitalo K and Harkonen PL (2002) VEGF-C induced lymphangiogenesis is associated with lymph node metastasis in orthotopic MCF-7 tumours. *International Journal of Cancer* **98**:946-951.

McHale JF, Harari OA, Marshall D and Haskard DO (1999) Vascular endothelial cell expression of ICAM-1 and VCAM-1 at the onset of eliciting contact hypersensitivity in mice: evidence for a dominant role for TNF-alpha. *Journal of Immunology* **162**:1648-1655.

McLaughlin F, Hayes BP, Horgan CMT, Beesley JE, Campbell CJ and Randi AM (1998) Tumour necrosis factor (TNF)-alpha and interleukin (IL)-1beta down-regulate intercellular adhesion molecule (ICAM)-2 expression on the endothelium. *Cell Adhesion Communications* **6**:381-400.

McLaughlin F, Ludbrook VJ, Kola I, Campbell CJ and Randi AM (1999) Characterisation of the tumour necrosis factor (TNF)alpha response elements in the human ICAM-2 promoter. *Journal of Cell Science* **112**:4695-4703.

McQuibban GA, Butler GS, Gong J-H, Bendall L, Power C, Clark-Lewis I and Overall CM (2001) Matrix metalloproteinase activity inactivates the CXC chemokine stromal cell-derived factor-1. *Journal of Biological Chemistry* **276**:43503-43508.

McQuibban GA, Gong J-H, Wong JP, Wallace JL, Clark-Lewis I and Overall CM (2002) Matrix metalloproteinase processing of monocyte chemoattractant proteins generates CC chemokine receptor antagonists with anti-inflammatory properties in vivo. *Blood* **100**:1160-1167.

Medvedev AE, Espevik T, Ranges G and Sundan A (1996) Distinct roles of the two tumor necrosis factor (TNF) receptors in modulating TNF and lymphotoxin alpha effects. *Journal of Biological Chemistry* **271**:9778-9784.

Metzelaar MJ, Wijngaard PLJ, Peters PJ, Sixma JJ, Nieuwenhuis HK and Clevers HC (1991) CD63. A novel lysosomal membrane glycoprotein, cloned by a screening procedure for intracellular antigens in eukaryotic cells. *Journal of Biological Chemistry* **266**:3239-3245.

Meyer K and Palmer JW (1934) The polysaccharide of the vitreous humor. *Journal of Biological Chemistry* **107**:629-634.

Middleton J, Neil S, Wintle J, Clark-Lewis I, Moore H, Lam C, Auer M, Hub E and Rot A (1997) Transcytosis and surface presentation of IL-8 by venular endothelial cells. *Cell* **91**:385-395.

Miettinen M, Lindenmayer AE and Chaubal A (1994) Endothelial cell markers CD31, CD34 and BNH9 antibody to H- and Y-antigens - evaluation of their specificity and sensitivity in the diagnosis of vascular tumors and comparison with von Willebrande factor. *Modern Pathology* **7**:82-90.

Modrowski D, Godet D and Marie PJ (1995) Involvement of interleukin 1 and tumour necrosis factor alpha as endogenous growth factors in human osteoblastic cells. *Cytokine* **7**:720-726.

Moe RE (1963) Fine structures of the reticulum and sinuses of lymph nodes. *American Journal of Anatomy* **112**:311-335.

Mortimer PS (1997) Lymphatics. *Recent Advances in Dermatology* **15**:175-192.

Moss ML, Jin SL, Milla ME, Bickett DM, Burkhart W, Carter HL, Chen WJ, Clay WC, Didsbury JR, Hassler D, Hoffman CR, Kost TA, Lambert MH, Leesnitzer MA, McCauley P, McGeehan G, Mitchell J, Moyer M, Pahel G, Rocque W, Overtone LK, Schoenen F, Seaton T, Su JL, Becherer JD and al. e (1997) Cloning of a disintegrin metalloproteinase that processes precursor tumour-necrosis factor-alpha. *Nature* **385**:733-736.

Mu FT, Callaghan JM, Steele-Mortimer O, Stenmark H, Parton RG, Campbell PL, McCluskey J, Yeo JP, Tock EP and Toh BH (1995) EEA1, an early endosome-associated protein. EEA1 is a conserved alpha-helical peripheral membrane protein flanked by cystine "fingers" and contains a calmodulin-binding IQ motif. *Journal of Biological Chemistry* **270**:13503-13511.

Muller AM, Hermanns MI, Skrzynski C, Nesslinger M, Muller K-M and Kirkpatrick CJ (2002) Expression of the endothelial markers PECAM-1, vWf and CD34 in vivo and in vitro. *Experimental and Molecular Pathology* **72**:221-229.

Muller WA (2003) Leukocyte-endothelial-cell interactions in leukocyte transmigration and the inflammatory response. *Trends in Immunology* **24**:326-333.

Muller WA, Ratti CM, McDonnell SL and Cohn ZA (1989) A human endothelial cell-restricted, externally disposed plasmalemmal protein enriched in intercellular junctions. *Journal of Experimental Medicine* **170**:399.

Muller WA, Weigl SA, Deng X and Phillips DM (1993) PECAM-1 is required for transendothelial migration of leukocytes. *Journal of Experimental Medicine* **178**:449-460.

Nakae S, Komiyama Y, Narumi S, Sudo K, Horai R, Tagawa Y-I, Sekikawa K, Matsushima K, Asano M and Iwakura Y (2003) IL-1-induced tumour necrosis factor-alpha elicits inflammatory cell infiltration in the skin by inducing IFN-gamma-inducible protein 10 in the elicitation phase of the contact hypersensitivity response. *International Immunology* **15**:251-260.

Nandi A, Estess P and Siegelman M (2004) Bimolecular complex between rolling and firm adhesion receptors required for cell arrest: CD44 association with VLA-4 in T cell extravasation. *Immunity* **20**:455-465.

Narindrasorasak S, Yao P and Sarkar B (2003) Protein disulfide isomerase, a multifunctional protein chaperone, shows copper-binding activity. *Biochemistry and Biophysics Research Communications* **311**:405-414.

Neish AS, Williams AJ, Palmer HJ, Whitley MZ and Collins T (1992) Functional analysis of the human vascular cell adhesion molecule 1 promoter. *Journal of Experimental Medicine* **176**:1583-1593.

Neubauer K, Ritzel A, Saile B and Ramadori G (2000) Decrease of platelet-endothelial cell adhesion molecule 1-gene-expression in inflammatory cells and in endothelial cells in the rat liver following CCl4-administration and in vitro after treatment with TNFalpha. *Immunology Letters* **74**:153-164.

Newman PJ (1994) The role of PECAM-1 in vascular cell biology. *Annals of the New York Academy of Sciences* **714**:165-174.

Newman PJ, Berndt MC, Gorski J, White 2nd GC, Lyman S, Paddock C and Muller WA (1990) PECAM-1 (CD31) cloning and relation to adhesion molecules of the immunoglobulin gene superfamily. *Science* **247**:1219-1222.

Newton JP, Buckley CD, Jones EY and Simmons DL (1997) Residues on both faces of the first immunoglobulin fold contribute to homophilic binding sites of PECAM-1/CD31. *Journal of Biological Chemistry* **272**:20555-20563.

Newton JP, Hunter AP, Simmons DL, Buckley CD and Harvey DJ (1999) CD31 (PECAM-1) exists as a dimer and is heavily N-glycosylated. *Biochemistry and Biophysics Research Communications* **261**:283-291.

Nibbs RJB, Kriehuber E, Ponath PD, Parent D, Qin S, Campbell JDM, Henderson A, Kerjaschki D, Maurer D, Graham GJ and Rot A (2001) The beta-chemokine receptor D6 is expressed by lymphatic endothelium and a subset of vascular tumors. *American Journal of Pathology* **158**:867-877.

Niki T, Iba S, Tokunou M, Yamada T, Matsuno Y and Hirohashi S (2000) Expression of vascular endothelial growth factors A, B, C, and D and their relationships to lymph node status in lung adenocarcinoma. *Clinical Cancer Research* **6**:2431-2439.

Nisato RE, Harrison JA, Buser R, Orci L, Rinsch C, Montesano R, Dupraz P and Pepper MS (2004) Generation and characterization of telomerase-immortalized human lymphatic endothelial cells.

Nocentini G, Giunchi L, Ronchetti S, Krausz LT, Bartoli A, Moraca R, Migliorati G and Riccardi C (1997) A new member of the tumor necrosis factor-nerve growth factor receptor family inhibits T cell receptor-induced apoptosis. *Proceedings of the National Academy of Sciences of the USA* **94**:6216-6221.

Nortamo P, Li R, Renkonen R, Timonen T, Prieto J, Patarroyo M and Gahmberg CG (1991) The expression of human intercellular adhesion molecule-2 is refractory to inflammatory cytokines. *European Journal of Immunology* **21**:2629-2632.

Nose K, Saito H and Kuroki T (1990) Isolation of a gene sequence induced later by tumor-promoting 12-O-tetradecanoylphrobol-13-acetate in mouse osteoblastic cells (MC3T3-E1) and expressed constitutively in ras-transformed cells. *Cell Growth and Differentiation* **1**:511-518.

Ohl L, Mohaupt M, Czeloth N, Hintzen G, Kiafard Z, Zwirner J, Blankenstein T, Henning G and Forster R (2004) CCR7 govern skin dendritic cell migration under inflammatory and steady-state conditions. *Immunity* **21**:279-288.

Okamoto I, Kawano Y, Murakami D, Sasayama T, Araki N, Miki T, Wong AJ and Saya H (2001) Proteolytic release of CD44 intracellular domain and its role in the CD44 signaling pathway. *Journal of Cell Biology* **155**:1-8.

Olive PL, Aquino-Parsons C, MacPhail SH, Liao S-Y, Raleigh J, Lerman MI and Stanbridge EJ (2001) Carbonic anhydrase 9 as an endogenous marker for hypoxic cells in cervical cancer. *Cancer Research* **61**:8924-8929.

Oliver G, Sosa-Pineda B, Geisendorf S, Spana E, Doe CQ and Gruss P (1993) Prox1, a prospero-related homeobox gene expressed during mouse development. *Mechanisms of Development* **44**:3-16.

O'Neill LAJ (2004) TLRs: Professor Mechnikov, sit on your hat. *Trends in Immunology* **25**:687-694.

Oppenheimer-Marks N, Davis LS, Tompkins Bogue D, Ramberg J and Lipsky PE (1991) Differential utilization of ICAM-1 and VCAM-1 during the adhesion and transendothelial migration of human T lymphocytes. *Journal of Immunology* **147**:2913-2921.

Osawa M, Masuda M, Harada N, Lopes RB and Fujiwara K (1997) Tyrosine phosphorylation of platelet endothelial cell adhesion molecule-1 (PECAM-1, CD31) in mechanically stimulated vascular endothelial cells. *European Journal of Cell Biology* **72**:229-237.

Paavonen K, Puolakkainen P, Jussila L, Jahkola T and Alitalo K (2000) Vascular endothelial growth factor receptor-3 in lymphangiogenesis in wound healing. *Americal Journal of Pathology* **156**:1499-1504.

Pajusola K, Aprelikova O, Armstrong E, Morris S and Alitalo K (1993a) Two human FLT4 receptor tyrosine kinase isoforms with distinct carboxy terminal tails are produced by alternative processing of primary transcripts. *Oncogene* **8**:2931-2937.

Pajusola K, Aprelikova O, Korhonen J, Kaipainen A, Pertovaara L, Alitalo R and Alitalo K (1992) FLT4 receptor tyrosine kinase contains seven immunoglobulin-like loops and is expressed in multiple human tissues and cell lines. *Cancer Research* **52**:5738-5743.

Pajusola K, Aprelikova O, Korhonen J, Kaipainen A, Pertovaara L, Alitalo R and Alitalo K (1993b) FLT4 receptor tyrosine kinase contains seven immunoglobulin-like loops and is expressed in multiple human tissues and cell lines. *Cancer Research* **53**:3845.

Palframan RT, Jung S, Cheng G, Weninger W, Luo Y, Dorf M, Littman DR, Rollins BJ, Zweerink H, Rot A and von Andrian UH (2001) Inflammatory chemokine transport and presentation in HEV: a remote control mechanism for monocyte recruitment to lymph nodes in inflamed tissue. *Journal of Experimental Medicine* **194**:1361-1373.

Park M-J, Park I-C, Lee H-C, Woo S-H, Lee J-Y, Hong Y-J, Rhee C-H, Lee Y-S, Lee S-H, Shim B-S, Kuroki T and Hong S-I (2003) Protein kinase C-alpha activation by phorbol ester induces secretion of gelatinase B/MMP-9 through ERK 1/2 pathway in capillary endothelial cells. *International Journal of Oncology* **22**:137-143.

Parks WC, Wilson CL and Lopez-Boado YS (2004) Matrix metalloproteinases as modulators of inflammation and innate immunity. *Nature Reviews Immunology* **4**:617-629.

Parsons RJ and McMaster PD (1938) The effect of the pulse upon the formation and flow of lymph. *Journal of Experimental Medicine* **68**:353-376.

Partanen TA, Arola J, Saaristo A, Jussila L, Ora A, Miettinen M, Stacker SA, Achen MG and Alitalo K (2000) VEGF-C and VEGF-D expression in neuroendocrine cells and their receptor, VEGFR-3, in fenestrated blood vessels in human tissues. *FASEB Journal* **14**:2087-2096.

Pennica D, Hayflick JS, Bringman TS, Palladino MA and Goeddel DV (1985) Cloning and expression in Escherichia coli of the cDNA for murine tumour necrosis factor. *Proceedings of the National Academy of Sciences of the USA* **82**:6060-6064.

Pennica D, Nedwin GE, Hayflick JS, Seeburg PH, Derynck R, Palladino MA, Kohr WJ, Aggarwal BB and Goeddel DV (1984) Human tumour necrosis factor: precursor structure, expression and homology to lymphtoxin. *Nature* **312**:724-729.

Petrova TV, Makinen T, Makela TP, Saarela J, Virtanen I, Ferrell RE, Finegold DN, Kerjaschki D, Yla-Herttuala S and Alitalo K (2002) Lymphatic endothelial reprogramming of vascular endothelial cells by the Prox-1 homeobox transcription factor. *EMBO Journal* **21**:4593-4599.

Piali L, Hammel P, Uherek C, Bachmann F, Gisler RH, Dunon D and Imhof BA (1995) CD31/PECAM-1 is a ligand for alpha v beta 3 integrin involved in adhesion of leukocytes to endothelium. *Journal of Cell Biology* **130**:451-460.

Pierce JW, Schoenleber R, Jesmok G, Best J, Moore SA, Collins T and Gerritsen ME (1997) Novel inhibitors of cytokine-induced IkappaBalpha phosphorylation and endothelial cell adhesion molecule expression show anti-inflammatory effects in vivo. *Journal of Biological Chemistry* **272**:21096-21103.

Poritz LS, Garver KI, Tilberg AF and Koltun WA (2004) Tumour necrosis factor alpha disrupts tight juction assembly. *Journal of Surgical Research* **116**:14-18.

Prescott AR, Lucocq JM, James J, Lister JM and Ponnambalam S (1997) Distinct compartmentalization of TGN46 abd beta 1,4-galactosyltransferase in HeLa cells. *European Journal of Cell Biology* **72**:238-246.

Prevo R, Banerji S, Ferguson DJP, Clasper S and Jackson DG (2001) Mouse LYVE-1 is an endocytic receptor for hyaluronan in lymphatic endothelium. *Journal of Biological Chemistry* **276**:19420-19430.

Protin U, Schweighoffer T, Jochum W and Hilberg F (1999) CD44-deficient mice develop normally with changes in subpopulations and recirculation of lymphocyte subsets. *Journal of Immunlogy* **163**:4917-4923.

Proudfoot AEI, Power CA and Wells TNC (2000) The strategy of blocking the chemokine system to combat disease. *Immunological Reviews* **177**:246-256.

Qu C, Edwards EW, Tacke F, Angeli V, Llodra J, Sanchez-Schmitz G, Garin A, Haque NS, Peters W, van Rooijen N, Sanchez-Torres C, Bromberg J, Charo IF, Jung S, Lira SA and Randolph GJ (2004) Role of CCR8 and other chemokine pathways in the migration of moncyte-derived dendritic cells to lymph nodes. *Journal of Experimental Medicine* **200**:1231-1241.

Qureshi MH, Cook-Mills J, Doherty DE and Garvy BA (2003) TNFalpha-dependent ICAM-1 and VCAM-1-mediated inflammatory responses are delayed in neonatal mice infected with Pneumocystis carinii. *Journal of Immunology* **171**:4700-4707.

Ramirez MI, Millien G, Hinds A, Cao Y, Seldin DC and Williams MC (2003) T1alpha, a lung type I cell differentiation gene, is required for normal lung cell proliferation and alveolus formation at birth. *Developmental Biology* **256**:61-72.

Randolph GJ (2001) Dendritic cell migration to lymph nodes: cytokines, chemokines, and lipid mediators. *Seminars in Immunology* **13**:267-274.

Randolph GJ, Beaulieu S, Lebecque S, Steinman RM and Muller AM (1998) Differentiation of monocytes into dendritic cells in a model of transendothelial trafficking. *Science* **282**:480-483.

Randolph GJ and Furie MB (1996) Mononuclear phagocytes egress from an in vitro model of the vascular wall by migrating across endothelium in the basal to apical direction: role of intercellular adhesion molecule 1 and the CD11/CD18 integrins. *Journal of Experimental Medicine* **183**:451-462.

Rischer CE and Easton TA (1995) *Focus on Human Biology*. HarperCollins College Publishers, New York.

Rishi AK, Joyce-Brady M, Fisher J, Dobbs LG, Floros J, VanderSpek J, Brody JS and Williams MC (1995) Cloning, characterization and development expression of a rat lung alveolar type I cell gene in embryonic endodermal and neural derivatives. *Developmental Biology* **167**:294-306.

Robbiani DF, Finch RA, Jager D, Muller AM, Sartorelli AC and Randolph GJ (2000) The leukotriene C4 transporter MRP1 regulates CCL19 (MIP-3beta, ELC)-dependent mobilization of dendritic cells to lymph nodes. *Cell* **103**:757-768.

Robinson B (1907) The Pathologic Physiology of (I.)Tractus Lymphaticus, (II.) Lymph, in *The Abdominal and Pelvic Brain*.

Romer LH, McLean NV, Yan HC, Daise M, Sun J and DeLisser HM (1995) IFN-gamma and TNF-alpha induce redistribution of PECAM-1 (CD31) on human endothelial cells. *Journal of Immunology* **154**:658206592.

Roscic-Mrkic B, Fischer M, Leemann C, Manrique A, Gordon CJ, Moore JP, Proudfoot AEI and Trkola A (2003) RANTES (CCL5) uses the proteoglycan CD44 as an auxiliary receptor to mediate cellular activation signals and HIV-1 enhancement. *Blood* **102**:1169-1177.

Rossi A, Kapahi P, Natoli G, Takahashi T, Chen Y, Karin M and Santoro MG (2000) Anti-inflammatory cyclopentenone prostaglandins are direct inhibitors of IkB kinase. *Nature* **403**:103-108.

Rothlein R, Dustin ML, Marlin SD and Springer TA (1986) A human intercellular adhesion molecule (ICAM-1) distinct from LFA-1. *Journal of Immunology* **137**:1270-1274.

Rotta G, Edwards EW, Sangaletti S, Bennett C, Ronzoni S, Colombo MP, Steinman RM, Randolph GJ and Rescigno M (2003) Lipopolysaccharide or whole bacteria block the conversion of inflammatory monocytes into dendritic cells in vivo. *Journal of Experimental Medicine* **198**:1253-1263.

Ryan TJ (1989) Structure and function of lymphatics. *Journal of Investigative Dermatology* **93**:18S-24S.

Sabin FR (1902) On the origin of the lymphatic system from the veins, and the development of the lymph hearts and thoracic duct in the pig. *American Journal of Anatomy* **1**:367-389.

Sabin FR (1904) On the development of the superficial lymphatics in the skin of the pig. *American Journal of Anatomy* **3**:183-195.

Saharinen P, Tammela T, Karkkainen MJ and Alitalo K (2004) Lymphatic vasculature: development, molecular regulation and role in tumor metastasis and inflammation. *Trends in Immunology* **25**:387-395.

Sassetti C, Van Zante A and Rosen SD (2000) Identification of endoglycan, a member of the CD34/podocalyxin family of sialomucins. *Journal of Biological Chemistry* **275**:9001-9010.

Satomaa T, Renkonen O, Helin J, Kirveskari J, Makitie A and Renkonen R (2002) O-glycans on human high endothelial CD34 putatively participating in L-selectin recognition. *Blood* **99**:2609-2611.

Satterthwaite AB, Burn TC, Le Beau MM and Tenen DG (1992) Structure of the gene encoding CD34, a human hematopoietic stem cell antigen. *Genomics* **12**:788-794.

Schacht V, Ramirez MI, Hong Y-K, Hirakawa S, Feng D, Harvey N, Williams M, Dvorak AM, Dvorak HF, Oliver G and Detmar M (2003) T1alpha/podoplanin deficiency disrupts normal lymphatic vasculature formation and causes lymphedema. *EMBO Journal* **22**:3546-3556.

Schacht V, Dadras SS, Johnson LA, Jackson DG, Hong YK, Detmar M (2005) Up-regulation of the lymphatic marker podoplanin, a mucin-type transmembrane glycoprotein, in human squamous cell carcinomas and germ cell tumors. *American Journal of Pathology* **166**:913-921.

Schall TJ, Lewis M, Koller KJ, Lee A, Rice GC, Wong GH, Gatanaga T, Granger GA, Lentz R and Raab H (1990) Molecular cloning and expression of a receptor for human tumor necrosis factor. *Cell* **61**:361-370.

Scheinecker C, McHugh R, Shevach EM and Germain RN (2002) Constitutive presentation of a natural tissue autoantigen exclusively by dendritic cells in the draining lymph node. *Journal of Experimental Medicine* **196**:1079-1090.

Schenkel AR, Mamdouh Z, Chen X, Liebman RM and Muller WA (2002) CD99 plays a major role in the migration of monocytes through endothelial junctions. *Nature Immunology* **3**:143-150.

Schlingemann RO, Rietveld FJ, de Waal RM, Bradley NJ, I. SA, Davies AJ, Greaves MF, Denekamp J and Ruiter DJ (1990) Leukocyte antigen CD34 is expressed by a subset of cultured endothelial cells and on endothelial abluminal microprocesses in the tumor stroma. *Laboratory Investigation* **62**:690-696.

Schmid-Schonbein GW (1990a) Mechanisms causing initial lymphatics to expand and compress to promote lymph flow. *Archives of Histology and Cytology* **53**:107-114.

Schmid-Schonbein GW (1990b) Microlymphatics and lymph flow. *Physiology Reviews* **70**:987-1028.

Schmits R, Filmus J, Gerwin N, Senaldi G, Kiefer F, Kundig T, Wakeham A, Shahinian A, Catzavelos C, Rak J, Furlonger C, Zakarian A, Simard JJL, Ohashi PS, Paige CJ, Gutierrez-Ramos JC and Mak TW (1997) CD44 regulates hematopoetic progenitor distribution, granuloma formation and tumorigenicity. *Blood* **90**:2217-2233.

Schneeberger EE, Vu Q, LeBlanc BW and Doerschuk CM (2000) The accumulation of dendritic cells in the lung is impaired in CD18-/- but not ICAM-1-/- mutant mice. *Journal of Immunology* **164**:2472-2478.

Schoppmann SF, Bayer G, Aumayr K, Taucher S, Geleff S, Rudas M, Kubista E, Hausmaninger H, Samonigg H, Gnant M, Jakesz R and Horvat R (2004) Prognostic value of lymphangiogenesis and lymphovascular invasion in invasive breast cancer. *Annals of Surgery* **240**:306-312.

Shaw SK, Perkins BN, Lim Y-C, Liu Y, Nusrat A, Schnell FJ, Parkos CA and Luscinskas FW (2001) Reduced expression of junctional adhesion molecule and platelet/endothelial cell adhesion molecule-1 (CD31) at human vascular endothelial junctions by cytokines tumour necrosis factor-alpha plus interferon-gamma does no reduce leukocyte tranmigration under flow. *American Journal of Pathology* **159**:2281-2291.

Shenoy RK (2002) Management of disability in lymphatic filariasis - an update. *Journal of Communicable Disease* **34**:1-14.

Sherman L, Wainwright D, Ponta H and Herrlich P (1998) A splice variant of CD44 expressed in the apical ectodermal ridge presents fibroblast growth factors to limb mesenchyme and is required for limb outgrowth. *Genes and Development* **12**:1058-1071.

Shirai T, Yamaguchi H, Ito H, Todd CW and Wallace RB (1985) Cloning and expression in Escherichia coli of teh gene for human tumour necrosis factor. *Nature* **313**:803-806.

Shreeniwas R, Koga S, Karakurum M, Pinsky D, Kaiser E, Brett J, Wolitzky BA, Norton C, Plocinski J, Benjamin W, Burns DK, Goldstein A and Stern D (1992) Hypoxia-mediated induction of endothelial cell interleukin-1alpha. An autocrine mechanism promoting expression of leukocyte adhesion molecules on the vessel surface. *Journal of Clinical Investigation* **90**:2333-2339.

Shtivelman E and Bishop JM (1991) Expression of CD44 is repressed in neuroblastoma cells. *Molecular and Cellular Biology* **11**:5446-5453.

Simmons DL, Satterthwaite AB, Tene DG and Seed B (1992) Molecular cloning of a cDNA encoding CD34, a sialomucin of human hematopoietic stem cells. *Journal of Immunology* **148**:267-271.

Skobe M and Detmar M (2000) Structure, function, and molecular control of the skin lymphatic system. *Journal of Investigative Dermatology Symposium Proceedings* **5**:14-19.

Skobe M, Hawighorst T, Jackson DG, Prevo R, Janes L, Velasco P, Riccardi L, Alitalo K, Claffey K and Detmar M (2001) Induction of tumor lymphangiogenesis by VEGF-C promotes breast cancer metastasis. *Nature Medicine* 7:192-198.

Sligh JE, Ballantyne CM, Rich SS, Hawkins HK, Smith CW, Bradley A and Beaudet AL (1993) Inflammatory and immune responses are impaired in mice deficient in intercellular adhesion molecule 1. *Proceedings of the National Academy of Sciences of the USA* **90**:8529-8533.

Smith RA and Baglioni C (1987) The active form of tumor necrosis factor is a trimer. *Journal of Biological Chemistry* **262**:6951-6954.

Solowiej A, Biswas P, Graesser D and Madri JA (2003) Lack of platelet endothelial cell adhesion molecule-1 attenuates foreign body inflammation because of decreased angiogenesis. *American Journal of Pathology* **162**:953-962.

Spillmann D, Witt D and Lindahl U (19998) Defining the interleukin-8-binding domain of heparan sulfate. *Journal of Biological Chemistry* **273**:15487-15493.

Springer TA (1990) Adhesion receptors of the immune system. *Nature* **346**:425.

Stacker SA, Caesar C, Baldwin ME, Thornton GE, Williams RA, Prevo R, Jackson DG, Nishikawa S-I, Kubo H and Achen MG (2001) VEGF-D promotes the metastatic spread of tumor cells via the lymphatics. *Nature Medicine* 7:186-191.

Stamenkovic I, Amiot M, Pesando JM and Seed B (1989) A lymphocyte molecule implicated in lymph node homing is a member of the cartilage link protein family. *Cell* **56**:1057-1062.

Staunton DE, Dustin ML and Springer TA (1989) Functional cloning of ICAM-2, a cell adhesion ligand for LFA-1 homologous to ICAM-1. *Nature* **339**:61-64.

Staunton DE, Marlin SD, Stratowa C, Dustin ML and Springer TA (1988) Primary structure of ICAM-1 demonstrates interaction between members of the immunoglobulin and integrin supergene families. *Cell* **52**:925-933.

Stoop R, Gál I, Glant TT, McNeish JD and Mikecz K (2002) Trafficking of CD44-deficient murine lymphocytes under normal and inflammatory conditions. *European Journal of Immunology* **32**:2532-2542.

Straume O, Jackson DG and Akslen LA (2003) Independent prognostic impact of lymphatic vessel density and presence of low-grade lymphangiogenesis in cutaneous melanoma. *Clinical Cancer Research* **9**:250-256.

Sun J, Paddock C, Shubert J, Zhang H-B, Amin K, Newman PJ and Albelda SM (2000) Contributions of the extracellular and cytoplasmic domains of platelet-endothelial cell adhesion molecule-1 (PECAM-1/CD31) in regulating cell-cell localization. *Journal of Cell Science* **113**:1459-1469.

Sun J, Williams J, Yan H-C, Amin KM, Albelda S and DeLisser HM (1996a) Platelet endothelial cell adhesion molecule-1 (PECAM-1) homophilic adhesion is mediated by immunoglobulin-like domains 1 and 2 and depends on the cytoplasmic domain and the level of surface expression. *Journal of Biological Chemistry* **271**:18561-18570.

Sun QH, DeLisser HM, Zukowski MM, Paddock C, Albelda SM and Newman PJ (1996b) Individually distinct Ig homology domains in PECAM-1 regulate homophilic binding and modulate receptor affinity. *Journal of Biological Chemistry* **271**:11090-11098.

Swartz MA (2001) The physiology of the lymphatic system. *Advanced Drug Delivery Reviews* **50**:3-20.

Tammi R, Rilla K, Pienimaki J-P, MacCallum DK, Hogg M, Luukkonen M, Hascall VC and Tammi M (2001) Hyaluronan enters keratinocytes by a novel endocytic route for catabolism. *Journal of Biological Chemistry*.

Tanaka Y, Adams DH, Hubscher S, Hirano H, Siebenlist U and Shaw S (1993) T-cell adhesion induced by proteoglycan-immobilized cytokine MIP-1 beta. *Nature* **361**:79-82.

Tanaka Y, Albelda SM, Horgan KJ, van Seventer GA, Shimuzu Y, Newman W, Hallam J, Newman PJ, Buck CA and Shaw S (1992) CD31 expressed on distinctive T cell subsets is a preferential amplifier of beta1 integrin-mediated adhesion. *Journal of Experimental Medicine* **176**:245-253.

Tartaglia LA, Ayres TM, Wong GH and Goeddel DV (1993) A novel domain within the 55 kd TNF receptor signals cell death. *Cell* **74**:845-853.

Tchelingerian JL, Le Saux F and Jacque C (1996) Identification and topography of neuronal cell populations expressing TNF alpha and IL-1 alpha in response to hippocampal lesion. *Journal of Neuroscience Research* **43**:99-106.

Teder P, Vandivier RW, Jiang D, Liang J, Cohn L, Puré E, Henson PM and Noble PW (2002) Resolution of lung inflammation by CD44. *Science* **296**:155-158.

Termeer CC, Hennies J, Voith U, Ahrens T, Weiss JM, Prehm P and Simon JC (2000) Oligosaccharides of hyaluronan are potent activators of dendritic cells. *Journal of Immunology* **165**:1863-1870.

Thelen M (2001) Dancing to the tune of chemokines. *Nature Immunology* **2**:129-134.

Thompson RD, Noble KE, Larbi KY, Dewar A, Duncan GS, Mak TW and Nourshargh S (2001) Platelet-endothelial cell adhesion molecule-1 (PECAM-1)-deficient mice demonstrate a transient and cytokine-specific role for PECAM-1 in leukocyte migration through the perivascular basement membrane. *Blood* **97**:1854-1860.

Toole BP (2004) Hyaluronan: from extracellular glue to pericellular cue. *Nature Reviews Cancer* **4**:528-539.

Traweek ST, Kandalaft PL, Mehta P and Battifora H (1991) The human hematopoietic progenitor cell antigen (CD34) in vascular neoplasia. *American Journal of Clinical Pathology* **96**:25-31.

Turley EA, Noble PW and Bourguignon LYW (2002) Signaling properties of hyaluronan receptors. *Journal of Biological Chemistry* **277**:4589-4592.

Van den Steen PE, Husson SJ, Proost P, Van Damme J and Opdenakker G (2003b) Carboxyterminal cleavage of the chemokines MIG and IP-10 by gelatinase B and neutrophil collagenase. *Biochemistry and Biophysics Research Communications* **310**:889-896.

Van den Steen PE, Proost P, Wuyts A, Van Damme J and Opdenakker G (2000) Neutrophil gelatinase B potentiates interleukin-8 tenfold by aminoterminal processing, whereas it degrades cTAP-III, PF-4 and GRO-alpha and leaves RANTES and MCP-2 intact. *Blood* **96**:2673-2681.

Van den Steen PE, Wuyts A, Husson SJ, Proost P, Van Damme J and Opdenakker G (2003a) Gelatinase B/MMP-9 and neutrophil collagenase/MMP-8 process the chemokines human GCP-2/CXCL6, ENA-78/CXCL5 and mouse GCP-2/LIX and modulate their physiological activities. *European Journal of Biochemistry* **270**:3739-3749.

Varela LM and Ip MM (1996) Tumor necrosis factor-alpha: a multifunctional regulatory of mammary gland development. *Endocrinology* **137**:4915-4924.

Varon D, Jackson DE, Shenkman B, Dardik R, Tamarin I, Savion N and Newman PJ (1998) Platelet/endothelial cell adhesion molecule-1 serves as a costimulatory agonist receptor that modulates integrin-dependent adhesion and aggregation of human platelets. *Blood* **91**:500-507.

Veikkola T, Jussila L, Makinen T, Karpanen T, Jeltsch M, Petrova TV, Kubo H, Thurston G, McDonald DM, Achen MG, Stacker SA and Alitalo K (2001) Signalling via vascular endothelial growth factor receptor-3 is sufficient for lymphangiogenesis in transgenic mice. *EMBO Journal* **20**:1223-1231.

Velendzas D, Dufel S and McGovern TW (2004) Plague, eMedicine.com, Inc.

Vermaelen KY, Carro-Muino I, Lambrecht BN and Pauwels RA (2001) Specific migratory dendritic cells rapidly transport antigen from the airways to the thoracic lymph nodes. *Journal of Experimental Medicine* **193**:51-60.

Voet D and Voet JG (1995) *Biochemistry*. John Wiley and Sons, Inc, New York.

von Andrian UH and Mackay CR (2000) T-cell function and migration. *New England Journal of Medicine*:1020-1034.

von der Weid P-Y and Zawieja DC (2003) Lymphatic smooth muscle: the motor unit of lymph drainage. *International Journal of Biochemistry and Cell Biology* **36**:1147-1153.

Wang AM, Creasey AA, Ladner MB, Lin LS, Strickler J, Van Arsdell JN, Yamamoto R and Mark DF (1985) Molecular cloning of the complementary DNA for human tumor necrosis factor. *Science* **228**:149-154.

Ware CF, Crowe PD, Grayson MH, Androlewicz MJ and Browning JL (1992) Expression of surface lymphotoxin and tumor necrosis factor on activated T, B and natural killer cells. *Journal of Immunology* **149**:3881-3888.

Weinlich G, Heine M, Stossel H, Zanella M, Stoitzner P, Ortner U, Smolle J, Koch F, Sepp NT, Schuler G and Romani N (1998) Entry into afferent lymphatics and maturation in situ of migrating murine cutaneous dendritic cells. *Journal of Investigative Dermatology* **110**:441-448.

Weiss JM, Renkl AC, Maier CS, Kimmig M, Liaw L, Ahrens T, Kon S, Maeda M, Hotta H, Uede T and Simon JC (2001) Osteopontin is involved in the initiation of cutaneous contact hypersensitivity by inducing Landerhans and dendritic cell migration to lymph nodes. *Journal of Experimental Medicine* **194**:1219-1229.

Weller PF, Rand TH, Goelz SE, Chi-Rosso G and Lobb RR (1991) Human eosinophil adherence to vascular endothelium mediated by binding to vascular cell adhesion molecule 1 and endothelial leukocyte adhesion molecule 1. *Proceedings of the National Academy of Sciences of the USA* **88**:7430-7433.

Wetterwald A, Hoffstetter W, Cecchini MG, Lanske B, Wagner C, Fleisch H and Atkinson M (1996) Characterization and cloning of the E11 antigen, a marker expressed by rat osteoblasts and osteocytes. *Bone* **18**:125-132.

Wigle JT, Chowdhury K, Gruss P and Oliver G (1999) Prox1 function is crucial for murine lens fiber elongation. *Nature Genetics* **21**:318-322.

Wigle JT, Harvey N, Detmar M, Lagutina I, Grosveld G, Gunn MD, Jackson DG and Oliver G (2002) An essential role for Prox1 in the induction of the lymphatic endothelial cell phenotype. *EMBO Journal* **21**:1505-1513.

Wigle JT and Oliver G (1999) Prox1 function is required for the development of the murine lymphatic system. *Cell* **98**:769-778.

Williams CSM, Leek RD, Robson AM, Banerji S, Prevo R, Harris AL and Jackson DG (2003) Absence of lymphangiogenesis and intratumoural lymph vessels in human metastatic breast cancer. *Journal of Pathology* **200**:195-206.

Williams MC, Cao Y, Hinds A, Rishi AK and Wetterwald A (1996) T1 alpha protein is developmentally regulated and expressed by alveolar type I cells, chororoid plexus, and ciliary epithelia of adult rats. *American Journal of Respiratory Cell and Molecular Biology* **14**:577-585.

Wykoff CC, Beasley NJP, Watson PH, Turner KJ, Pastorek J, Wilson GD, Turley H, Maxwell PH, Pugh CW, Ratcliffe PJ and Harris AL (2001) Hypoxia inducible regulation of tumour associated carbonic anhydrases. *Cancer Research* **60**:7075-7083.

Xu H, Guan H, Zu G, Bullard D, Hanson J, Slater M and Elmets CA (2001) The role of ICAM-1 molecule in the migration of Langerhans cells in the skin and regional lymph node. *European Journal of Immunology* **31**:3085-3093.

Yagi T and Takeichi M (2000) Cadherin superfamily genes: functions, genomic organization, and neurologic diversity. *Genes and Development* **14**:1169-1180.

Yamada K, Takane N, Otabe S, Inada C, Inoue M and Nonaka K (1993) Pancreatic beta-cell-selective production of tumor necrosis factor-alpha induced by interleukin-1. *Diabetes* **42**:1026-1031.

Yan H-C, Baldwin HS, Sun J, Buck CA, Albelda SM and DeLisser HM (1995a) Alternative splicing of a specific cytoplasmic exon alters the binding characteristics of murine platelet/endothelial cell adhesion molecule-1 (PECAM-1). *Journal of Biological Chemistry* **270**:23672-23680.

Yan HC, Pilewski JM, Zhang Q, DeLisser HM, Romer L and Albelda SM (1995b) Localization of multiple functional domains on human PECAM-1 (CD31) by monoclonal antibody epitope mapping. *Cell Adhesion Communications* **3**:45-66.

Yoon Y-S, Murayama T, Gravereaux E, Tkebuchava T, Silver M, Curry C, Wecker A, Kirchmair R, Hu CS, Kearney M, Ashare A, Jackson DG, Kubo H, Isner JM and Losordo DW (2003) VEGF-C gene therapy augments postnatal lymphangiogenesis and ameliorates secondary lymphedema. *Journal of Clinical Investigation* **111**:717-725.

Young AJ (1999) The physiology of lymphocyte migration through the single lymph node *in vivo*. *Seminars in Immunology* **11**:73-83.

Young AJ, Seabrook TJ, Marston WL, Dudler L and Hay JB (2000) A role for lymphatic endothelium in the sequestration of recirculating gamma-delta T cells in TNFalpha-stimulated lymph nodes. *European Journal of Immunology* **30**:327-334.

Yuan J (1997) Transducing signals of life and death. *Current Opinions in Cell Biology* **9**:247-251.

Zhang M, Singh RK, Wang MH, Wells A and Siegal GP (1996) *Clinical and Experimental Metastasis* **14**:268-276.

Zhang M, Wang MH, Singh RK, Wells A and Siegal GP (1997) Epidermal growth factor induces CD44 gene expression through a novel regulatory element in mouse fibroblasts. *Journal of Biological Chemistry* **272**:14139-14146.

Zheng Z, Katoh S, He Q, Oritani K, Miyake K, Lesley J, Hyman R, Hamik A, Parkhouse ME, Farr AG and Kincade PW (1995) Monoclonal antibodies to CD44 and their influence on hyaluronan recognition. *Journal of Cell Biology* **130**:485-495.

Zhou B, Weigel JA, Fauss L and Weigel PH (2000) Identification of the hyaluronan receptor for endocytosis (HARE). *Journal of Biological Chemistry* **275**:37733-37741.

Zhou LJ and Tedder TF (1995) A distinct pattern of cytokine gene expression by human CD83+ blood dendritic cells. *Blood* **86**:3295-3301.

Zinkernagel RM (1996) Immunology taught by viruses. *Science* **271**:173-178.

Zinman B, Hanley AJG, Harris SB, Kwan J and Fantus IG (1999) Circulating tumour necrosis factor-alpha concentrations in a native Canadian population with high rates of type 2 diabetes mellitus. *Journal of Clinical Endocrinology and Metabolism* **84**:272-278.

Appendix I

Preliminary characterisation of the LYVE-1 gene

A1.1 Introduction

The generation of a LYVE-1$^{-/-}$ knock-out mouse to study the phenotype and establish the physiological role of LYVE-1 was part of the original project undertaken in this PhD. However, when it became known that such a transgenic mouse was in the later stages of being produced by Regeneron, this aspect of the project was terminated. Instead, preliminary mapping of the LYVE-1 promoter was performed and this may provide a basis for further studies.

A1.2 Results

A1.2.1 Identification of LYVE-1 genomic clones from a mouse PAC library

To isolate clones containing LYVE-1 sequence, a mouse 129 strain genomic library, spotted on seven separate filters was used. This library (from the UK Human Genome Mapping Centre) had been prepared from female 129/SvevTACfBr mouse spleen and uses a pPAC$_4$ vector based on a P1 plasmid, a large single-copy plasmid containing large inserts averaging in size at 147Kb.

The DNA sequence used to probe this PAC library was derived by PCR amplification of embryonic (E13.5) balb/c cDNA using the primers 157F (GAACTCTCCATCCAGCTTGGTG) and 471R(CTGCGCTGACTCTACCTGGTC) and comprised mouse LYVE-1 exon 1, part of exon 2 and the intervening intron. This DNA was used as a probe for Southern blotting of the filters. Of the seven filters probed, three displayed positive results and a total of five clones were

identified as containing the desired sequence. These were named 457P18, 493O10, 530D13, 565L9 and 497B1, each over 20kb.

The intended strategy was to knock-out exon 1 which encodes the leader peptide and ideally also exons 2 and 3, which together encode the Link domain. PCR analysis of the clones selected from the library revealed that they all contained sequences from exon 1 through exon 5 and were therefore appropriate for the preparation of the knock-out construct.

Further studies proceeded with mapping one of the clones, 457P18 using a range of 6-base cutter restriction endonucleases in single digests. The fragments generated were separated by agarose gel electrophoresis and transferred to nitrocellulose membrane for Southern blotting using LYVE-1 probes generated by PCR amplification of balb/c genomic DNA by the primers 290F (CTAGGCACCCAGTCCAAGG) and 471R (CTGCGCTGACTCTACCTGGTC); and 451F (GACCAGGTAGAGTCAGCGCAG) and 528R (GATGACAGAGAACTGTTCTCCAAC), as probes for exon 1, (figure A1.1) and exon 2, (figure A1.2) respectively.

The results (figures A1.1 and A1.2) showed that each probe hybridised to the same 7-kb *Kpn*I fragment, which was therefore selected for cloning into pBluescript. However, this was not used for the knock-out construct as at this stage it became known that Regeneron were generating such a mouse and the emphasis of this part of the PhD changed to characterising the LYVE-1 gene.

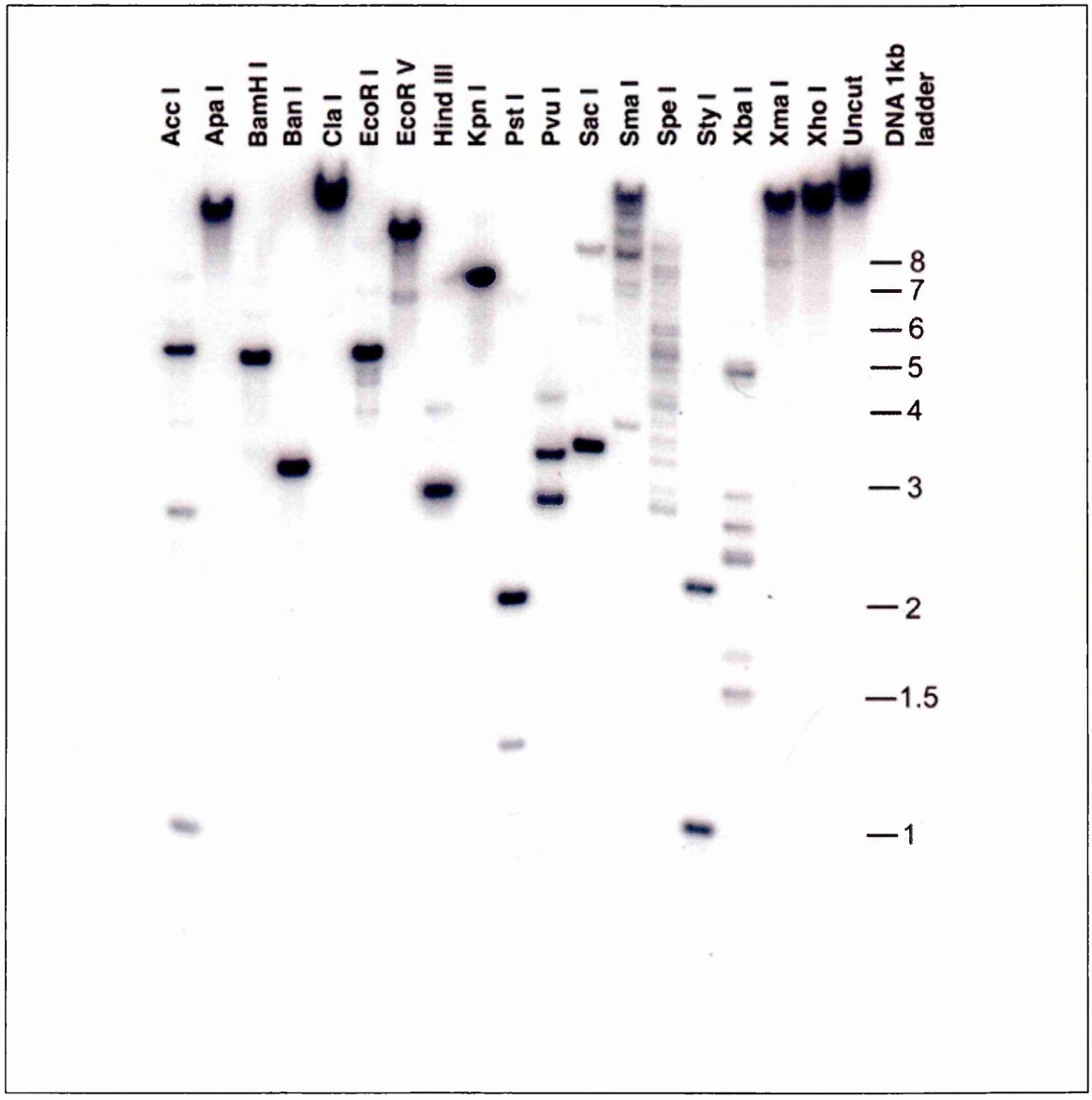

Figure A1.1 Southern blotting of fragments of PAC clone 457P18 with a LYVE-1 exon 1 probe. Fragments were generated by a panel of restriction enzymes and separated by agarose gel electrophoresis prior to transfer onto Hybond N+ membrane and probing using a DNA probe generated by PCR of LYVE-1 exon 1.

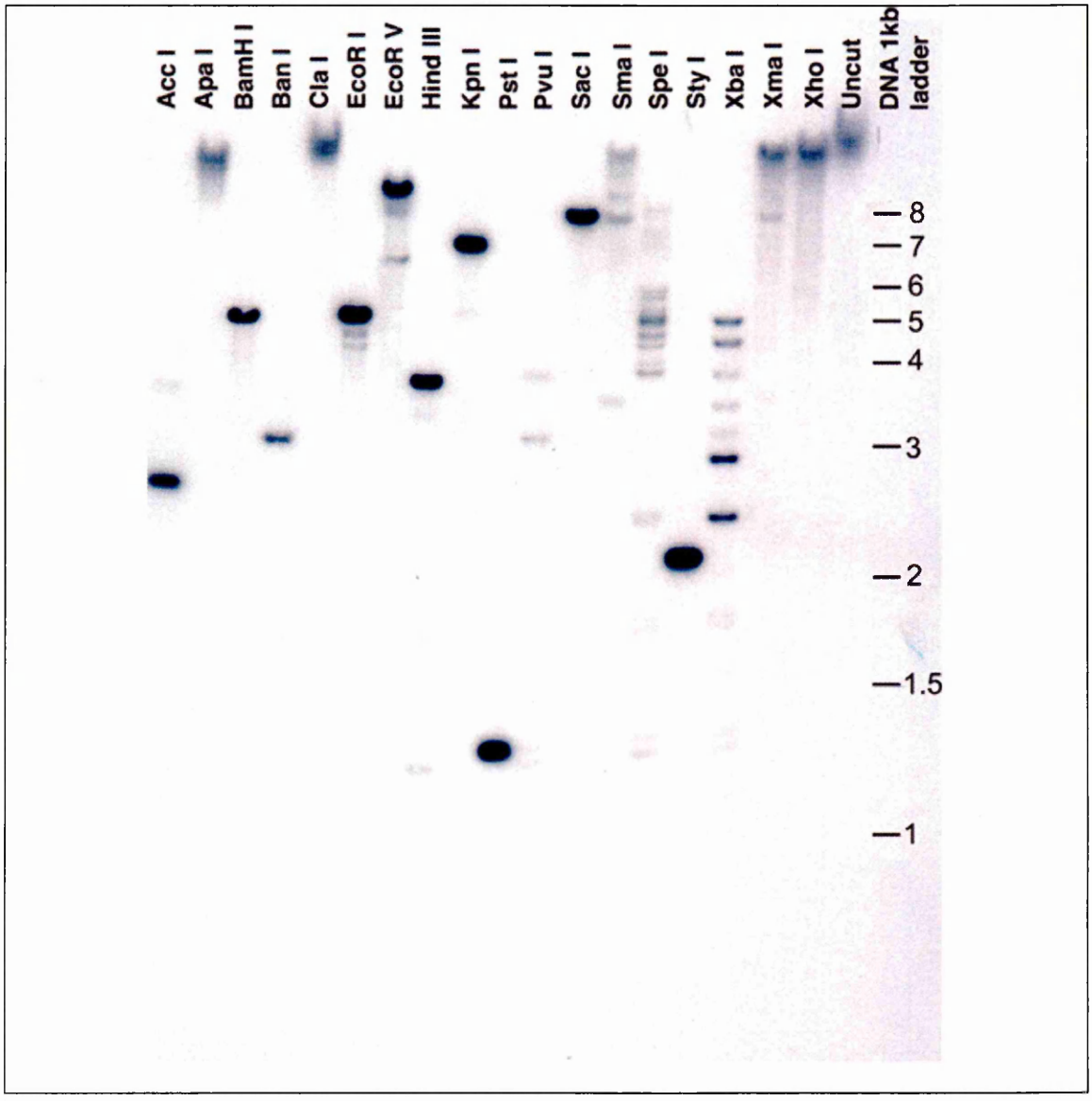

Figure A1.2 Southern blotting of fragments of PAC clone 457P18 with a LYVE-1 exon 2 probe. Fragments were generated by a panel of restriction enzymes and separated by agarose gel electrophoresis prior to transfer onto Hybond N+ membrane and probing using a DNA probe generated by PCR of LYVE-1 exon 2.

A1.2.2 Mapping of the LYVE-1 transcription start site by primer extension analysis

To map the 5′ end transcription start site of LYVE-1, primer extension was performed whereby oligonucleotides complementary to sequence at the 5′ of exon 1 were radiolabeled at the 5′ end and used to prime synthesis of cDNA within the 5′ UT of the LYVE-1 mRNA, extending from the primer to the 5′ terminus of the LYVE-1 mRNA. Products were subjected to polyacrylamide electrophoresis and the length of product from each primer was used to determine the distance of the primer from the transcription initiation site of the mRNA.

As a positive control for the primer extension reaction, the 5′UT of CD44 was extended using a CD44 primer designed previously for primer extension analysis of the human CD44 gene (Shtivelman and Bishop, 1991) on commercially available human spleen RNA (Clontech). The reaction yielded a product of the expected size of 163 nucleotides from the initiation site (figure A1.3). As expression of LYVE-1 is mostly restricted to lymphatic endothelium, only a small number of tissues proved abundant sources of RNA. This experiment pre-dated the availability of commercially available HDLEC from PromoCell (chapter 4 of this thesis) and due to lack of human tissue readily obtainable, primer extension analysis was performed on RNA isolated from mouse lung tissue, which was shown to contain abundant LYVE-1 message by reverse-transcriptase PCR (data not shown). To define the most suitable primers for primer extension analysis, 5 different primers were used (shown in figure A1.4), which all yielded products (figure A1.5) and enabled the 5′ end transcription start site of mouse LYVE-1 to be mapped, as indicated in figure A1.4.

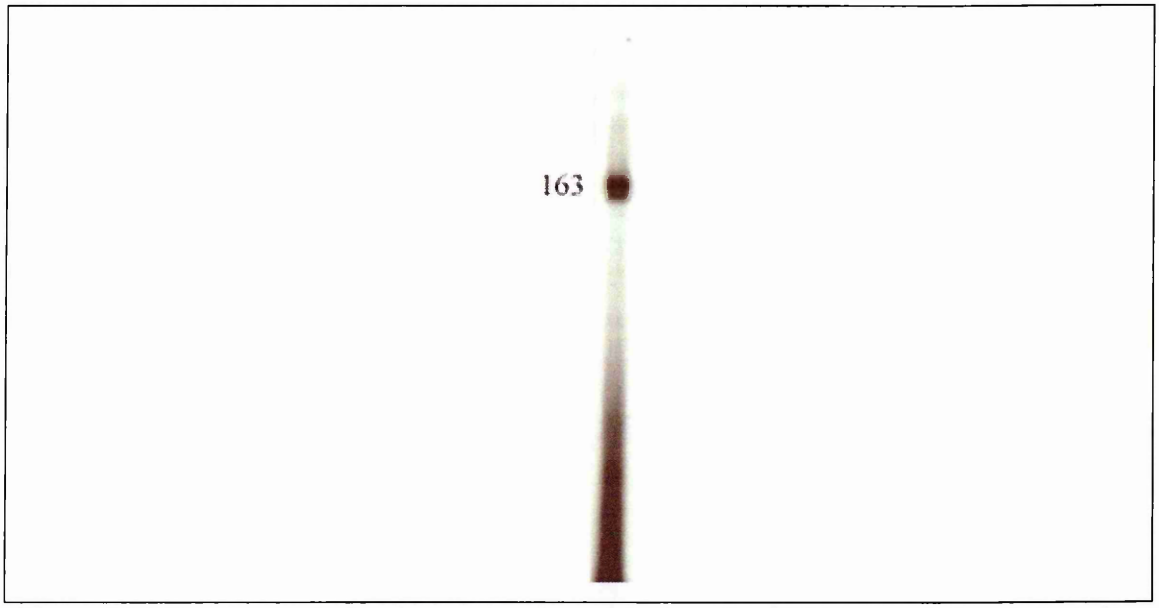

Figure A1.3 Positive control: primer extension analysis of the CD44 transcriptional start site. The CD44 primer used by Shtivelman and Bishop (1991) was used to generate a product of the expected size of 163 nucleotides from the primer to the initiation site, from commercially available human spleen RNA (Clontech), 30μg, detected by autoradiography.

TAGAACTCTCCATCCAGCTTGGTGATTGAACATCTGTCTCCCTTACTGCGG

GTGGCCAGCCACAGTGCCCCG**GAGGGATCTGCACA**ATGCCCAGCACAC

TA[1]GCCTGGTGTTACTC**CTCGCCTCTATTTGGACCACTAGGCACCCAGT**[2]

CCAAGGTGCCGACCTCGTGCAAGACCTTTCCATTT**CTACATGCAGAATC**

ATGGGCGTTGCCCTT[3]GTGGGCAGAAACAAAAACCCACAGATGAAT**TTC**

ACAGAAGCCAACGAGGCCTGTAAGATG[4]CTGGGACTGACTCTGGCCAG

CAGGGACCAGGTA**GAGTCAGCGCAGAAATCTGGCTTTGAGACT**[5]TGC…

….Exons 3, 4, 5 and 6.

Figure A1.4 Positions of primers (1-5) used for primer extension to map the transcription site of mouse LYVE-1 sequence. Complementary primer sequence is underlined, untranslated sequence is shown in black, exon 1 in red and exon 2 in blue. Sequence commences with the transcription initiation site mapped by primer extension (figure A1.5). The intron between exons 1 and 2 is not shown.

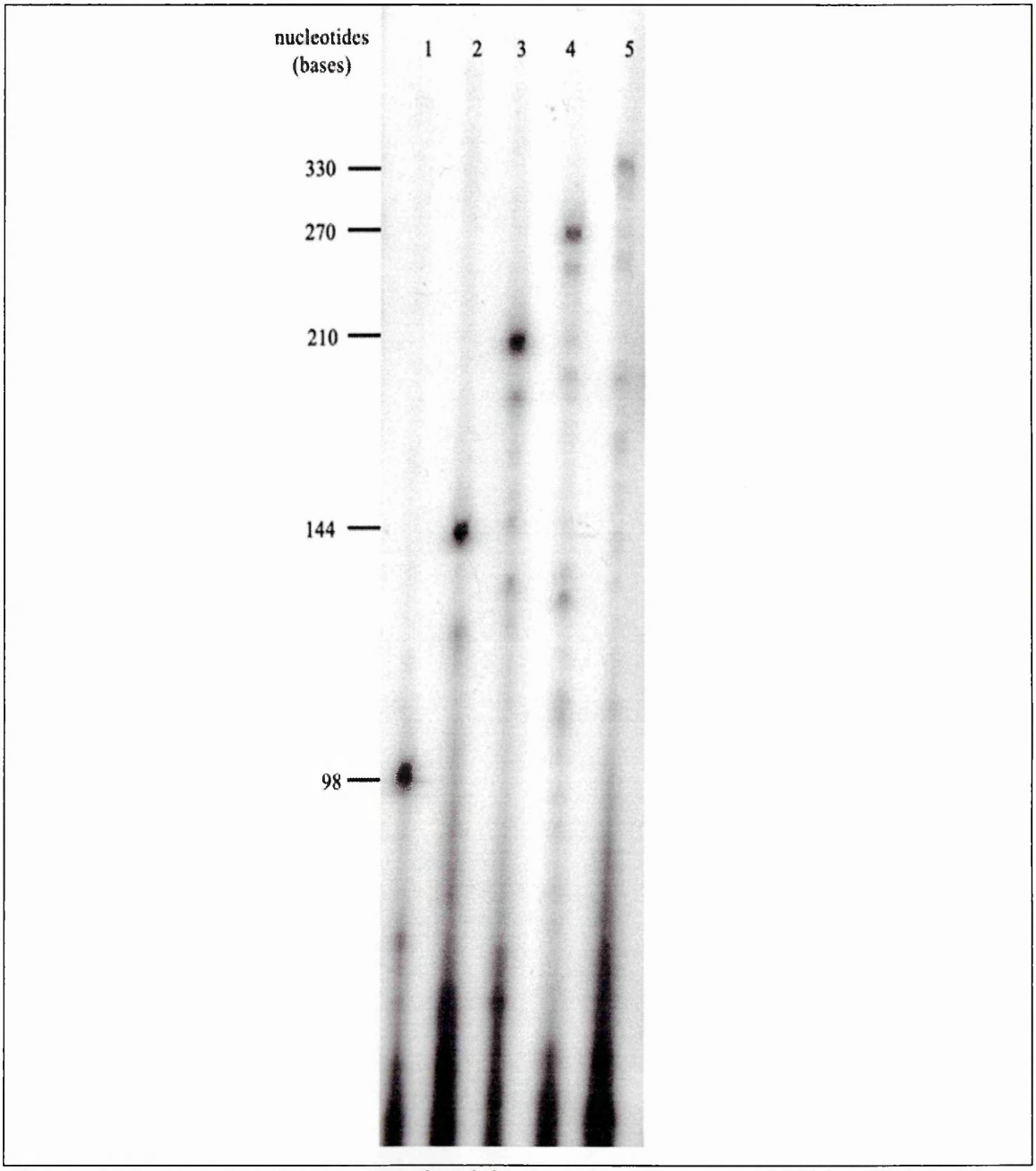

Figure A1.5. Mapping the transcription initiation site of mouse *LYVE-1* mRNA. Primer extension analysis was performed using 40μg of total RNA from mouse lung using primers 1-5. Products were electrophoresed in the corresponding lanes and detected by autoradiography. The sizes of each are indicated (bases). Lower molecular weight, feint bands which migrated faster than the main bands of products and are thus visible lower down the gel represent incomplete extensions caused by premature dissociation of the reverse transcriptase enzyme. The over-exposure at the bottom of the gel represents unextended primers.

A1.2.3 Identification of putative promoter sequences in human LYVE-1

Cloning potential upstream regulatory sequences into luciferase reporter constructs

To identify promoter sequences upstream of the *LYVE-1* gene, segments of the human gene immediately upstream of the transcription start site were cloned into reporter constructs. Studies were performed on the human gene due to greater availability of sequence data. The transcription start site in the human gene was assumed to be the same as in the mouse gene, identified through primer extension, as the two genes share similar organisation of exons and introns (data not shown). The two reporter vectors, pGL3Basic and pGL3Enhancer, encoding the luciferase gene, downstream of a multiple cloning site were used (figure A1.6). One construct, pGL3 Enhancer, also contained an additional downstream SV40 enhancer element, to increase the activity of the promoter. As a positive control, a chicken β-actin promoter was excised from pBR-β-actin-Luc (a kind gift from Dr. Katya Simon) using *Xho*I and *Hin*dIII, and cloned into both constructs for transfection efficiency, for the validation of the luciferase assay. Initially a sequence of 2.0 kb was amplified from human genomic DNA using the primers HuLYVE1-91561F*Xho*I (GACTACTGCTCGAGTAGAGAGCTCTGCTTGAGCC) and 93610R*Hind*III (GTCATCAGAAAGCTTCCAGGCTGAAGCACCTGGCCATC), with TaqPlus polymerase, a mixture of high fidelity polymerase and high efficiency polymerase. Following digestion with *Xho*I and *Hin*dIII the 2-kb product was cloned into the two *Xho*I/*Hin*dIII-cut luciferase reporter constructs, for transfection in to cell lines.

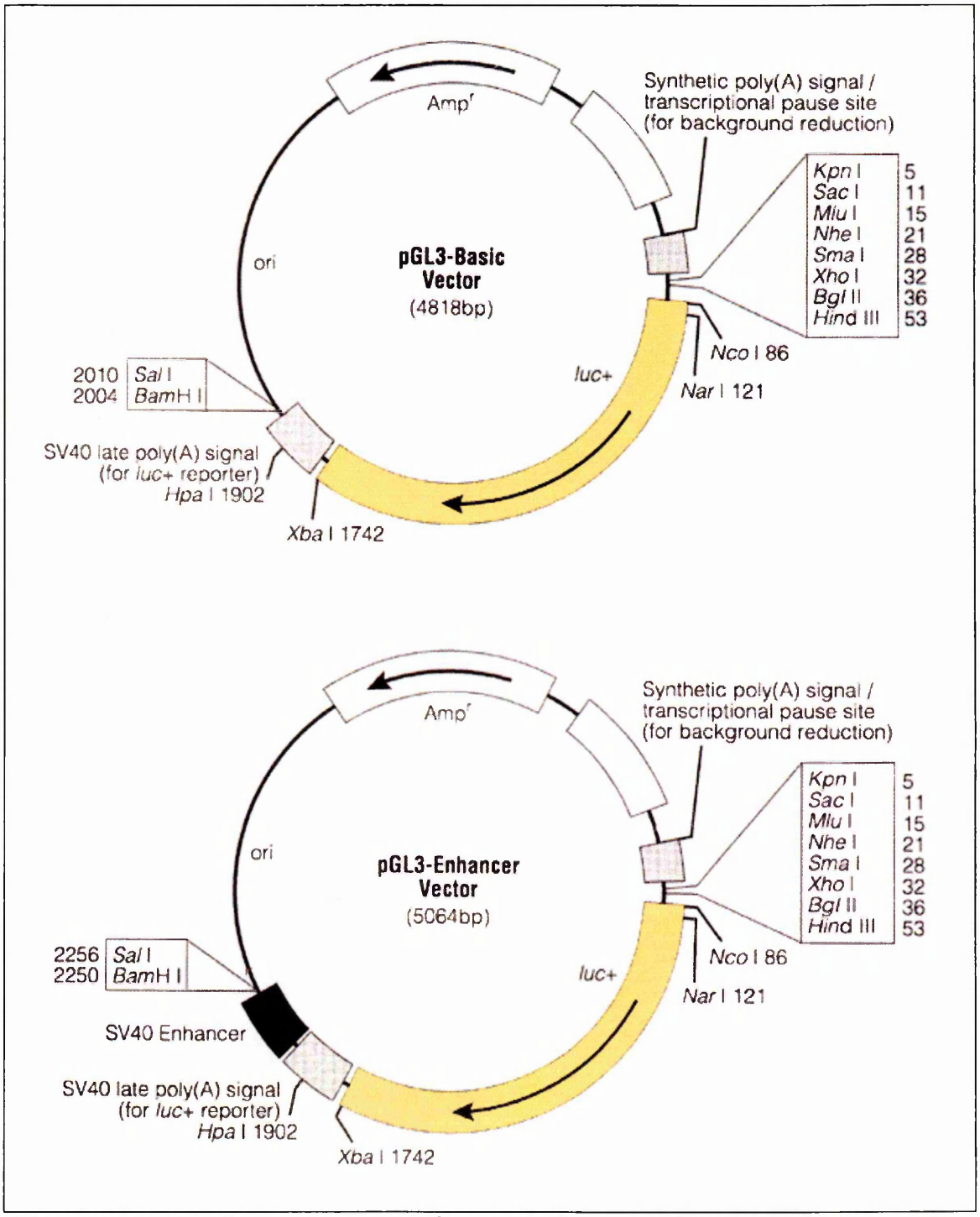

Figure A1.6 pGL3 luciferase vector maps. Sequence indicated *luc+* (shown in yellow) represents cDNA encoding the modified firefly luciferase; Amp^r, the gene conferring ampicillin resistance in E. coli; ori, origin of replication in E. coli. Arrows within *luc+* and the Amp^r gene indicate the direction of transcription. (Adapted from the Promega catalogue).

Analysis of LYVE-1 promoter activity in transfected cell lines

To assay for LYVE-1 promoter activity of genomic DNA upstream of the LYVE-1 coding sequence, reporter constructs were transfected into a range of cell lines. Ideally the choice of candidate cell line should endogenously express LYVE-1 and be readily transfectable. However, primary lymphatic endothelial cells (LEC) only became available at a later stage of this thesis and therefore could not be used for these experiments. Therefore in these preliminary studies, the first cell line selected for transfection was the human embryonic kidney fibroblast cells 293T. These have the advantage of high transfection efficiency by calcium phosphate, although they do not express LYVE-1. The second cell line used was the mouse monocyte-macrophage cell line RAW264.7. LYVE-1 expression has been detected on a subpopulation of macrophages isolated from mouse peritoneal cavities (for example, see figure A1.7) and although no basal LYVE-1 expression was detected in RAW264.7 (data not shown), it was considered possible that these cells might have the necessary transcription factors to recognise the human LYVE-1 promoter. Finally transfection of the endothelial cell line HUVEC was performed because these cells represented the closest lineage to LEC available at the time these assays were performed. Indeed LYVE-1 was originally cloned from a HUVEC cDNA library (Banerji et al., 1999) and LYVE-1 is expressed on blood vasculature in the embryo.

293T

The luciferase constructs generated were used to transfect 293T by calcium phosphate, alongside negative controls of empty vector. Luciferase activity was observed in cells transfected with β-actin positive controls but the LYVE-1 constructs displayed luciferase activity that was not significantly greater than that of the negative controls (empty vectors), (table A1.1). In fact, both basic and enhancer constructs containing the 2kb fragment actually induced less luciferase activity than the vector alone. The lack of a positive result from the 2kb

constructs could be due to either this sequence lacking promoter activity or, more likely due to an inability of 293T cells to transcribe LYVE-1, a protein that has never been shown to be expressed in these cells.

RAW264.7

The luciferase constructs were used to transfect RAW 264.7 by lipofectin and lysates were assayed for luciferase activity. Results showed that the 2kb constructs displayed less luciferase activity than that of empty vectors, although both data from empty vectors and LYVE-1 constructs showed very low activity in comparison to that from β-actin constructs (table A1.2).

HUVEC

The endothelial cell line, HUVEC were transfected with the luciferase constructs by Nucleofector™ electroporation (Amaxa). However, as with the other cell lines, transfection with the 2kb LYVE-1 construct displayed luciferase activity that was not significantly greater than that of the empty vectors, although the positive controls indicated that transfection had been efficient in parallel samples (table A1.3).

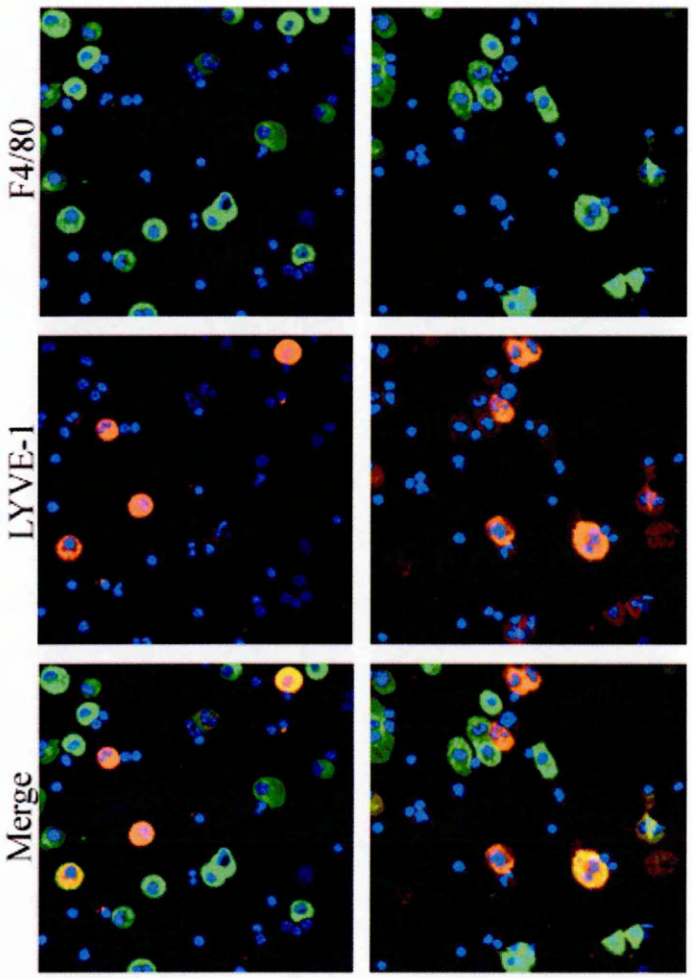

Figure A1.7 Expression of LYVE-1 in a subpopulation of mouse peritoneal macrophages. Slides of cells obtained by peritoneal lavage were prepared by cytospin and stained using the anti-mannose receptor mAb, F4/80 (a kind gift from Prof. Simon Gordon, Sir William Dunn School of Pathology, Oxford) and rabbit anti-LYVE-1 antisera. The appropriate AlexaFluor® 488 and 594-conjugated goat antibodies were used for secondary detection and nuclei counter-stained with DAPI. Images were captured at magnification: x 32.

Construct	Mean luciferase activity (arbitary units)	Standard error
pGL3Basic	78.72	3.56
pGL3Basic+2kb	24.44	18.36
pGL3Basic+β-actin	>9999	-
pGL3Enh	45.98	9.92
pGL3Enh+2kb	23.58	19.06
pGL3Enh+β-actin	>9999	-

Table A1.1 Luciferase activity from 2kb LYVE-1 sequence in 293T transfectants. Cells in 6-well dishes were transfected with 1 μg/well DNA by calcium phosphate precipitation, in duplicate for each construct. Following 24h incubation, cell lysates were prepared using reporter lysis buffer (Promega) and luciferase assays were performed using luciferase substrate and buffer (Promega) in a luminometer. Values >9999 indicate activity beyond the detection range of the luminometer.

Construct	Mean luciferase activity (arbitary units)	Standard error
pGL3Basic	0.24	0.10
pGL3Basic+2kb	0.07	0.01
pGL3Basic+β-actin	781.90	3.90
pGL3Enh	1.42	0.17
pGL3Enh+2kb	0.113	0.01
pGL3Enh+β-actin	674.20	4.10

Table A1.2 Luciferase activity from 2kb LYVE-1 sequence in RAW 264.7 transfectants. Cells in 6-well dishes were transfected with 1 μg/well DNA by lipofectin reagent (Life Technologies), in duplicate for each construct. Following 72h incubation, cell lysates were prepared using reporter lysis buffer (Promega) and luciferase assays were performed using luciferase substrate and buffer (Promega) in a luminometer.

Construct	Mean luciferase activity (arbitary units)	Standard error
pGL3Basic	0.123	0.059
pGL3Basic+2kb	0.077	0.001
pGL3Basic+β-actin	229.0	57.8
pGL3Enh	0.288	0.181
pGL3Enh+2kb	0.334	0.051
pGL3Enh+β-actin	250.8	108.5

Table A1.3 Luciferase activity from 2kb LYVE-1 sequence in HUVEC transfectants. Cells in 6-well dishes were transfected with 5 μg/well DNA by electroporation (Amaxa), in duplicate for each construct. Following 72h incubation, cell lysates were prepared using reporter lysis buffer (Promega) and luciferase assays were performed using luciferase substrate and buffer (Promega) in a luminometer.

The lack of promoter activity shown with these cells indicates the promoter elements in the LYVE-1 gene most likely lie further upstream than the 2kb segment analysed. For this reason, a larger fragment of 5kb was amplified from the LYVE-1 5'UT region in human genomic DNA, using the primers 88361*Xho*I (GACTACTGCTCGAGAGTTATGGAGAGCTCCTGCAC) and 93610*Hin*dIII (detailed earlier) and following digestion with *Xho*I and *Hind*III, cloned into the the *Xho*I/*Hind*III-cut luciferase reporter pCL3Enhancer. Transfection of HUVEC was then performed (table A1.4).

Construct	Mean luciferase activity (arbitary units)	Standard error
pGL3Enh	0.338	0.052
pGL3Enh+5kb	0.121	0.040
pGL3Enh+β-actin	445.45	99.85

Table A1.4 Luciferase activity from 5kb LYVE-1 sequence in HUVEC transfectants. Cells in 6-well dishes were transfected with 5 μg/well DNA by electroporation (Amaxa), in duplicate for each construct. Following 72h incubation, cell lysates were prepared using reporter lysis buffer (Promega) and luciferase assays were performed using luciferase substrate and buffer (Promega) in a luminometer.

However, the results (table A1.4) revealed that this larger fragment of sequences displayed no luciferase activity significantly greater than that of the negative controls. Although this indicated that the promoter may be further upstream, the possible presence of a repressor element in the 2kb and 5kb segments also had to be considered. Therefore, smaller sequences of 0.4, 0.7 and 1.1 kb were amplified from human genomic DNA using 93610*Hin*dIII (detailed earlier) and the primers 92991F*Kpn*I (GACTACTGGACTACTGGGTACCGGAAGGCAGAAG GTTCTAGACTC); 92731F*Kpn*I (GACTACTGGACTACTGGGTACCAGGTGGA GTCTGACTTGAATTCTG) and 92369F*Kpn*I (GACTACTGGACTACTGGGTAC CGTGCTCACCCAGATCATGAGGTC) respectively. The amplified sequences were digested with *Hin*dIII and *Asp*718 (a more efficient isoschizomer of *Kpn*I), cloned into the *Hin*dIII/*Asp*718-cut pCL3Enhancer vector and transfected into HUVEC (table A1.5). However no promoter activity was detected in any of the LYVE-1 fragments cloned into the luciferase reporter construct.

Construct	Mean luciferase activity (arbitary units)	Standard error
pGL3Enh	0.116	0.101
pGL3Enh+0.4kb	0.000	0.000
pGL3Enh+0.7kb	0.025	0.005
pGL3Enh+1.1kb	0.000	0.000
pGL3Enh+2kb	0.029	0.005
pGL3Enh+5kb	0.008	0.008
pGL3Enh+β-actin	247.55	98.05

Table A1.5 Luciferase activity from LYVE-1 sequence in HUVEC transfectants. Cells in 6-well dishes were transfected with 5 μg/well DNA by electroporation (Amaxa), in duplicate for each construct. Following 72h incubation, cell lysates were prepared using reporter lysis buffer (Promega) and luciferase assays were performed using luciferase substrate and buffer (Promega) in a luminometer.

A1.3 Discussion

Despite initial success in identifying a PAC clone containing the LYVE-1 gene, efforts towards generating a LYVE-1 knock-out mouse were abandoned upon discovering that the US company Regeneron were at an advanced stage of creating such a mouse. Consequently efforts were diverted to characterisation of the promoter.

The 5′ end of mouse LYVE-1 was successfully mapped using primer extension of five independent primers. However, the mapping of promoter elements proved to be more problematic as the luciferase assays employed rely on LYVE-1 being actively transcribed within a transfectable cell line. It is possible that the promoter sequences in LYVE-1 lie much further upstream from the transcription start site than those sequences of up to 5kb which were cloned into the reporter

constructs. Another possibility is that a repressor element is present. An example of this lies within the VCAM-1 gene, in which upstream sequences contain negative regulatory activity (Neish et al., 1992). Future experiments would require cloning of defined segments of 5'UT region into the reporter constructs. The HDLEC cell line from PromoCell, Heidelberg may prove a better candidate as these cells constitutively express LYVE-1 (described in Chapters 4, 5 and 6). However methods for transfecting these cells must be optimised before such experiments could be successful. Detection of DNase hypersensitivity sites would also be an effective method to identify regions of the gene involved in active transcription of LYVE-1 in HDLEC. The main advantage of such a technique is that it involves no assumptions as to where putative promoter sequences and enhancer elements may lie.

As a footnote, the LYVE-1$^{-/-}$ mouse developed by Regeneron has proved not to be embryonic lethal and thus far exhibits no obvious phenotypic characteristics or reductions in life-span. However, the ability of the mouse to perform under certain physiological challenges such as inflammation may well be compromised and is the subject of current research in the Jackson laboratory.

Appendix II

Expression of Podoplanin-Fc for the Generation of Antisera

The aim of this work was to clone the extracellular domain of human podoplanin into pCDM7Ig and transfect the construct into human 293T cells using calcium phosphate prior to purifying the secreted protein from the supernatant by protein A–Sepharose chromatography. This was then used to generate polyclonal antisera in rabbits, as a stable marker for lymphatic endothelium in tissue samples (see appendix III) and in LEC. The fusion protein was also used to screen for reactivity of the mAb D2/40. The latter was carried out as a collaboration with Prof. Michael Detmar's laboratory in the Cutaneous Biology Research Centre, Harvard.

A2.1 RT-PCR and Preparation of Podoplanin cDNA

RNA was isolated from commercially available cultured human dermal microvascular endothelial cells, PromoCell, Heidelberg (described in chapters 4 and 5) and first strand synthesis performed. The podoplanin coding sequence was amplified by PCR with the primers hPodo156F*Hin*dIII (GTCAGCAGGAAGCTTCCAGGAGAGCAACAACTCAAC) and hPodo 570R *Bam*HI (TCGGCTCCGGATCCACTGTTGACAAACCATCTTTCTC) using *Pyrococcus furiosus* (Pfu) DNA polymerase. Following digestion with *Hin*dIII and *Bam*HI the product was cloned into a *Hin*dIII/*Bam*HI cut IgFc vector pCDM7Ig, to yield a construct encoding podoplanin fused at the COOH terminus to the Fc region of human IgG1.

A2.2 Expression of Podoplanin as a Soluble IgFc Fusion Protein

For expression and purification of podoplanin-Fc fusion protein, the construct was transfected into 293T cells using calcium phosphate and the secreted fusion protein purified from the supernatant by affinity chromatography on a column of protein A-Sepharose.

A2.3 Detection of Podoplanin Fusion Protein by D2/40 in ELISA

To identify the antigen of the mAb D2/40 as podoplanin, an ELISA was performed. Microtitre plates were coated with 5µg of either human podoplanin-Fc or human LYVE-1-Fc (included as a negative control). The mouse mAb anti-human podoplanin, D2-40 was applied at a series of dilutions and bound antibody was detected by incubation for 1h with horseradish-peroxidase-conjugated goat anti-mouse IgG followed by *O*-phenylenediamine (OPD) substrate and quantitated by spectrophotometry at 490 nm (see also Schacht et al., 2005).

A2.4 Detection of Podoplanin Fusion Protein by Western Blot

To further confirm the specificity of D2/40 for podoplanin, a Western blot was performed. 200ng human podoplanin-Fc and human LYVE-1-Fc were subjected to SDS-PAGE and transferred to nitrocellulose membrane. The blot was incubated with D2-40 and developed with horseradish peroxidase-conjugated goat anti-mouse IgG, using chemiluminescent detection and exposing to Kodak BioMax MR film, (see also Schacht et al., 2005).

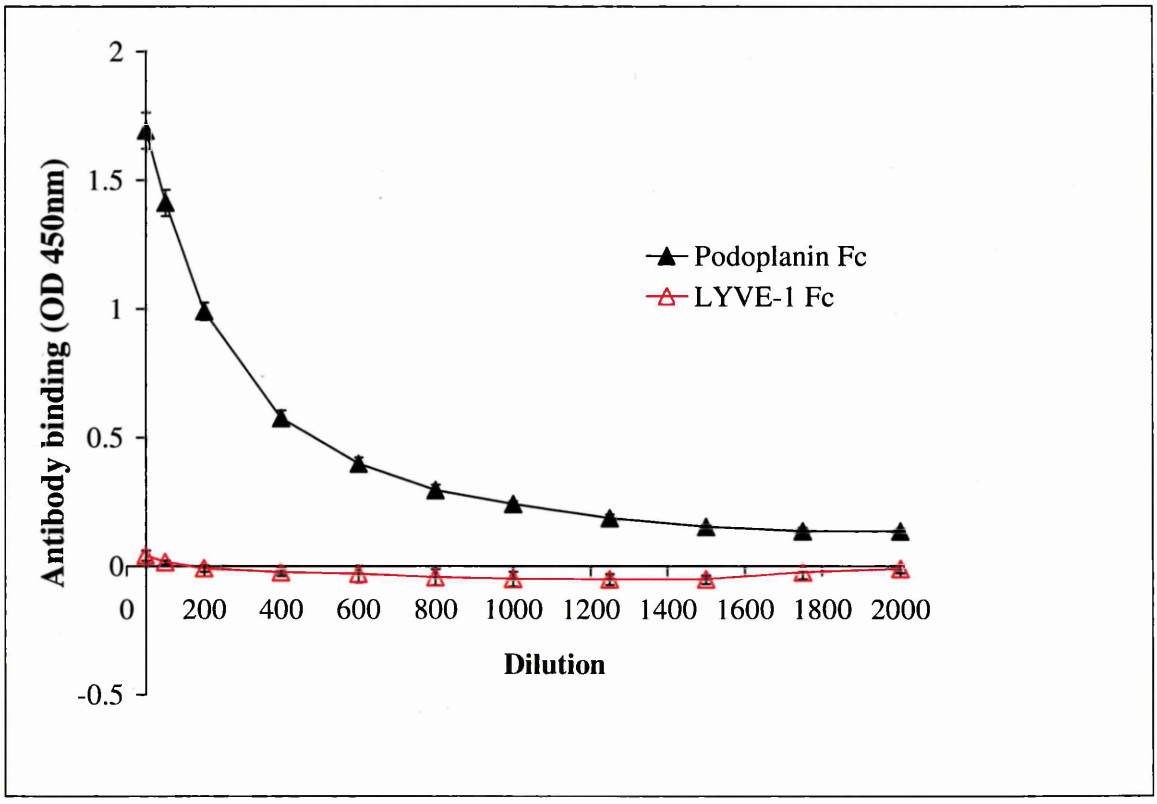

Figure A2.1 Specificity of D2/40 for podoplanin in ELISA. Microtitre plates were coated with 5µg of either the putative human podoplanin-Fc or human LYVE-1-Fc (included as a negative control). The mouse mAb anti-human podoplanin, D2-40 was applied at a series of dilutions and bound antibody was detected by incubation for 1h with horseradish-peroxidase-conjugated goat anti-mouse IgG followed by *O*-phenylenediamine (OPD) substrate and quantitated by spectrophotometry at 490 nm.

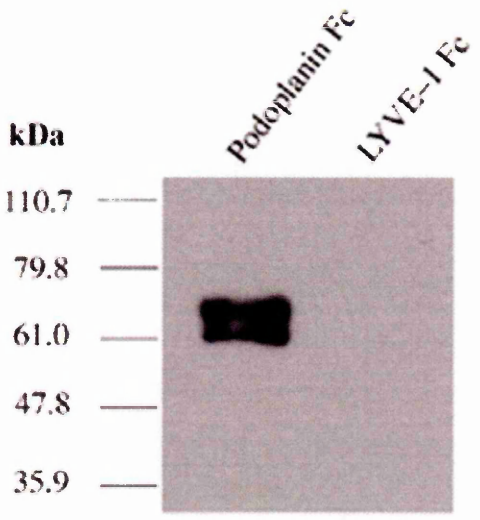

Figure A2.2 Specificity of D2/40 for podoplanin by Western blotting. The putative podoplanin Fc protein was subjected to polyacrylamide gel electrophoresis in parallel with LYVE-1 Fc, included as a negative control, then transferred to Hybond C+ membrane. The anti-podoplanin mAb D2-40 and HRP conjugated goat anti mouse IgG were applied, prior to detection using ECL reagent (Pierce) and X-ray film. Molecular weight standards (kDa) are shown on the left.

A2.5 Generation of podoplanin antisera in rabbits

To generate human podoplanin antisera, podoplanin Fc fusion protein was used to immunize two rabbits. Two test bleeds were taken one week after consecutive boost immunizations and antibody responses of the rabbits were monitored by ELISA. A microtitre plate was coated with either podoplanin Fc or LYVE-1 Fc, as an irrelevant fusion protein to assess the proportion of immune response which had been raised against the Fc domain of the immunogen. Serum prepared from animals following immunisation and also from the same animals before the immunisation schedule had commenced (as preimmune controls), were applied to the microtitre plate. Bound antibody was detected by peroxidase-conjugated goat anti-rat IgG and *O*-phenylenediamine (OPD) substrate and quantitated by spectrophotometry at 490 nm. As shown in figure A2.3, the antiserum from both rabbits showed reactivity against both fusion proteins and hence was directed towards the Fc region. Therefore neither could be used as a podoplanin polyclonal antibody although proved useful in detecting the Fc portion of human IgG (Branwen Hide, PhD student).

Future attempts to generate antibodies against podoplanin should either involve cloning into a vector that permits efficient cleavage and thus removal of the Fc portion. Alternatively rabbit, mouse or rat (depending on the host species) Fc could be used in the fusion construct in place of human Fc.

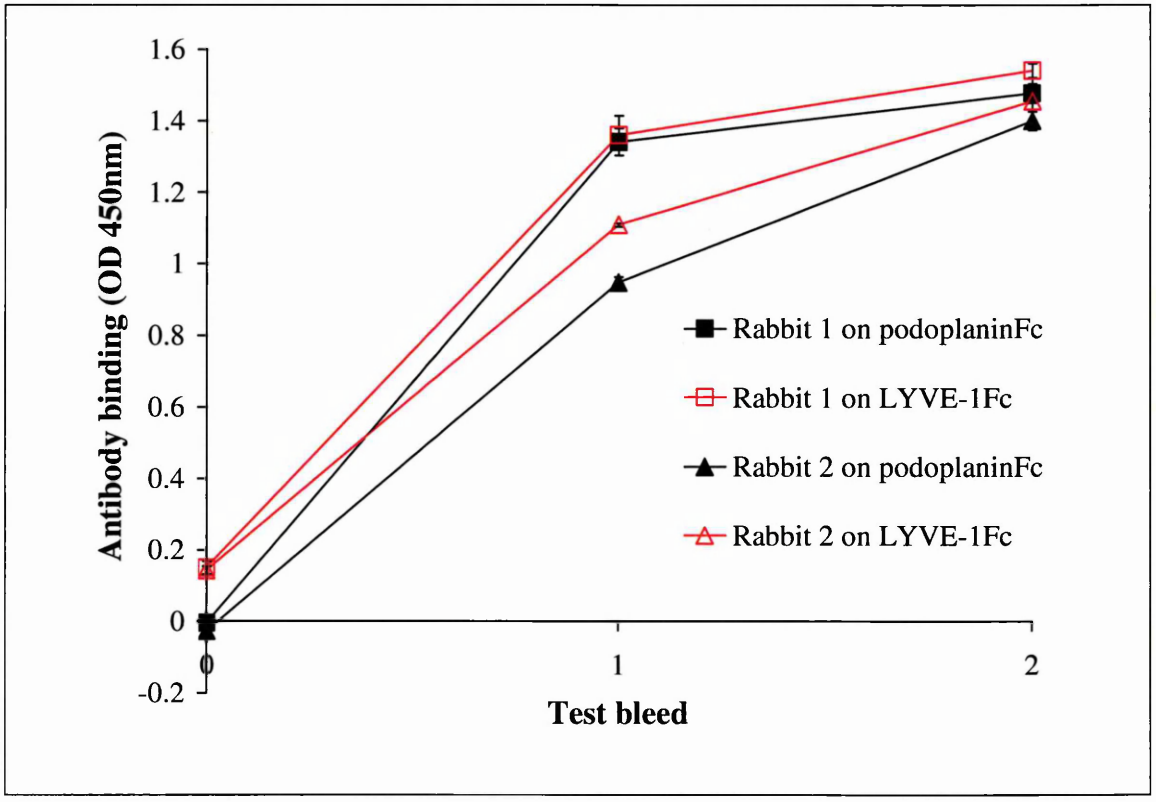

Figure A2.3 Test bleed of rabbit podoplaninFc immunised rabbits. Sera from both animals, from either the preimmune test bleed as negative controls or from the two test bleeds were diluted 1:50 and applied to a microtitre plate precoated with either LYVE-1 Fc or podoplanin Fc at 5 µg/ml. Bound antibody was detected with HRP-conjugated goat anti-rat antibody and OPD substrate, measuring the absorption at 490nm. Values are the mean ± standard deviation for triplicate wells.

Appendix III

Heterogeneity of LYVE-1 Expression by Tissue Lymphatics

Squamous cell carcinoma is known to have a considerable inflammatory infiltrate associated with it and the development of such lesions in mice has been shown to be mediated through TNFR1 signalling, as well as an up-regulation of TNFα (Lind et al., 2004). Experiments described in chapter 4 of this thesis showed that TNFα induces marked down-modulation of LYVE-1 in primary lymphatic endothelial cells derived from three different sources. Therefore to investigate whether such a decrease in expression occurs *in vivo*, lymphatic vessels within frozen sections of squamous cell carcinoma tissue were stained using podoplanin, a stable marker for lymphatic endothelium and LYVE-1. Frozen sections of squamous cell carcinomas and surrounding healthy tissue were prepared from 5 patients and kindly donated by Abigail King and Dr. Graham Ogg, MRC Human Immunology Unit, Weatherall Institute of Molecular Medicine, Oxford for this preliminary study.

Whereas the normal skin surrounding the lesion showed colocalisation of LYVE-1 with podoplanin and strong expression of LYVE-1, tissue from the lesions showed numerous podoplanin-positive vessels which were LYVE-1 negative (figure A3.1). Although some LYVE-1 expression was detected in squamous cell carcinoma tissue (for example in patient 5), it was feint and only on a minority of vessels. A study by Schacht et al. (2005) has shown that although podoplanin is absent from normal human epidermis, it can be strongly induced in squamous cell carcinoma. Therefore, some of the podoplanin-positive structures shown in

figure A3.2 which do not appear to have typical lymphatic vessel morphology, may be epithelial tissue and hence LYVE-1-negative. Further studies into this potentially interesting avenue were restricted by patient numbers.

Many human cancers are associated with pre-existing chronic infectious or inflammatory conditions (Schacter et al., 2002). Inflammatory infiltrates of tumour-associated macrophages, DCs and T cells result in the high concentration of pro-metastatic cytokines, MMPs and reactive oxygen intermediates and although squamous cell carcinoma is not highly metastatic, a substantial inflammatory infiltrate has been reported. The apparent down-regulation of LYVE-1 observed in squamous cell carcinoma may be in response to the pro-inflammatory infiltrate and cytokines such as TNFα, shown in chapters 4 and 5 of this thesis to reduce expression of LYVE-1 dramatically *in vitro* and in chapter 6 to down-regulated LYVE-1 in intact lymphatic vessels *in vivo*. Although hypoxia was also shown to reduce LYVE-1 expression in cultured HDLEC (chapter 4), the effect was marginal in comparison to that induced by TNFα and the images captured by immunofluorescence microscopy suggest a more significant loss of LYVE-1 in tissues than that precipitated by hypoxia. Immunofluorescence microscopy could be used to indicate whether or not the tissue is hypoxic and expressing CA9, known to be up-regulated on endothelium under conditions of low oxygen tension, or whether TNFα could be detected. Clearly if the down-regulation of LYVE-1 apparent in this preliminary study is borne out in an extended investigation examining more samples of human tissue, the use of LYVE-1 as a marker in conditions of inflammation could have led to an underestimation of lymphatic vessel density in previous studies.

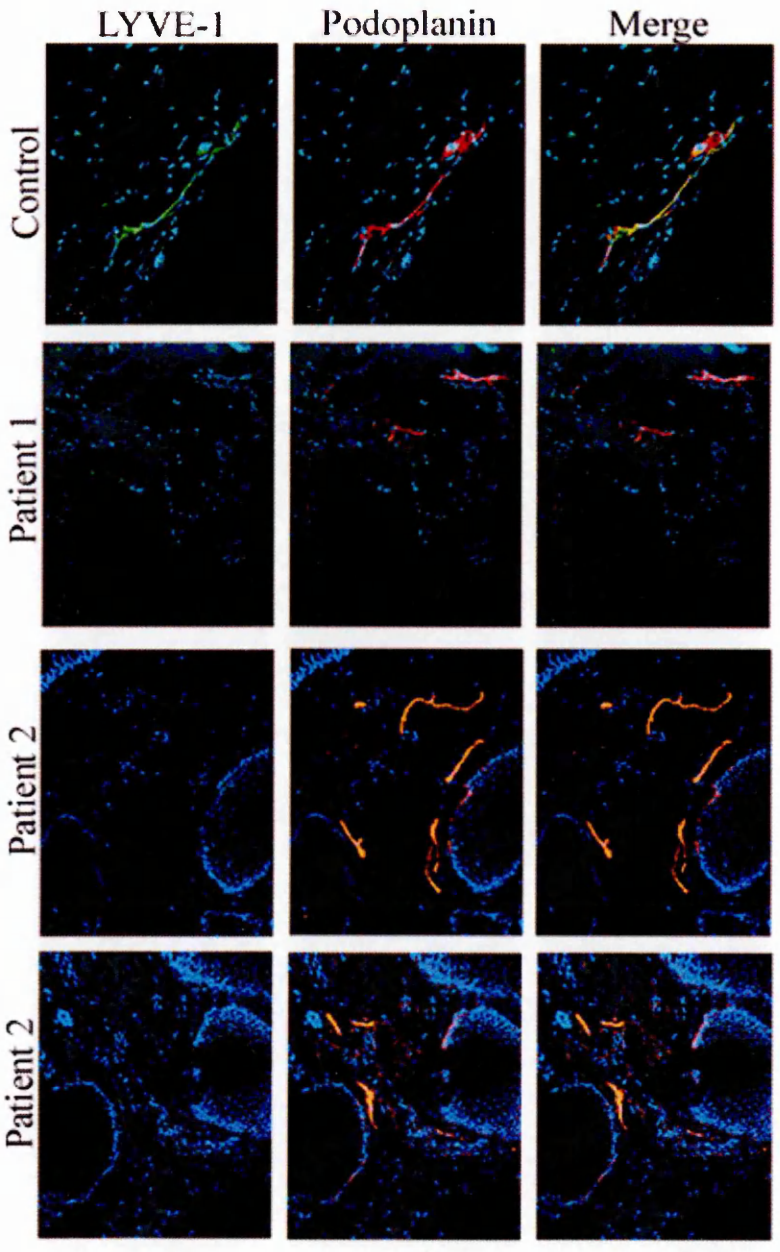

Figure A3.1 Reduced expression of LYVE-1 on podoplanin-positive lymphatic endothelial vessels in squamous cell carcinoma tissue. Frozen tissue sections were stained with anti-LYVE-1 mAb and rabbit anti-podoplanin, with AlexaFluor® conjugates 488 (green) and 594 (red) respectively. Nuclei were counterstained with DAPI. Immunofluorescence microscopy of normal healthy geriatric skin tissue from patient 1 is shown in the upper panels whilst a representative image from the carcinoma lesion of that patient is shown in panels beneath, as well representative images from the lesion of a second patient. Images were captured at magnification: X 320.